1975-1

Compilation and Summation of Historical and Existing Physical Oceanographic Data from the Eastern Gulf of Mexico

FINAL REPORT
Contract No. 08550-CT4-16

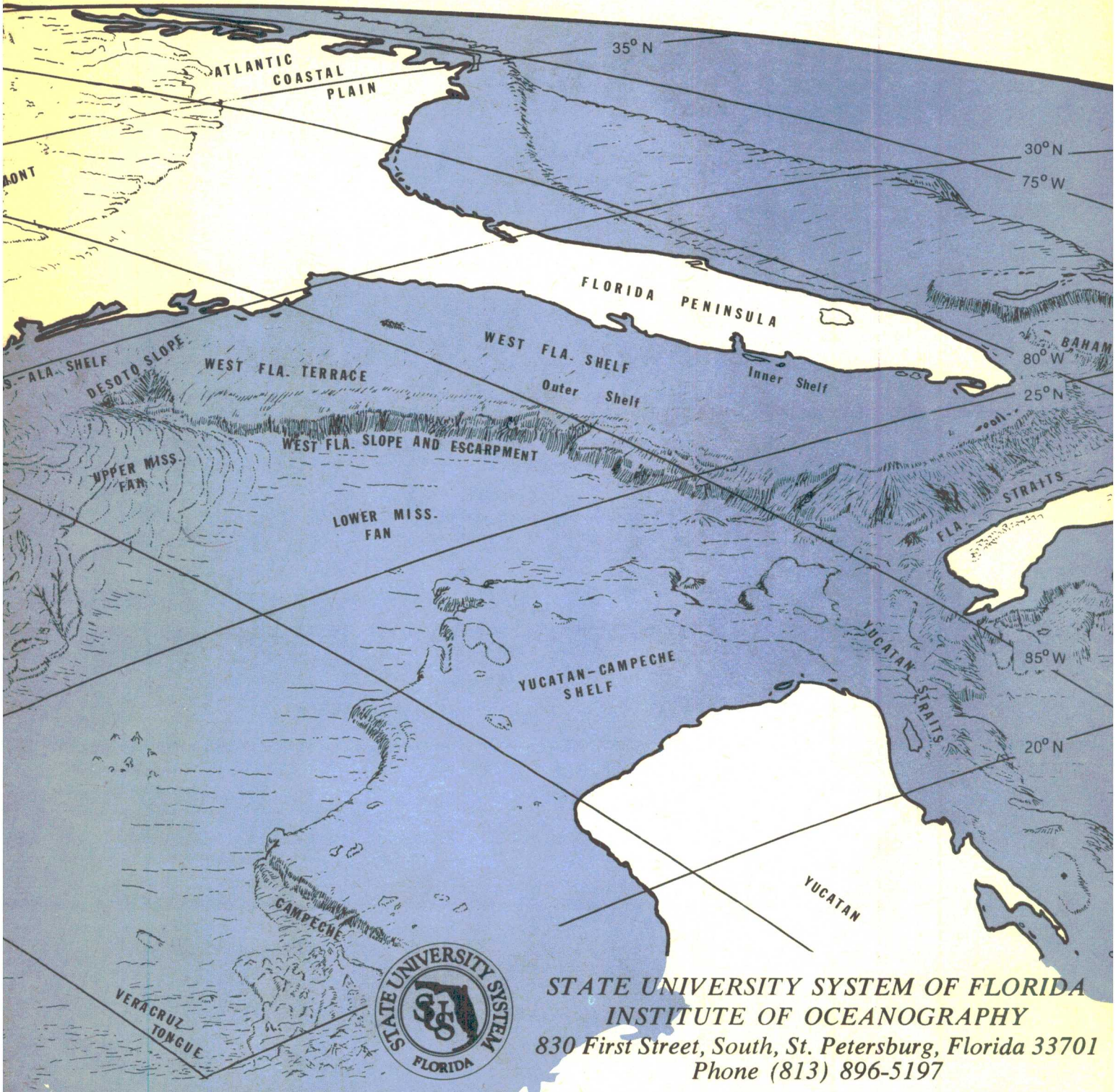

STATE UNIVERSITY SYSTEM OF FLORIDA
INSTITUTE OF OCEANOGRAPHY
830 First Street, South, St. Petersburg, Florida 33701
Phone (813) 896-5197

University of Florida, Gainesville · *Florida State University, Tallahassee* · *Florida A. & M. University, Tallahassee* · *University of South Florida, Tampa* · *Florida Atlantic University, Boca Raton*
University of West Florida, Pensacola · *Florida Technological University, Orlando* · *University of North Florida, Jacksonville* · *Florida International University, Miami*

Compilation and Summation of Historical and Existing Physical Oceanographic Data from the Eastern Gulf of Mexico in Support of The Creation of a MAFLA Sampling Program

A Report Submitted to the
Bureau of Land Management
under BLM Contract No. 08550-CT4-16

July 15, 1975

Participating scientists and agencies

University of Miami

C. N. K. Mooers
E. D. Houde
J. Fernandez-Partegas
J. Price
H. Perkins
J. Van Leer

University of Alabama

W. W. Schroeder

Texas A&M University

J. D. Cochrane

NOAA/EDS/NODC

R. C. Lockerman
D. Knoll

Nova University

P. P. Niiler
R. Plaisted

NOAA/AOML

R. L. Molinari (Scientific Coordinator)
G. A. Maul
D. V. Hansen

SUSIO

M. Rinkel (Contract Administrator)

NOAA/NMFS

J. Brucks

Table of Contents

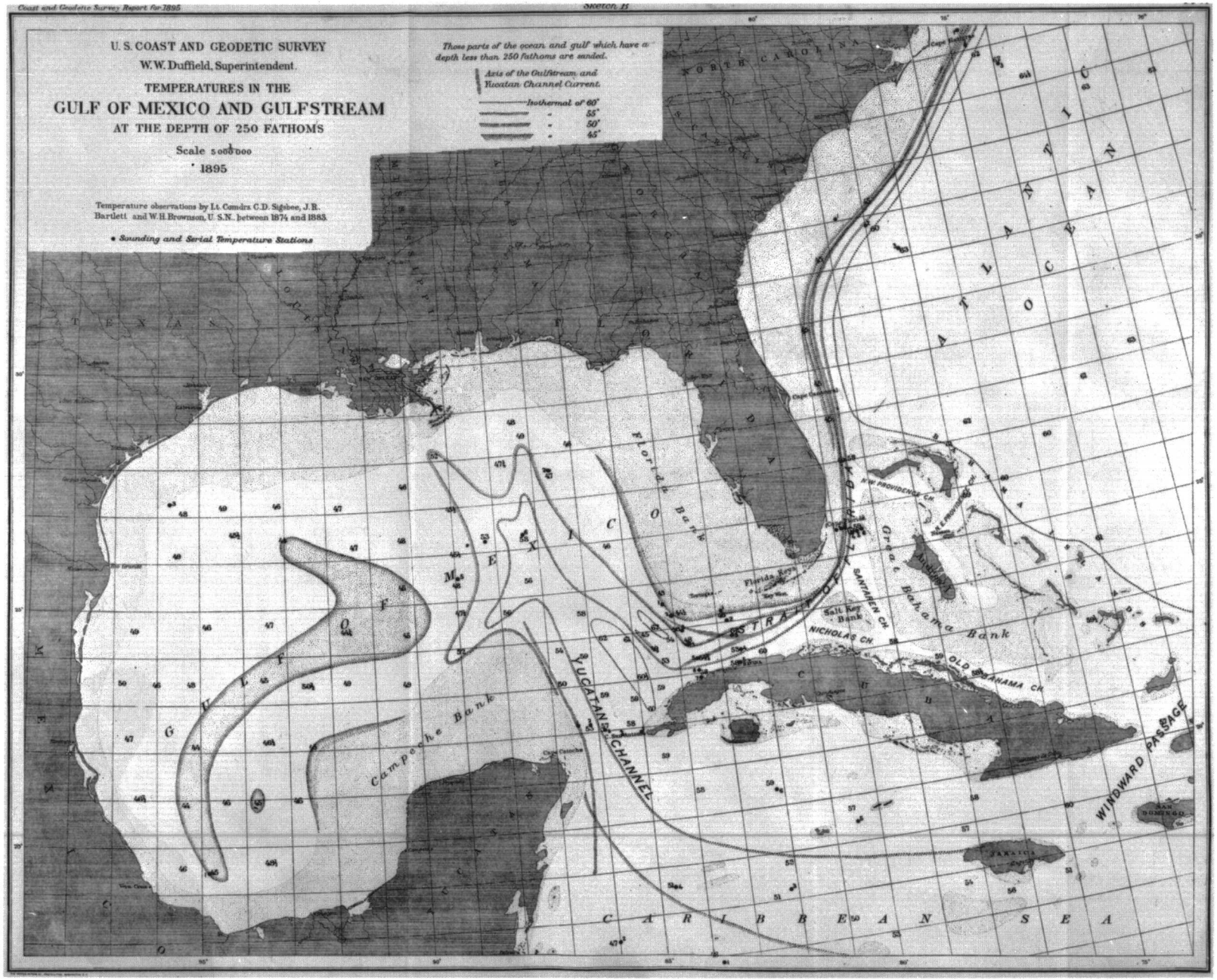

Historical Background: 1895 Map of the Temperatures (°F) in the Gulf of Mexico at the Depth of 250 Fathoms.

I. Introduction

Physical oceanography has a dual role in determining the environmental implications of development of the Outer Continental Shelf (OCS). It is intrinsically important to determine physical parameters to predict dispersion of materials in OCS waters, but the role of physical oceanography is equally important in the support it must give to other oceanographic disciplines. In fact, it is highly unlikely that meaningful interpretations of bio-geo-chemical data, or the ecosystem structure can be made without adequate knowledge of the advective field, for instance.

Cognizant of the importance of understanding the circulation of the eastern Gulf of Mexico, the Bureau of Land Management (BLM) commissioned a group of oceanographers familiar with the area:

a) to "assemble the historical and contemporary physical and associated meteorological data of the northeast Gulf of Mexico... for submission to the National Oceanographic Data Center (NODC)";

b) to "construct a zero-order synthesis of oceanographic conditions in the northeast Gulf of Mexico and have them graphically displayed";

c) to "describe the general circulation and oceanographic conditions on the continental shelf area of the northeast Gulf of Mexico and in the Loop Current of the deeper Gulf areas";

d) to "describe qualitatively the interaction between the shelf circulation of the northeast Gulf of Mexico and the Loop Current";

e) to "describe the seasonal distribution of the intensity of fish spawning and zooplankton productivity on the western Florida continental shelf and relate these to temperature and salinity data";

f) to "develop a first-order understanding of the trajectory of a pollutant in the northeast Gulf of Mexico"; and

g) to "provide recommendations on sampling locations for future biological, geological, chemical, and physical oceanographic investigations".

Objective (a) was required because at the inception of this program a considerable portion of the data collected in the Gulf of Mexico had not been submitted to NODC. Phase 1 of this study therefore consisted of an accelerated reduction of existing data, and submission of the data to the national repository. Table 1 lists the data-set at NODC in the region 21°N to 30°N, and 81°W to 90°W (figure I-1), before the completion of this phase, and those data forwarded to NODC as a result of this phase.

Table 1.
Results of accelerated reduction and submission of data to NODC

Type of data	Previously at NODC	Submitted to NODC
STD-Hydrocast	3,363	5,602
XBT	2,500	2,569
MBT	12,078	811
Cyclesonde stations		5,740
Current meter days		2,899

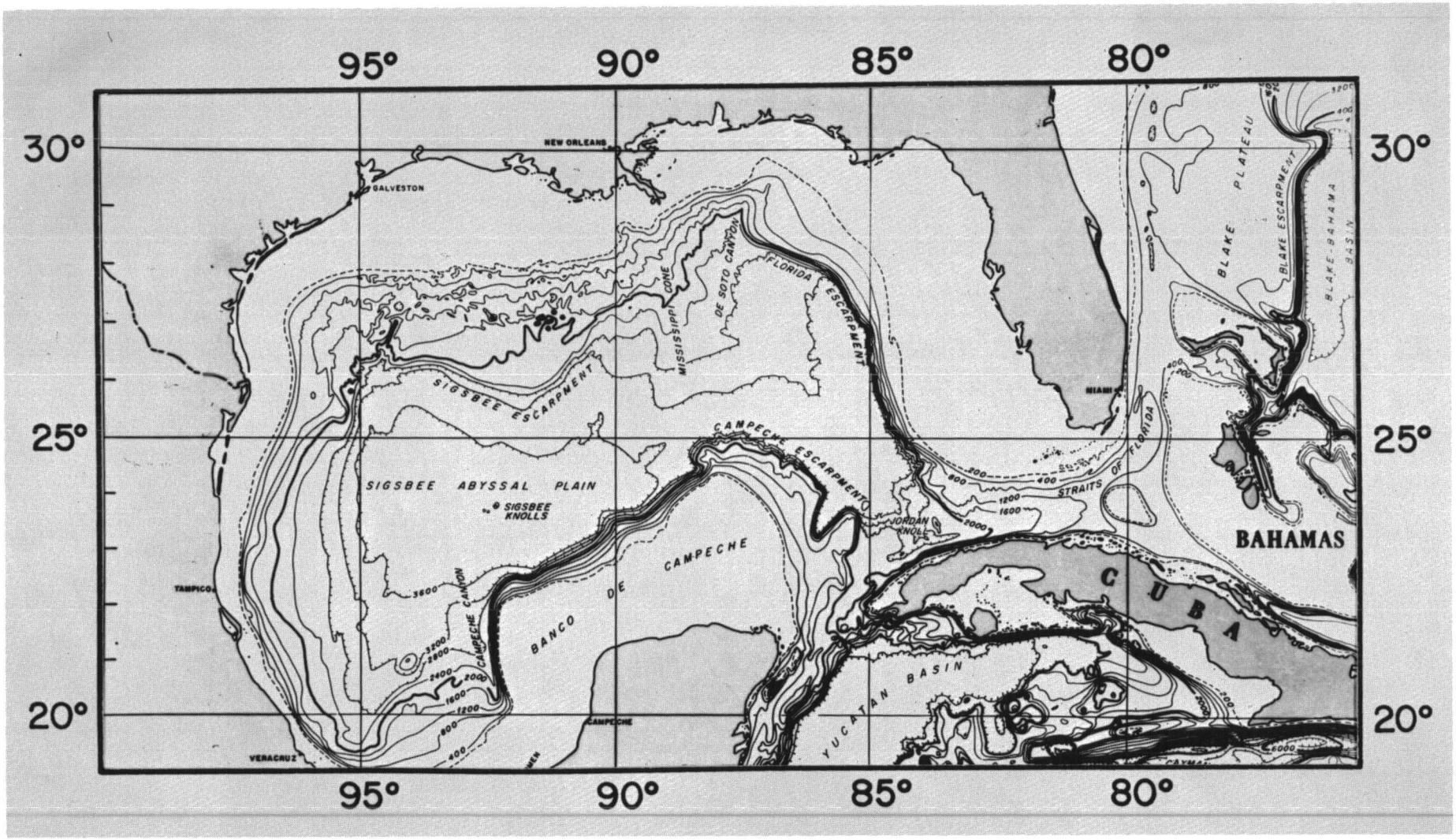

Figure I-1. Bathymetric map of the Gulf of Mexico, with isobaths in meters. (Uchupi, 1971).

It should be noted that a portion of the data submitted includes data previously forwarded to NODC, but not yet processed.

NODC established a separate data-file in which the MAFLA data were stored. At the request of the individual investigators certain analyses and graphic displays were produced from this data-set to meet objectives (b) through (g) above. The list of products provided is given in Appendix I.

The following sections are summary statements of the group's individual and/or collective thoughts on objectives (c) to (g) above. First, a description of the atmospheric conditions over the eastern Gulf of Mexico, the tides, the river run-off, and the hydrography and circulation of the shelf and deep-basin are given in the summary of knowledge (objective c). The mechanisms by which atmospheric disturbances, the Loop Current, tides and river run-off can induce shelf motions are then discussed (objective d). Discussion of the modes of motion induced by these forcing functions is given when data are available. A section on biological patterns and variability, and the red tides are included to indicate the importance of the supportive role physical measurements play (objective e).

Some of the difficulties encountered when attempting to predict pollutant trajectories using climatological data are described. Possible pollutant trajectories based on previous studies, and analyses of the NODC products are then presented (objective f). The proposed sampling grid (objective g) explicitly establishes a program to monitor shelf and deep basin circulation, to describe processes important in determining dispersion, and to obtain data for input to a numerical model. Also implicit in the design of the sampling grid is information pertinent to the establishment of bio-geo-chemical grids.

A list of other recommendations is given, based on knowledge gained during the course of this program, to aid other groups planning similar studies. These recommendations include thoughts on insuring the successful implementation of BLM objectives by continuing the efforts initiated in this preliminary study.

Several appendices are attached which present in greater detail the data-sets considered in the summary discussions. These appendices are particularly useful in delineating the spatial and temporal extent of the available data-set.

II. Summary of Knowledge

The eastern Gulf of Mexico is defined herein as the region bounded on the west by 90°W, on the east by the west Florida coastline, on the south by 21°N, and on the north by the Mississippi, Alabama, Florida (MAFLA) coastline. Figure I-1 presents a schematic diagram of the bottom topography of this region. The shelf is usually considered that region shoreward of the 200 meter isobath, and the deep basin, those regions with depths greater than 200 m.

A summary of the geological oceanography of the region is given by Brooks (1973), who also lists a partial bibliography. Those topographic features which directly affect shelf motions will be discussed where appropriate.

The sections to follow include summary statements on atmospheric disturbances, shelf and deep-basin hydrography and circulation, and biological variability. Although a wealth of information is available in the NODC products, time constraints prohibited a complete analysis of this information. Therefore, that portion of the available data relevant both to defining those processes active in dispersing shelf waters, and to determining a sampling grid was given particular attention.

A. Meteorological Disturbances

Jose Fernandez-Partagas

Atmospheric fronts which affect the continental shelf of the eastern Gulf of Mexico have a space-scale of several thousand kilometers, and a time-scale of several days. Data were obtained from the National Climatic Center (NCC) to compute statistical characteristics of these frontal passages over the eastern Gulf of Mexico.

Appendix II presents some preliminary results of the analysis performed on these data. The more salient results, as well as a discussion of more persistent atmospheric features, are given below.

Meteorologically, there are two distinct seasons in the eastern Gulf of Mexico and over the surrounding land-masses: the winter season and the summer season. The transition of one season to the other usually occurs in April or May, and in October or November. A progressive vector diagram of winds at 26°N, 86°W is given in figure IIA-1 for two successive years; the two years were remarkably similar, showing winter disturbances and summer persistence of the Southeast Trades.

1. Winter Disturbances

Over the eastern Gulf of Mexico, the atmospheric circulation in winter is chiefly controlled by synoptic-scale disturbances which have a space-scale of several thousand kilometers and a time-scale of several days. The main synoptic-scale disturbances in winter are the atmospheric fronts which separate two air-masses of different characteristics: a cold, dry air-mass and a warm, relatively moist air-mass. Depending upon the relative velocity of these two air-masses, the fronts are classified as (1) cold fronts; (2) warm fronts; (3) stationary fronts; and (4) occluded fronts. Cold fronts and warm fronts are the most frequently observed. Stationary fronts are observed over short periods (usually for less than 24 hours), and occluded fronts rarely affect the eastern Gulf of Mexico. Cold fronts in winter move predominantly toward the southeast at an average speed of 15-20 knots. Warm fronts move basically toward the north at an average speed of 5 knots or less.

Occasionally, an extratropical cyclone (which is associated with different air-masses) shows a significant development over the eastern Gulf of Mexico. Such an extratropical cyclone usually moves to the northeast or to the east at a high speed (25-30 knots), crosses northern Florida, and reaches its maximum intensity over the Atlantic Ocean.

2. Summer Disturbances

The atmospheric circulation over the eastern Gulf of Mexico in summer is primarily controlled by a quasi-permanent feature: the east-west oriented high pressure ridge which elongates westward from the Bermuda-Azores high. Different wind flow regimes (easterlies, westerlies, or light and variable winds) over specific locations in the eastern Gulf of Mexico are associated with the latitudinal fluctuations of this

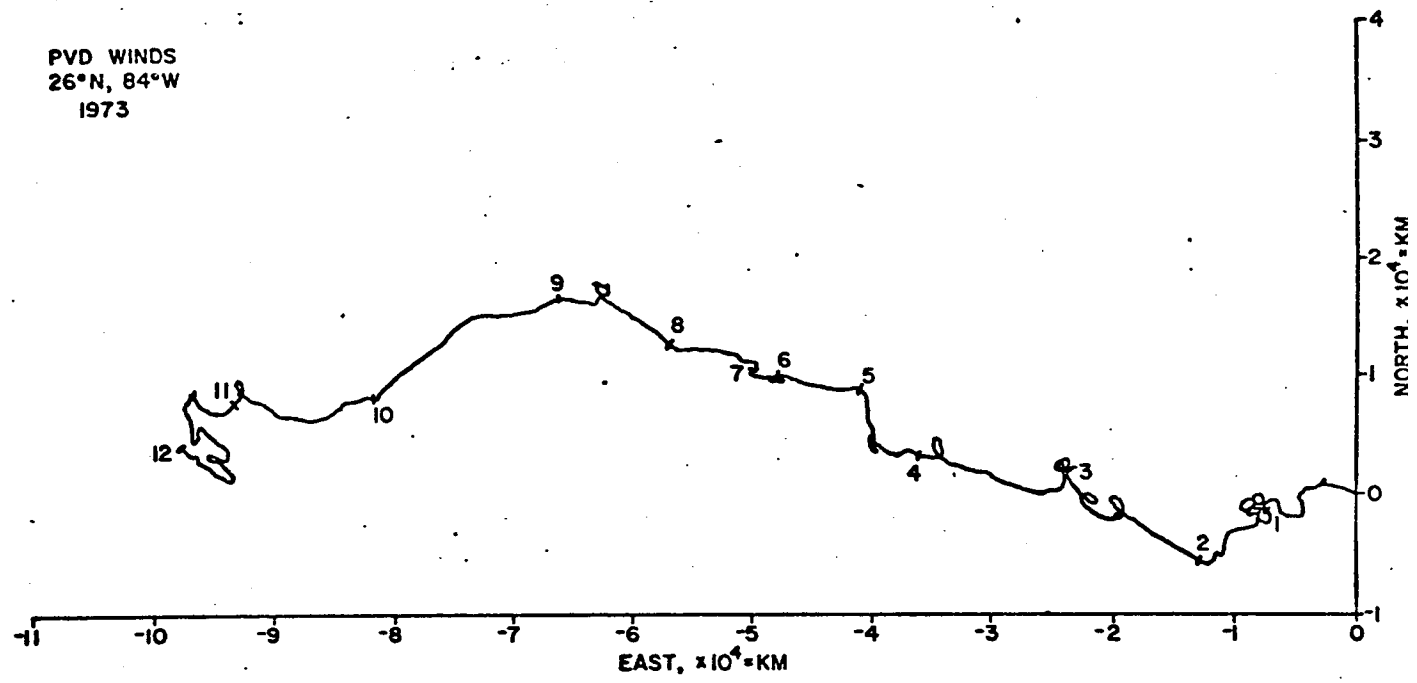

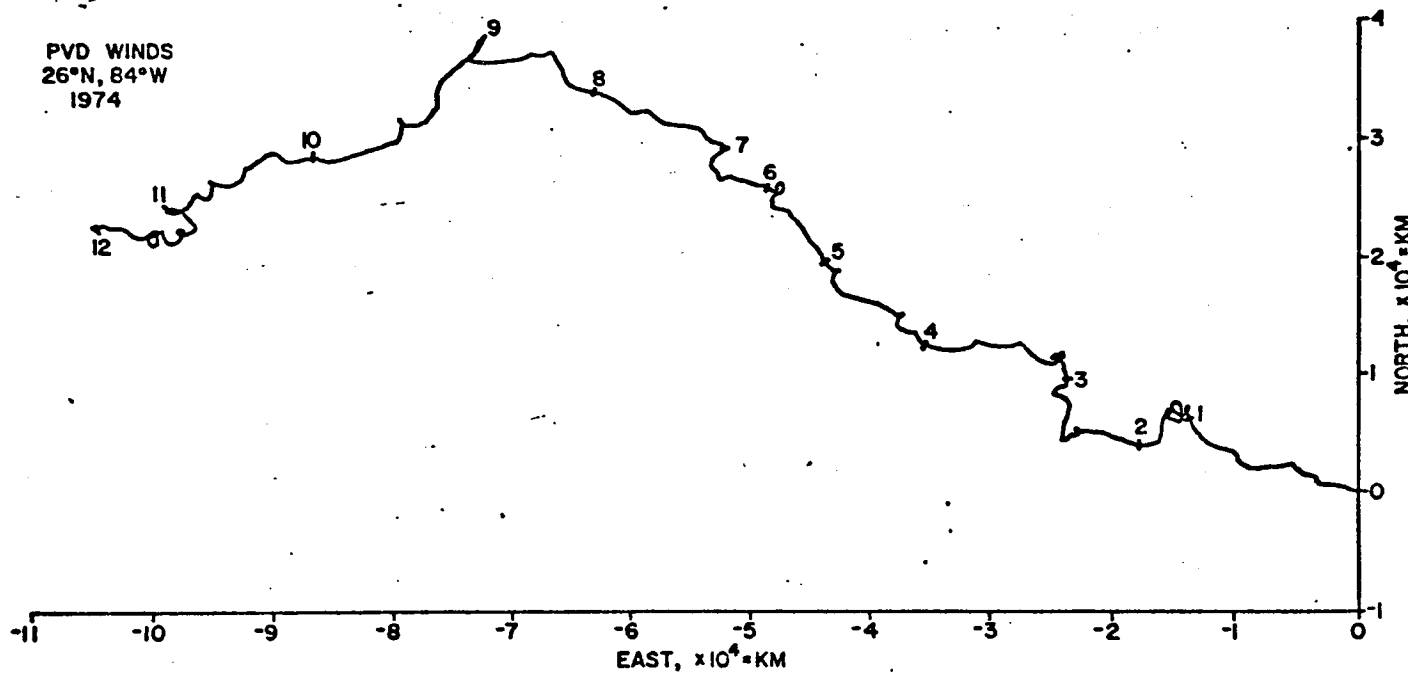

Figure II A-1. Progressive vector diagram of winds deduced from synoptic weather charts for 26°N, 84°W, for two years. The numbers denote the end of months. The distance between the numbers is proportional to the mean speed for the month.

ridge. The prevailing flow at specific locations depends upon the relative position of the ridge axis.

The summer disturbances in the eastern Gulf of Mexico are basically of tropical origin and are classified as (1) tropical waves; and (2) tropical cyclones.. Tropical waves tend to be quite weak, especially near the sea-surface. Conditions necessary for the development of tropical storms and hurricanes are not frequently found. However, at least one or two tropical storms and/or hurricanes may affect the eastern Gulf of Mexico every year. While in this area, tropical storms and hurricanes tend to show a northwest to northeast movement, and in many cases, their forward speed is 15 knots or less.

B. Tides

Christopher N. K. Mooers

A comprehensive review of the surface tides in the Gulf of Mexico has been given by Zetler and Hansen (1972). They note that the diurnal tides of the Gulf of Mexico tend to co-oscillate with those of the North Atlantic. The range of the surface tides in the Gulf is of the order of 15 cm, with the diurnal tides dominant over the semidiurnal tides in most locales. Though numerous coastal tide gauges exist in the Gulf, there is very little tidal current data. In such a case, numerical models are a possible recourse. Grijalva (1964), Garner (1966), and Mikhailov, Meleshko, and Sheheveleva (1969) have produced numerical models for the semidiurnal tides and tidal currents in the Gulf of Mexico. The models reveal patterns of tidal currents which vary considerably through the Gulf.

Because internal (baroclinic) tides can exist where and when strong density stratification exists, internal tides can be expected to be more prevalent in summer than winter. Internal tides lead to enhanced tidal velocities with large velocity changes in the vertical across the thermocline, and are thus important in mixing processes. Internal tides will become incoherent where there are irregularities in bottom topography, hydrography, and currents. Thus, in the winter season, the season of large-scale transient circulation patterns produced by meteorological disturbances, very irregular internal tides can be expected (Price and Mooers, 1974). Tidal velocities of 5 to 20 cm/sec were observed in their study at 26°N. The diurnal ellipses were oriented north-south, and the semidiurnal ellipses were oriented east-west. Both tidal species were very baroclinic and irregular; i.e., their amplitudes and phases varied with depth and time due to modulation by transient circulations.

An important part of the short-term circulation is the inertial motion, which has a period dependent upon latitude. On the West Florida Shelf, the inertial period varies from about 28 hours at Key West to about 24 hours at Mobile Bay. Thus, the diurnal tides are near-inertial motions in the Northeastern Gulf, which will lead to further irregular diurnal tidal behavior. As noted previously, inertial motions are predominantly excited by meteorological disturbances. They have been observed to have horizontal velocities of 10 to 30 cm/sec on the West Florida Shelf (Price and Mooers, 1974, and Mooers and Van Leer, 1975).

In conclusion, it can be stated with some confidence that tidal and inertial motions produce particle orbits with a radius of the order of several kilometers and an orbital period of the order of 12 to 28 hours in the Eastern Gulf of Mexico. Such particle motions are likely to play a significant role in horizontal dispersion. The baroclinic components of these motions are a very important mechanism for producing vertical mixing through shear instabilities.

C. River Run-off

William W. Schroeder

River discharge data for the MAFLA area, excluding the Yucatan Peninsula and Cuba, are summarized in Table 2. A Cumulative total of 663,361 ft^3/sec (18,784 m^3/sec) is received by the study area. This is equivalent to approximately 21×10^{12} ft^3/yr (60×10^{10} m^3/yr), or .02% of the Gulf of Mexico's volume, or .07% of the annual volume of the Florida Current.

The MAFLA area can be divided conveniently into four geographical sub-areas, on the basis of river discharge characteristics, west, northwest, northeast, and east. The river discharge associated with each area is listed in Table 3. A decrease in runoff, from west to east is very apparent in these data. The western sub-area is dominated by the Mississippi Delta land mass, and characterized by the Mississippi River which accounts for 72% of the total discharge into the MAFLA area. The Mississippi Delta protrudes into the Gulf of Mexico to 29°N latitude, while the Mississippi, Alabama, and Northwest Florida coastlines parallel 30.5°N latitude. The geographical point of discharge for the Mississippi River is only 20 km from the 200 m isobath and 45 km from the 1000 m isobath. The broad Mississippi-Alabama continental shelf lies to the north and east. This can result in a condition where the discharged waters may be easily entrained by the Loop Current.

The northwestern sub-area encompasses the coastline from Chandeleur Sound to Cape San Blas. It is characterized by a number of river discharges dominated by the Mobile Delta River System (Table 3). The combined discharges amount to only 20% of the Mississippi River discharge. All of the discharged waters enter the MAFLA area in coastal regions boardering a broad shallow continental shelf.

The northeastern sub-area extends from Cape San Blas east to Tarpon Springs. This region is commonly known as "The Big Bend". It is characterized by an extensive shallow inner continental shelf. The Chipola River at Apalachicola Bay and the Suwannee River at Suwannee Sound are responsible for the major discharges. This sub-area received less than 7% of the total river discharge in the MAFLA area and is equivalent to just over 9% of the Mississippi River discharge. All of the discharge in this sub-area, however, flows into the shallow coastal area.

The eastern sub-area includes the remainder of the MAFLA area from Tarpon Springs south to Florida Bay. This region can be appropriately labeled "the desert" because it accounts for less than 1% of the total river discharge.

The monthly average discharges for the Mississippi, Amite-Pearl, Pascagoula, and Mobile Bay Delta System are shown in Figure IIC-1. The Mississippi River reaches a maximum discharge in April, while the Pascagoula and Mobile Bay Delta System peak in March and the Amite-Pearl in February-March. Minimum discharges occur during the August-September-October period for all of the rivers.

TABLE 2

RIVER DISCHARGE IN THE STUDY AREA
(MODIFIED FROM CORPS OF ENG. DATA, ROSS, 1973 AND CHERMOCK, 1974)

Receiving body of Water	Mean Discharge (c.f.s.)	
Gulf of Mexico (Mississippi River Delta, Louisiana)		
Mississippi River	478,028	
Mississippi Sound (Louisiana, Mississippi, Alabama)		
Pascagoula River	15,200	
Old Fort Bayou	90	
Biloxi River	1,110	
Bayou Bernard	150	
Wolf River	760	
Jourdan River	700	
Pearl River	12,900	
Additional	520	(1)
Subtotal (Direct input)	31,430	
Amite (via Lake Maurepus, Lake Pontchartrain and Lake Borgne)	1,891	
TOTAL	33,321	
Mobile Bay System (Alabama)		
Montlimer Creek	18	
Fish River	107	
Additional	600	(1)
Alabama River	31,870	
Tombigbee River	36,230	
East Basset Creek — Mobile Delta River System	276	
Chickasaw Creek	260	
Additional	3,715	(1)
TOTAL	73,076	
Perdido Bay (Alabama & Florida)		
Perdido River	740	
Jacks Branch	27	
Styx River	170	
Additional	931	(1)
TOTAL	1,868	
Pensacola Bay System (Florida)		
Escambia River	6,544	
Pine Barren	144	
Yellow River	2,228	
Shoal River	1,092	
Blackwater River	305	
Big Juniper Creek	70	
Big Coldwater Creek	532	
Pond Creek	82	
Additional	1,605	(1)
TOTAL	12,602	

TABLE 2
(continued)

Receiving body of Water	Mean Discharge (c.f.s.)
Choctawhatchee Bay (Florida)	
Choctawhatchee River	7,063
Additional	1,289 (1)
TOTAL	8,352
St. Andrew Bay (Florida)	
Econfina Creek	535
Additional	5,832 (1)
TOTAL	6,367
Apalachicola Bay (Florida)	
Chepola River	24,960
Apalachicola River	1,531
Additional	144 (1)
TOTAL	26,635
Apalachee Bay (Florida)	
Ochlockonee River	1,832
St. Marks River	736
Aucilla River	385
Econfina River	134
Fenholloway River	125
Additional	2,232 (1)
TOTAL	5,444
Deadman Bay (Florida)	
Steinhatchee River	326
Additional	419 (1)
TOTAL	745
Suwannee Sound (Florida)	
Suwannee River	10,560
Additional	868 (1)
TOTAL	11,428
Waccasassa Bay (Florida)	
Waccasassa River	80
Additional	120 (1)
TOTAL	200
Tampa Bay System (Florida)	
Sweetwater Creek	25
Rock Creek	45
Double Branch	40
Lake Tarpon (Brooker Creek)	29
Hillsborough River	671
Palm River	62
Alafia River	384
Little Manatee River	186
Manatee River	109
Additional	263 (1)
TOTAL	1,814

TABLE 2
(continued)

Receiving body of Water	Mean Discharge (c.f.s.)
Charlotta Harbor (Florida)	
Myakka River	359
Peach River	1,267
Additional	639 (1)
TOTAL	2,255
San Carlos Bay	
Caloosahatchee River	1,044
Additional	182 (1)
TOTAL	1,226
Florida Bay (Florida)	
NO DATA	

(1) Estimated

Table 3

MAFLA Subareas based on River Discharge Characteristics

West		
Mississippi River		478,028
Northwest		
Mississippi Sound	33,321	
Mobile Bay System	73,076	
Perdido Bay	1,868	
Pensacola Bay System	12,602	
Choctawhatchee Bay	8,352	
St. Andrew Bay	6,367	
TOTAL		135,586
Northeast		
Apalachicola Bay	26,635	
Apalochee Bay	5,444	
Deadman Bay	745	
Suwannee Sound	11,428	
Waccasassa Bay	200	
TOTAL		44,452
East		
Tampa Bay System	1,814	
Charlotta Harbor	2,255	
San Carlos Bay	1,226	
Florida Bay	N.D.	
TOTAL		5,295
		663,361

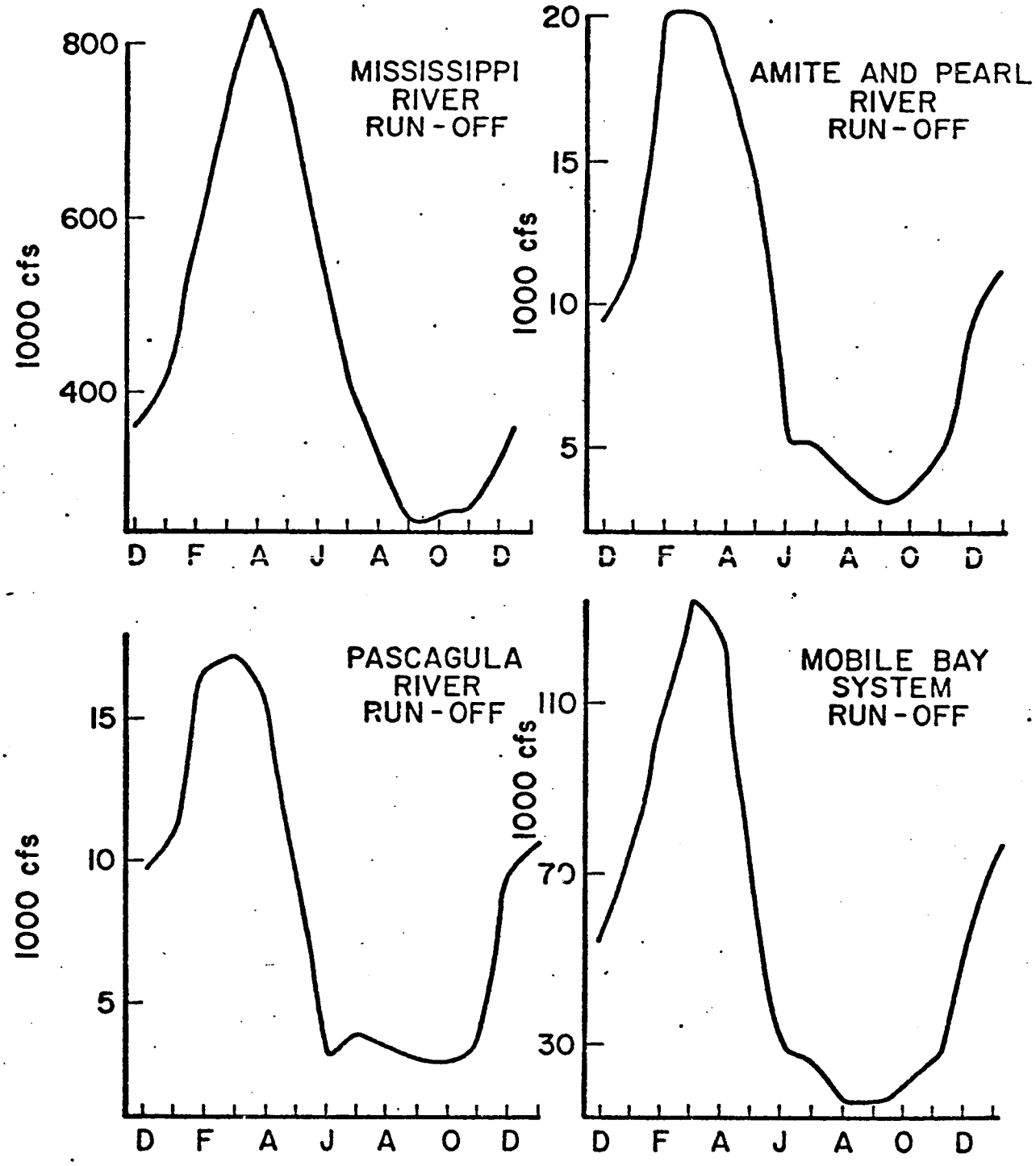

Figure II C-1. Annual cycle of river discharge for four rivers in the MAFLA area.

The plumes created by river discharges, particularly in the western and northwestern sub-areas do not necessarily assume a fixed or regular horizontal distribution pattern. Drennan (1963) clearly shows the variability that can exist. Each plume will create, in some degree, horizontal density gradients and, thus, pressure gradients, which will induce a secondary circulation until the plume has been dissipated through cross-shelf mixing.

During extreme discharge periods the impact of river-runoff can greatly increase. In 1973 the Mississippi River, as well as most other rivers in the MAFLA area, flooded at a record high. Data from numerous cruises and shore stations, taken during the latter part of 1973, to be discussed, indicate that a large lens of low salinity water became entrained by the Loop Current. Its movement was traced along the west Florida continental shelf to the Florida Keys. Atkinson and Wallace (1975) hypothesized that the Mississippi River was the source of low salinity waters observed in the Gulf Stream off Georgia in September 1973.

D. Deep Basin Oceanographic Conditions and General Circulation

Robert L. Molinari
John D. Cochrane
George A. Maul

Although an intense and continuous current, that portion of the North Atlantic gyre found in the eastern Gulf of Mexico historically has been studied as four distinct circulation regimes. In particular, early studies at Texas A&M University concentrated on the Yucatan Current in the vicinity of the eastern Campeche Bank (Figure I-1). Separate studies have considered the northern extension of the Yucatan Current, the Loop Current; or the south-flowing eastern boundary current, the West Florida Current; or the Florida Current. However, recent multi-ship efforts have provided quasi-synoptic pictures of the entire area's circulation. (For purposes of this section a quasi-synoptic data-set will be one collected within a two-week to one month period. For purposes of analysis it will be assumed that no significant temporal variability occurred in the fields measured during this interval.) Most of the available deep-basin data are used in this section to describe qualitatively the deep-basin circulation and oceanographic conditions.

The large temporal and spatial variability which has been observed in the Loop Current will be stressed in this section. This variability must be considered when models are developed to predict the deep-basin circulation, if any measure of success is to be attained.

1. Oceanographic Conditions

Due to inadequate sampling, no definitive temporal variation, if one exists, in the water masses entering the Gulf of Mexico has been discerned. However, there are definite spatial variations in the cross-stream distribution of water masses, particularly in the upper 300 m.

Figure IID-1 gives representative T-S and T-O_2 curves for waters in the western Caribbean Sea, the center of the Loop Current, and the western Gulf of Mexico. Such curves are frequently used in physical oceanography to identify water masses (see Sverdrup, Johnson and Fleming (1942), for instance). The Loop Current and Caribbean Sea waters have very similar properties as the Loop Current is an extension of the currents originating south of the Yucatan Strait. The water mass properties determined from samples collected to the west of the Loop Current at station 35 are considerably different. Nomenclature, and possible origins of the Gulf water masses have been given by Nowlin and McClellan (1967), Wust (1964), and others. The spatial variability of the water mass properties has been described statistically by Nowlin (1972) and Caruthers (1972).

In particular, two water masses studied by these authors are useful both in describing the spatial variability of the water mass properties, and as a tracer for the Loop Current. The Subtropical

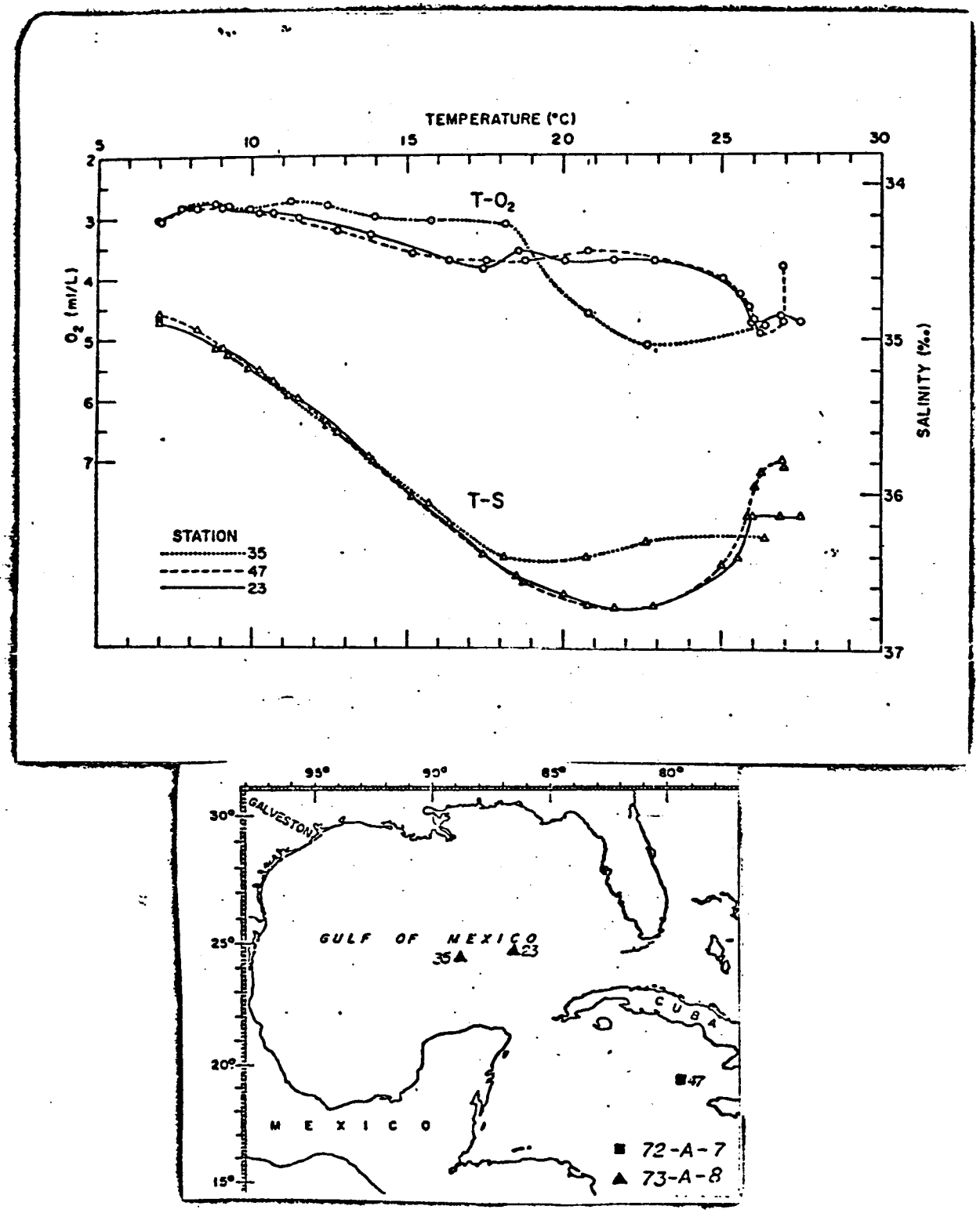

Figure II D-1. Characteristic T-S, and T-O_2, relations for stations in the western Caribbean Sea (station 47), the center of the Loop Current (station 23), and to the west of the Loop Current (station 35).

Underwater (SUW) is characterized by a salinity maximum in the upper 200 m of the Gulf of Mexico. The maximum salinities of approximately 36.75°/oo (Nowlin,1972) normally occur near 22°C. The Antarctic Intermediate Water (AIW) is characterized by a salinity minimum which occurs on the average at 6.25°C.

Although the characterization of the Loop Current as a river of water flowing through the ambient Gulf of Mexico waters is somewhat simplistic, it has some value when describing the distribution of SUW and AIW. The Loop Current salinities in the SUW and AIW are extremes; i.e., the maximum salinities at 22°C and minimum salinities at 6.25°C occur in the core of this flow. However, because of vertical mixing, horizontal mixing, and/or water mass formation, these extremes are eroded along the edge of the Loop Current. Thus at radial distances(to be defined) from the Loop core,the salinity maximum decreases and the minimum increases.

This spatial variability, particularly in the upper layers, is apparent qualitatively in the T-S and T-O_2 histograms given in Appendix III for various regions of the eastern Gulf of Mexico. The histograms were computed at NODC by summing all the observations of temperature and salinity, or oxygen in 1°C and 0.3 °/oo, or 0.4 ml/l bands. Percent of observations within each 0.3 °/oo or 0.4 ml/l band were then calculated using the total number of realizations in the entire 1°C interval . Mean values for salinity and oxygen in each interval are marked by x's on the plots.

The eastern Gulf was divided into four depth zones for purposes of describing water mass characteristics; > 200 m, 200-100 m, 100-50 m and 50-0 m. The histogram for depths >200 m represents the characteristics of the deep-basin waters,i.e. the area of the Loop Current. The histograms illustrate the decrease in maximum salinity at 22°C, and the increased variability in water mass properties at distances from the core of the Loop Current.

Appendix IV includes vertical sections of salinity and oxygen through the core of the Loop Current, and geostrophic velocity profiles relative to 500 m computed for these sections. These data show the radial extent of the Loop Current waters as a function of distance from the core.

The SUW to the right of the current axis looking downstream has salinities greater than 36.5°/oo. Thus, the center of the Loop Current, be it in the continuous or detached eddy mode, is characterized at 200 m by a pool of high salinity water. This pool is seen in the vertical sections of February 1962 and 1966 and June 1966 when the Loop extended continuously from the Yucatan to the Florida Strait, and in September 1965 and August 1968 when detached eddies had formed. The station just to the left of speed-axis during these months seldom had salinities greater than 36.5°/oo.

There are, however, salinities greater than 36.5°/oo to the left of the speed-axis in eddies which have apparently spun-off from the Loop Current. For instance, anticyclonic eddies are found to the north of the main flow in September 1965 and June 1966 (Appendix IV). Although these eddies have water mass properties similar to those of the main flow, they are shallower, less intense features.

2. General Circulation

Leipper (1970) proposed an annual cycle of the Loop Current based on his analysis of a 1965-1966 data-set Maul (1974) showed Leipper's suggestion to be qualitatively correct with a year-long experiment. Support for the existence of such a cycle can also be found in the climatological studies of Whitaker (1971) and Linn (in preparation). The former considered monthly averaged temperature data, and the latter averaged monthly ship drift data (Figure IID-2).

The annual cycle, as proposed by Leipper (1970), is characterized by a spring intrusion of the Loop Current into the basin. The maximum penetration of this current occurs in the summer, followed by the separation of an anticyclonic eddy from the main flow. During the fall, the Loop recedes, with minimum penetration in the winter.

The annual cycle's temporal variability, is reexamined in light of a preliminary analysis of the data on file at NODC. Topographies of the 20°C isotherm surface can be used to approximate the density distribution and therefore the geostrophic current distribution in the deep basin. In particular, the 150 m contour of the 20°C topography closely parallels the core of the current, much as the 200 m contour of the 15°C topography approximates the Gulf Stream speed axis (e.g. Parker, 1972) off New England.

The surface velocity distribution of the Loop Current is asymetric. Facing downstream, the speed axis is to the left of the current core. The width of the current is approximately 100 km in the Yucatan Strait. As the flow turns anticyclonically, the current slows down, and spreads out (Chew, 1974). The width of the current is approximately 150 km in the anticyclonic turn which is adjacent to the MAFLA area. As the current turns south, the width decreases and reaches a minimum in the Straits of Florida due to both topographic constraints (Cuba) and the dynamics of cyclonic turning Chew (1974); a minimum of 75 km width is found there.

Complete topographies of the 20°C surface are given in Appendix IV. Superimposed on the October, 1970 and August 1971 topographies are surface drogue trajectories. Dynamic height contours, when available, relative to 500 m, also are given in Appendix IV. The 150 m contour of the 20°C topography is seen to closely parallel the core of the current as indicated by the dynamic height contours, and the drogue measurements. A 75 km band exists on each side of this isopleth wherein the current speed is greater than 25 cm/sec.

Figures IID-3 to IID-6 show the 150 m contour of the 20°C surface determined from quasi-synoptic surveys conducted in 5 separate years. Some aspects of the cycle proposed by Leipper are present in all years. However, a more important feature in terms of being able to predict the circulation is the year-to-year variability in the current patterns. For instance:

a) The first clear-cut indication of a separated eddy in 1966, 1968, 1969, and 1973 occurs in either July or August or September. However, by May 1972 (see Appendix IV) an eddy had already detached.

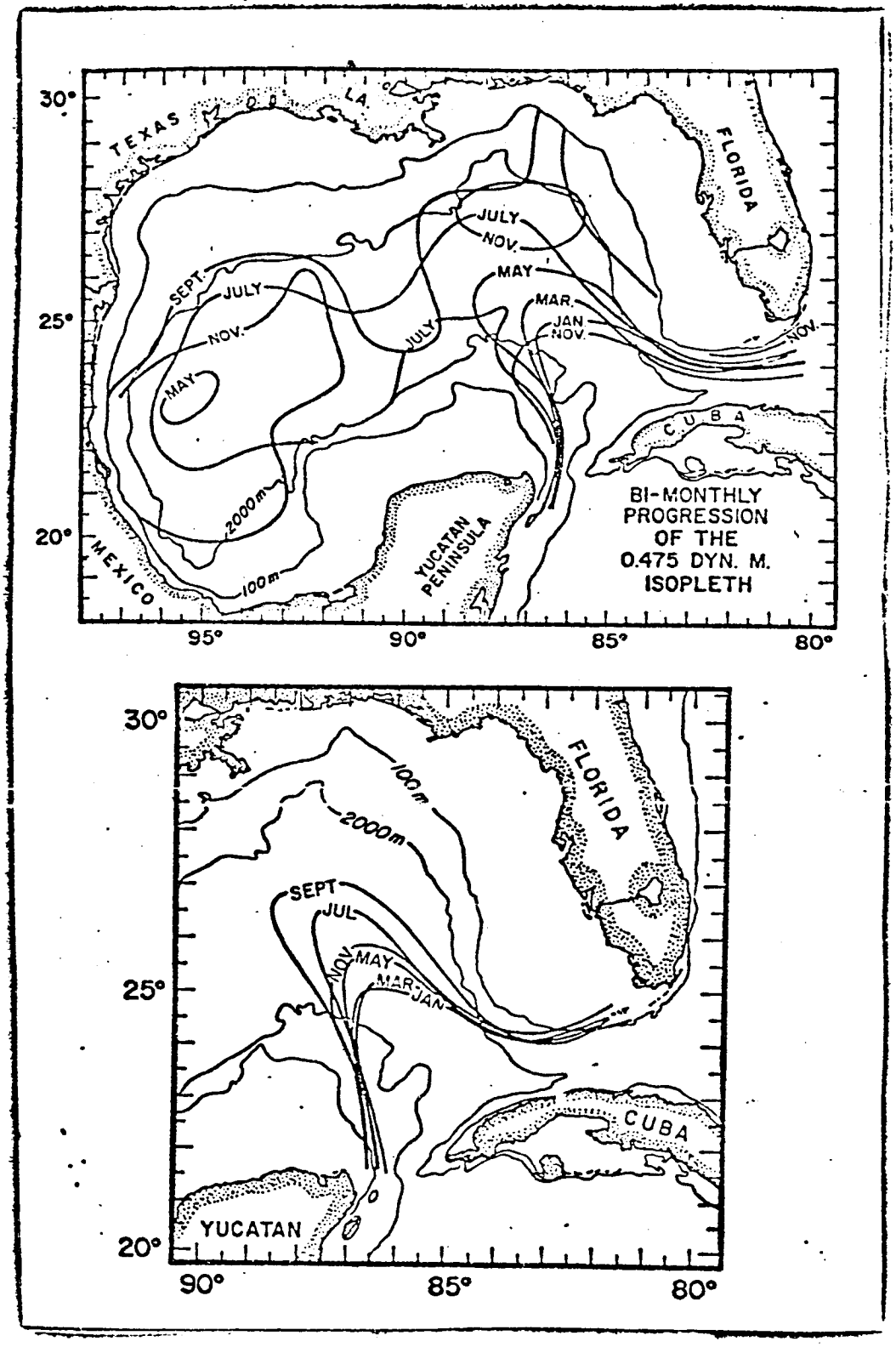

Figure II D-2. Upper panel. Seasonal sequence of positions of the Loop Current as indicated by the 0.475 dyn-m contour (relative to 150 db) determined from the average temperature and salinity structure (Whitaker 1971). Lower panel. Seasonal sequence of positions of the Loop Current as indicated by the 1.4 dyn-m contour (relative to 1000 db) determined by "geostrophic levelling" from average ship drifts (Linn, in preparation).

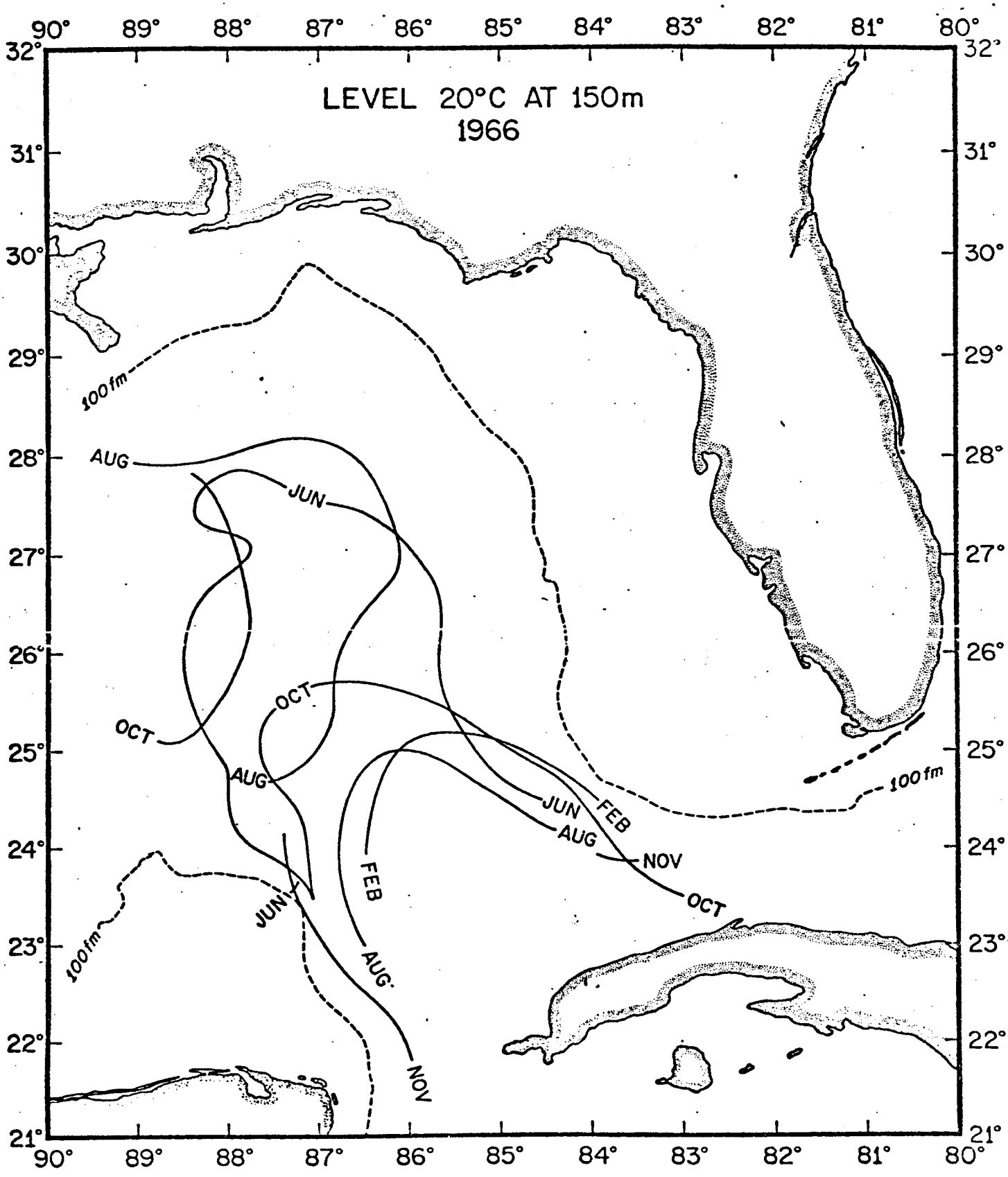

Figure II D-3. The 150 m contour of the 20°C surface taken from the complete 20°C topographies given in appendix IV. The data were collected in 1966 during the months indicated on the figure.

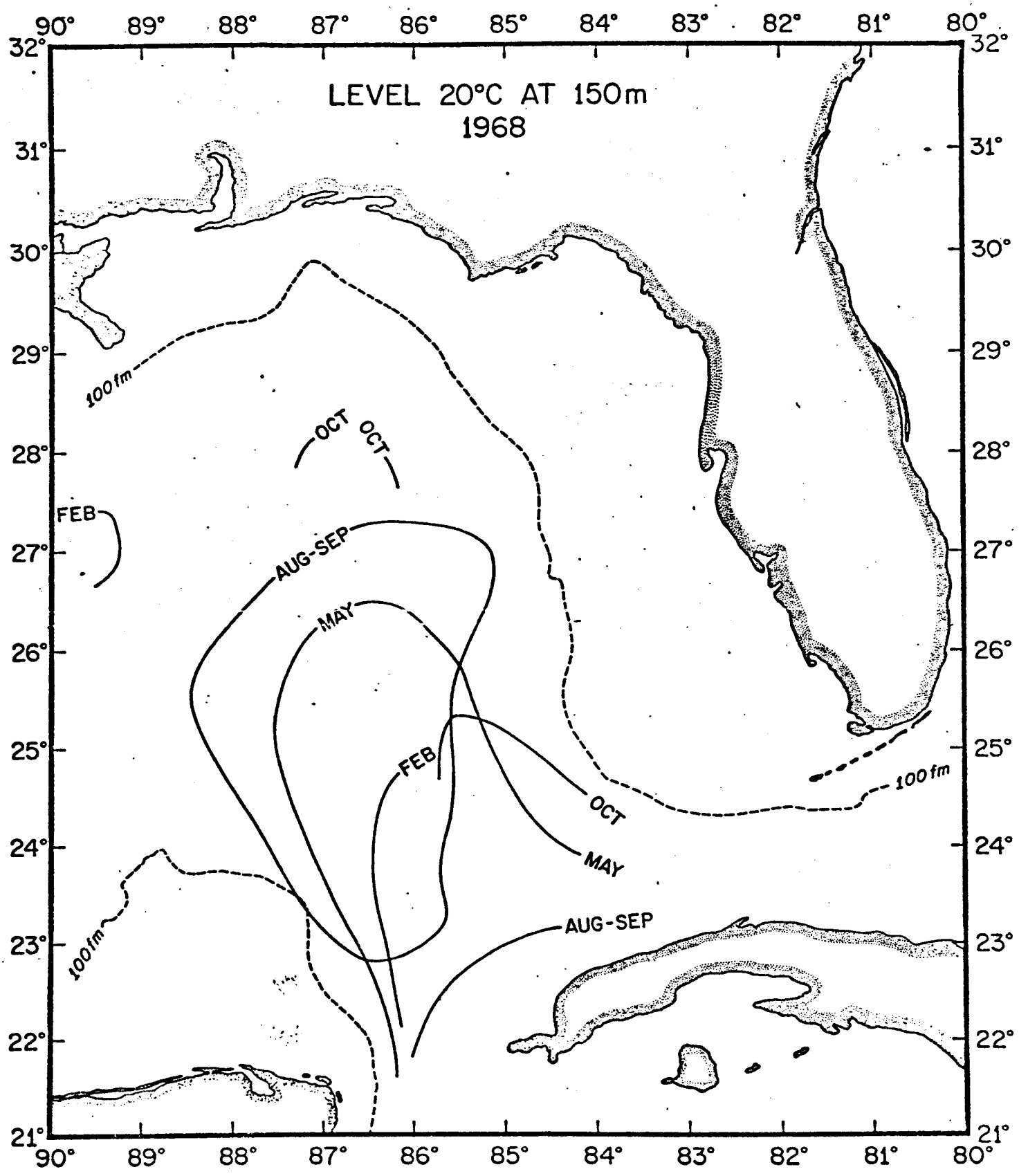

Figure II D-4. Same as in Figure II D-3, except for 1968.

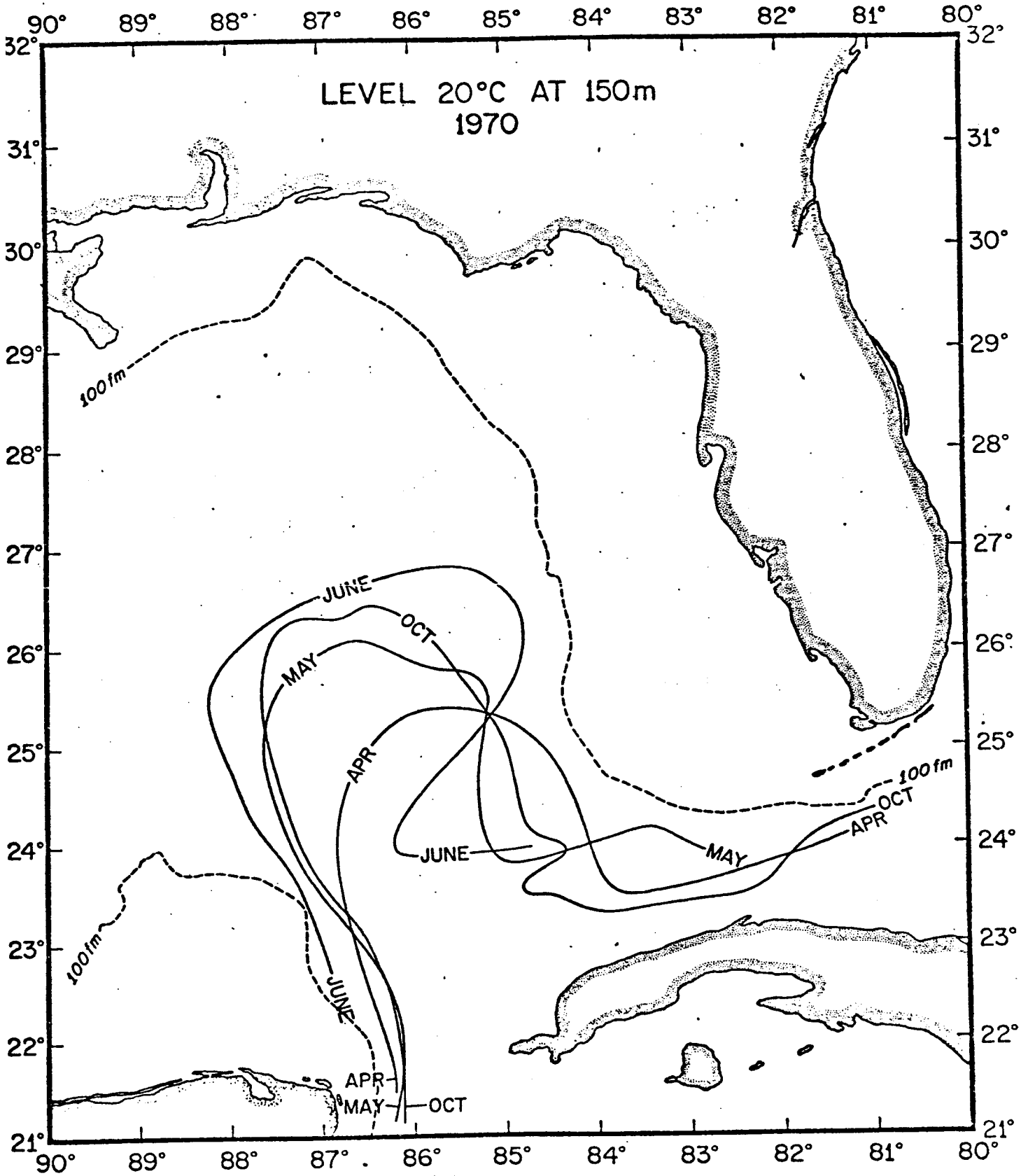

Figure II D-5. Same as in figure II D-3, except for 1970.

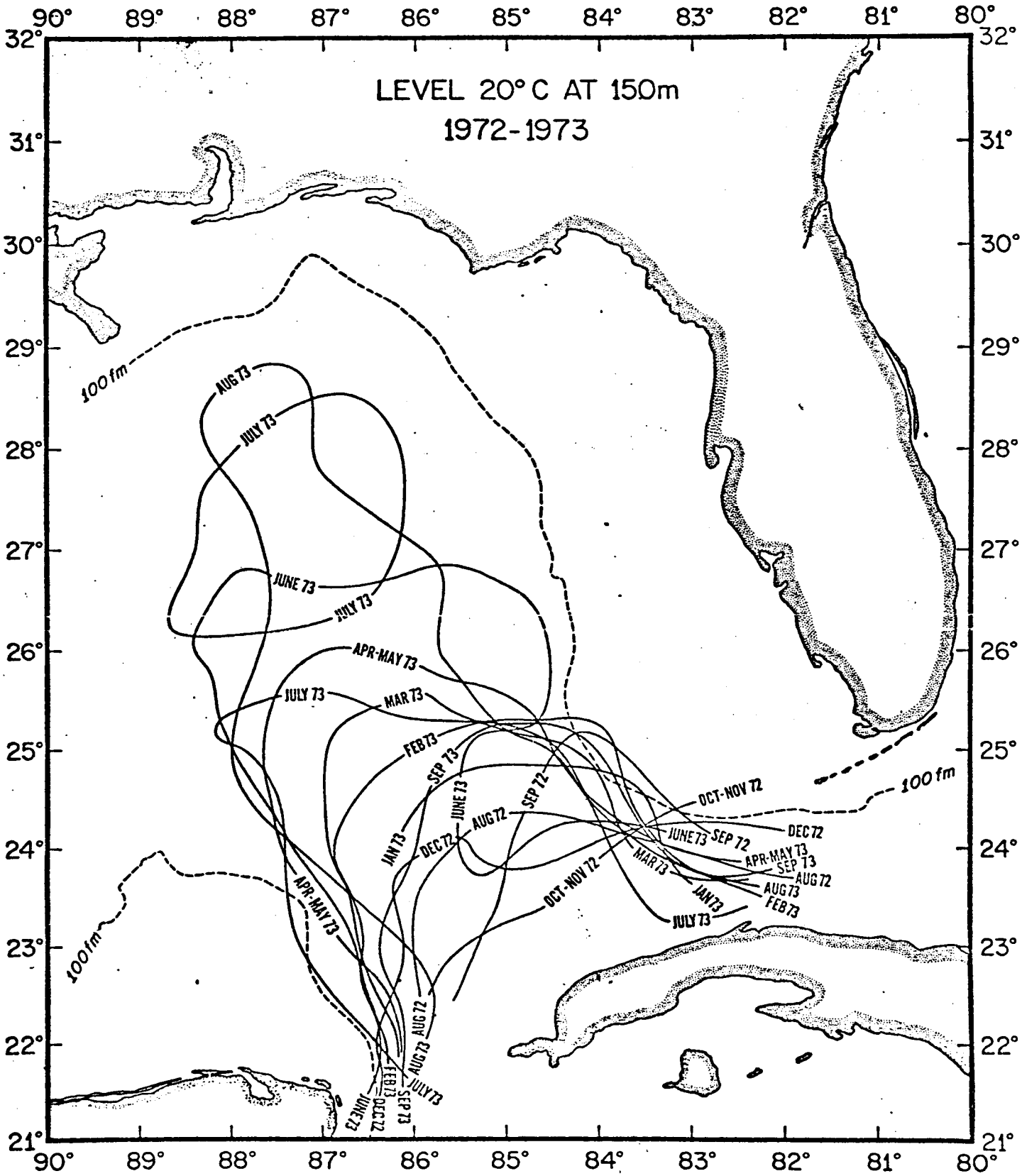

Figure II D-6. Same as in figure II D-3, except for 1972-1973.

b) The size and shape of the separated eddies vary considerably. For instance the 1966 and 1968 eddies are much larger than the 1973 eddy.

c) The secondary intrusion of the main current, which can occur after an eddy separation, results in various fall penetrations of the Loop into the Gulf, e.g. the Loop is much farther to the north in August 1973, than in August 1972 (Figure IID-7).

A bi-monthly climatology for the position of the core of the Loop Current was constructed from data supplied by NODC. NODC produced listings of monthly averages of temperature by 1^{o}squares of latitude and longitude and 5 meter-depth intervals using only MBT and XBT data. Depths of the $20^{o}C$ isotherm, to the nearest 5 m interval, for each month and 1^{o} square were determined from these listings. The figures in Appendix V give the climatological $20^{o}C$ topographies for each month, as well as an annual mean $20^{o}C$ topography. The number of data points in each 1^{o}square are also given on these figures.

Two-month averages of the depth of the $20^{o}C$ isotherm then were computed because of the small number of data points available in some months. The climatological 150 m contour of the $20^{o}C$ surface for each two-month period is given on Figures IID-7 to IID-12. Superimposed on the climatological curves are 150 m contours derived from data obtained during quasi-synoptic cruises to the region.

Assuming that the bi-monthly Loop Currents possesses the same approximate properties as the quasi-synoptic currents (i.e., 150 km wide, velocities greater than 25 cm/sec, and centered on the 150 m contour of the $20^{o}C$ topography), then some qualitative statements about a mean annual cycle can be made. It should be stressed that the $20^{o}C$ surfaces were subjectively contoured, and the data set was quite limited during some time periods (see Appendix IV).

The annual cycle as proposed by Leipper is evident in the climatological Loop Currents given in Figures IID-7 to IID-12. The spring intrusion is followed by an eddy separation in the summer, which in turn is followed by a smaller intrusion in the winter. The following table summarizes the penetration results presented in Figures IID-7 to IID-12. The penetration of the Loop is taken as the northernmost latitude of the 150 m contour; as previously indicated, the current can extend approximately 75 km to the north of this latitude.

Months	Loop Penetration	
	Main flow	Detached Eddy
January-February	$25.50^{o}N$	
March-April	$26.75^{o}N$	
May-June	$27.00^{o}N$	
July-August	$25.25^{o}N$	$27.75^{o}N$
September-October	$26.25^{o}N$	$27.25^{o}N$
November-December	$26.25^{o}N$	

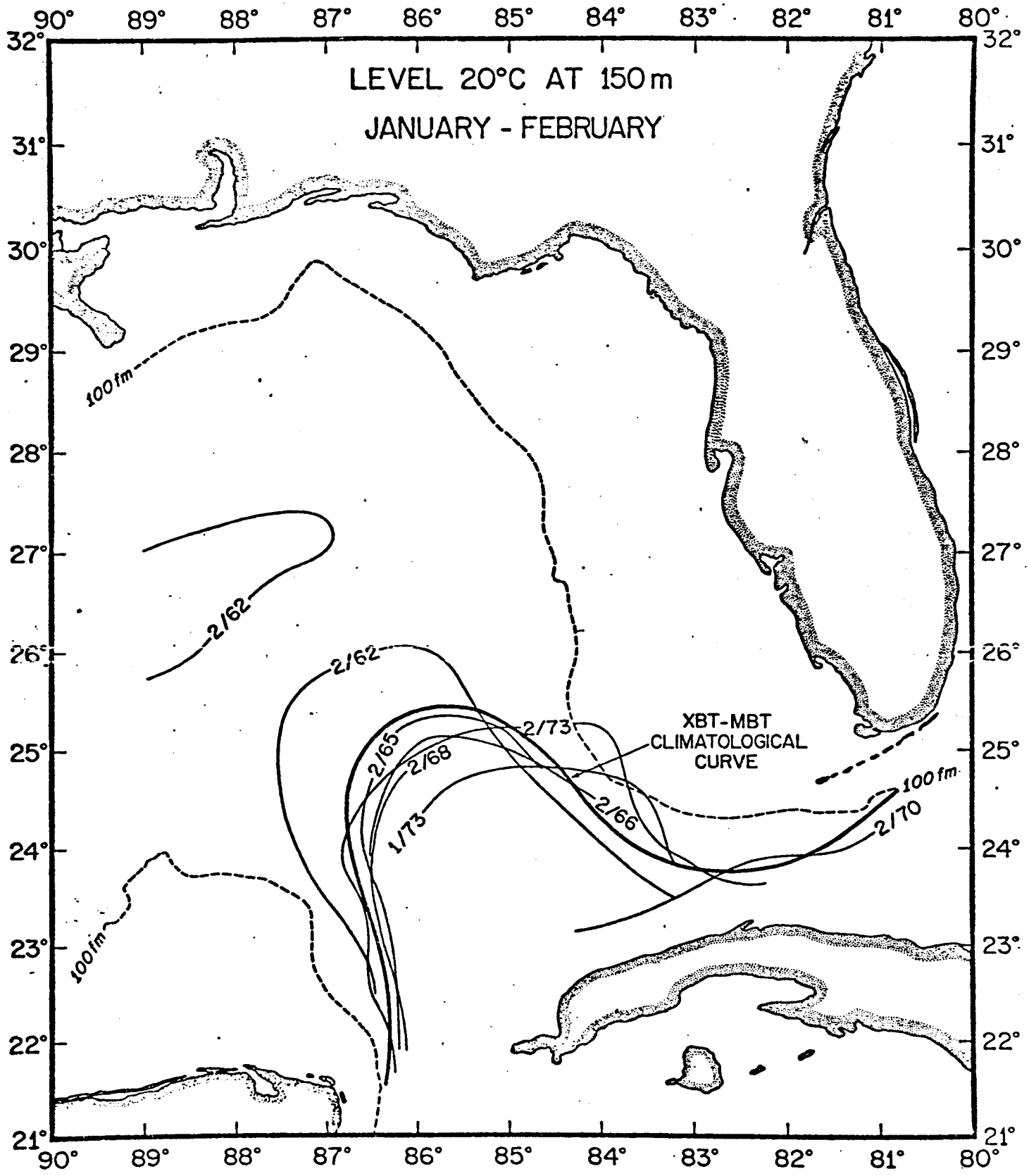

Figure II D-7. Bi-monthly climatological 20°C topographies were determined by overlaying two months of mean temperature data supplied by NODC (see Appendix V for monthly average 20°C surfaces). The 150 M contour of the January-February 20°C surface is given as the XBT-MBT climatological curve above. The 150 m contours of the 20°C surface for individual cruises (denoted by month and year of the cruise) are taken from the complete 20°c topographies given in Appendix IV.

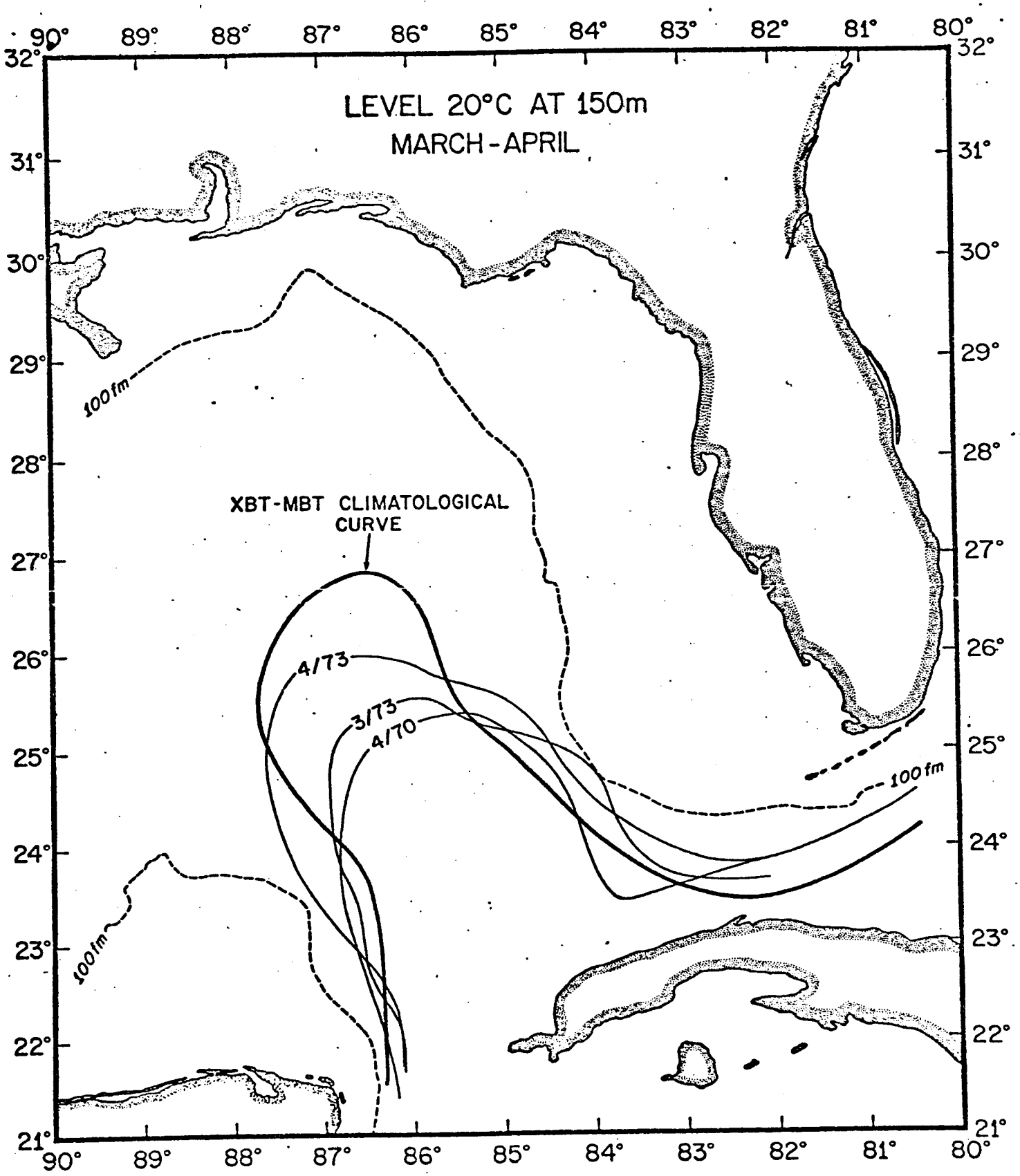

Figure II D-8. Same as in figure II D-7, except for March-April.

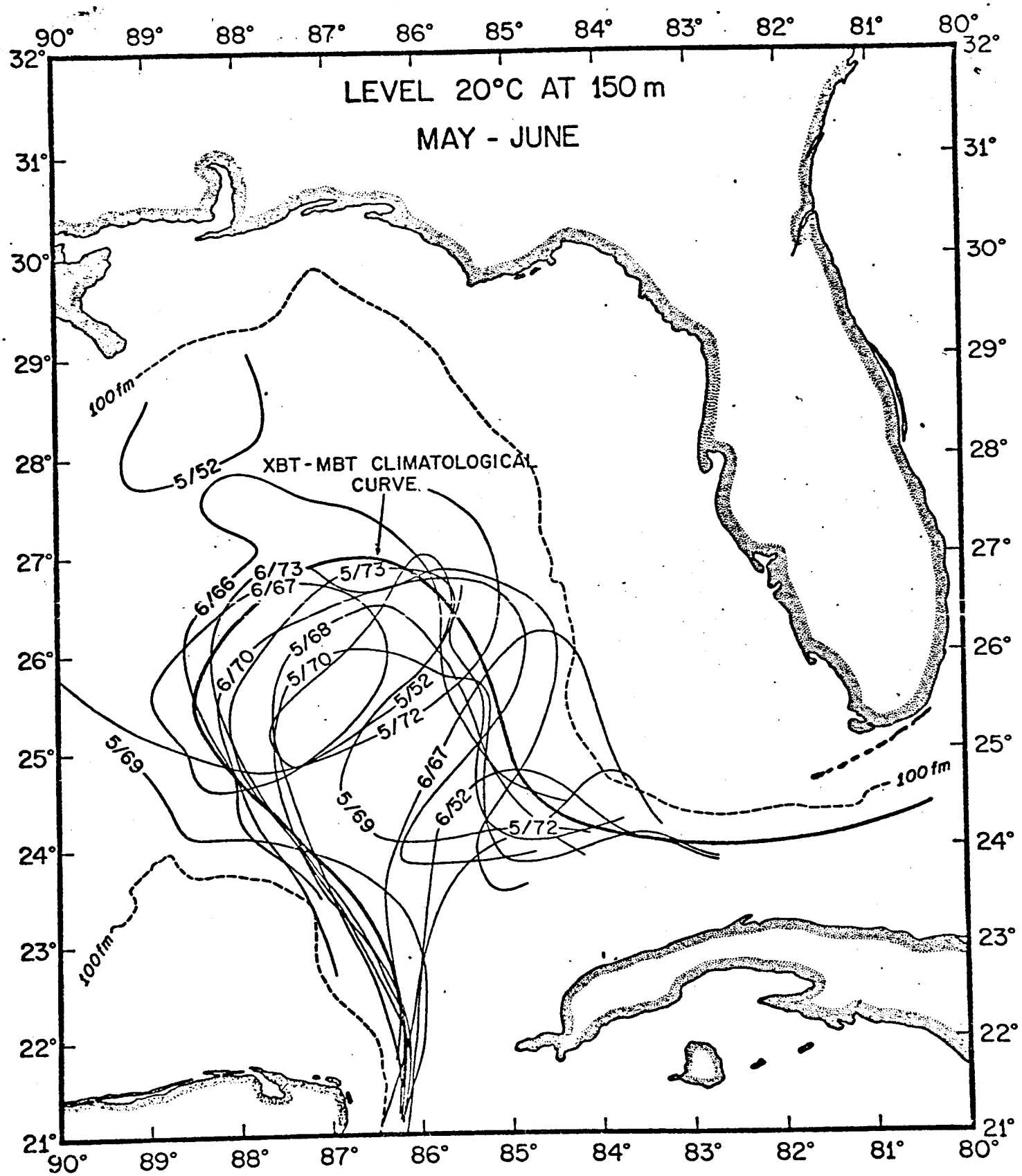

Figure II D-9. Same as in figure II D-7, except for May-June.

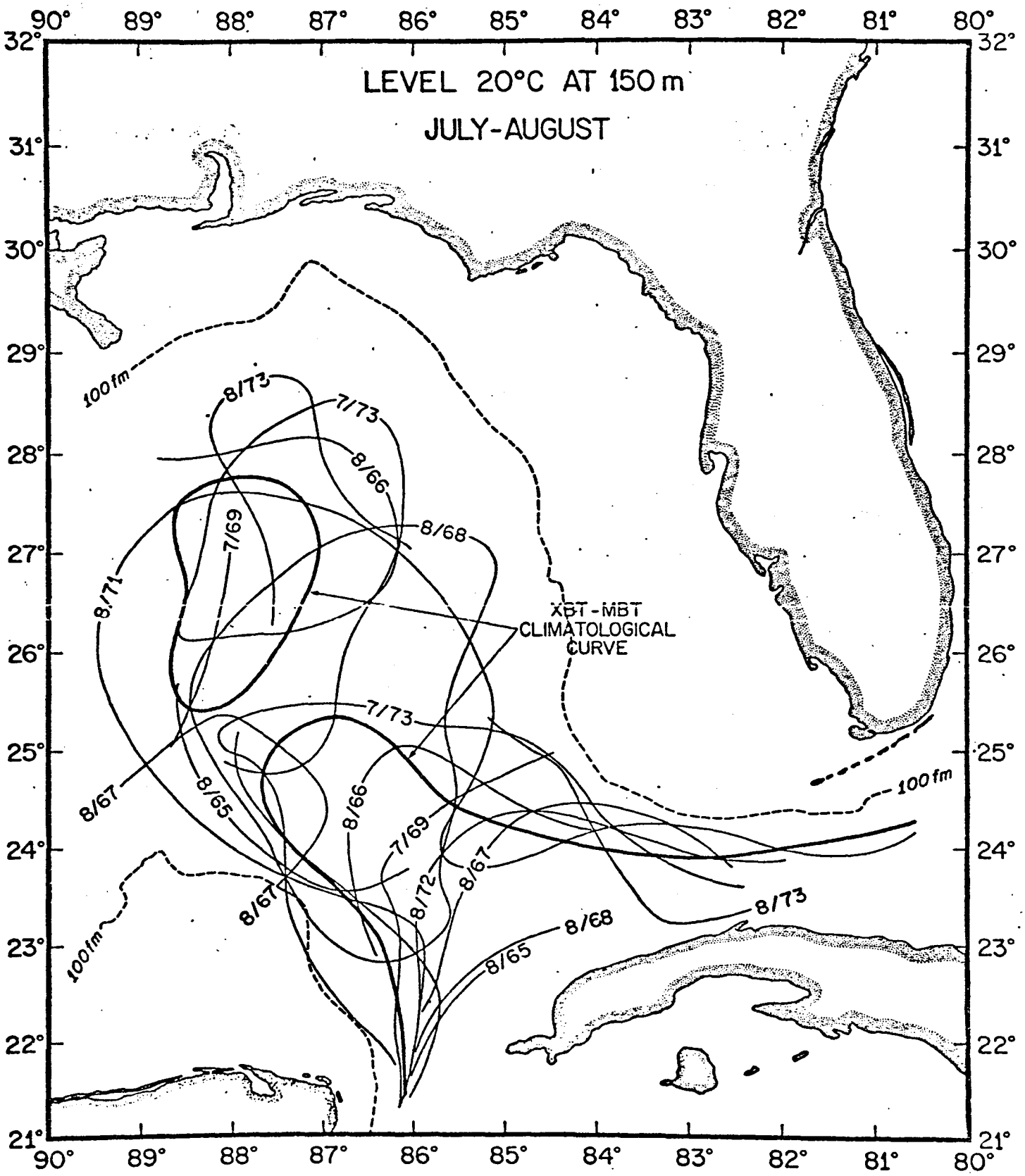

Figure II D-10. Same as in figure II D-7, except for July-August.

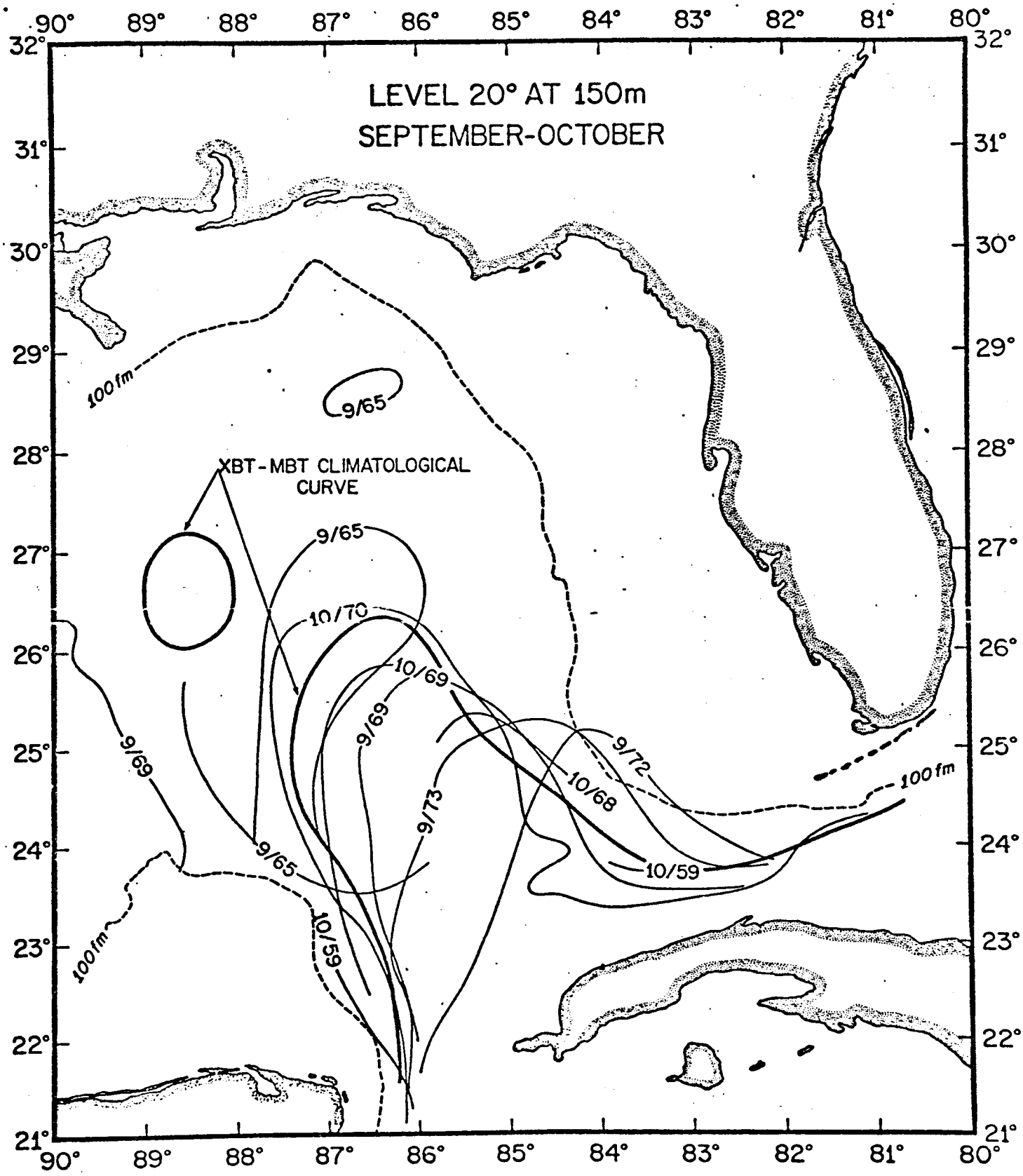

Figure II D-11. Same as in figure II D-7, except for September-October.

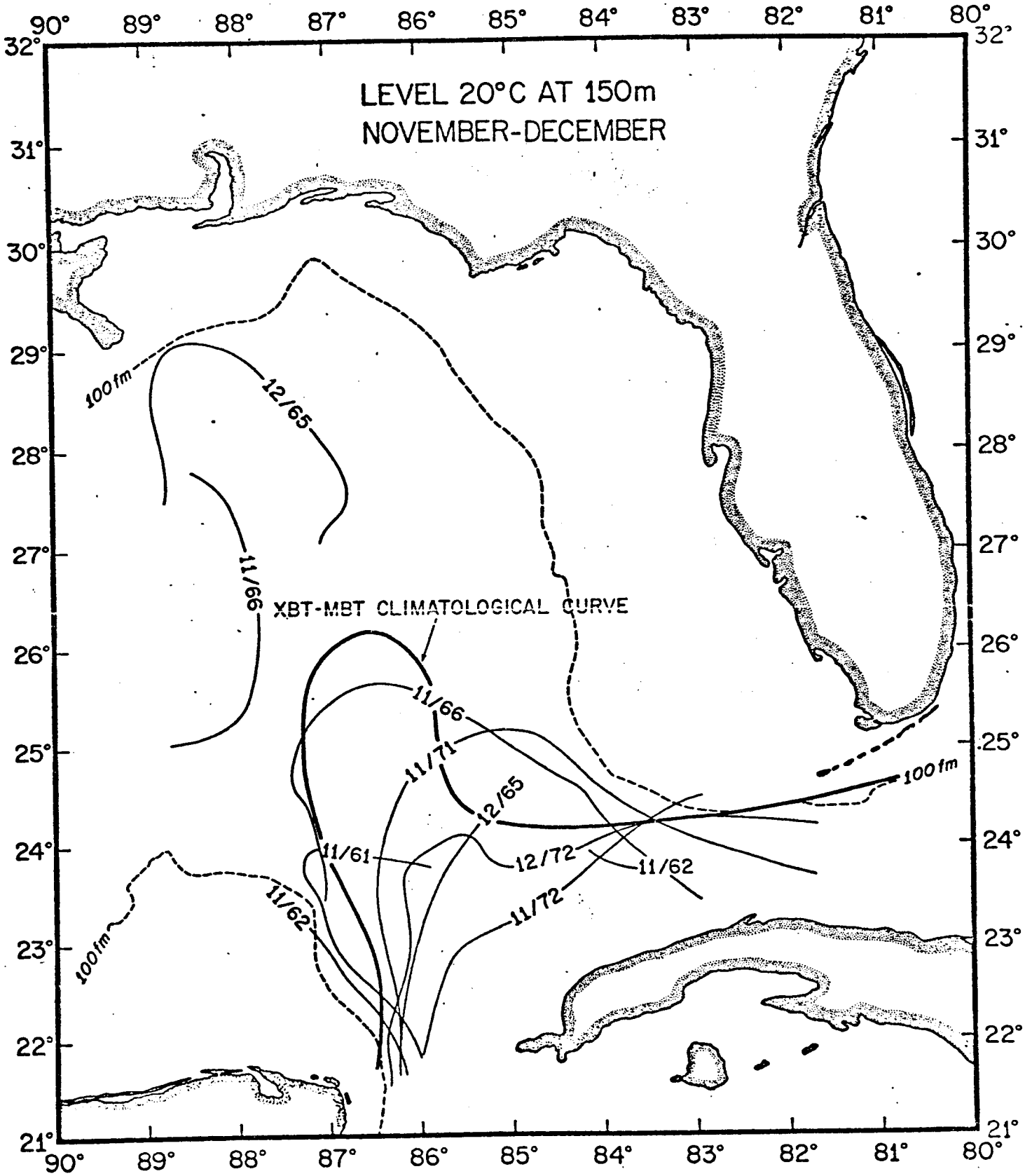

Figure II D-12. Same as in figure II D-7, except for November-December.

In addition, the Loop intrudes into the basin at approximately a 30° angle west of due north measured from the western tip of Cuba. The climatological Loop appears widest in May-June, having a width of approximately 300 km.

Finally, a climatological eddy separates in July-August and is centered at approximatley 26 30'N. The eddy is elliptical with a major axis of approximately 250 km, and a minor axis of 150 km. The eddy diminishes in size from July-August to September-October.

The problems that can arise if these climatologies are used in any prediction efforts become obvious if the 150 m contours determined from quasi-synoptic cruises and other data are considered. For instance, the few contour lines available in the January-February, and March-April (Figures IID-7 and IID-8), suggest that the climatological curves are good approximations to the conditions in the basin during these months. However, an early March satellite image to be presented in a later section suggests a circulation pattern more typical of the summer climatological currents.

When large data-sets are available, such as in May-June and July-August , the variability becomes obvious. For instance, eddies detached in May 1972 and June of 1952 and 1967. The current pattern at 25°N during these events is completely different from the climatological flow given in Figure IID-9. The size of the broken-off eddies varies considerably from the July-August mean (Figure IID-10). The August 1968 eddy extends over four degrees of latitude whereas the July 1973 eddy only three.

During September 1972 and 1973 the core of the current appears to run directly onto the continental shelf at 25°N before turning south. Again the climatological current possesses different characteristics. The detached eddies, and the current apparently flowing directly onto the continental shelf are two features which can influence shelf circulation.

The preceding discussions have dealt primarily with the temporal variability of the deep basin circulation with limited discussion of the spatial variability either in the vertical or the horizontal. Most investigators of the deep-basin have assumed that the flow is geostrophic with some deep level-of-no-motion, and there have been only a few isolated experiments designed to measure the deep flow (see Pequenat (1972), for instance). Until additional data are collected and analyses performed, little can be said about the deeper flow in the basin except that which can be inferred from water mass properties (Nowlin, 1972).

Except for the discussions on separated eddies of various scales, little has been said of the flow outside the 150-km band of the Loop Current. For instance, how far to the north of this band does the velocity structure of the Loop extend? Do the eddies which separate from the Loop still advect as part of the Loop Current system or do they drift in response to other forces? These and similar questions require additional analysis to ascertain if the existing data-set is sufficient to answer them, or if more observations are required.

Two examples of the effects of spatial variability are shown in Figures IID-13 and IID-14. The inferred circulation fields were deduced

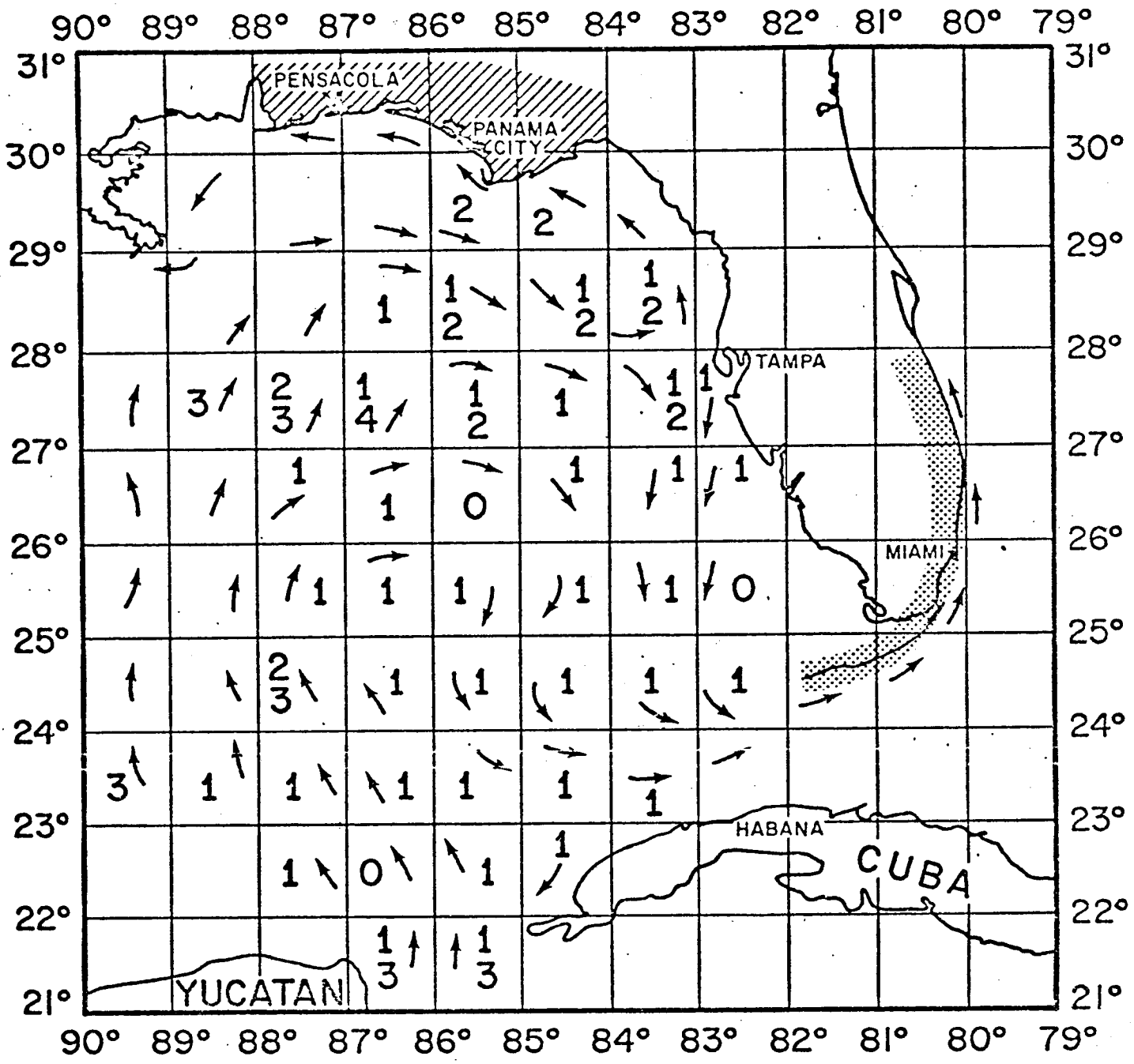

1 EAST FLORIDA AREA
2 MAFLA AREA
3 WEST LOUISIANA AREA
4 TEXAS AREA
5 WEST FLORIDA AREA
6 EAST DELTA AREA
7 WEST MISSISSIPPI AREA
8 ST. PETE - TAMPA AREA
9 HONDURAS AREA
0 NO RETURNS

MAFLA AREA
EAST FLORIDA AREA

igure II D-13. Drift bottle returns for releases within 1° squares of atitude and longitude. The numbers within the 1° squares indicate the egions of return, as listed on the figure. The bottles were released in ay 1970. The circulation pattern as given by the arrows was deduced from n analysis of drift bottle return, dynamic height, and thermal data.

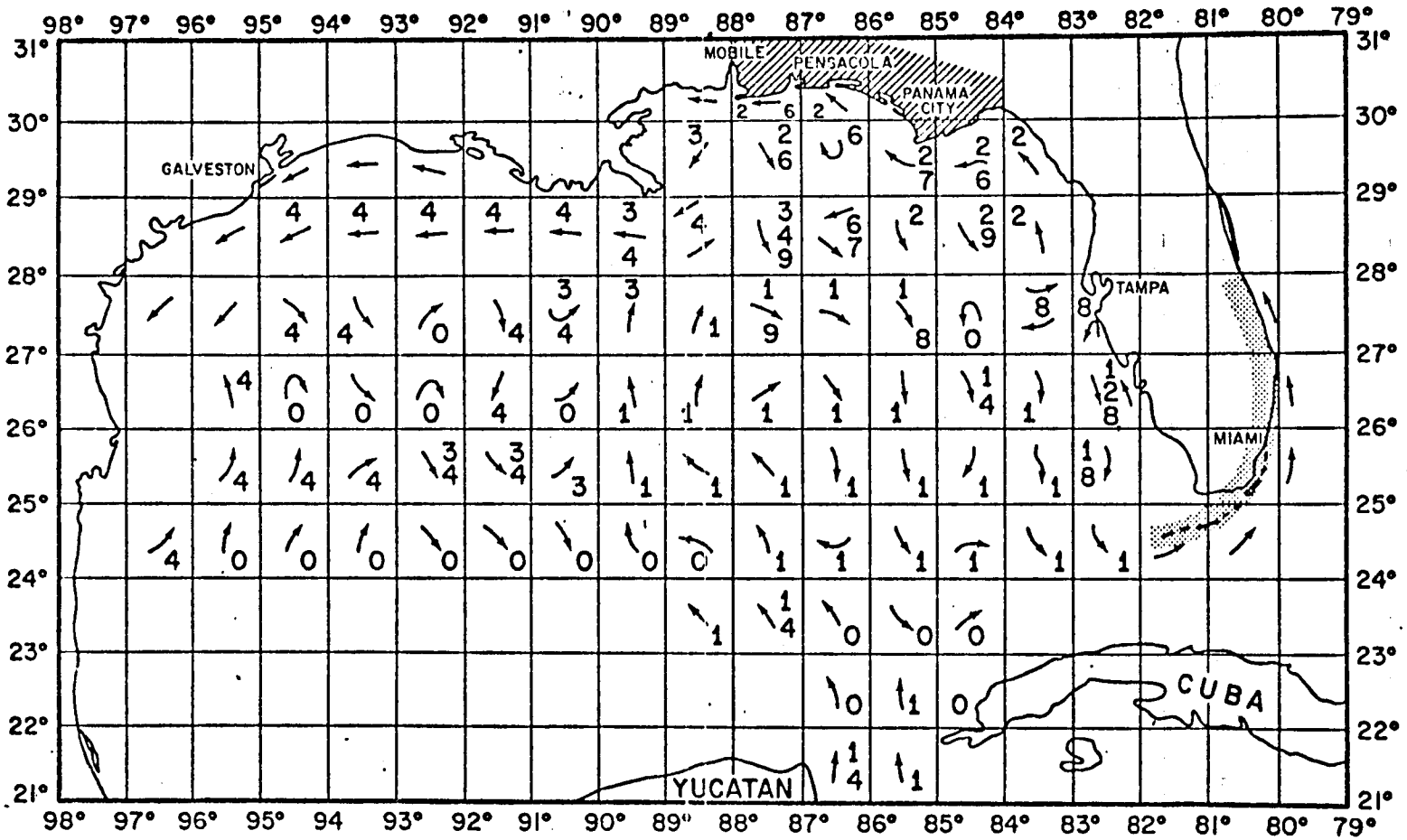

1 EAST FLORIDA AREA
2 MAFLA AREA
3 WEST LOUISIANA AREA
4 TEXAS AREA
5 WEST FLORIDA AREA
6 EAST DELTA AREA
7 WEST MISSISSIPPI AREA
8 ST. PETE - TAMPA AREA
9 HONDURAS AREA
0 NO RETURNS

MAFLA AREA
EAST FLORIDA AREA

Figure II D-14. Same as in figure II D-13, except for drift bottle releases in August 1971.

from drift bottle, temperature, and density data. The corresponding $20^{o}C$ topographies are given in Appendix IV. Drift bottle releases within a 1^{o} square of latitude and longitude frequently have several recovery sites indicating the importance of the spatial variability in determining parcel trajectories.

E. Shelf Oceanographic Conditions and General Circulation

Data collected in the few systematic studies of the oceanographic conditions of the Gulf of Mexico's continental shelf (Department of Natural Resources, 1969 , Rinkel, 1972 , Price and Mooers 1974 a, b, c, 1975 ,for instance) frequently have been subjected to only preliminary analysis. Therefore, much of the discussion in this section is of a qualitative nature. Again, as in the deep basin section, those processes active in the dispersion of shelf waters and relevant to the establishment of a sampling grid are emphasized.

The continental shelf of the eastern Gulf of Mexico can be divided into four sub-regions, each bounded by a major topographic feature. The MAFLA shelf extends from the Mississippi Delta (90°W) to Cape San Blas (85°W); the Big Bend area or Florida Middle Ground from Cape San Blas to Tampa Bay (28°N); the west Florida Shelf from Tampa Bay to Cape Romano (26°N); and Florida Bay from Cape Romano to the Florida Keys. Gaul (1967) conducted a four-year study on the MAFLA shelf. No systematic data have been collected on the Middle Ground; both the Hourglass Program (Florida Department of Natural Resources, 1969), and the Western Florida Continental Shelf Program (Rinkel, 1972) focused on the west Florida Shelf, and the NSF Continental Shelf Dynamics Program (Price and Mooers, 1974a, b, c, 1975, and Plaisted, Waters, and Niiler, 1975) obtained long term current meter records at 26°N. These seasonal and other data are used in this section to describe qualitatively the oceanographic conditions on the eastern Gulf of Mexico continental shelf.

1. Oceanographic Conditions

Robert L. Molinari
Murice Rinkel
Christopher N. K. Mooers
William W. Schroeder

In the summer season the density stratification intensifies in the shoreward direction, i. e., the thermocline intensifies shoreward from the deep Gulf, reaching a nearly two-layered state near shore, and becoming nearly horizontally homogeneous. In the winter season, the shelf water is nearly vertically homogeneous over the inner shelf due to wind stirring and cooling, but it shows a strong horizontal gradient.

NODC performed a thermocline analysis on their bathythermograph (BT) files. The eastern Gulf shelf was segmented into irregular sectors bounded by topographic contours (0 m, 50 m, 100 m, 200 m), and latitude and/or longitude lines. The thermocline depth was defined for a particular BT station as that level at which the greatest temperature change occurred over a 10 m interval. The mean thermocline depth was then determined within each sector for one-month time intervals. Because of the paucity of data, two-month averages were obtained, and the results are given on Figures IIE-1 to IIE-3.

Only qualitative statements can be made about these figures, because in many areas the contours of the thermocline depth are determined by only a few data points. The 25 m thermocline depth contour advances towards the shore over most of the shelf from January-February to May-June, consistent with the hypothesis of shoreward intensification of the thermocline. However, for an unexplained reason the 25 m contour moves seaward in July-August (Figure IIE-2). The 0 m contours during January-February and November-December encompass regions of no thermocline, a common winter feature on most shelves.

The 20°C topographies for the area off Panama City, Florida given in Appendix VI, and the vertical sections along 28°30'N, 27°30'N, and 26°N given in Appendix VII depict synoptic scale thermal and density conditions. The summer thermocline intensification is characterized on the horizontal plots of Appendix VI by an increase in the contour gradients; in June-July 1964, and May 1965, for instance. The two-layered density stratification is seen in the sigma-t sections of Appendix VII at 28°30'N during May 1971, at 27°30'N and 26°N during June 1972, for example. Typical winter patterns exist at all three latitudes during January 1973 (Appendix VII).

The seasonal transitions have never been precisely "captured" or documented, but they are believed to be rapid. The transition from summer to winter regime is believed to occur with the first intense cold air outbreak of the winter, soon after the autumnal equinox. The transition from winter to summer regime is suspected to occur after the last cold air outbreak of the winter, soon after the vernal equinox.

There is a year-to-year variability in the seasonal transition on the MAFLA shelf. The 20°C topographies of Appendix VI indicate the winter-to-summer transition had occurred by 10-11 May 1965, but had not

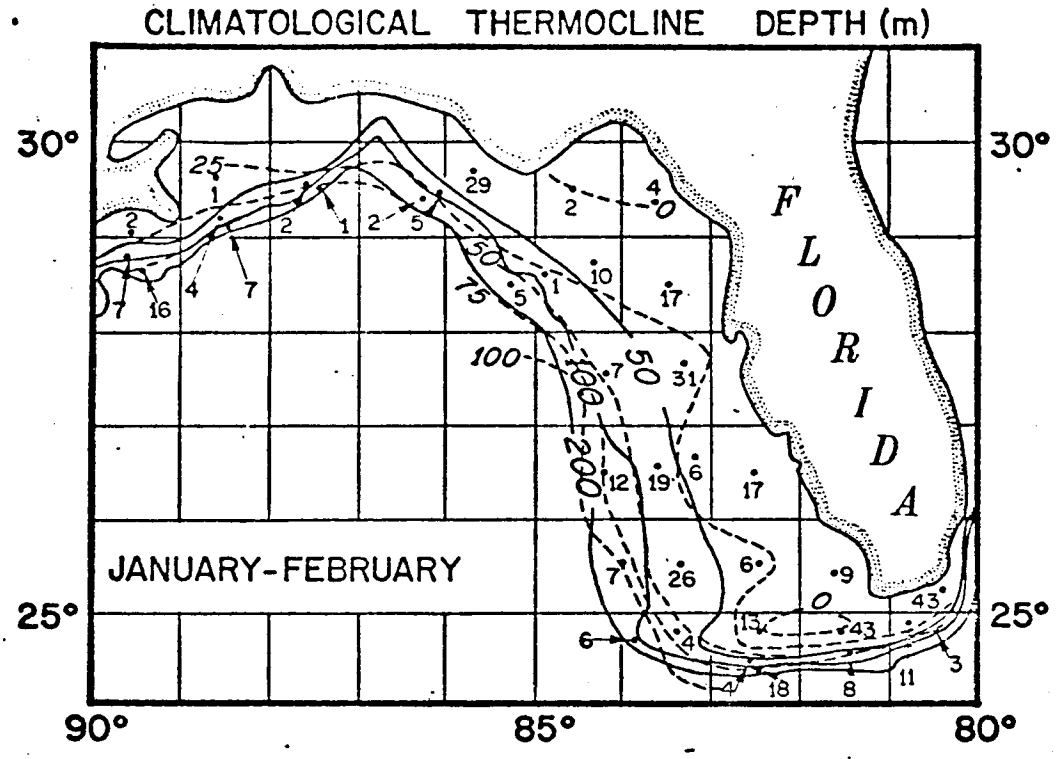

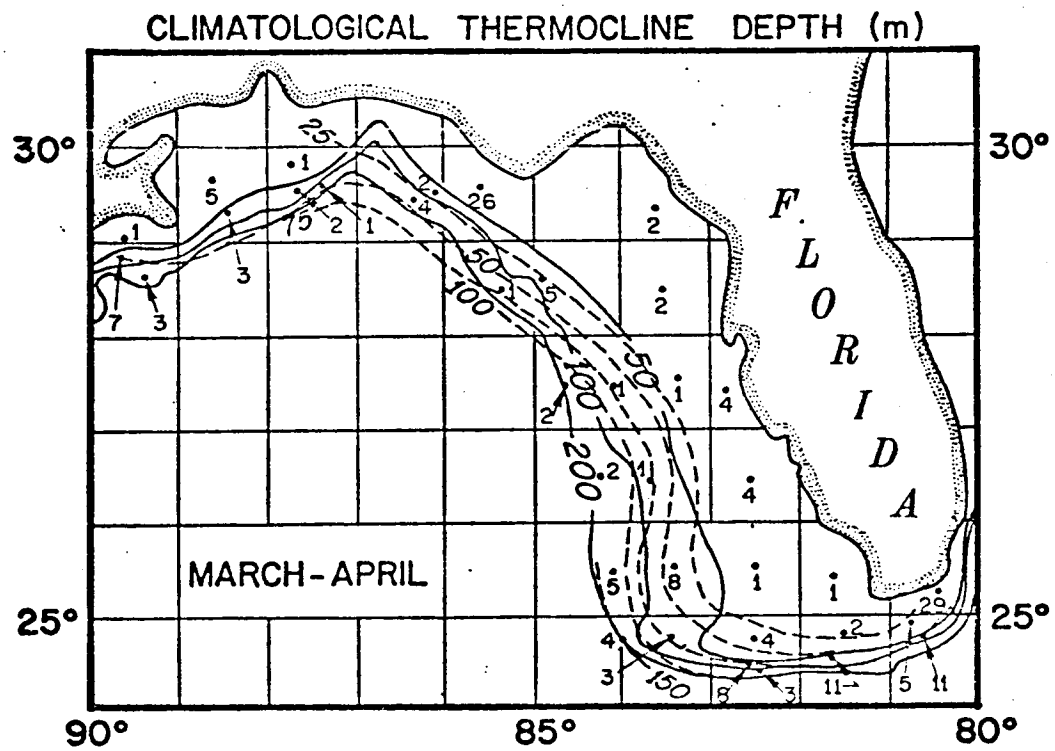

Figure II E-1. Monthly average thermocline depths were determined by NODC for regions of various shapes. The solid lines representing isobaths, 0 m, 50 m, 100 m, 200 m and 1σ latitude and longitude lines are the boundaries of these regions. The dashed lines are contours (in m) of thermocline depth. The number within each region represents the data points used to determine the average thermodine depth.

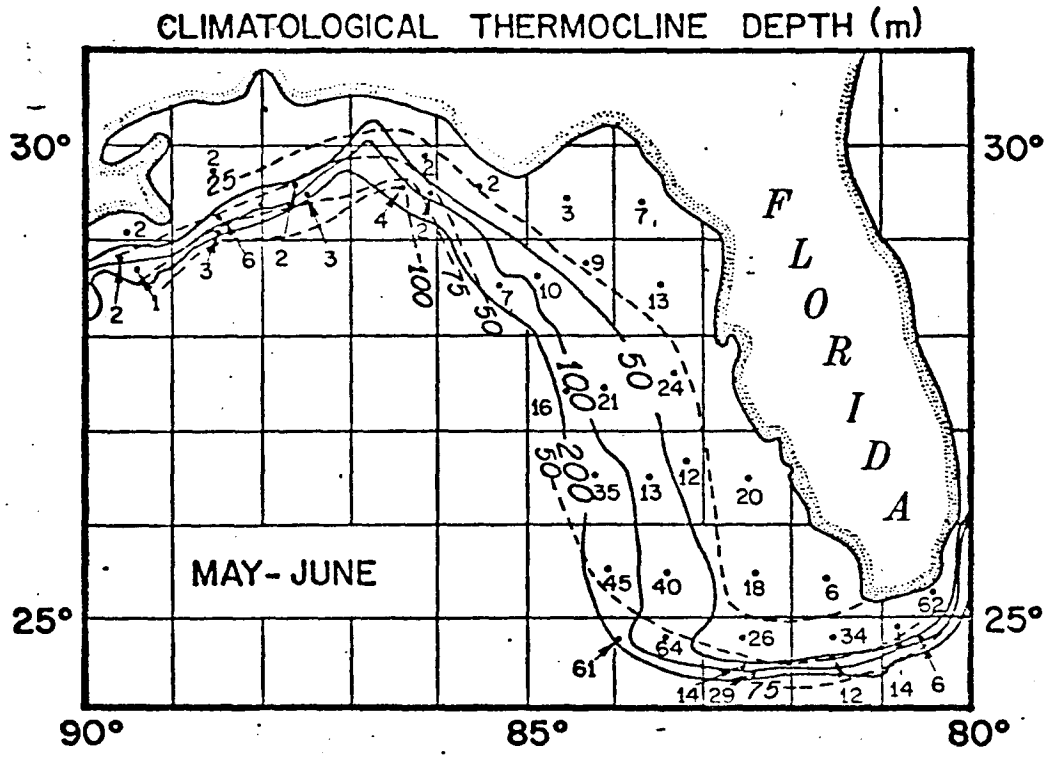

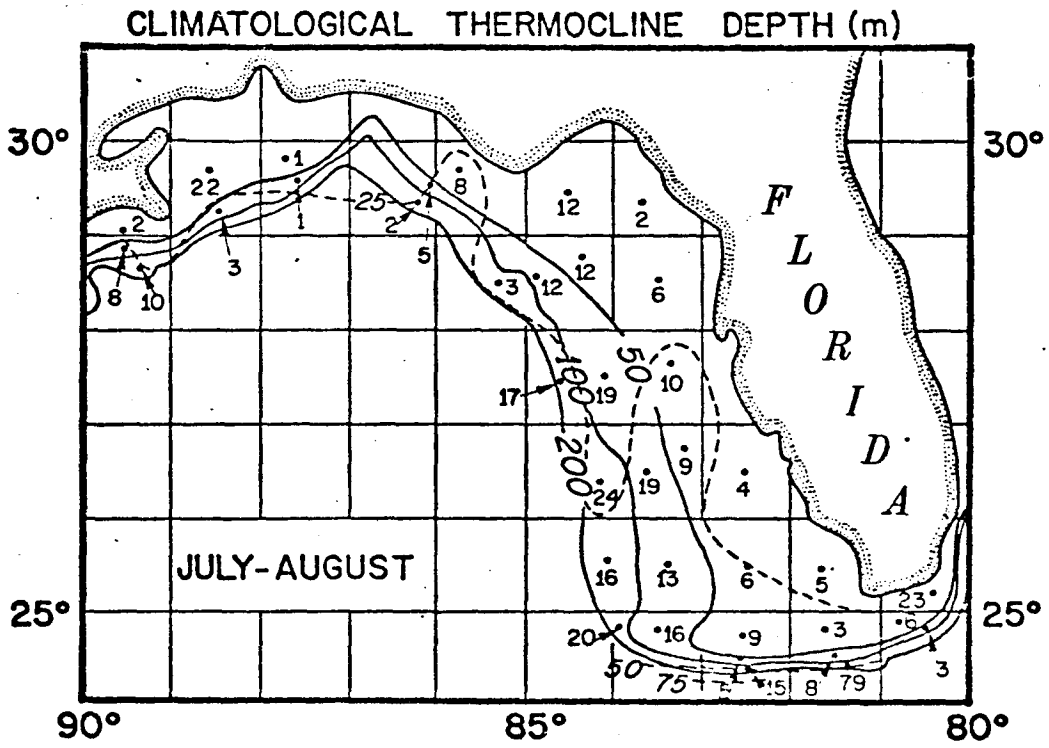

Figure II E-2. Same as in figure II E-1, except for May-June and July-August.

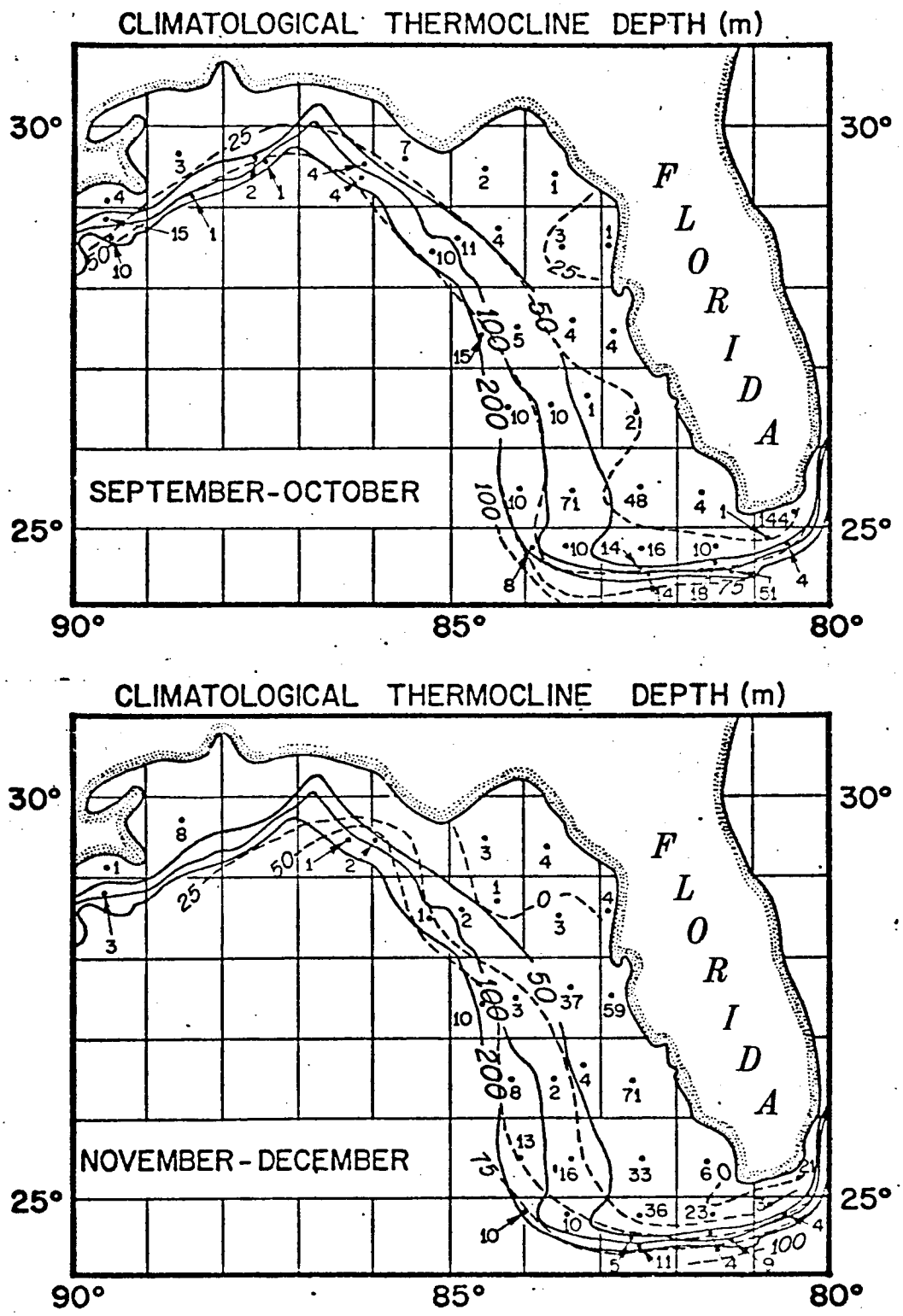

Figure II E-3. Same as in figure II E-1, except for September-October and November-December.

yet occurred by 20 June-3 July 1964. The summer-to-winter transition had occurred sometime after December in both years.

Average monthly surface and bottom salinity values were determined for blocks 1 to 6 (Figure IIE-4); in addition, average monthly salinities at 30.5 m were calculated for blocks 5 and 6. The data base utilized to calculate these salinities is a combination of NODC listings (as of 1973), University of Alabama data recently submitted to NODC, and selected data supplied to this study by the Mississippi Gulf Coast Research Laboratory. Plots of these data are depicted in Figure IIE-5.

The lowest average salinities, 21.8 and 22.1 ‰, occur at the surface in blocks 1 and 2 respectively during March. The lowest average values for both bottom and 30.5 meter waters never drop below 30‰ and in general fall within the range of open Gulf waters. The annual cycles observed in Figure IIE-5, blocks 1, 2, 3, and 4, particularly in the surface waters, closely parallel the annual cycles of river discharges (Figure IIC-1). The cycles from blocks 5 and 6, however, do not follow this trend. Both have two shorter periods of minimum salinity which slightly precede and then follow the months of maximum river discharge. Because block 5 boarders the eastern portion of the Mississippi River Delta and receives at least a portion of the Mississippi discharge, the cycles' configuration suggests (1) a non-uniform discharge from the four major distributaries over the maximum discharge period, and/or (2) other forces are in part responsible for the horizontal distribution patterns.

Similar salinity averages have not been computed using the data of Gaul (1964, 1965, 1966) or the Hourglass or West Florida Shelf data-set. However, T-S, and T-O_2 histograms have been constructed for hydro-biological regions, further subdivided into three depth zones, 0-50 m, 50-100 m, and 100-200 m using all the hydrological data in the MAFLA file. These histograms and a map of the hydrobiological regions are given in Appendix III. The histograms do not contain information on the temporal variability of the water mass characteristics but rather the spatial variability.

Spatial variability increases with distance from the deep basin as the effects of river run-off and meteorological disturbances become more pronounced. This is particularly evident at 22°C where SUW is found in the deep basin. The salinity maximum at 22°C decreases towards the coast in all zones, as the variability at this temperature increases.

2. General Shelf Circulation

Christopher N. K. Mooers
James F. Price

As is generally true of the continental shelves of the United States, very little systematic knowledge of the general shelf circulation of the eastern Gulf of Mexico exists. Here the term "general shelf circulation" refers to circulation components on the shelf with time scales greater than a day. Comprehensive circulation studies employing direct current measurements (readers unfamiliar with the basic characteristics of modern recording current meters and/or the basic time series analysis methods commonly employed in the analysis of physical oceano-

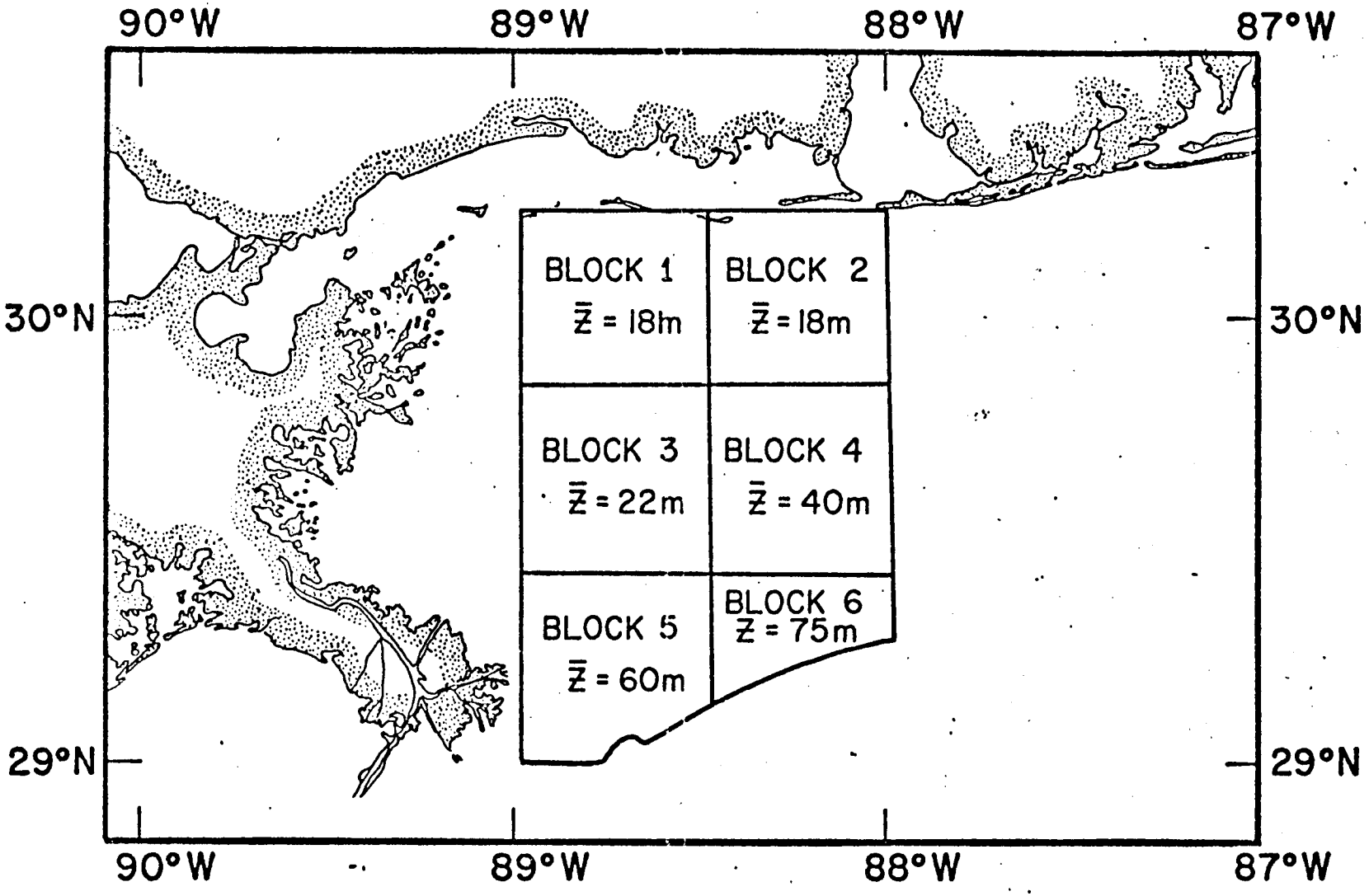

Figure.II E-4. Unequal area blocks used in the discussion of average salinities of the region. The mean depth for each block is given.

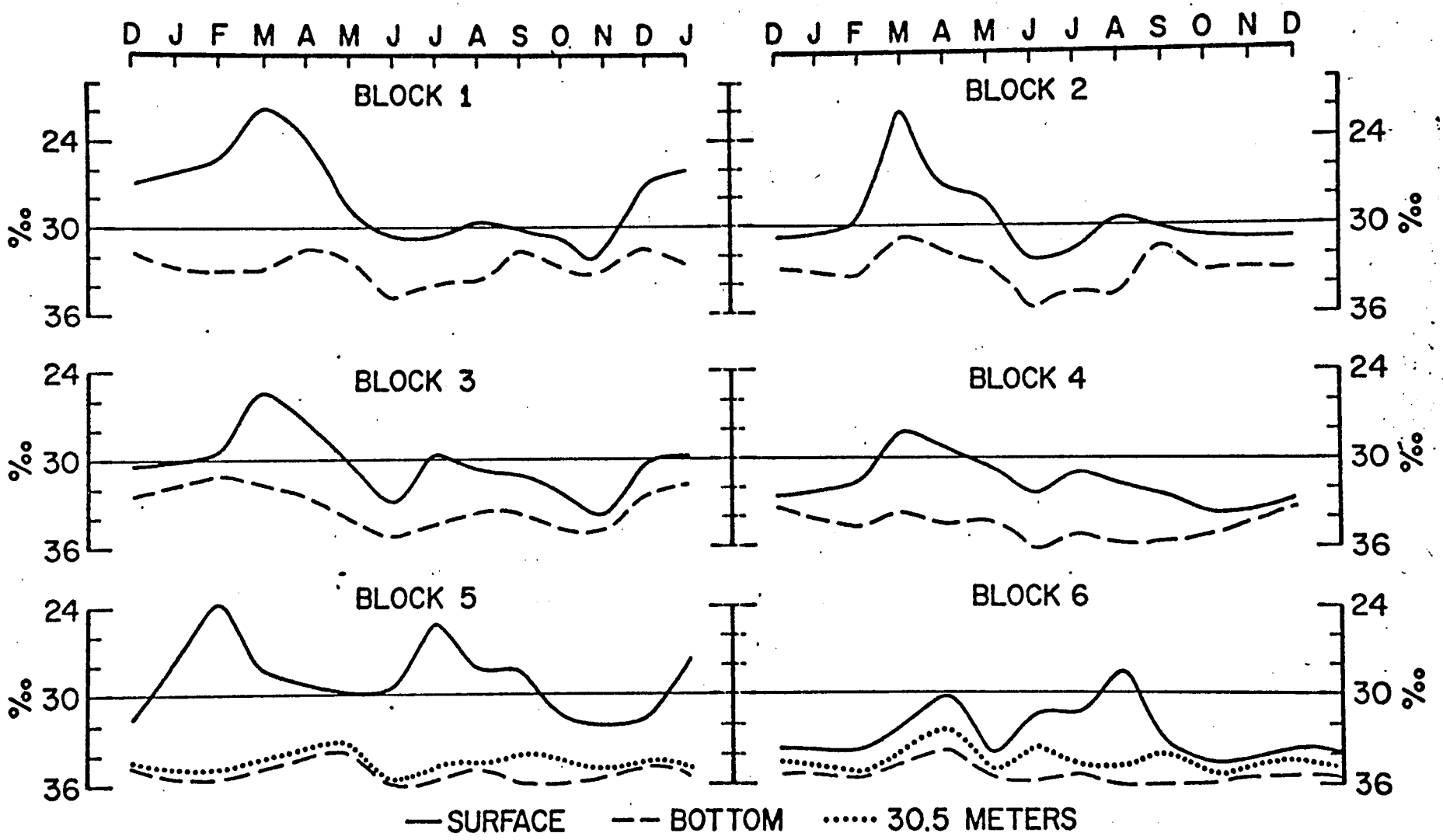

Figure II E-5. Annual cycle of average salinity for the blocks given in figure II E-4.

graphic data are urged to first read Appendix VIII before proceeding with the following section) have been performed only in recent years. We will focus attention here primarily on two intensive experiments conducted in February-March 1973, and October-December 1973.

These experiments have been documented in detail by Price and Mooers (1974 and 1975). During each of these experiments, ten or more current meters were deployed on the inner and outer West Florida Continental Shelf in the vicinity of 26°N. From these studies, and the work reported by Plaisted, Waters, and Niiler (1975), several conclusions are drawn which may have general applicability to the entire region.

The mean current, averaged over periods of a month or longer, tends to flow approximately parallel to the isobaths, although near the surface over the outer shelf there may occur significant cross-isobath mean flow (Figure II-E6). Frequently in winter the mean flow over the inner shelf is nearly uniform with depth in both direction and magnitude. In contrast, the mean flow over the outer shelf has different orientations in the top and bottom layer. Thus, a system of surface currents and undercurrents exists, (Figure IIE-7).

The low frequency (period greater than 1 day) fluctuating component of the flow is in general 5 times larger than the monthly mean flow, (50 cm/sec RMS value versus 10 cm/sec) Figure IIE-8. These fluctuating currents are weakly polarized in a plane parallel to the isobaths. The polarization is strongest near the bottom and over the inner shelf. Nevertheless, over the inner shelf, where the current most nearly parallels the topography, the current has been observed to flow directly across the isobaths for a period of several days at a speed of 10 cm/sec (Price and Mooers, 1974).

Energy spectra computed from the current meter records described show that the most important components of the low frequency fluctuating flow have periods of from 5 to 20 days, Figure IIE-9. A mean velocity computed over a record length of only several-to-ten days duration may, therefore, be seriously biased by these energetic fluctuations and may bear no relation to the mean flows shown. The tendency for both the mean and fluctuating flow to occur along the isobaths is the result of averaging over several or more cycles of the fluctuating flow.

The low frequency flow is well correlated in the vertical over distances of approximately 50 meters or less, Figure IIE-10. That is, two fixed-level current meters separated by 50 meters or less on the same mooring would be expected to yield rather similar records (correlation approximately 0.6 or higher). Two current meters at the same depth in the water column on different moorings and separated by 20 kilometers across the shelf would yield about the same correlation. The alongshelf correlation scale is roughly 100 kilometers, and the temporal correlation scale is of the order of 5 days (Price and Mooers, 1974). Hence, samples taken less frequently than 50 meters in the vertical, 20 kilometers across the shelf, 100 kilometers along the shelf, and 5 days in time are unlikely to be related in any systematic (statistical or causal) fashion. These considerations translate directly into sampling requirements.

The fluctuating flow may cause oscillatory particle displacements of the order of 100's of kilometers in the time scale of several weeks.

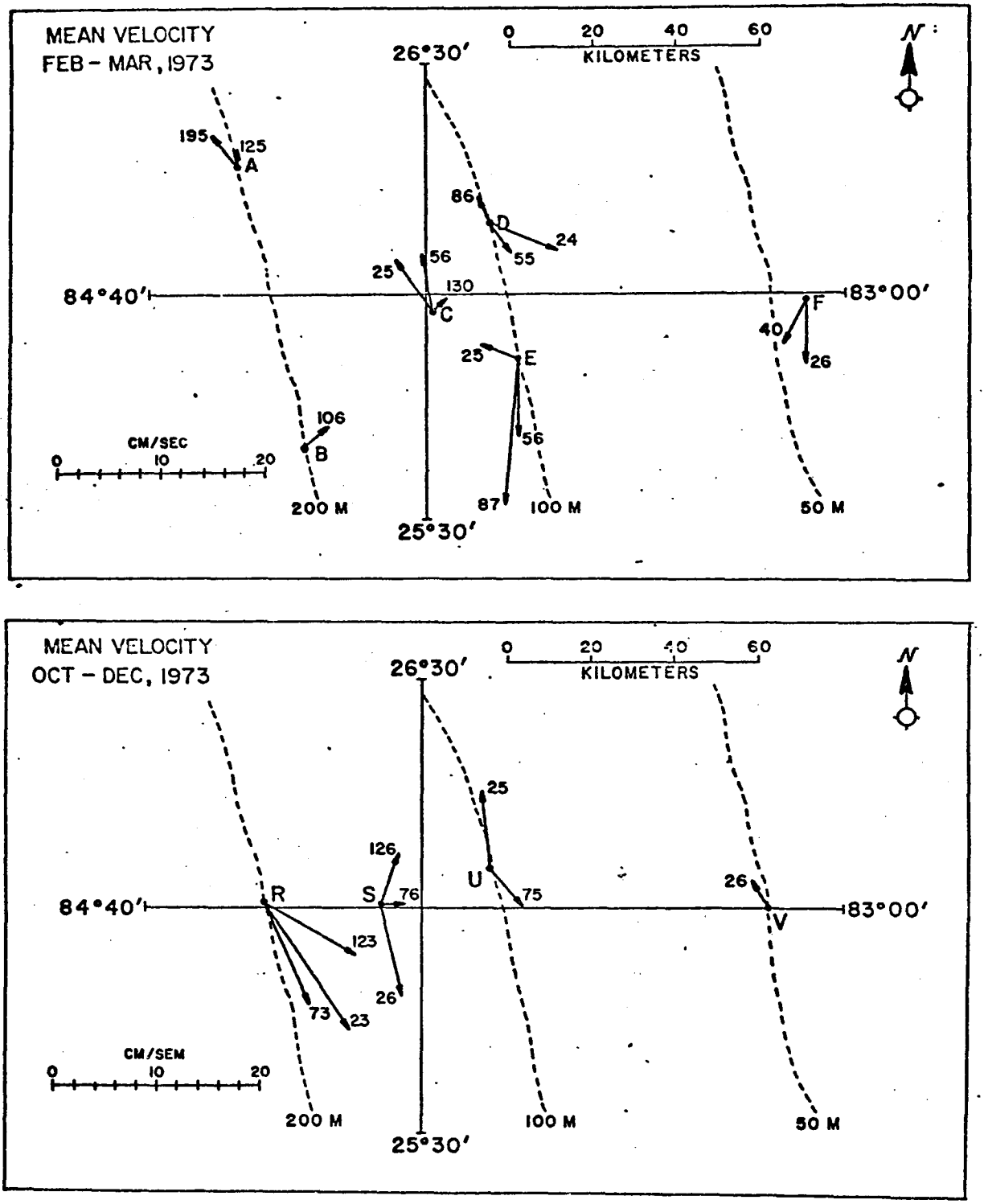

Figure II.E-6. Mean velocity measured over approximately five-week periods in February-March 1973, and in October-December 1973. The number at the head of each vector is the depth of the current meter.

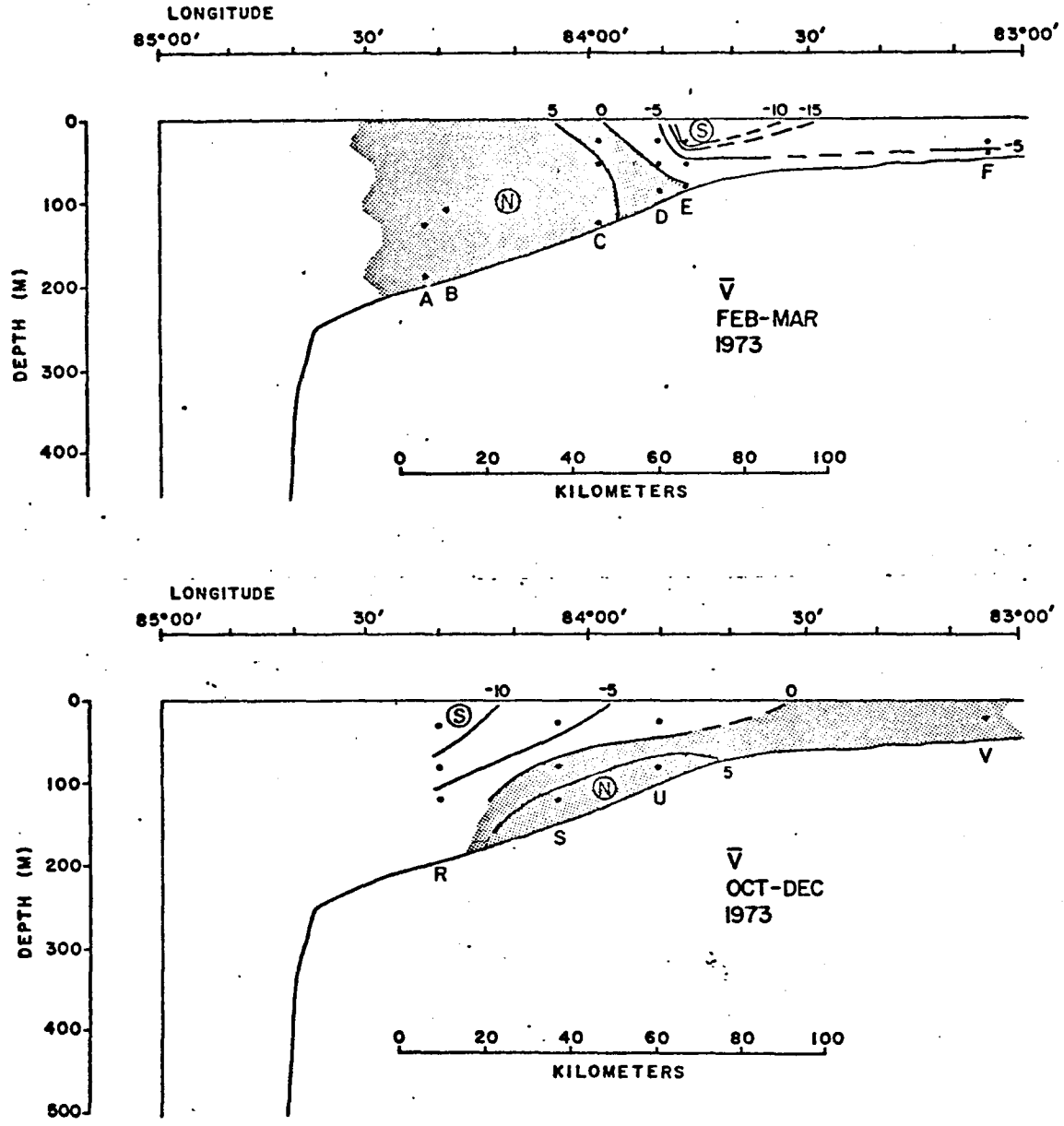

Figure II E-7. Vertical sections of longshore velocity component from the data shown in figure II E-6.

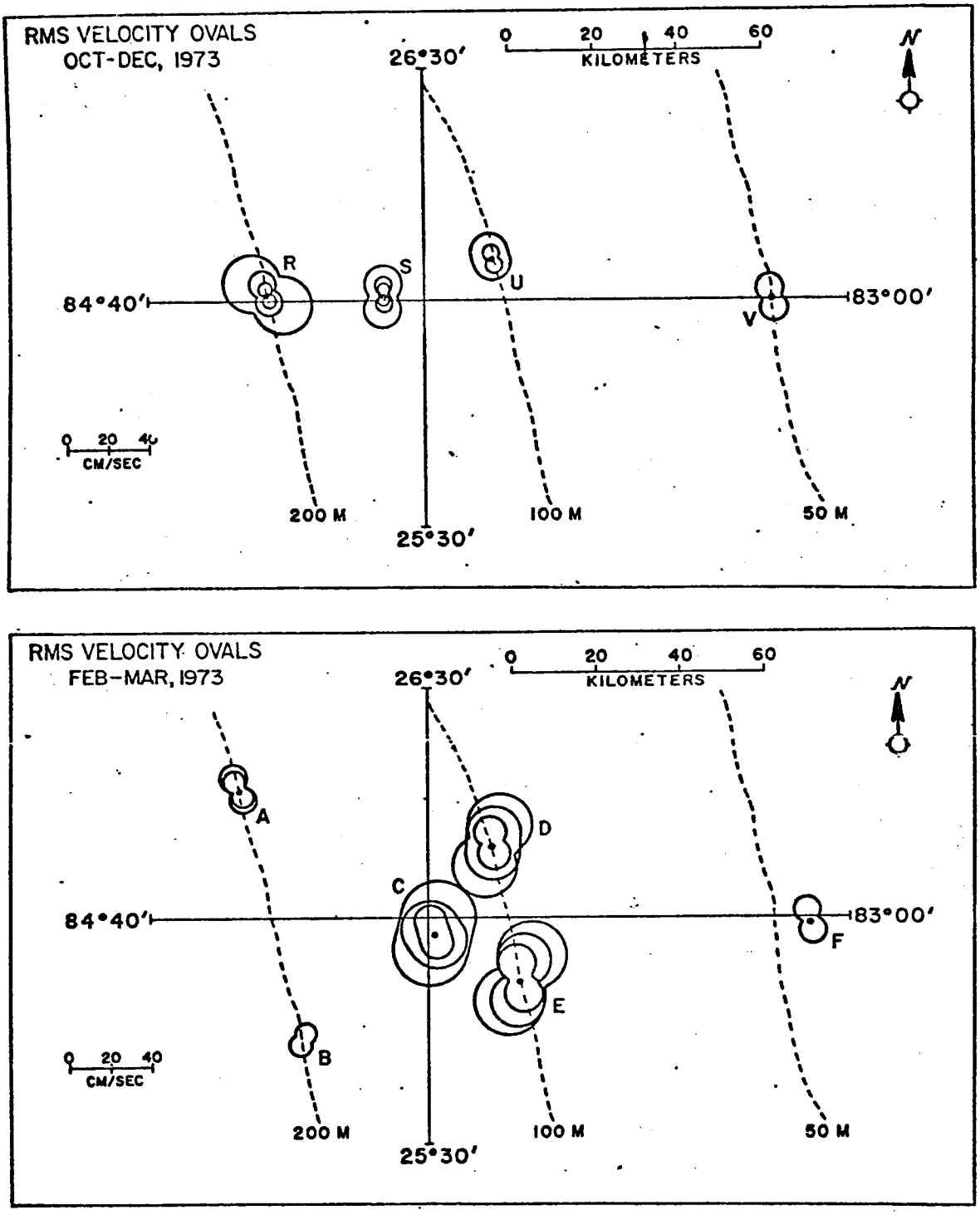

Figure II E-8. RMS velocity ovals computed from the current meter data shown as averages in figures II E-6 and II E-7. The distance from the oval center to any point on the circumference is proportional to the RMS value of the fluctuating component of velocity in that direction. The data were filtered to remove tidal and inertial motions.

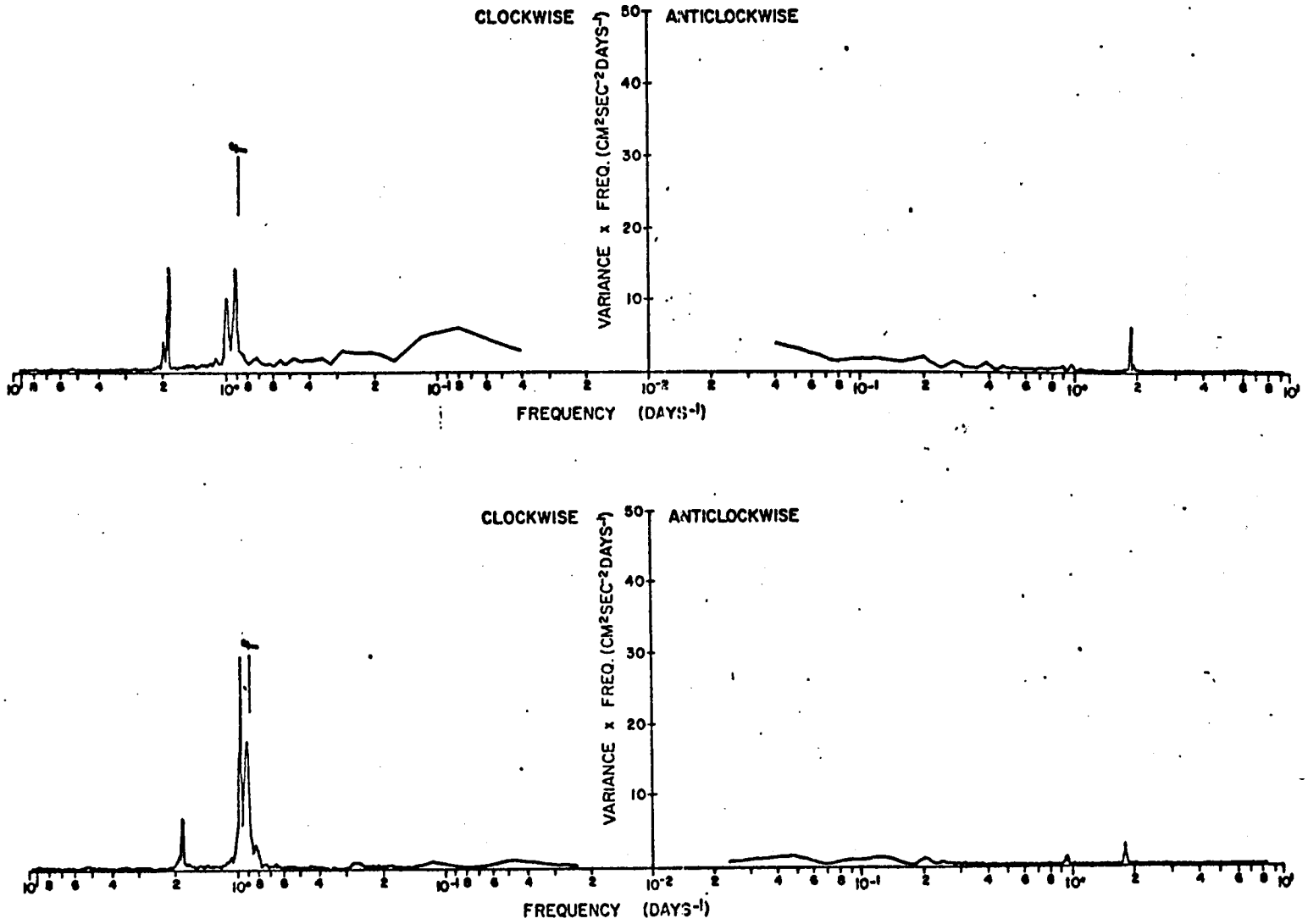

Figure II E-9. Top panel. The average of 15 separate horizontal current spectra computed from data taken in February-March 1973 (see figure II E-6 for station locations. The area under the curve is directly proportional to the energy in the frequency band. See Appendix. Lower panel. A similar average for data taken in October-December 1973 (see figure II E-6 for station locations). The spectra have been divided into components which rotate clockwise and counterclockwise.

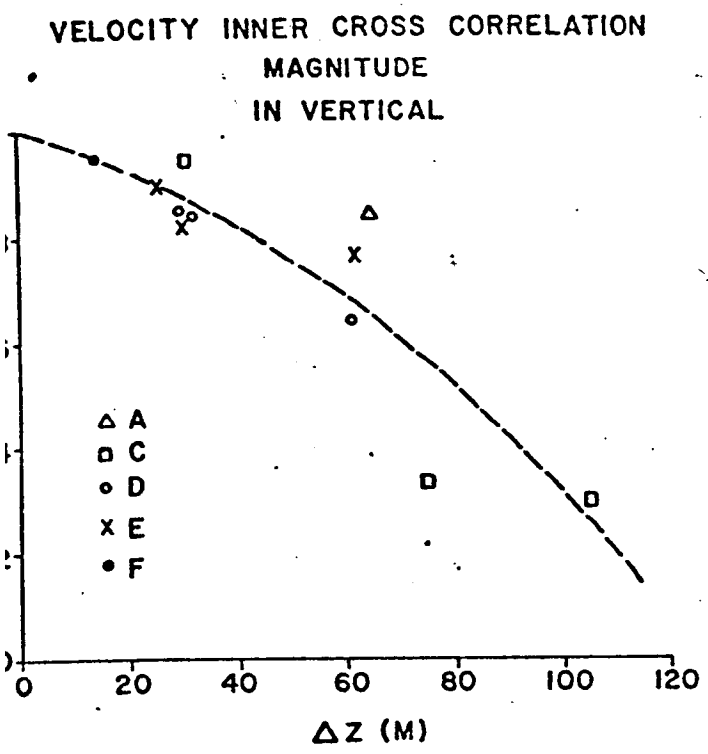

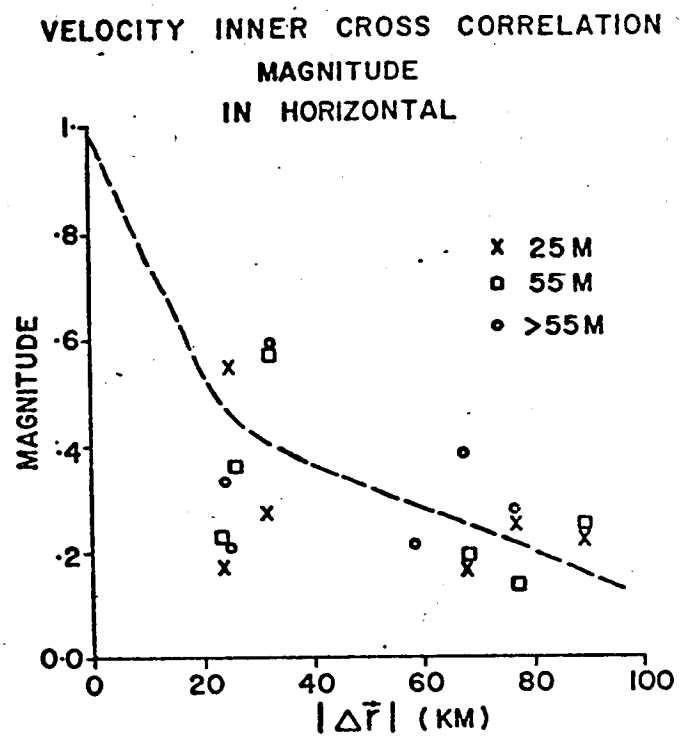

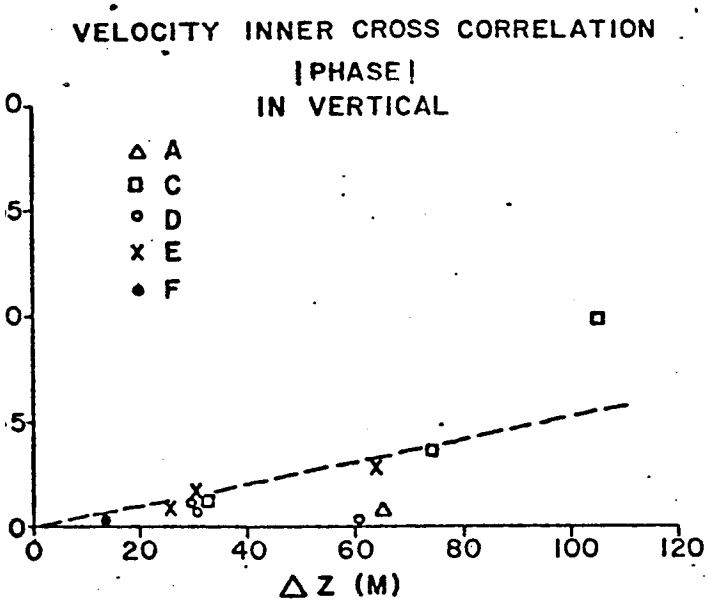

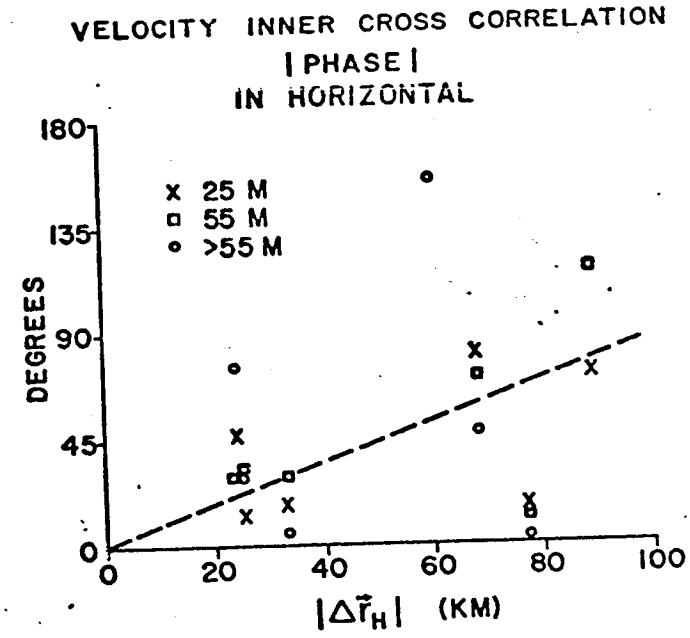

Figure II E-10. Correlation functions computed from records of horizontal current taken in February-March 1973. The correlations were computed between data separated in the vertical, and in the horizontal. The dashed lines indicate the trend of correlation as the separation distance between the observation points increases. See appendix 8 for a discussion of correlation.

By contrast, tidally induced flows are both weaker (approximately 10 cm/sec versus 50 cm/sec) and of such short persistence (roughly half a day for the diurnal tide) that tidally induced particle displacements are only some 5 kilometers.

The extreme values of currents occur with the superposition of seasonal mean flow, storm-induced, several-day to several-week oscillations, storm-induced inertial oscillation, and tidal oscillations. Extreme values can reach 100 cm/sec .

Nearly two years of current meter, temperature, and bottom pressure data from various locations on the West Florida shelf, between about 25° N and 28°N, have been or are being acquired by Nova University. Records from the fifteen months of this current monitoring project have been presented in graphical and tabular form (Plaisted, Waters, and Niiler, 1975). These records are in general accord with the description of variability given above.

The forcing mechanism of the large amplitude, low frequency (approximately .1 cpd) currents observed by both the University of Miami and Nova University is not understood, though transient wind systems and Loop Current meanders are possible forcing mechanisms. However, these current oscillations have been observed propagating northwards along the continental shelf at a speed of approximately 20-40 kilometers/day. Therefore, the currents observed at any particular point on the shelf may be due to forcing at a large distance (order of 100's of kilometers) from the observation site. This is a significant feature of the West Florida Continental Shelf which must be kept in mind when designing future monitoring studies. It strongly suggests that instruments should be deployed over a wide area along the shelf, not simply in the area of immediate interest.

The direct current measurements summarized here clearly show the significance of the low-frequency component of the currents. The time-averaged mean current is small when compared to the low-frequency fluctuating flow. The tidal and inertial motions, though energetic, are not capable of producing large particle displacements (greater than say 20 kilometers) because of their high frequency. On a time scale of several days to a week, the advective flow field is dominated by the low-frequency fluctuations. The tidal and inertial motions play a turbulent dispersive role on this time scale.

F. Motion Inducing Forces Active on the Eastern Gulf of Mexico Continental Shelf

The Loop Current, atmospheric disturbances, tides, and the effects of river run-off are presented as "forces" which can impart momentum to the shelf waters of the eastern Gulf of Mexico. The forcing can be accomplished through lateral momentum exchange from the Loop Current to the shelf waters; through vertical momentum exchange from the winds to the shelf waters; through the gravitational effects of the sun or moon; or through pressure gradients established by river run-off.

The current meter studies on the West Florida Shelf described previously are among the first experiments to investigate the forcing of shelf motions by atmospheric disturbances. Historically, deep-basin studies have discontinued operations at the 200 m isobath, while shelf studies have been bounded by the coastline and the 200 m contour. Therefore, the discussion of these forces must be more descriptive than dynamical, in the sense that effects of the Loop Current, for instance, have been observed, but not dynamically described.

Tidal motions have been described in the section on shelf circulation. The effects of river run-off on the shelf circulation have not been documented. Qualitatively, the fresh water discharge should establish horizontal pressure gradients and motion, but the authors are unaware of any observational or theoretical studies which describe quantitatively this effect on the eastern Gulf of Mexico shelf. Therefore neither tides nor river run-off are considered in this section.

1. Atmospheric Disturbances

James F. Price
Christopher N. K. Mooers

The effects of atmospheric disturbances and semi-permanent meteorological features on shelf circulation are many. For example, the summer Southeast Trades are strong and persistent in the southern Gulf but weak and variable in the northern Gulf. The Trades induce a northward surface Ekman drift which is convergent towards the north, hence there must be some form of compensatory flow, presumably at depth. The occasional summer hurricanes and tropical cyclones can be expected to mix the upper layers substantially and to produce strong currents trapped on the outer shelf in their northward progression. The winter Trades are less persistent and are frequently interrupted by vigorous atmospheric frontal systems.

In advance of a cold air outbreak from the continent, an atmospheric warm front proceeds northward. These warm fronts are capable of causing coastal downwelling in the eastern Gulf and exciting topographically trapped waves which move northward. Then an atmospheric cold front advances rapidly from the northwest, producing a rapid clockwise turning of the winds and a sharp drop in air temperature. These developments may produce inertial oscillations and convective cooling, both of which can deepen the wind-mixed layer. Mooers and Van Leer (1975) describe a

case in which a strong cold front deepened the mixed-layer to 50 meters from an initial depth of 25 meters. The surface layer was cooled by $1^{o}C$.

Following the frontal passage, a period of intense southward winds, a "norther", occurs, which can produce transient coastal upwelling. This winter sequence of winds favorable to downwelling, windstirring, and upwelling occurs on a weekly time scale, but with considerable variability in frequency of occurrence and intensity. Nonetheless, such agitation can be expected to produce vigorous transient circulations and exchange of shelf and Gulf waters, back and forth across the outer shelf.

The direct, local response of the ocean surface layer to winds may be estimated by modeling the surface layer as a time-dependent Ekman layer. The winds shown in Figure IIA-1 were used to force motions in a Ekman layer 20 meters deep. The results model the wind-driven current averaged over the top 20 meters of the water column. Near coastlines the current will be modified considerably, since at the coastline the flow perpendicular to the coast must vanish. The winter months clearly show transient inertial oscillations driven by cold front systems, Figure IIF-1. These oscillations have up to 50 cm/sec half-amplitudes and would thus cause oscillatory particle displacements on the order of 10 kilometers. Direct current measurements on the West Florida Shelf reported by Price and Mooers (1974) show very similar large amplitude inertial oscillations having a similar phase relation to cold front systems.

2. Loop Current

Robert L. Molinari
John D. Cochrane
George A. Maul
Murice Rinkel
William W. Schroeder

Deep basin processes which can affect the shelf circulation and dispersion of shelf waters include

1) momentum and water mass transfer from the Loop Current to the shelf,

2) direct incursions of the Loop Current, and its associated momentum and water masses, onto the shelf,

3) incursions of Loop related eddies, and their associated momentum and water masses, onto the shelf, and

4) fluxes of mass from the shelf to the deep basin instigated by Loop Current features.

To date there have been no observational or theoretical studies addressing the question of momentum transfer from the Loop Current to the shelf. Therefore, the mechanism of exchange between the two regions when the core of the Loop Current is some distance from the shelf is not considered in this section.

There are occasions when the Loop Current runs directly onto the West Florida Shelf (Figure IIF-2) transferring momentum and water masses from the deep basin onto the shelf. Again there have been no direct

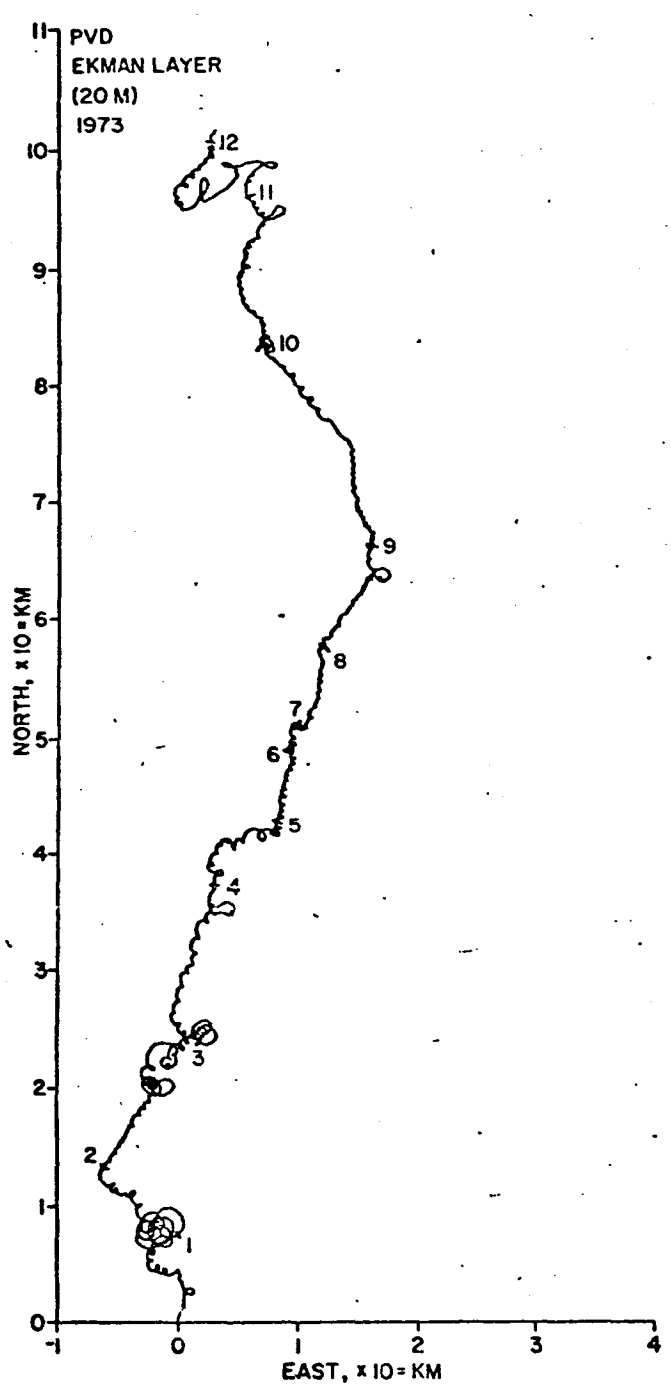

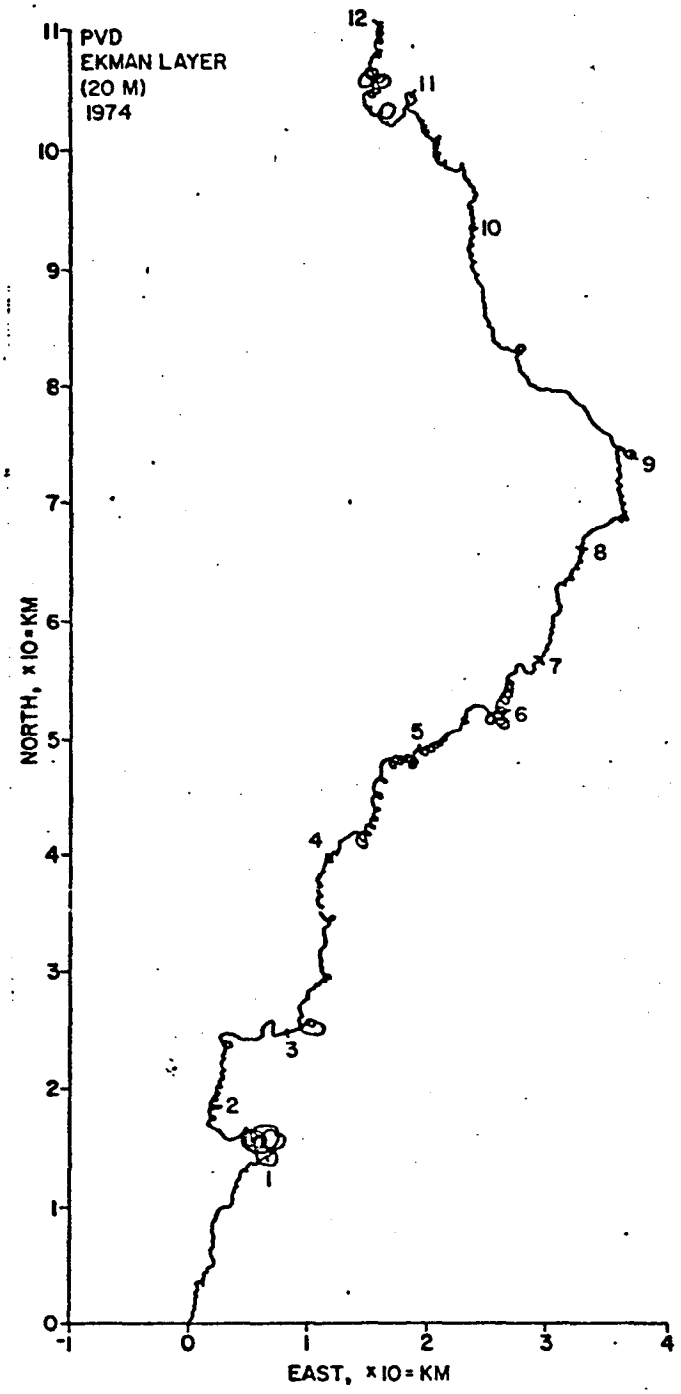

Figure II F-1. Ekman layer response for a 20 meter thick layer driven by the winds shown in figure II A-1. The numbers denote the end of the month as in that figure.

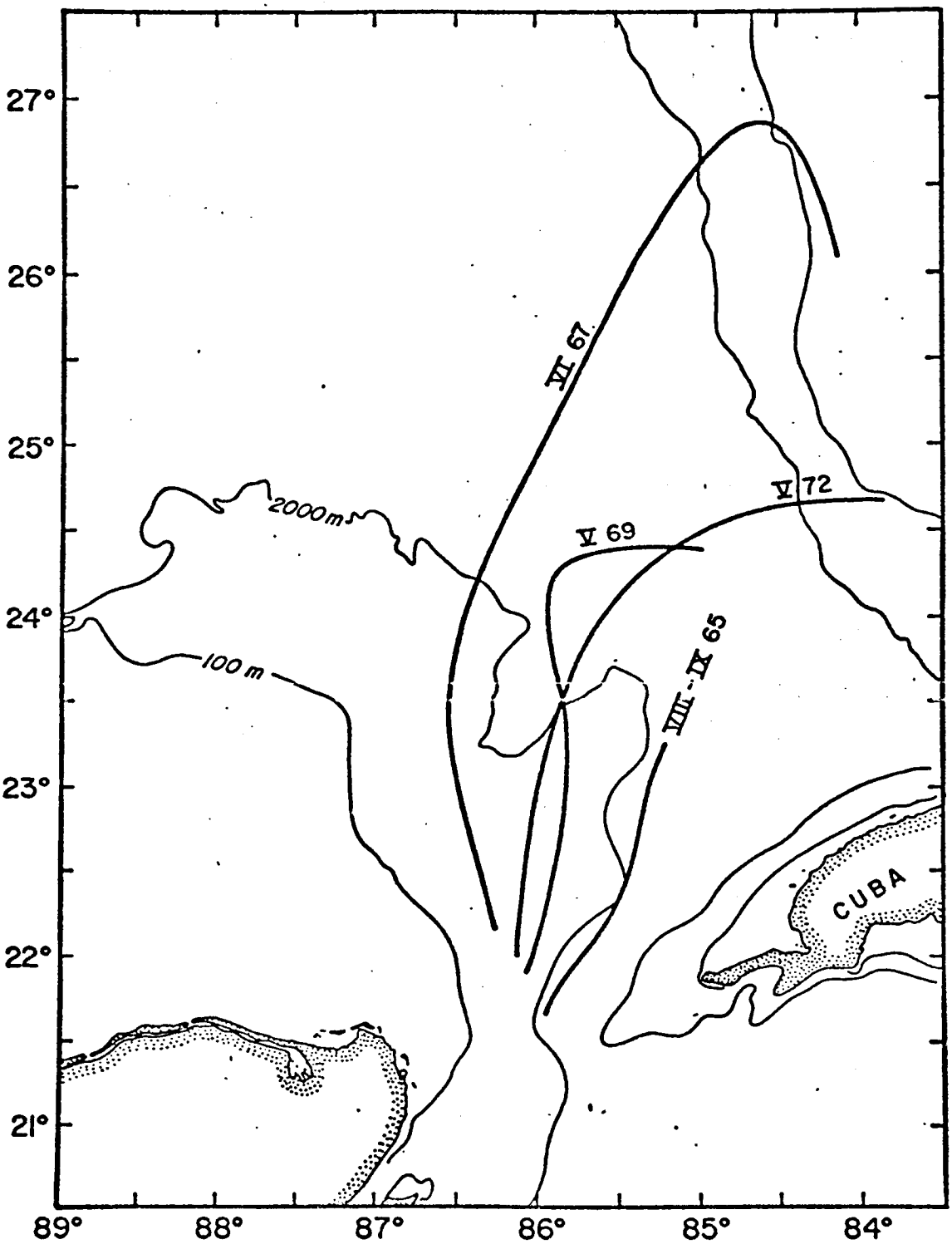

Figure II F-2. Intrusions of the Loop Current onto the west Florida Shelf as indicated by the 100 m contour of the 22°C topography. Maul (1974) has shown that this contour of the 22°C surface can be used as a indicator for the core of the current.

measurements of the spatial extent of the motions induced. However, water mass distributions give some indication of the frequency and extent of these overflows.

The 16 seasonal distributions of temperature, salinity, and sigma-t from the Western Florida Continental Shelf Program have been examined for evidence of Loop Current waters. In particular the distribution of salinity core maxima, an indication of SUW, have been plotted, and are given in Appendix IX. Fourteen of these maps include stations far enough offshore to be of use in this discussion. Loop Current waters are defined as those having salinities greater than 36.5°/oo (see Loop Current discussion).

In September 1972 and January 1973 there were direct incursions of the Loop onto the shelf between 24°N and 26°N (see Appendix IV for 20°C topographies). The salinity maximum maps of Appendix IX indicate an intrusion of deep basin water some 80 to 90 km wide. Salinity data indicate a similar intrusion of Loop waters, but there are no supporting deep-basin data. In the deep basin, salinities greater than 36.5°/oo were found only to the right of the core, facing downstream. However, the relation between current core and salinities greater than 36.5°/oo has not been defined for water on the shelf. Comparison of the 150 m contour of the 20°C topography and the salinity distribution on the shelf suggests that the deep-basin current core-salinity relation may not be valid on the shelf, that is, salinities greater than 36.5°/oo on the shelf may not be correlated with the right speeds associated with the core of the current.

The 20°C topographies given in Appendix IV include no clear-cut indications of a continuous Loop Current extending past 28°N. The August 1973 topography can be contoured to indicate either a continuous Loop Current or a detatched eddy. However, there are definite indications of the large eddies which separate from the main flow extending far north onto the MAFLA shelf.

Particularly dramatic eddy penetrations occurred in 1965 and 1973. The 1965 eddy persisted on the shelf through December 1965. The shelf topographies of Appendix VI suggest that the eddy drifted west towards the Mississippi Delta. Remnants of this eddy are found in the February 1966 20°C topography (Appendix IV) off the Delta.

Figure IIF-3 shows the salinity maximum distribution for August 1973. SUW has penetrated well onto the continental; shelf but again the relation between the current core and the salinity maximum has not been defined. The 20°C topography for August 1973 (Appendix IV) indicates the core of the current is south of 29°N. Additional large scale intrusions of SUW onto the MAFLA Shelf are found in August 1971 and November 1971 and 1972.

Smaller scale eddies also have been found on the eastern Gulf shelf. A vertical salinity and oxygen section through the smaller northern eddy found in September 1965 (see Appendix IV) shows this gyre has the same water mass characteristics as the southern flow. The eddy is approximately 100 km wide, and it is somewhat shallower with slower speeds than the southern gyre.

These features are also found on the West Florida Shelf. Examples of these high salinity intrusions are found in salinity maximum distributions

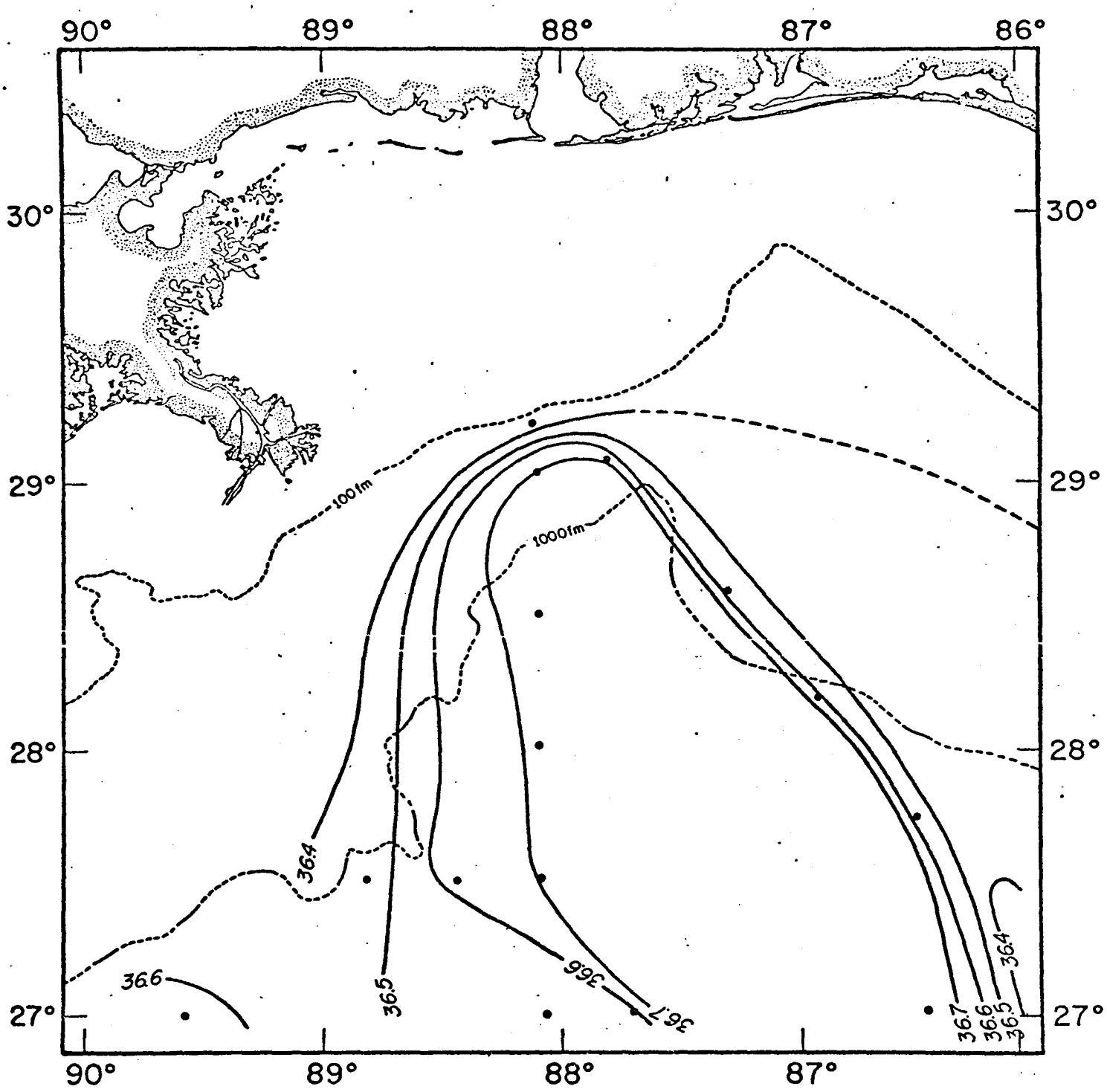

Figure II F-3. Distribution of the salinity values at the core of the salinity maximum during August 1973, showing the penetration of deep basin water onto the MAFLA shelf. The dots indicate station positions.

during May 1972, May 1973, and June 1973 (Appendix IX) between 26°N and 28°N. These eddies have spatial scales of 60 to 100 km.

The Loop Current water may be present on the shelf along the bottom as a tongue of water intruding up the continental slope, toward the coast. These features are illustrated in the vertical sections of Appendix VII. For instance, parcels of high salinity water are found either along the bottom or at mid-water in August 1971, September 1972, January 1973 at 28°30'N; in May 1971, June-July 1973, at 27°30'N; and in May 1971, June 1973 at 26°00'N. To date no seasonal variability to the occurrence of these features has been determined.

The intrusion of these deep basin features has two obvious effects on the shelf water masses and circulation which should be stressed. Not only do they bring deep basin chemical and biological species onto the shelf, but to conserve mass they must cause an offshore movement of the shelf water somewhere along the shelf.

The meanders associated with the Loop Current can be expected to entrain shelf waters. Off the west Florida Shelf a meander is frequently found between 24°N and 26°N and 84°W and 86°W (figure II-F) Large amounts of shelf water can be transported over the deep basin through the interaction of this feature and the shelf.

In addition, it appears that the formation of such a meander is a necessary step in the sequence which can culminate in the separation of an eddy. FigureIIF-5 gives the 20°C topography after such a separation occurs. In fact, the separation is characterized by a ridge of shelf water separating the main flow, and the cut-off eddy. Salinity cross-section across the gyre and into the main flow (June 1966 August 1968, June 1970, (Appendix III) for instance) show the near-surface low salinities characteristic of this shelf water. Additional analysis is required to ascertain if shelf waters entrained by the edge of a separated eddy remain in the Gulf or are transported out.

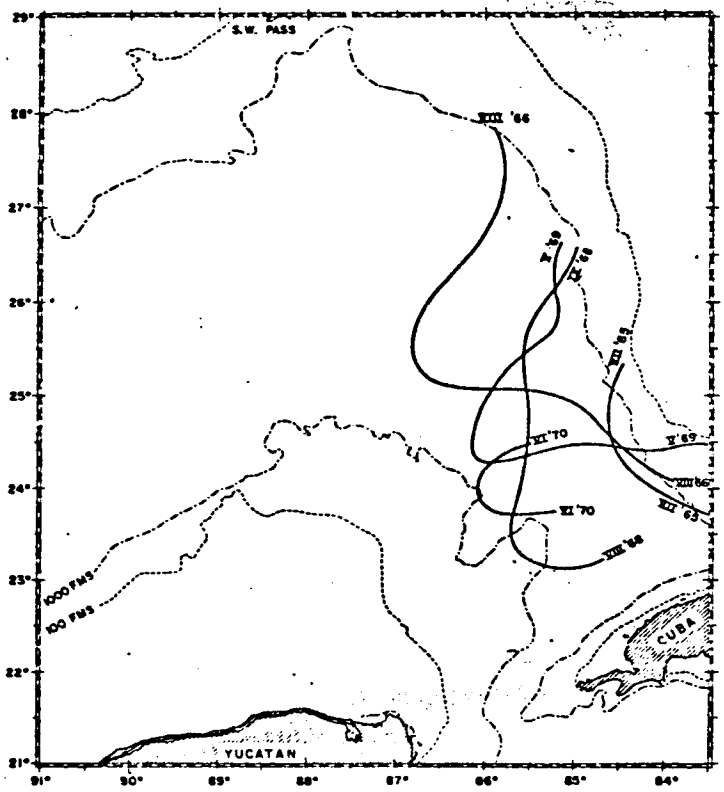

Figure II F-4. The west Florida Shelf meander as indicated by the 100 m contour of the 22°C topography (from Cochrane 1972). Maul (1974) has shown that this contour of the 22°C surface can be used as an indication for the core of the current.

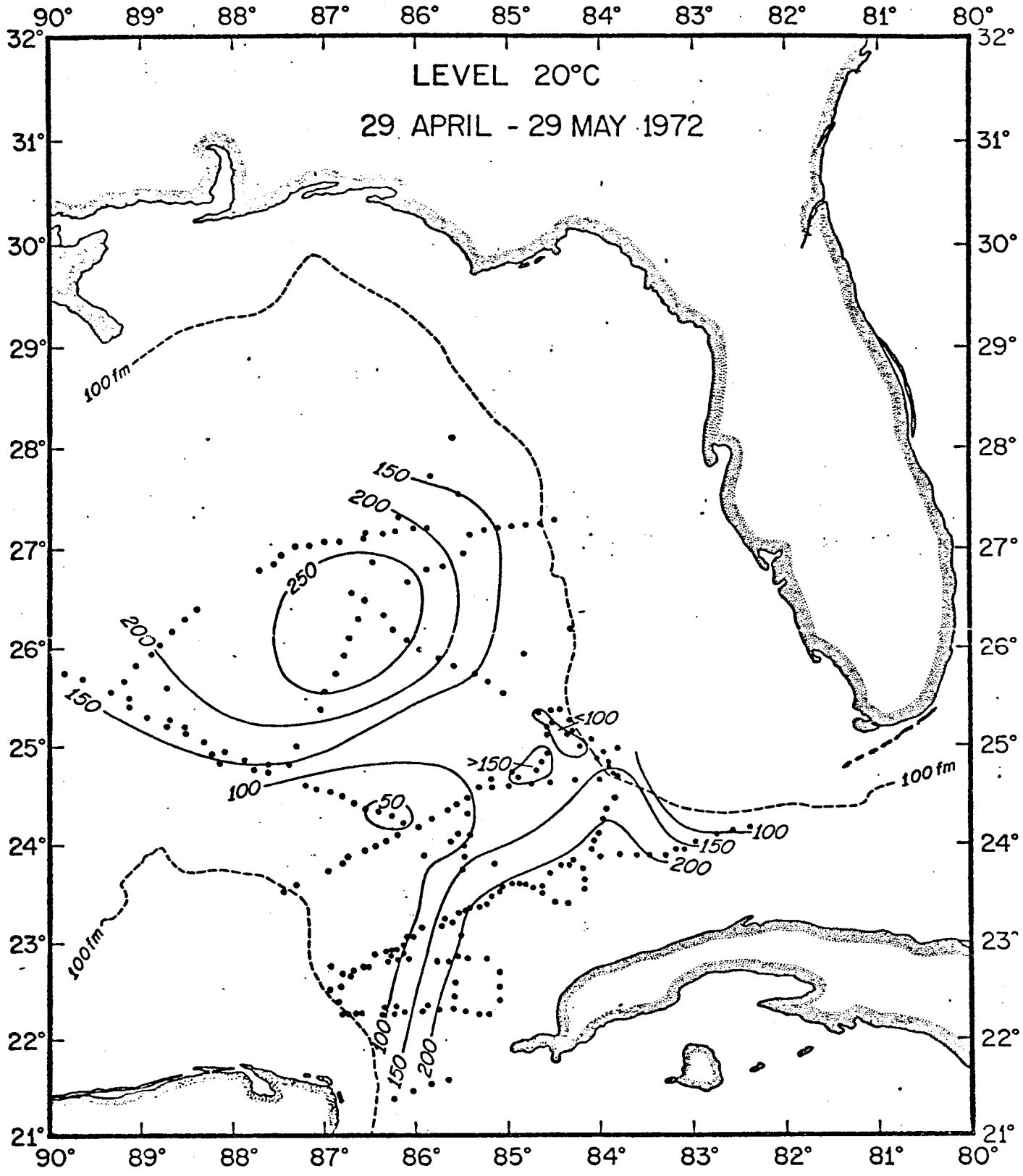

Figure II F-5. The 20°C topography during May 1972, a detached eddy is shown with the ridge separating the eddy and the main flow extending from the west Florida Shelf to the Campeche Bank.

G. Biological Considerations

1. Seasonal Abundance and Distribution of Zooplankton, Fish Eggs and Fish Larvae in the Eastern Gulf of Mexico

Edward Houde

Standing crops of zooplankton (measured as ml per 1000 m^3 filtered) and both abundance (no. under 10 m^2 of sea surface) and concentration (no. per 100 m^3 filtered) of fish eggs and larvae were examined from eastern Gulf of Mexico plankton collections made during 12 cruises in 1972-1974. Zooplankton volumes were examined to provide an index of productivity, while occurrence of fish eggs and larvae was used to delimit spawning areas and times. Objectives were to determine if some areas of the eastern Gulf had relatively high plankton productivity, and if there were areas where fish spawning was intense. Such information would be useful to predict probable impacts of an oil spill or other pollutant discharged into the eastern Gulf.

Collections were made by oblique tows of paired 60 cm Bongo net plankton samplers at stations spaced 15 or 30 mi. apart on a grid that extended from the Dry Tortugas (lat. 24°30'N) to Cape San Blas (lat. 29°30'N), and from the 10 m contour near the west Florida coast to approximately the 200 m contour at the shelf edge. The number of stations per cruise ranged from 13 to 51. A total of 482 zooplankton samples were analyzed from the 333 μ mesh net; 483 fish egg and larvae samples were analyzed from the 505 μ mesh net. Because individual species among the zooplankton were not identified, and because catches of fish eggs and larvae were not indentiied beyond those categories, these results can be used to define areas of productivity on the western Florida shelf only in a relative sense.

a. The Nature of Distribution: Distributions of zooplankton, fish eggs, and larvae are patchy in the eastern Gulf. When the mean abundance or concentrations for all stations on a given cruise were examined, their standard errors and coefficients of variation were high, reflecting contagion in distribution of the organisms. Fish egg concentrations had a higher degree of contagion than either fish larvae concentrations or zooplankton volumes in the eastern Gulf. Examples of contour charts for zooplankton volumes from four cruises are given in Figure IIG-1.

Mean zooplankton volumes for the 12 cruises ranged from 69.1 to 287.8 ml per 1000 m^3, the pooled mean for all cruises equalling 153.4 ml per 1000 m^3. Mean fish egg abundances ranged from 163.1 to 927.1 under 10 m^2 of sea surface, pooled mean equalling 510.1 under 10 m^2. Mean concentrations of fish eggs ranged from 100.0 to 1079.3 per 100 m^3, pooled mean equalling 365.4. Mean fish larvae abundances were 55.3 to 825.4 under 10 m^2 of sea surface, pooled mean equalling 435.5 and mean concentrations ranged from 58.4 to 353.3 per 100 m^3, pooled mean equalling 164.4.

b. Seasonality: Zooplankton production and spawning by fishes have a distinct seasonal pattern in the eastern Gulf. Figure IIG-2 illustrates the seasonal increase of zooplankton standing crop during spring that reached a peak during summer, and then decreased to a winter minimum.

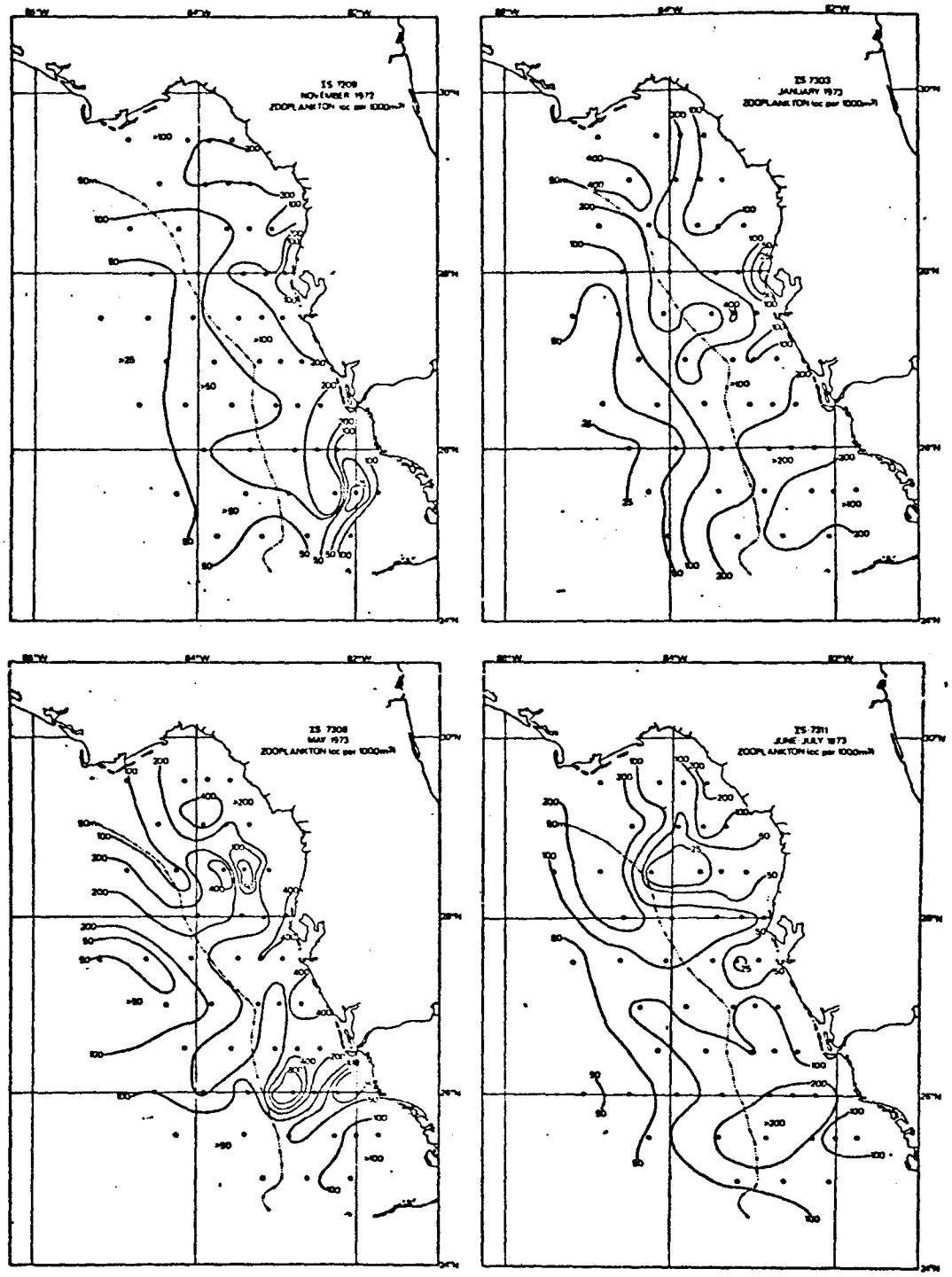

Figure II G-1. Contour charts of zooplankton volumes (cc per 1000 m^3) for four cruises to the Eastern Gulf of Mexico, 1972-1973.

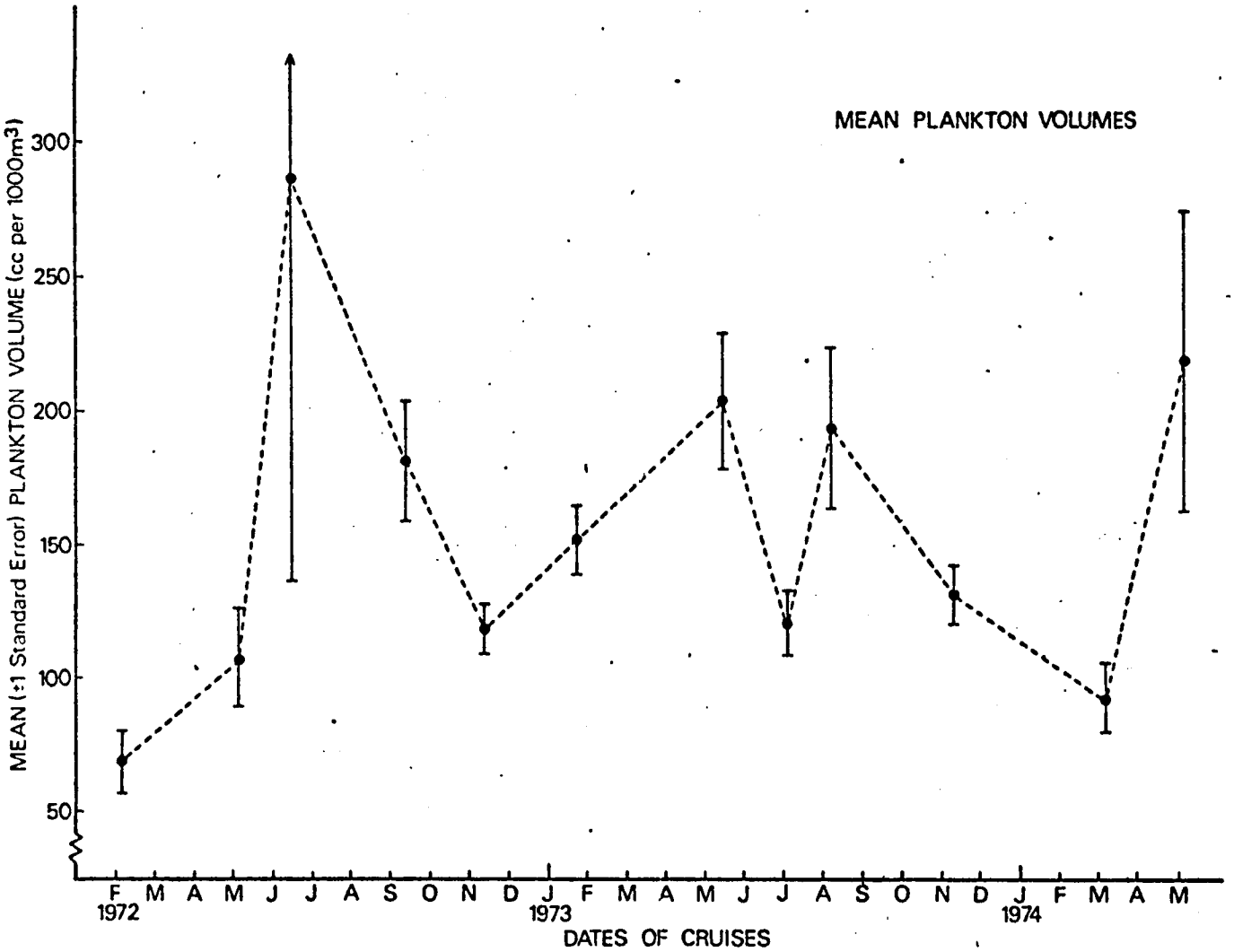

Figure II G-2. Mean zooplankton volumes for each of 12 cruises to the Eastern Gulf of Mexico, 1972-1974.

Egg and larvae abundance followed the same pattern. Mean zooplankton volumes were less than 125 ml per 1000 m^3 for winter cruises (November through March), but summer cruise means (May through September) increased to 200 ml per 1000 m^3 or more. The increases in fish eggs and larvae from winter to summer were even more pronounced than those observed for zooplankton, the mean concentrations (no. per 100 m^3) more than doubling between seasons.

c. North-South Distribution and Abundance: The eastern Gulf Study area was roughly bisected by latitude 27°15'N. Zooplankton and ichthyoplankton were examined relative to this latitude for each cruise. In general, all three components were more concentrated in the northern half of the study area, although pooled means over all cruises did not differ greatly between sectors. Mean zooplankton volumes in the northern sector were higher relative to mean volumes from the southern sector for winter cruises. In summer, the mean zooplankton volumes frequently were higher in the southern sector (Figure IIG-3). There were no seasonal differences in the patterns of occurrence for fish egg and larvae concentrations between the two sectors. Larval abundance (no. under 10 m^2) usually was highest in the southern sector.

The overall seasonality of production that was observed for the whole shelf area was also present in each of the two sectors. The degree of seasonal change in ichthyoplankton concentrations was greater in the northern sector of the shelf. Zooplankton volumes increased more in the southern sector during the spring and summer months.

d. Distribution and Abundance Relative to the 50 m Isobath: Zooplankton and ichthyoplankton catches were examined in relation to the 50 m isobath, which divides the shelf study area into approximate halves. Mean zooplankton volumes (Figure IIG-4), and fish egg and larvae concentrations were greatest at stations less than 50 m deep. Mean egg abundance also was greatest in the shallow nearshore areas. But, the mean abundance of larvae was highest at deeper stations on all 12 cruises. The seasonal pattern of zooplankton and ichthyoplankton occurrence was most apparent at stations less than 50 m deep. Ichthyoplankton concentrations, in particular, increased most at nearshore stations during spring and summer months.

Pooled mean zooplankton volumes at stations less than 50 m deep exceeded those at deeper stations by a factor of 1.8. Pooled mean fish egg concentrations were 7.3 times higher at the shallow stations and larvae concentrations were 2.1 times higher there. But, when abundance was considered, larvae were 2.2 times more abundant at stations deeper than 50 m. Because discrete depth strata were not sampled, it is possible that larvae could have been highly concentrated in certain depth-strata at the deeper stations, but the oblique tow sampling technique allows determination only of the mean concentration over the enitre water column.

e. Specific Areas of Abundunce: The patchy nature of zooplankton and ichthyoplankton distributions made it difficult to determine if any areas were consistently highly productive. Dense patches of eggs (1600 under 10 m^2) usually occurred at depths of 20 to 100 m during spring and summer, but no specific areas had consistently high numbers. Localized patches of larvae also were present, but these were not as commonly observed as dense egg patches.

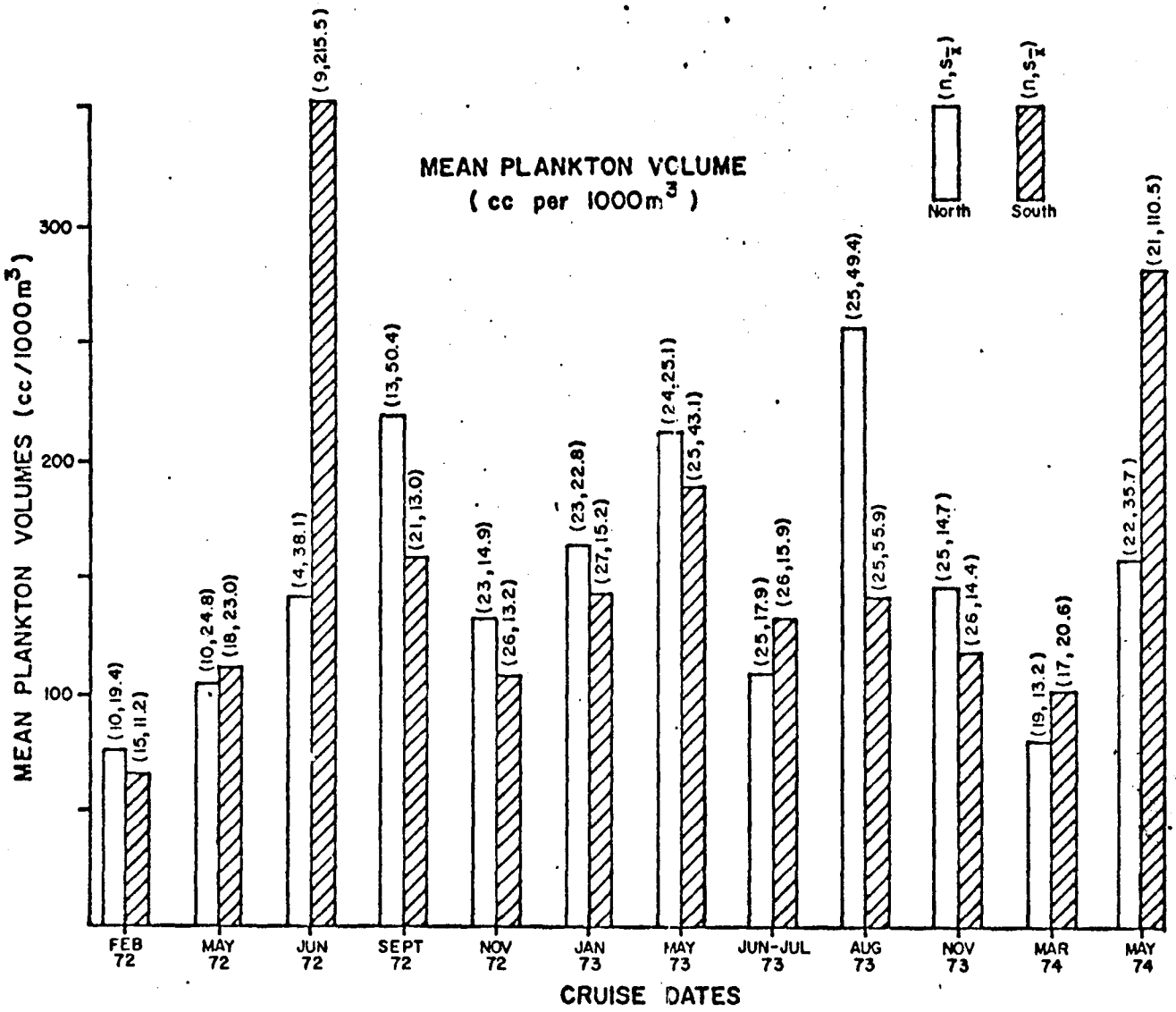

Figure II G-3. Mean zooplankton volumes compared between stations sampled north of latitude 27°15'N and stations south of that latitude for 12 cruises, 1972-1974. Numbers of stations and standard errors of the mean are given in parentheses above bar graphs.

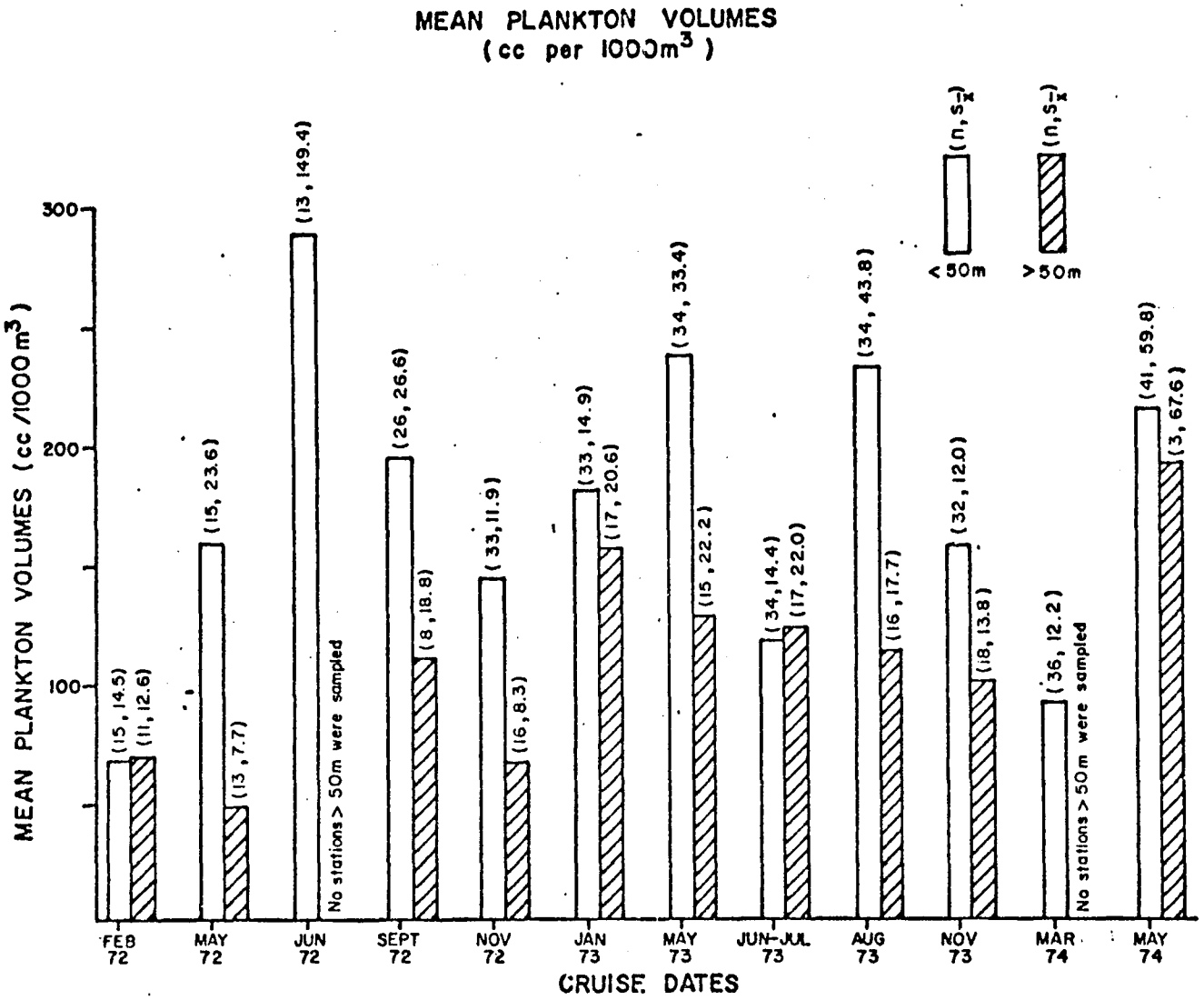

Figure II G-4. Mean zooplankton volumes compared between stations at depths less than 50 m and greater than 50 m for 12 cruises, 1972-1974. Numbers of stations and standard errors of the mean are given in parentheses above bar graphs.

Zooplankton volumes frequently were higher than the mean volume for given cruises between latitudes 25°30'N to 27°30'N and longitudes 82°30'W to 84°00'W. Another area having relatively high zooplankton standing crops was located in the northeast Gulf between latitudes 28°00'N to 29°00'N and longitudes 84°00'W to 85°00'W. Previous research on Gulf of Mexico plankton biomass also had indicated that these areas were relatively productive. Upwelling has been suggested as a possible cause of the relatively high productivity in these areas (Bogdanov, et al. 1968).

f. Correlations Among Biological Variables: Correlations among the biological variables using $\log_{10}$- transformed concentrations and abundances usually were positive, and many of these were significant. Zooplankton volumes and larval fish concentrations were positively correlated for all 12 cruises, 9 of these being significant ($P<0.05$). Zooplankton volumes and fish egg concentrations were positively correlated on 8 cruises, 7 of these being significant.

It seems probable that there are factors in the eastern Gulf that tend to concentrate zooplankton, fish eggs, and larvae in the same areas; although significant correlations do not imply cause and effect relationships it is possible that larval fishes were most concentrated in areas of dense zooplankton because feeding conditions and survival were best in those areas.

g. Effects of Temperature and Salinity: Correlations between each of the biological variables and the mean value of either temperature or salinity from surface, 10 m, and 20 m depths were examined for each cruise. No obvious relationships were found, except that the onshore-offshore distribution of organisms previously observed in relation to the 50 m isobath was apparent in correlations with temperature and salinity. Because abundance or concentration of organisms, except for larval abundance, was greatest near shore at all seasons, correlations with temperature tended to vary seasonally. High and positive correlations of larval abundance with temperature were observed for fall and winter cruises, which reflected the relative abundance of larvae at offshore stations during fall and winter when larval production was reduced in cooler, nearshore areas.

When contour charts of temperature and salinity were compared with those for zooplankton, fish eggs, and larvae, there were no obvious associations among unusual temperature and salinity conditions and the distribution of organisms. Such associations might be largely species dependent; because this analysis examined only the categories zooplankton, fish eggs, and fish larvae, strong associations between the organisms and temperature-salinity conditions could not be distinguished. The patchy nature of egg and larvae distributions also made it difficult to show relationships with either temperature or salinity. Even in summer 1973, when a lens of low salinity water from Mississippi floods was located over the shelf study area, its effects on production were not obvious. Zooplankton volumes, fish eggs, and larval abundance were all observed at reduced levels during the June-July 1973 cruise (Figure IIG-2), but had recovered by August 1973, although salinities remained low in the area. Because this low salinity water was present only from the surface to 15 m depth, it is possible that many planktonic organisms below were not seriously affected by it.

2. Red Tides of the West Florida Shelf

George A. Maul

Periodically, a plankton bloom of Gymnodinium breve occurs off the west coast of Florida. When massive amounts ($\gg 10^3$ cells liter^{-1}) of this dinoflagellate occur, the water takes on a characteristically reddish-brown color. The plant community seems to drift onto the beaches near the southern limit of the MAFLA area with the flood tide, and hence the colloquialism "red tide". It appears that red tides are natural events, since they have been recorded for more than 100 years in this area.

G. breve is known to exist in these waters in low concentrations at all times. For reasons not clearly understood, a plankton bloom is initiated in a zone parallel to the coast, 16-64 km offshore (12-37 m depth). Usually this occurs in early autumn, but cases have been documented in other seasons. As G. breve are drifted towards shore, massive fish kills occur due to the toxicity of the organism. In estuarine waters, the shellfish become contaminated and have been known to cause neurotoxicity in humans; airborne toxins are known to cause eye and upper respiratory irritation. Further, the masses of dead fish are a major public health nuisance and economic hardship to the tourist industry ($20,000,000 in lost revenues during the 1971 outbreak).

Research into the life and growth cycle of G. breve is still incomplete. It is possible that the sexual stage is a bottom resting benthic cyst. If G. breve does have such cysts, there is the distinct possibility that seed populations exist within this offshore initiation zone. Then the conditions that cause changes in the nutrients, vitamins, bacteria, insolation, temperature, salinity, and circulation of this zone are a primary consideration as to whether or not a bloom may occur. In artificial cultures, G. breve have been shown to grow when the water was enriched with phosphate, ammonium, disodium EDTA, and vitamin B_1, B_3, and B_{12}. In addition, growth was further enhanced when chelated iron was added to the medium. The iron may be added to the ocean during periods of heavy summer rains as river run-off, or through submarine springs which seem to lie along the same 16-64 km offshore "initiation zone."

Water circulation and mixing appear to play a vital role in the process leading to the initiation and subsequent effects of a bloom of G breve. Horizontal transport into a region can provide the required environment to cause or sustain a bloom. Similarly, vertical mixing processes alter an environment locally, particularly with respect to the distribution of water parcels within the euphotic zone. For example, detatched eddies from the Gulf Loop Current, which are known to exist on the shelf in the shallow waters, (Maul, 1974) could not only transport in foreign materials, but also enhance the mixing of these materials throughout the water column. Murphy et al. (1975) report that an interaction of the Gulf Loop Current with the shelf waters is suspected to have transported G. breve from the west Florida shelf to the Florida east coast resulting in 1972 in that area's first documented red tide. This implies that other materials, naturally or artificially occurring in the water may also be so transported.

The red tide of Gymnodinium breve is an important economic, public health, and political issue affecting the MAFLA area. The influence of man's activities is not understood, but the conditions which trigger, and the environment which supports such an event may well be modified by changes in the sedimentation rate or type, by changes in the dissolved materials in sea water, and by changes in the natural circulation of the water(Joyce, 1975). Transport of materials due to man's activities that must be monitored include the suspended sediments and the chemical by-products of drilling and spills. In addition the background nutrients, organisms, and water mass characteristics must be known in order to assess changes to the environment.

III. Pollutant Trajectories

George A. Maul
Robert L. Molinari

A particle trajectory is a line tangent to the instantaneous velocity vectors of a particle. The trajectory represents the time dependent integral of the response to forces acting on a particle. The frequency domain of these forces on the shelf at 26°N was discussed above (Figure IIE-9). Most of the energy is contained in the low frequency movements, but there are peaks at the inertial, diurnal, and semidiurnal frequencies. These higher frequency movements add little translatory motion to a particle since they are cyclical in nature. The lower frequency motions, (Loop Current meanders, eddy separation events, and the annual cycle of the flow in the eastern Gulf of Mexico) are primarily responsible for particle trajectories over distances in excess of 20 km. Motions discussed in earlier sections will here be reviewed for their implication for transport and dispersal of pollutants.

Table 4 summarizes the forces active on the eastern Gulf of Mexico continental shelf, the effect of that force on the shelf waters, the shelf area affected, the seasonality, the spatial and temporal scale of the induced motion, and the adequacy of the data base. Numerical and/or statistical predictions necessarily require a data base from which to initialize the model's fields and with which to test the results. Table 4 shows that in all cases the data base is inadequate, and indeed there may be classes of forcing not yet discovered due to the lack of proper measurements (i.e. secular trends). The inadequacy of the data-base is even more evident in attempting to predict water parcel trajectories from existing knowledge.

Certain aspects of the circulation as discussed in Section I and II, are well enough understood to present a zero-order synthesis. There is a well documented annual cycle of the Gulf Loop Current, although the variability about that cycle is large. The wind system over the Gulf of Mexico is reasonably well known to the extent that the persistence of the southeast trades and the time and space scale of frontal passages are known. It is known that the Loop Current interacts with the coastal waters, and that eddies of several scales detach from the flow and also interact with these inshore waters. Finally, although the gross effects of river run-off are not understood, the low salinity water can be used as a tracer to document the advection of water parcels.

Figure III-1 is represented here from Section I to discuss the annual variability of the Loop Current which might be expected in an analysis of particle trajectories, based only on interaction between the deep basin and shelf waters. Clearly for the data in this figure, the possible interaction of a particle in the MAFLA area with the Loop Current depends on the season. During the winter, when the Loop Current is far to the south, a parcel would have to take an entirely different route to leave the Gulf of Mexico than one in summer when the current is close to the northeastern shelf. Significant variability from year to year is also clear: The August 1972 pathline shows that the main current was at 24½°N, whereas in August 1973, the main current was at 28½°N. Similarly in 1972 an eddy had separated in May, whereas in 1973 the eddy had definitely separated by September, but could have been separated as early as July.

Table 4
Summary of Forcing Functions

Force	Affect on Shelf	Shelf Area Affected	Seasonality	Spatial Scale of Induced Motion	Temporal Scale of Induced Motion	Data Available
1) Loop Current						
a) Direct incursions of Loop Current	Advection of momentum and deep basin waters onto the shelf, flushing of shelf waters and possible entrainment by Loop Current.	west Florida	Occurences noted in summer and fall.	Shelf-wide?	?	Observations of events are available in deep-basin, few measurements on shelf.
b) Incursions of separated eddies and smaller scale features	Same as 1a but on smaller scale	MAFLA, west Florida	Large-scale eddies found on MAFLA Shelf in summer fall, and winter. Smaller scale eddies?	Large-eddies shelfwide Small-eddies 50-100 km	Months	Observations of eddies of all scales available on MAFLA, and west Florida shelf. Little data on frequency of occurrence, seasonality, motion of eddies on shelf, entrainment of shelf waters.
c) Large scale eddy separation	Entrains shelf water in vicinity of Florida meander. These waters probably not transported out of Gulf	west Florida	Summer, Fall	Shelf-wide?	Months	Observations available of shelf waters in ridge across deep basin. No data available on effects of MAFLA shelf, i.e., for mass conservation are these waters transported south?

Table 4 contd.
Summary of Forcing Functions

Force	Affect on Shelf	Shelf Area Affected	Seasonality	Spatial Scale of Induced Motion	Temporal Scale of Induced Motion	Data Available
2) Wind Forcing						
a) Trade Winds	Convergences and divergences in the trades induce downwelling, upwelling in the surface layers.	?	latitudinal variations in the trades are greatest in the summer	?	?	Wind data exist to identify where surface layer effects should occur. No direct ocean data available
b) Frontal passages	Fronts can produce downwelling, upwelling, excite shelf waves and inertial motions, and deepen the mixed layer	MAFLA, west Florida	winter-cold fronts summer-warm fronts	shelf-wide	week	Statistics of frontal passages exist. Direct measurements of the effect of cold front passage at 26 N have been collected
3) Tides and inertial motions	Internal tides and inertial motions can produce horizontal motions of shelf waters	MAFLA, west Florida	Internal tide generation-summer Inertial motions-winter	several kilometers	day	Surface tide data available around Gulf. Direct measurement of phenomena at 26°N.
4) River run-off	Fresh water inflow produces horizontal pressure gradients which establish local motions	MAFLA, west Florida	Maximum discharge-spring Minimum discharge-late summer	?	?	River discharge data available. Few measurements of run-off effects.

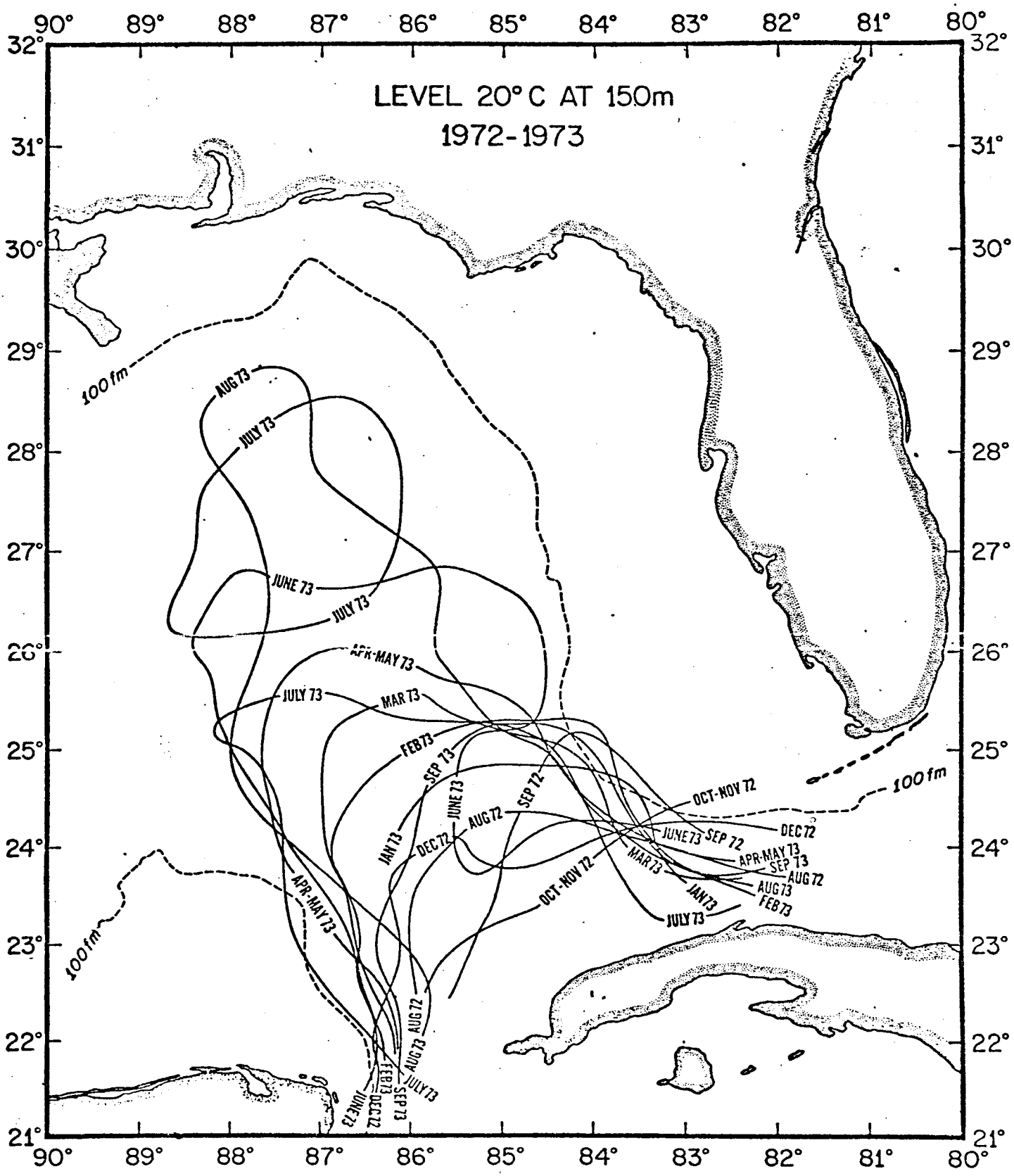

Figure III-1. The 150 m contour of the 20°C surface taken from the complete 20°C topographies given in Appendix IV. The data were collected in 1972-1973 during the months indicated on the figure.

Although trajectories cannot be determined for a particular location during a particular interval, some general scenarios can be established for the paths of water parcels on the MAFLA shelf from Cape San Blas to the Mississippi Delta. The scenarios are based on data collected in this region, and illustrate the problems associated with predicting pollutant trajectories. In addition, the possible effects of wind forcing in determining parcel trajectories are presented.

Assuming that drift bottles approximate the drift characteristics of surface water parcels, the data of Gaul (1964, 1965, 1966) and others can be used to establish the scenarios.

Gaul's drift bottles were launched from an area southwest of Panama City. The figures of Appendix VI show drift bottle returns from the launch sites noted. The returns are divided into four zones:

Zone 1 - east coast of Florida,
Zone 2 - west coast of Florida,
Zone 3 - MAFLA coast, west to 90°W
Zone 4 - Texas and Mexico coast.

Recovery summaries for zones 1, 3, and 4 are given on Figure III-2, and below.

Month	Areas of Maximum Returns
December to March	Zone 1 (all years)
April	Zone 3 (all years)
	Zone 1 (1963, 1964)
May and June	Zone 1 (1963, 1964)
	Zone 3 (1965)
August	Zone 3 (all years)
September and October	Zone 4 (all years)

The data show that during the winter, when the climatological winds are from the north, surface water parcels can be advected south to be entrained into the Loop Current, even though the current is at its southernmost position. Drift bottle studies by Chew, Drennan, and Demoran (1962), and Tolbert and Salsman (1964), provide further evidence for the importance of wind drift currents in the winter. Their releases were closer to the shore than Gaul's. The majority of recoveries on the east Florida Coast were also from winter launches.

The summer recoveries can also be interpreted in terms of the climatological wind field. Although the climatological Loop Current is at its northernmost penetration, there are few summer recoveries in zone 1, but rather most recoveries are in zones 3 and 4. Northern trajectories are also implied in the drift bottle results presented in Figures IID-12 and IID-13. The trade winds have penetrated farther to the north, and thus the MAFLA recoveries could be interpretated as the result of surface wind drift. An alternative hypothesis is that some shelf water parcels become entrained onto a detached eddy. The September to October recoveries of drifters on the Mexican coast could be explained by such an occurrence.

Figure III-2 also shows a high degree of variability in the arrival of these surface drifters. The large number of drifters found

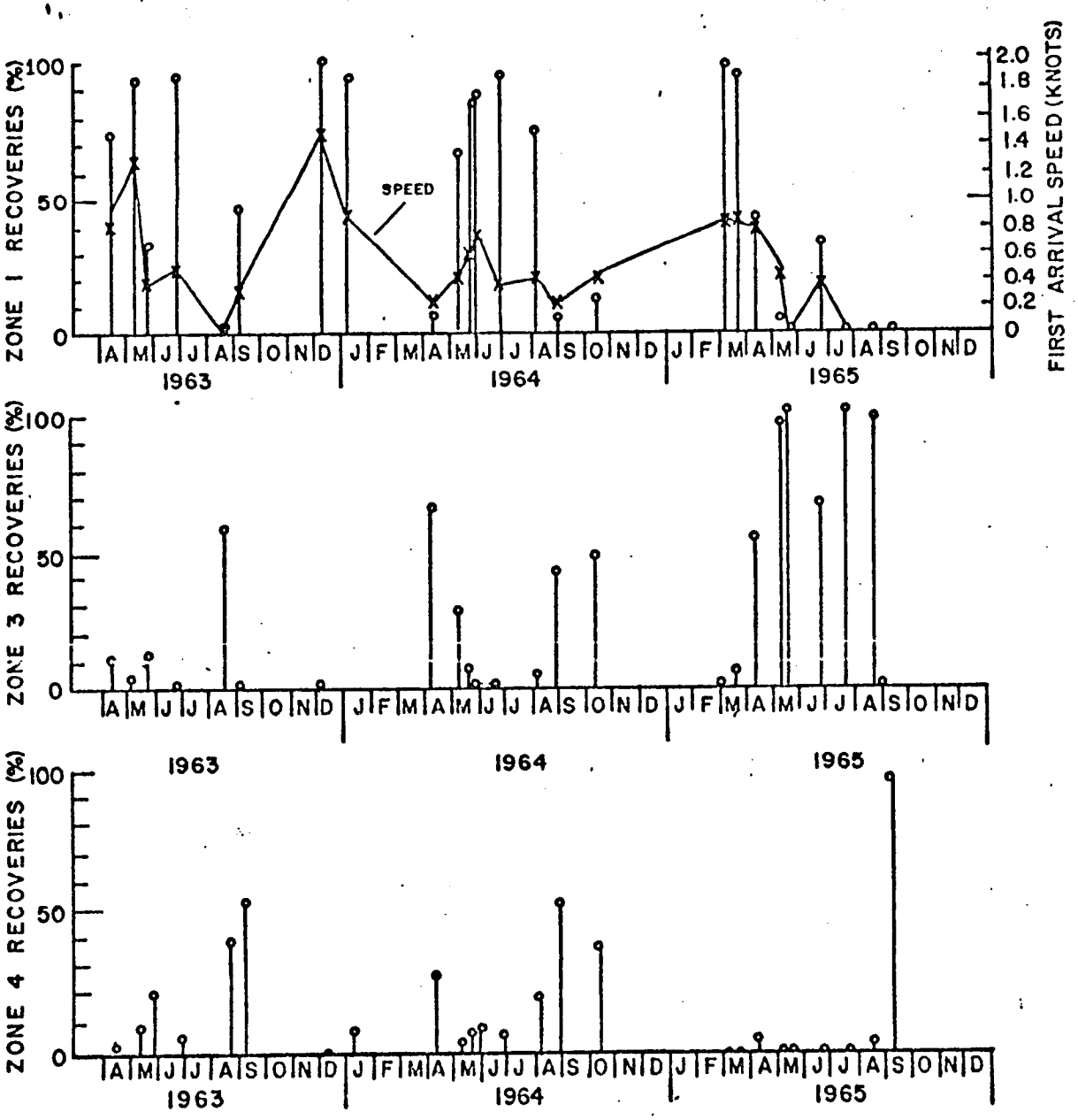

Figure III-2. Drift bottle recovery statistics from releases at 29°22'N, and 86°38.7'W. Zone 1 is the east coast of Florida, zone 3 the MAFLA coast, and zone 4 the Texas-Mexico coasts. First recovery speeds were computed using a hypothetical trajectory.

in zone 1 in the summer of 1964 is not seen in the summers of 1963 or 1965. This same degree of variability is seen in the location of pathlines and times of eddy separation discussed above in Figure III-1. Thus, if the prediction of the location of the Loop Current based only on a climatological analysis (such as given in Appendix V) were used to develop a water parcel trajectory, large errors could result.

The question remains then, what is the spatial and temporal variation of the circulation? Conventional oceanographic observations can never provide resolution to describe all the nuisances of water motion, if indeed that is even a desirable goal. A hint at the high spatial variability can be extracted from the very high resolution scanning radiometer aboard the NOAA-3 spacecraft. Figure III-3 is an infrared image of the northern Gulf of Mexico made on 2 March 1975 at a spatial resolution of about 1 km. The figure illustrates the complication of trajectory computation by spatial variability.

The infrared signal at the spacecraft is the net radiance from the earth and the atmosphere, and therefore, the cold clouds (which block surface radiation) appear white. The major clouds are identified on the overlay, as are the land and water masses. The warm Gulf Loop Current and a major detached eddy appear dark; the coastal waters are in intermediate shades of gray. The cold plume of the Mississippi River can be seen as a spreading white feature in the delta region. Between Cape San Blas and the Mississippi Delta, a mass of warm (dark) water can be seen to have penetrated the cool (gray) coastal water almost to the coast at Pensocola. An interpretation of the circulation associated with this complex pattern is given in the overlay. The basic assumption in this interpretation is that the surface thermal patterns reflect the deeper thermal structure; in turn, the deep thermal structure is assumed to reflect the density field. Hansen and Maul (1970) showed that this was true for the Gulf Stream, and it will be assumed applicable on the shelf. It must be emphasized that this assumption has not been tested in shallow water, and that while the analysis may err in detail, the complexity of the thermal patterns suggests a spatial complexity in currents as well.

The main coastal intrusion near Pensocola is in the vicinity of the DeSoto Canyon, an area well known for upwelling, (Gaul 1967). This intrusion may have an anticyclonic rotation, and may be deep Gulf water in origin. The basic flow pattern is interpreted to be easterly along the coast, but with counter flows and eddies superimposed. Given this circulation pattern, a particle trajectory would be very sensitive to the starting point and to the steadiness of the current pattern.

To particularize this discussion, consider a particle at the sea surface in the region east of the mouth of the Mississippi River at the time of Figure III-3. Two entirely different paths are possible for a few kilometers difference in initial location. If the flow pattern remains stationary, the particle could flow offshore to the southwest, and possibly interact with the detached eddy and remain in the Gulf for many weeks. On the other hand, if the initial position were slightly farther to the east, the particle could flow around the DeSoto Canyon intrusion, perhaps influencing the productive fishery at its head. This particle could continue to flow southeasterly, and either influence the Florida coast east of Cape San Blas, or interact with the main flow of

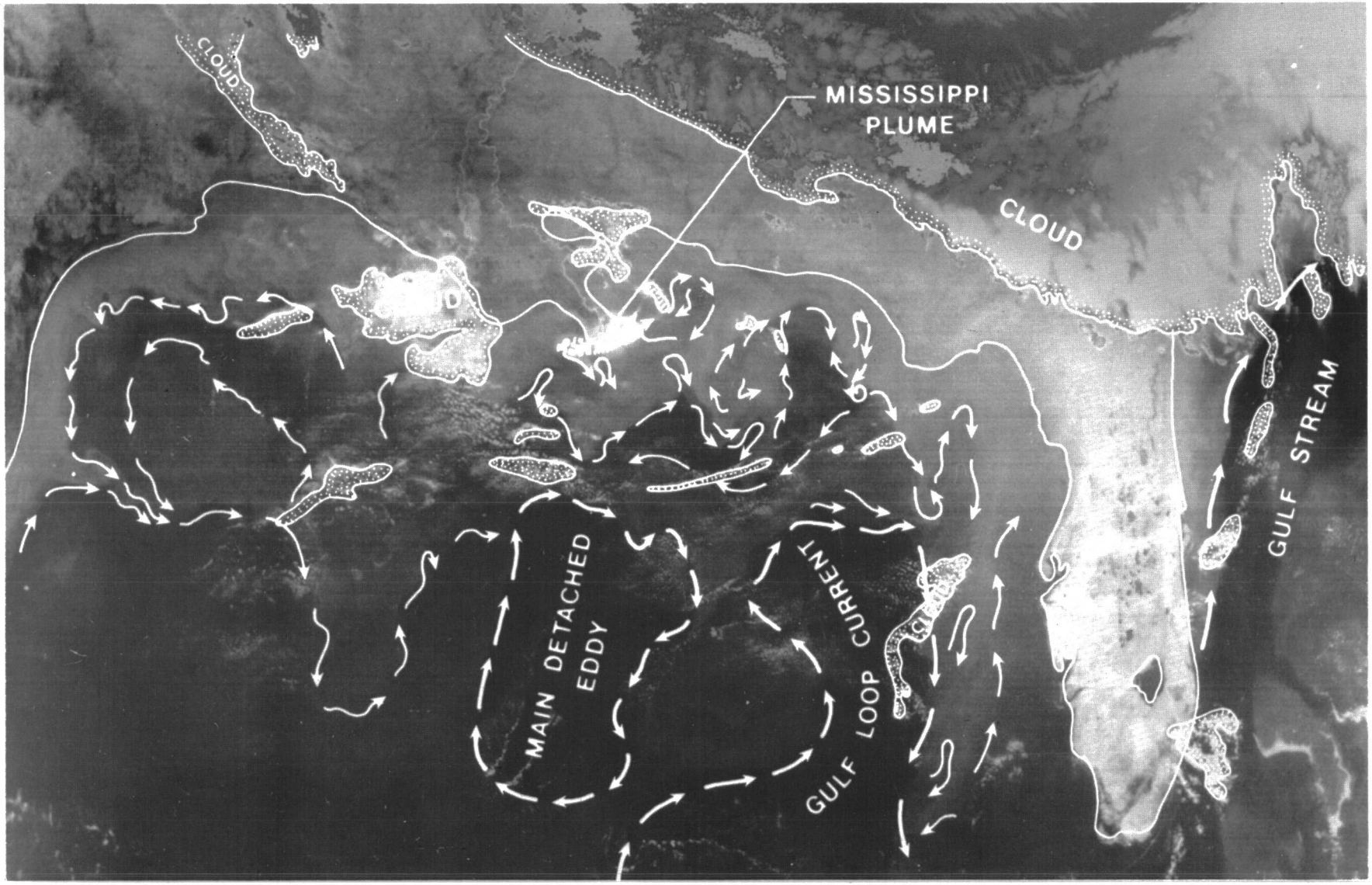

Figure III-3. High resolution infrared satellite image of northern Gulf of Mexico. Overlay is a schematic of one possible interpretation of the flow regime.

the Loop Current and leave the Gulf of Mexico through the Straits of Florida. As seen from Figure III-1, if the Loop Current were not this far north, the particle might not leave the Gulf at all.

Another satellite image taken 17 days later (not included) shows that this discussion would be completely different had that image been used as an illustration. For example, the flow around the DeSoto Canyon appears to have completely detached from the deep water, and the area of the Gulf Loop Current in Figure III-3 north of the word "Loop" appears to have also detached into a second eddy. This is further demonstration of the temporal and spatial variability. Present state-of-knowledge and analysis do not permit detailed definition of this spatial variability. The problem is amplified on the shelf where the variability is more intense.

Recent satellite techniques using the geosynchronous meterological satellite have led Maul and Baig (1975) to believe that composite pictures of the thermal patterns can be made every three to five days for 8 months of the year. These detailed images, coupled with properly placed measuring devices, could provide sufficient data to make short-range forecasts based on synoptic ocean "weather" observations. No single system is capable of measuring this complex circulation pattern; a substantial and coordinated effort is mandatory.

These results, the inadequacy of the existent data sets, and the discussions of the preceding sections argue for intensive monitoring and process-oriented studies to meet BLM's requirement of assessing the environmental impact of developing the outer continental shelf. The recommended sampling grid, to follow, attempts to specify a rational approach to the physical oceanographic portion of the MAFLA program.

IV. Recommended Sampling Grid

Physical oceanographic studies should lay a solid observational base for formulating and testing models, biological, chemical, and geological as well as physical, for hindcasting and forecasting, and for diagnostic purposes in evaluating an environmental calamity. The most efficient sampling grid for meeting these objectives can be devised through a program of data analysis and numerical modeling. First, the temporal and spatial persistence of the important scales of motion would be determined as a function of position in the basin. Then, statistical and/or dynamical modeling tests using these data as input would be used to derive an efficient sampling grid. Finally, real-time data received from the grid would up-date the model fields so as to provide initial conditions for any required diagnostic or forecasting attempts.

As described in previous sections, the data-set in the Gulf of Mexico is adequate neither in the deep basin nor on the shelf for rigorously defining the circulation cycle. Furthermore, the data-set that does exist has not been analyzed to meet regional needs but rather has been analyzed to consider only limited areas and their circulation. Therefore, additional data analysis is necessary, as will be recommended, concurrently, with the initiation of a sampling program. This sampling program should satisfy two needs:

a) provide a monitoring capability, and

b) obtain the data necessary to develop a predictive capability.

To meet these objectives, the physical sampling program for the MAFLA region logically breaks down into two categories: (i) a general circulation study, and (ii) process—oriented studies. The general circulation study is designed initially to monitor and eventually to define the spatial structure of the time-varying flow and hydrography on time scales of several days to seasonal over the course of several years. In a sense, this study is the physical analogue to chemical, geological, and biological baseline studies because it concerns itself with the advection field on a regional spatial scale.

In contrast, the process-oriented studies on the shelf are concerned with time and space scales which are generally associated with turbulent dispersion, and in the deep basin with scales which can force shelf motions, i.e., those processes which need to be parameterized for inclusion in numerical models. Of particular importance are those processes involved with extreme events such as hurricane passages, large freshwater intrusions, cold front passages, etc.

A. General Circulation Study

The general circulation monitoring study is presented in terms of "nested" control volumes. Each volume interacts with an enclosed or enclosing volume through lateral boundaries. Such a nested grid has proved to be a useful concept in numerical modeling efforts, wherein boundary conditions for a finer resolution grid are determined through interpolation of coarser grid results.

The smallest grid to be considered is that to be monitored in the immediate vicinity of the drilling rigs. Here the physical oceano-

graphic measurements play primarily a supportive role to the observational programs of other disciplines. In determining the station and current meter locations for the bio-geo-chemical studies, the following results, previously discussed, should be considered:

a) the flow tends to be along isobaths;

b) most state-of-the-art moorings are ineffective near the surface because of mooring motions, therefore, a current meter placed directly on a rig is necessary to obtain surface current measurements;

c) the surface flow is a combination of wind-induced and other motions, therefore, meteorological observations should be obtained from instrumented rigs;

d) state-of-the-art moorings are available for near-bottom monitoring, therefore a meter should be placed a maximum of 3 m from the bottom boundary;

e) the flow field will be reasonably coherent over transhelf horizontal scales of the order of 25 km, which should dictate the transhelf horizontal spacing of moorings;

f) the flow field will be reasonably coherent over longshelf horizontal scales of the order of 100 km, which should dictate the longshelf horizontal spacing of moorings.

The continental shelf from the Mississippi Delta to the Florida Keys comprises the next control volume. If such a large volume is impractical for initial program goals, the shelf can be divided into smaller volumes using geological boundaries for terminal points. For instance three possible control volumes are:

a) Mississippi Delta to Cape San Blas,

b) Cape San Blas to Tampa Bay,

c) Tampa Bay to Florida Keys. The danger in not considering the shelf as a whole is that little is known of the interaction between these regions, and feedback from one area to the next could be important in establishing the circulation.

The observational program of the general circulation of the MAFLA-west Florida Shelf should have six major components: meteorology, hydrography, horizontal currents, sea level, bottom pressure, and river run-off. With these components, the primary kinematic, thermodynamic, and dynamic properties and forces can be determined. Each component will be discussed below. It is estimated that one-to-two years would be required to activate such a monitoring array in its entirety. On 3-to-6 months notice, it could commence in a significant way.

The meteorological component should consist of approximately ten NWS coastal meteorological stations; two NDBO meteorological buoys (Figure IVA-1), and auxiliary meteorological data from surface synoptic charts, NCC (Asheville, N. C.) archives, and the FNWC (Monterey, Calif.) data banks via NMFS/Monterey. The utility of the NDBO buoys is discussed in Appendix X. These data sets are generally available on an hourly to six-hourly basis and should be adequate for determining the primary meteorological influences on the shelf circulation.

The hydrographic component should consist of the monthly occupancy of about ten standard stations on each of about five grid lines across the shelf and slope regions (Figure IVA-1). Standard CTD/STD casts

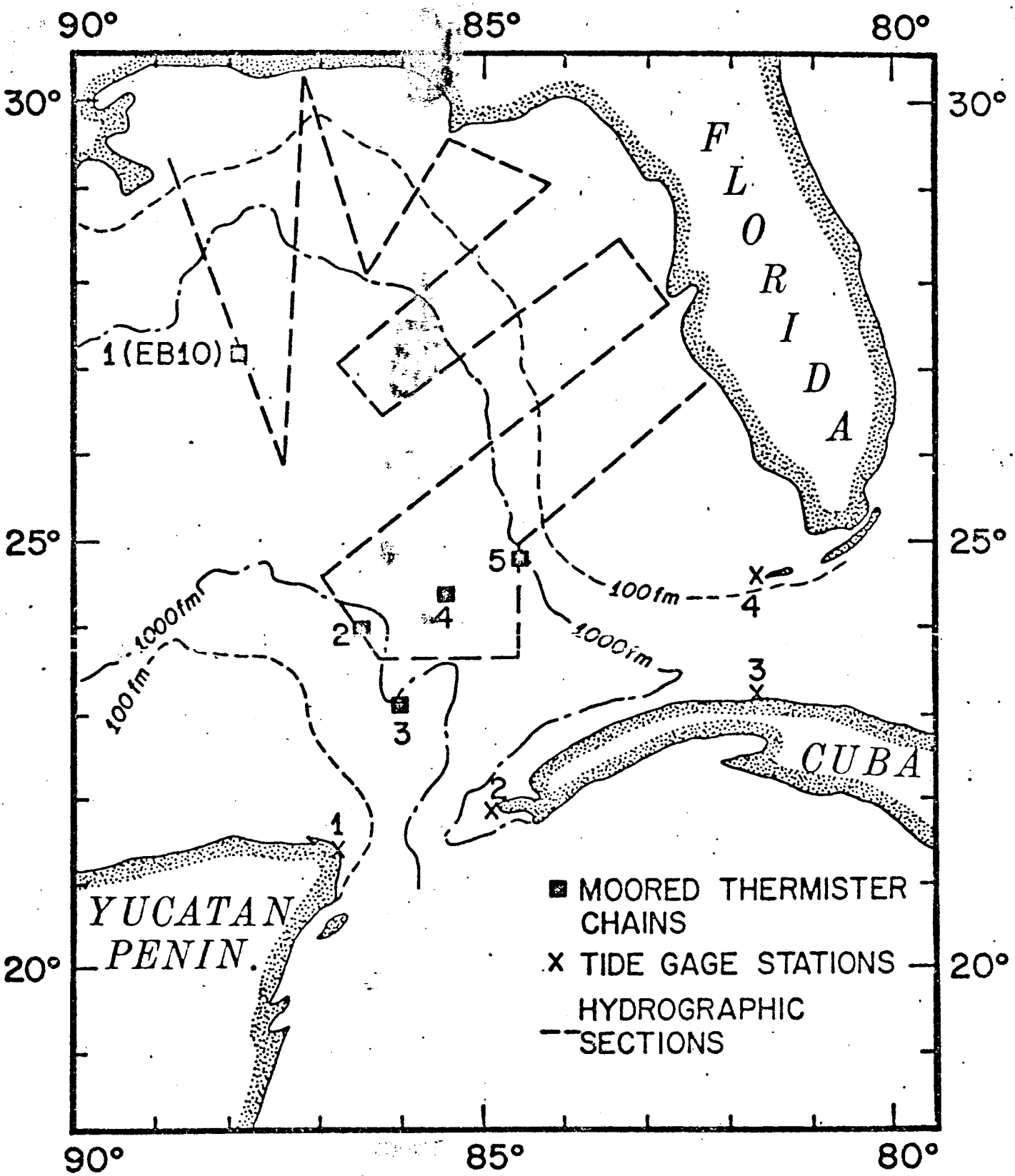

Figure IV A-1. Recommended hydrological sections, and moored buoy (instrumented with thermister chanins) positons. Moored buoy EB-10 is also on NDBO meteorological buoy.

plus occasional water bottle samples for dissolved oxygen and nutrients should be adequate. From this effort, the major features of the seasonal evolution of the hydrographic fields can be determined.

The horizontal current component should consist of an array of six moorings on each of four transhelf lines plus selected additional stations along the shelf break (Figure IVA-2). The details of a typical transhelf array (see Figure IVA-3) are based on recently acquired knowledge of circulation and exchange processes, and of correlation scales. The array is designed with the following criteria in mind:

a) points a, b, d, e, and f of the rig-monitoring discussion are directly applicable;

b) the velocity structure is baroclinic, especially on the outer shelf, thus, vertical resolution is required through the water column, but decreasing with depth; for data analysis convenience and effectivness, current meters are located on common levels;

c) because there exists neither persistent nor coherent energy at high frequencies, a sampling rate of once per 20 to 30 minutes is adequate; with these sampling rates, record durations of six months are feasible with standard current meters;

d) similar thinking dictates the locus of the hydrographic lines;

e) emphasis has been placed on the outer shelf and the shelf break, because in these regions deep-basin exchanges take place, and boundary conditions for numerical models must be specified;

f) additional stations along the shelf break are intended to monitor the propagation of eddy-wave events from the disturbance area south of 26°N.

A total of 80 current meters should be in operation at all times, with 40 current meters in reserve for replenishment of the array. Since the moorings and current meters can be maintained in place for six months at a time, half of the current meters should be replaced at quarterly intervals. An additional 10 current meters would be kept in reserve for replacement of losses. From this component, the general features of the subtidal frequency circulation would be determined throughout the water column.

The sea level component should consist of six standard NOS stations. The primary task of this component would be to analyze the sea level data for non-barometric effects in order to estimate longshore and cross-shelf surface pressure gradients.

The bottom pressure component should consist of five installations on the outer shelf. They should be maintained in place for periods of six months at a time, being replaced in the same fashion as the current meters. From this component, cross-shelf and longshelf pressure gradients, as well as tidal and other pressure disturbances, would be determined.

The river run-off component should consist of analysis of the run-off data available through federal and state agencies. This component would provide the information on seasonal and storm generated freshwater discharges onto the shelf.

It should be stressed that for numerical modeling irrespective of the size of the array, the control volume concept should be employed. That is, the monitoring array should enclose the area to be studied. The data from such an array can then serve as boundary conditions for a numerical model.

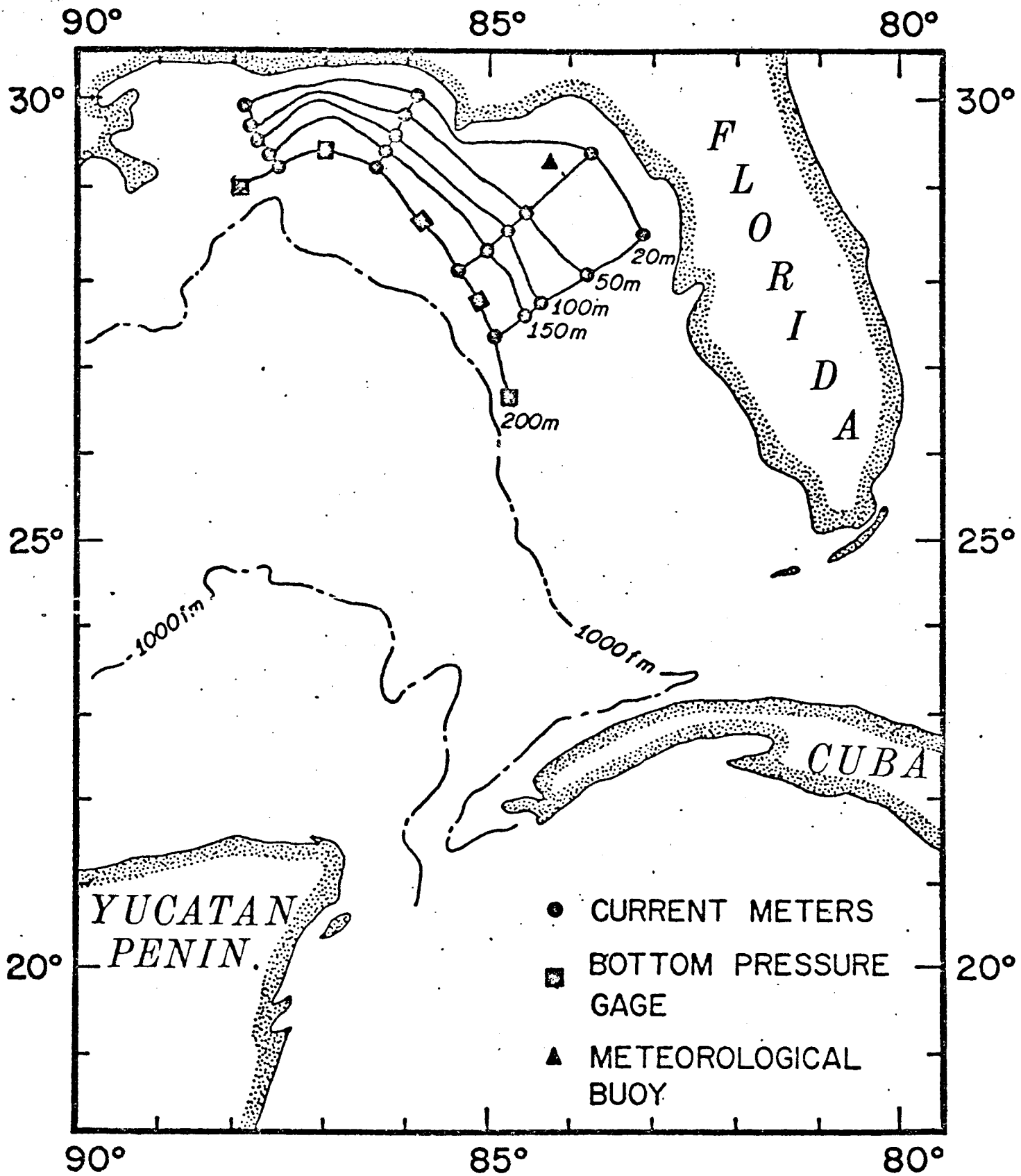

Figure IV A-2. Recommended current meter mooring, and bottom tide gauge positions, and a proposed meteorological buoy location.

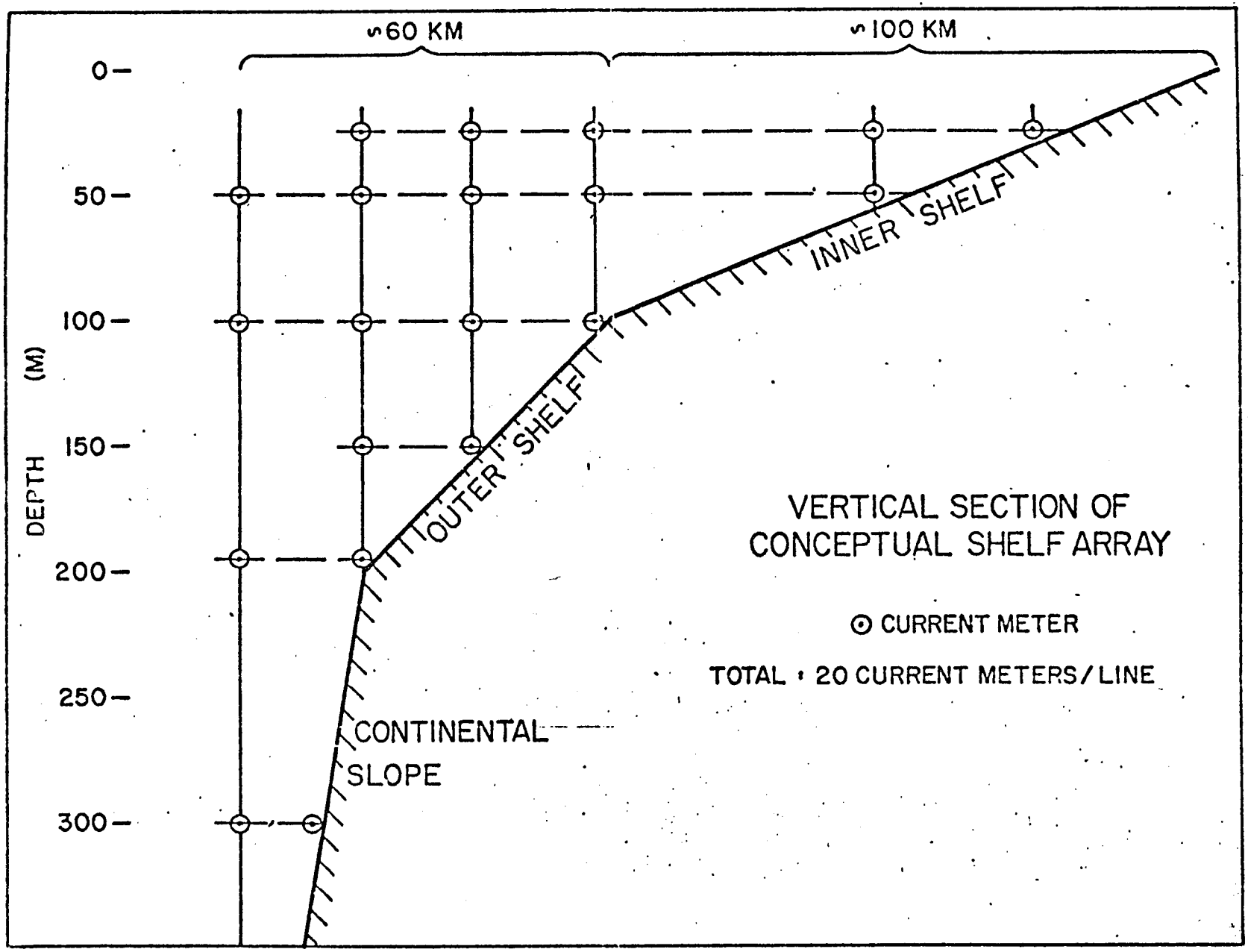

Figure IV A-3. Recommended vertical deployment of current meters.

The general circulation study of the final control volume, the deep basin, is based primarily on continuous monitoring of those parameters required to describe the spatial and temporal variability of the surface flow. Extension of the shelf hydrographic sections into the deep basin, and certain process oriented studies will provide information pertinent to the deeper flow.

The monitoring tools to be used for this portion of the program are satellite imagery, satellite altimeters, moored buoys, and tide stations. The satellite IR imagery process is operational. To determine the feasibility of using the other methods requires one year of research and development.

a) Satellite Imagery. Figure IVA-4 is an enhanced IR image of the eastern Gulf of Mexico. The image clearly outlines the edge of the Loop Current, as well as defining meanders and possible eddies along the edge of the flow. It has been shown that this boundary approximates the depth of the 22°C at 100 m, a good indicator of the Loop Current axis (Maul,1974).

This image was obtained from the NOAA-3 satellite. The satellite should provide, on the average, one good IR image of the Gulf every five days from October to May. The lack of surface temperature gradients precludes the use of IR images in the summer. The visible channel on the NOAA satellites and several NASA vehicles provide useful data in summer. Acquisition and enhancement of these data are recommended so that a year-round monitoring capability is established.

It is necessary to enhance the image received from the satellite to obtain the clarity of the photograph shown in Figure IVA-4. This enhancement was done by the National Environmental Satellite Service. It is recommended that a program be established with NESS, so that investigators concerned with the position of the Loop Current can receive the latest image enhanced for ocean radiances.

b) Satellite Film Loops. A film Loop technique which uses images in the IR band from the SMS-GOES satellite to monitor current edges has been developed (Maul & Baig, 1975). This method provides a means of reducing the effect of clouds when images of the sea-surface are required. The film-loop technique has been successfully applied to obtain images of the north edge of the Gulf Stream.

An attempt is underway to apply this method to images obtained from the Gulf of Mexico. If the results are positive,it is recommended that this tool be included in any monitoring effort.

c) Satellite Altimeter. An experimental altimeter is being placed aboard the GEOS-C satellite to obtain sea-surface topographies. It has been recently shown that the altimeter return pulse strength is sensitive to sea state, and sea state has also been shown to be a useful indicator of the Gulf Loop Current. In addition, the microwave sensors of other spacecraft will return useful sea surface information on the Gulf. It is planned to evaluate the effectiveness of the microwave sensors in defining the Loop Current sea surface topography and sea state during a series of cruises to the region. If the test results are positive, the year-round monitoring of the Loop Current position could be significantly augmented.

Figure IV A-4. An enhanced IR image of the eastern Gulf of Mexico obtained from the NOAA-3 satellite.

d) Moored Buoys. The NOAA Data Buoy Office (NDBO) plans to moor a meteorological buoy at site EB-10 (Figure IVA-1). A request to NDBO should be made to instrument the buoy with a thermister chain. Information from the buoy, when correlated with the satellite imagery, should define the northern penetration of the Loop.

The configuration of the Loop, eddy or non-eddy mode, determines the trajectories of parcels entrained on the north and northeastern continental shelves. The monitoring of the eddy breakoff zone should indicate when an eddy break-off event will occur. It is recommended that NDBO be queried about the feasibility of mooring four buoys in this area. The minimum instrumentation of these buoys would be a thermister chain.

e) Tide Gauges. Many investigators have hypothesized that the circulation in the Gulf of Mexico is forced by the flow through the Yucatan Strait. Tide gauge data across the channel provide an inexpensive means of monitoring one component of this input. These data may also be useful in specifying the boundary conditions for a planned numerical model of the Gulf.

Figure IVA-1 also gives the positions of the CICAR tide stations. CICAR is the acronym for the group of countries who have been, and will continue studying cooperatively the oceanography of the Caribbean Sea and Gulf of Mexico. A recommendation will be made at the next CICAR meeting to take the sea level data from tide stations on opposite sides of the Yucatan Strait (stations 1 and 2, Figure IVA-1). In addition, it will be recommended that a tide gauge be deployed at position 3 to monitor the outflow from the Gulf.

f) Hydrographic Sections. The hydrographic sections given in Figure IVA-1 extend into the deep basin. The CTS/STD casts should be taken as close to the bottom as possible to fully define the offshore conditions.

B. Process Oriented Studies

1. Shelf Circulation

As examples of process oriented studies, we cite (i) surface and bottom mixed layer dynamics during strong meteorological events, (ii) surface gravity wave dynamics during strong meteorological events, (iii) air-sea, heat and moisture transfers during cold air outbreaks, (iv) dispersal of surface and subsurface materials and (v) bottom sediment transport dynamics. Many of these studies can be conducted from or in the vicinity of oil drilling rigs.

The aforementioned process studies are of a general nature and could therefore be conducted in almost any shelf region. There are other process studies which are relatively unique to the MAFLA shelf: (i) The circulation in the massive De S oto Canyon deserves special attention. It can be expected to be a major "conduit" for upwelled deep Gulf water (Gaul, 1967). (ii) The influence of Cape San Blas on the shelf circulation, presently unknown, may be profound. For example, it may serve to support either a setup or setdown of sea level, providing longshore and offshore pressure gradients to be balanced by longshore coastal flows. Thus, local studies in the vicinity of Cape San Blas are called for. (iii) The intense winter storms (cyclones and cold fronts) may lead to significant cooling and downward convection of shelf waters, ultimately cascading into the Gulf (Nowlin and Parker, 1974). Conversely, the Loop Current penetrates far enough into the Gulf to allow some of its waters to penetrate into the MAFLA area. Hence, studies of water mass exchange across the shelf break are required. (iv) The occasional penetration of the Mississippi River plume into the MAFLA area may lead to significant entrainment of ambient shelf waters, as discussed. In turn, the plume may be subsequently entrained into the Loop Current. Thus, detailed studies of the plume's interaction with shelf, deep Gulf, and Loop Current waters would be of some importance. From these studies, the mechanisms of dispersal would be considerably illuminated, and dispersal models could be formulated and tested.

2. Deep Basin Circulation

The Loop Current sampling grid is designed to define and/or sample those Loop Current features which are known or have been hypothesized to have, a direct bearing on the shelf circulation and the transport of shelf waters. These features include but are not limited to:

a) direct incursions of the Loop Current on the shelf,

b) large scale perturbations of the Loop Current, such as eddy detachments,

c) smaller scale perturbations (order of a 100 km) frequently found on the northern edge of the Loop, and

d) meanders of the Loop Current which may be responsible for initiating shelf motions.

These features are inherently important because of their flushing action on the shelf waters. But they also have an intrinsic importance to sampling programs of other disciplines, in the sense that deep basin waters can transport chemical and biological species onto the shelf that

are not normally located there. No coherent spatial or temporal baseline distributions could be developed without the minimal knowledge of the type of water mass present.

The continuous monitoring program will provide an early warning system for the occurrence of such events. This warning will give scientists the opportunity to marshall their efforts in an efficient manner.

It is important to stress the interrelations between the shelf and deep basin, and the monitoring and process studies, and the need for coordination among investigators. Only through such coordination will efficient observational programs be implemented and full utilization of the resulting data-sets be realized. As an example, the separation of an eddy from the main flow would appear at first glance to be strictly a deep-basin process study. However, such an event is characterized by the entrainment of shelf water into the Gulf basin. The effect of this entrainment on the dispersion of MAFLA shelf waters is not known, but somewhere on the shelf this water must be replaced, possibly by deep basin water. Thus to define the process will require close coordination of shelf and deep-basin studies.

C. Parameter Range Resolution and Accuracy

The following table specifies parameter ranges and resolution/accuracies which should be attained in all deep-basin/shelf studies.

Parameter	Range (extreme)	Resolution/Accuracy
Temperature	5°to 32°C	0.02°C
Salinity	20 to 40°/oo	0.02°/oo
Current Speed	2 to 200 cm/sec	2 cm/sec
Current direction	0°to 360°	5°
Bottom pressure	1 to 50 bars	1 millibar

In terms of spatial and temporal scales to be resolved on the shelf, the following table is presented.

Dimension	Span	Resolution
Time	1 year	30 minutes
Depth	20 to 500 meters	1/3 depth
Onshore-Offshore	200 km	25 km
Longshore	600 km	100 km

D. Miscellaneous Sampling Recommendations

1) Provide for precision navigation capability (HIFIX, Raydist, etc.) during the conduct of all shelf cruises.

2) Deploy surface and bottom drifters from all hydrographic stations.

3) Attempt to involve the Coast Guard in MAFLA sampling through aircraft and ship support.

4) Attempt to involve NDBO in oceanographic/meteorological buoy support in the MAFLA region.

5) Attempt to incorporate shipofopportunity XBT reports in all monitoring efforts.

E. Other Recommendations

These recommendations are proposed on the basis of lessons learned during the course of this study, and to enumerate certain key steps required to insure a rational observational program and full utilization of the data-set already collected in the MAFLA area.

1) The following timetable is recommended to insure the most efficient use of time.

If a considerable amount of data is to be reduced and submitted to NODC, it is recommended that NODC begin work on those products not dependent on the new data submittals. Although the time required for this phase is a function of the outstanding data, six months should provide enough time for analysis and submittal.

During the second phase, NODC would produce the output requested by the individual investigators, while these scientists concentrate on their particular area of interest. Phase 2 should be a three-month study.

During the final phase, the NODC products would be reviewed and combined with the individual products to arrive at a summary of knowledge of the study area. The minimum time required for this phase is six months to insure complete synthesis of all the data available. A major problem with the present study was that insufficient time was available to review the NODC products. This was through no fault of NODC, who met all their deadlines, but rather was a flaw in the original timetable established by the other participating scientists.

2) It is recommended that formal lines of communication be established with other disciplines involved in the particular BLM regional study at the inception of the program.

One of the difficulties encountered in defining the supportive role physical oceanography must play in the area was the lack of knowledge of the requirements of other disciplines. Only at our last workshop were members of all the other groups present to discuss our mutual problems and goals. The experience was enlightening and gave us some clues to their physical oceanographic needs.

3) All sampling in the MAFLA area should be coordinated through a federally sponsored office, committee, or administrator to insure dissemination of all plans and coordination of data collection efforts whenever possible.

Many observational programs are planned for the Gulf of Mexico in the near future. In addition, many groups are presently collecting data in the region. These programs are under the auspices of various institutions and funding agencies, such as the Coast Guard, NOAA Data Buoy Office, and National Ocean Survey, and all will be obtaining valuable environmental data on the circulation and its causes. However, each group has its own mission, and there is little intergroup coordination at most organizational levels. The coordination that does exist, occurs by fortuitous scientist-to-scientist contacts.

To eliminate the haphazard nature of these serendipitous meetings, a central clearinghouse for Gulf research programs is recommended. Initially this center could be notified of impending studies and would disseminate the information to other interested parties. However, as the monitoring efforts become operational, it will become necessary to

identify a scientist or scientists who are willing to combine the diverse data sets to arrive at circulation patterns. Eventually a regional Fleet Numerical Weather Central type group should be established to prepare the data for input to operational numerical models.

4) It is recommended that BLM continue to support NODC maintenance, expansion, and update of MAFLA data files.

The establishment of the MAFLA data file, primarily through the efforts of NODC personnel, is one of the major benefits to evolve from this effort. To provide the data base for future BLM studies in the MAFLA area, it is essential that the MAFLA file continue with its present interactive capability. The file must be able to respond to new requirements for data analysis and presentations, as well as accept new data sets. Particular attention should be devoted to establishing and maintaining quality control procedures and to developing the capability to handle chemical data.

5) It is recommended that further climatological studies by NCC be sponsored.

The importance of meteorological forcing has been stressed throughout this document. Additional studies, such as determining the climatological properties of cyclones and anticyclones in the northeast Gulf of Mexico, are necessary to evaluate the effect of meteorological disturbances on the circulation.

6) It is recommended that the continuing analysis of the historical data set be sponsored with the eventual goal of developing and publishing a physical oceanographic climatology of the Gulf of Mexico.

7) It is recommended that numerical modeling efforts on the MAFLA shelf be sponsored.

References

Atkinson, L. P., and D. Wallace (1975). The source of unusually low surface salinities in the Gulf Stream off Georgia. Submitted to Deep-Sea Research.

Bogdanor, D. V., V. A. Sokolov, and N. S. Khromov (1968). Regions of high biological and commercial productivity in the Gulf of Mexico and Caribbean Sea. Oceanology 8: 371-381.

Brooks, H. K. (1973). Geological Oceanography. In: A Summary of Knowledge of the Eastern Gulf of Mexico 1973. Coordinated by the State University System of Florida Institute of Oceanography. IIE-1 to IIE-50.

Caruthers, J. W. (1972). Water masses at intermediate depths. In: Contribution on the Physical Oceanography of the Gulf of Mexico, Capurro and Reid Editors, Gulf Publishing Company, pp 53-64.

Chermock, R. L. (1974). An environmental study of offshore Alabama as related to drilling for gas and oil. Geological Survey of Alabama. 290 pgs.

Chew, F. (1974). The turning process in meandering currents: A case study. Jour. Phys. Ocn. 4 (1), pp 21-57.

Chew, F., K. L. Drennan, and W. J. Demoran, 1962). Some results of drift bottle studies off the Mississippi Delta. Limnology and Oceanography 1, pp 252-257.

Cochrane, J. D. (1972). Separation of an anticyclone and subsequent developments in the Loop Current (1969). In: Contributions on the Physical Oceanography of the Gulf of Mexico, Texas A & M University. Oceanographic Studies, Capurro and Reid, Editors, pp 91-106.

Drennan, K. L. (1963). Surface circulation in the northeastern Gulf of Mexico Gulf Coast Res. Lab. Ocn. Sec. Tech. Rept. 1. 110 pgs.

Florida Department of Natural Resources (1969). Memoirs of the Hourglass Cruises. Marine Research Laboratory St. Petersburg, Florida. Volumes 1 and 2.

Gainer, H. J. (1966). A theoretical investigation of the M2 constituent of the tide in the Gulf of Mexico. Masters Thesis, U.S. Naval Post-graduate School. 94pgs.

Gaul, R. D., and R. E. Boykin (1964). Northeast Gulf of Mexico hydrographic data collected in 1963. Texas A & M Univ. Dept. of Ocn. and Met. Ref. 64-26T, 81 pgs.

Gaul, R. D., and R. E. Boykin (1965). Northeast Gulf of Mexico hydrographic survey data collected in 1964. Texas A & M Univ. Dept. of Ocn. and Met., Ref. 65-8T.

Gaul, R. D., R. E. Boykin, and D. E. Letzring (1966). Northeast Gulf of Mexico hydrographic survey data collected in 1965. Texas A & M Univ. Dept. of Ocn. and Met., Ref. 66-8T. 202 pgs.

Gaul, R. D. (1967). Circulation over the continental margin of the northeastern Gulf of Mexico. Doctoral dissertation, Texas A & M Univ., 172 pgs.

Grijalva, N. O. (1964). Numerisch - Hydrodynamische untersuchungen im Golf von Mexico. Dissertation, Naturwissenschaftlichen Fakul tat der Universitat Hamburg.

Hansen, D. V. and G. A. Maul (1970). A note on the use of sea surface temperature for observing ocean currents. Remote Sensing of Environment, 2, pp 161-164.

Joyce, E. A., Jr., Editor, (1975). Proceedings of the Florida Red Tide Conference, 10-12 October 1974. Florida Dept. of Natural Resources, Marine Res. Lab., Pub. No. 8, 18 pgs.

Leipper, D. F. (1970). A sequence of current patterns in the Gulf of Mexico. Jour. Geo. Res., 75 (3), pp 637-657.

Linn, J. B. (1975). Seasonal sequence of positions of the Loop Current as determined by geostrophic levelling from average ships' drifts. In preparation.

Maul, G. A. (1974). An Evaluation of the Use of the Earth Resources Technology Satellite for Observing Ocean Current Boundaries in the Gulf Stream System, NOAA Technical Report (in press).

Maul, G. A. and S. R. Baig (1975). A new technique for observing mid-latitue ocean currents from space. Proceedings of the 1975 ASP/ACSM Convention, Washington, D.C. pp 713-716.

Michaelov, V. D., V. P. Melishko, and G. I. Shchereleva (1969). Estimation of the tides and tidal currents in the Gulf of Mexico and Caribbean Sea. Trans. G.O.I.N., 96, 146-173.

Mooers, C. N. K., and J. F. Price (1974). Tidal and inertial motions on the West Florida Shelf: winter 1973 abstract in: Trans. Am. Geo. Un., 55, 295.

Mooers, C. N. K., and J. C. Van Leer (1975). Motion induced by an atmospheric cold front on the edge of the West Florida Shelf on 9 February 1973. Submitted to Jour. Phys. Ocn.

Murphy, E. K. Steidinger, B. Roberts, J. Williams, and J. Jolley (1975). An Explanation of the Florida East Coast Gymnodinium breve Red Tide, November, 1972. Limn. and Oceano. (in press).

National Ocean Survey. 1973. Surface Water Temperature and Density. Atlantic Coast; North and South America. National Oceanic and Atmospheric Administration. 109pgs.

Nowlin, W. D., and H. J. McLellan (1967). A characterization of the Gulf of Mexico waters in winter. Jour. Mar. Res. 25 (1), 29-59.

Nowlin, W. D. (1972). Winter circulation patterns and property distributions. In: Contributions on the Physical Oceanography of the Gulf of Mexico, Capurro and Reid, Editors, Gulf Publishing Company, pp 3-51.

Parker, C. E. (1972). Some direct observations of currents in the Gulf Stream. Deep-Sea Research, 19, pp 879-893.

Pequegnat, W. E. (1972). A deep bottom current on the Mississippi Cone. In: Contributions on the Physical Oceanography of the Gulf of Mexico, Capurro and Reid, Editors, Gulf Publishing Company. pp 65-87.

Plaisted, R. O., K. M. Waters, and P. P. Niiler (1975). Current meter data report from the NSF continental shelf dynamics program 1973-1974. Nova University Scientific Data Report.

Price, J. F., and C. N. K. Mooers (1974a). Hydrographic data report from the winter 1973 experiment NSF Continental Shelf Dynamics Program. RSMAS University of Miami Scientific Report. UM-RSMAS-74006; 61 pgs.

Price, J. F. and C. N. K. Mooers (1974b). Current meter data report from the winter 1973 experiment, NSF Continental Shelf Dynamics. RSMAS University of Miami Scientific Report. UM-RSMAS-74020, 78 pgs.

Price, J. F. and C. N. K. Mooers (1974c). Current meter data report from the fall 1973 experiment, NSF Continental Shelf Dynamics Program. RSMAS Universtiy of Miami Scientific Report. UM-RSMAS-74035, 59 pgs.

Price, J. F. and C. N. K. Mooers (1975). Hydrographic data report from the fall 1973 experiment, NSF Continental Shelf Dynamics Program. RSMAS University of Miami Scientific Data Reprot. UM-RSMAS-75018, 52 pgs.

Rinkel, M. O. (1974). Western Florida Continental Shelf Program. In: Proceedings of Marine Environmental Implications of Offshore Drilling, Eastern Gulf of Mexico, 1974. Edited by Robert E. Smith, SUSIO

Robinson, M. K. (1973). Atlas of Monthly Mean Sea Surface and Sub-surface Temperature and Depth of the Top of the Thermocline Gulf of Mexico and Caribbean Sea. Scripps Institute of Oceanography. Ref. 73-8. 105 pgs.

Schroeder, W. W. and G. F. Crozier (1974). Hydrographic and Current Structure on the Western Continental Shelf of the Northeastern Gulf of Mexico. In: Proceedings of Marine Environmental Implications of Offshore Drilling in the Eastern Gulf of Mexico. The State University System of Florida Institute of Oceanography. 455 pgs.

Sverdrup, H. U., M. W. Johnson, and R. H. Fleming (1942). The Oceans, Their Physics, Chemistry, and General Biology. Prentice Hall, Inc. 1087 pgs.

Tolbert, W. H. and G. C. Salsman (1964). Surface circulation of the eastern Gulf of Mexico as determined by drift bottle studies. Jour. of Geophys. Res. V. 69, p. 225. p. 1. No. 2.

Uchupi, E. (1971). Bathymetric Atlas of the Atlantic, Caribbean, and Gulf of Mexico. Woods Hole Ocn. Instit. Ref. No. 71-72.

Whitaker, R. E. (1971). Seasonal variations of steric and recorded sea level of the Gulf of Mexico. Master's Thesis, Texas A & M University, Department of Oceanography, 109 pgs.

Whitehouse, U. G. and A. N. Brown (1956). Analysis of Air-Sea Surface Boundary Layer Temperature Records. TAMU Department of Oceanography. Ref. 56-14T. 50 pgs.

Wust, G. (1964). Stratification and circulation in the Antilles-Caribbean Basins. Columbia University Press, New York, 201 pgs.

Zetler, B. D. and D. V. Hansen (1972). Tides in the Gulf of Mexico. In: Contributions on the Physical Oceanography of the Gulf of Mexico, Capurro and Reid, Editors. Gulf Publishing Company, Houston, pp 265-275.

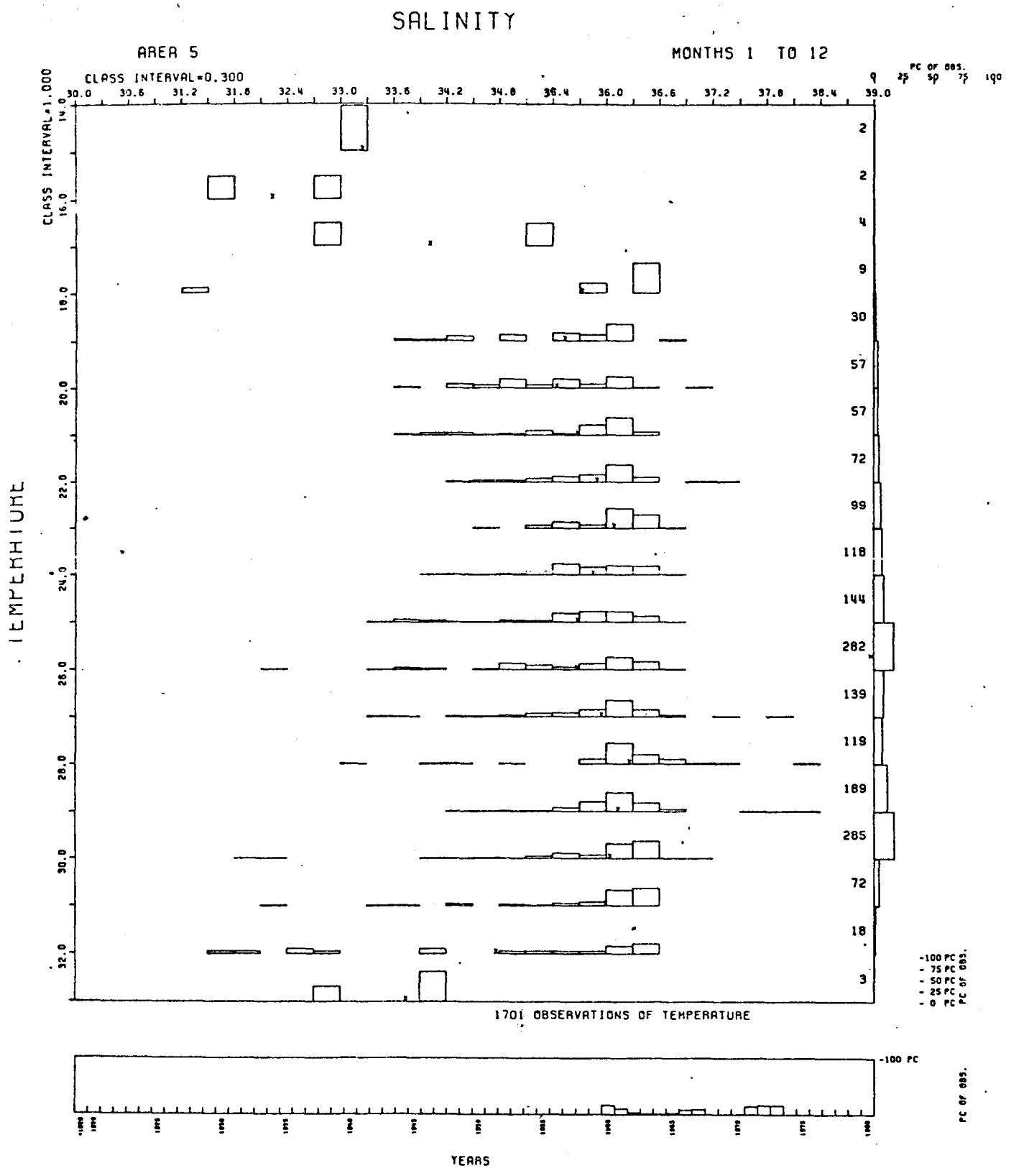

TEMPERATURE

AREA C DEPTH 0-50 METERS

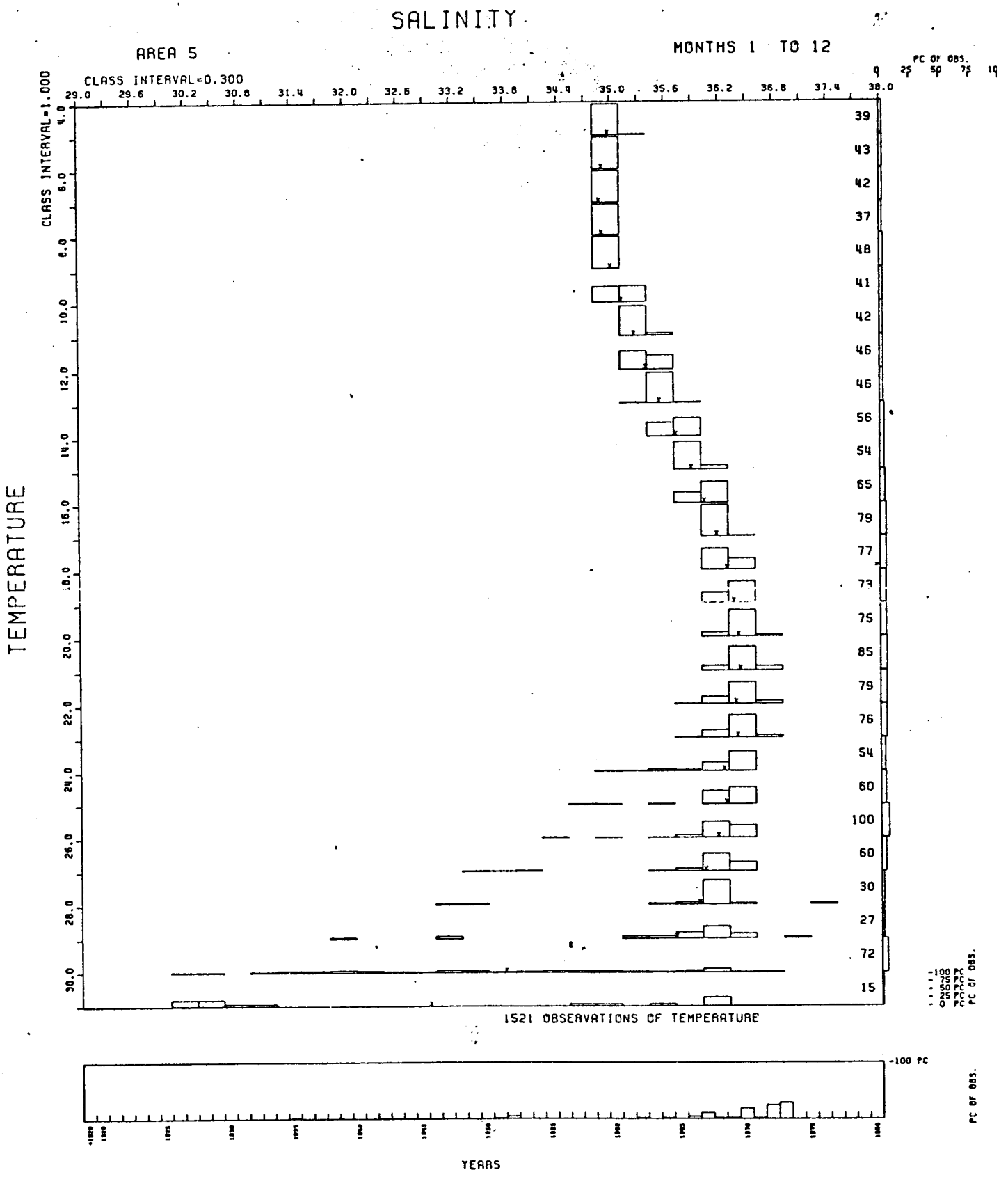

AREA B DEPTH > 200 METERS

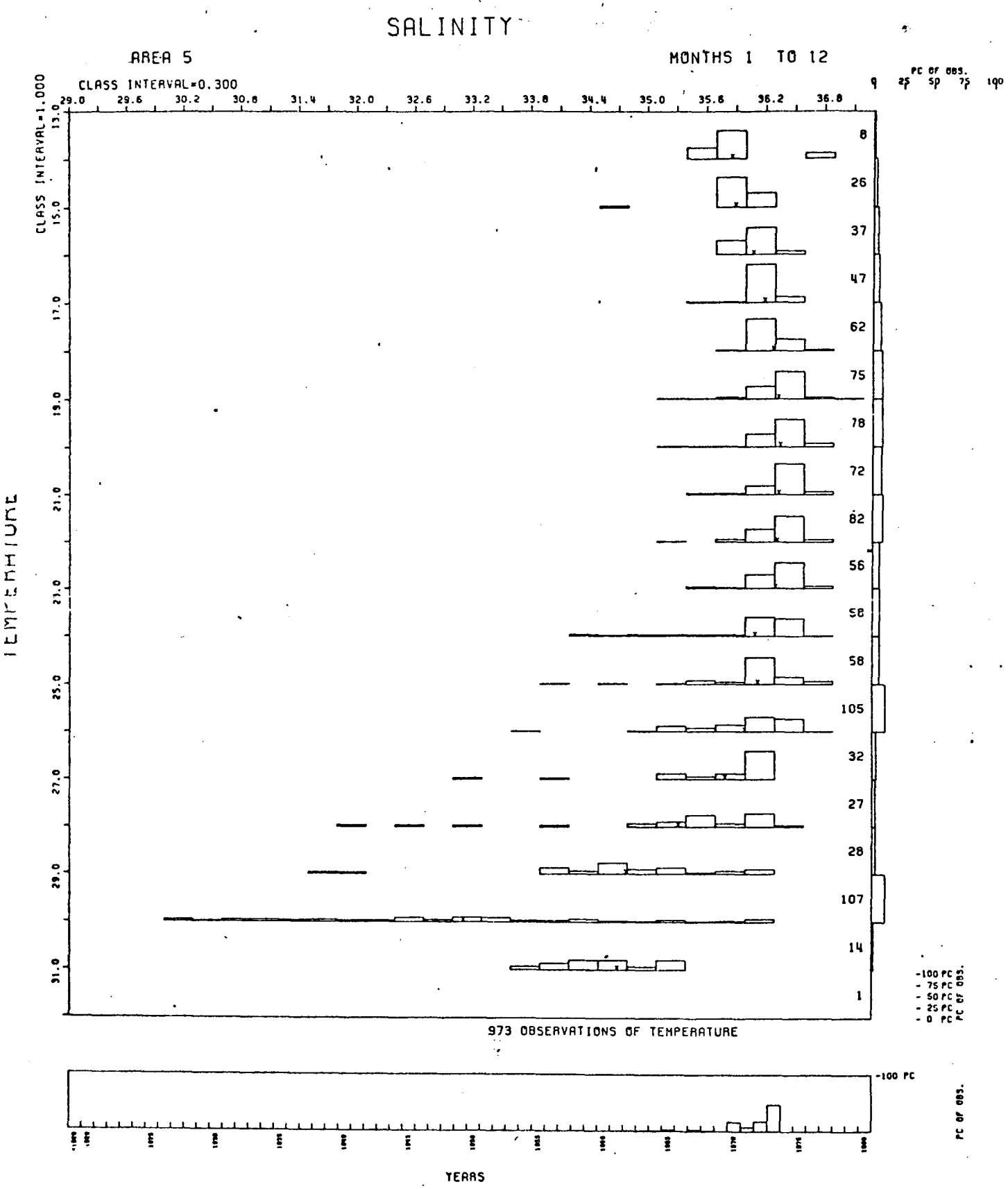
SALINITY
AREA 5
MONTHS 1 TO 12
CLASS INTERVAL=0.300
CLASS INTERVAL=1.000
TEMPERATURE
PC OF OBS.
973 OBSERVATIONS OF TEMPERATURE
YEARS
AREA B DEPTH 100-200 METERS

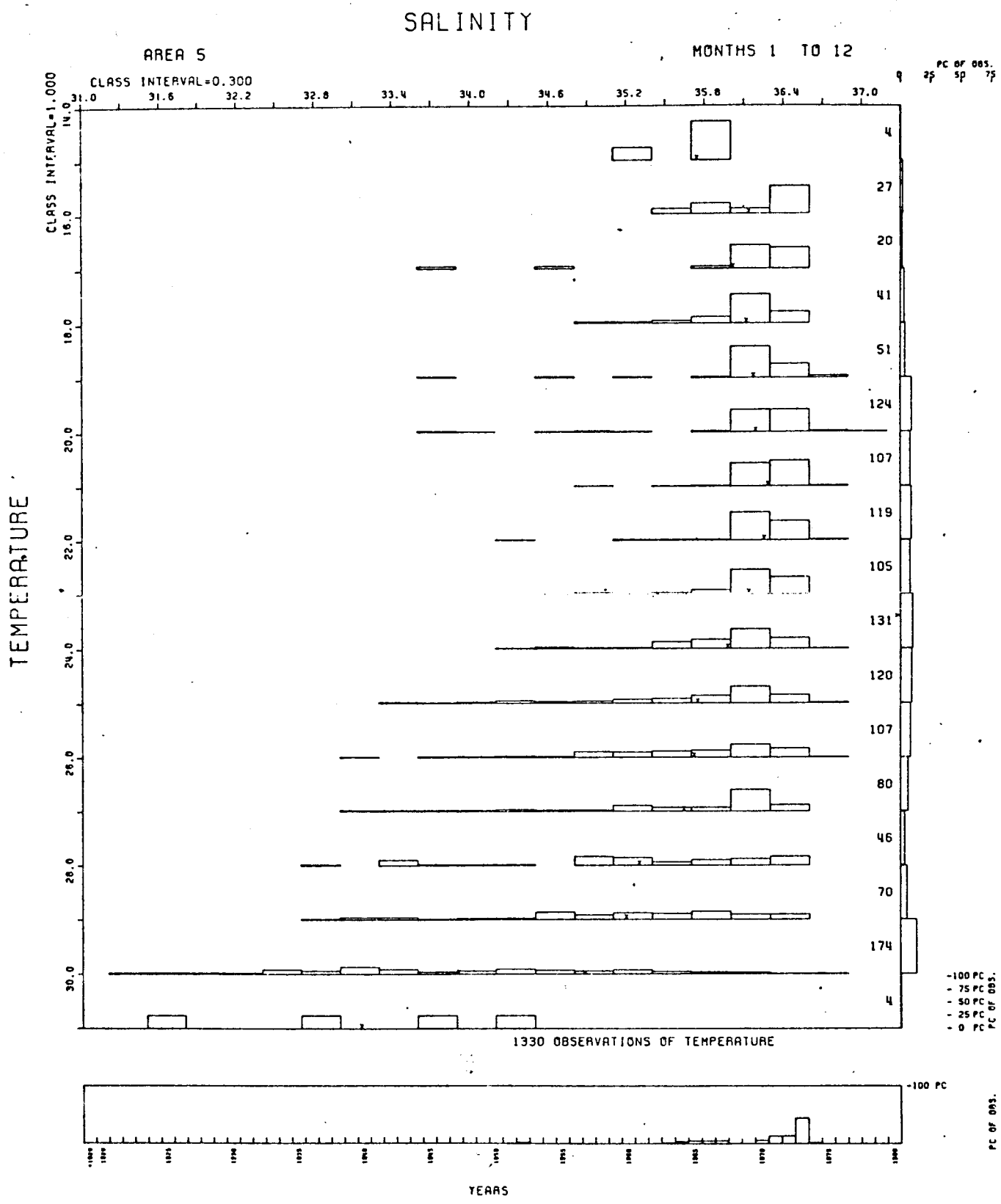

AREA B DEPTH 50-100 METERS

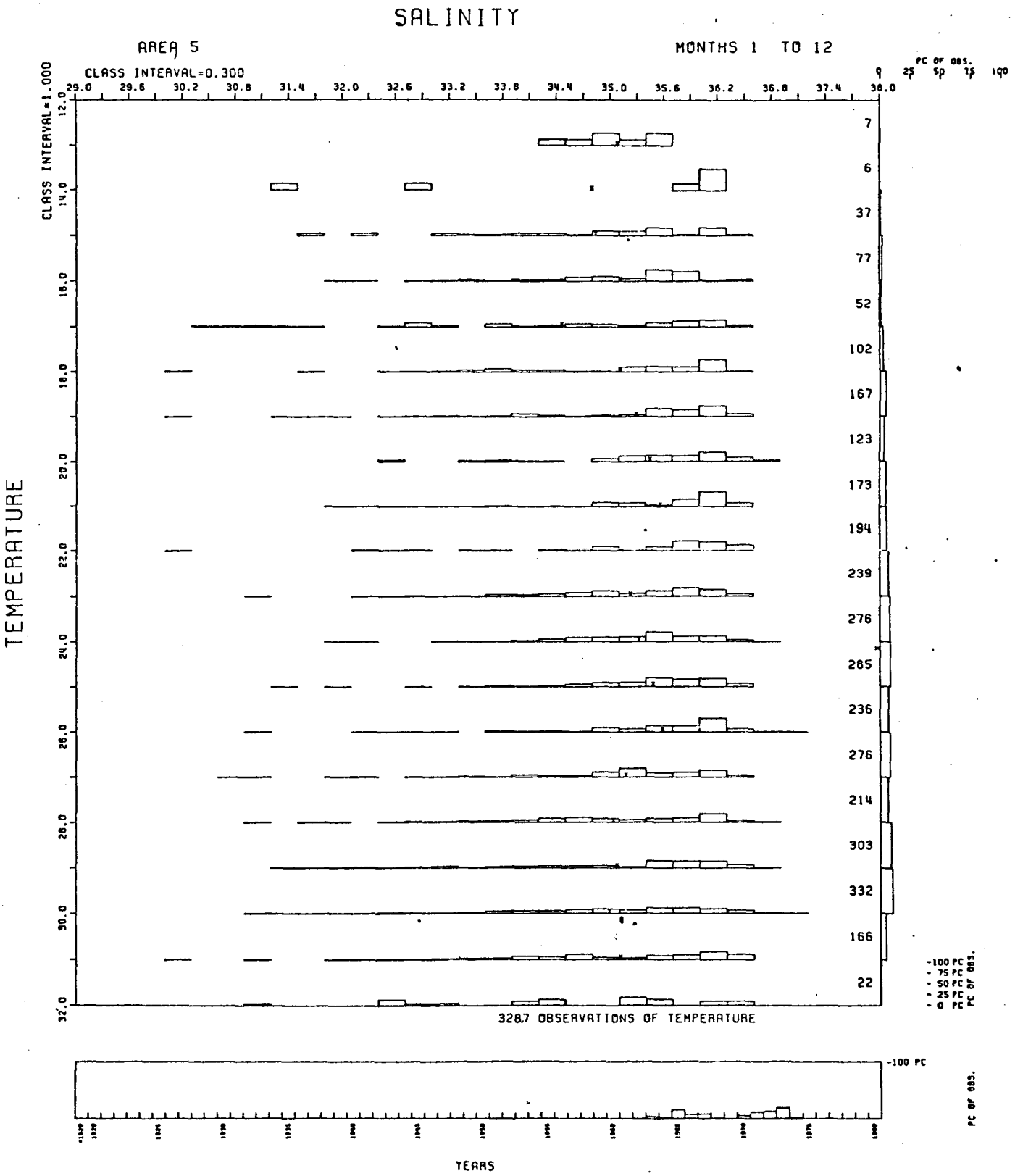

AREA B DEPTH 0-50 METERS

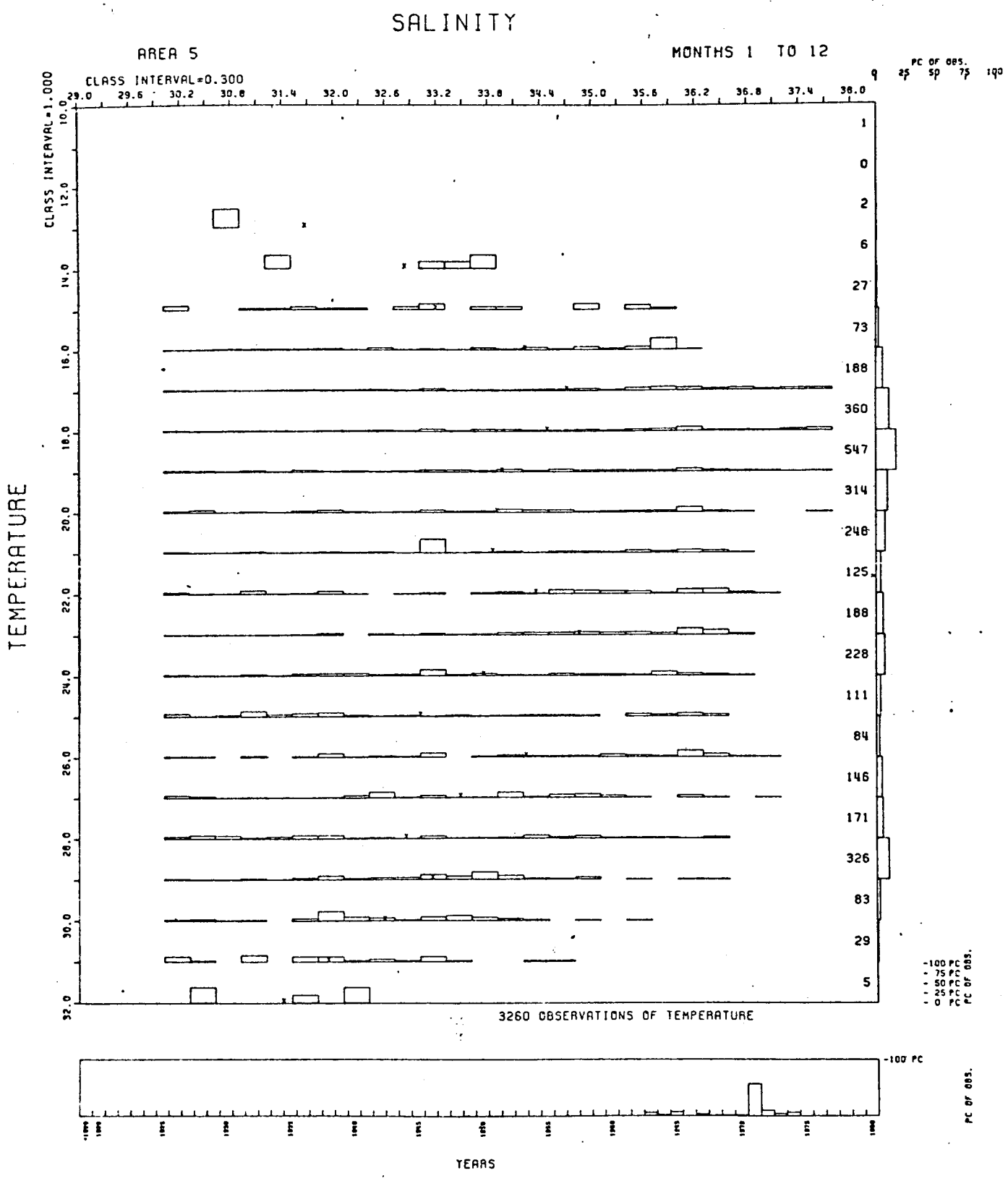

AREA A 0-50 METERS

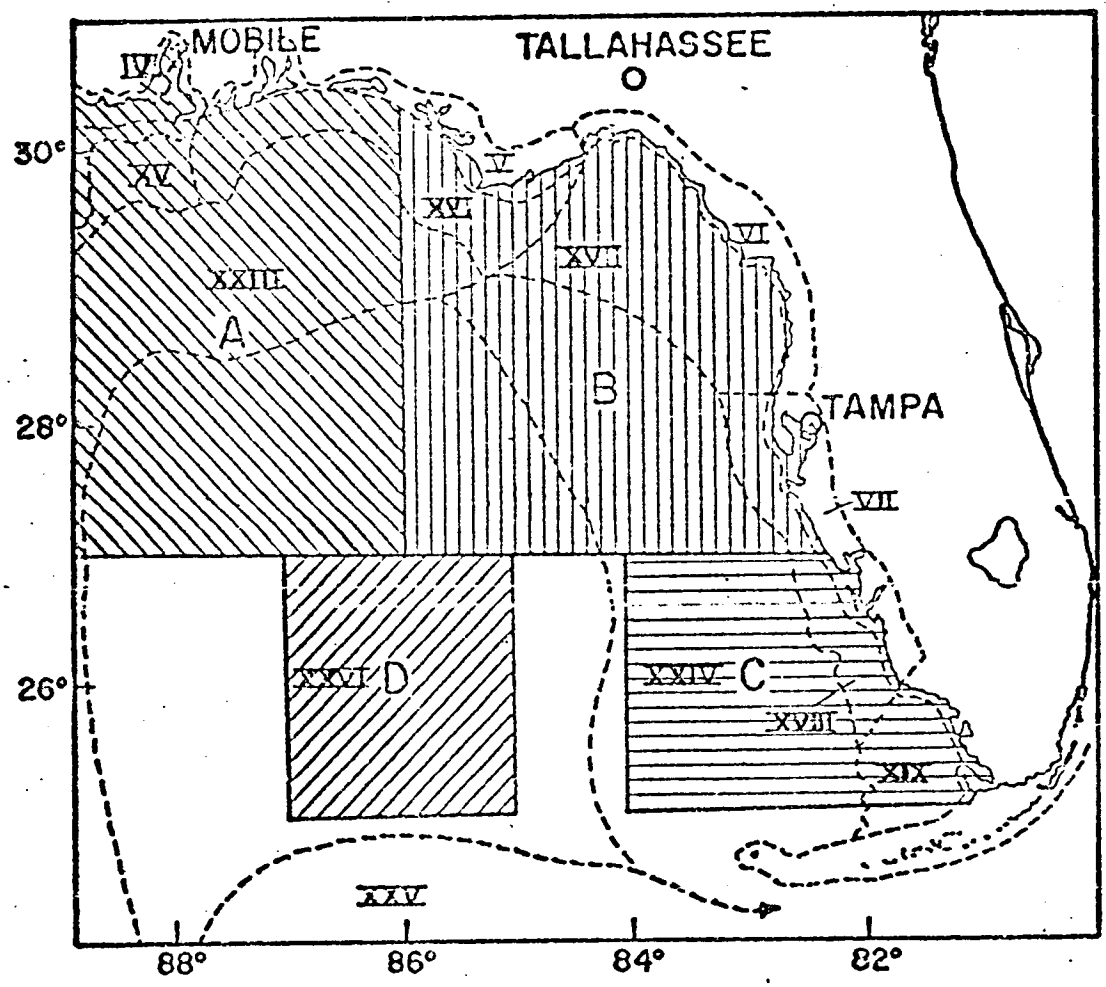

HYDROBIOLOGICAL ZONES

Appendix III

T-S, $T-O_2$ Histograms

Hydrobiological zones have been established in the eastern Gulf of Mexico based on biological and geological speciation. These zones are delineated on the first figure of this Appendix. The hydrobiological zones were further divided into 4 regions by depth, 0-50 m, 50-100 m, 100-200 m, and $>$ 200 m. T-S and $T-O_2$ histograms were produced for each subdivision. The depths of zone D are greater than 200 m, thus only two histograms are given for this zone.

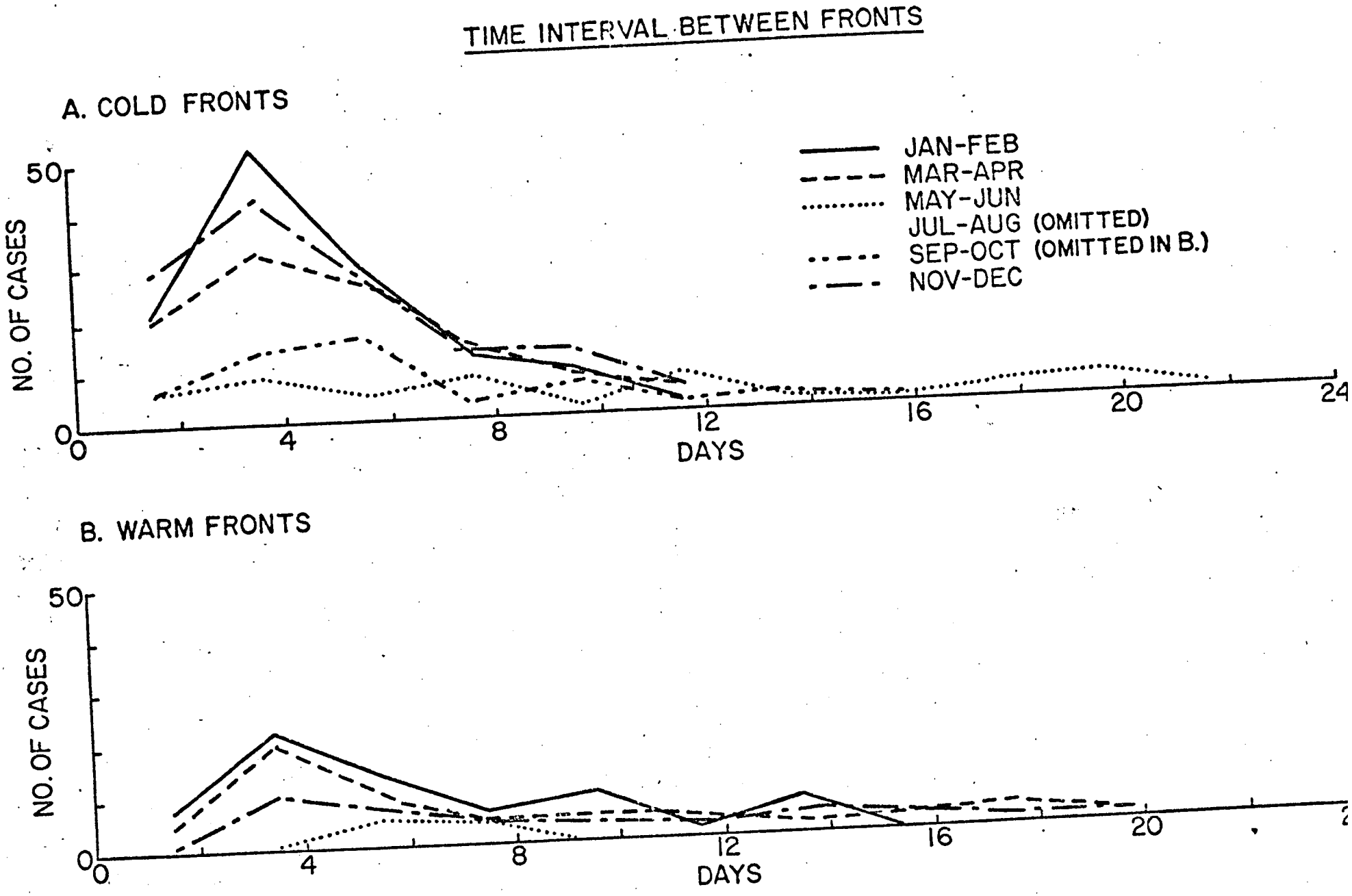

Figure 10. Frequency distribution (by bimesters) for the time-interval between fronts.

Time-interval Between Fronts

The frequency distribution by bimesters of the time-interval between fronts is illustrated in Figure 10. In this figure, the time-interval is classed by intervals of two days; the number of cases in each class is plotted only if it is found to be two or greater than two. The time interval for cold fronts is shown in graph A (top) and the time-interval for warm fronts is shown in graph B (bottom). Note that, for the winter months (November to April) both cold and warm fronts show a peak frequency in the 3-to-4 day range. For the summer months, the frequency distribution is not always shown because of the criterion imposed on the minimum number of cases required to be plotted. However, the time interval between fronts is known to be large and to vary considerably for the few summer-season fronts.

Graphs A and B in Figure 10 are known to underestimate the actual time interval between fronts. The underestimate can be of about twenty-four hours, somewhat larger (but less than 48 hours) in some cases. Therefore, a correction of at least +24 hours to the time-intervals appears to be in order.

It should suffice to indicate, in conclusion, that the well known annual cycle of the upper-air circulation in the tropics and subtropics is reasonably reflected on the cold front and warm front characteristics which are described in this climatological study.

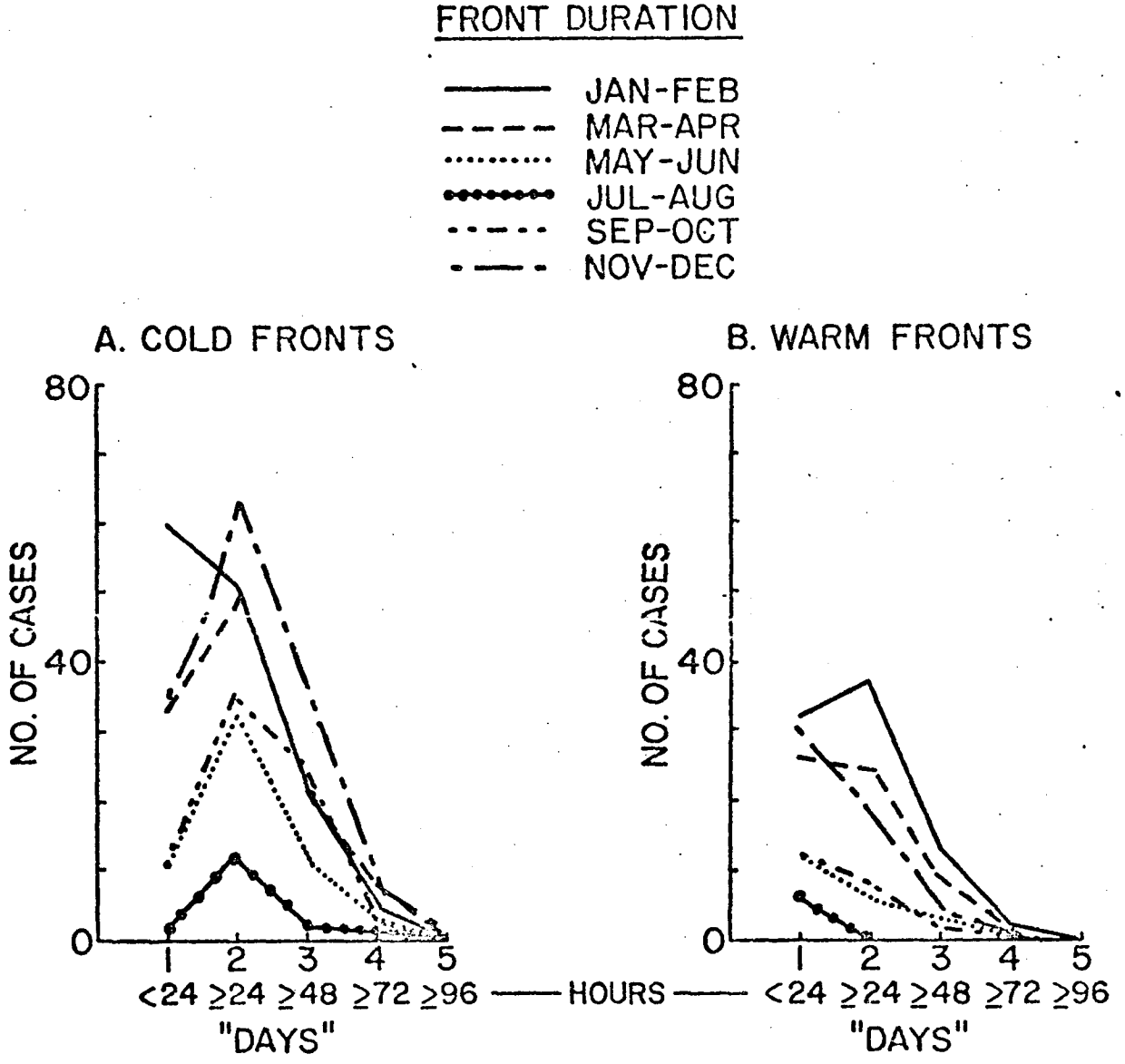

Figure 9. Frequency distribution for the front duration by bimesters throughout the year. In graphs A and B, "days" denotes time ranges as following: 1, less than 24 hr.; 2, from 24 hr. to less than 48 hr.; 3, from 48 hr. to less than 72 hr.; etc.

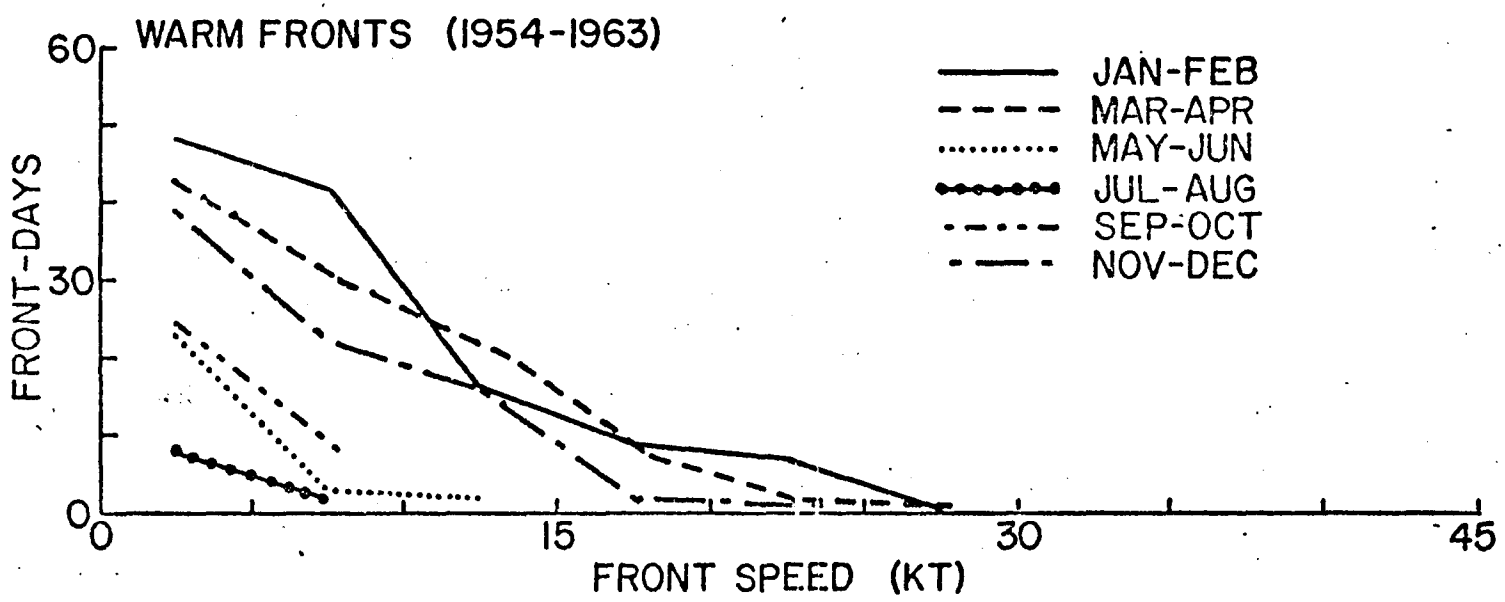

Figure 8. Same as Figure 7 but for the warm front speed.

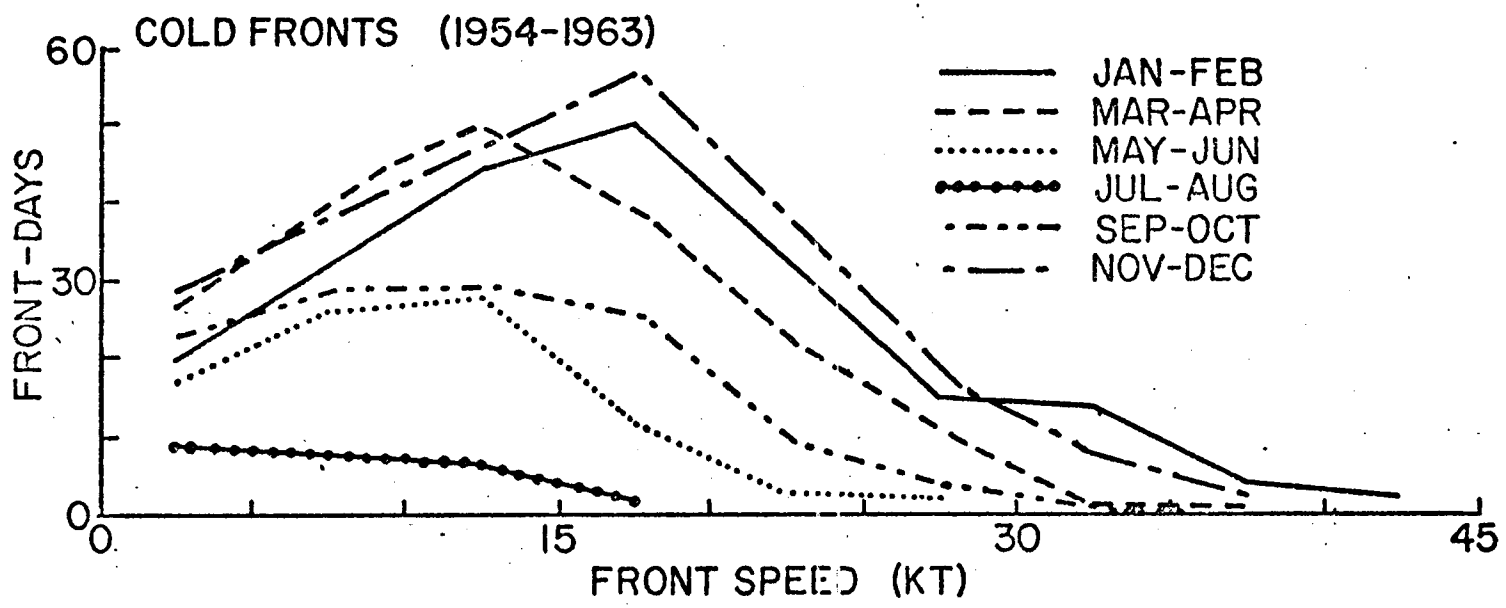

Figure 7. Frequency distribution for the cold front speed by bimesters throughout the year.

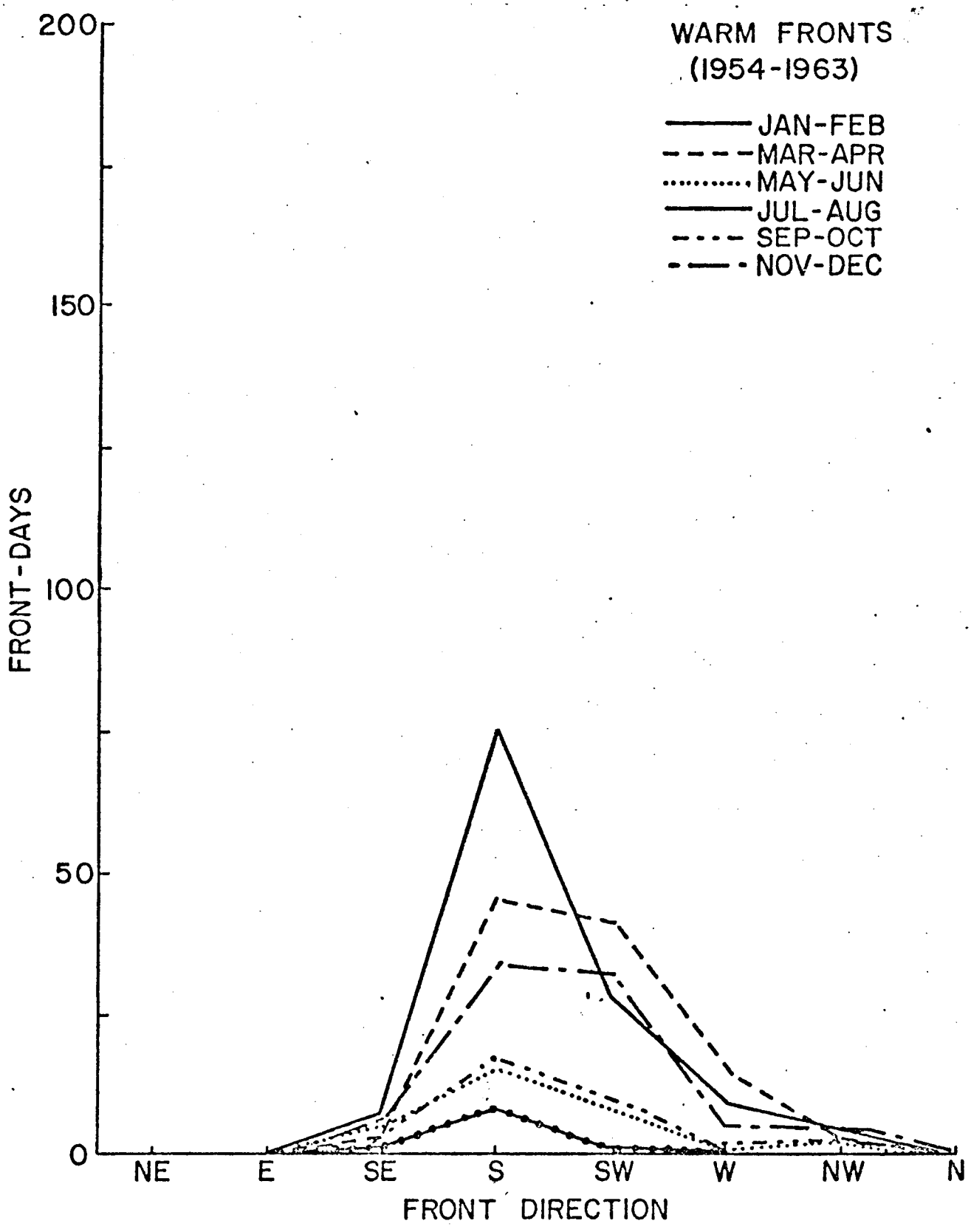

Figure 6. Same as Figure 5 but for the warm front direction.

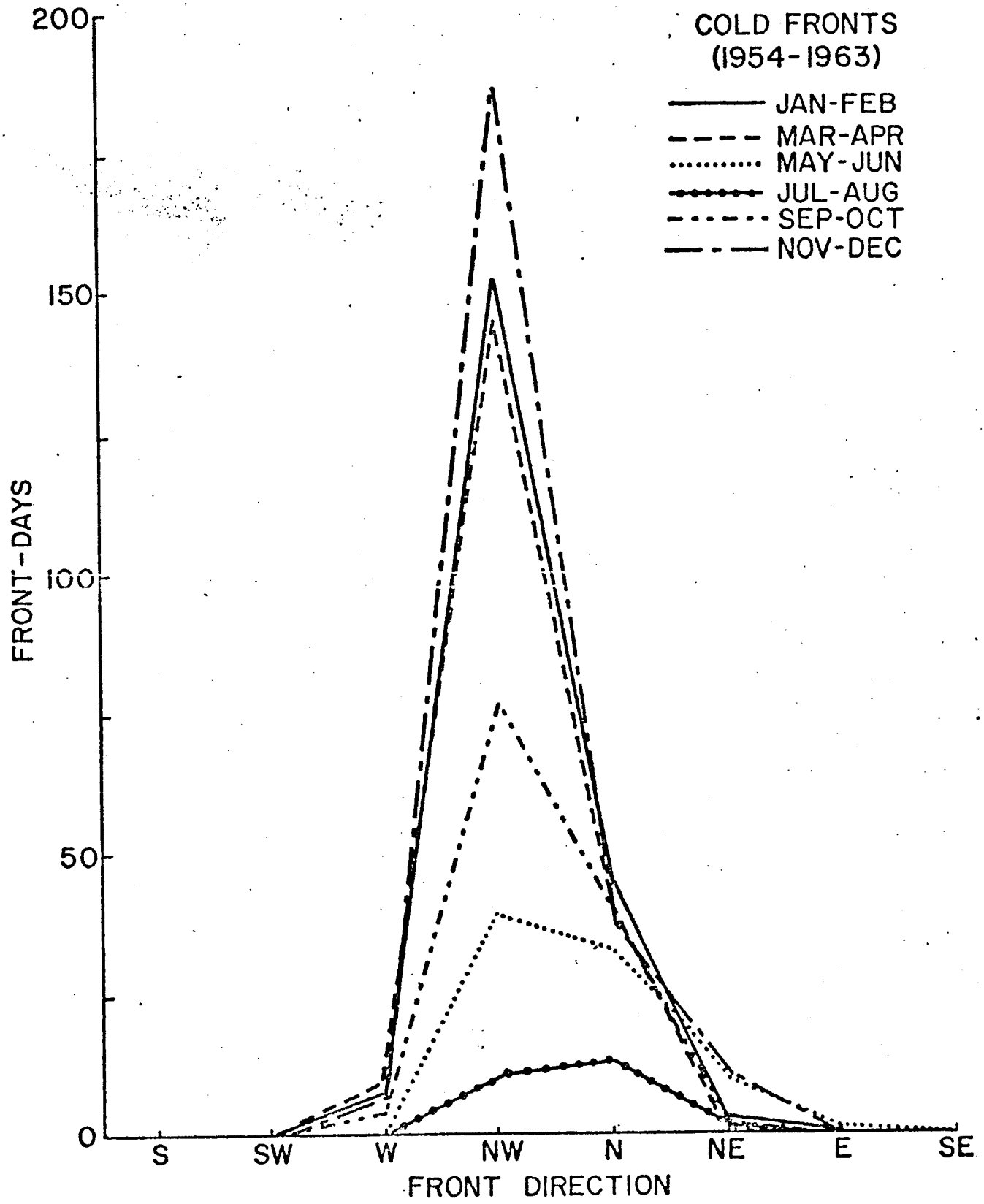

Figure 5. Frequency distribution for the cold front direction by bimesters throughout the year.

Front Direction

The frequency distribution for the cold front direction by bimesters throughout the year is illustrated in Figure 5. This figure, aside from indicating a very substantial decrease in frequency during the summer, indicates a shift in the cold front direction from the northwesterly to the northerly direction in summer and a shift back to the northwesterly direction in fall.

Figure 6 presents the frequency distribution by bimesters for the warm front direction. Note that the prevailing warm front direction is southerly throughout the year but with the southwesterly direction being almost as large as the southerly direction in spring and early winter.

Front Speed

Figures 7 and 8 show the frequency distribution for the front speed. This speed is classed in five-knot intervals. Figure 7 illustrates the frequency distribution by bimesters for the cold front speed. Note that the predominant frequency changes from the 15-20 knot range in the winter months to the less than 10-knot ranges in summer.

Figure 8 is analogous to Figure 7 but for the warm front speed. The predominant frequency (less than 5-knot range) does not change range throughout the year but frequencies for all speed ranges reach an expected minimum in summer.

Front Duration

The frequency distribution by bimesters for the front duration is illustrated in Figure 9. Graph A (left) refers to cold fronts and graph B (right) refers to warm fronts. Peak frequencies in graph A denote that the predominant front duration for cold fronts is the range from 24 to less than 48 hours (corresponding to fronts which are identified in the area on two consecutive maps). This is observed throughout the year with the exception of January-February. The predominant frequency in the less than 24-hour range for January-February appears to reflect the fastest moving mid-winter cold fronts. Graph B indicates that the predominant duration of warm fronts is less than twenty-four hours. An exception is found for January-February when the predominant duration shifts to the range from 24 to less than 48 hours. This longer duration of warm fronts in the area reflects the fact that the southernmost location of warm fronts occurs in mid-winter.

Graphs A and B are known to underestimate the actual duration of fronts in the area. This is because, normally, some time (less than 24 hours) elapses before the front is first detected in the area (on maps at 24-hour intervals) and some time (less than 24 hours) elapses after the front is last detected in the area. Consequently, a correction of about +24 hours to the time values in the previous paragraph seems to be pertinent.

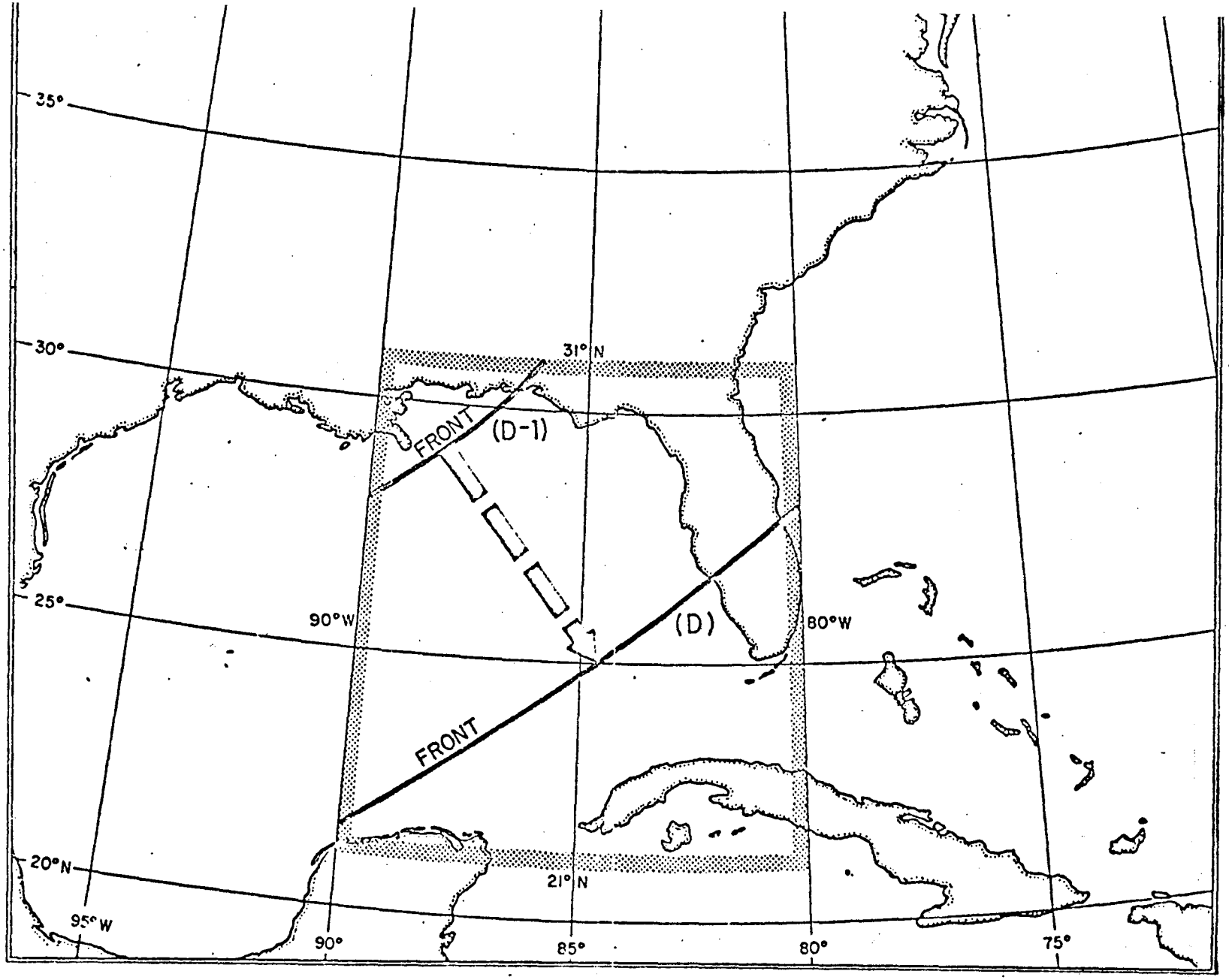

Figure 4. Map showing the 24 hr. displacement of a front based upon the front location on two consecutive days (D-1 and D).

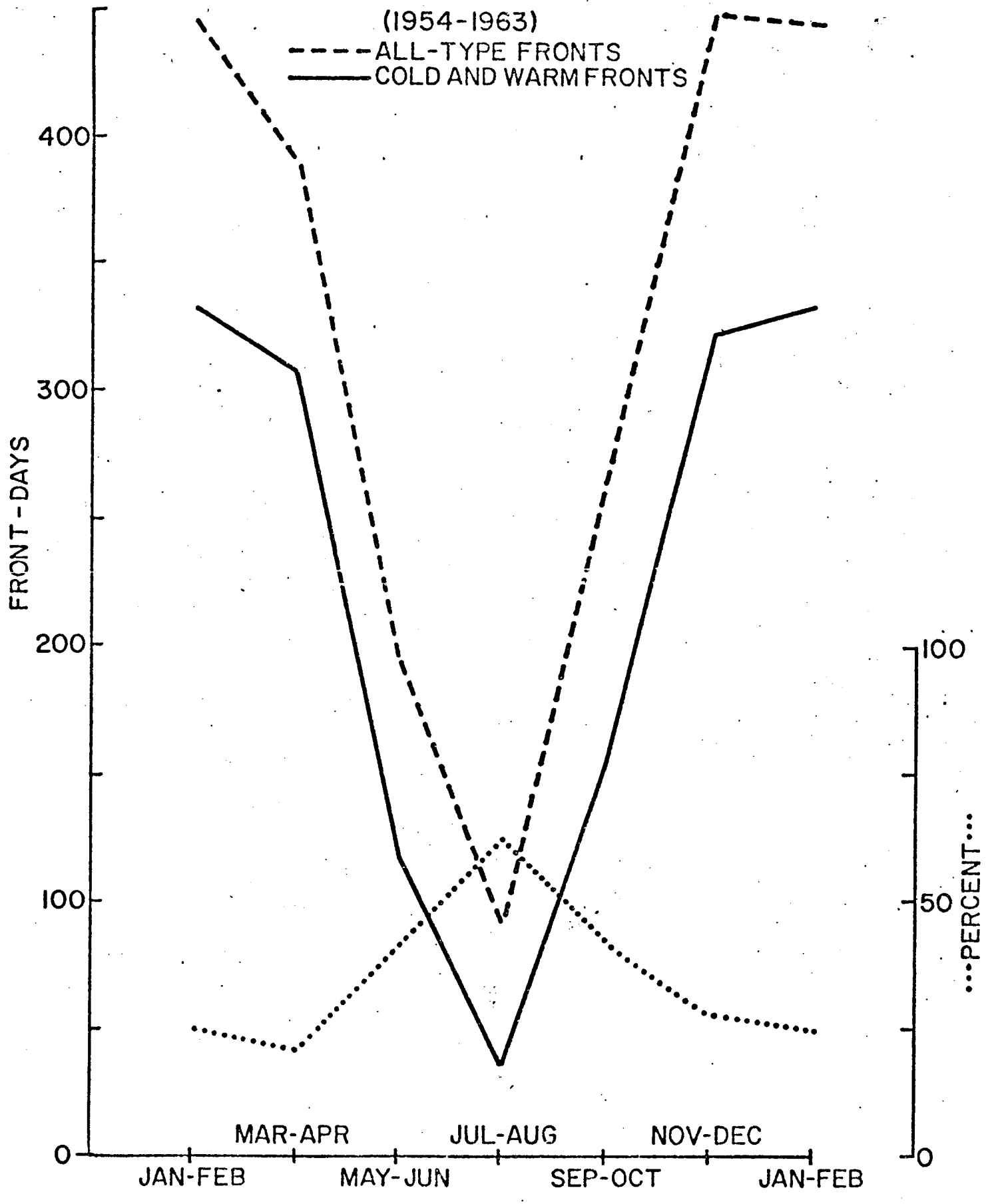

Figure 3. Same as Figure 2 but for front-days (frequency).

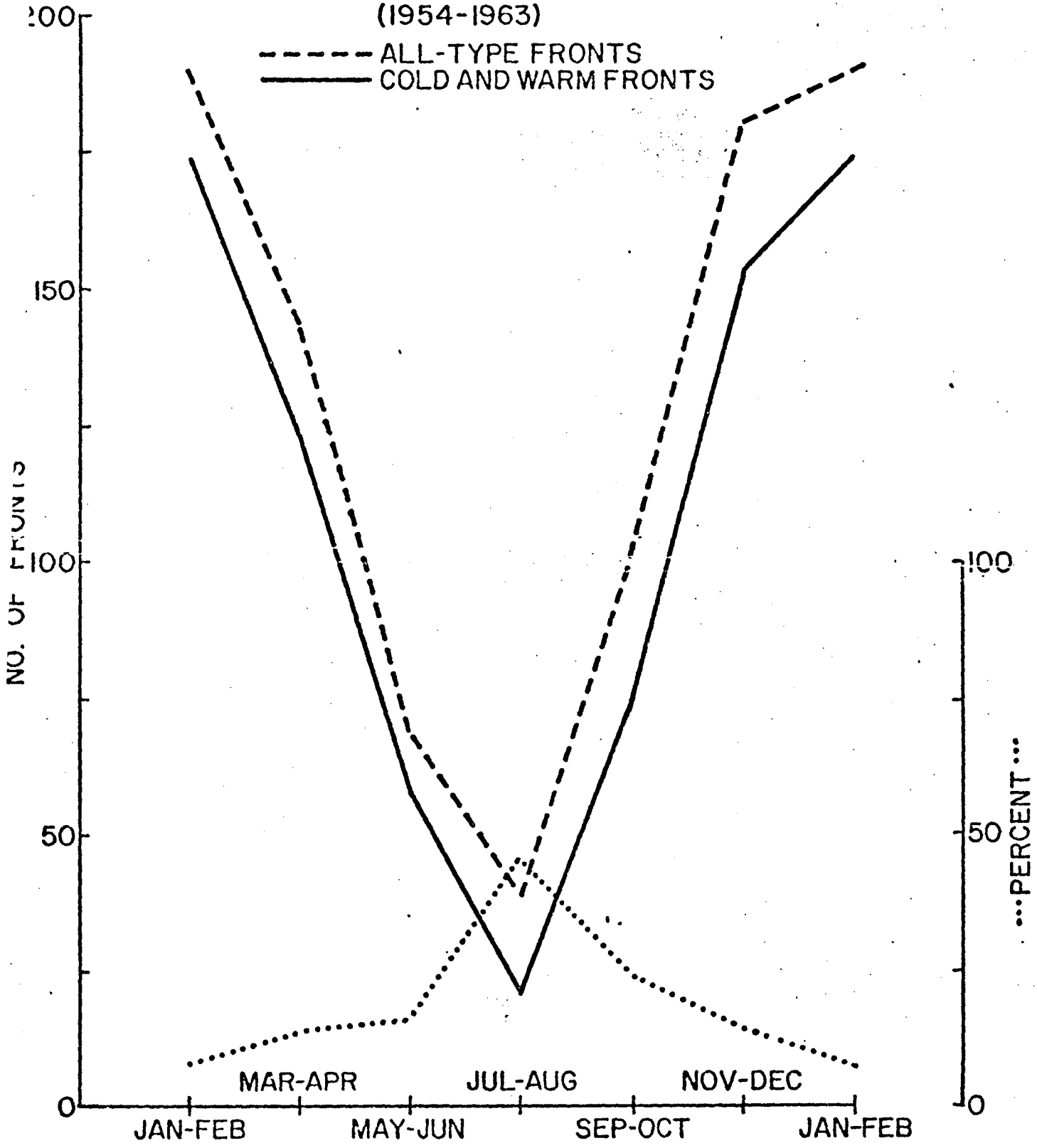

Figure 2. Graph showing the distribution of fronts by bimesters. The dotted line indicates the percent of fronts other than cold and warm fronts.

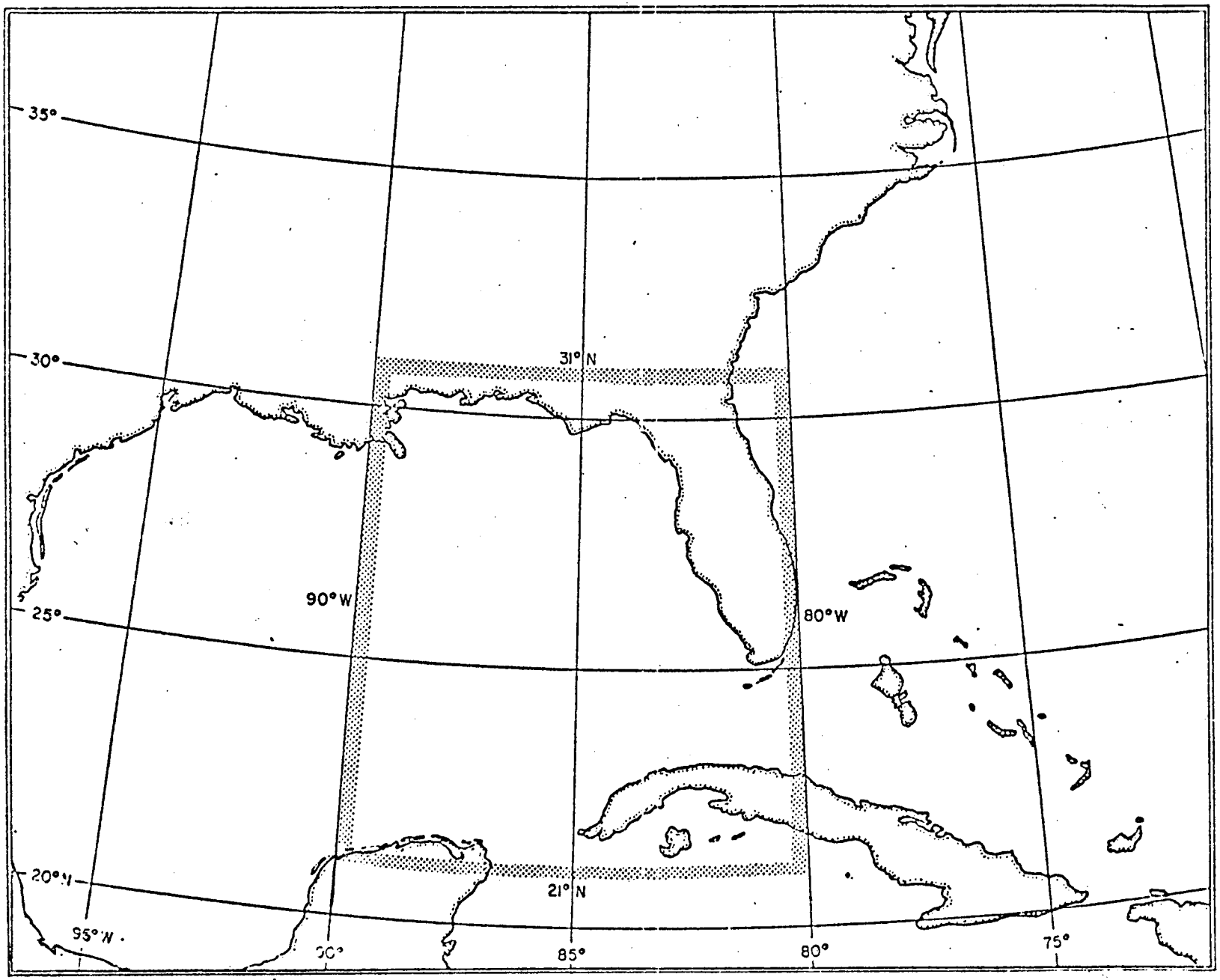

Figure 1. Map showing the area of frontal studies.

Appendix II

Some Frontal Characteristics over the Eastern Gulf of Mexico and Surrounding Land Areas

Jose Fernandez-Partagas
Christopher N. K. Mooers

This study is motivated primarily by the need for a climatology of frontal characteristics to be used in describing and modeling the ocean response to atmospheric forcing. From a meteorological standpoint, however, the present study is a contribution to areal weather forecasting by statistical methods.

This study describes some characteristics of the atmospheric fronts affecting the eastern Gulf of Mexico and surrounding land areas over a ten-year period. The frontal characteristics which are studied are the annual variations of (1) front direction; (2) front speed; (3) front duration; and (4) time-interval between fronts. Although various types of fronts can be recognized on surface weather charts only the cold and warm fronts are found to be suitable for this study.

Fronts were extracted by NCC (Asheville, North Carolina) from the Daily Series Synoptic Weather Maps (Northern Hemisphere) which are available at 24-hour intervals (daily at 1200 GMT). All maps for the years 1954 to 1963 were used. The fronts used in this study were those located within the area limited by the 21°N and the 31°N parallels and the 80°W and the 90°W meridians (fig. 1). Cold, warm, stationary, and occluded fronts were found in the ten-year sample. Frontogenesis and frontolysis causes of all types were also found.

The examination of individual fronts and of the front-days (frequency) by bimesters allows us to conclude that cold and warm fronts are the most important fronts in the area over most of the year. This is shown in Figures 2 and 3. The figures show that fronts other than cold and warm fronts are predominant only in summer when all fronts are known to be weakest in a year cycle of front intensity. This finding appears to justify, statistically, the elimination of fronts other than the cold and the warm fronts in this study. But even a more valid reason for the elimination is the unrealistic characteristics which would be obtained for stationary fronts, frontogenesis, and frontolysis cases whose existence is normally less than twenty-four hours.

This location of cold and warm fronts on two consecutive maps (24-hour intervals) allows us to determine the front direction and the front speed. A vector displacement is assessed as indicated in Figure 4. The direction of motion is approximated to eight points of the compass and the front speed is calculated in knots. The front duration is approximated by the number of consecutive maps on which an individual cold or warm front can be identified in the area. The time-interval between fronts is defined by the number of days between the first appearance in the area of two consecutive cold or warm fronts.

Appendix I

List of NODC Products

1) 230 station location plots for all stations in the MAFLA file by year/month.
2) 20 thermocline and mixed layer listings by depth zones.
3) 15 thermocline and mixed layer listings by hydrobiological areas.
4) 35 listings of monthly minimum, maximum, average, and standard deviation of temperature by 1^{o} square and 5 meter intervals using MBT/XBT data.
5) 4 joint histogram plots of temperature/salinity by designated depth zones.
6) 3 joint histogram plots of temperature/salinity by designated hydrobiological areas.
7) 4 joint histogram plots of temperature/oxygen by designated depth zones.
8) 3 joint histogram plots of temperature/oxygen by designated hydorbiological areas.
9) 180 plots of the depth occurrence of the $10^{o}C$, $15^{o}C$, and $20^{o}C$ isotherms using combined MBT, XBT, and station data input.
10) 540 listings of data used to generate the above plots (one set per each plot of MBT/XBT/and hydro data).

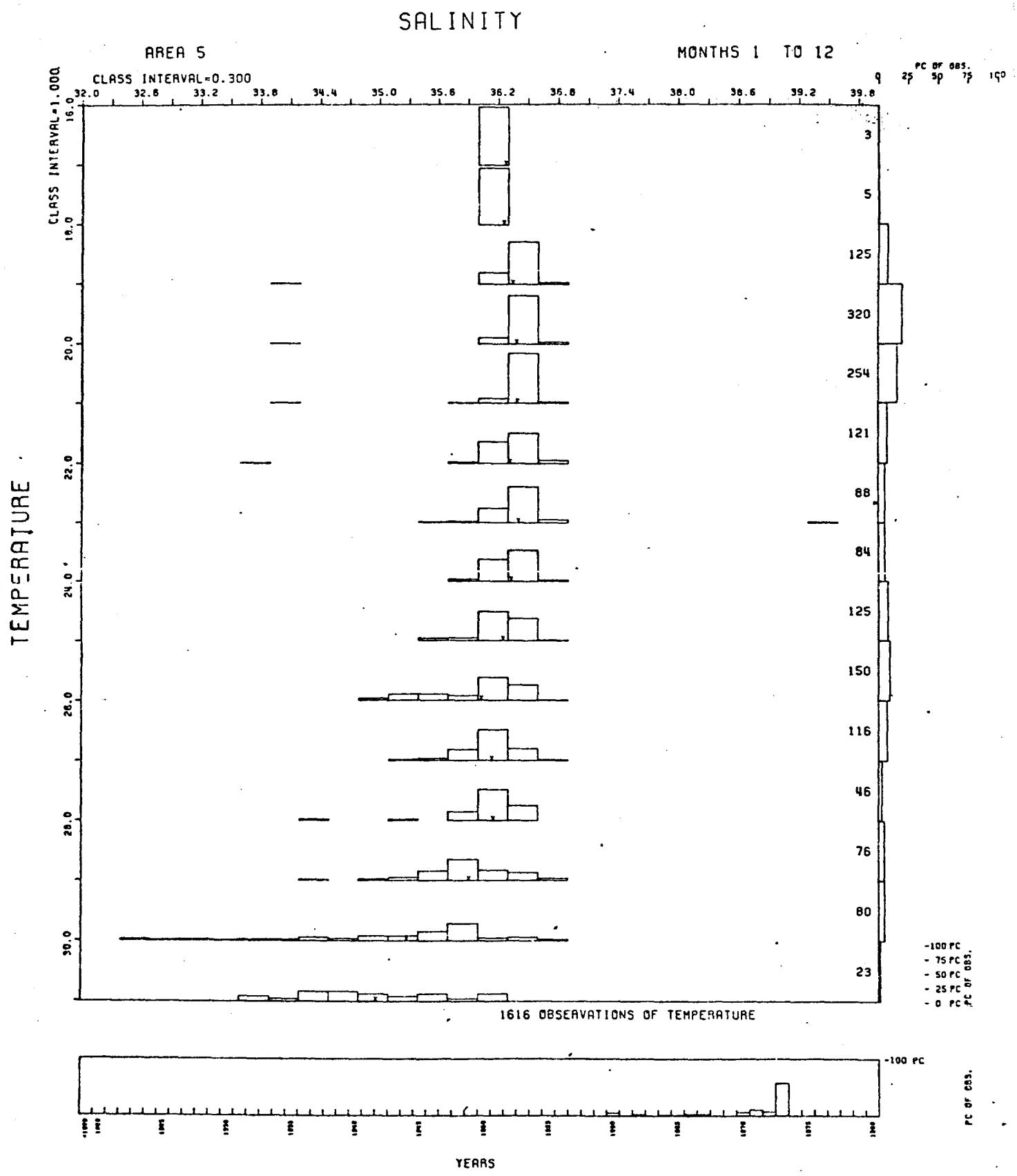

AREA C DEPTH 50-100 METERS

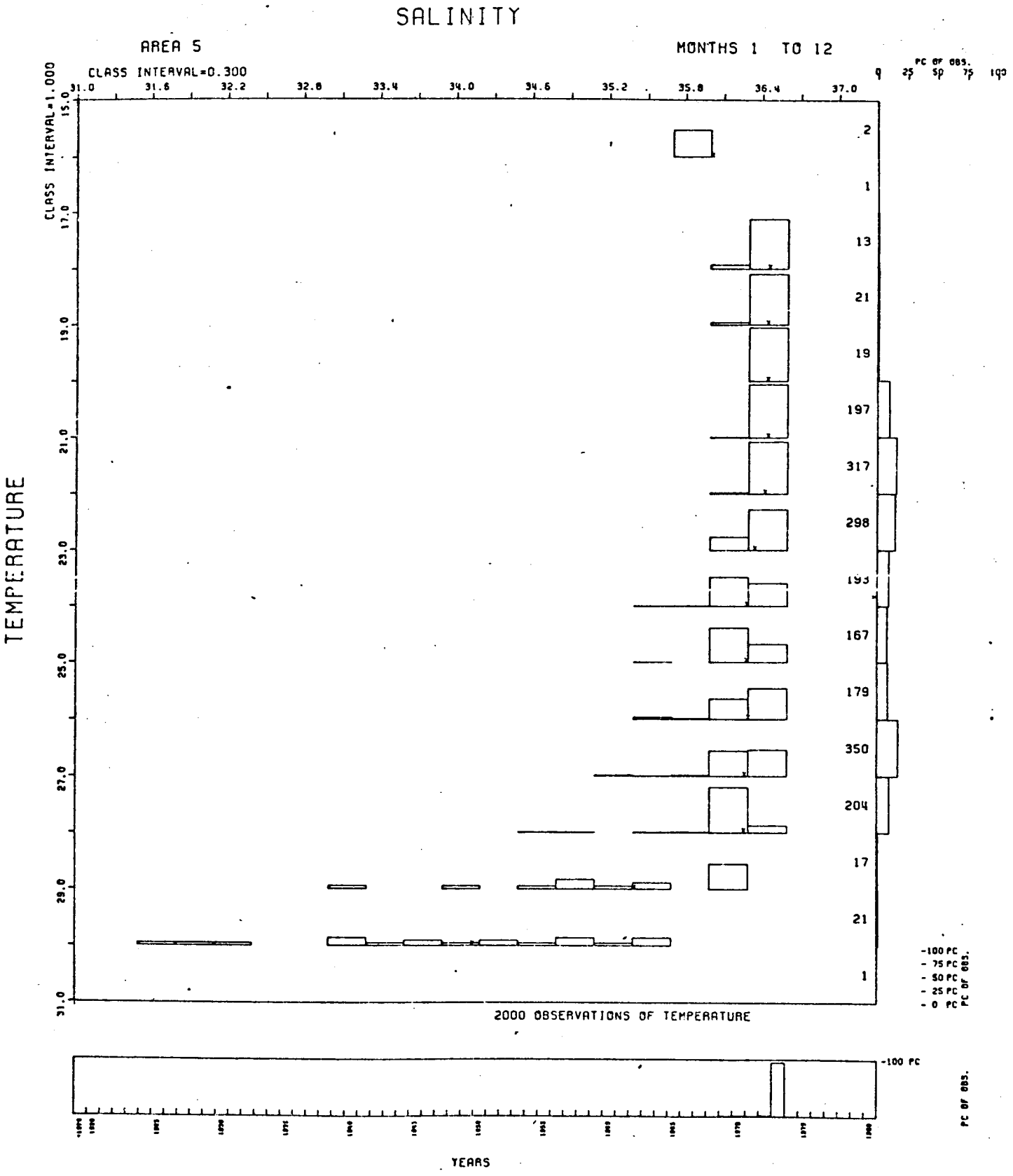

AREA C DEPTH 100-200 METERS

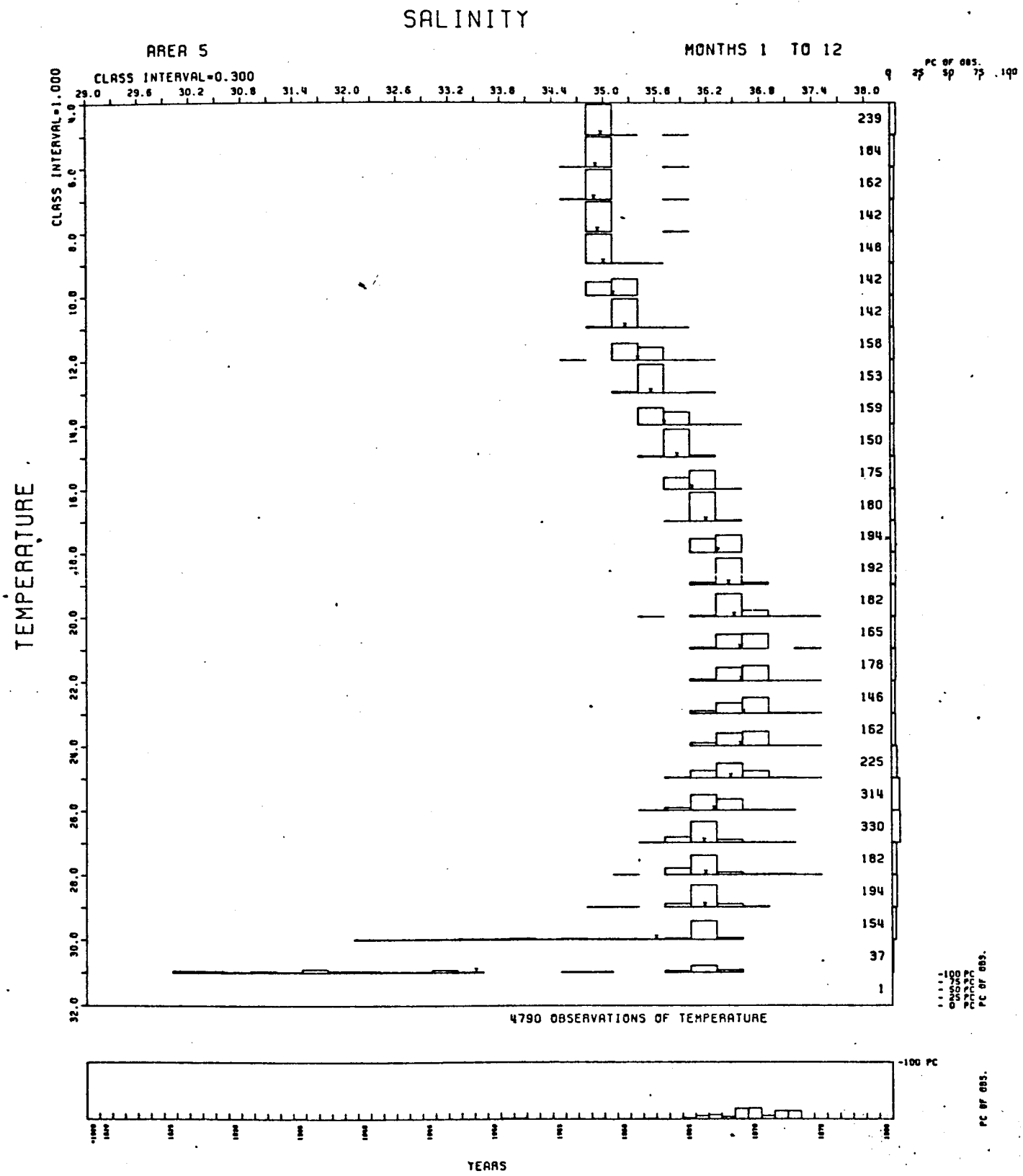

AREA D > 200 METERS

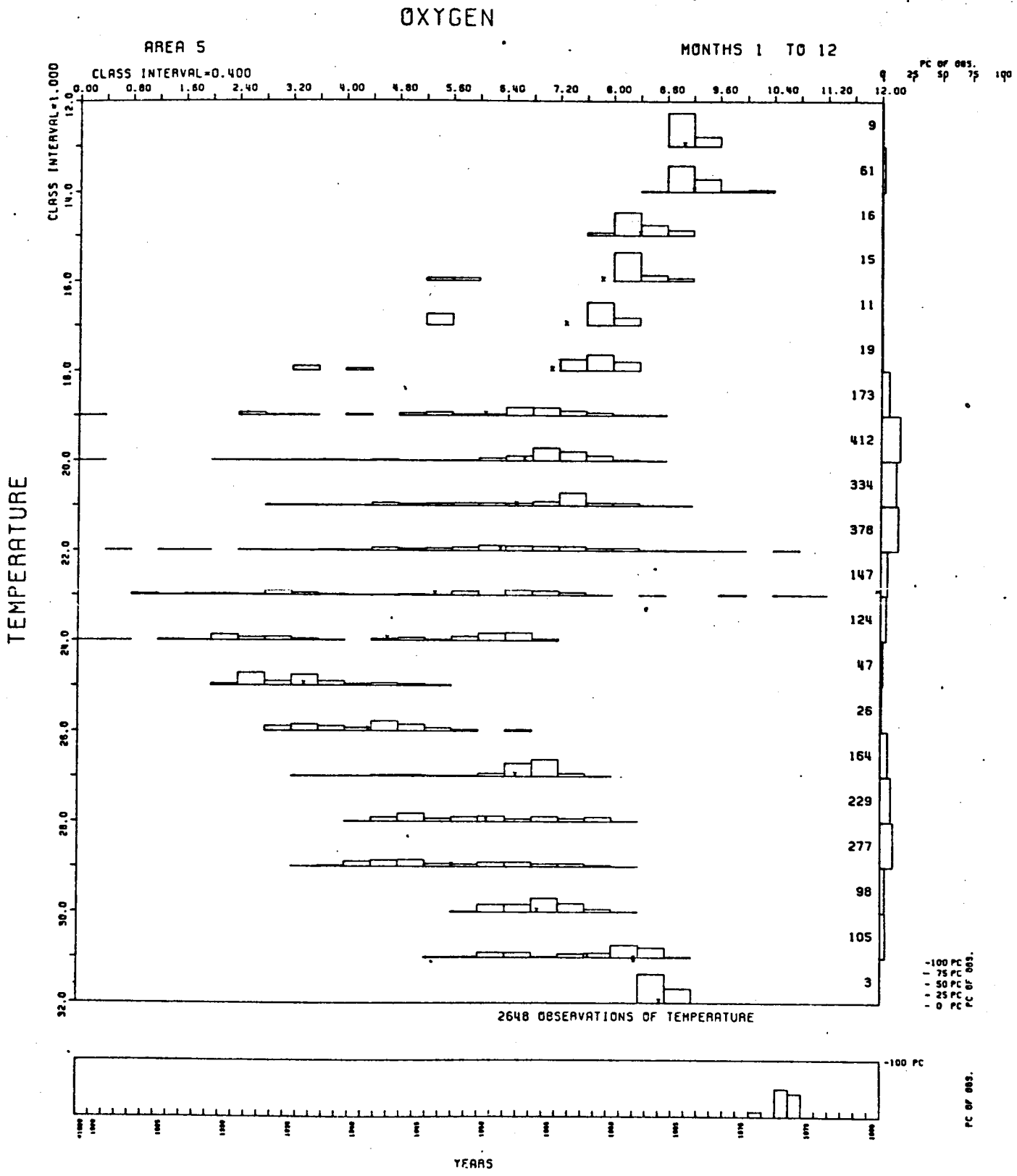

AREA A DEPTH 0-50 METERS

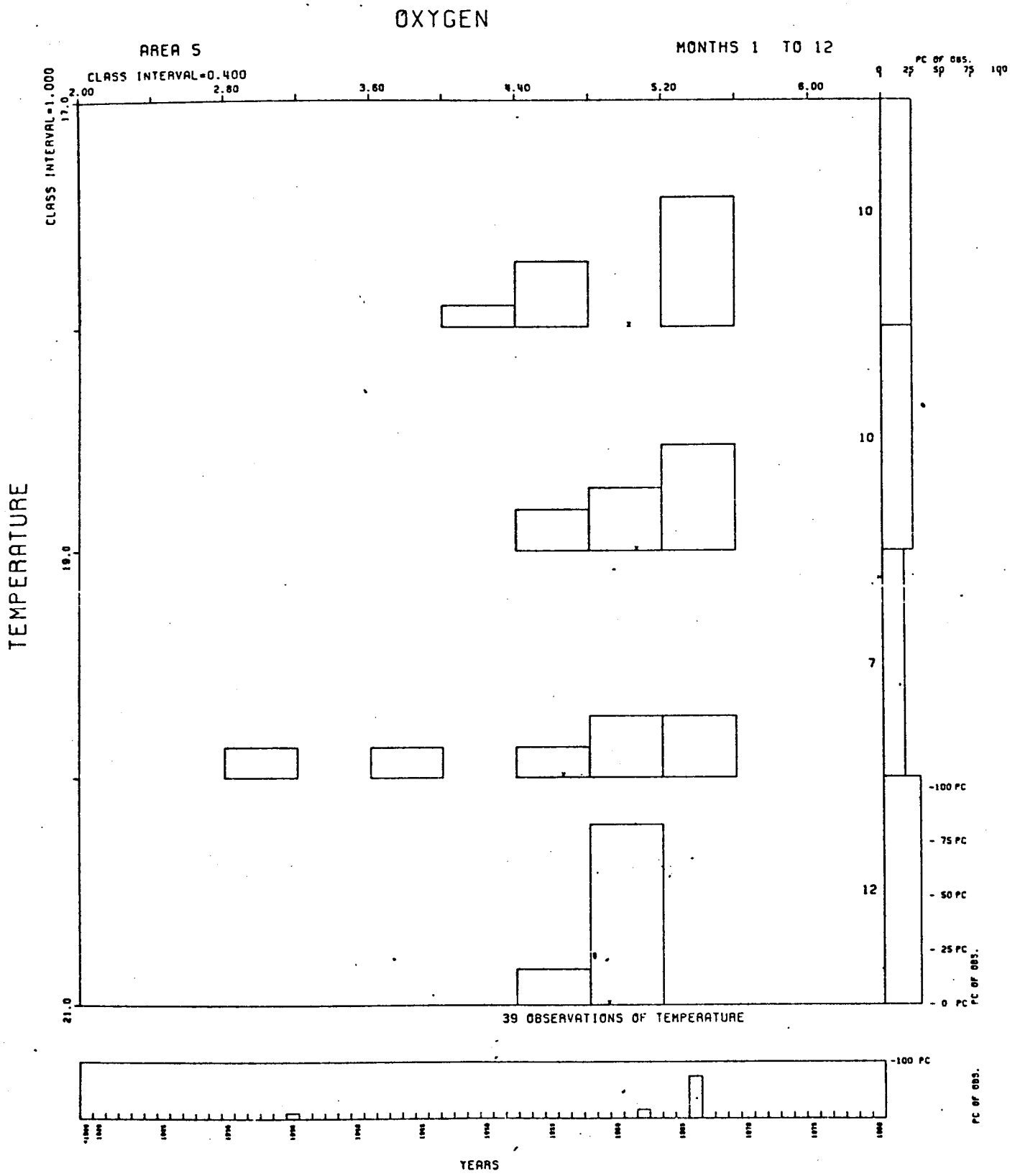

AREA A DEPTH 50-100 METERS

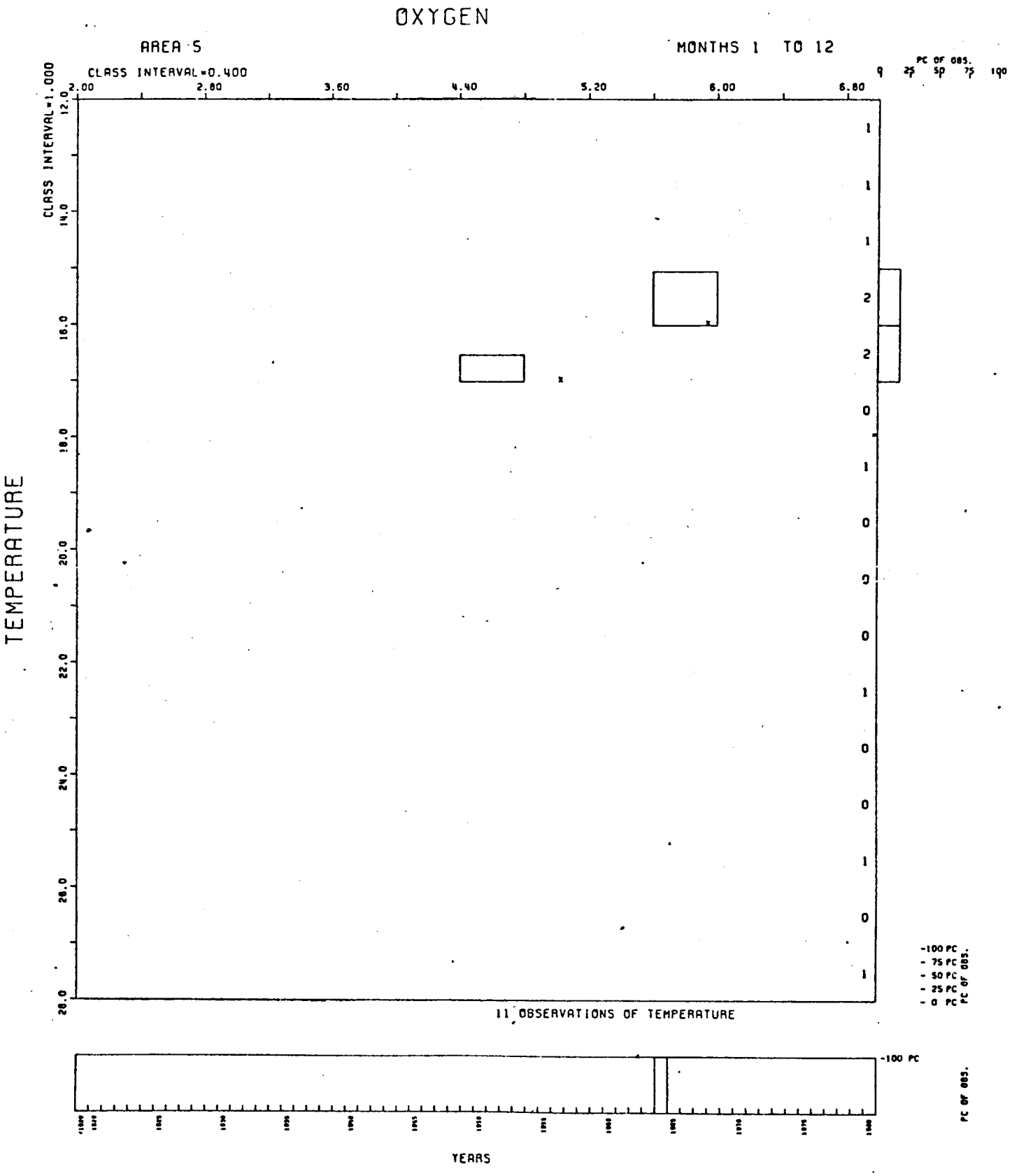

AREA A DEPTH 100-200 METERS

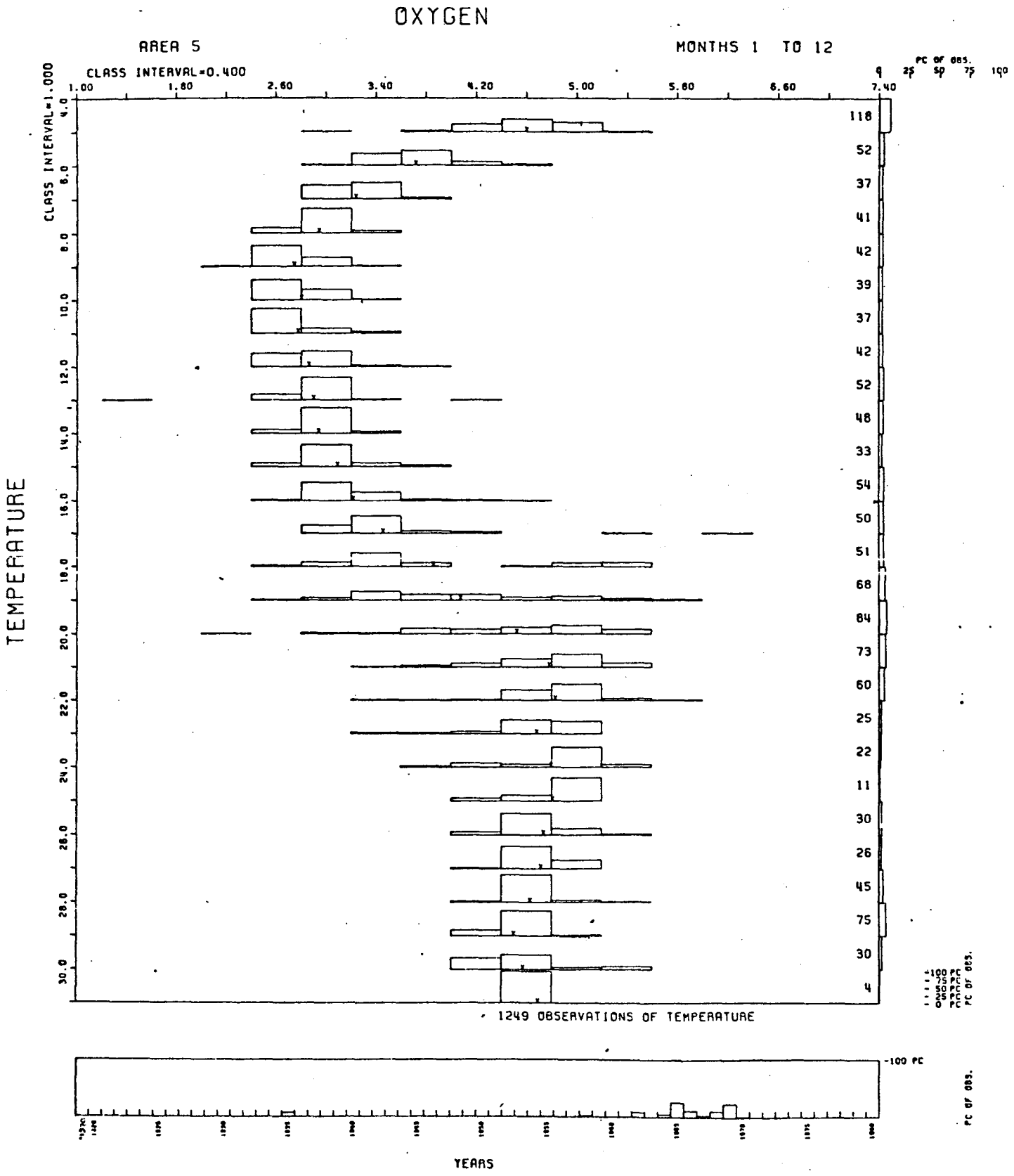

AREA A DEPTH > 200 METERS

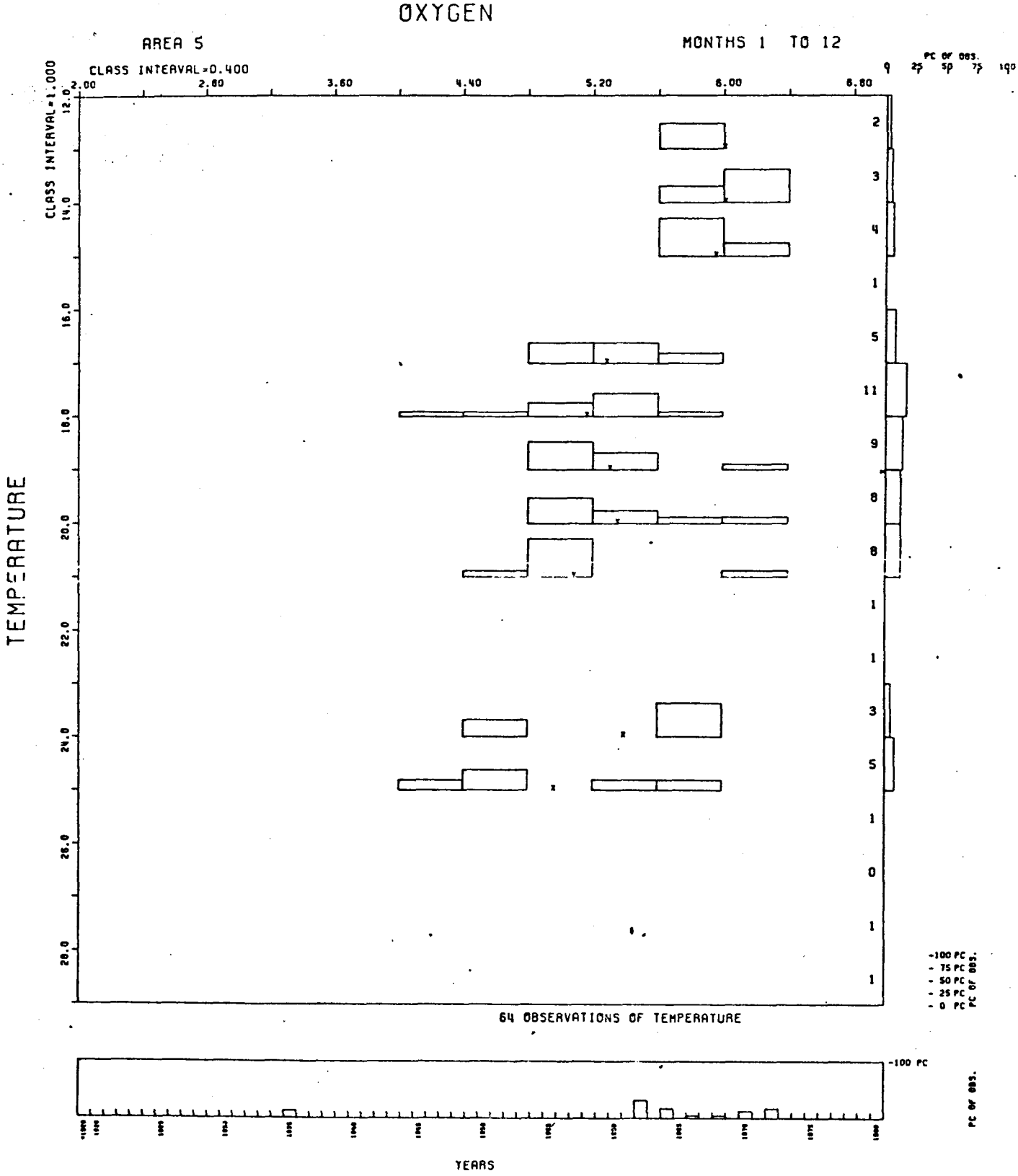

AREA B DEPTH 0-50 METERS

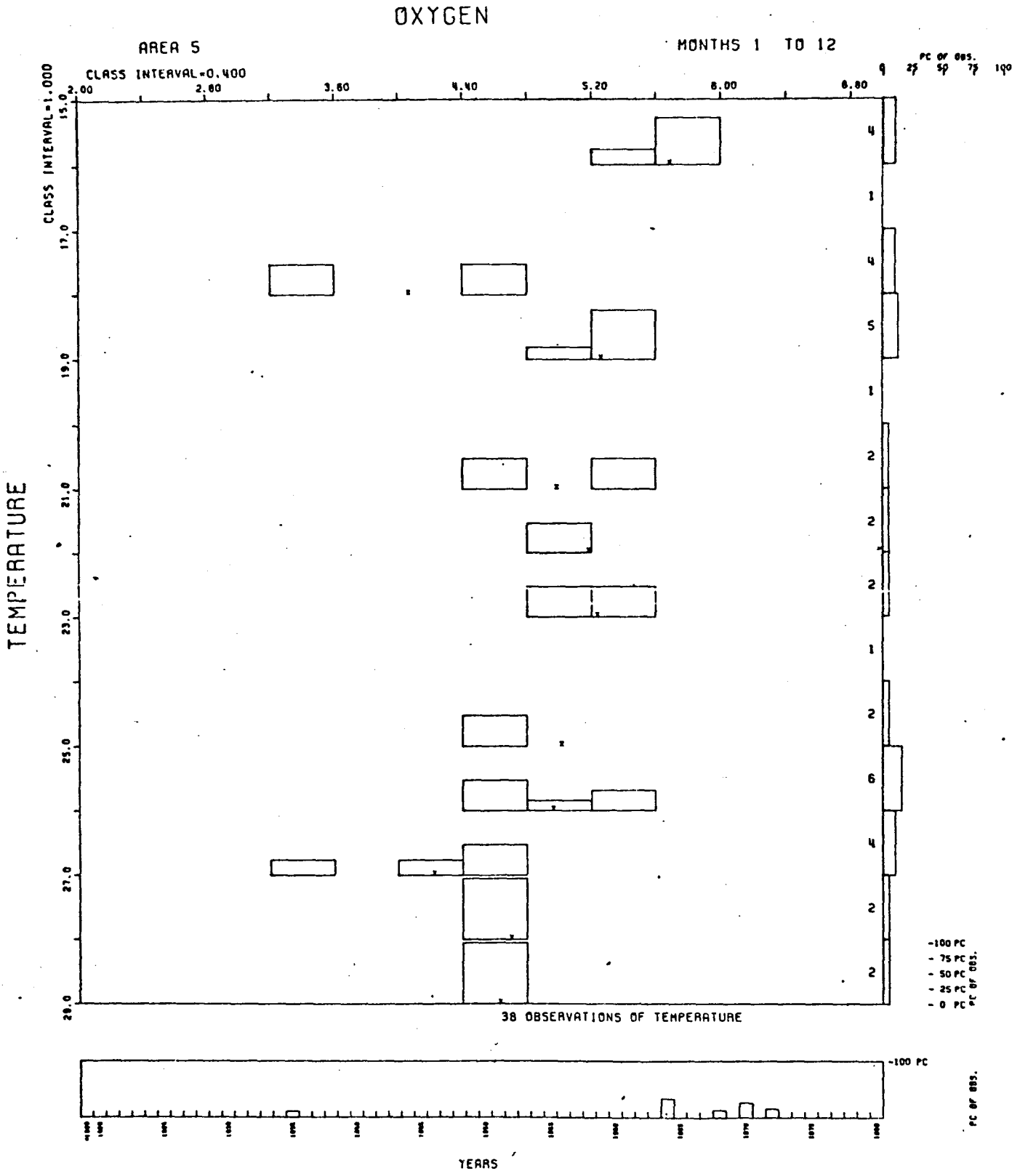

AREA B DEPTH 50-100 METERS

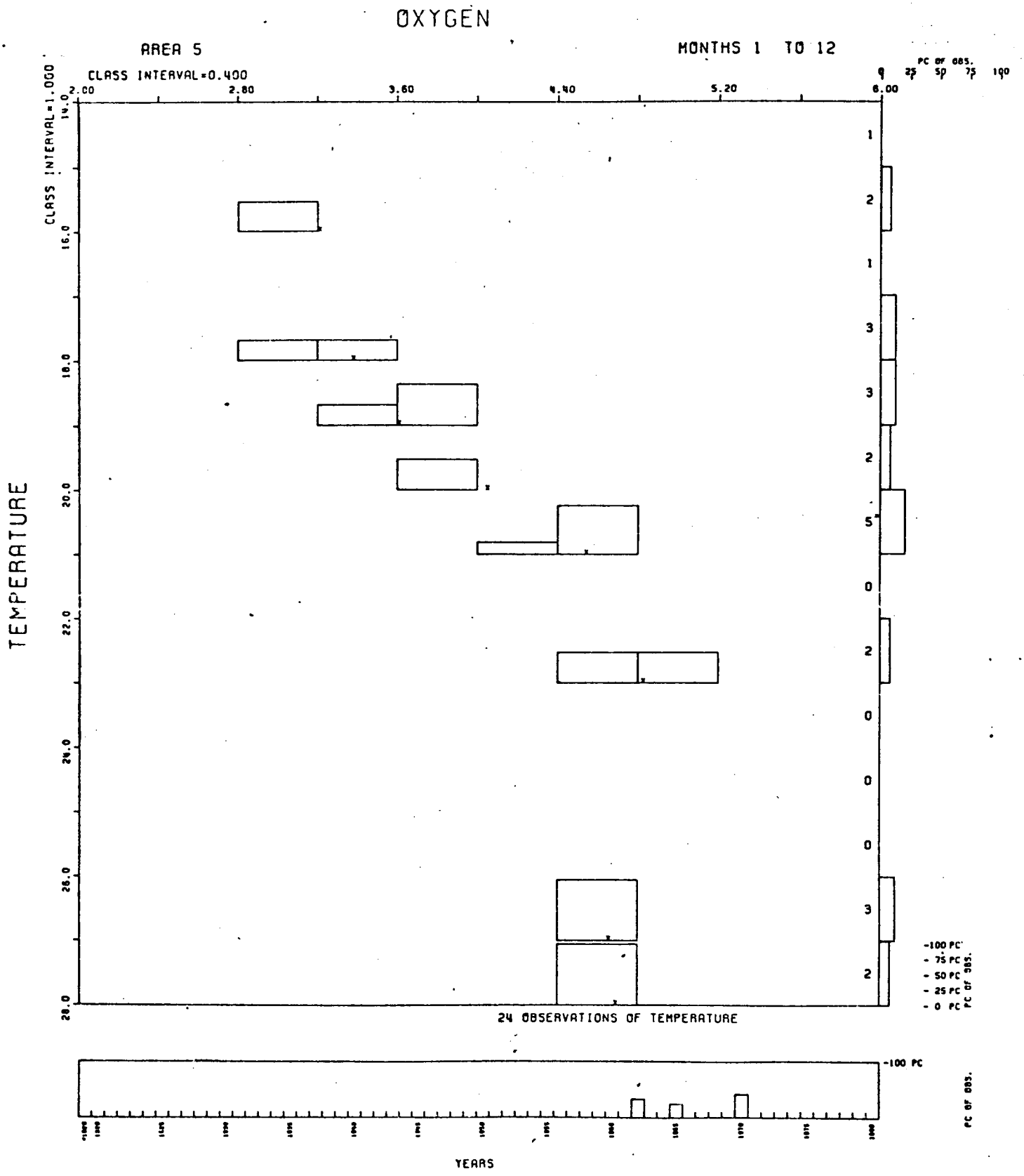

AREA B DEPTH 100-200 METERS

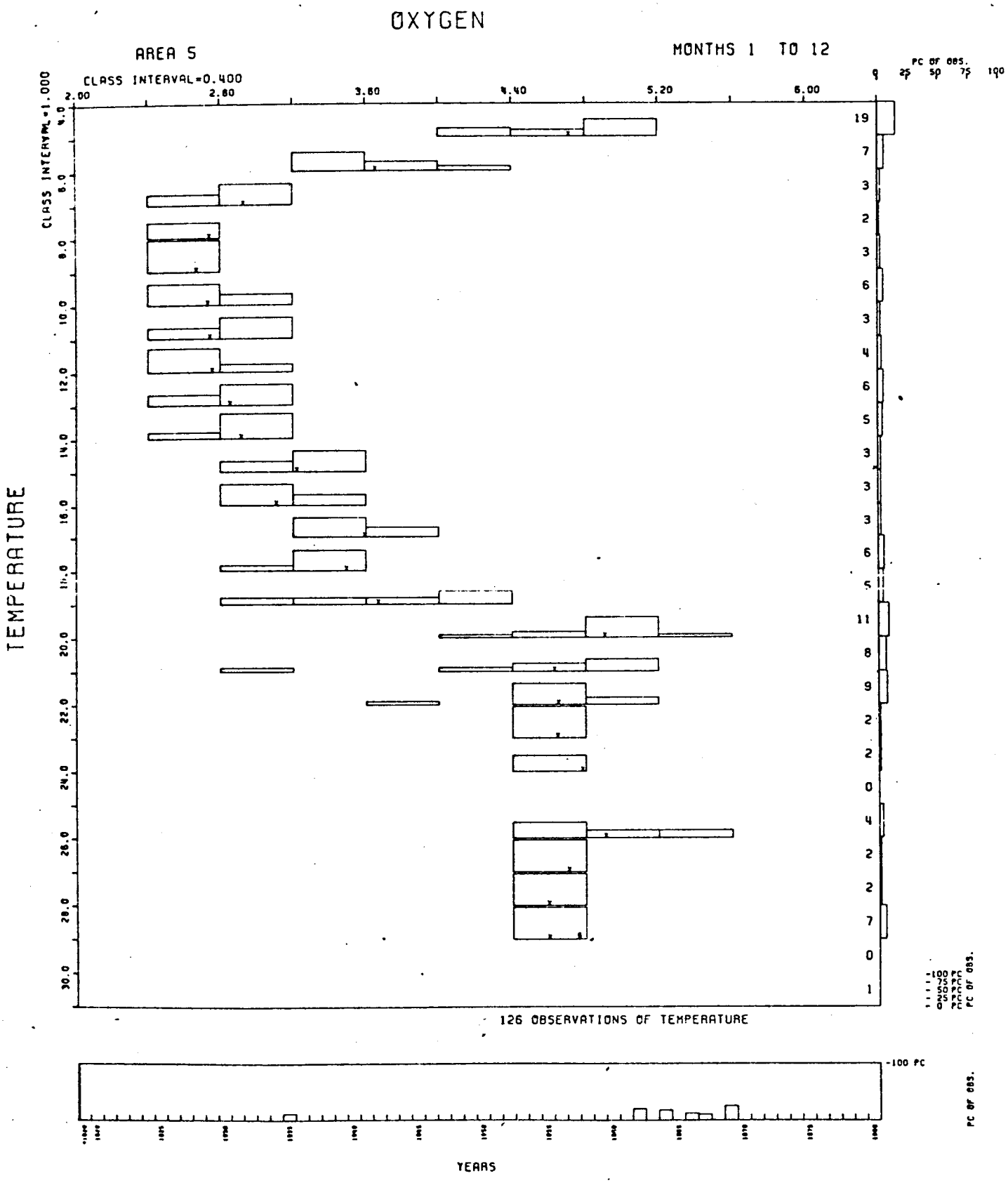

AREA B DEPTH > 200 METERS

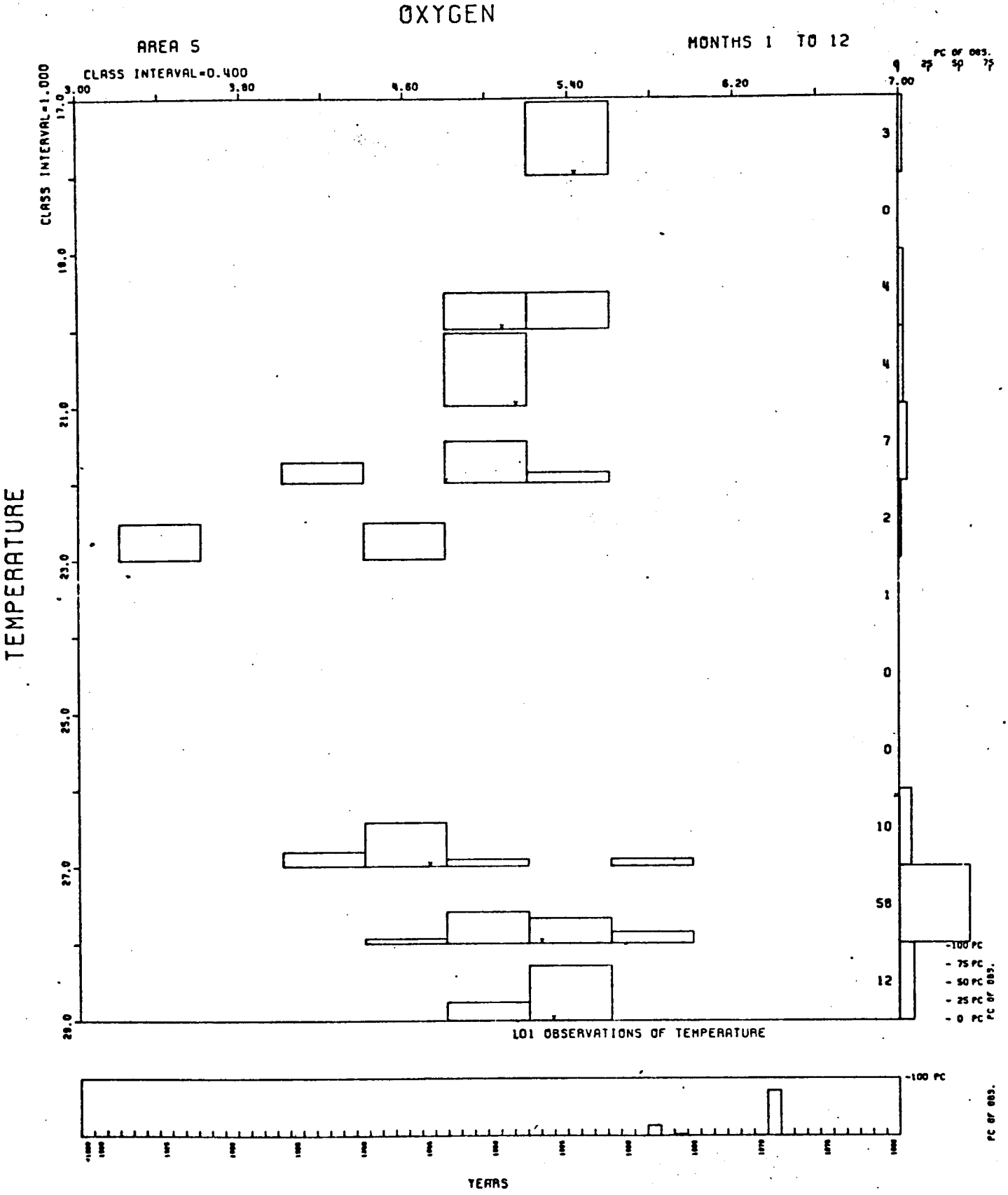

AREA C DEPTH 0-50 METERS

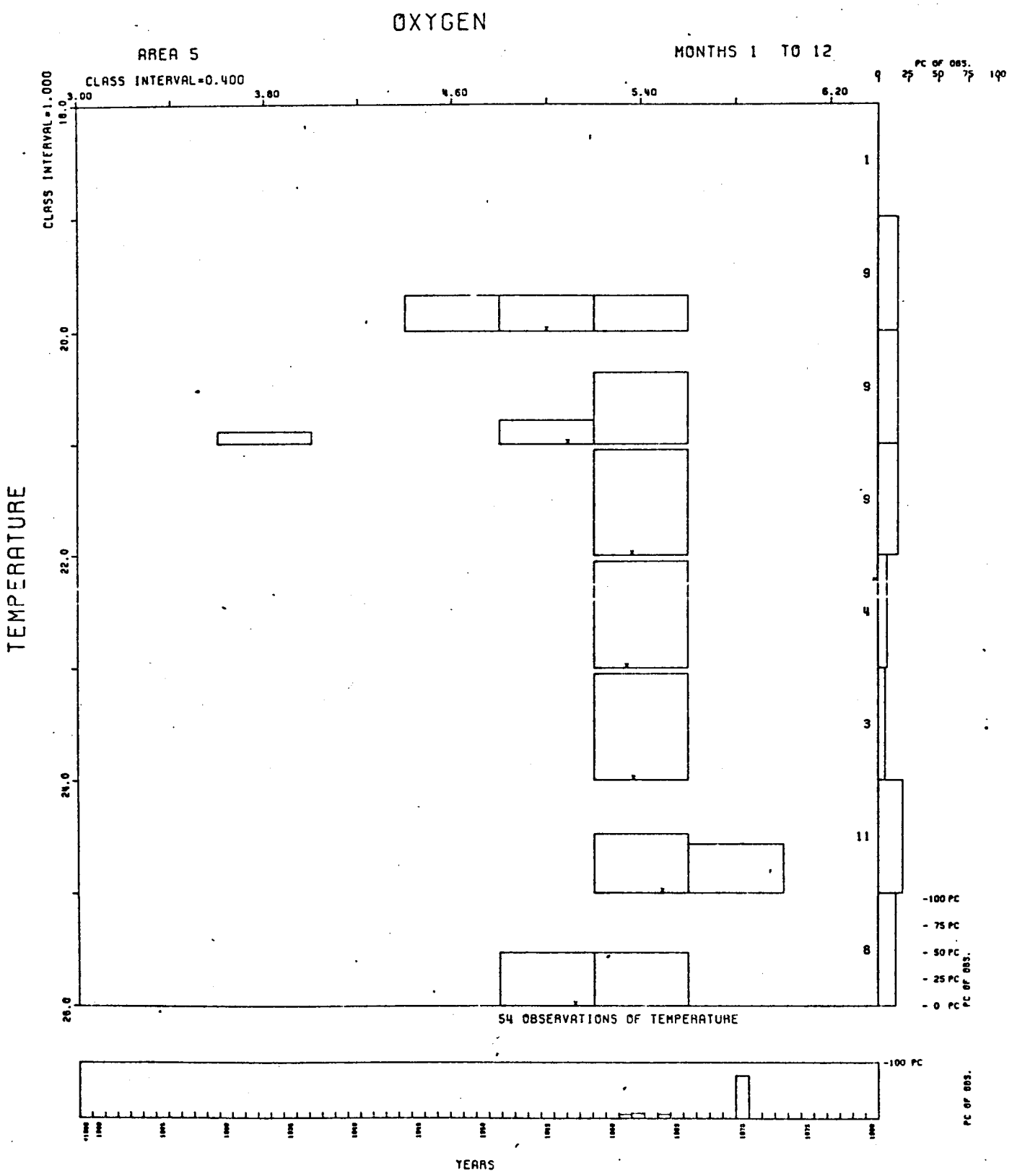

AREA C DEPTH 50-100 METERS

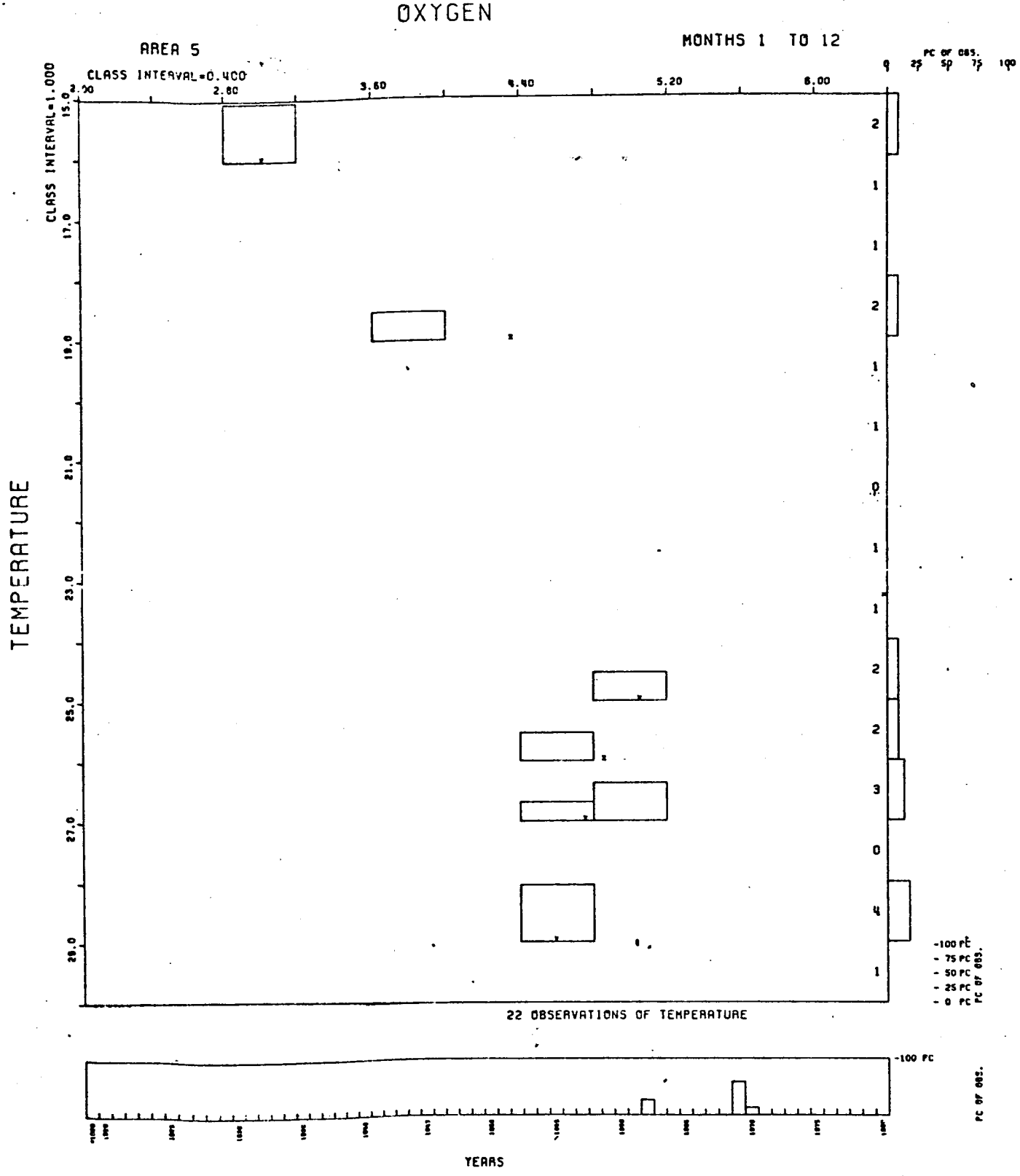

AREA C DEPTH 100-200 METERS

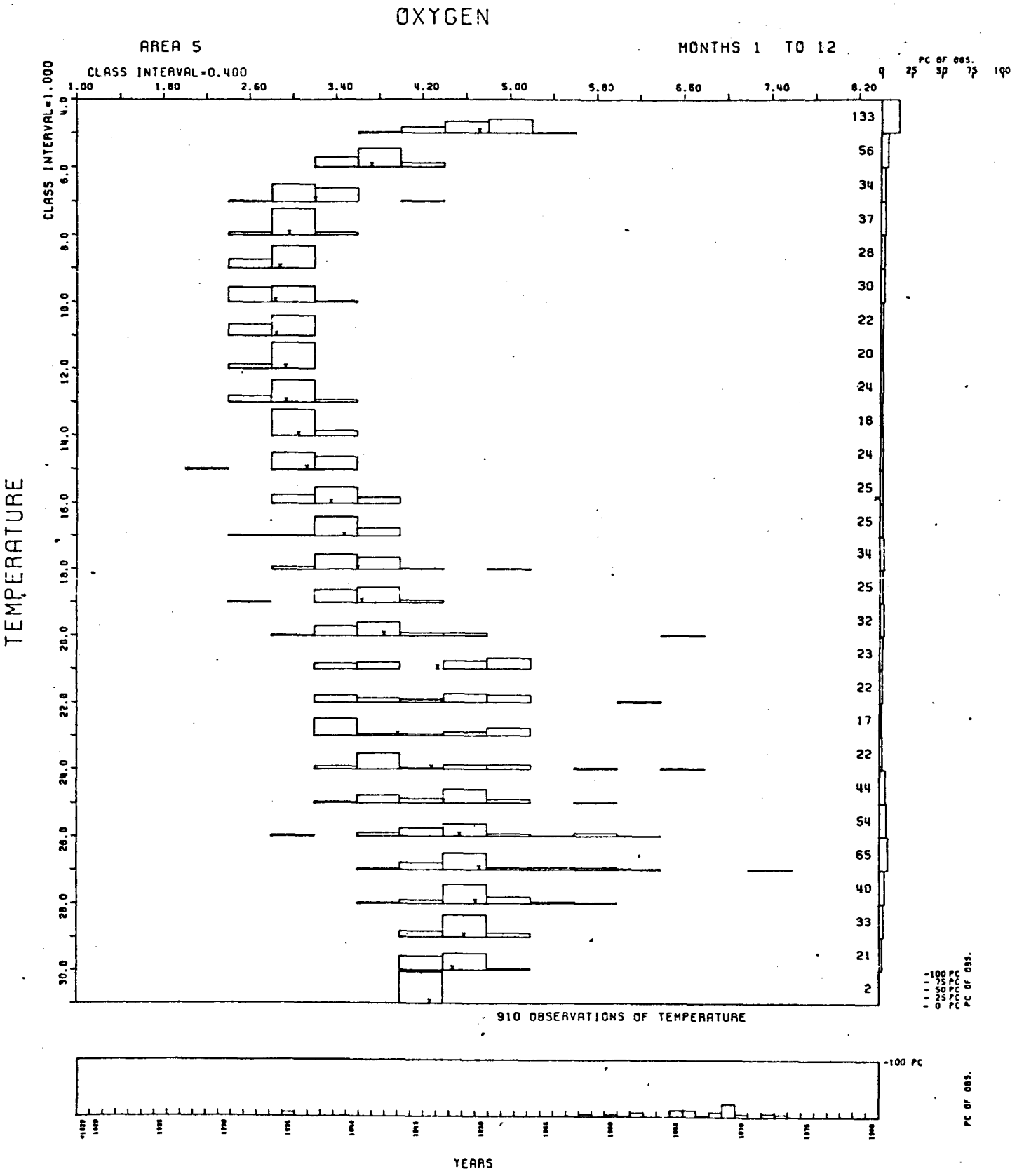

AREA D DEPTH > 200 METERS

Appendix IV

20° C Topographies in the Deep Basin

Charts indicating the depth of 10°C, 15°C, and 20°C isotherm levels as observed during individual and multi-ship operations in the eastern Gulf of Mexico have been produced by NODC. The data-sets include measurements taken by MBT, XBT, STD, and Nansen cast. In each case, a linear interpolation over the layer in which the desired isotherm occurred was performed to obtain the corresponding depth.

The 20°C topographies have been contoured, and are presented in chronological order. Although the type of measurement, i.e., XBT, STD, etc., was indicated on the NODC chart by different symbols, only the station position, irrespective of type, is given on the following charts.

Dynamic topographies relative to 500 db are given also for those cruises in which it was felt that the spatial coverage warranted this presentation. The dynamic height values and station positions were obtained from the NODC listings provided.

Vertical sections of salinity, and oxygen, if available, are provided for those cruises in which specific features were considered. For instance, those sections through the ridge separating the main flow and a detached eddy are considered particularly informative. These sections also include geostrophic velocities relative to 500 db to define the horizontal extent of the current cores.

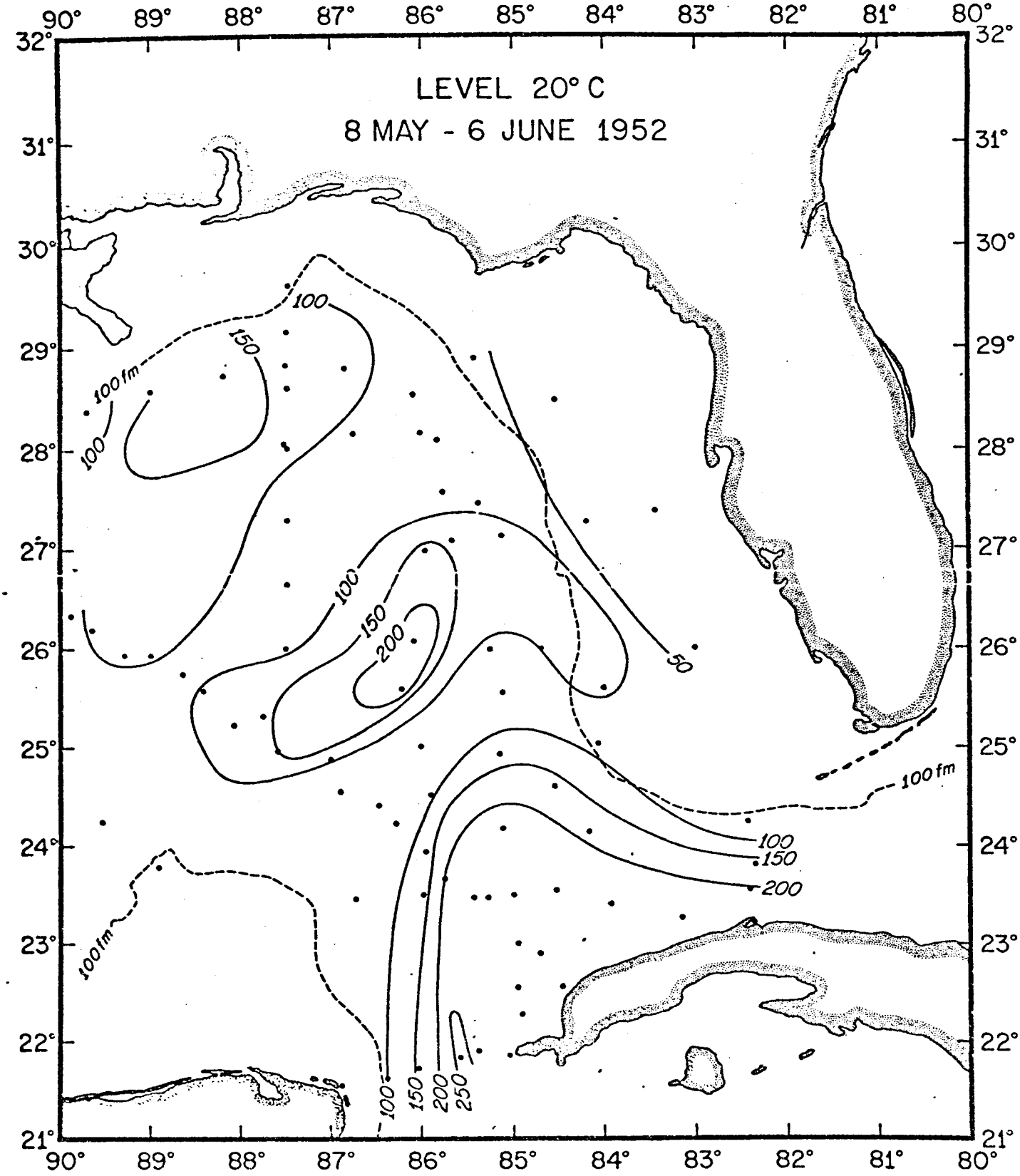
LEVEL 20° C
8 MAY - 6 JUNE 1952
90°
89°
88°
87°
86°
85°
84°
83°
82°
81°
80°
32°
31°
30°
29°
28°
27°
26°
25°
24°
23°
22°
21°
100 fm
100
150
200
250
50

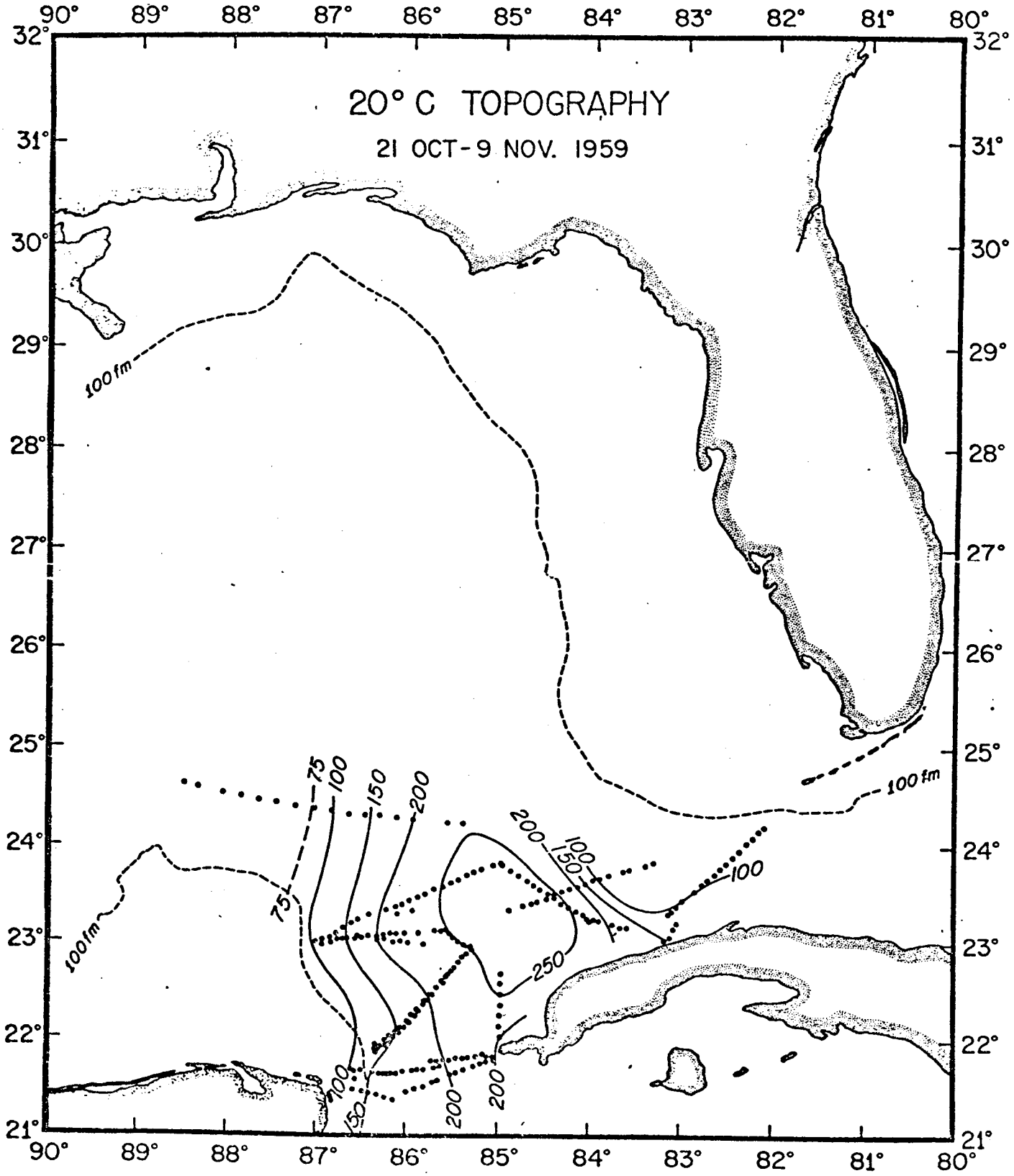
20° C TOPOGRAPHY
21 OCT-9 NOV. 1959
90° 89° 88° 87° 86° 85° 84° 83° 82° 81° 80°
32° 31° 30° 29° 28° 27° 26° 25° 24° 23° 22° 21°
100 fm
75
100
150
200
250

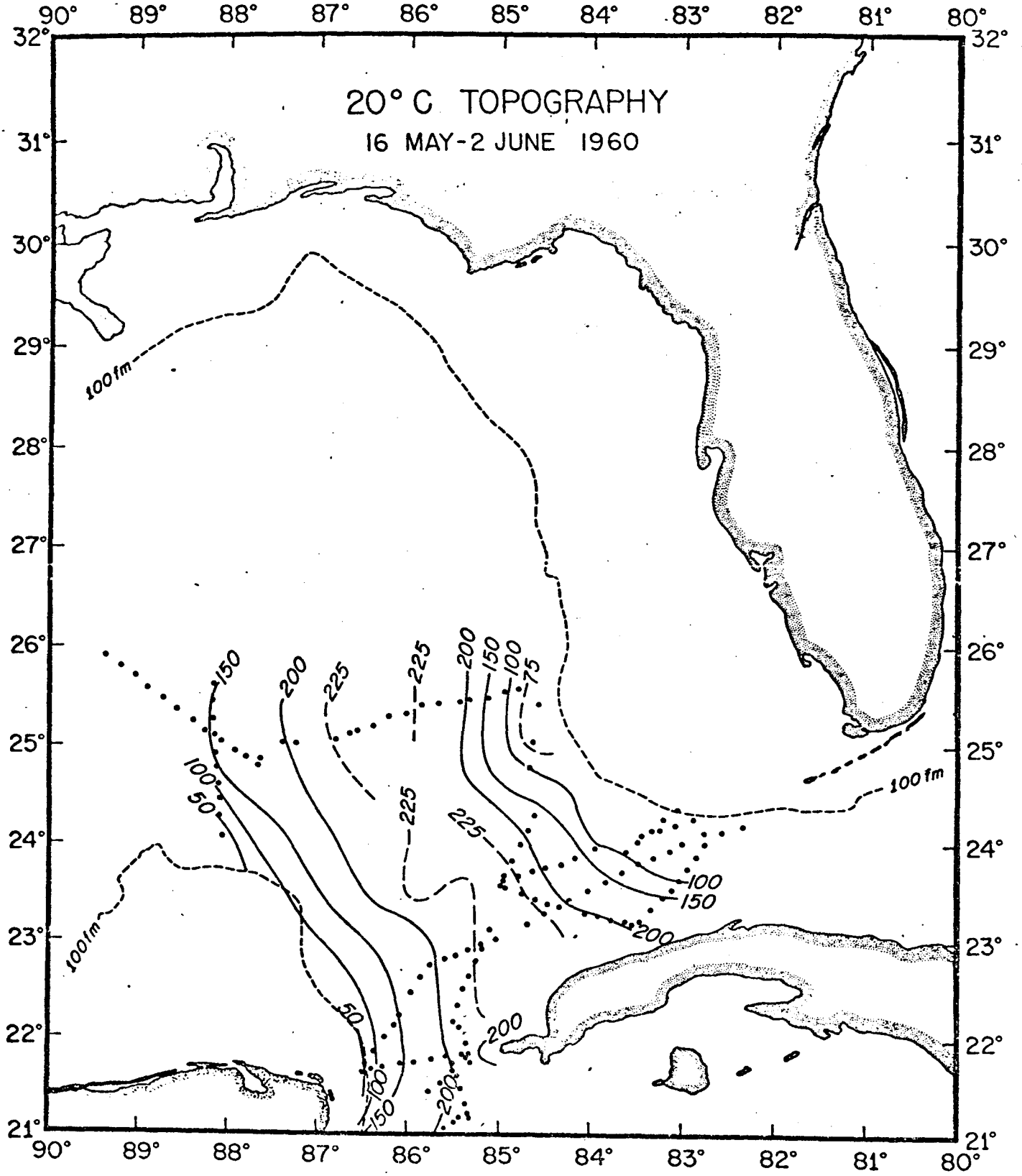
20° C TOPOGRAPHY
16 MAY-2 JUNE 1960
90° 89° 88° 87° 86° 85° 84° 83° 82° 81° 80°
32° 31° 30° 29° 28° 27° 26° 25° 24° 23° 22° 21°
100 fm
150
200
225
225
200
150
100
75
100
50
225
225
100
150
200
100 fm
100 fm
50
100
150
200
200

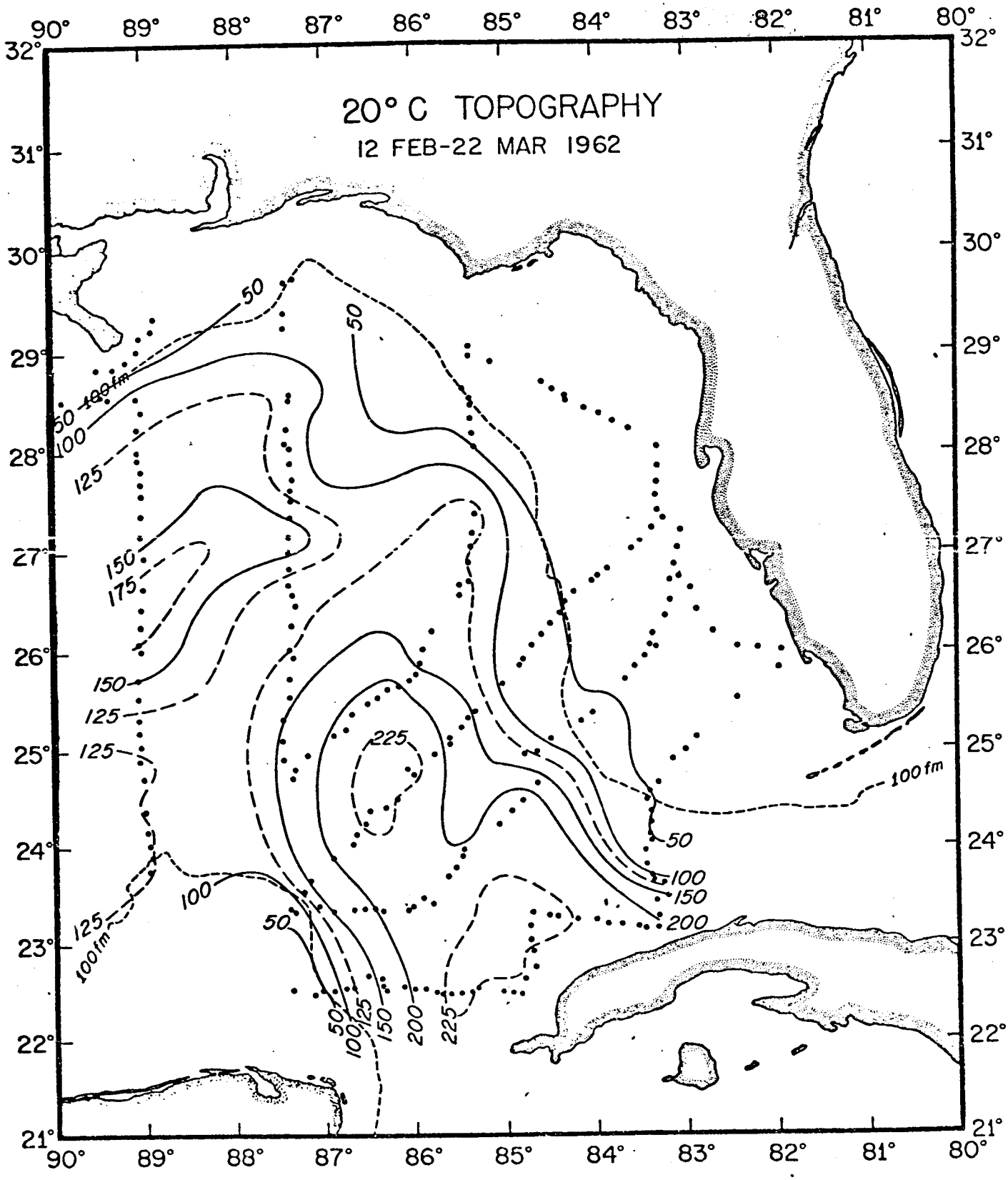
20° C TOPOGRAPHY
12 FEB-22 MAR 1962
90° 89° 88° 87° 86° 85° 84° 83° 82° 81° 80°
32° 31° 30° 29° 28° 27° 26° 25° 24° 23° 22° 21°
50
100 fm
125
150
175
225
100
200

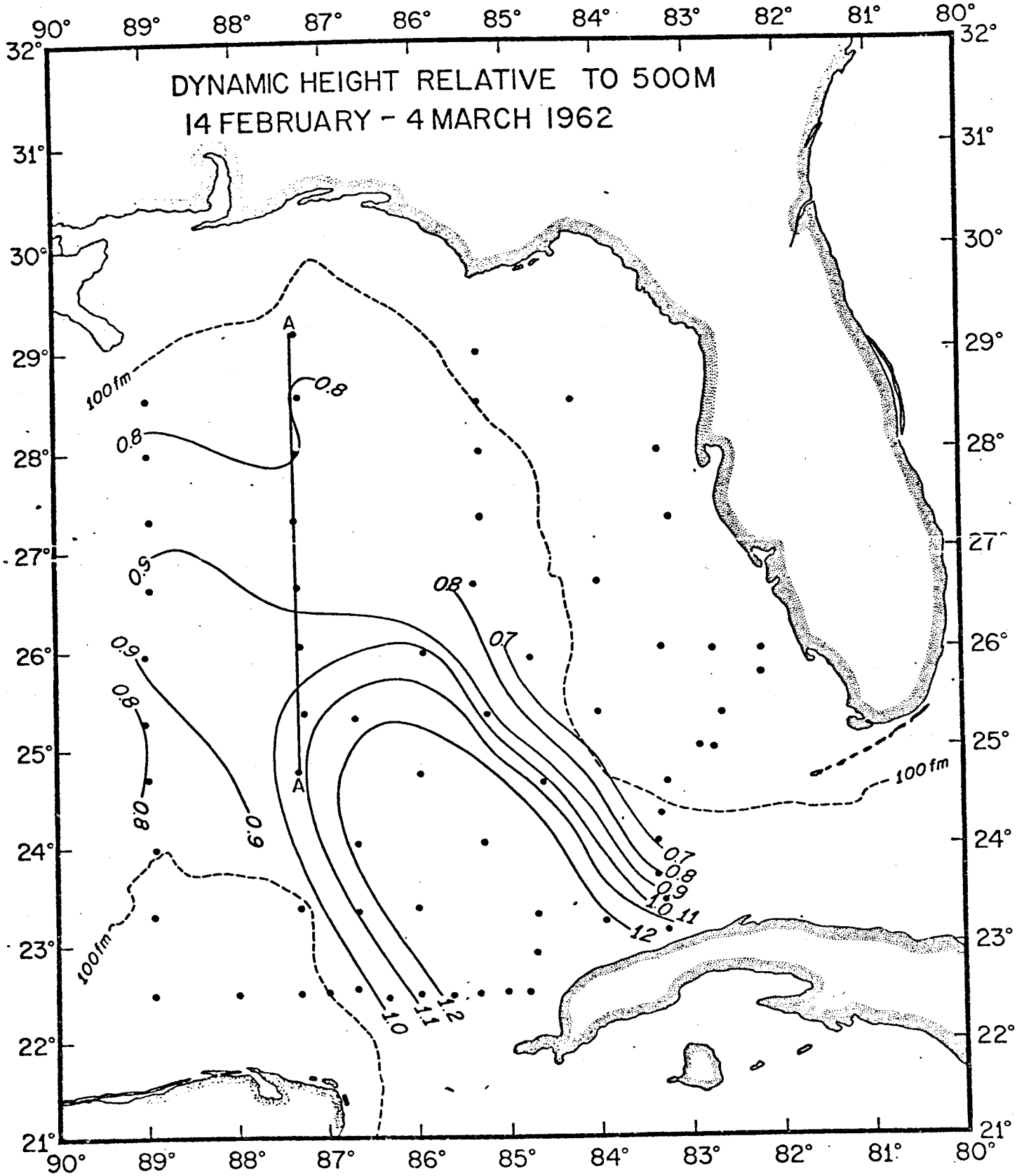
DYNAMIC HEIGHT RELATIVE TO 500M
14 FEBRUARY - 4 MARCH 1962
90° 89° 88° 87° 86° 85° 84° 83° 82° 81° 80°
32° 31° 30° 29° 28° 27° 26° 25° 24° 23° 22° 21°
A
A
100 fm
0.8
0.9
0.7
1.0
1.1
1.2

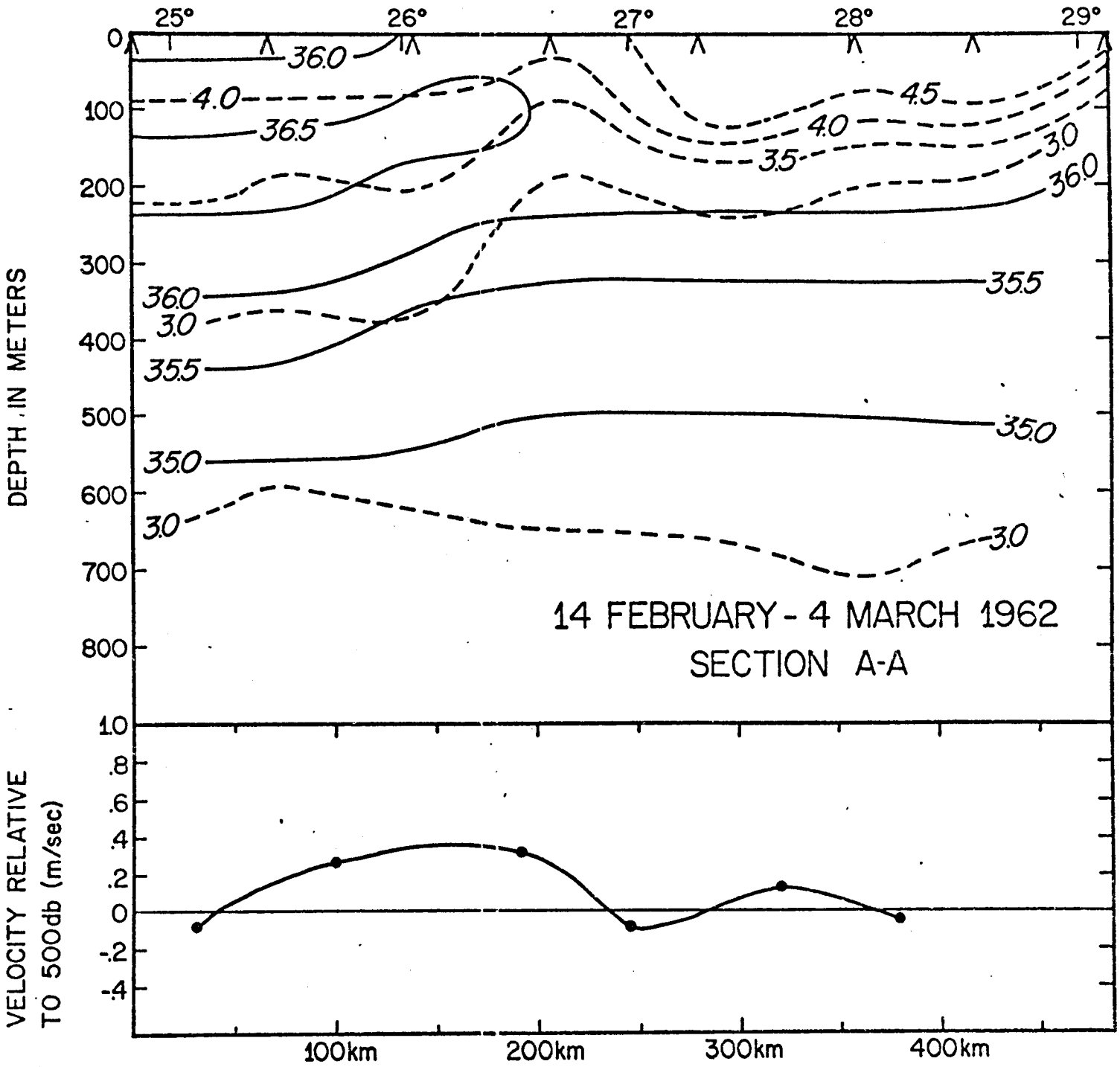
25°
26°
27°
28°
29°
0
100
200
300
400
500
600
700
800
DEPTH IN METERS
36.0
4.0
36.5
4.5
4.0
3.5
3.0
36.0
36.0
3.0
35.5
35.5
35.0
3.0
3.0
14 FEBRUARY - 4 MARCH 1962
SECTION A-A
1.0
.8
.6
.4
.2
0
-.2
-.4
VELOCITY RELATIVE
TO 500db (m/sec)
100km
200km
300km
400km

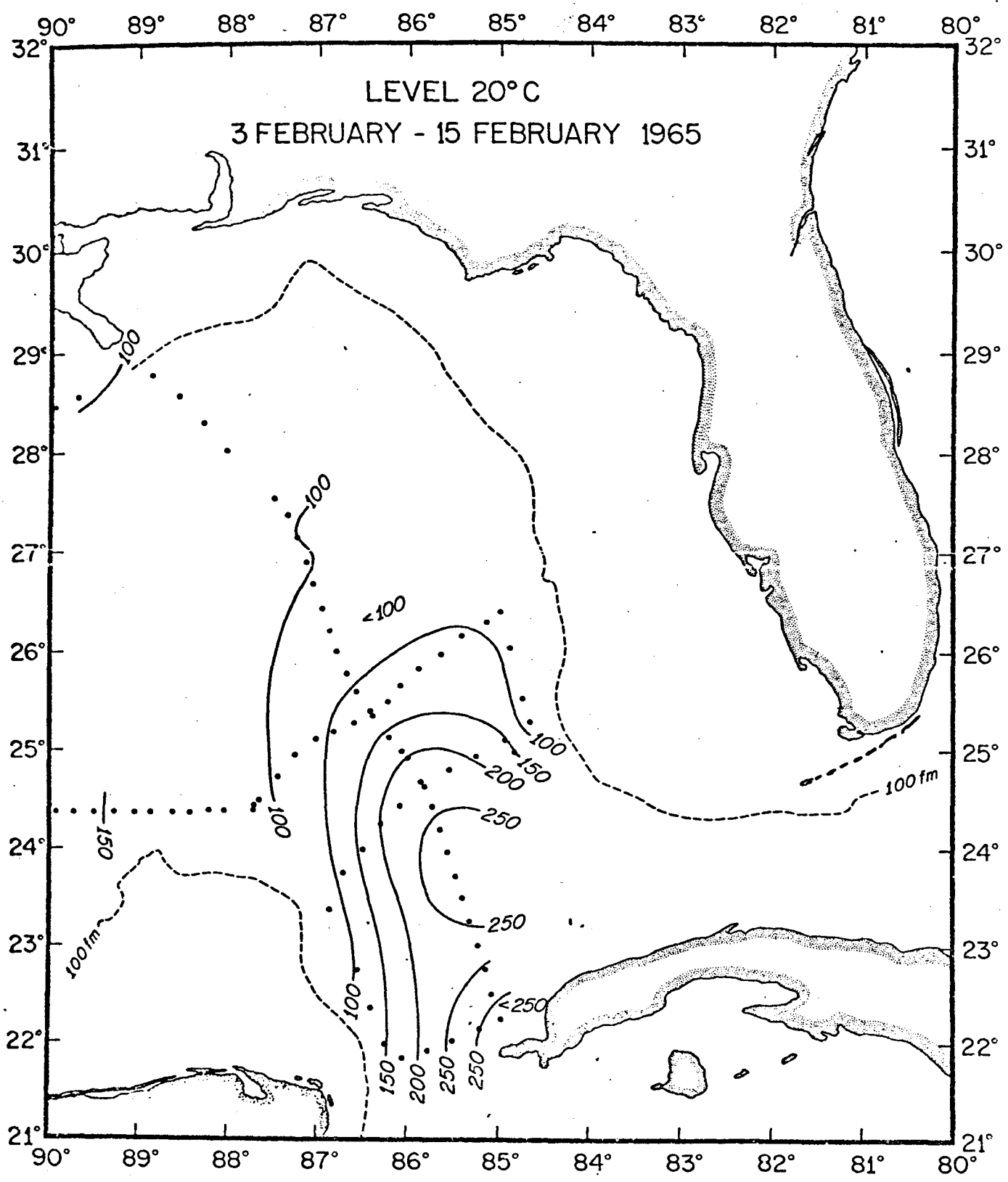
LEVEL 20° C
3 FEBRUARY - 15 FEBRUARY 1965
90° 89° 88° 87° 86° 85° 84° 83° 82° 81° 80°
32° 31° 30° 29° 28° 27° 26° 25° 24° 23° 22° 21°
100
100
100
100
150
200
250
250
250
250
100 fm
100 fm

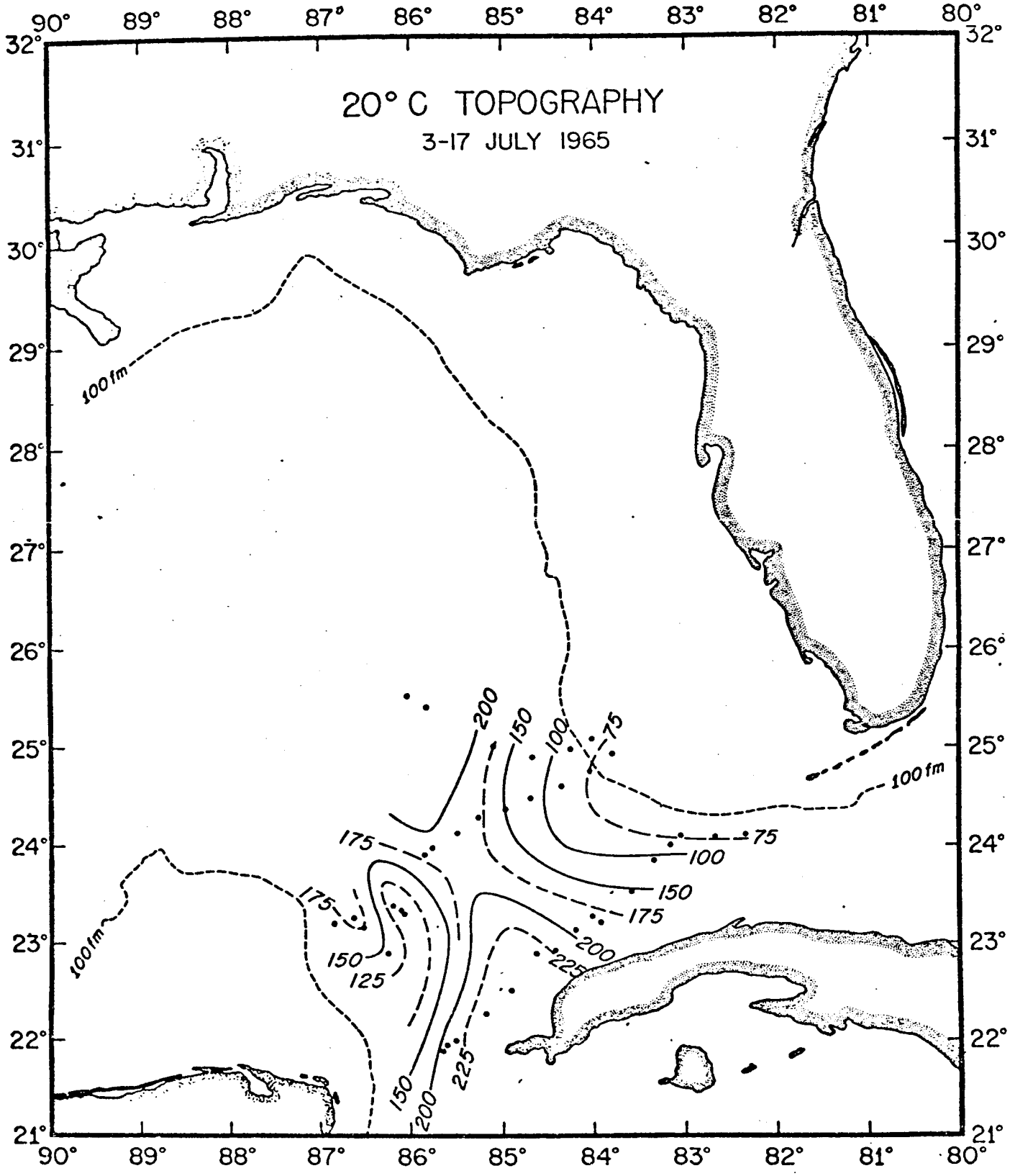
20° C TOPOGRAPHY
3-17 JULY 1965
90° 89° 88° 87° 86° 85° 84° 83° 82° 81° 80°
32° 31° 30° 29° 28° 27° 26° 25° 24° 23° 22° 21°
100 fm
200
150
100
75
175
225
125

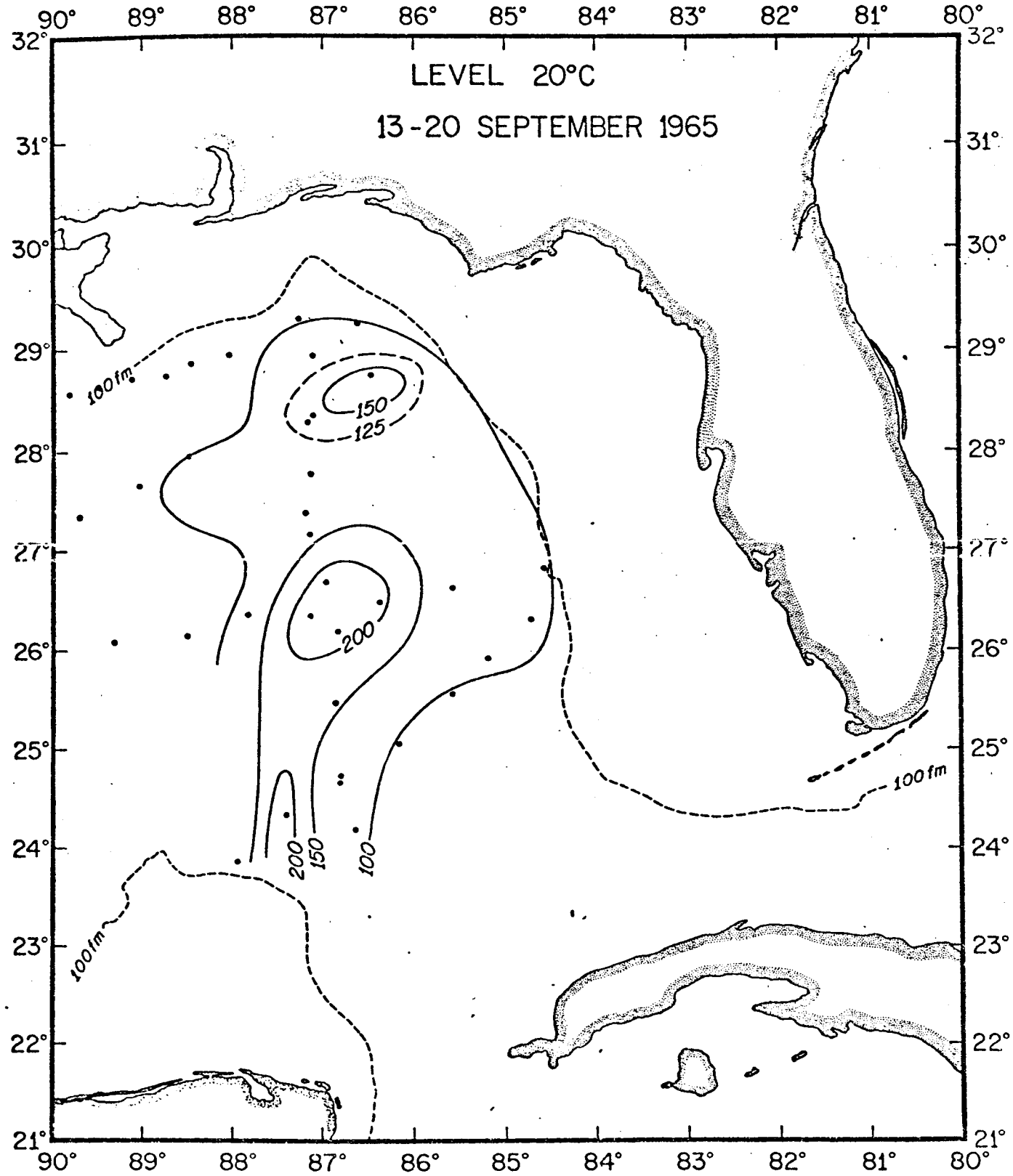
LEVEL 20°C
13-20 SEPTEMBER 1965
90° 89° 88° 87° 86° 85° 84° 83° 82° 81° 80°
32° 31° 30° 29° 28° 27° 26° 25° 24° 23° 22° 21°
100 fm
150
125
200
200
150
100
100 fm
100 fm

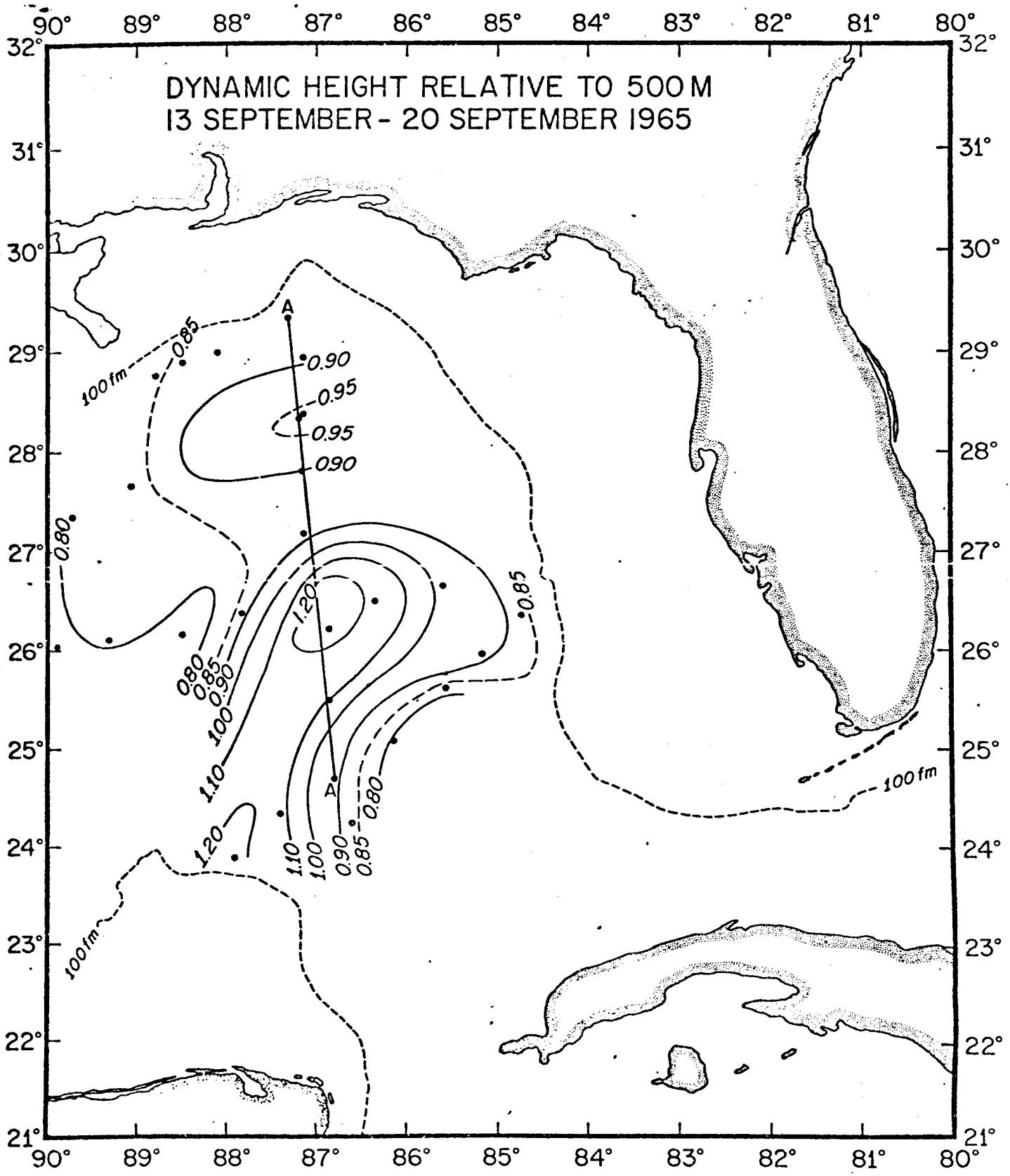
DYNAMIC HEIGHT RELATIVE TO 500 M
13 SEPTEMBER - 20 SEPTEMBER 1965
90°
89°
88°
87°
86°
85°
84°
83°
82°
81°
80°
32°
31°
30°
29°
28°
27°
26°
25°
24°
23°
22°
21°
A
A
0.90
0.95
0.95
0.90
0.85
100 fm
0.80
0.80
0.85
0.90
100
1.10
1.20
1.20
1.10
1.00
0.90
0.85
0.80
0.85
100 fm
100 fm

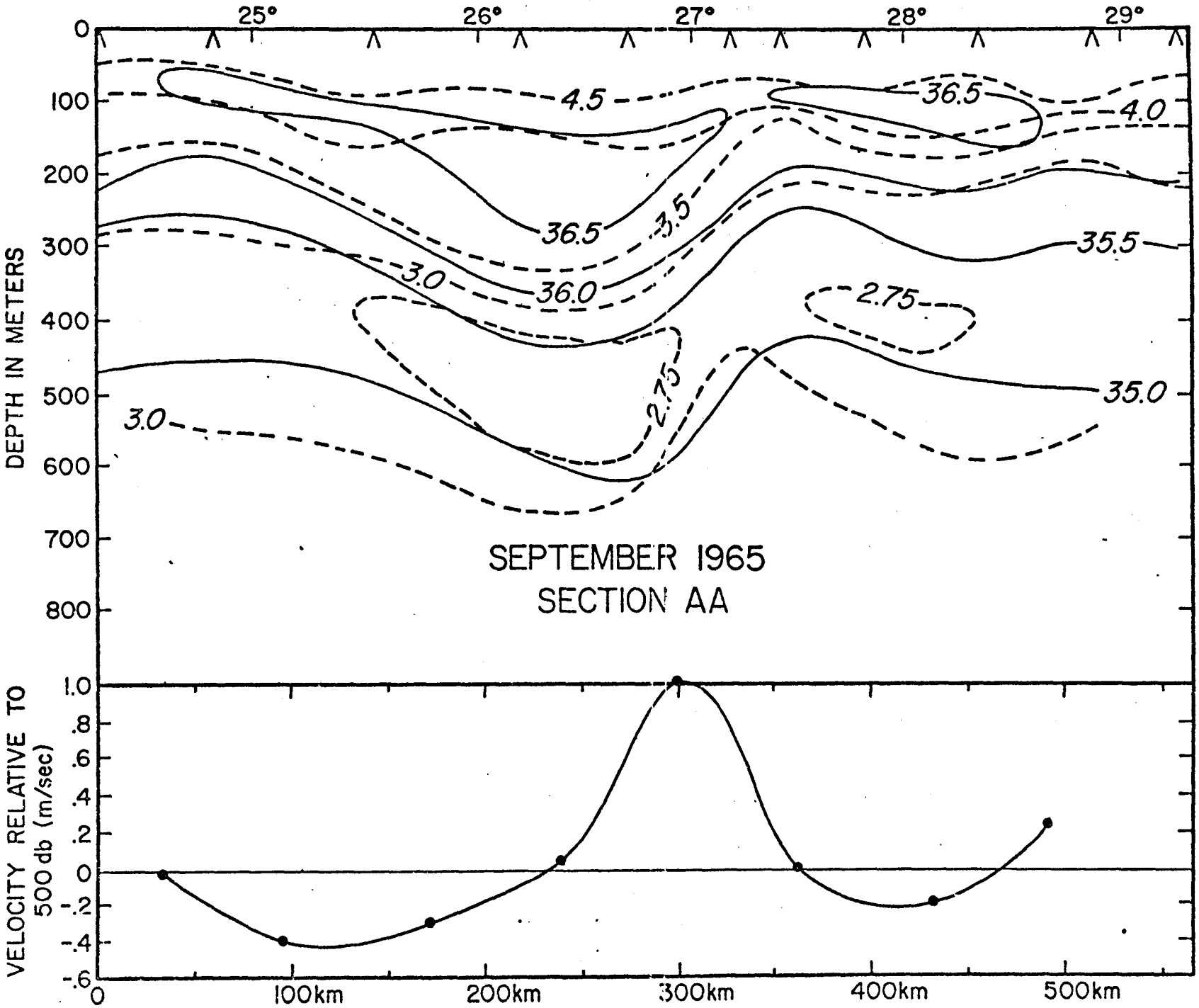
25°
26°
27°
28°
29°
0
100
200
300
400
500
600
700
800
DEPTH IN METERS
4.5
36.5
4.0
36.5
3.5
35.5
3.0
36.0
2.75
2.75
35.0
3.0
SEPTEMBER 1965
SECTION AA
1.0
.8
.6
.4
.2
0
-.2
-.4
-.6
VELOCITY RELATIVE TO 500 db (m/sec)
0
100km
200km
300km
400km
500km

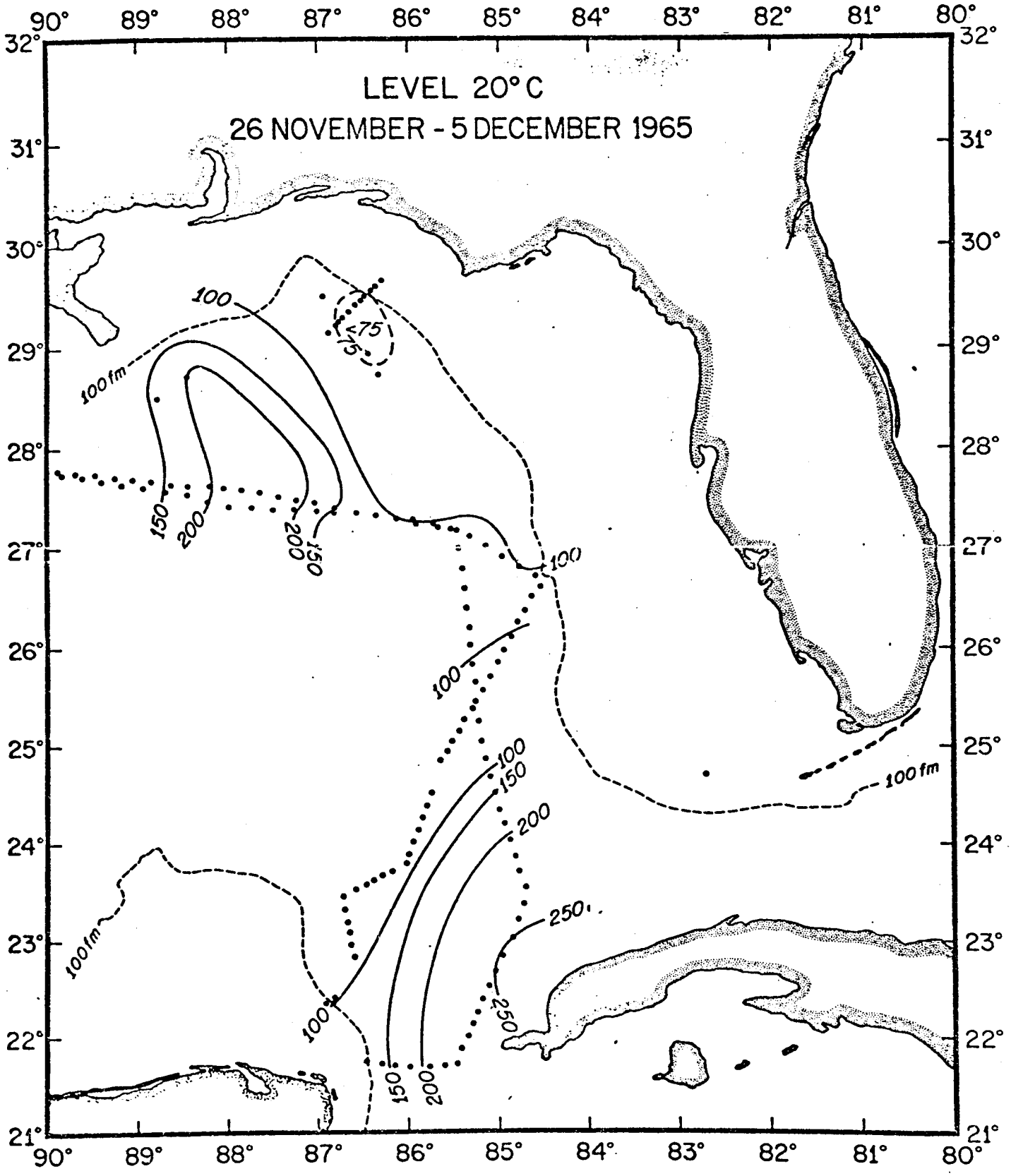
LEVEL 20° C
26 NOVEMBER - 5 DECEMBER 1965
90° 89° 88° 87° 86° 85° 84° 83° 82° 81° 80°
32° 31° 30° 29° 28° 27° 26° 25° 24° 23° 22° 21°
100
100 fm
75
150
200
250

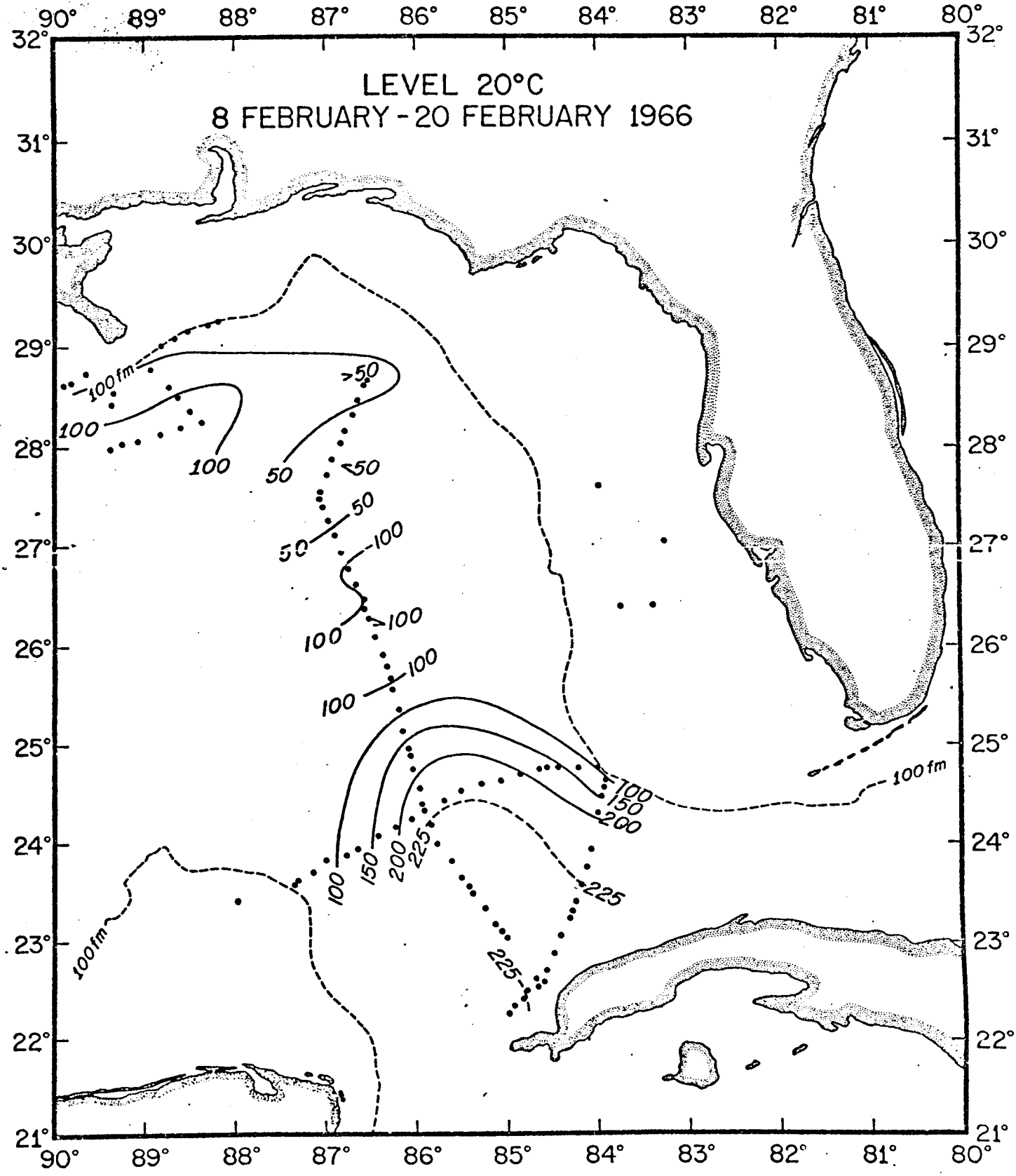
LEVEL 20°C
8 FEBRUARY - 20 FEBRUARY 1966
90°
89°
88°
87°
86°
85°
84°
83°
82°
81°
80°
32°
31°
30°
29°
28°
27°
26°
25°
24°
23°
22°
21°
100 fm
>50
100
50
<50
100
150
200
225

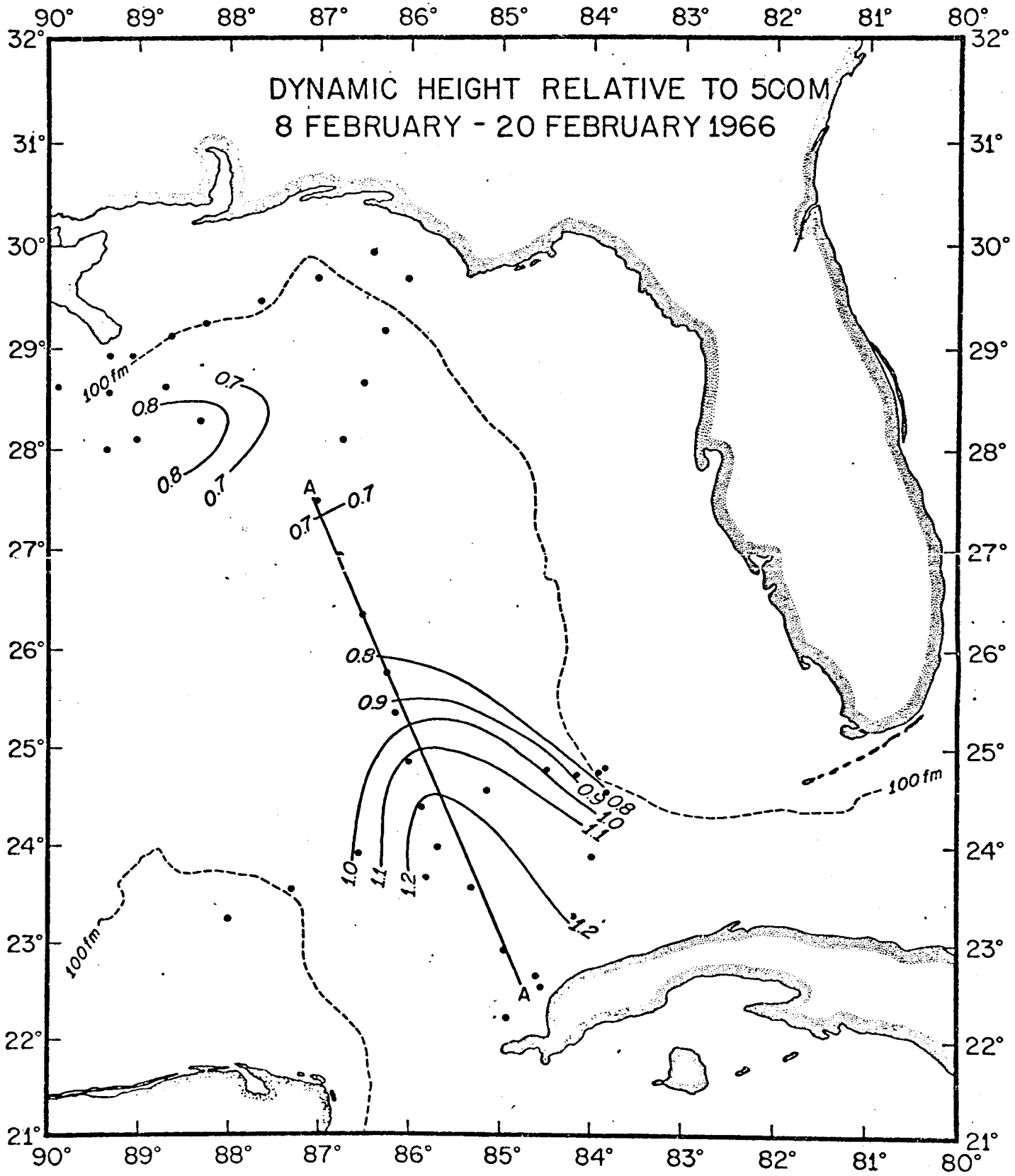
DYNAMIC HEIGHT RELATIVE TO 500M
8 FEBRUARY - 20 FEBRUARY 1966
90° 89° 88° 87° 86° 85° 84° 83° 82° 81° 80°
32° 31° 30° 29° 28° 27° 26° 25° 24° 23° 22° 21°
100 fm
0.7
0.8
0.8
0.7
A
0.7
0.7
0.8
0.9
1.0
1.1
1.2
0.9
0.8
1.0
1.1
1.2
A
100 fm
100 fm

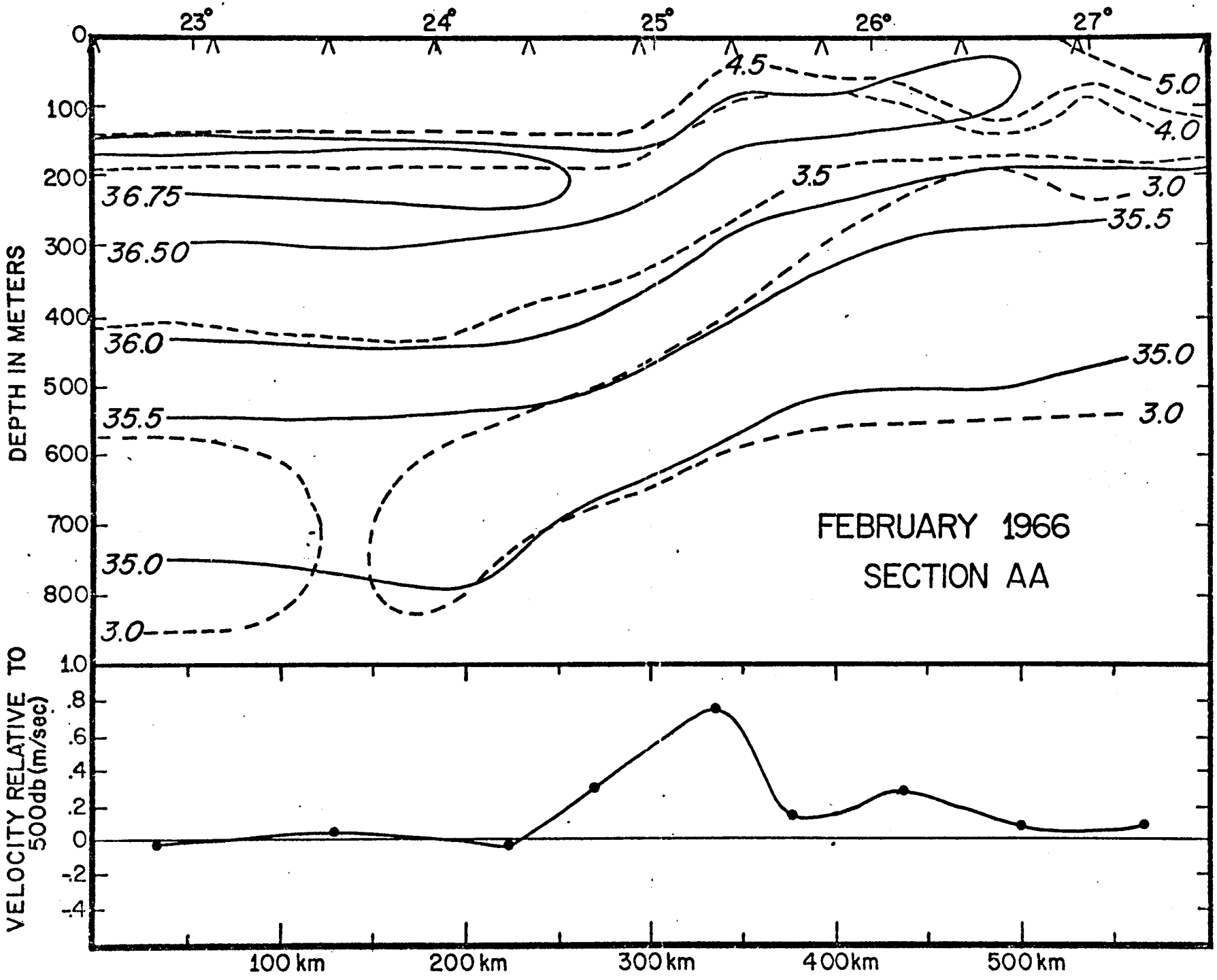
23°
24°
25°
26°
27°
0
100
200
300
400
500
600
700
800
1.0
DEPTH IN METERS
4.5
5.0
4.0
3.5
3.0
35.5
36.75
36.50
36.0
35.5
35.0
3.0
35.0
3.0
FEBRUARY 1966
SECTION AA
VELOCITY RELATIVE TO 500db (m/sec)
.8
.6
.4
.2
0
-.2
-.4
100 km
200 km
300 km
400 km
500 km

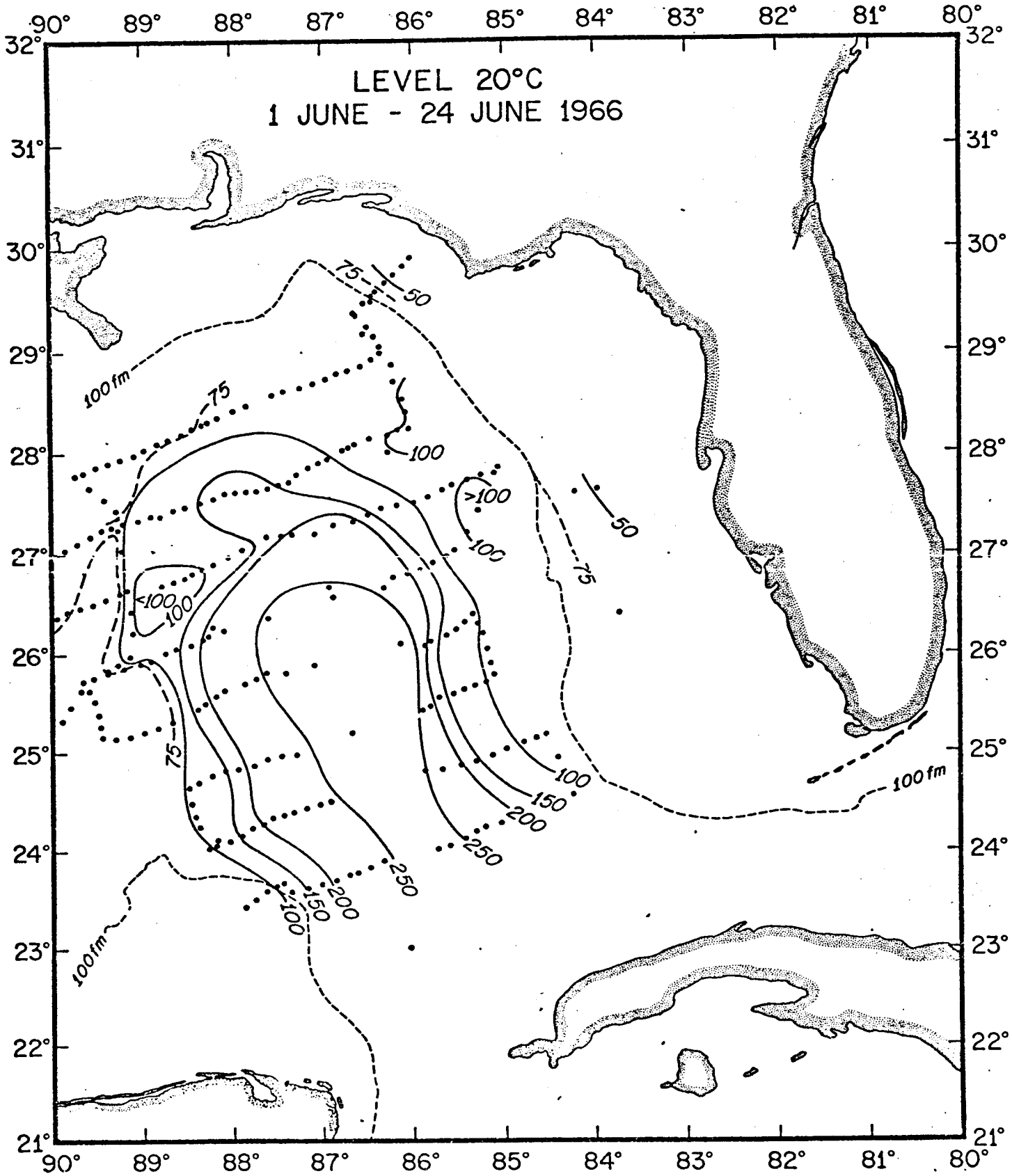
LEVEL 20°C
1 JUNE - 24 JUNE 1966
90° 89° 88° 87° 86° 85° 84° 83° 82° 81° 80°
32° 31° 30° 29° 28° 27° 26° 25° 24° 23° 22° 21°
100 fm
75
50
100
>100
<100
150
200
250

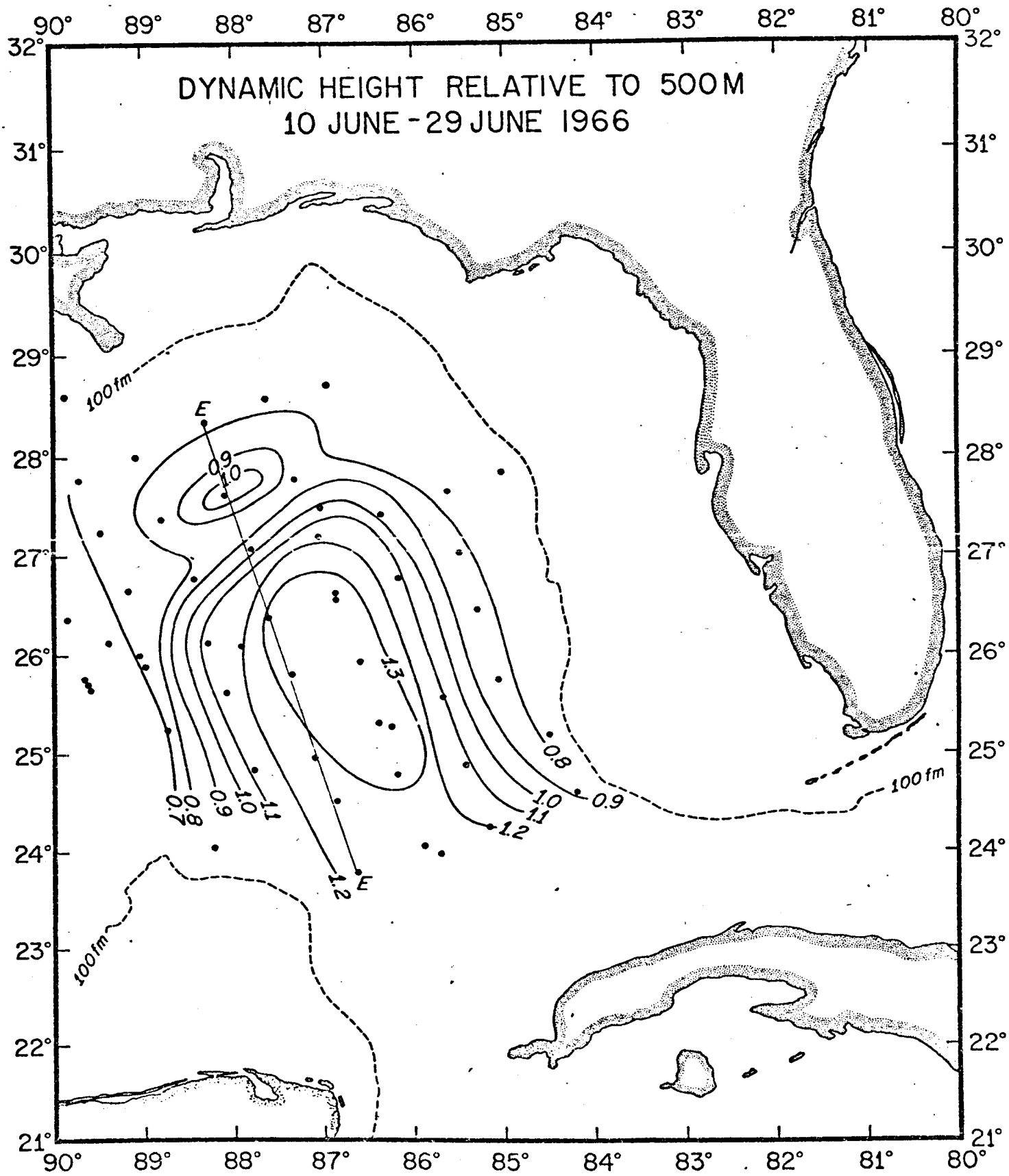
DYNAMIC HEIGHT RELATIVE TO 500M
10 JUNE - 29 JUNE 1966
90° 89° 88° 87° 86° 85° 84° 83° 82° 81° 80°
32° 31° 30° 29° 28° 27° 26° 25° 24° 23° 22° 21°
100 fm
E
0.9
1.0
0.7
0.8
0.9
1.0
1.1
1.2
1.3
0.8
0.9
1.0
1.1
1.2
E
100 fm
100 fm

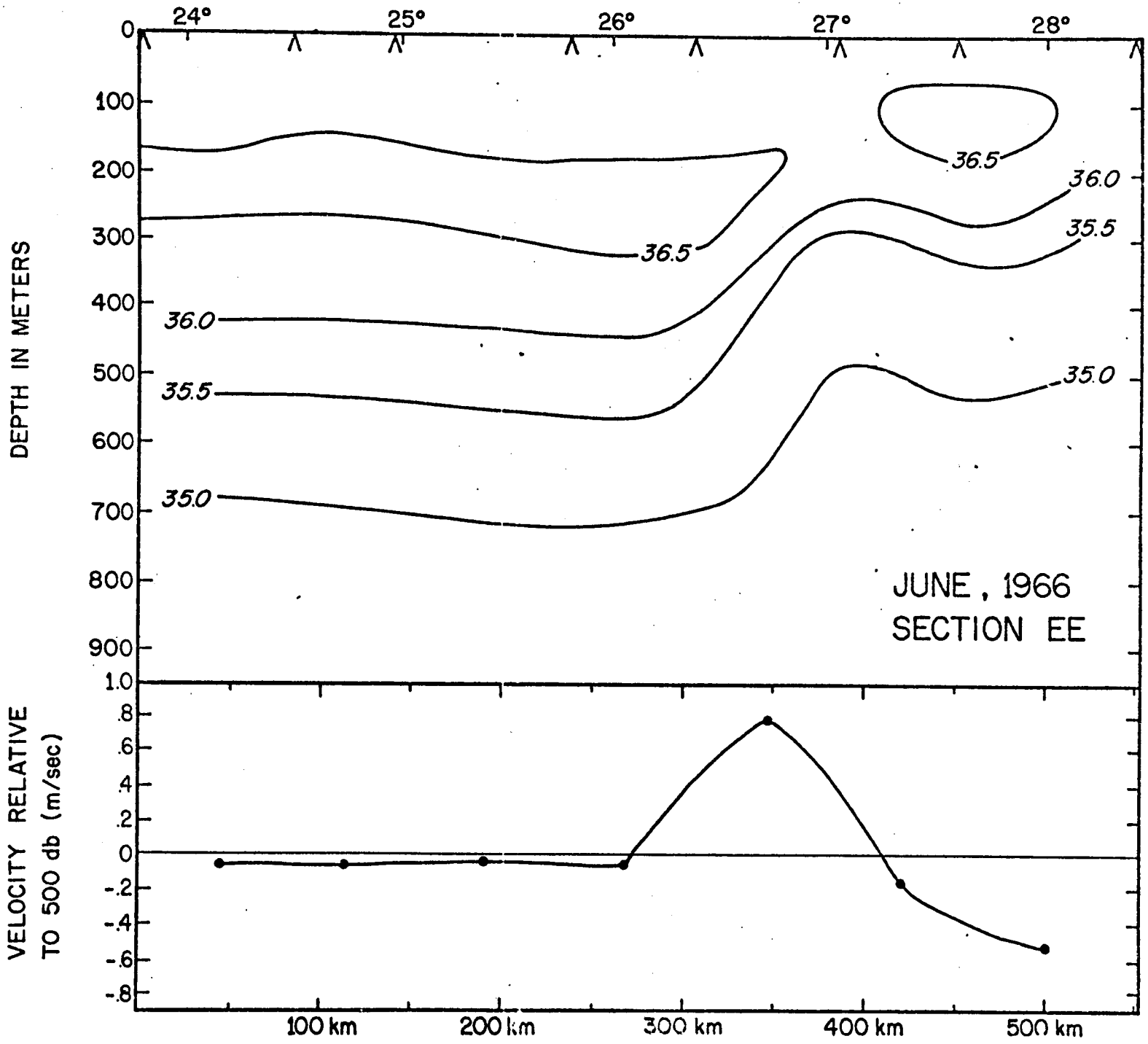
24°
25°
26°
27°
28°
0
100
200
300
400
500
600
700
800
900
1.0
DEPTH IN METERS
36.5
36.0
35.5
35.0
JUNE, 1966
SECTION EE
VELOCITY RELATIVE
TO 500 db (m/sec)
.8
.6
.4
.2
0
-.2
-.4
-.6
-.8
100 km
200 km
300 km
400 km
500 km

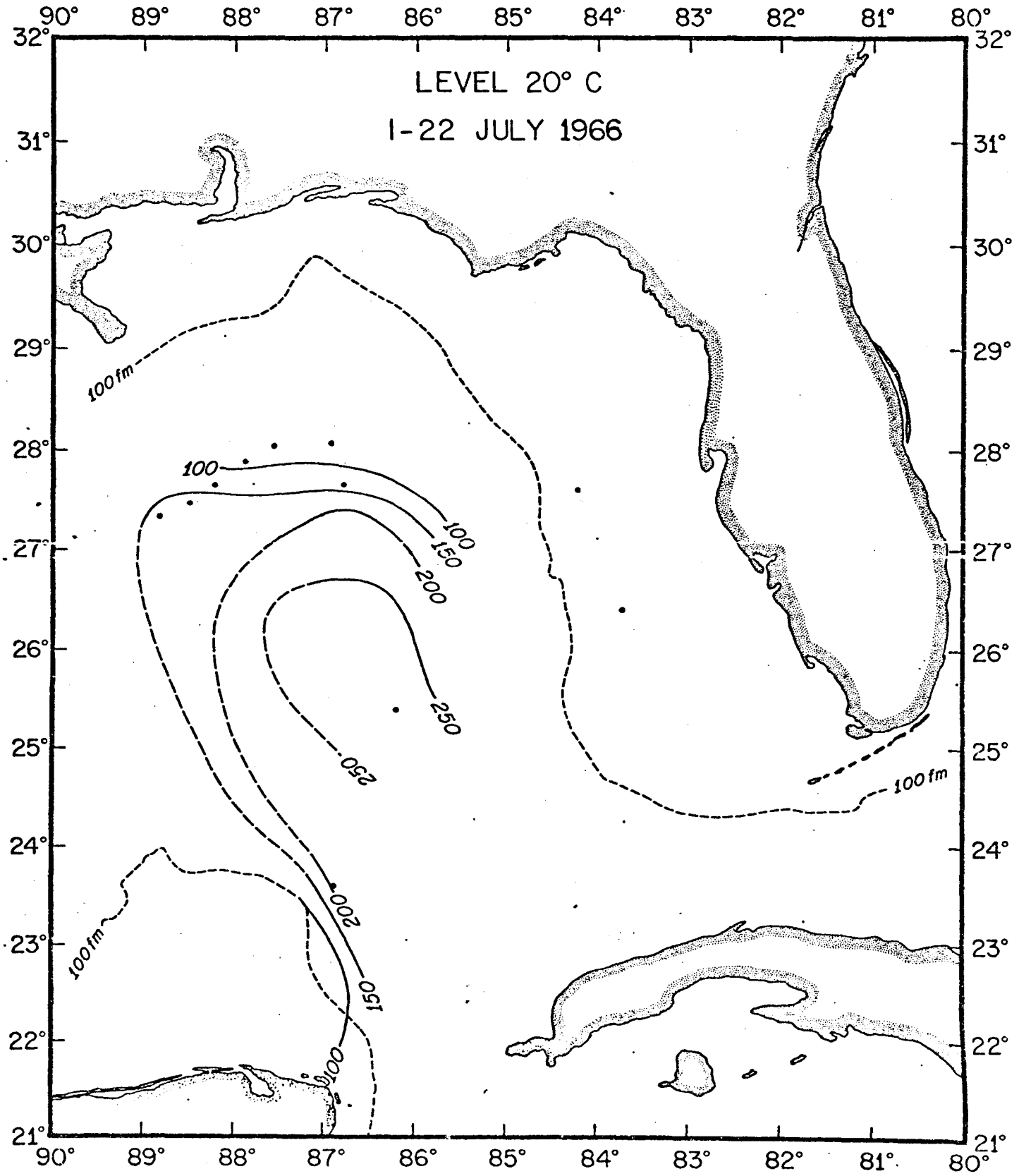
LEVEL 20° C
1-22 JULY 1966
90° 89° 88° 87° 86° 85° 84° 83° 82° 81° 80°
32° 31° 30° 29° 28° 27° 26° 25° 24° 23° 22° 21°
100 fm
100
150
200
250
250
200
150
100
100 fm
100 fm

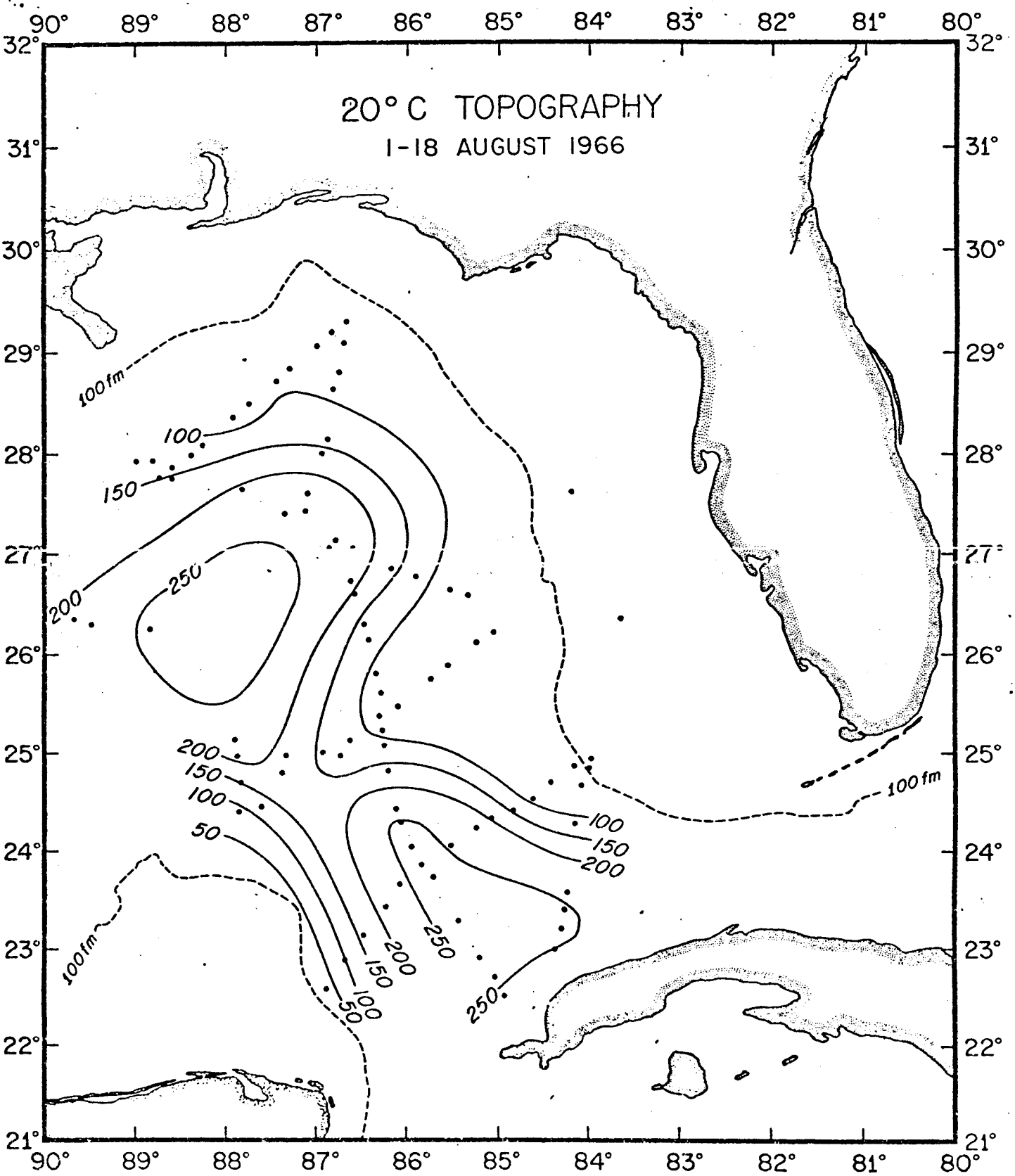
20° C TOPOGRAPHY
1-18 AUGUST 1966
90° 89° 88° 87° 86° 85° 84° 83° 82° 81° 80°
32° 31° 30° 29° 28° 27° 26° 25° 24° 23° 22° 21°
100 fm
100
150
200
250
200
150
100
50
100 fm
100
150
200
250
200
150
100
50
100 fm
250

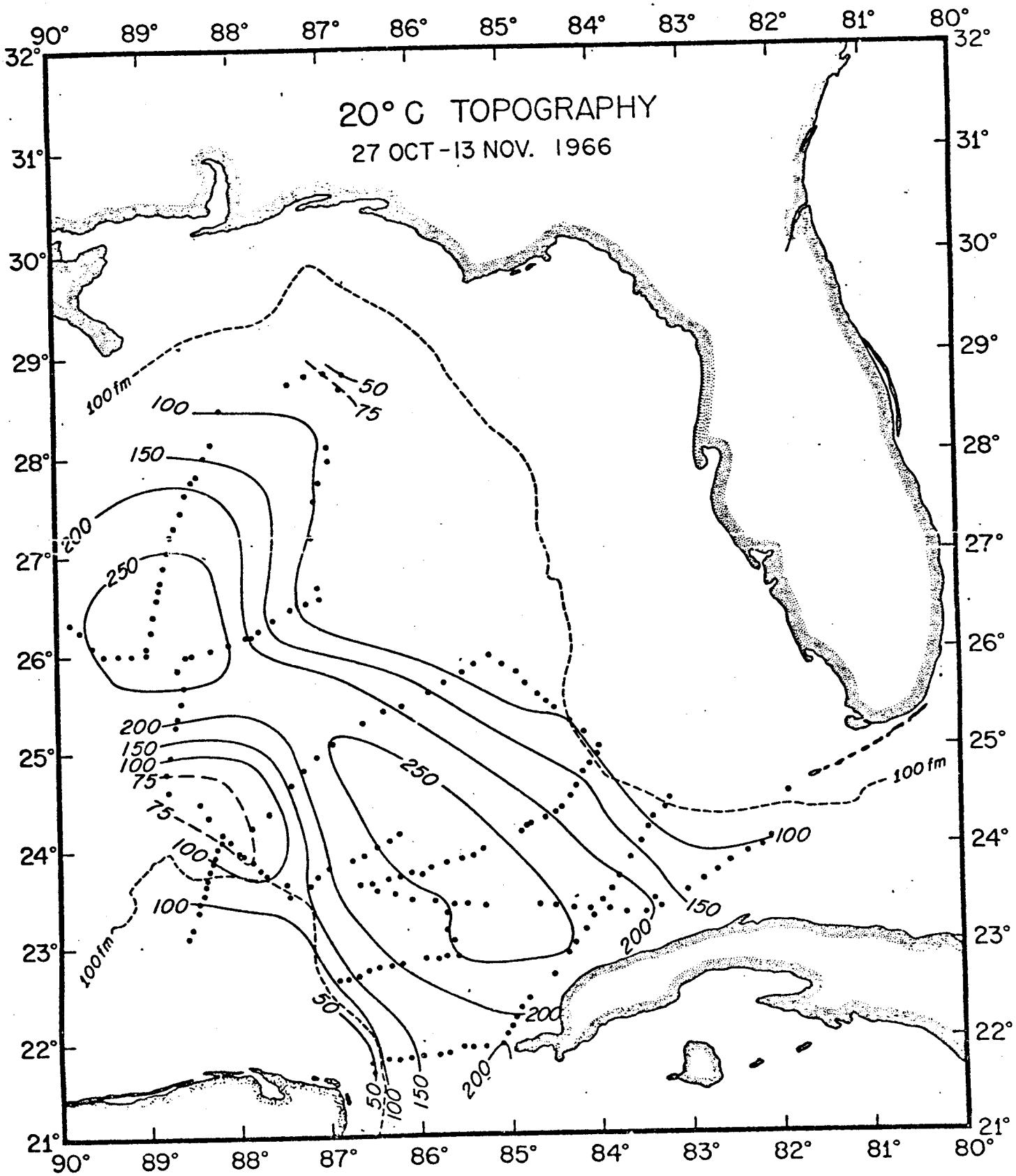
20° C TOPOGRAPHY
27 OCT - 13 NOV. 1966
90° 89° 88° 87° 86° 85° 84° 83° 82° 81° 80°
32° 31° 30° 29° 28° 27° 26° 25° 24° 23° 22° 21°
100 fm
50
75
100
150
200
250
100 fm

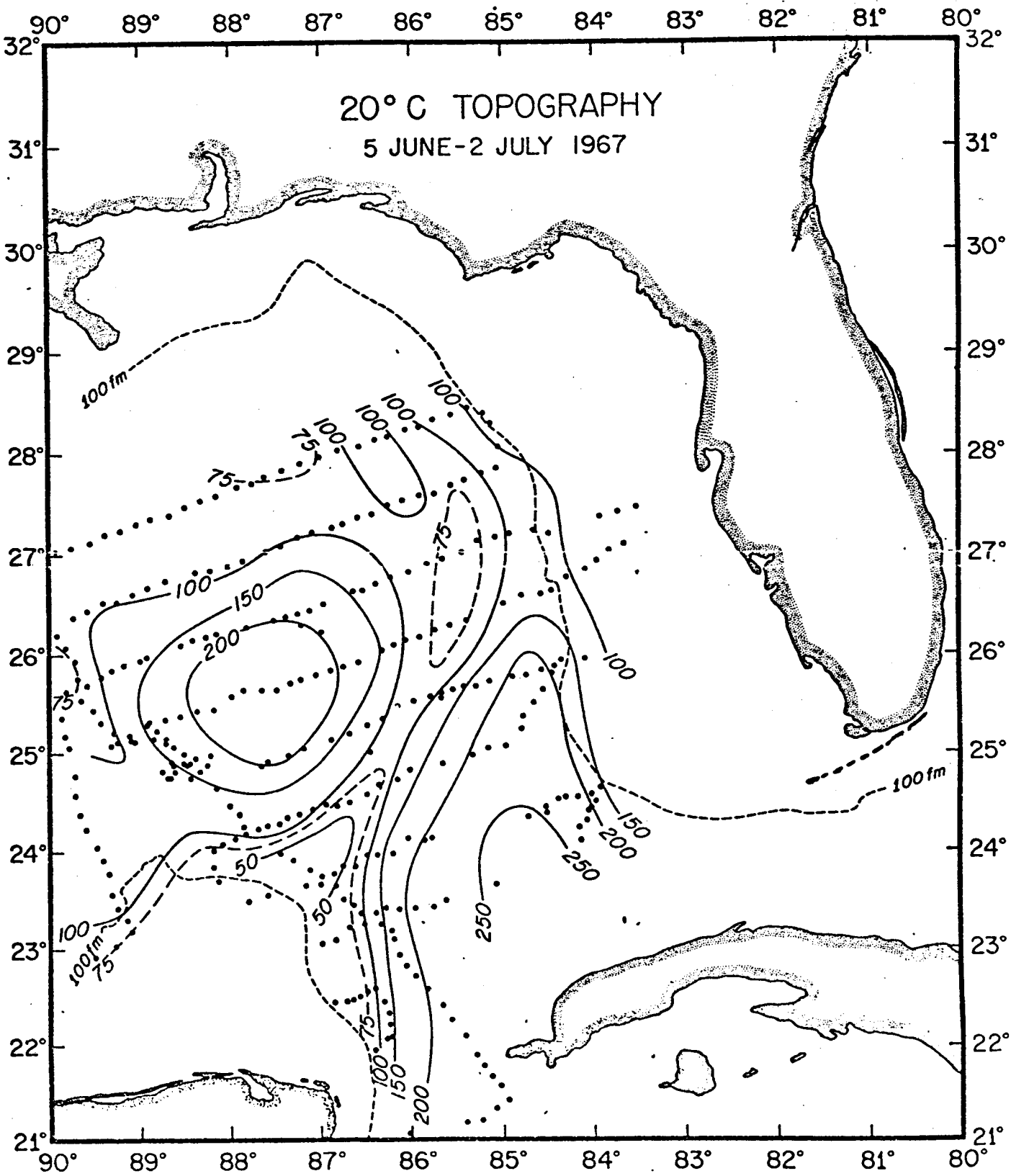
20° C TOPOGRAPHY
5 JUNE-2 JULY 1967
90° 89° 88° 87° 86° 85° 84° 83° 82° 81° 80°
32° 31° 30° 29° 28° 27° 26° 25° 24° 23° 22° 21°
100 fm
75
100
150
200
250
50

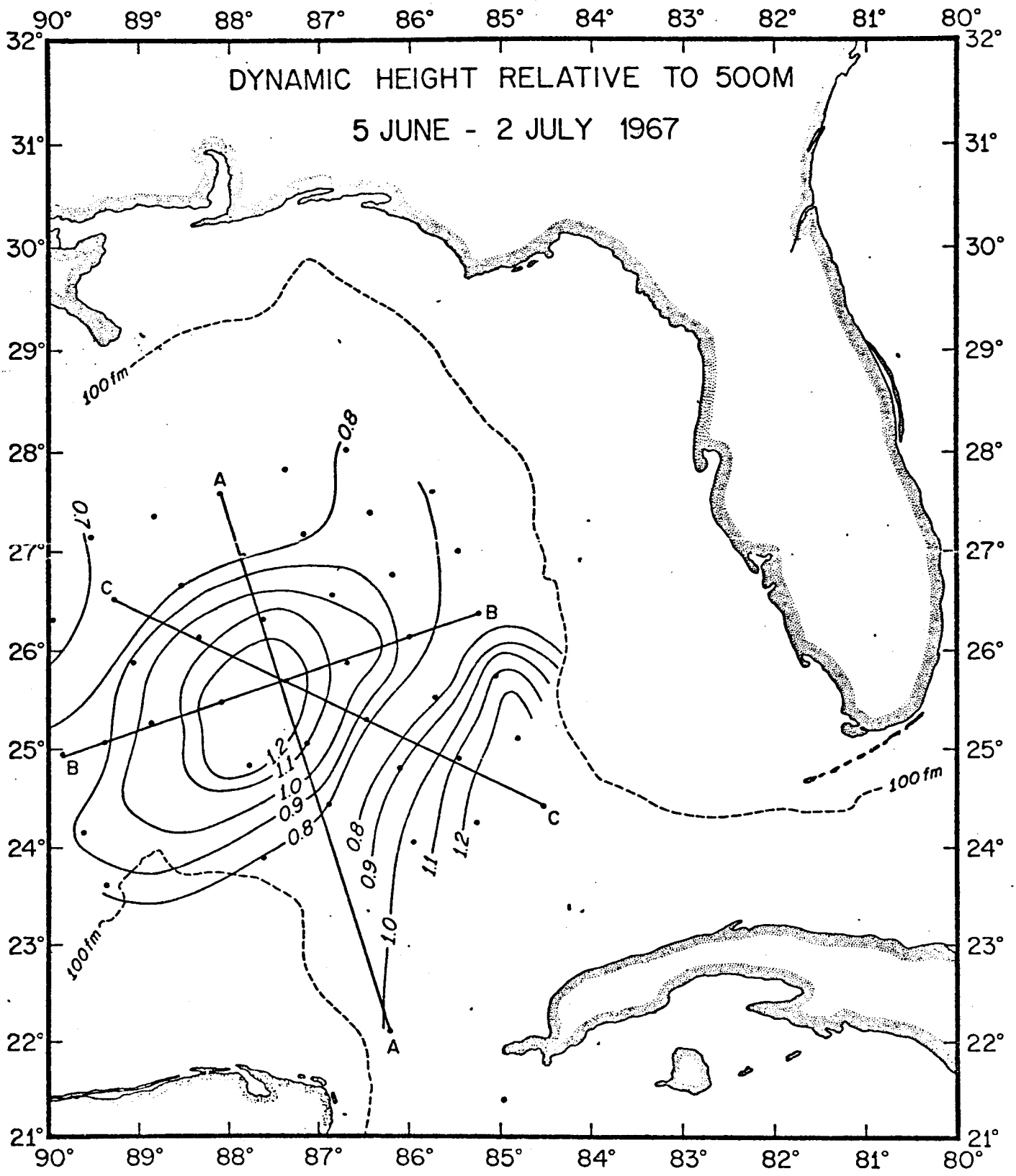
DYNAMIC HEIGHT RELATIVE TO 500M
5 JUNE - 2 JULY 1967
90° 89° 88° 87° 86° 85° 84° 83° 82° 81° 80°
32° 31° 30° 29° 28° 27° 26° 25° 24° 23° 22° 21°
100 fm
0.7
0.8
1.0
1.2
1.1
0.9
A
B
C

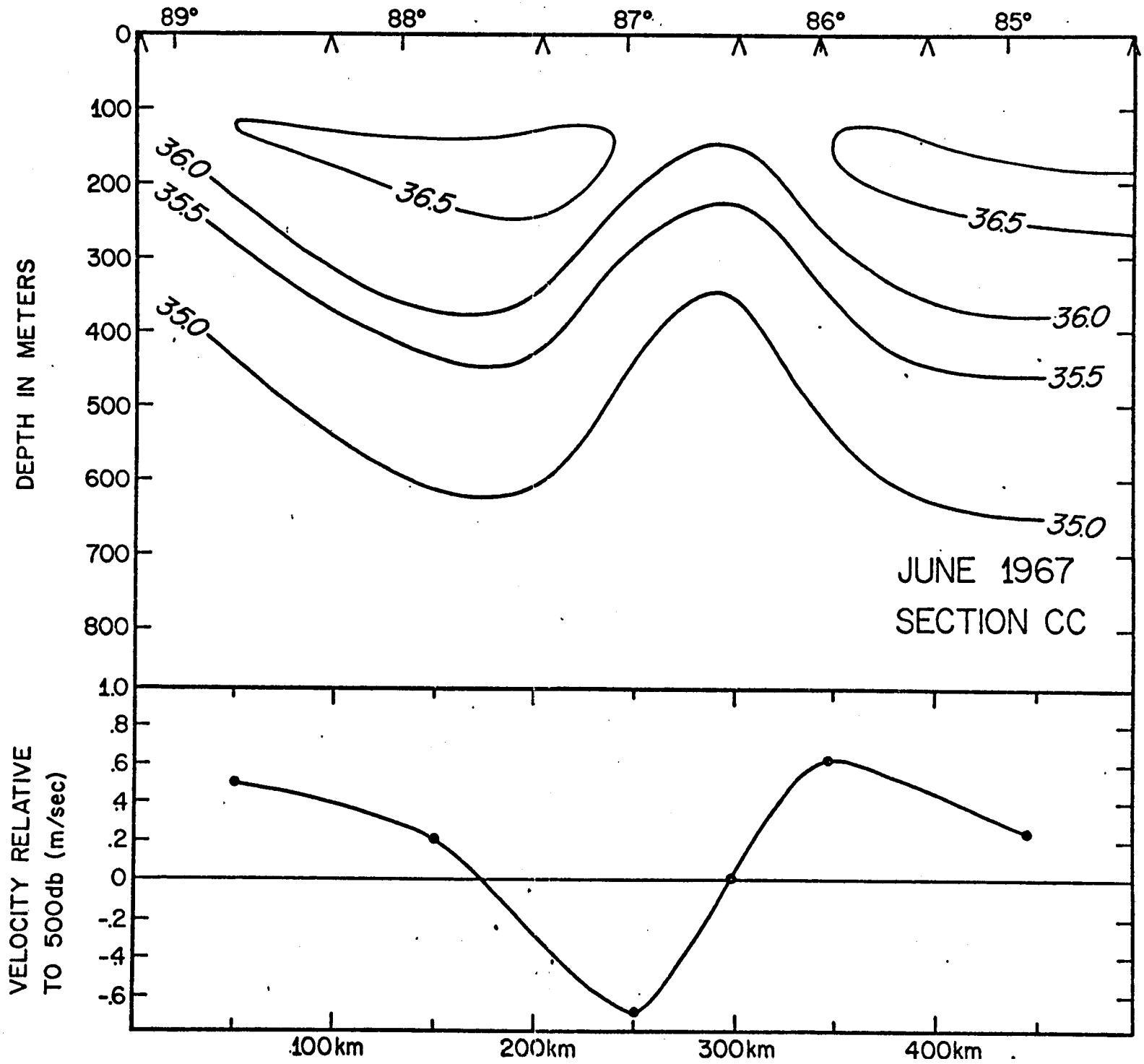
89°
88°
87°
86°
85°
0
100
200
300
400
500
600
700
800
1.0
.8
.6
.4
.2
0
-.2
-.4
-.6
DEPTH IN METERS
VELOCITY RELATIVE TO 500db (m/sec)
36.0
36.5
35.5
35.0
36.5
36.0
35.5
35.0
JUNE 1967
SECTION CC
100km
200km
300km
400km

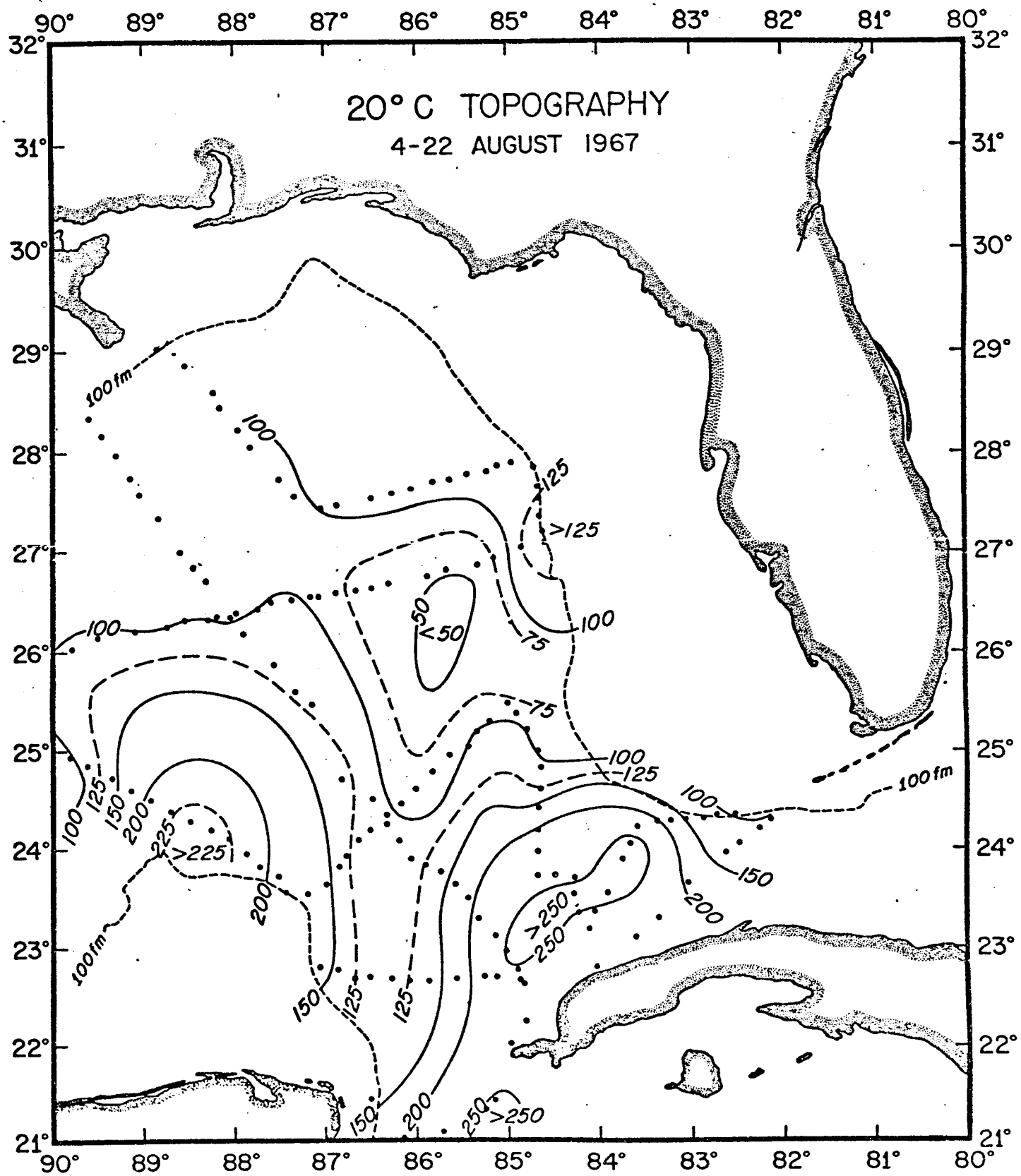
20° C TOPOGRAPHY
4-22 AUGUST 1967
90° 89° 88° 87° 86° 85° 84° 83° 82° 81° 80°
32° 31° 30° 29° 28° 27° 26° 25° 24° 23° 22° 21°
100 fm
100
125
>125
50
<50
75
150
200
225
>225
250
>250

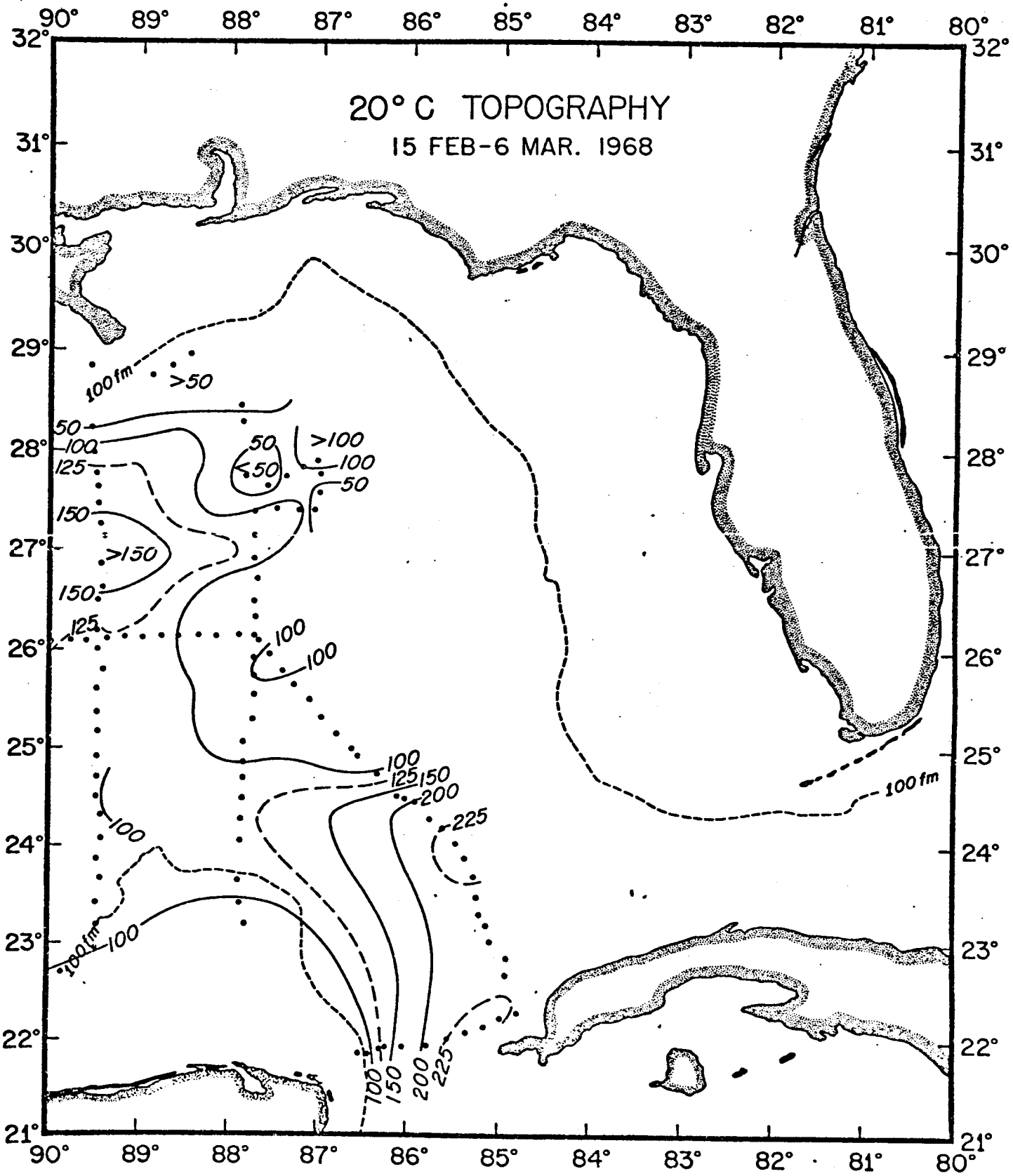
20° C TOPOGRAPHY
15 FEB-6 MAR. 1968
90° 89° 88° 87° 86° 85° 84° 83° 82° 81° 80°
32° 31° 30° 29° 28° 27° 26° 25° 24° 23° 22° 21°
100 fm
>50
50
100
125
150
>150
<50
>100
100 fm
225
700

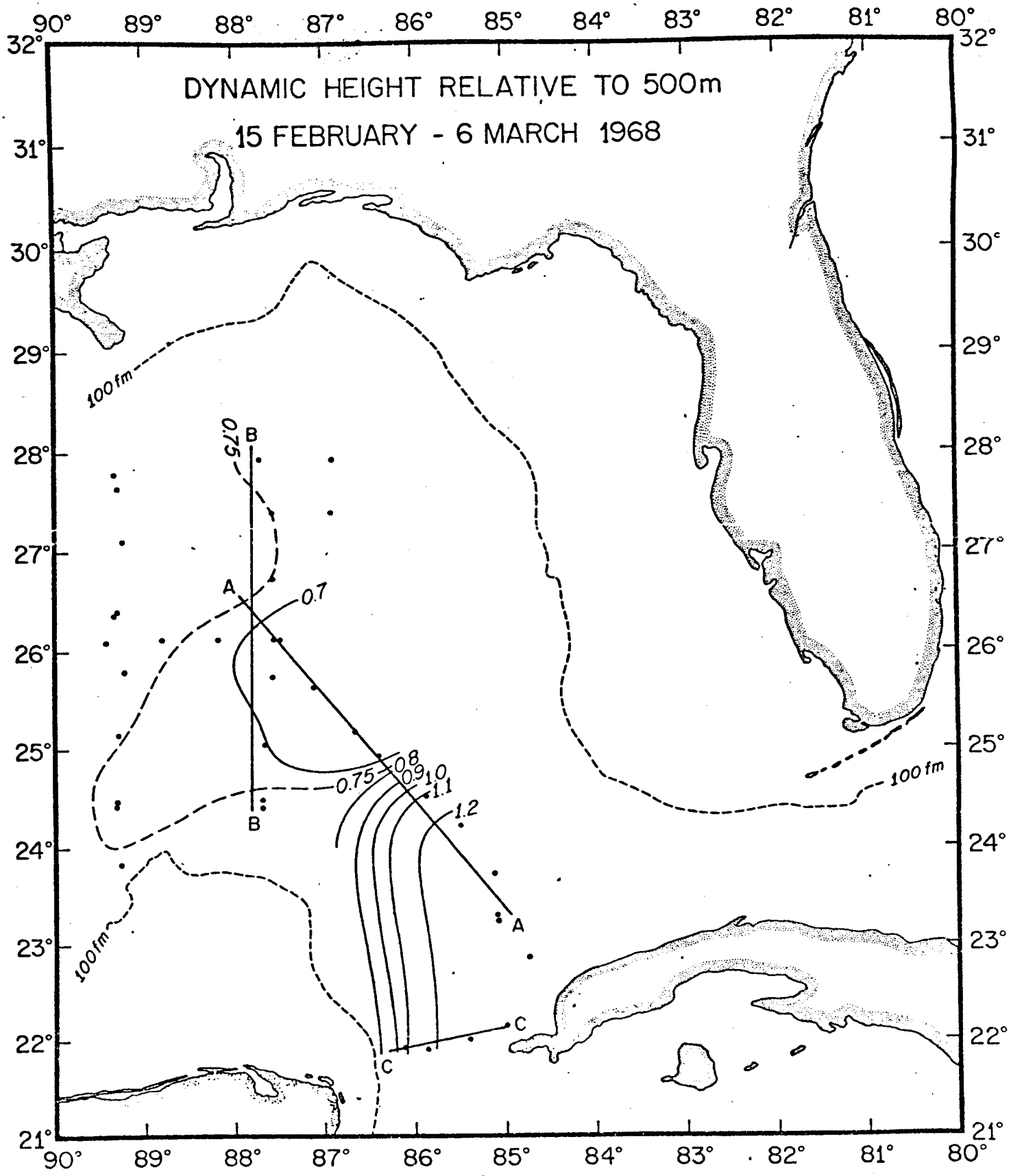
DYNAMIC HEIGHT RELATIVE TO 500m
15 FEBRUARY - 6 MARCH 1968
90° 89° 88° 87° 86° 85° 84° 83° 82° 81° 80°
32° 31° 30° 29° 28° 27° 26° 25° 24° 23° 22° 21°
100 fm
0.75
0.7
0.75
0.8
0.9
1.0
1.1
1.2
A
B
C

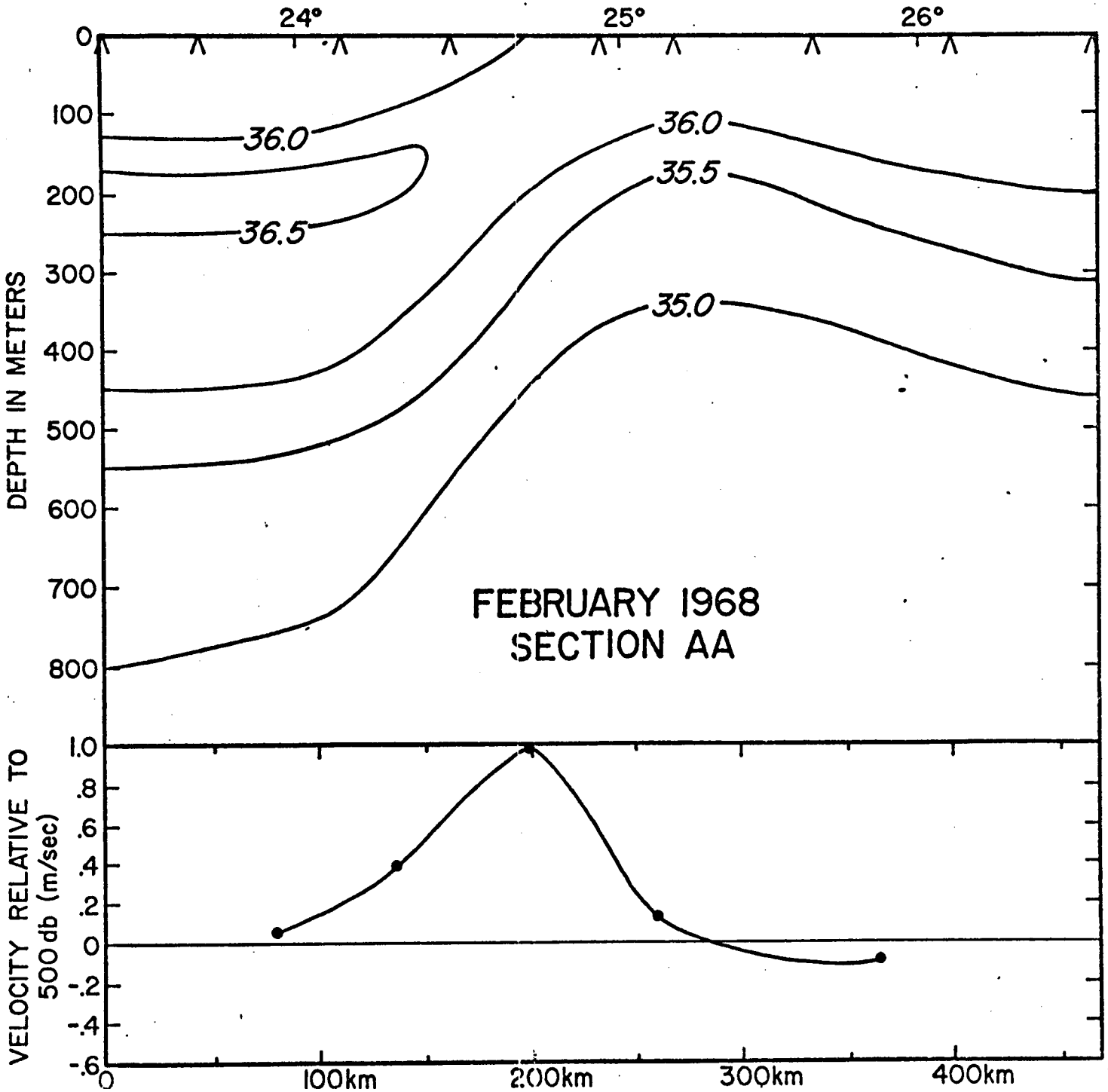
24°
25°
26°
0
100
200
300
400
500
600
700
800
DEPTH IN METERS
36.0
36.5
36.0
35.5
35.0
FEBRUARY 1968
SECTION AA
VELOCITY RELATIVE TO
500 db (m/sec)
1.0
.8
.6
.4
.2
0
-.2
-.4
-.6
0
100km
200km
300km
400km

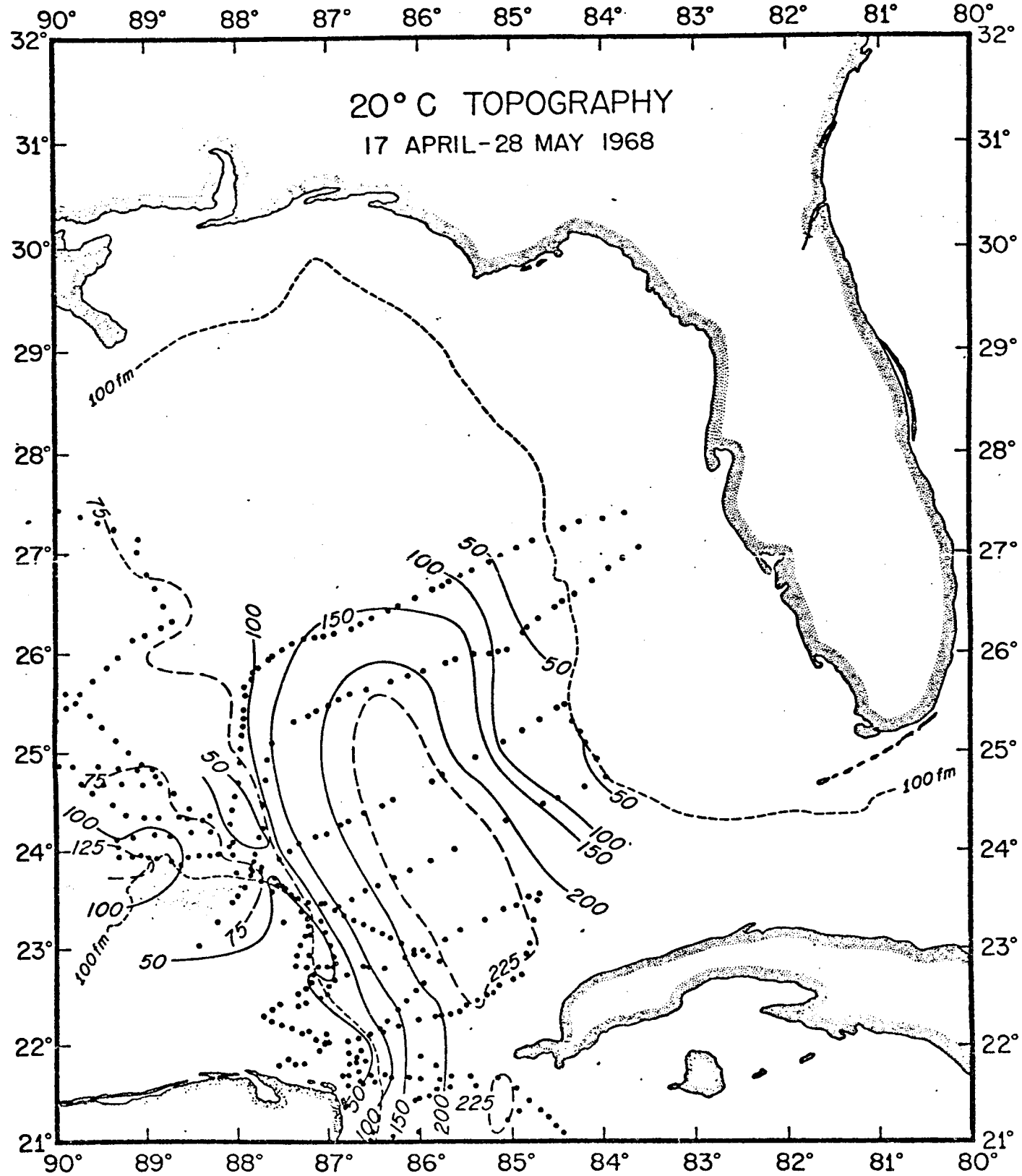
20° C TOPOGRAPHY
17 APRIL-28 MAY 1968
90° 89° 88° 87° 86° 85° 84° 83° 82° 81° 80°
32° 31° 30° 29° 28° 27° 26° 25° 24° 23° 22° 21°
100 fm
75
50
100
150
125
200
225

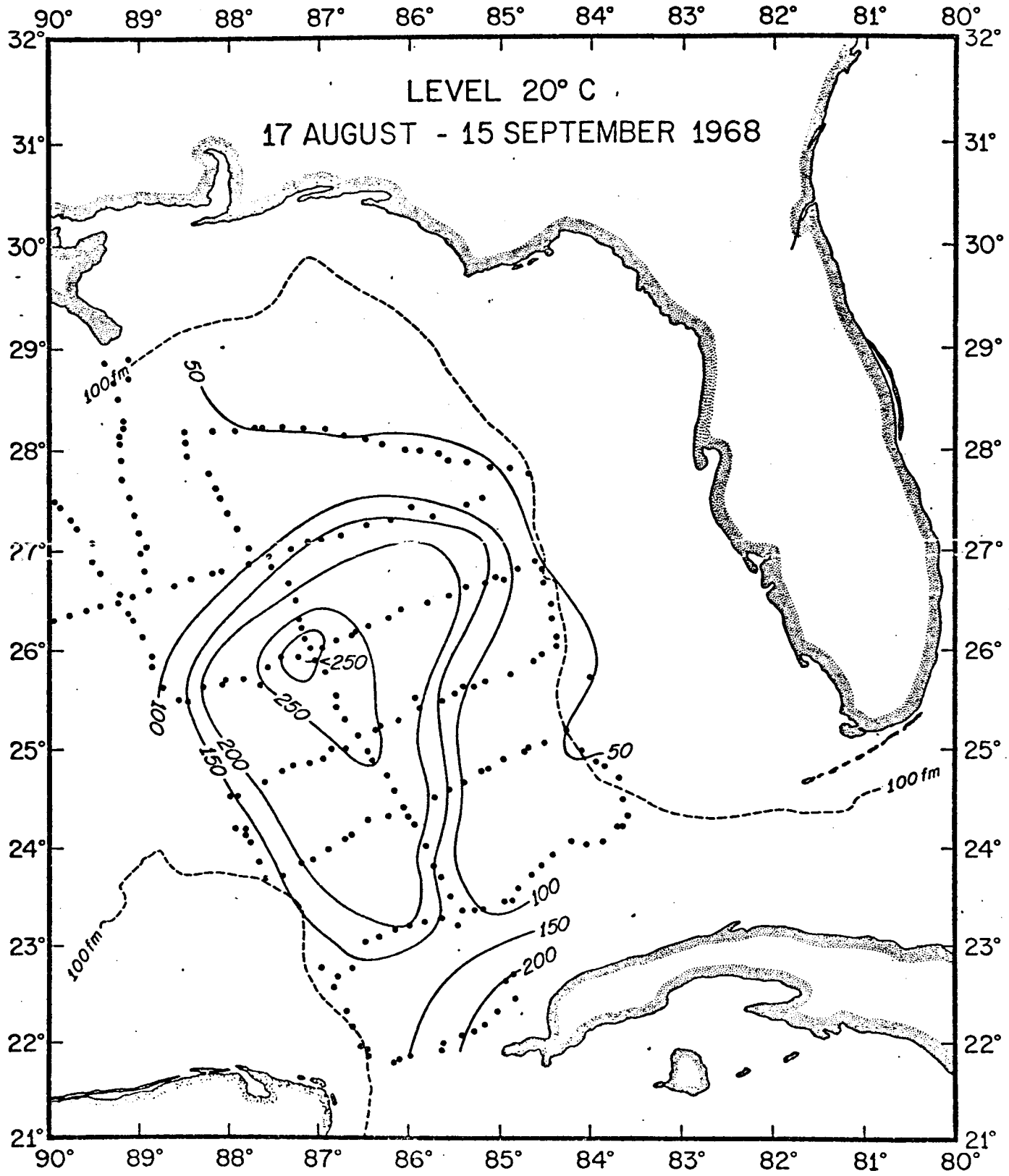
LEVEL 20° C
17 AUGUST - 15 SEPTEMBER 1968
90° 89° 88° 87° 86° 85° 84° 83° 82° 81° 80°
32° 31° 30° 29° 28° 27° 26° 25° 24° 23° 22° 21°
100fm
50
100
150
200
250
<250
50
100 fm
100
150
200
100fm

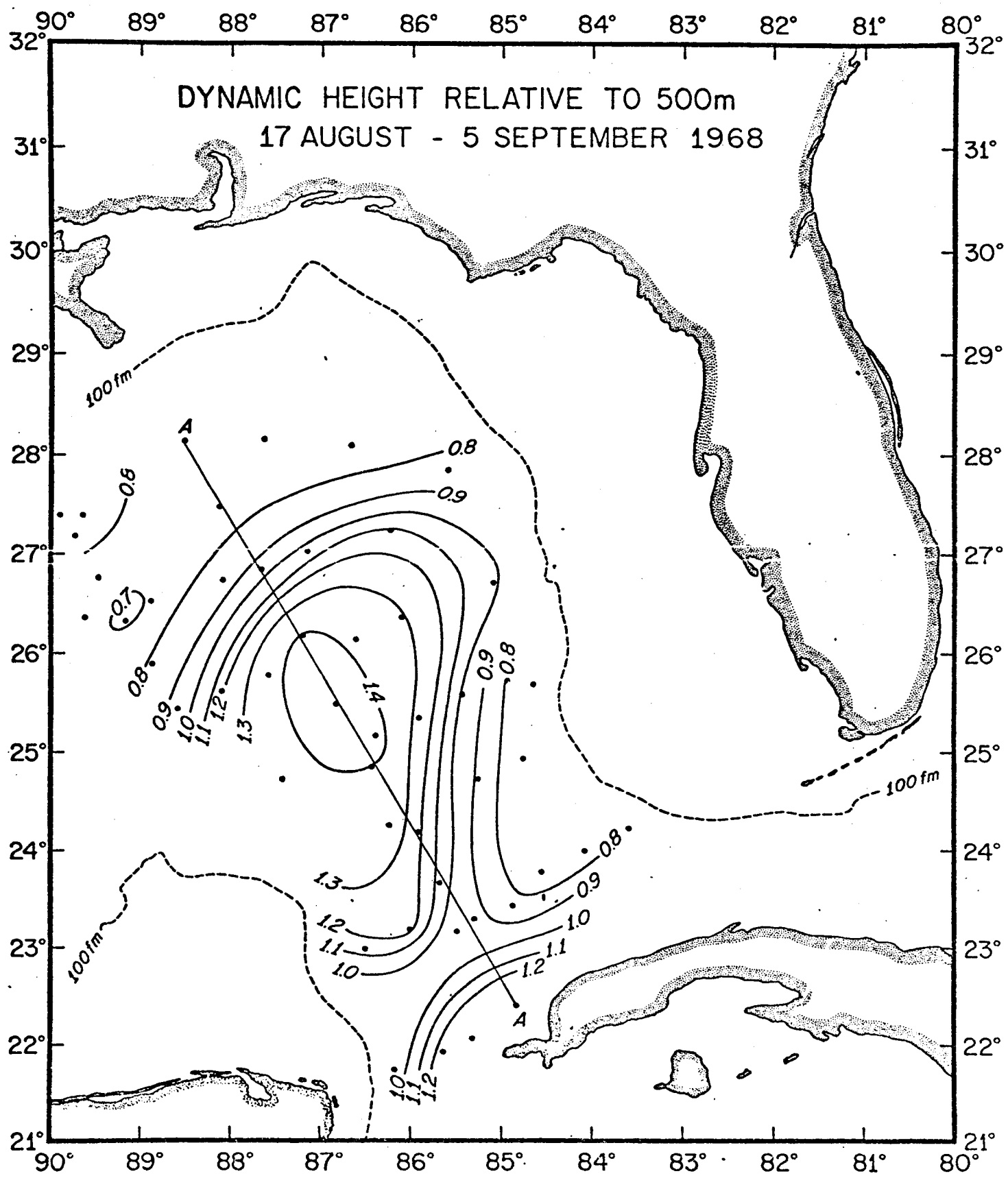
DYNAMIC HEIGHT RELATIVE TO 500m
17 AUGUST - 5 SEPTEMBER 1968
90° 89° 88° 87° 86° 85° 84° 83° 82° 81° 80°
32° 31° 30° 29° 28° 27° 26° 25° 24° 23° 22° 21°
100 fm
A
A
0.6
0.7
0.8
0.9
1.0
1.1
1.2
1.3
1.4

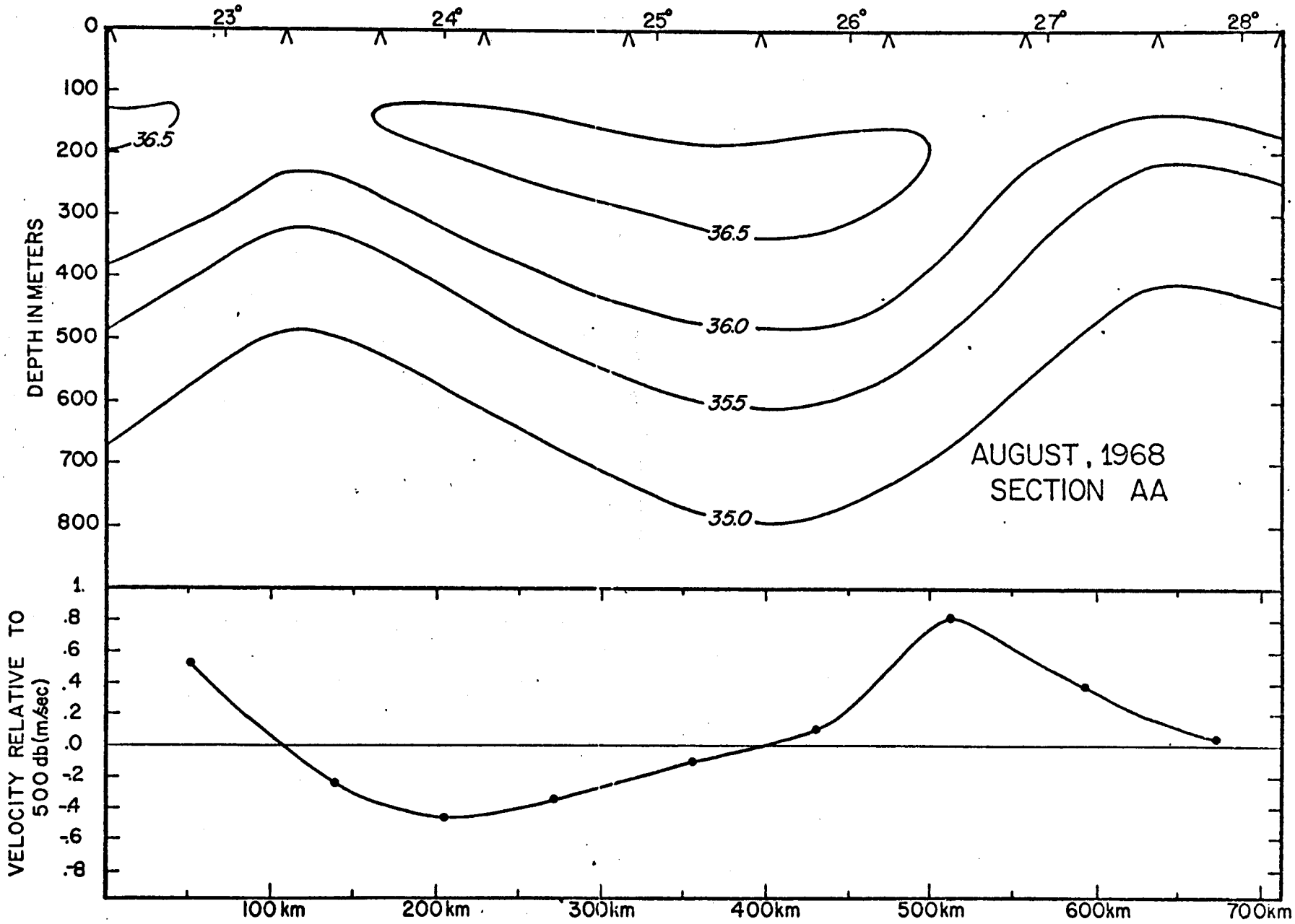
23°
24°
25°
26°
27°
28°
0
100
200
300
400
500
600
700
800
DEPTH IN METERS
36.5
36.5
36.0
35.5
35.0
AUGUST, 1968
SECTION AA
1.
.8
.6
.4
.2
.0
-.2
-.4
-.6
-.8
VELOCITY RELATIVE TO
500 db (m/sec)
100 km
200 km
300km
400km
500km
600km
700km

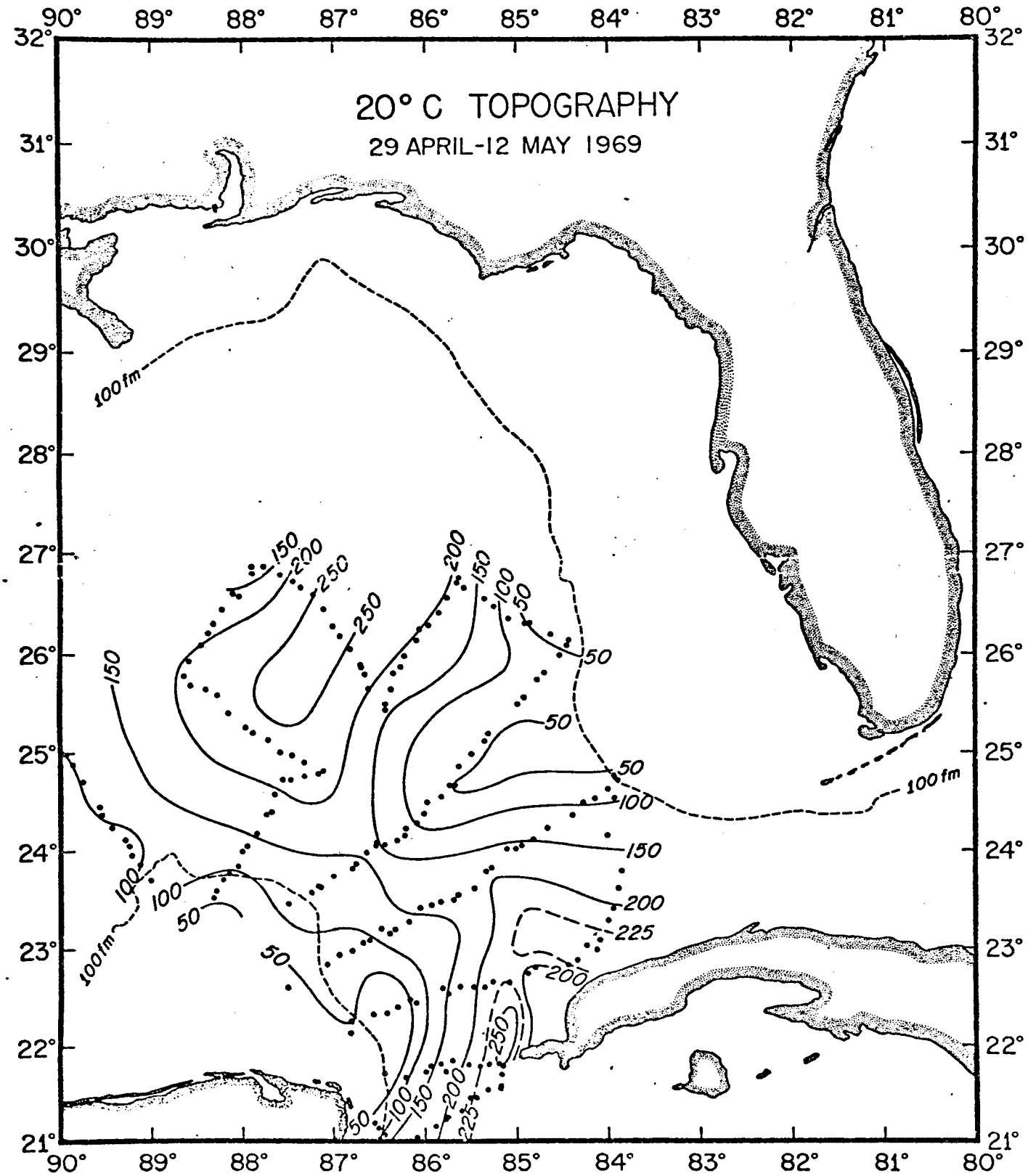
20° C TOPOGRAPHY
29 APRIL-12 MAY 1969
90° 89° 88° 87° 86° 85° 84° 83° 82° 81° 80°
32° 31° 30° 29° 28° 27° 26° 25° 24° 23° 22° 21°
100 fm
150
200
250
100
50
225

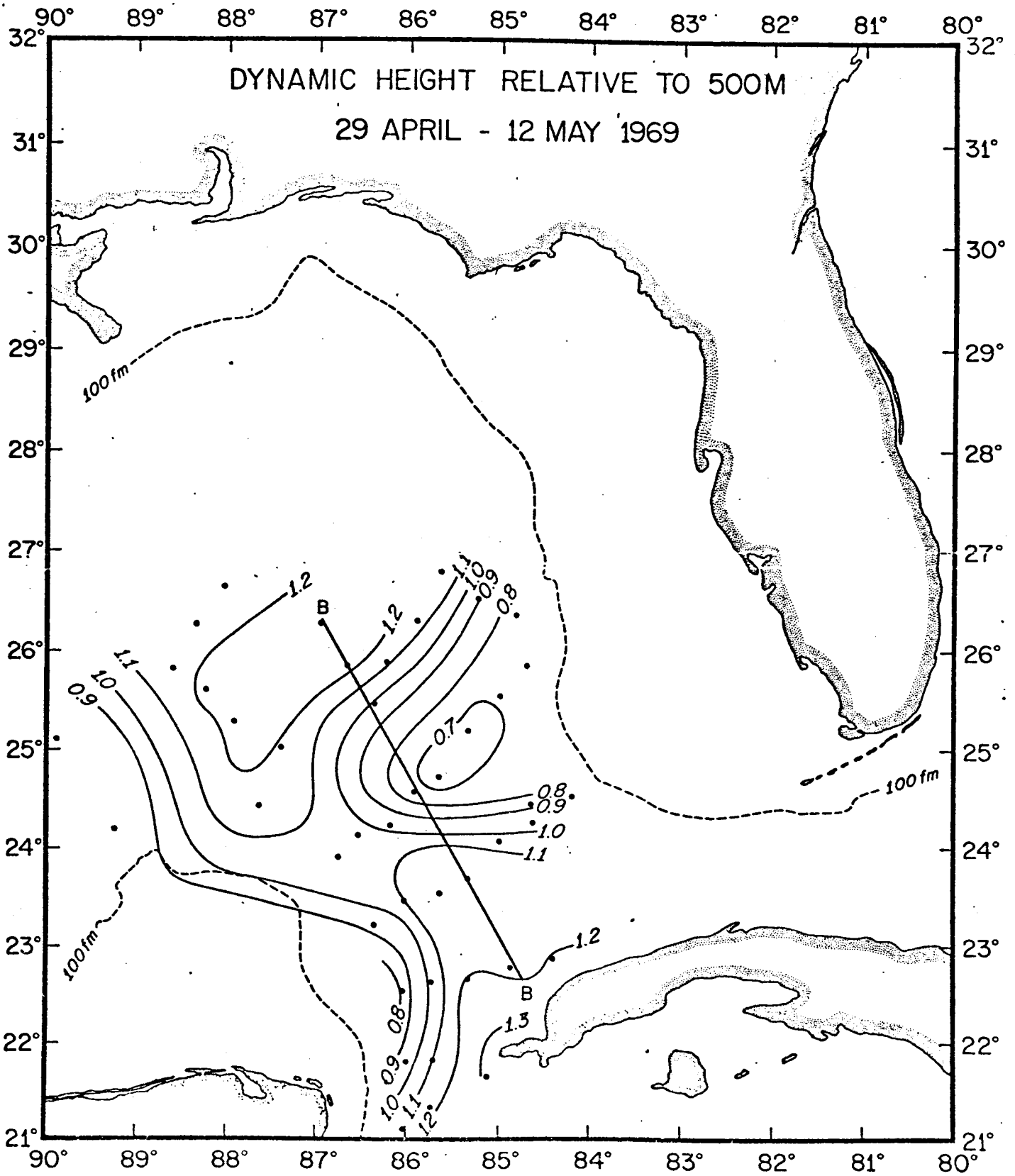
DYNAMIC HEIGHT RELATIVE TO 500M
29 APRIL - 12 MAY 1969
90° 89° 88° 87° 86° 85° 84° 83° 82° 81° 80°
32° 31° 30° 29° 28° 27° 26° 25° 24° 23° 22° 21°
100 fm
0.7
0.8
0.9
1.0
1.1
1.2
1.3
B

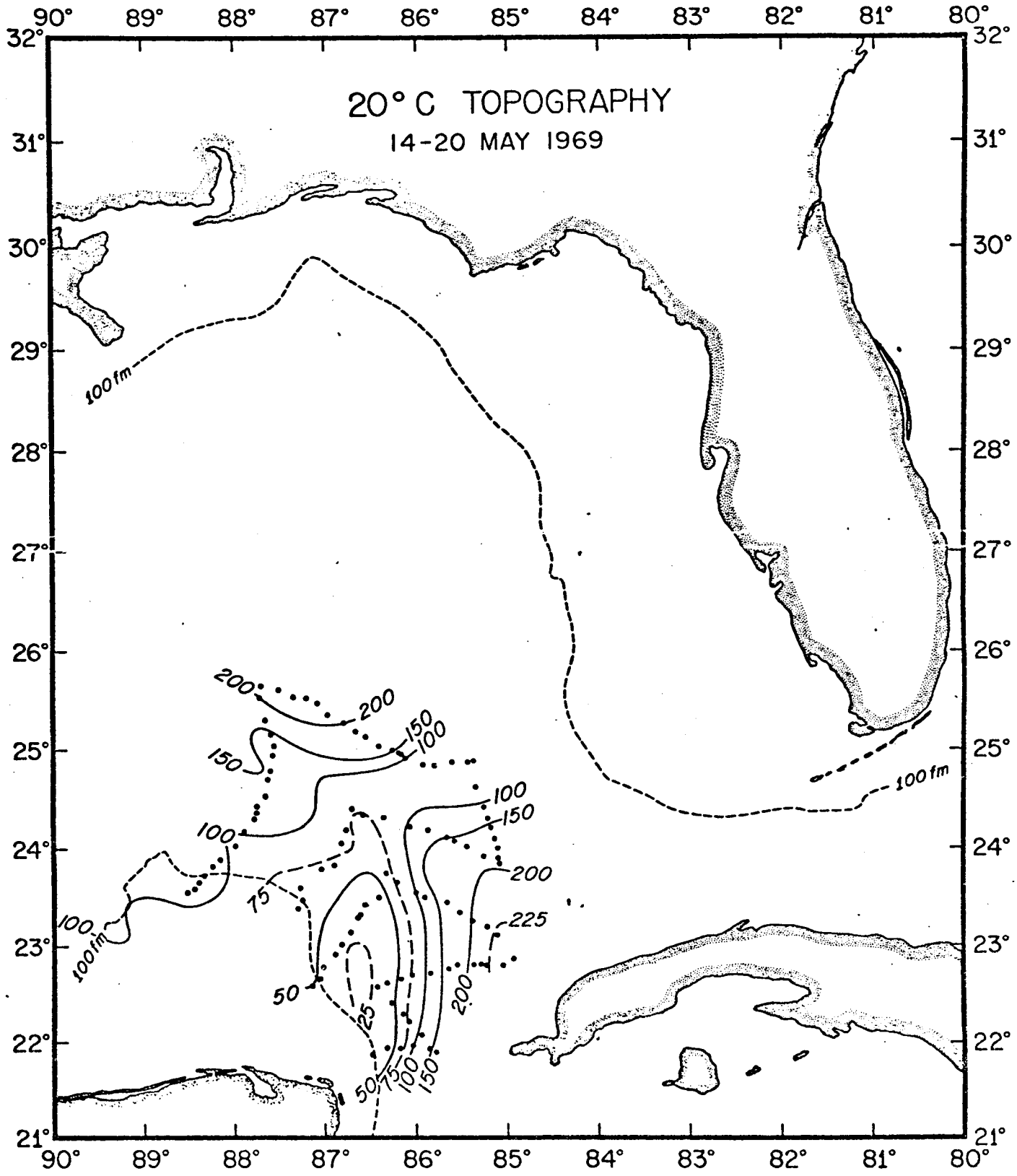
20° C TOPOGRAPHY
14-20 MAY 1969
90° 89° 88° 87° 86° 85° 84° 83° 82° 81° 80°
32° 31° 30° 29° 28° 27° 26° 25° 24° 23° 22° 21°
100 fm
100 fm
100 fm
200
200
150
100
150
100
100
150
200
225
75
50
25
50
75
100
150
200

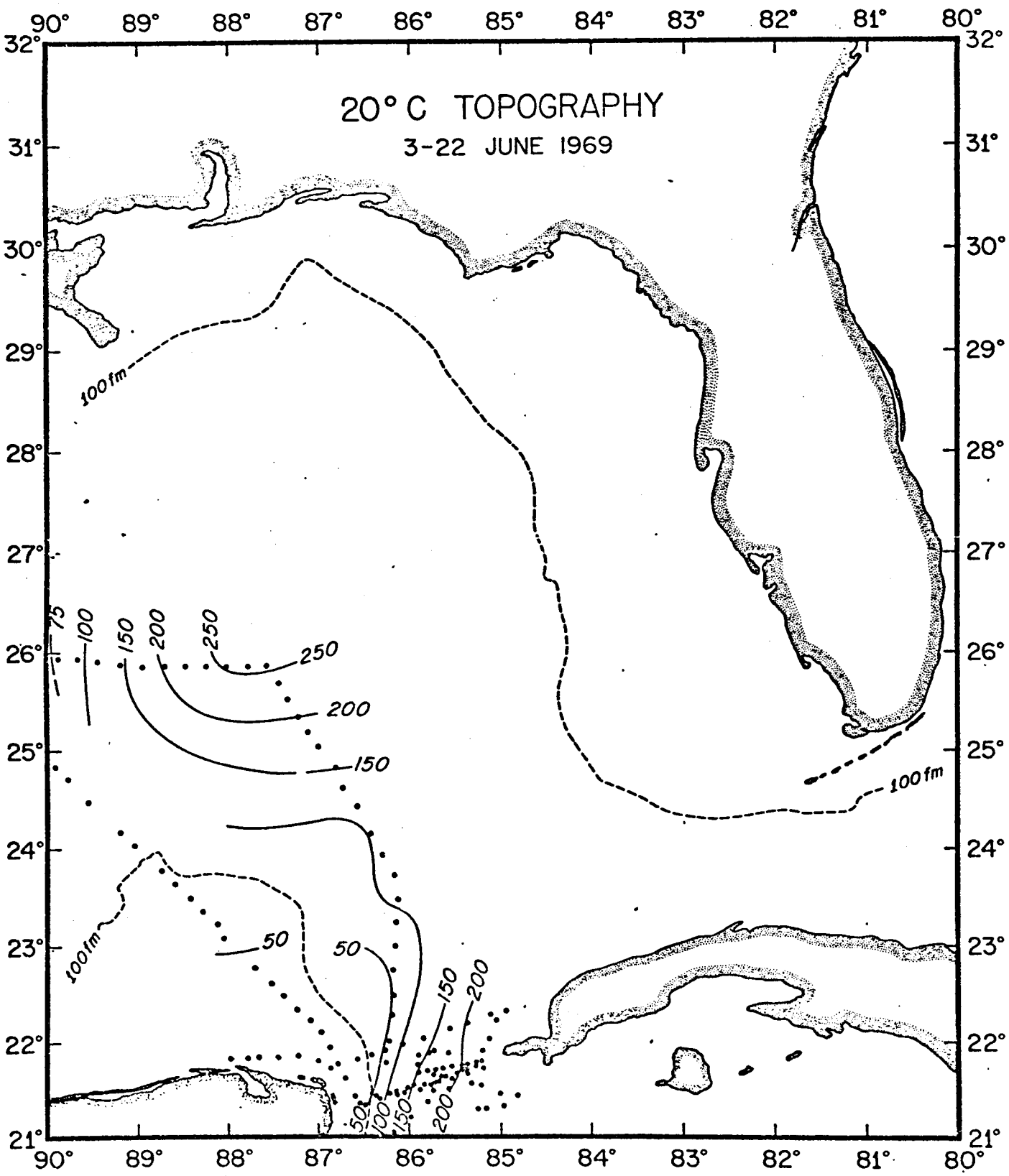
20° C TOPOGRAPHY
3-22 JUNE 1969
90° 89° 88° 87° 86° 85° 84° 83° 82° 81° 80°
32° 31° 30° 29° 28° 27° 26° 25° 24° 23° 22° 21°
100 fm
75
100
150
200
250
250
200
150
100 fm
50
50
100
150
200
50
100
150
200

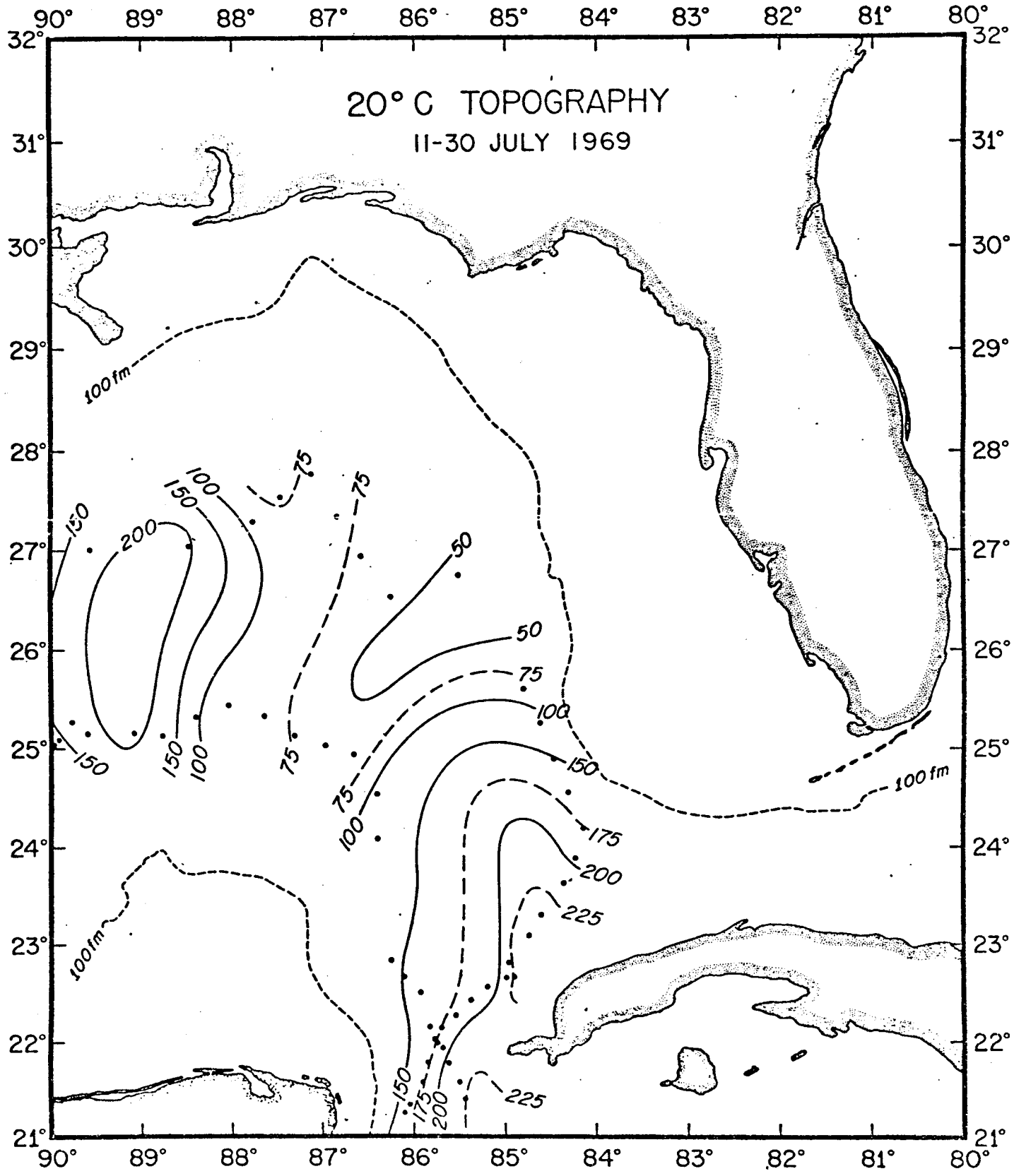
20° C TOPOGRAPHY
11-30 JULY 1969
90° 89° 88° 87° 86° 85° 84° 83° 82° 81° 80°
32° 31° 30° 29° 28° 27° 26° 25° 24° 23° 22° 21°
100 fm
150
200
100
75
50
75
100
150
175
200
225

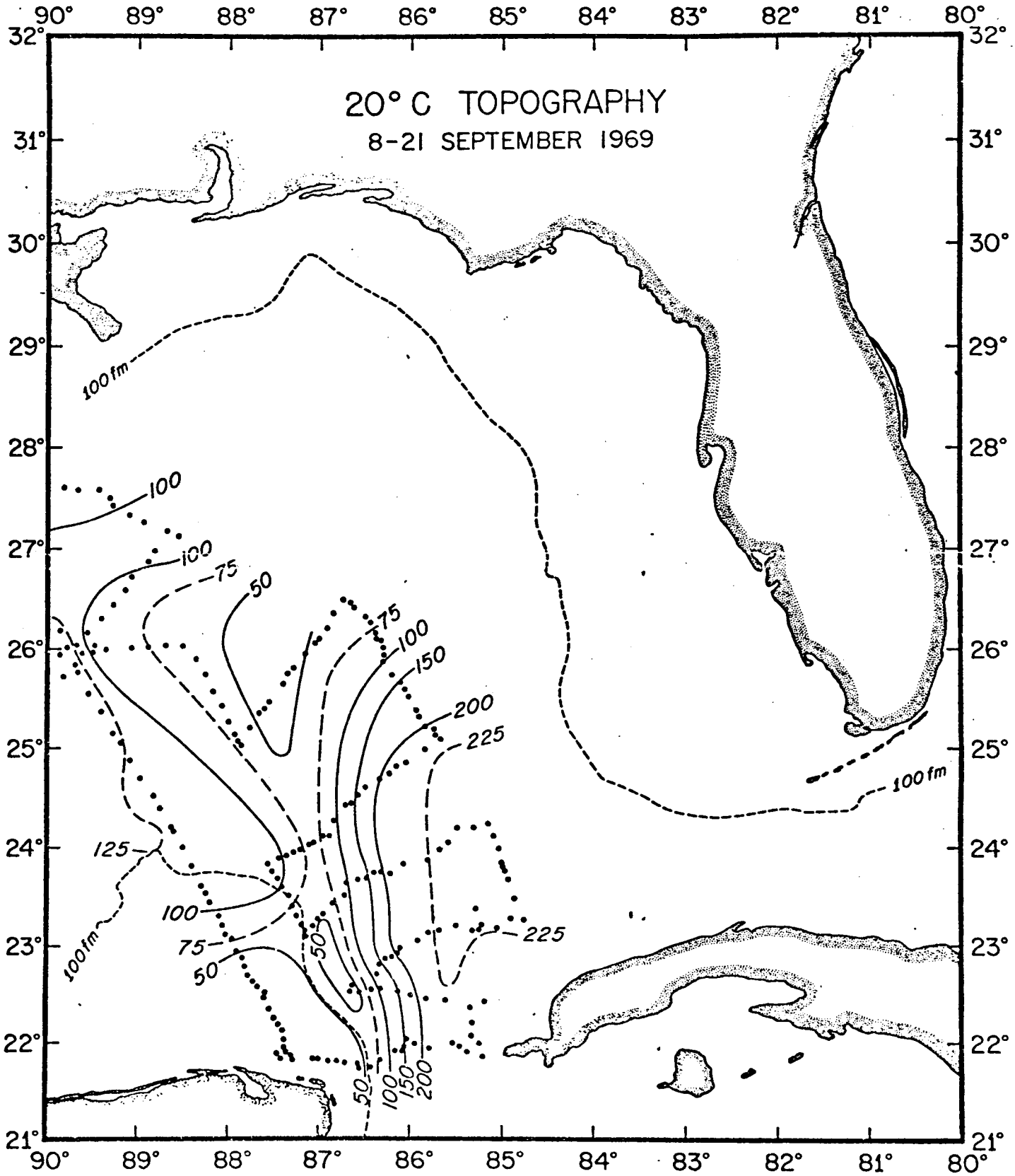
20° C TOPOGRAPHY
8-21 SEPTEMBER 1969
90° 89° 88° 87° 86° 85° 84° 83° 82° 81° 80°
32° 31° 30° 29° 28° 27° 26° 25° 24° 23° 22° 21°
100 fm
100
100
75
50
75
100
150
200
225
100 fm
125
100
75
50
100 fm
50
225
50
100
150
200

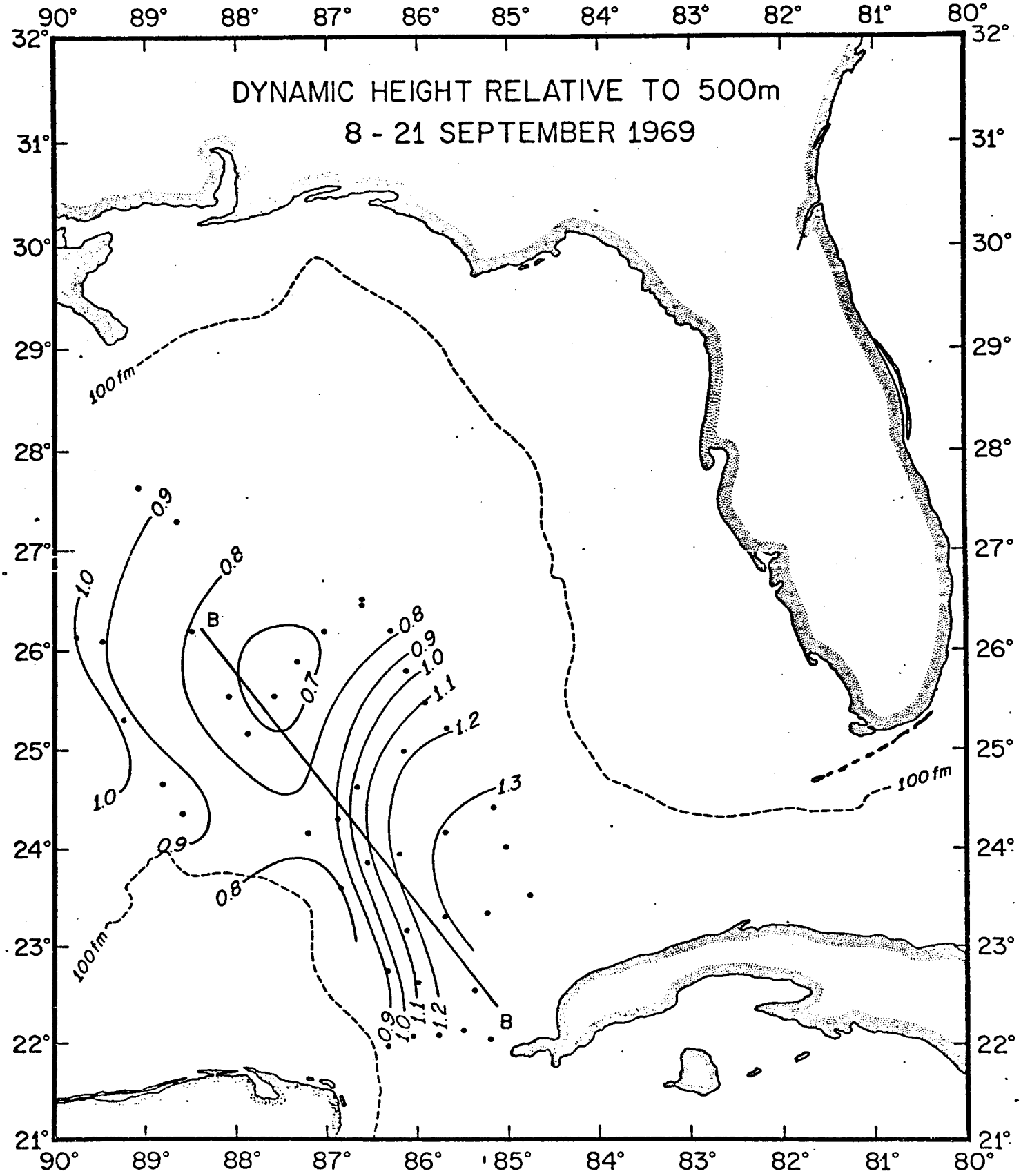
DYNAMIC HEIGHT RELATIVE TO 500m
8 - 21 SEPTEMBER 1969
90° 89° 88° 87° 86° 85° 84° 83° 82° 81° 80°
32° 31° 30° 29° 28° 27° 26° 25° 24° 23° 22° 21°
100 fm
0.9
1.0
0.8
0.7
B
1.1
1.2
1.3

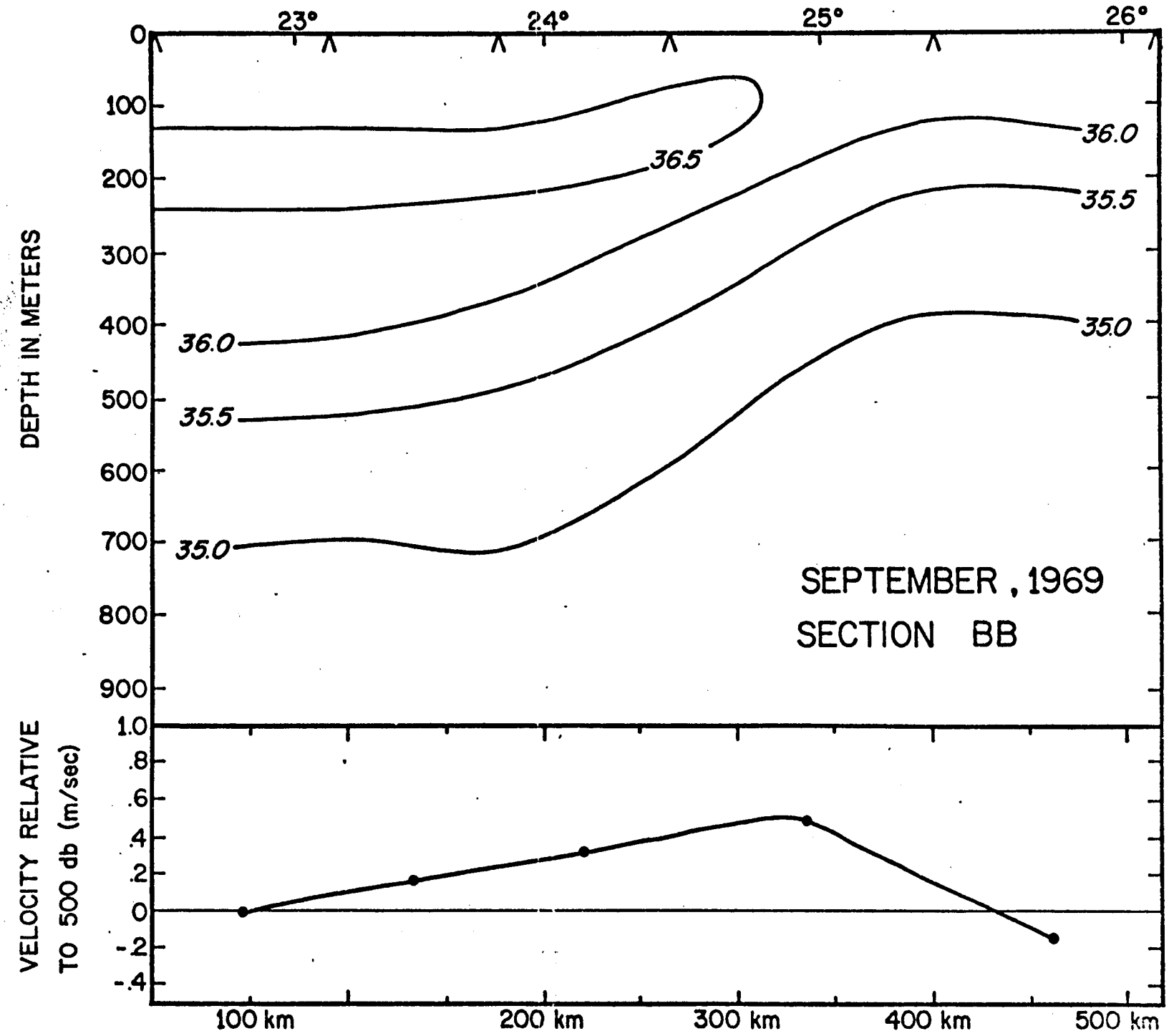
23°
24°
25°
26°
0
100
200
300
400
500
600
700
800
900
1.0
.8
.6
.4
.2
0
-.2
-.4
DEPTH IN METERS
VELOCITY RELATIVE
TO 500 db (m/sec)
36.5
36.0
35.5
35.0
36.0
35.5
35.0
SEPTEMBER, 1969
SECTION BB
100 km
200 km
300 km
400 km
500 km

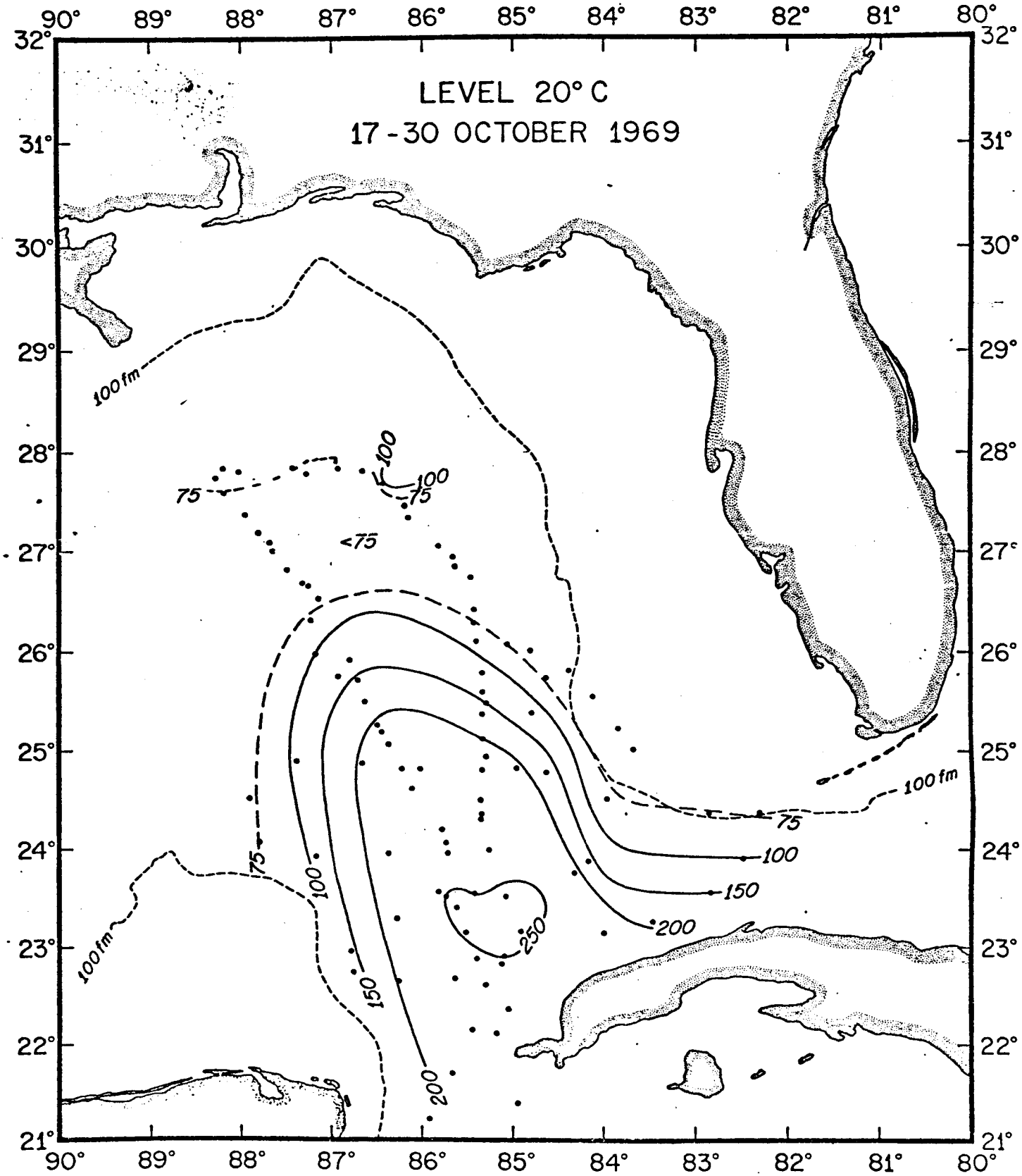
LEVEL 20° C
17 - 30 OCTOBER 1969
90°
89°
88°
87°
86°
85°
84°
83°
82°
81°
80°
32°
31°
30°
29°
28°
27°
26°
25°
24°
23°
22°
21°
100 fm
75
100
75
<75
100
150
200
250
100 fm
75
100
150
200
100 fm

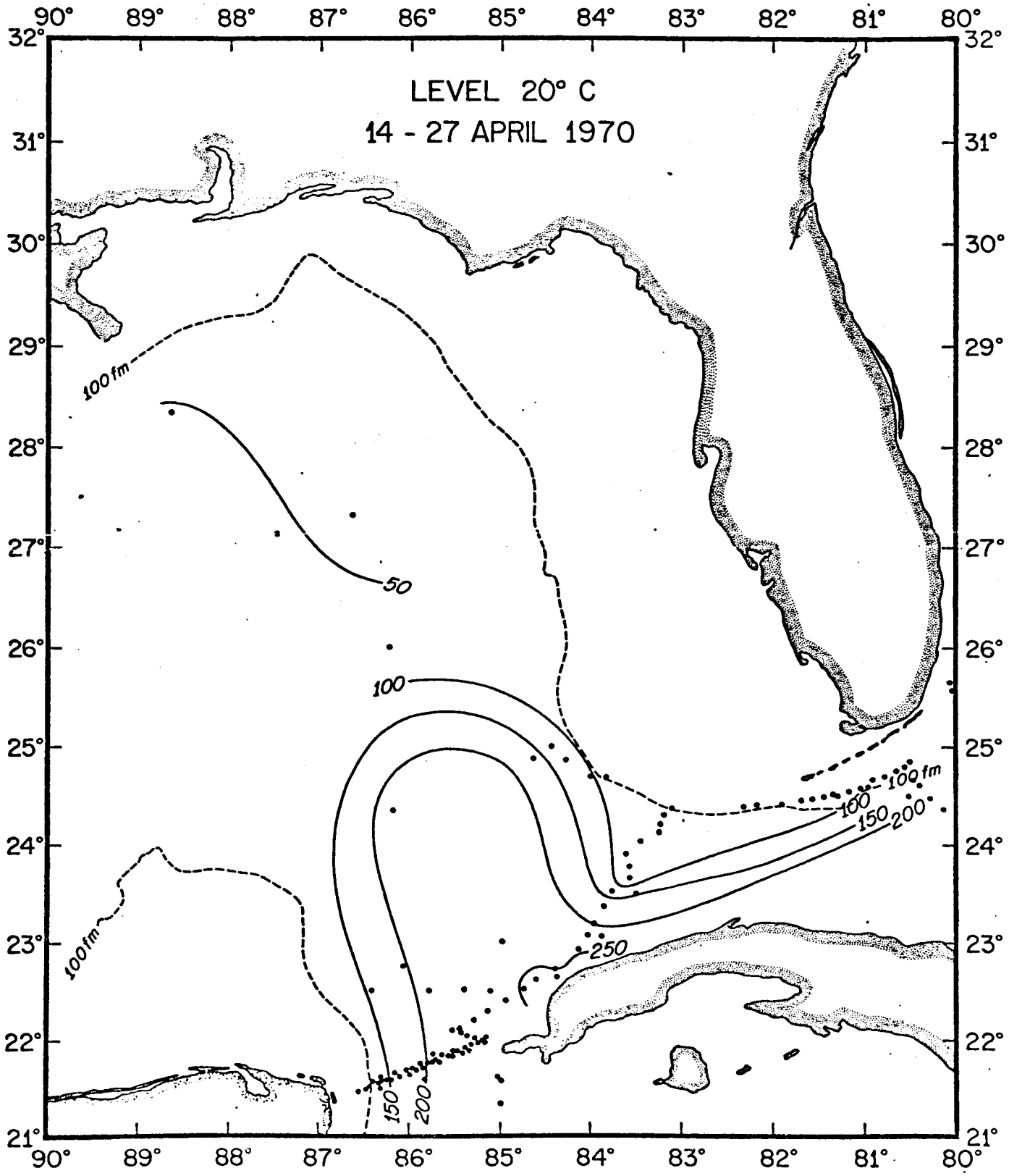
LEVEL 20° C
14 - 27 APRIL 1970
90° 89° 88° 87° 86° 85° 84° 83° 82° 81° 80°
32° 31° 30° 29° 28° 27° 26° 25° 24° 23° 22° 21°
100 fm
50
100
100 fm
100
150
200
250
100 fm
150
200

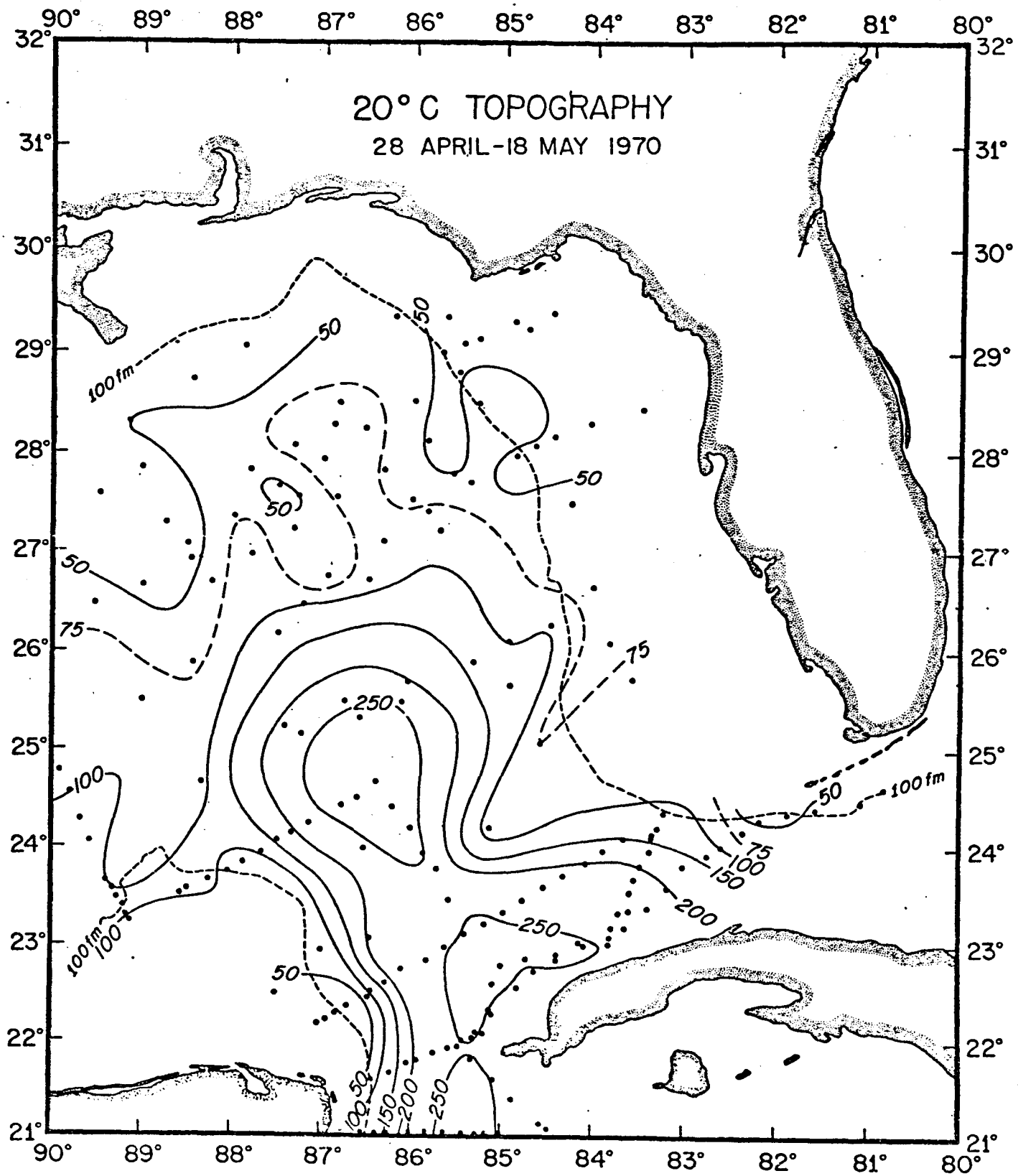
20° C TOPOGRAPHY
28 APRIL-18 MAY 1970
90° 89° 88° 87° 86° 85° 84° 83° 82° 81° 80°
32° 31° 30° 29° 28° 27° 26° 25° 24° 23° 22° 21°
50
75
100
150
200
250
100 fm

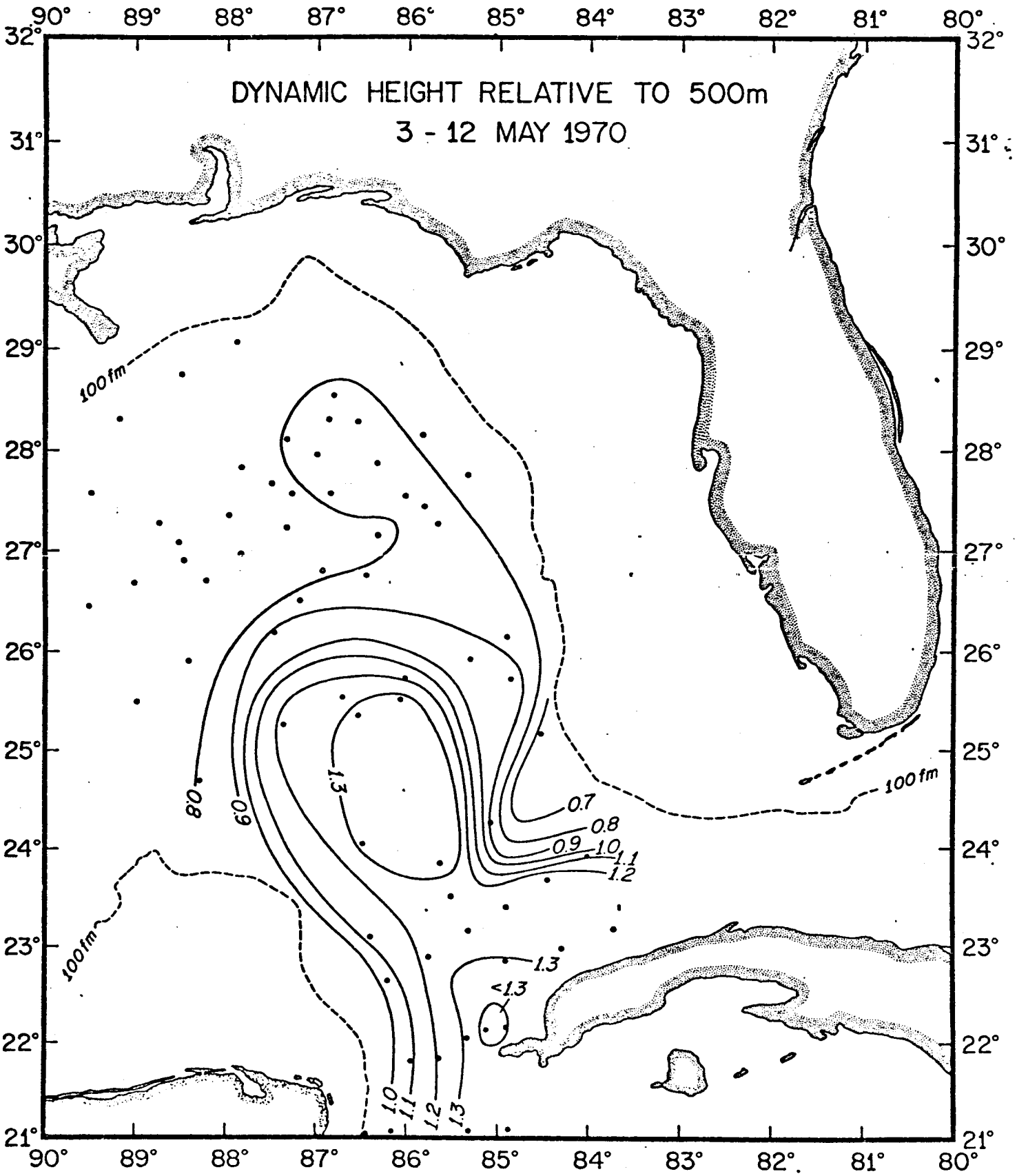
DYNAMIC HEIGHT RELATIVE TO 500m
3 - 12 MAY 1970
90° 89° 88° 87° 86° 85° 84° 83° 82° 81° 80°
32° 31° 30° 29° 28° 27° 26° 25° 24° 23° 22° 21°
100 fm
100 fm
100 fm
0.8
0.9
1.3
0.7
0.8
0.9
1.0
1.1
1.2
1.3
<1.3
1.0
1.1
1.2
1.3

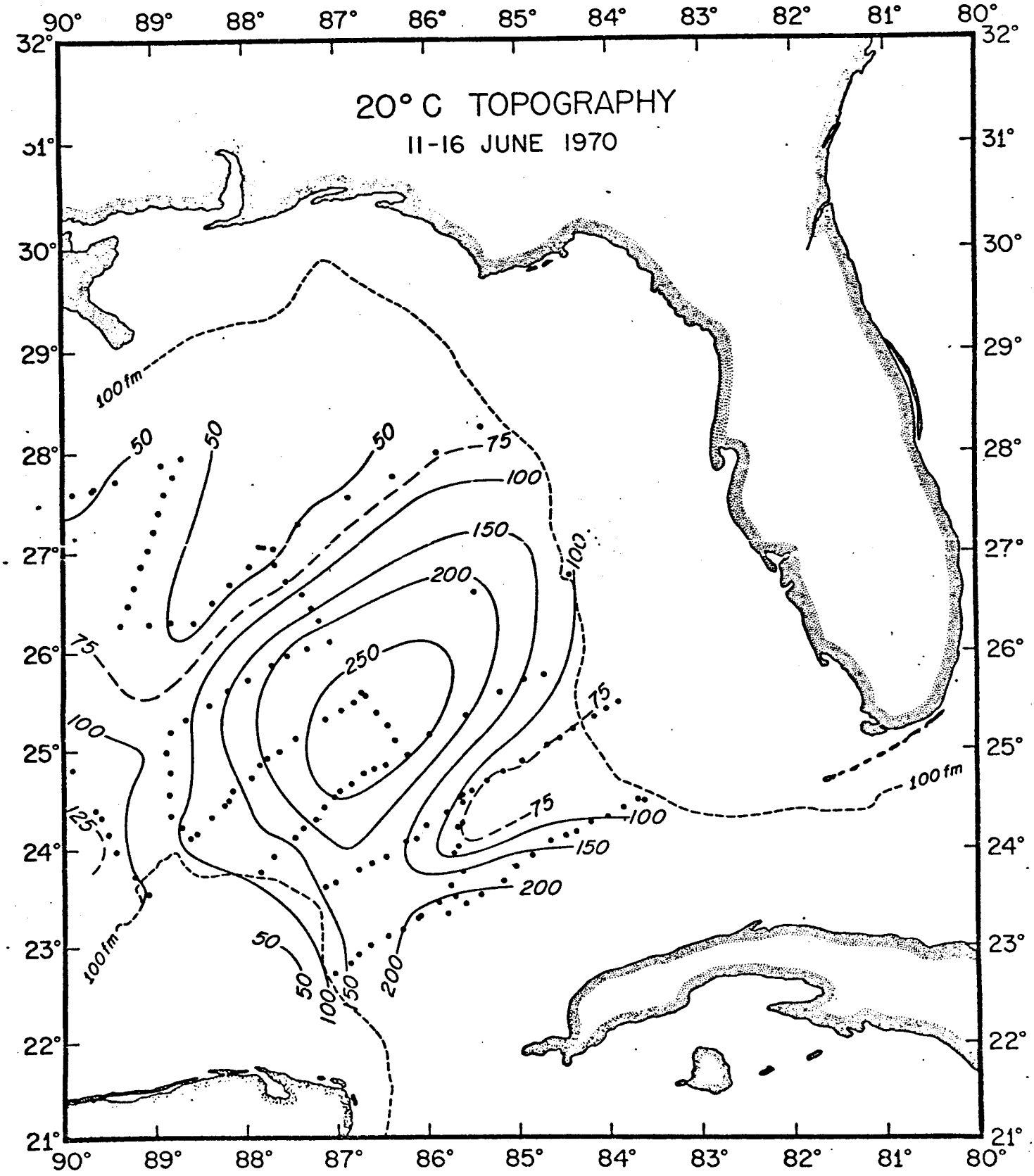
20° C TOPOGRAPHY
11-16 JUNE 1970
90° 89° 88° 87° 86° 85° 84° 83° 82° 81° 80°
32° 31° 30° 29° 28° 27° 26° 25° 24° 23° 22° 21°
100 fm
50
75
100
150
200
250
125

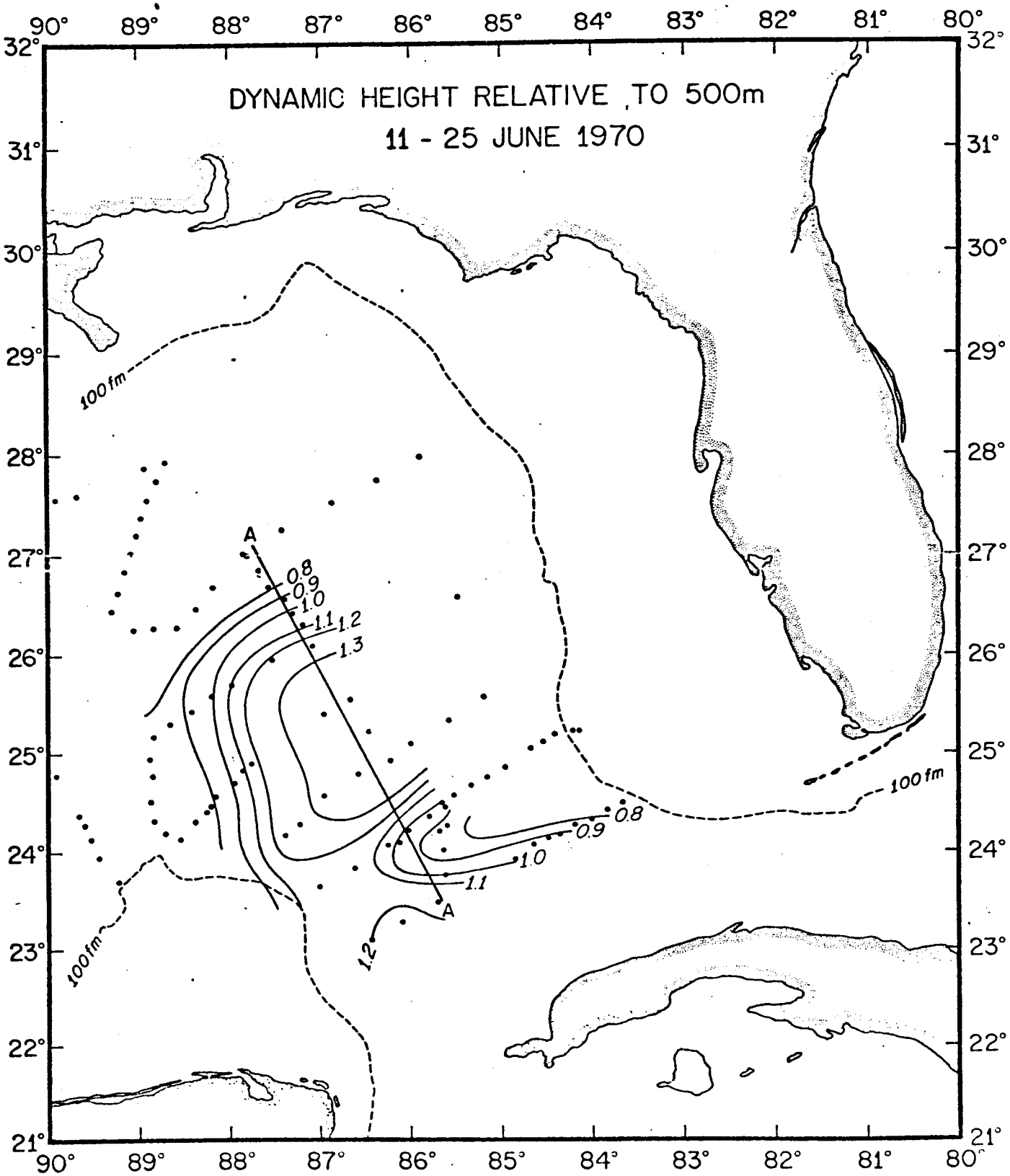
DYNAMIC HEIGHT RELATIVE TO 500m
11 - 25 JUNE 1970
90° 89° 88° 87° 86° 85° 84° 83° 82° 81° 80°
32° 31° 30° 29° 28° 27° 26° 25° 24° 23° 22° 21°
100 fm
A
0.8
0.9
1.0
1.1
1.2
1.3
A
0.8
0.9
1.0
1.1
1.2
100 fm
100 fm

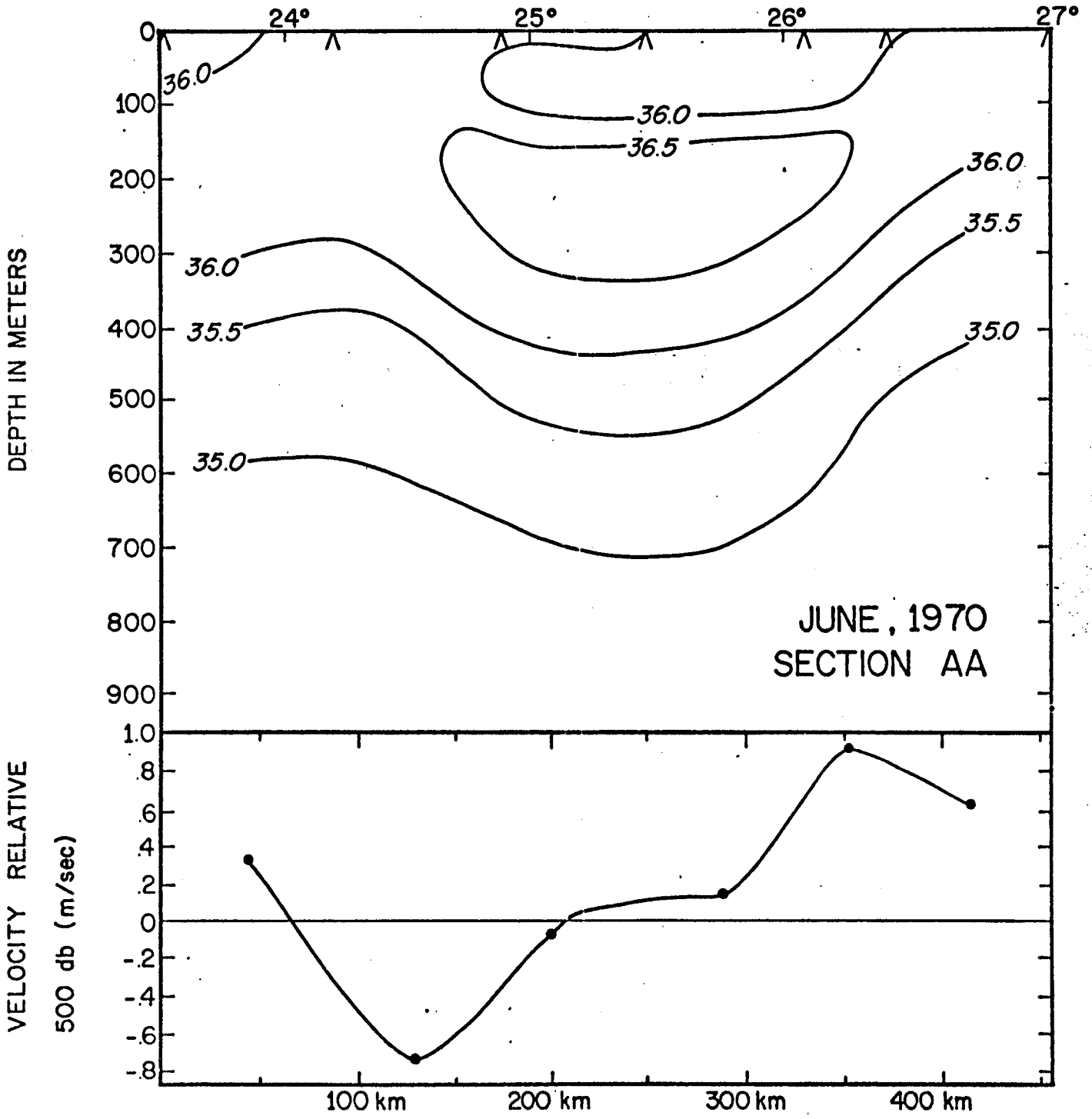
24°
25°
26°
27°
0
100
200
300
400
500
600
700
800
900
36.0
36.0
36.5
36.0
35.5
36.0
35.5
35.0
DEPTH IN METERS
JUNE, 1970
SECTION AA
1.0
.8
.6
.4
.2
0
-.2
-.4
-.6
-.8
VELOCITY RELATIVE
500 db (m/sec)
100 km
200 km
300 km
400 km

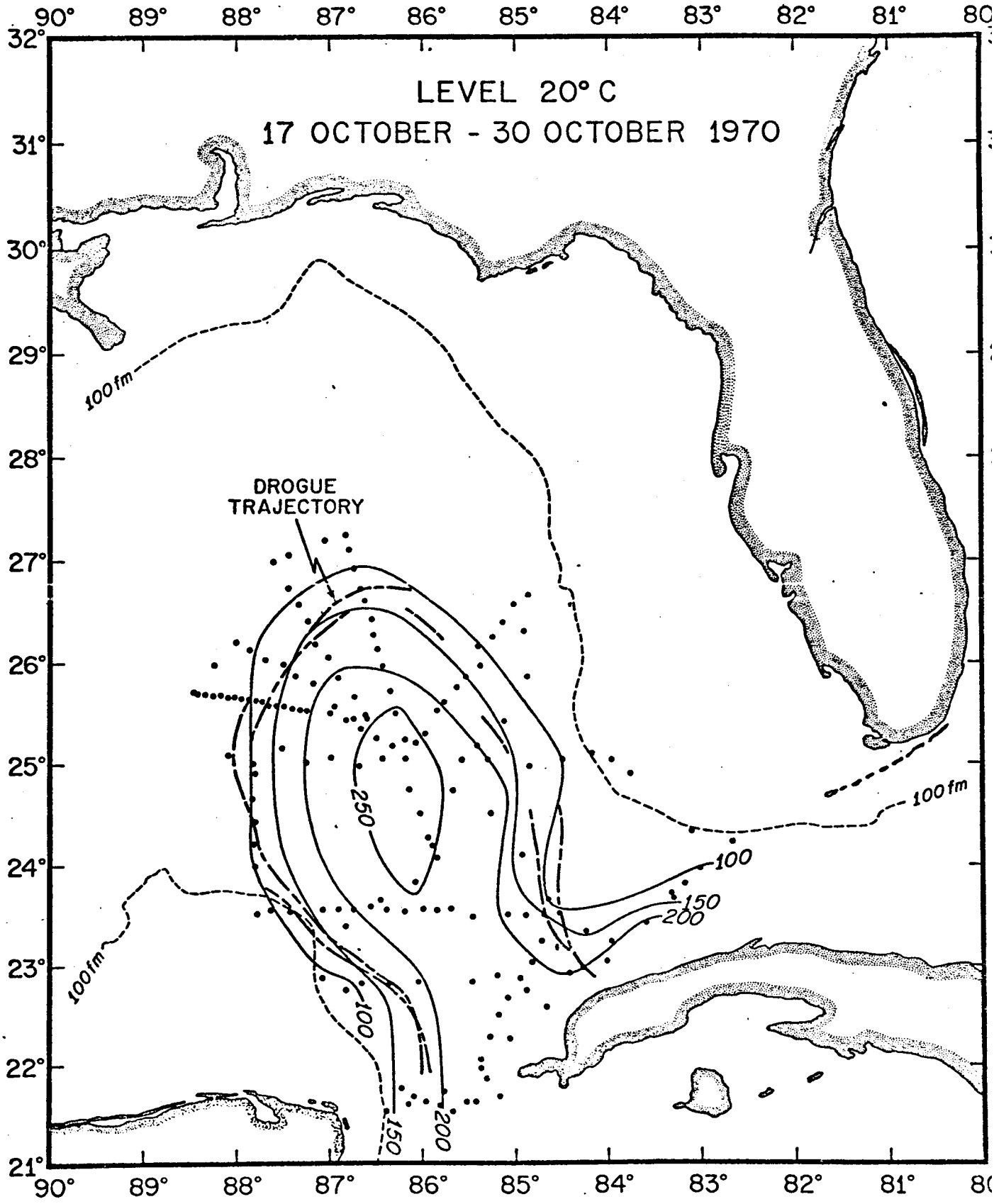
LEVEL 20° C
17 OCTOBER - 30 OCTOBER 1970
DROGUE TRAJECTORY
100 fm
100 fm
100 fm
250
100
150
200
100
150
200
90°
89°
88°
87°
86°
85°
84°
83°
82°
81°
32°
31°
30°
29°
28°
27°
26°
25°
24°
23°
22°
21°

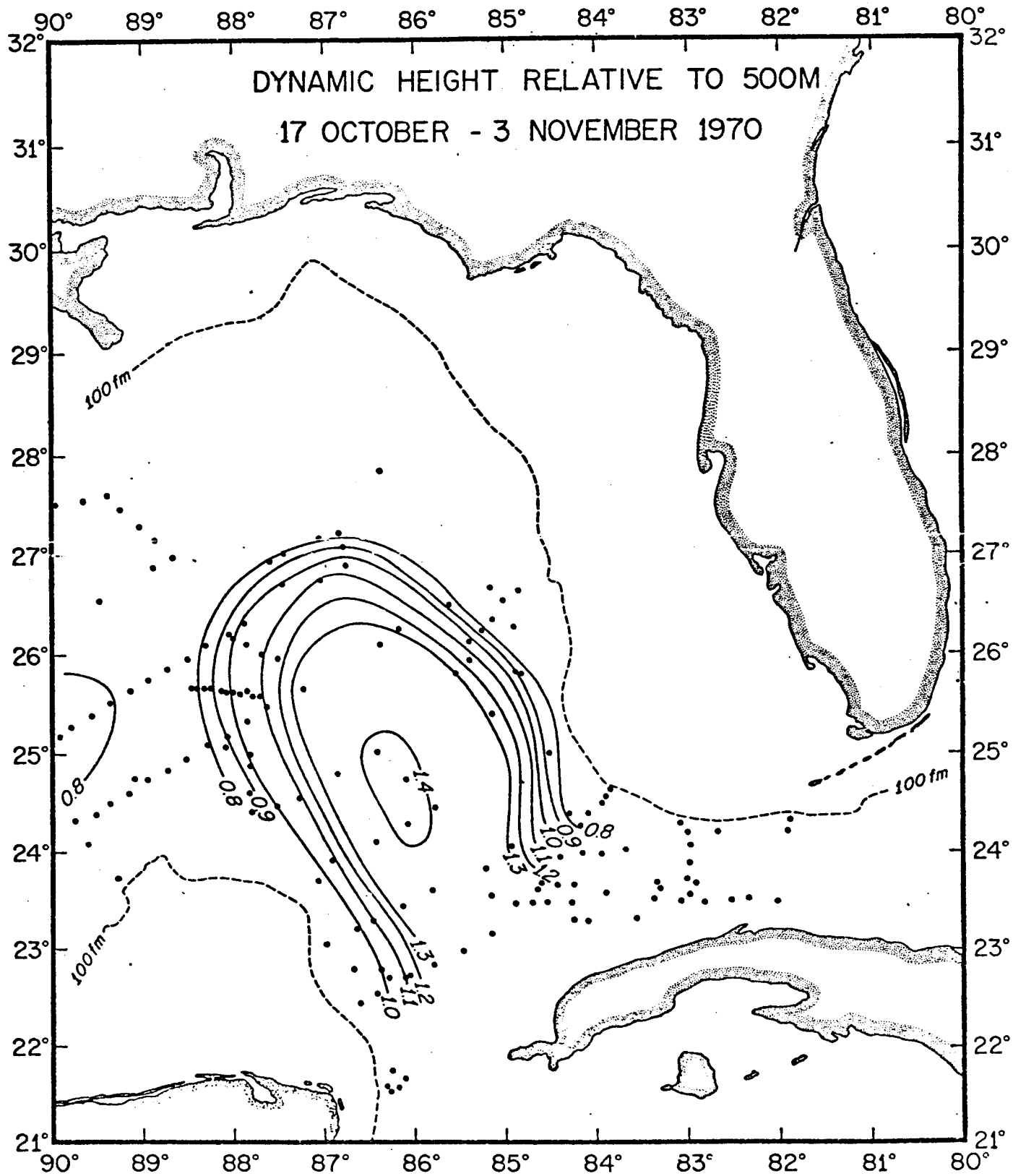
DYNAMIC HEIGHT RELATIVE TO 500M
17 OCTOBER - 3 NOVEMBER 1970
90° 89° 88° 87° 86° 85° 84° 83° 82° 81° 80°
32° 31° 30° 29° 28° 27° 26° 25° 24° 23° 22° 21°
100 fm
100 fm
100 fm
0.8
0.8
0.9
0.8
0.9
1.0
1.1
1.2
1.3
1.4
1.3
1.2
1.1
1.0

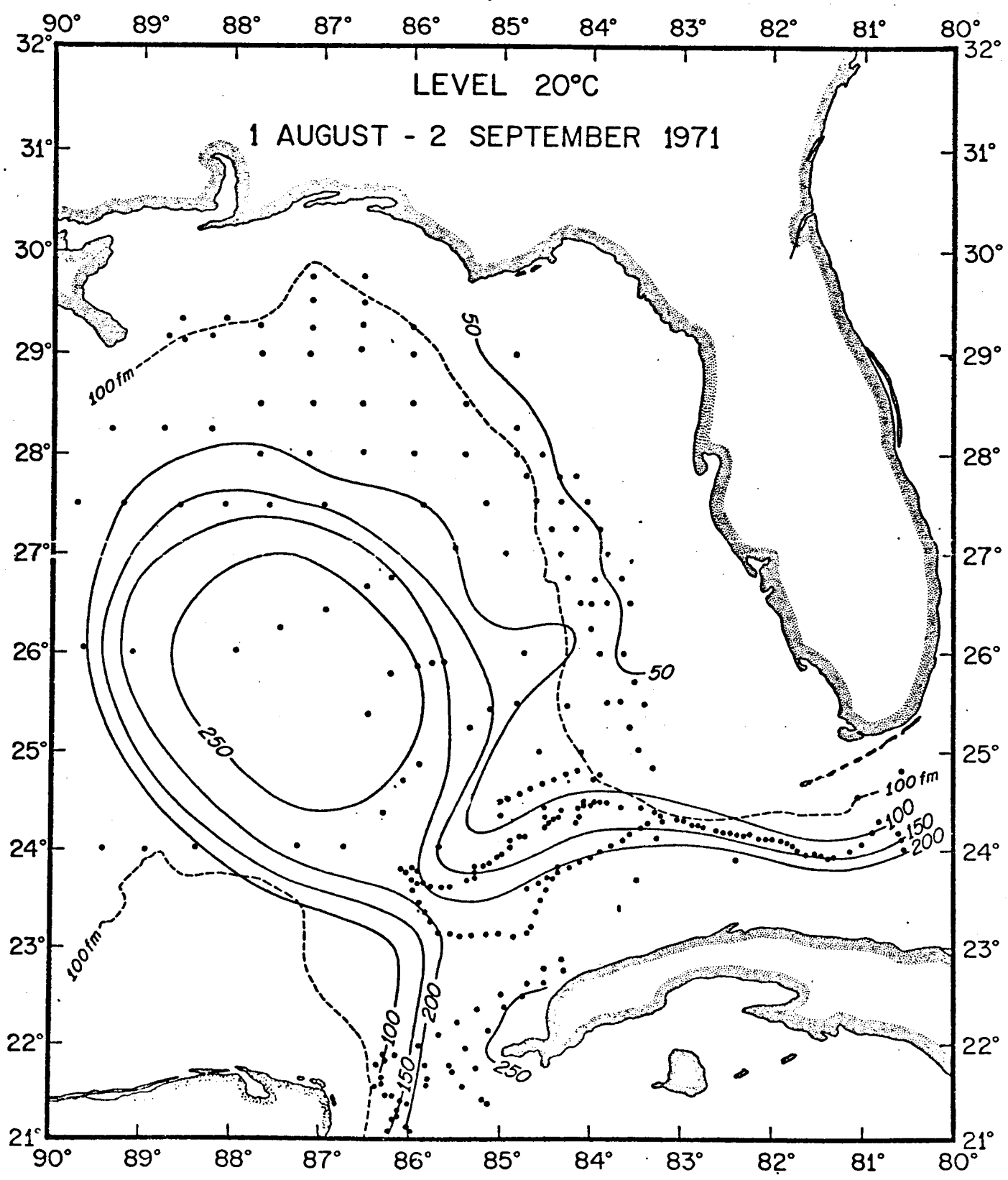
LEVEL 20°C
1 AUGUST - 2 SEPTEMBER 1971
90° 89° 88° 87° 86° 85° 84° 83° 82° 81° 80°
32° 31° 30° 29° 28° 27° 26° 25° 24° 23° 22° 21°
100 fm
50
250
100
150
200

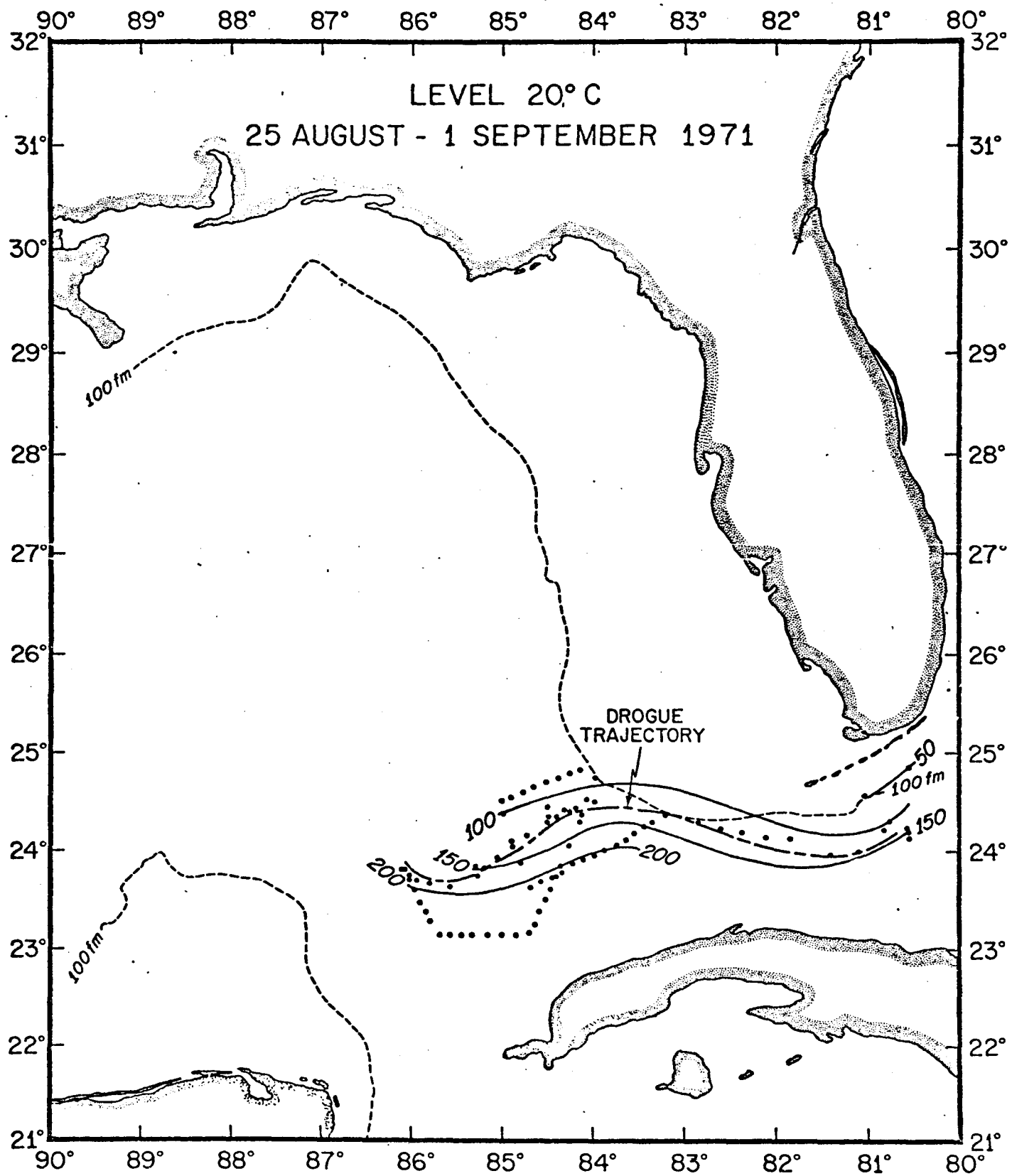
LEVEL 20° C
25 AUGUST - 1 SEPTEMBER 1971
90° 89° 88° 87° 86° 85° 84° 83° 82° 81° 80°
32° 31° 30° 29° 28° 27° 26° 25° 24° 23° 22° 21°
100 fm
100 fm
DROGUE TRAJECTORY
50
100 fm
100
150
200
150
200

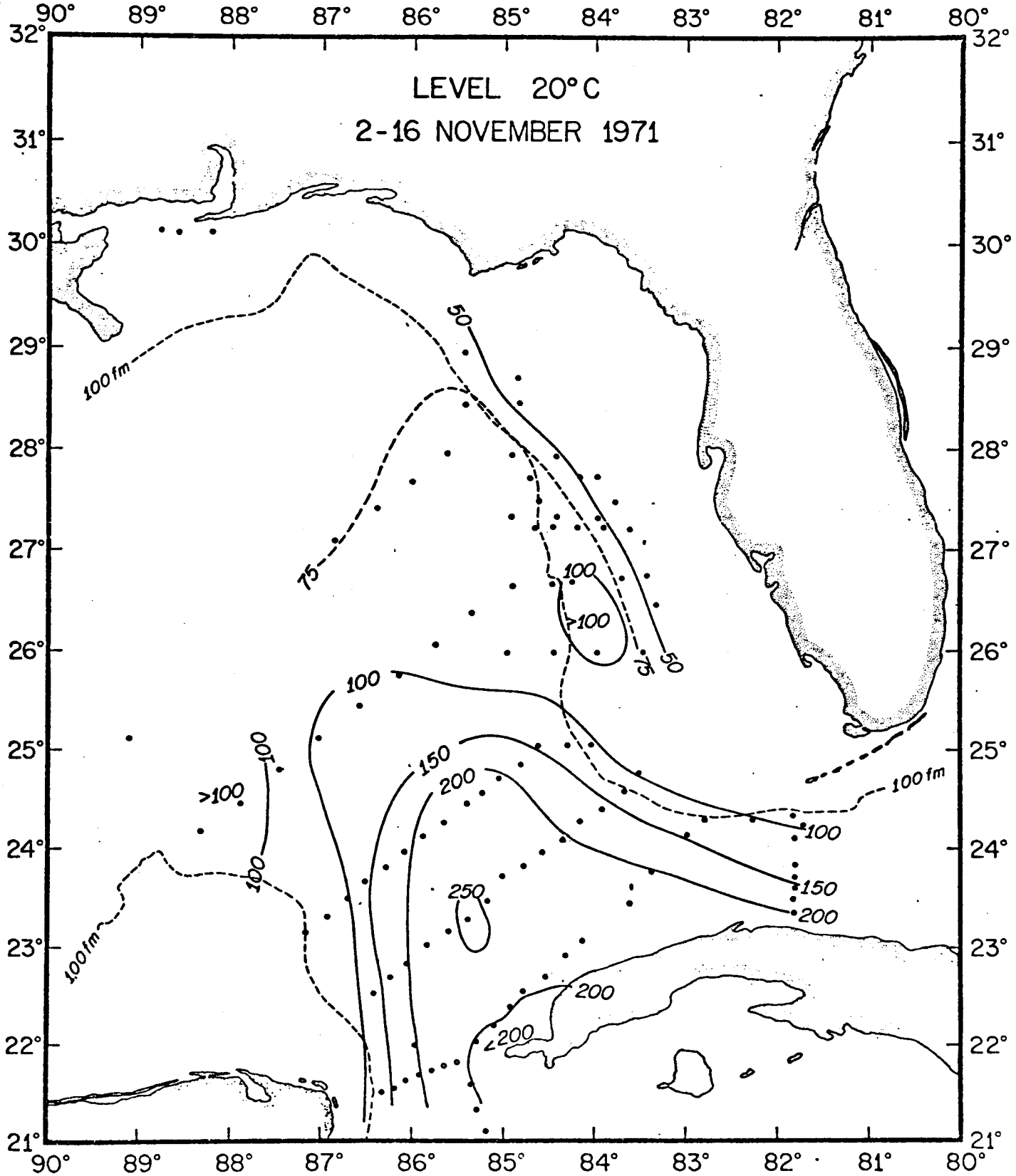
LEVEL 20°C
2-16 NOVEMBER 1971
90° 89° 88° 87° 86° 85° 84° 83° 82° 81° 80°
32° 31° 30° 29° 28° 27° 26° 25° 24° 23° 22° 21°
100 fm
50
75
100
>100
150
200
250

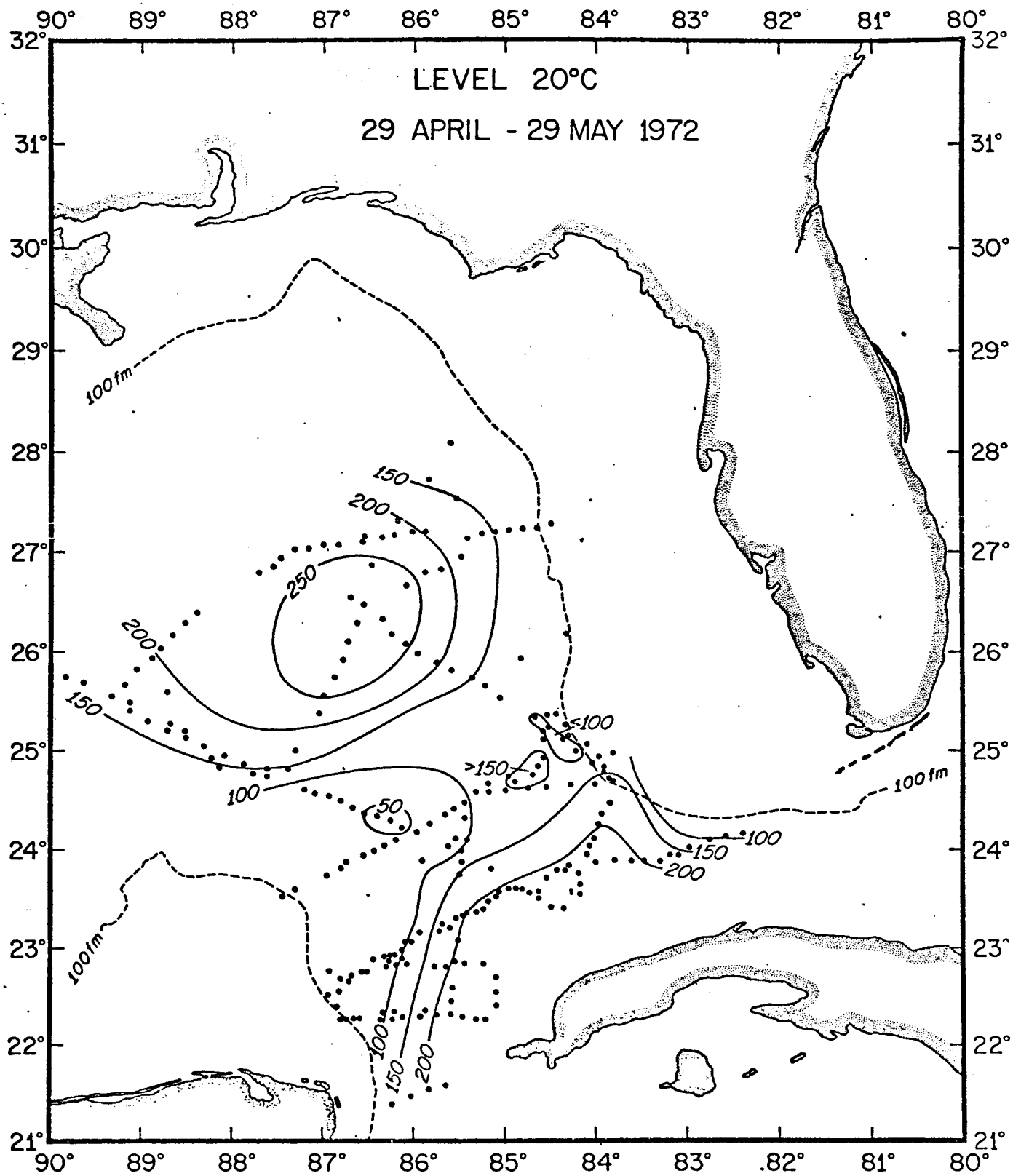
LEVEL 20°C
29 APRIL - 29 MAY 1972
90° 89° 88° 87° 86° 85° 84° 83° 82° 81° 80°
32° 31° 30° 29° 28° 27° 26° 25° 24° 23° 22° 21°
100 fm
150
200
250
200
150
100
50
<100
>150
100 fm
100
150
200
100 fm
100
150
200

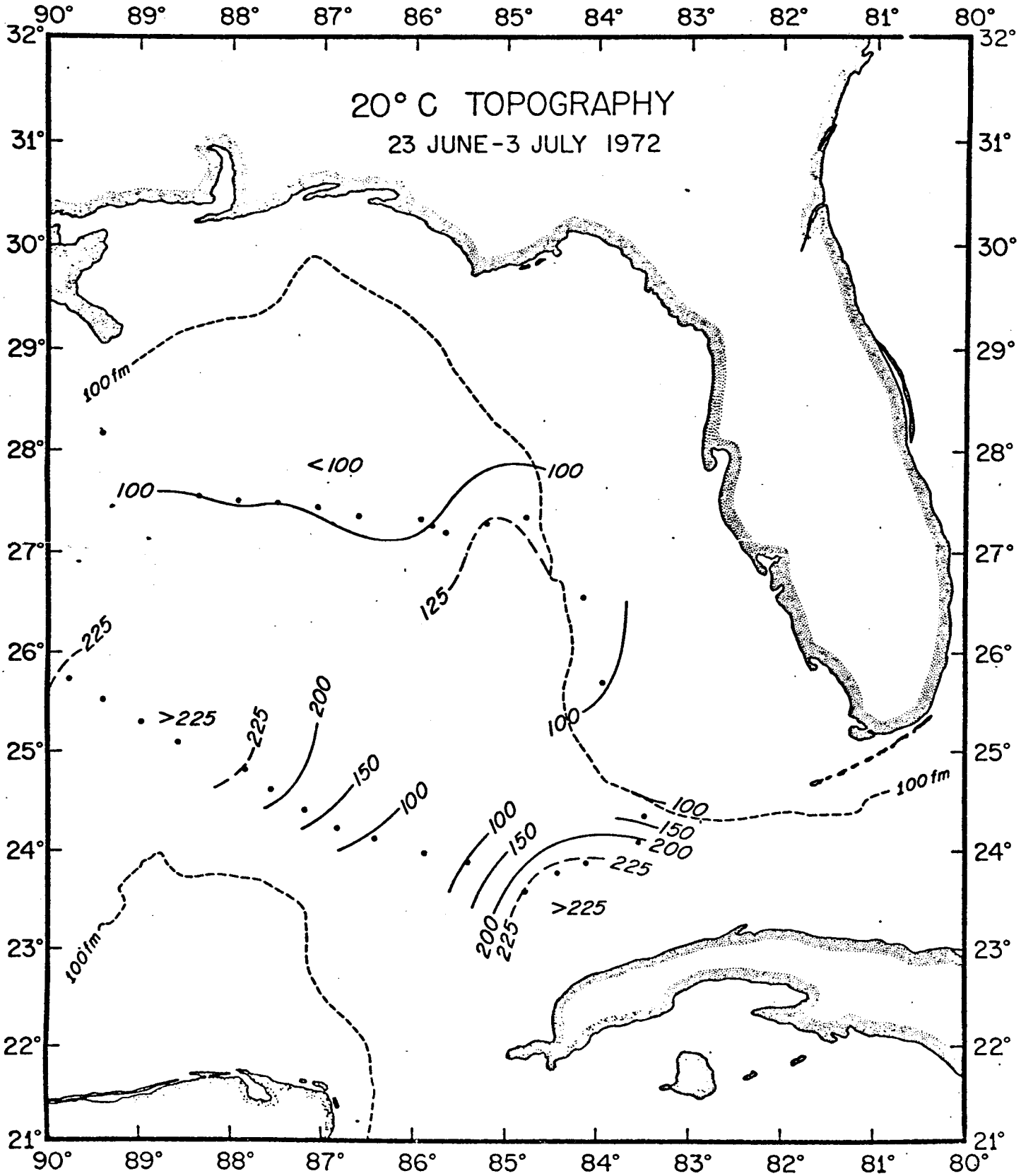
20° C TOPOGRAPHY
23 JUNE-3 JULY 1972
90° 89° 88° 87° 86° 85° 84° 83° 82° 81° 80°
32° 31° 30° 29° 28° 27° 26° 25° 24° 23° 22° 21°
100 fm
< 100
100
125
225
> 225
200
150
100
100 fm

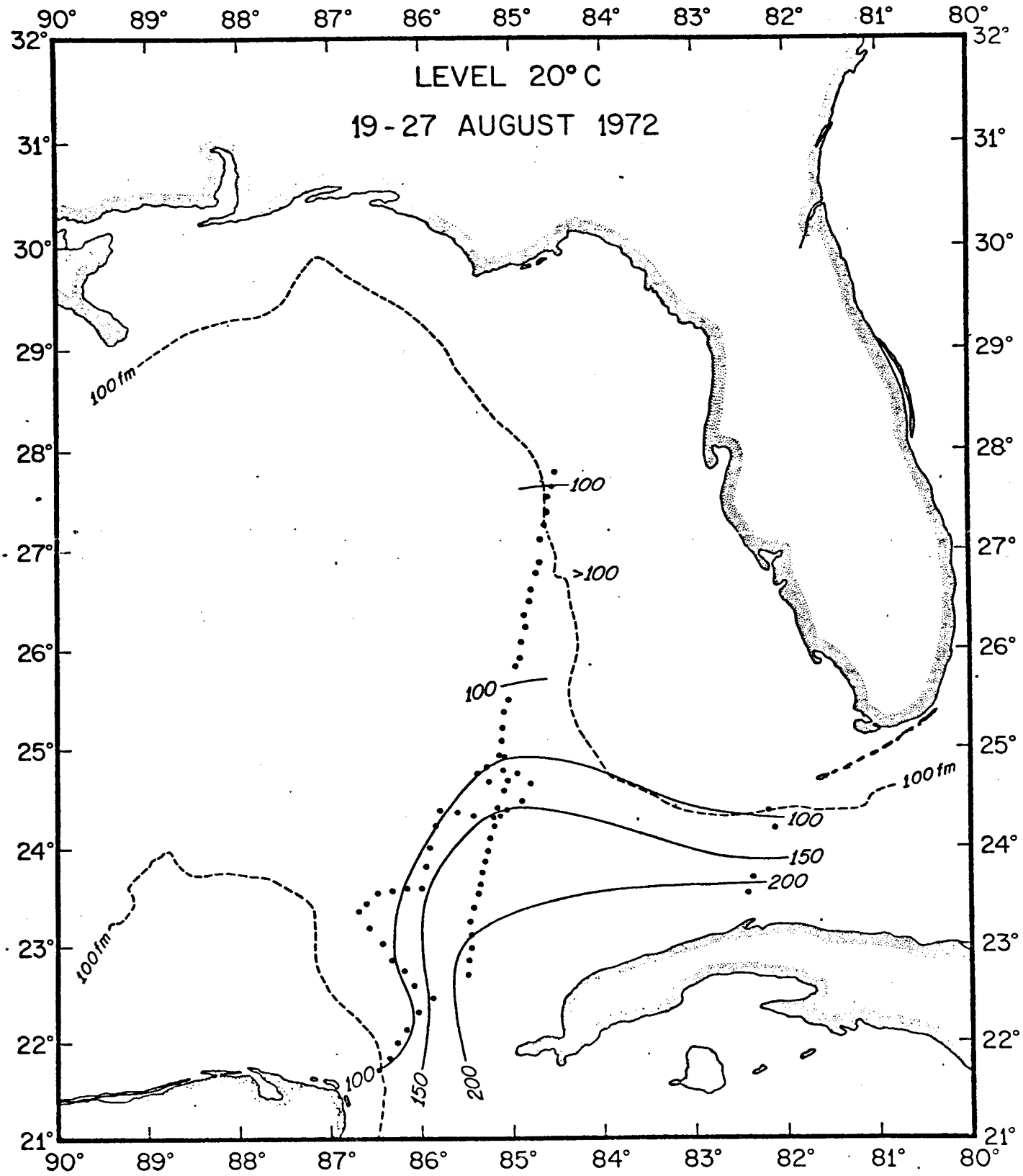
LEVEL 20° C
19 - 27 AUGUST 1972
90°
89°
88°
87°
86°
85°
84°
83°
82°
81°
80°
32°
31°
30°
29°
28°
27°
26°
25°
24°
23°
22°
21°
100 fm
100
>100
100
100 fm
100
150
200
100 fm
100
150
200

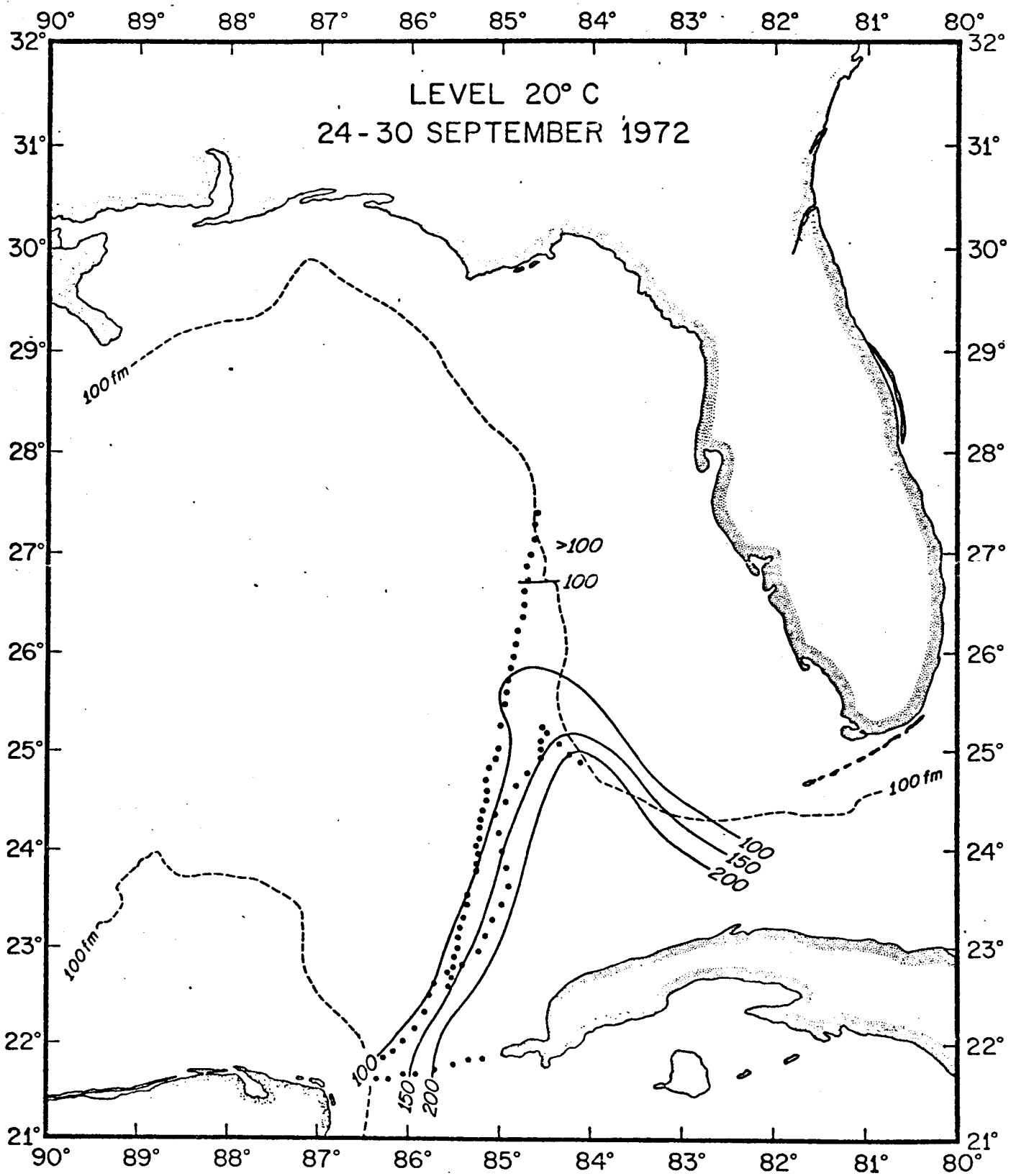
LEVEL 20° C
24-30 SEPTEMBER 1972
90° 89° 88° 87° 86° 85° 84° 83° 82° 81° 80°
32° 31° 30° 29° 28° 27° 26° 25° 24° 23° 22° 21°
100 fm
>100
100
100
150
200
100 fm
100 fm
100
150
200

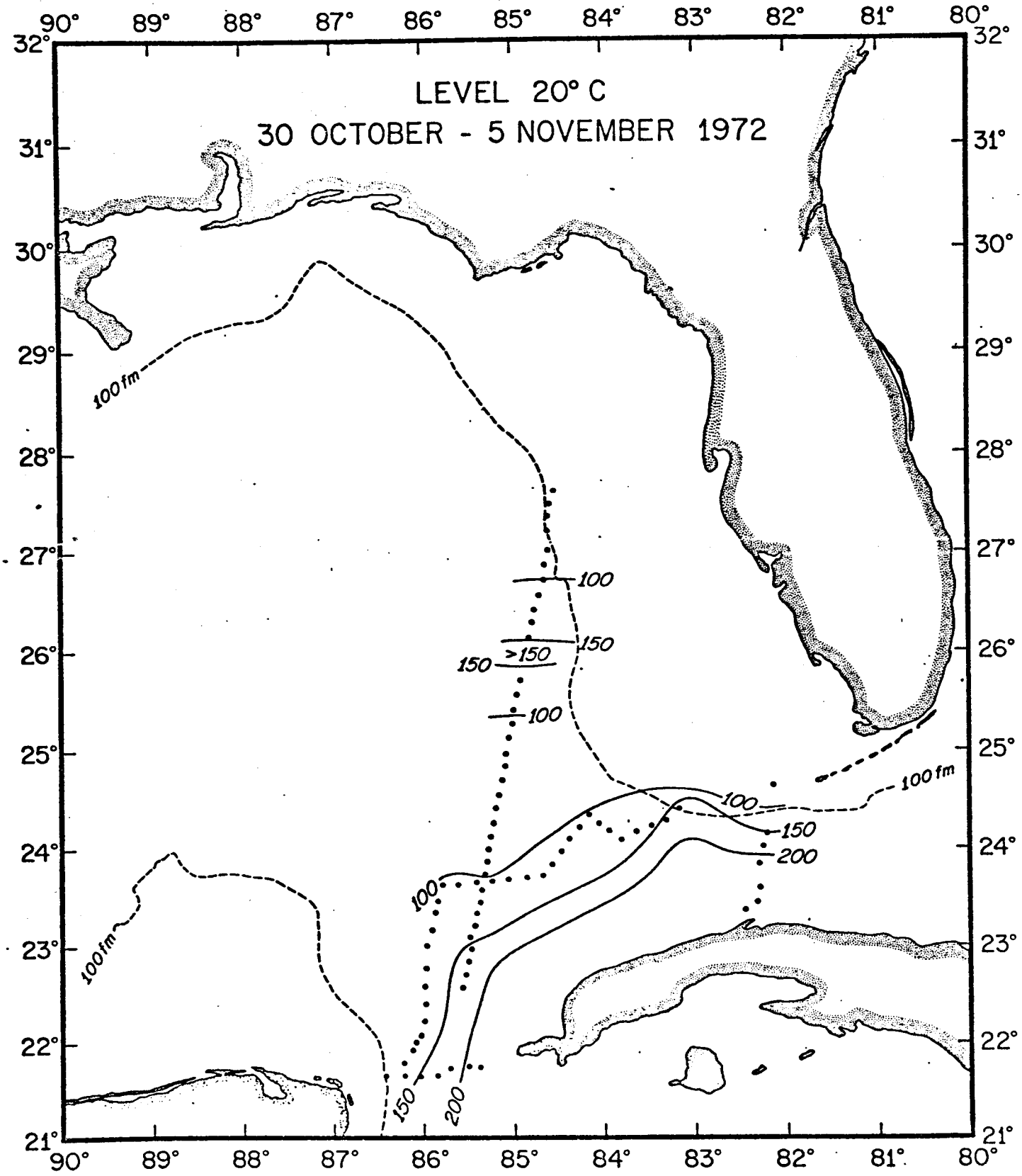
LEVEL 20° C
30 OCTOBER - 5 NOVEMBER 1972
90° 89° 88° 87° 86° 85° 84° 83° 82° 81° 80°
32° 31° 30° 29° 28° 27° 26° 25° 24° 23° 22° 21°
100 fm
100
150
>150
150
100
100 fm
100
150
200
100
150
200
100 fm

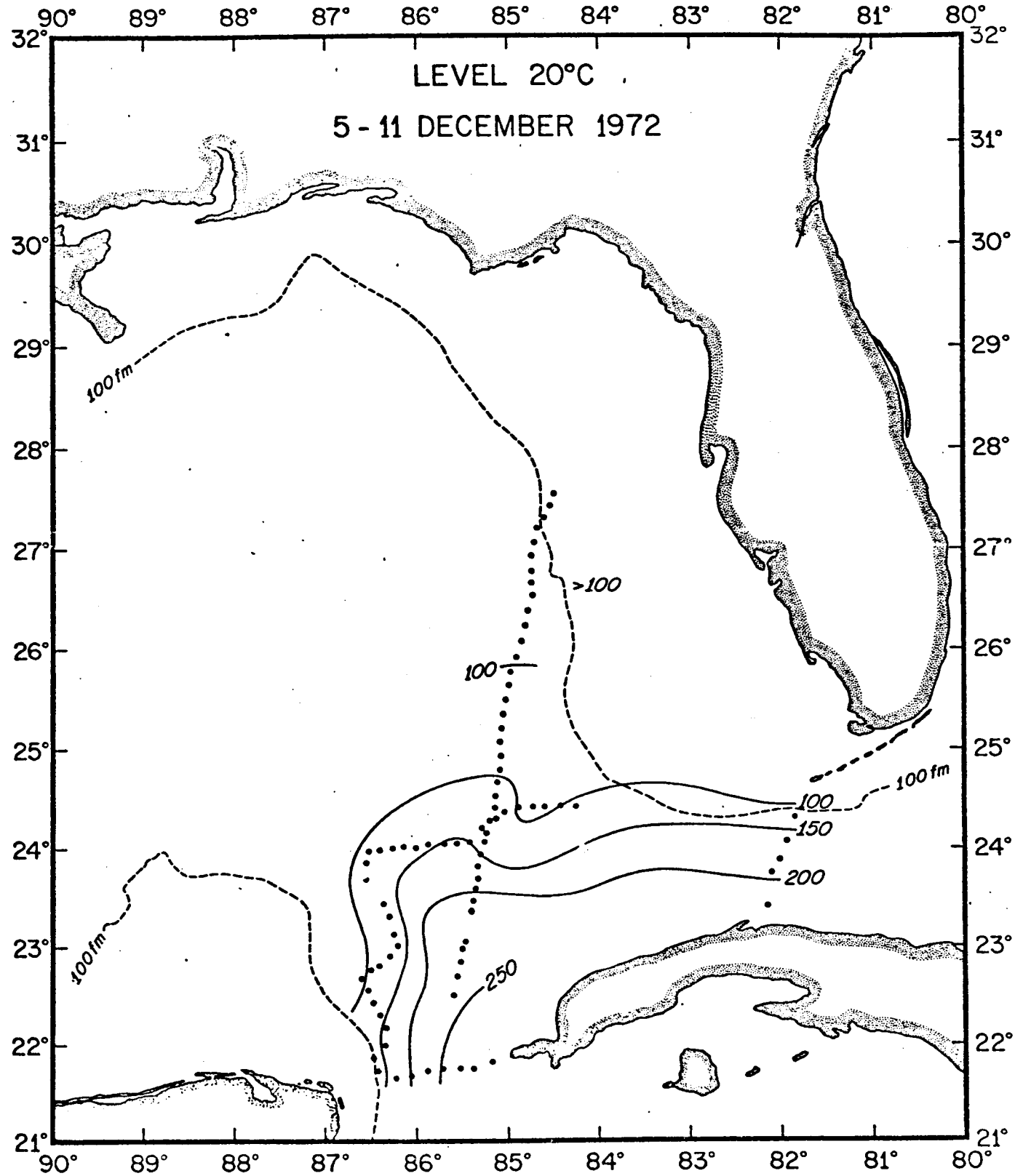
LEVEL 20°C
5 - 11 DECEMBER 1972
90° 89° 88° 87° 86° 85° 84° 83° 82° 81° 80°
32° 31° 30° 29° 28° 27° 26° 25° 24° 23° 22° 21°
100 fm
>100
100
100 fm
100
150
200
250
100 fm

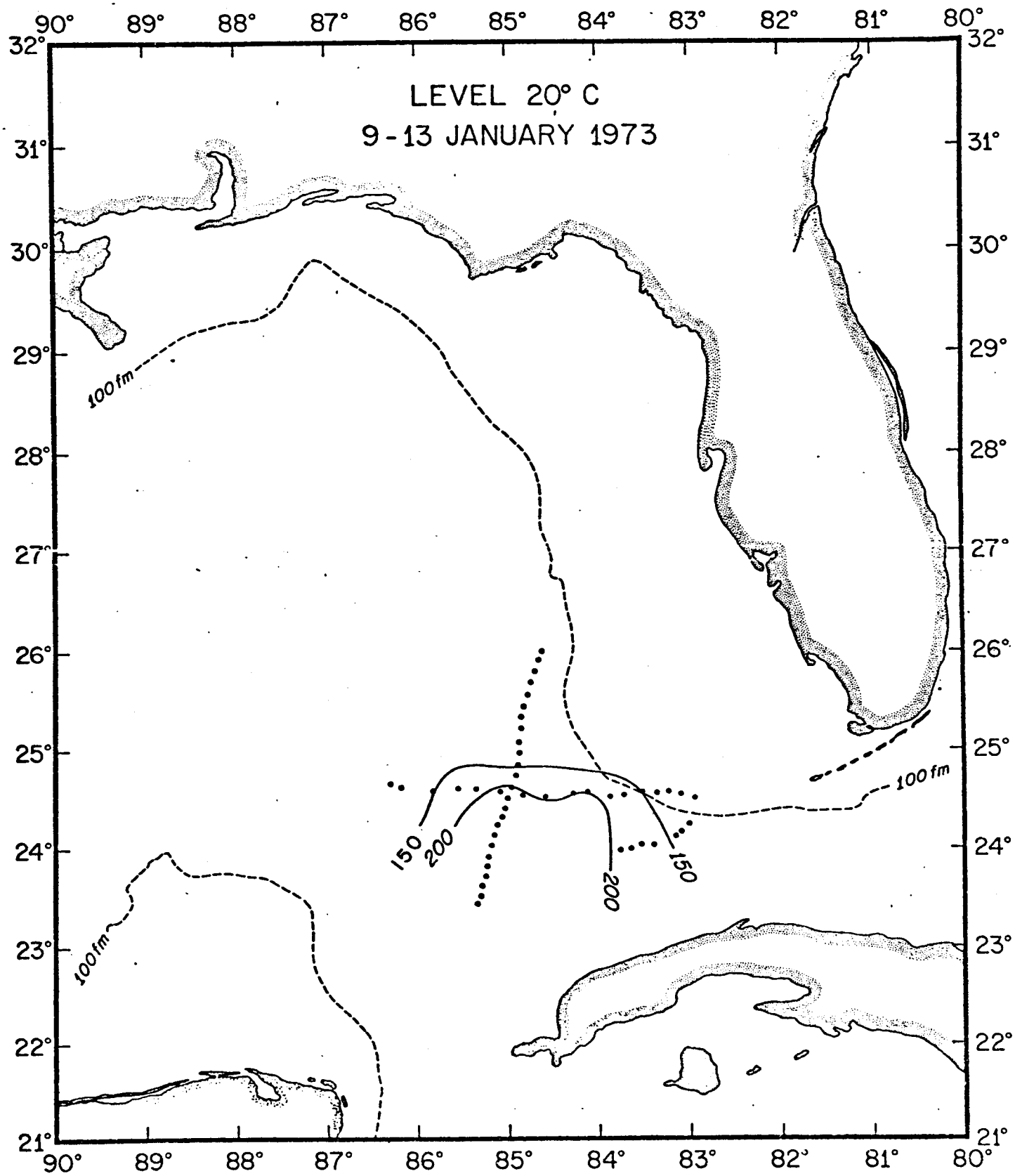
LEVEL 20° C
9-13 JANUARY 1973
90° 89° 88° 87° 86° 85° 84° 83° 82° 81° 80°
32° 31° 30° 29° 28° 27° 26° 25° 24° 23° 22° 21°
100 fm
100 fm
100 fm
150
200
200
150

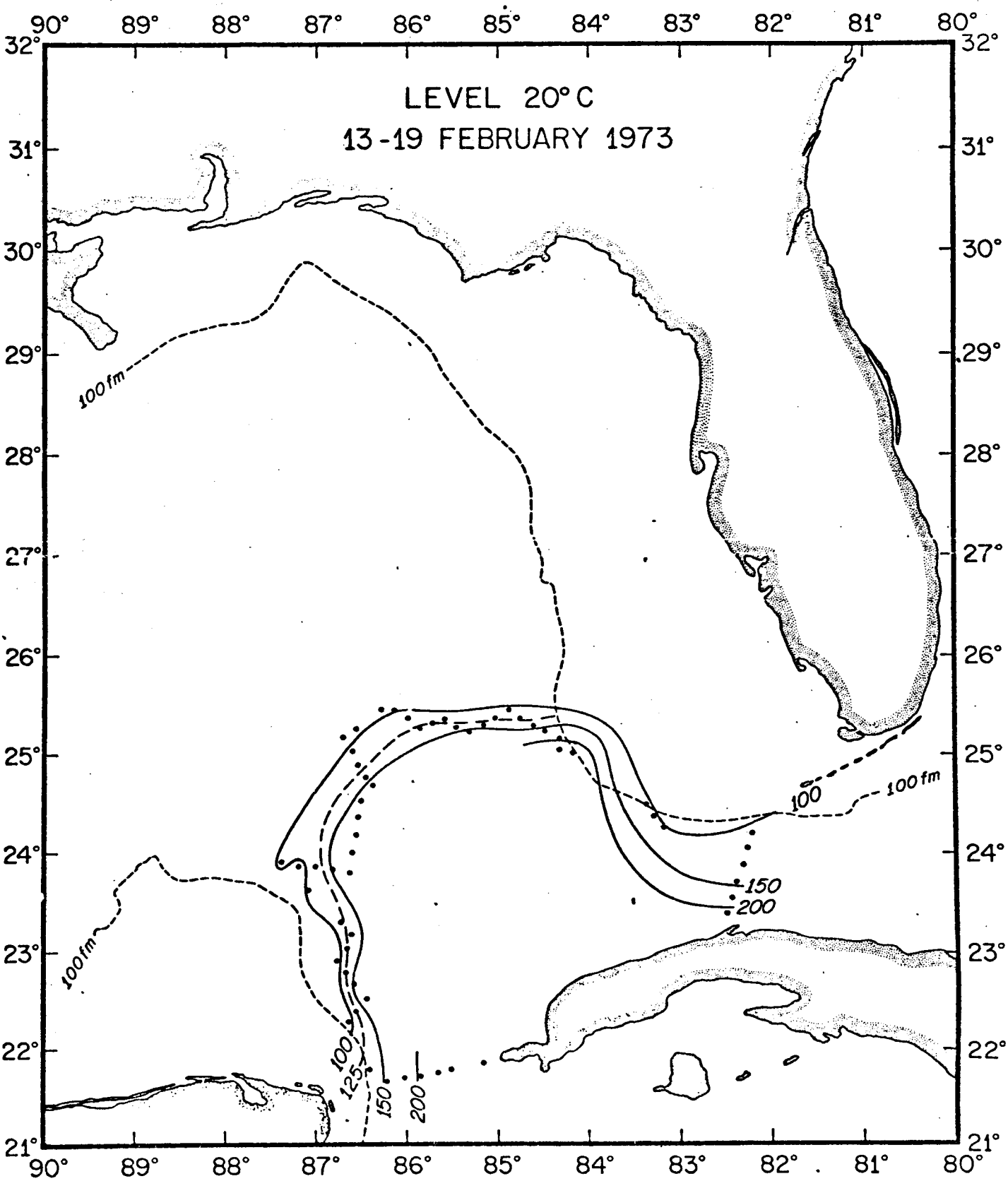
LEVEL 20°C
13-19 FEBRUARY 1973
90° 89° 88° 87° 86° 85° 84° 83° 82° 81° 80°
32° 31° 30° 29° 28° 27° 26° 25° 24° 23° 22° 21°
100 fm
100 fm
100 fm
100
125
150
200
150
200

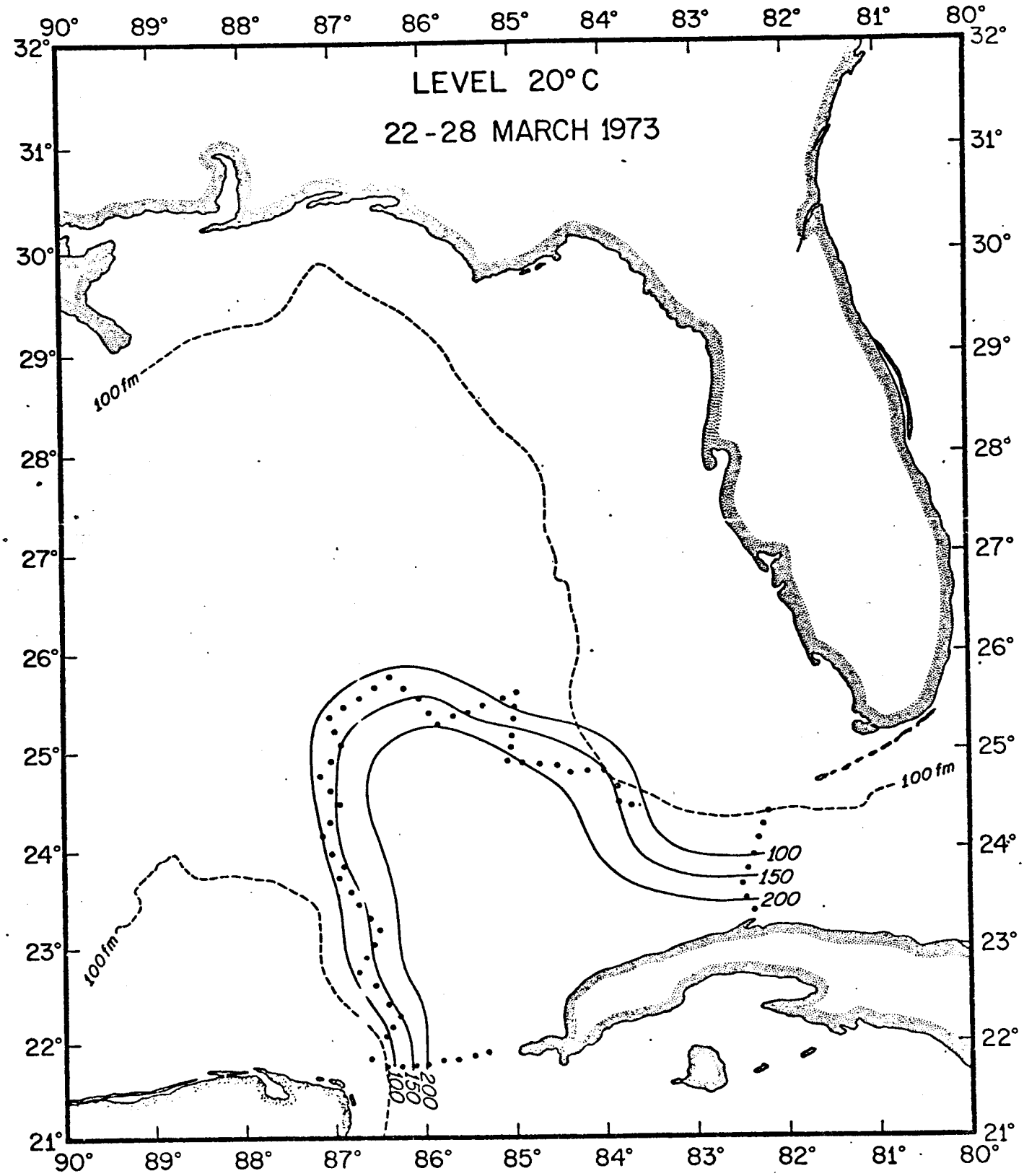
LEVEL 20°C
22-28 MARCH 1973
90° 89° 88° 87° 86° 85° 84° 83° 82° 81° 80°
32° 31° 30° 29° 28° 27° 26° 25° 24° 23° 22° 21°
100 fm
100 fm
100 fm
100
150
200
200
150
100

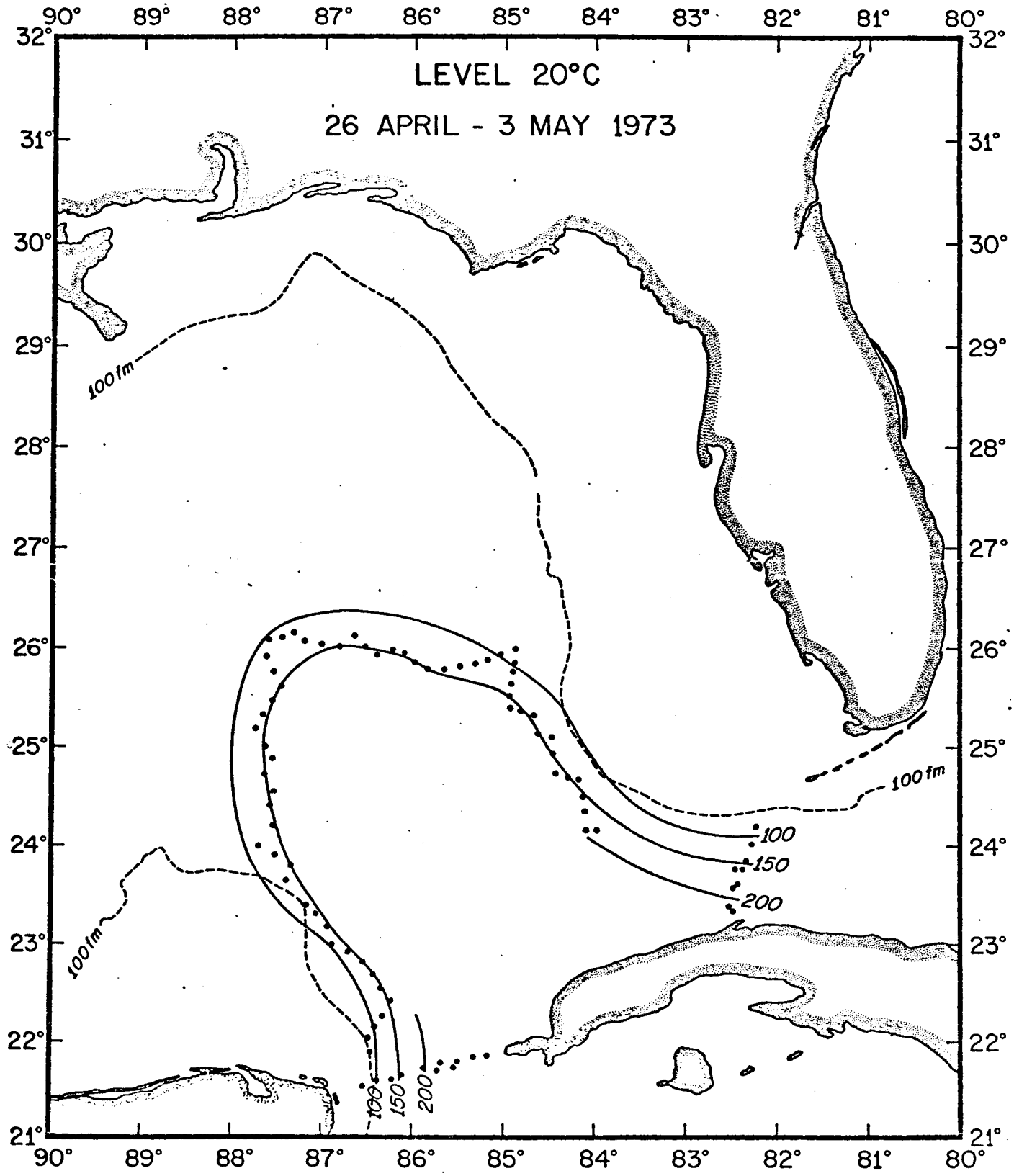
LEVEL 20°C
26 APRIL - 3 MAY 1973
90° 89° 88° 87° 86° 85° 84° 83° 82° 81° 80°
32° 31° 30° 29° 28° 27° 26° 25° 24° 23° 22° 21°
100 fm
100 fm
100 fm
100
150
200
100
150
200

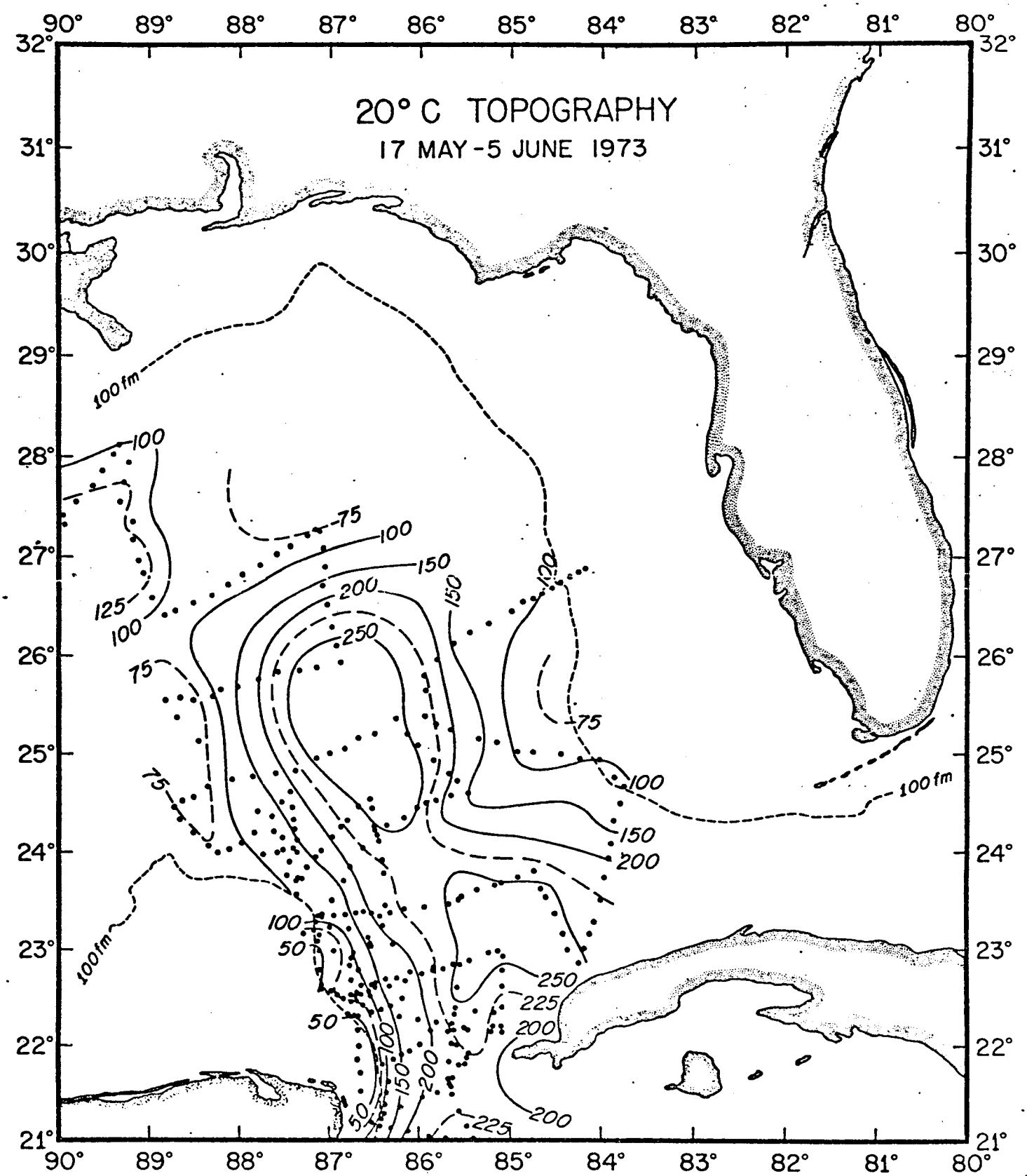
20° C TOPOGRAPHY
17 MAY - 5 JUNE 1973
90° 89° 88° 87° 86° 85° 84° 83° 82° 81° 80°
32° 31° 30° 29° 28° 27° 26° 25° 24° 23° 22° 21°
100 fm
100
75
125
150
200
250
120
50
225

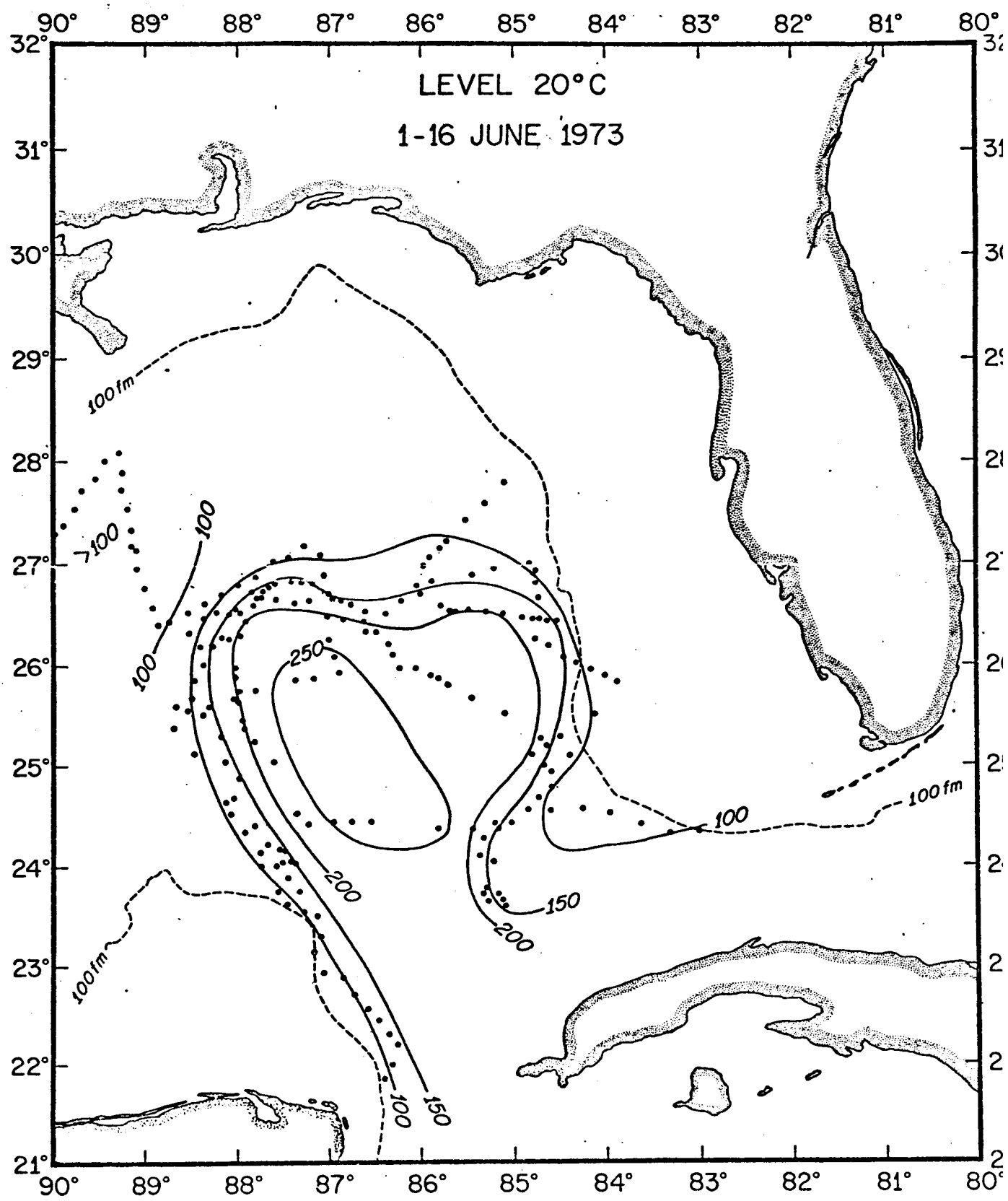
LEVEL 20°C
1-16 JUNE 1973
90°
89°
88°
87°
86°
85°
84°
83°
82°
81°
80°
32°
31°
30°
29°
28°
27°
26°
25°
24°
23°
22°
21°
100 fm
100
250
200
150

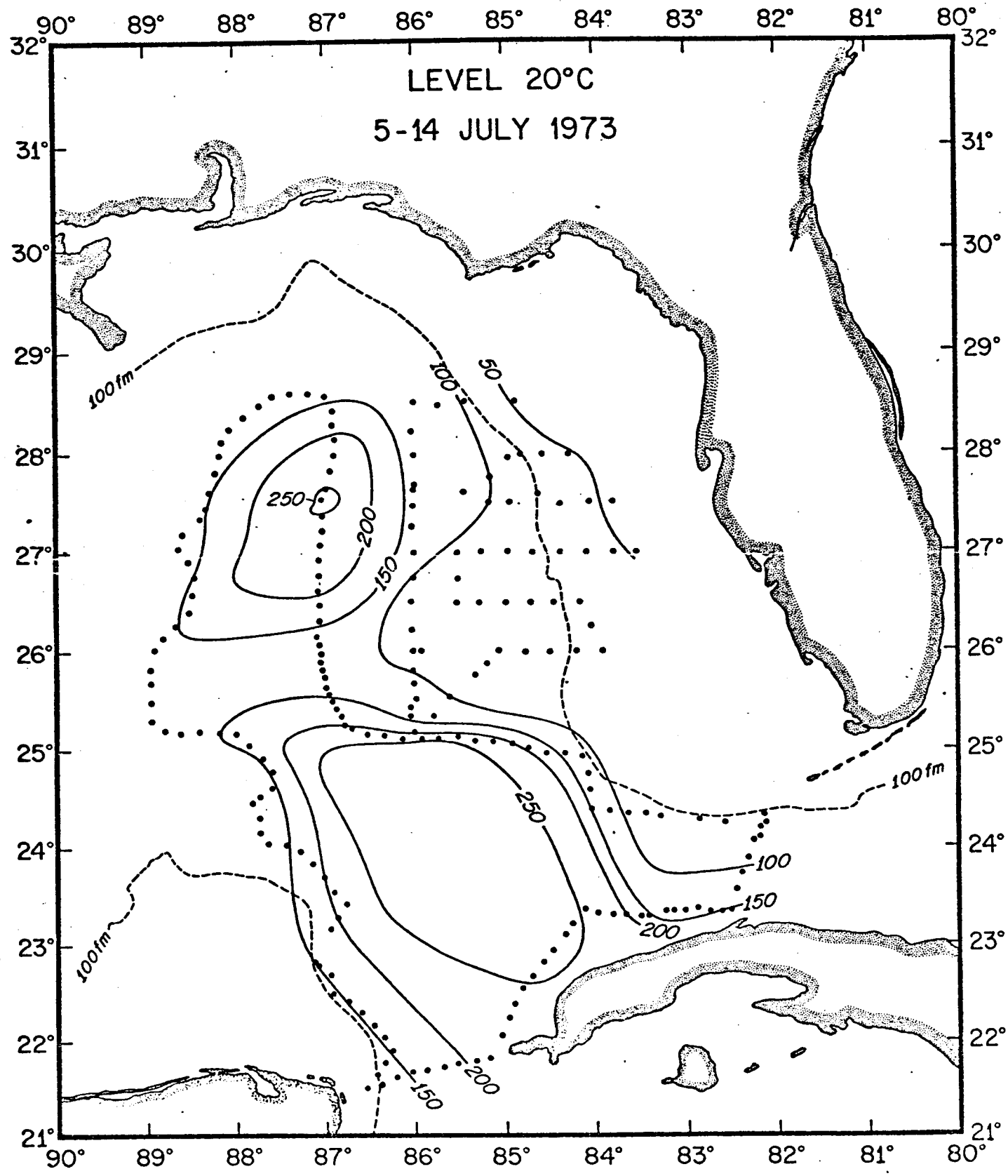
LEVEL 20°C
5-14 JULY 1973
90°
89°
88°
87°
86°
85°
84°
83°
82°
81°
80°
32°
31°
30°
29°
28°
27°
26°
25°
24°
23°
22°
21°
100 fm
50
100
150
200
250
100 fm
100
150
200
250
100 fm
150
200

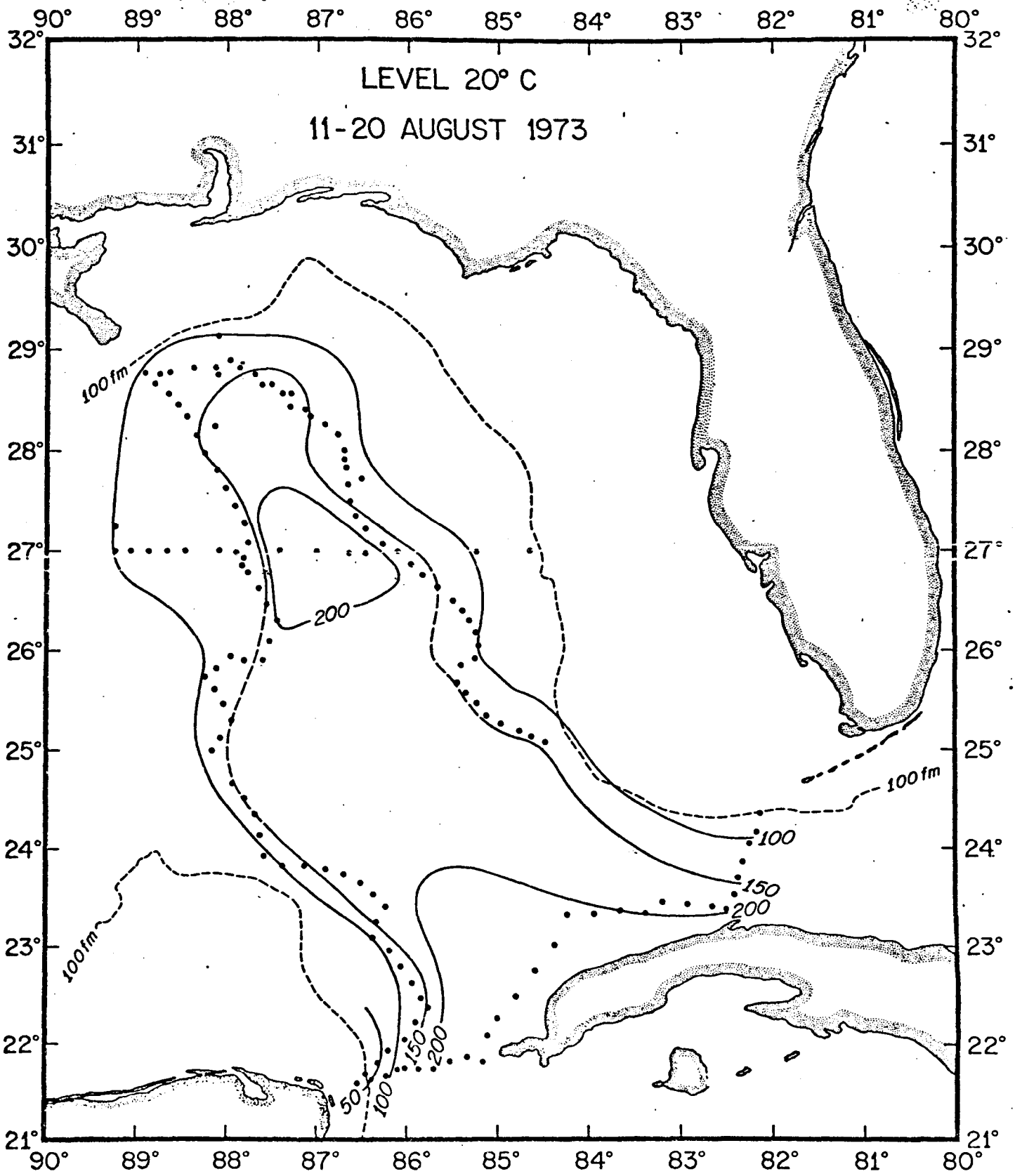
LEVEL 20° C
11-20 AUGUST 1973
90° 89° 88° 87° 86° 85° 84° 83° 82° 81° 80°
32° 31° 30° 29° 28° 27° 26° 25° 24° 23° 22° 21°
100 fm
200
100 fm
100
150
200
100 fm
50
100
150
200

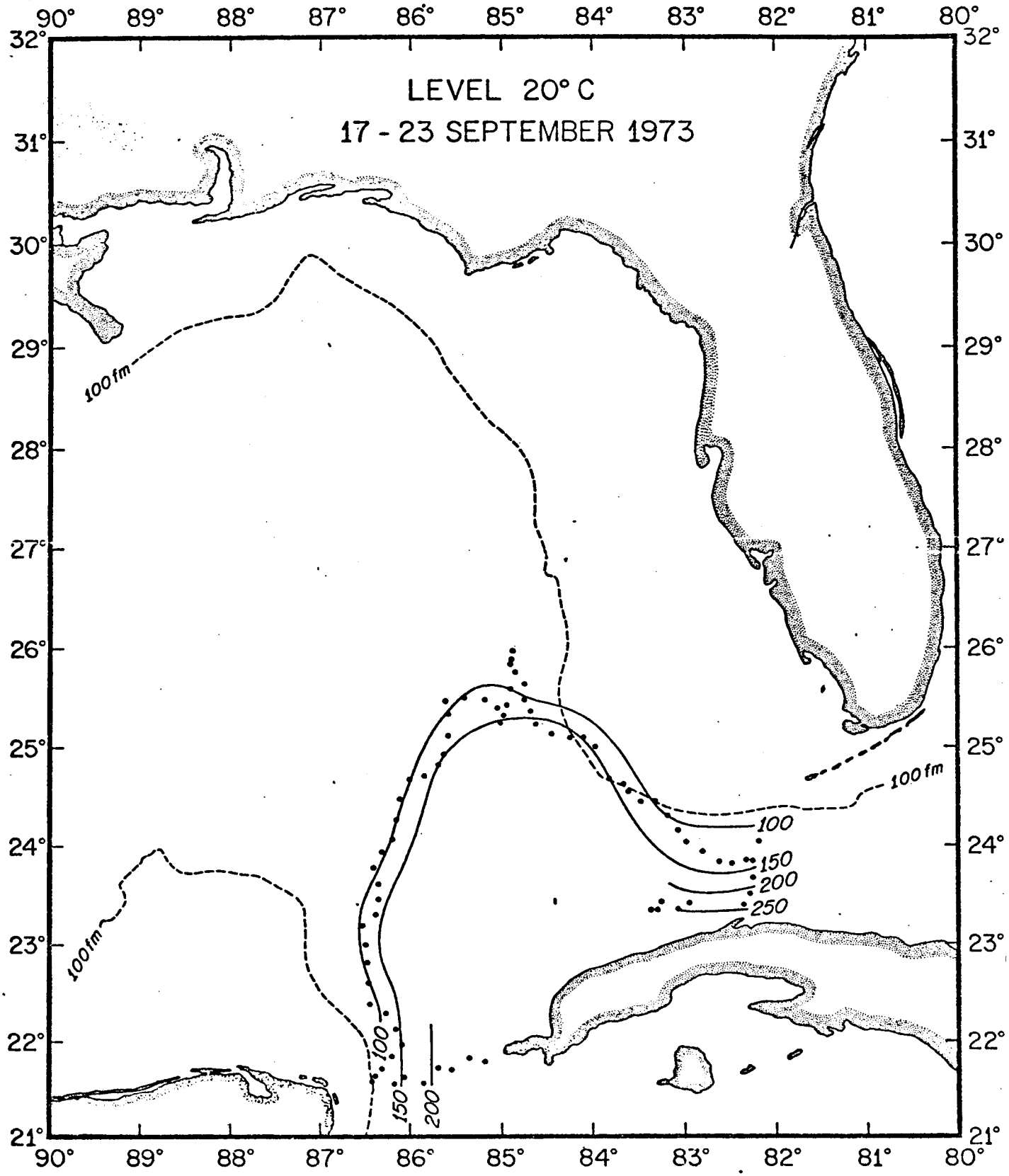
LEVEL 20° C
17 - 23 SEPTEMBER 1973
90° 89° 88° 87° 86° 85° 84° 83° 82° 81° 80°
32° 31° 30° 29° 28° 27° 26° 25° 24° 23° 22° 21°
100 fm
100 fm
100 fm
100
150
200
250
100
150
200

Appendix V

Monthly climatologies of the depth of the 20°C surface produced from NODC listings of average temperature by 5 m depth intervals, and 1° squares of latitude and longitude. The numbers within each 1° square represent the data points available. The contours are dashed in regions of few observations.

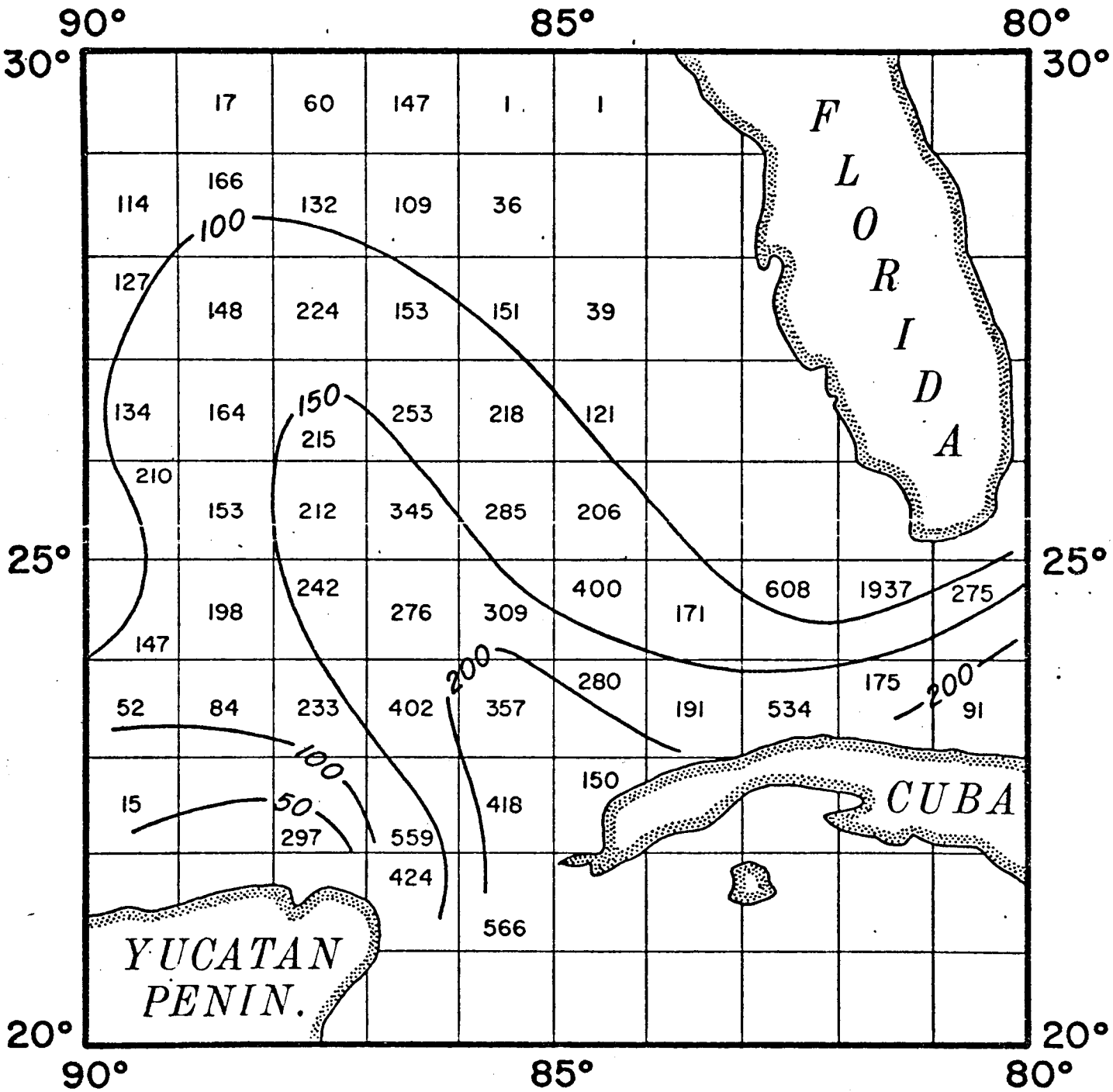

20°C TOPOGRAPHY
ANNUAL MEAN

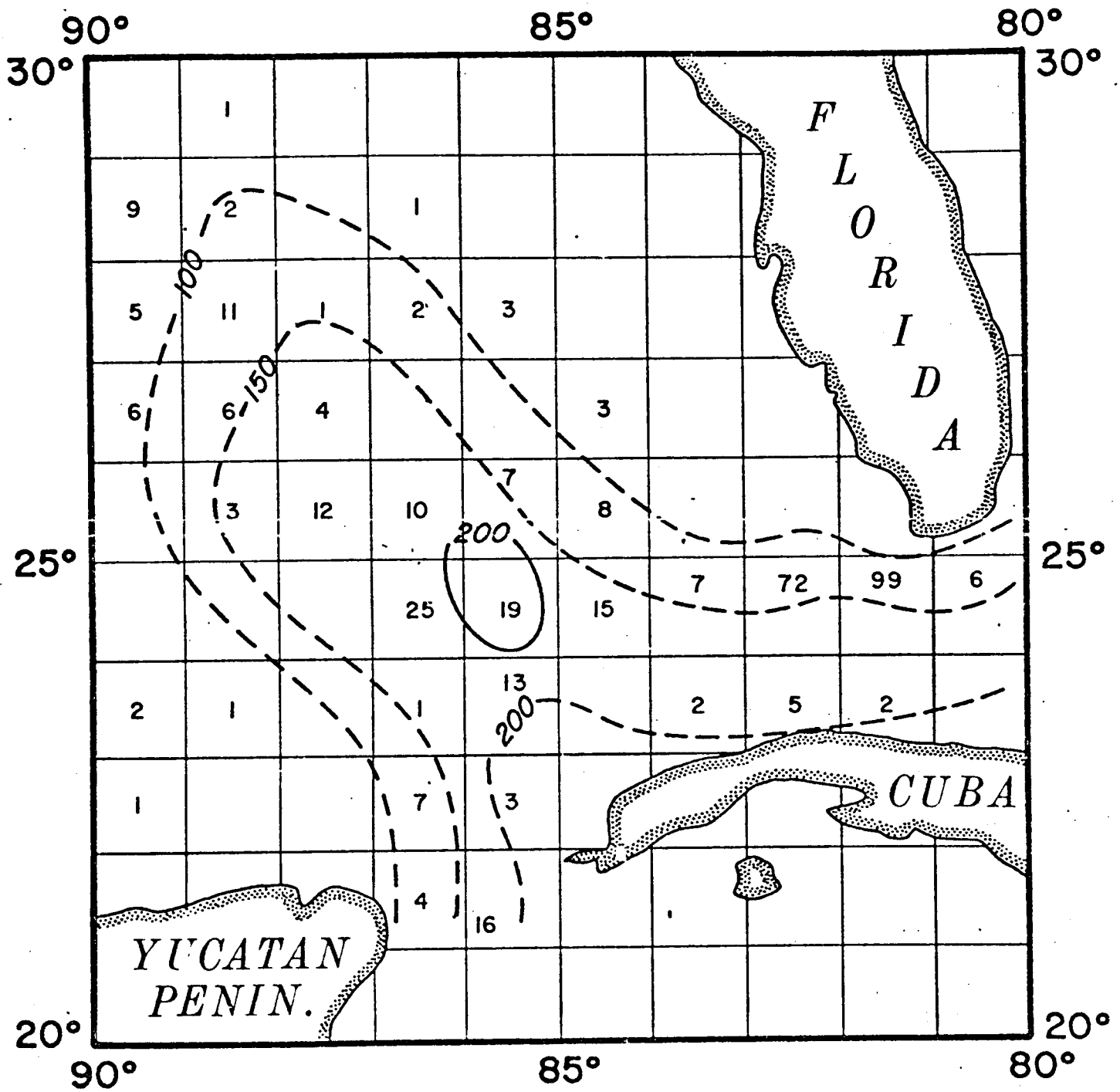

20°C TOPOGRAPHY
JANUARY

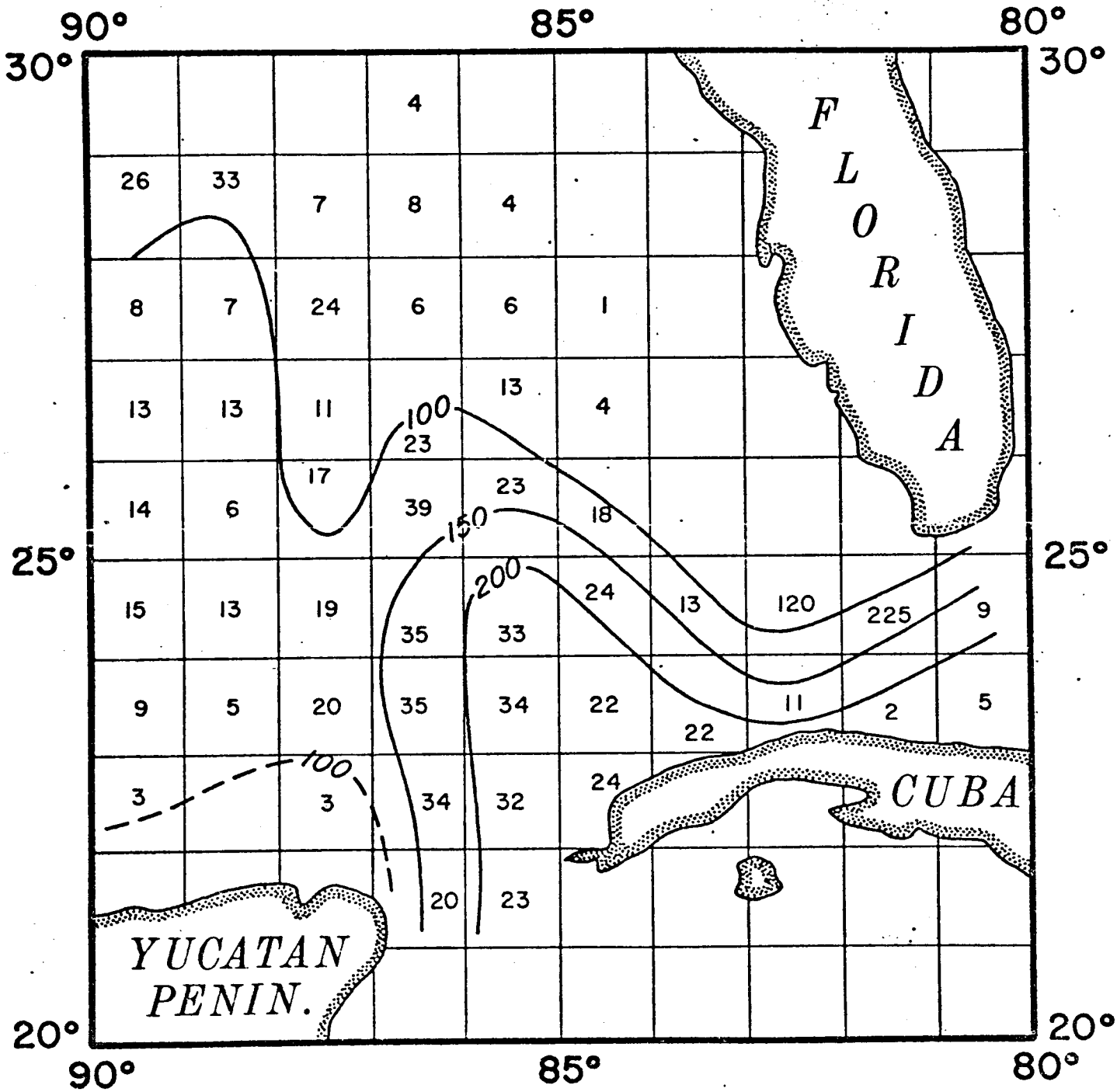

20°C TOPOGRAPHY
FEBRUARY

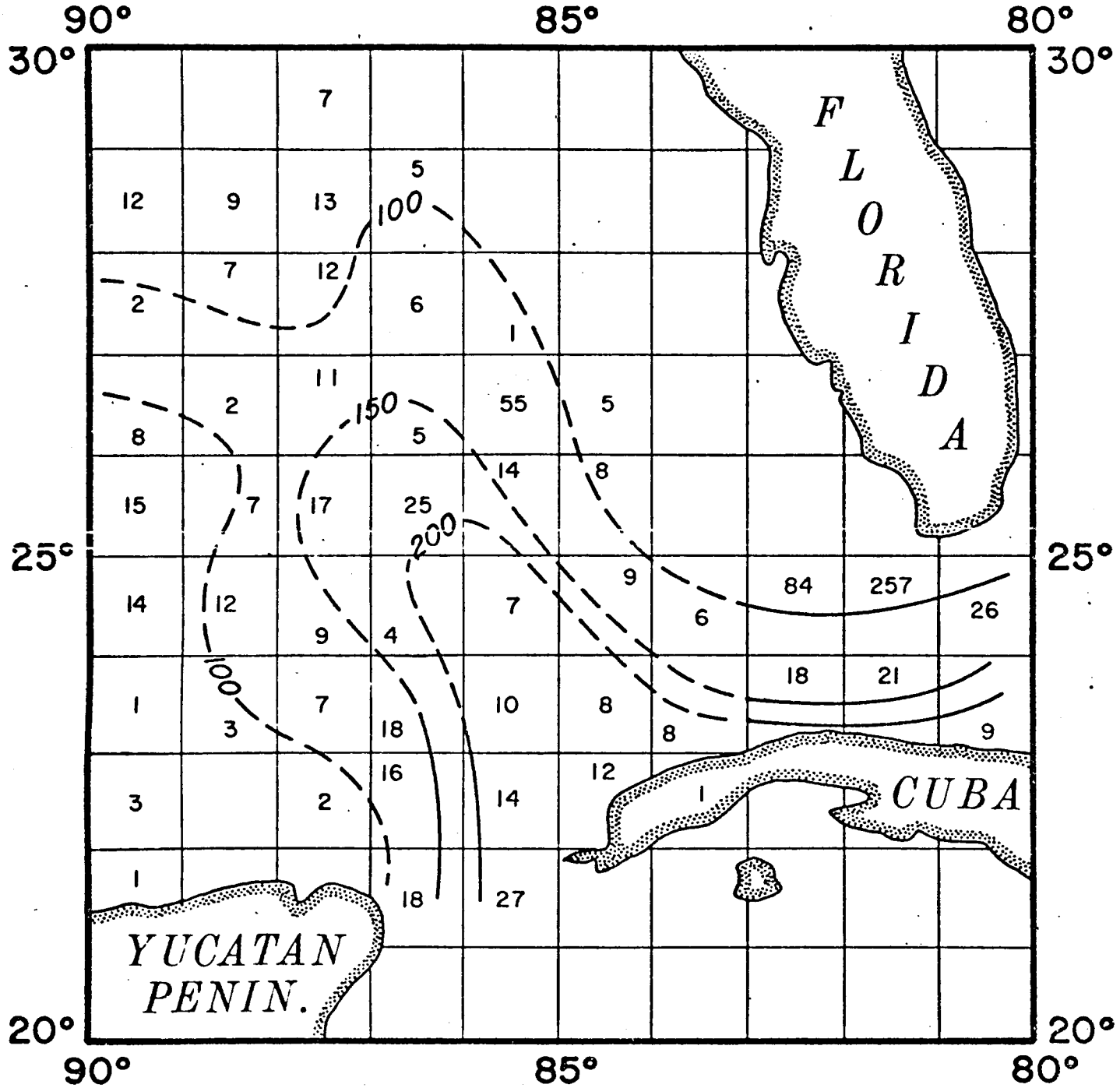

20°C TOPOGRAPHY
MARCH

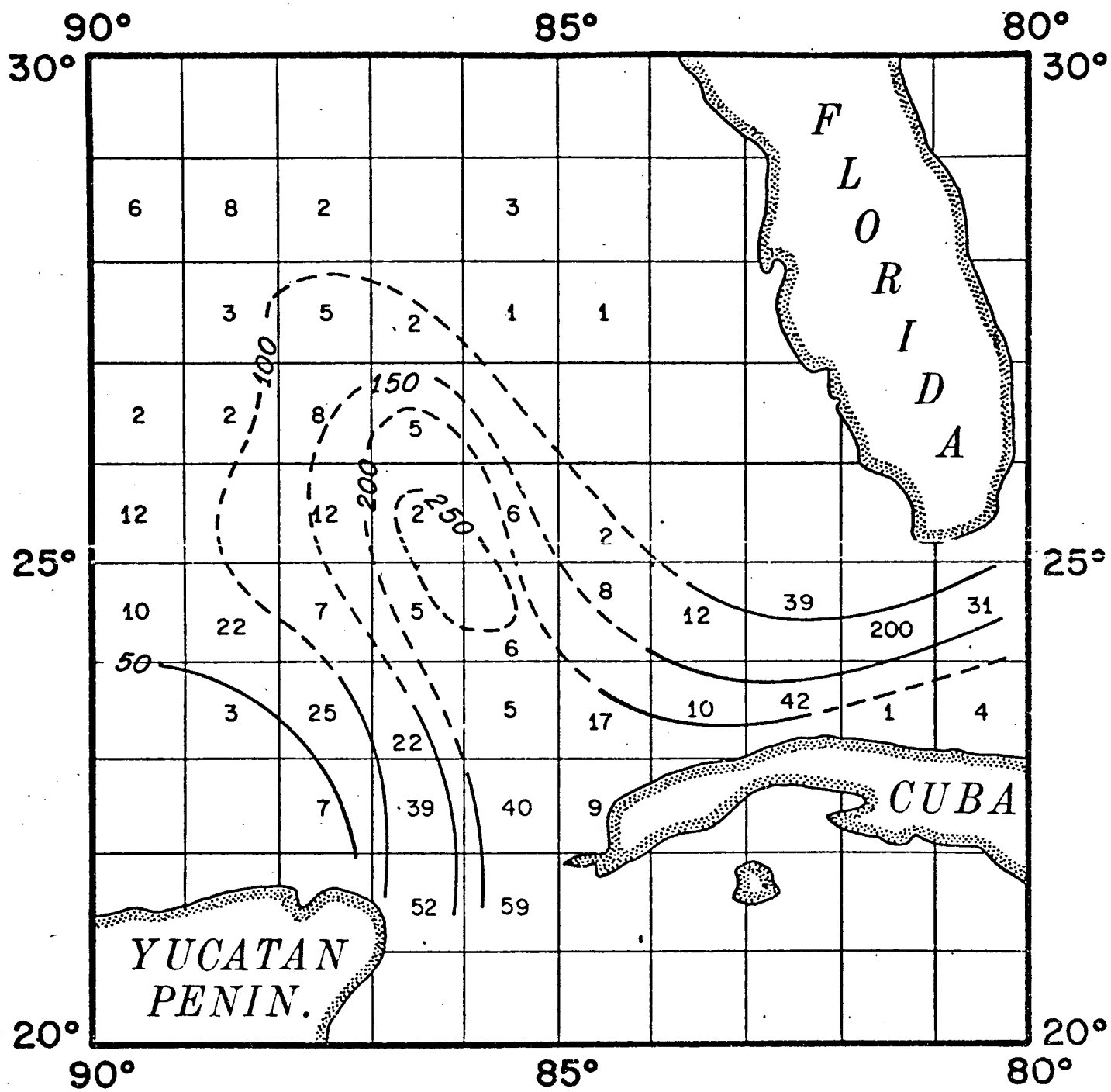

20°C TOPOGRAPHY
APRIL

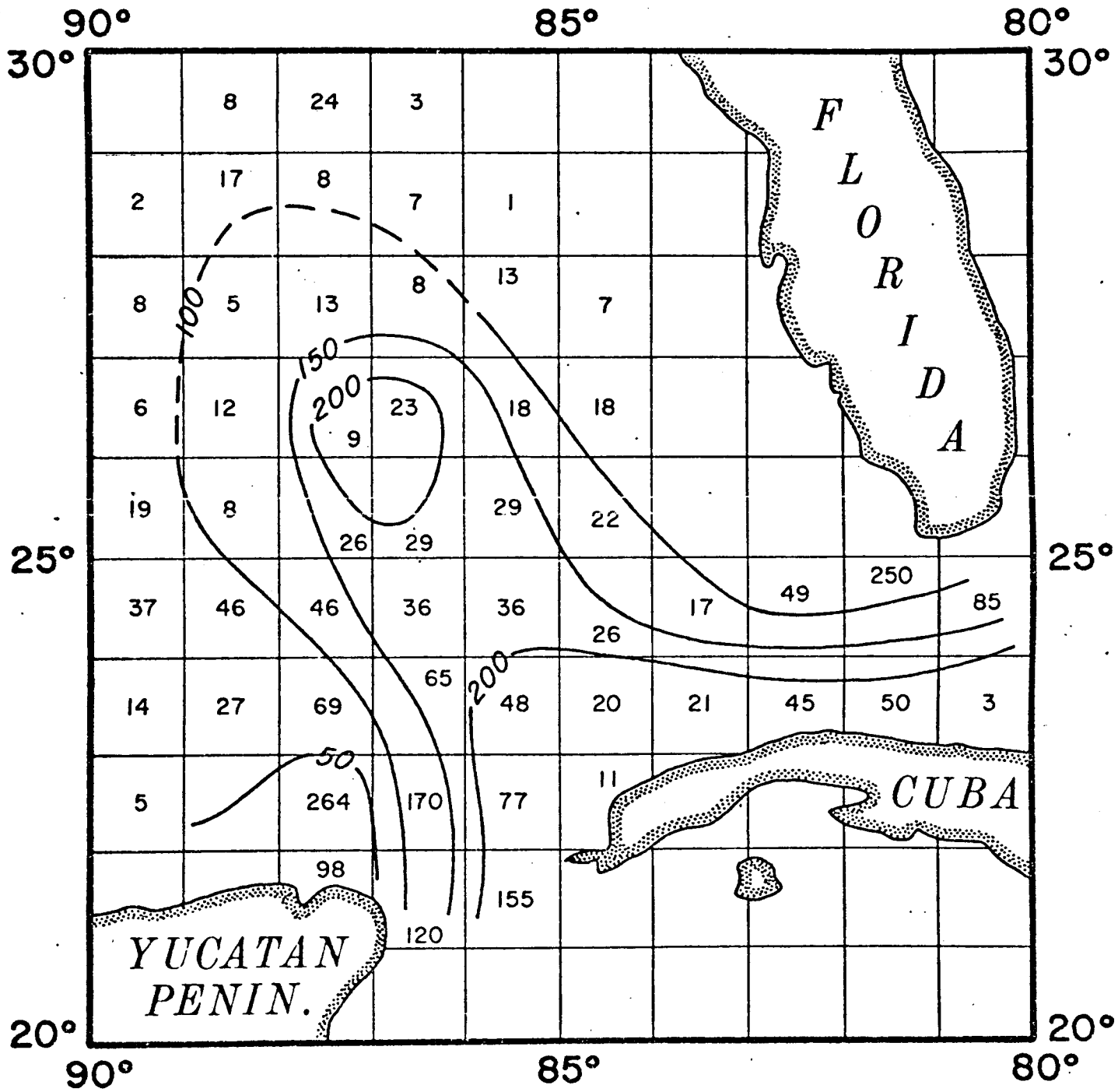

20°C TOPOGRAPHY
MAY

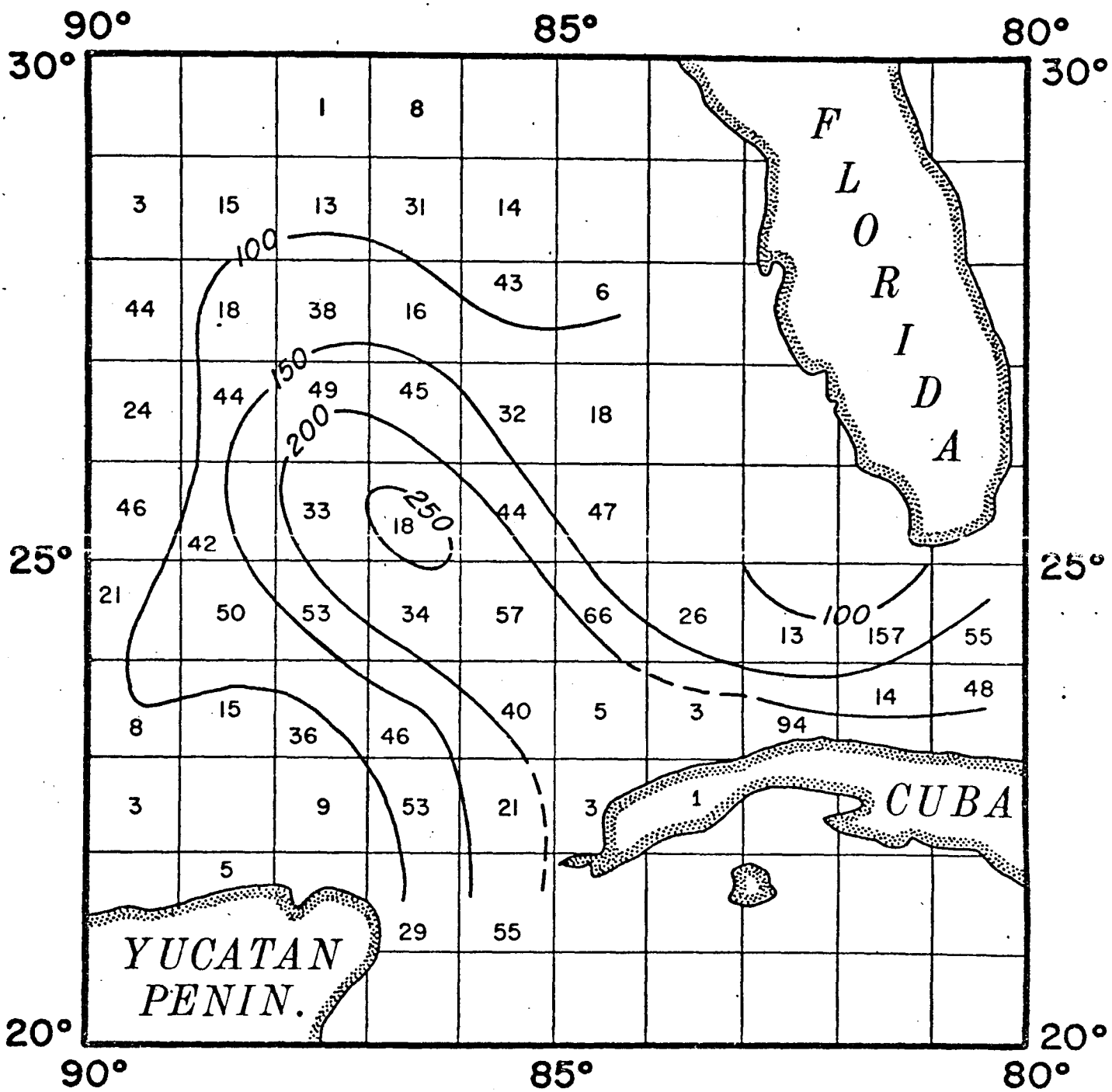

20°C TOPOGRAPHY
JUNE

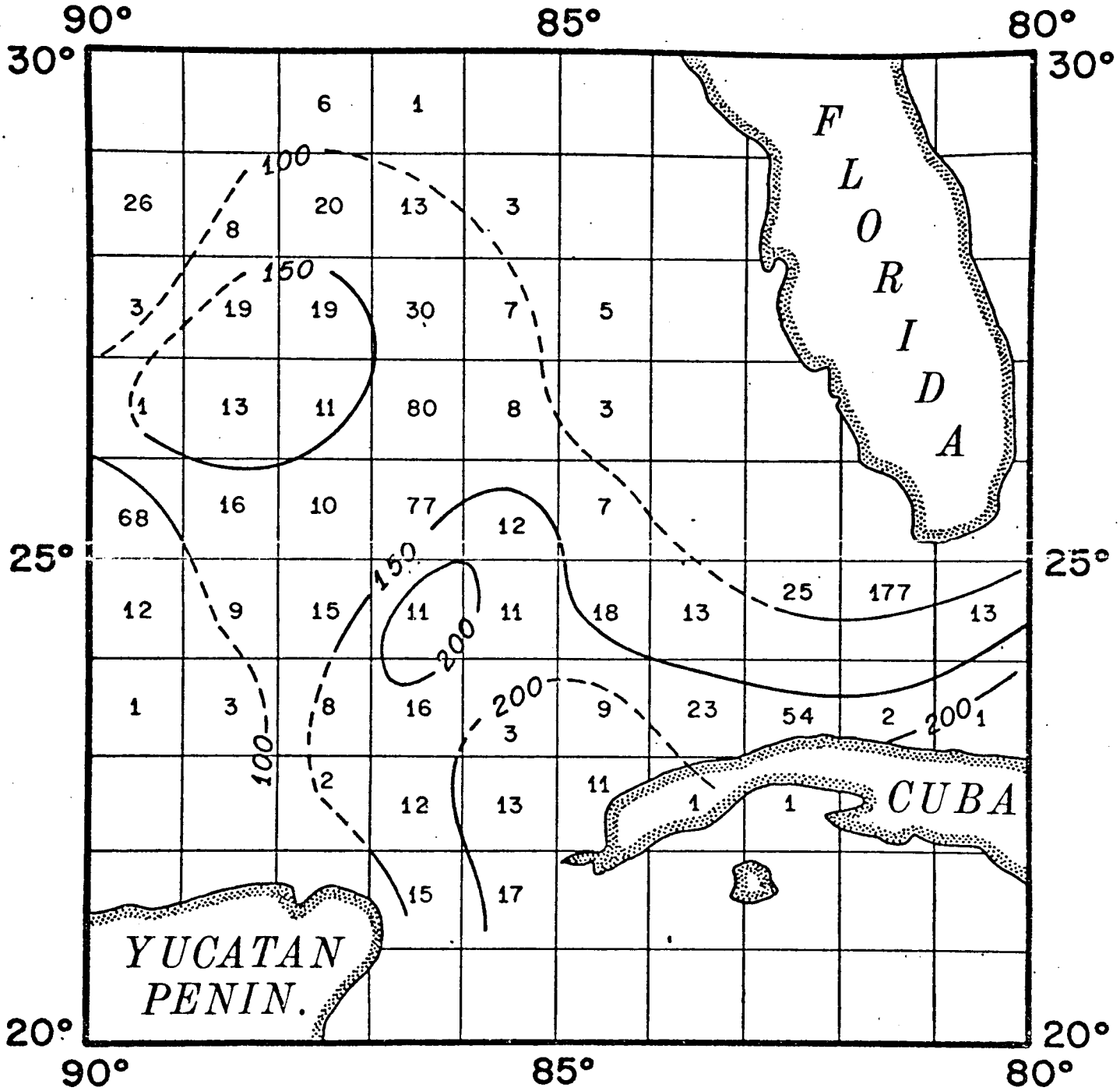

20°C TOPOGRAPHY
JULY

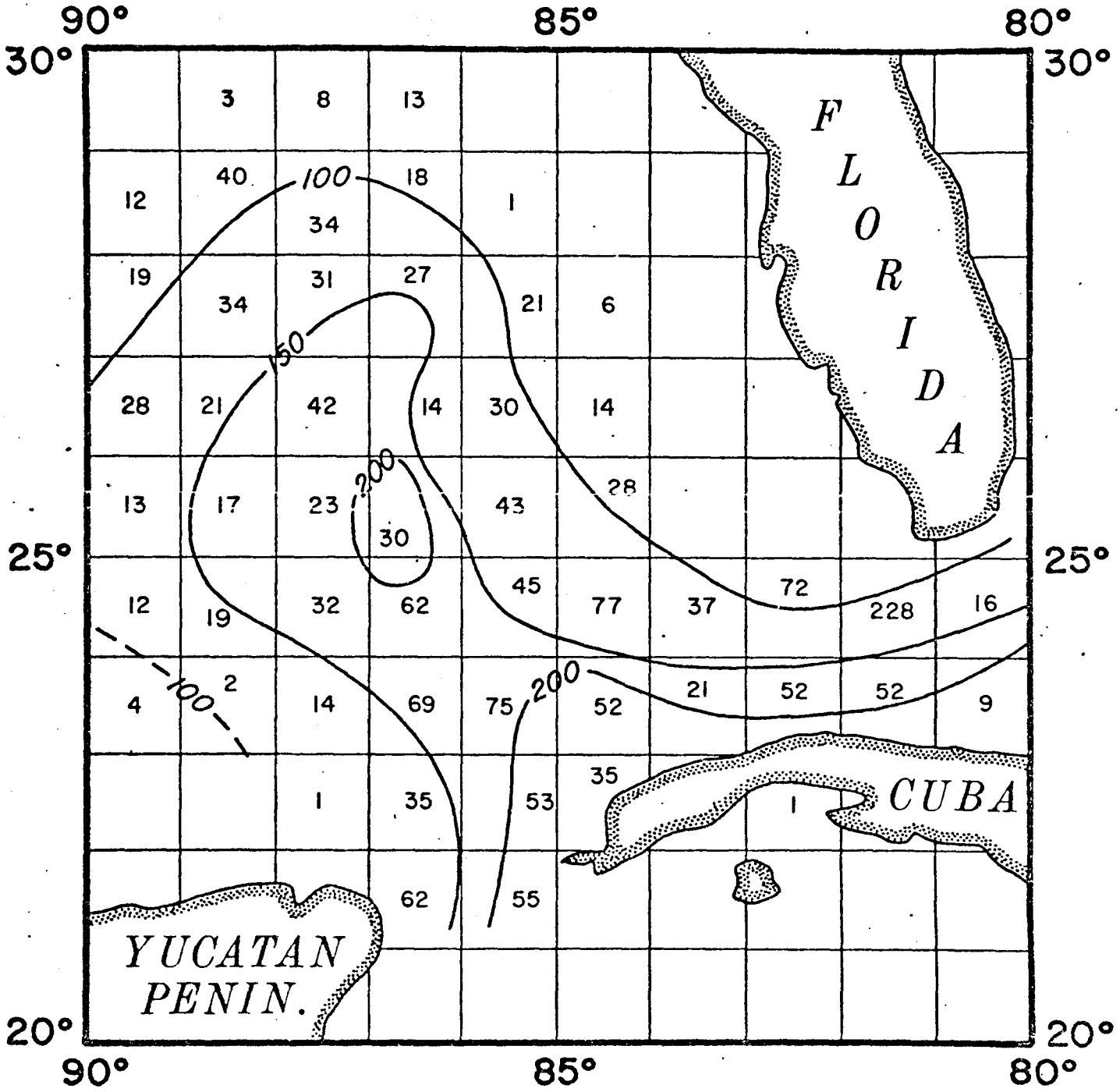

20°C TOPOGRAPHY
AUGUST

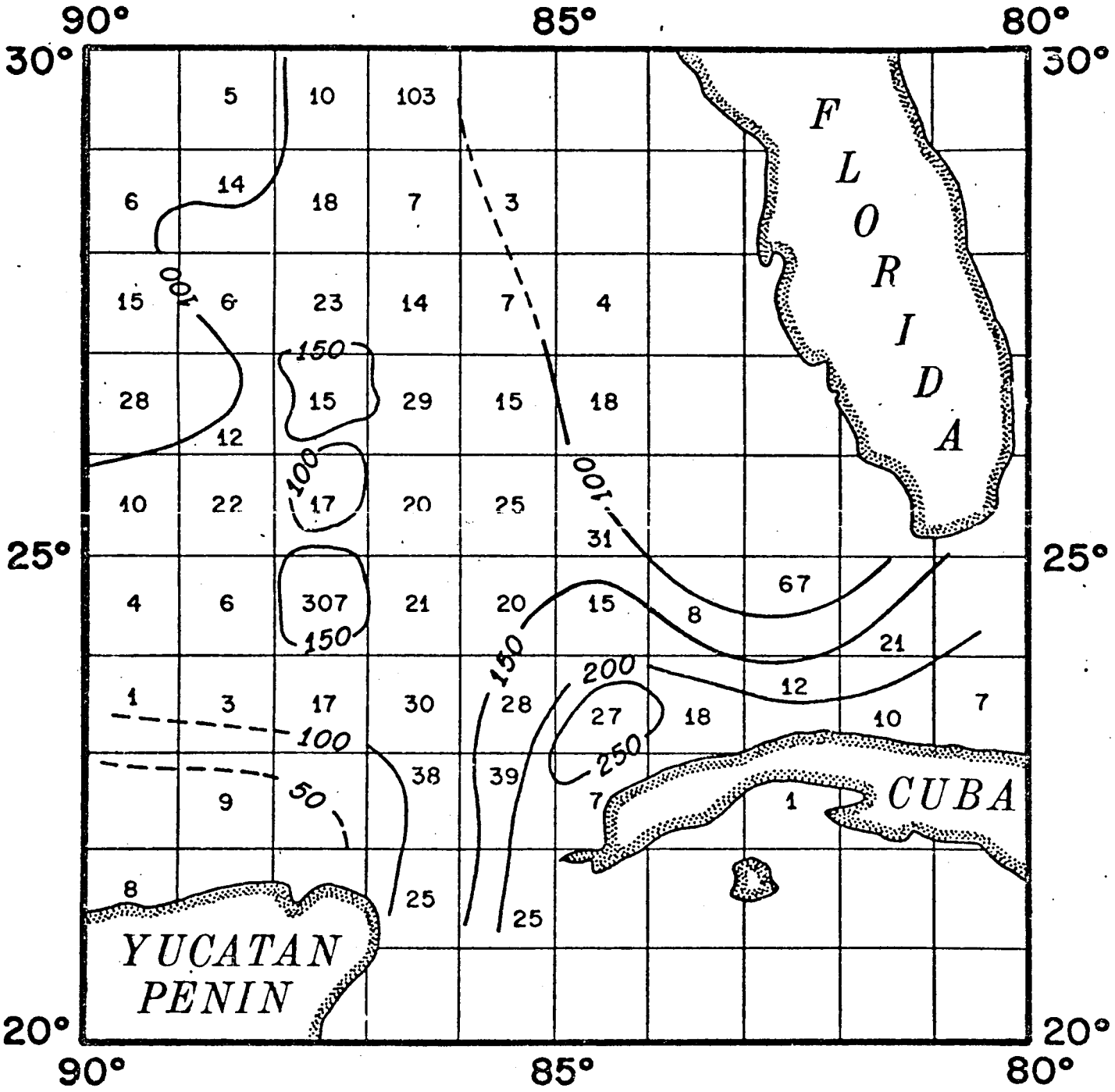

20°C TOPOGRAPHY
SEPTEMBER

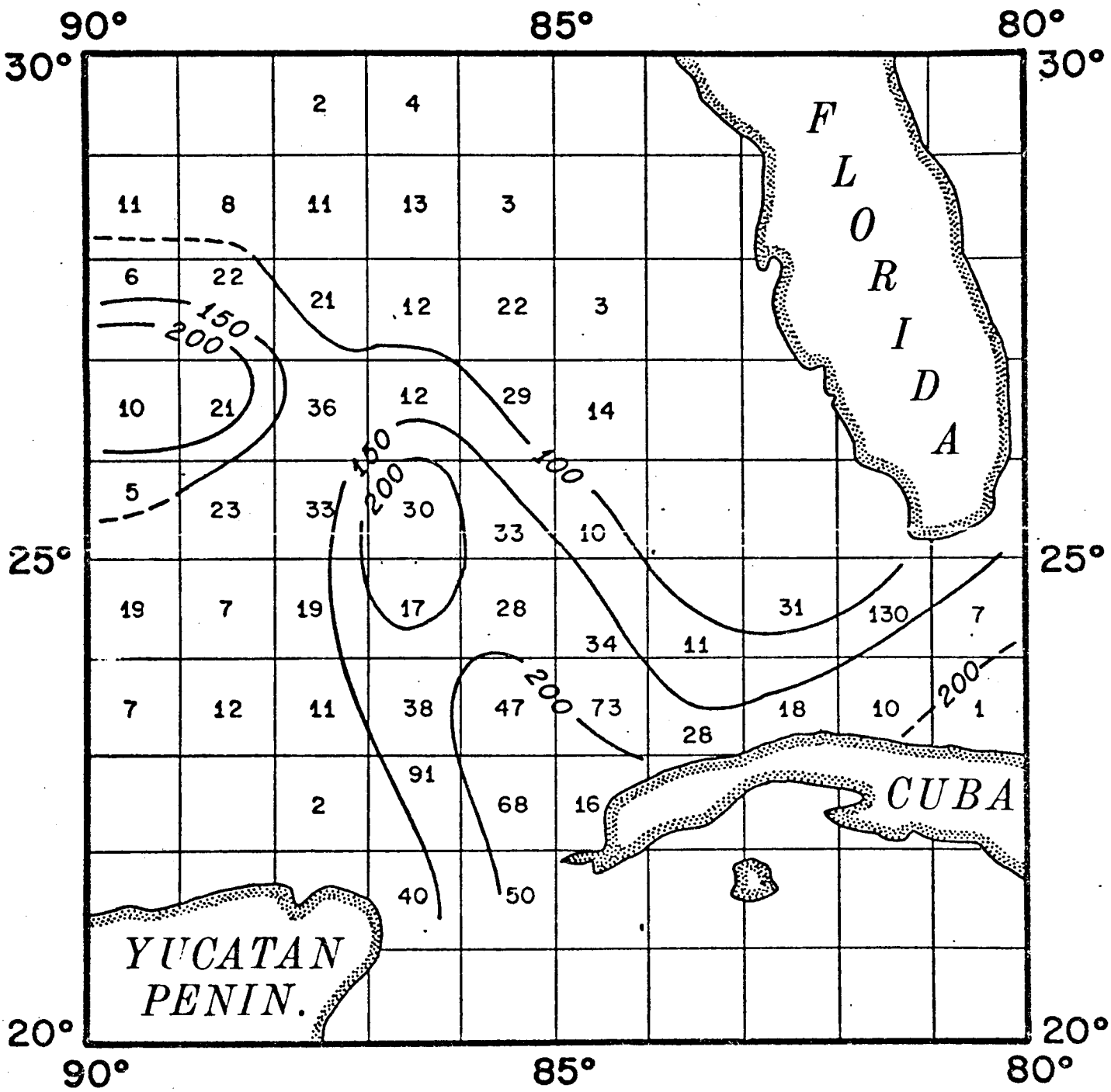

20°C TOPOGRAPHY
OCTOBER

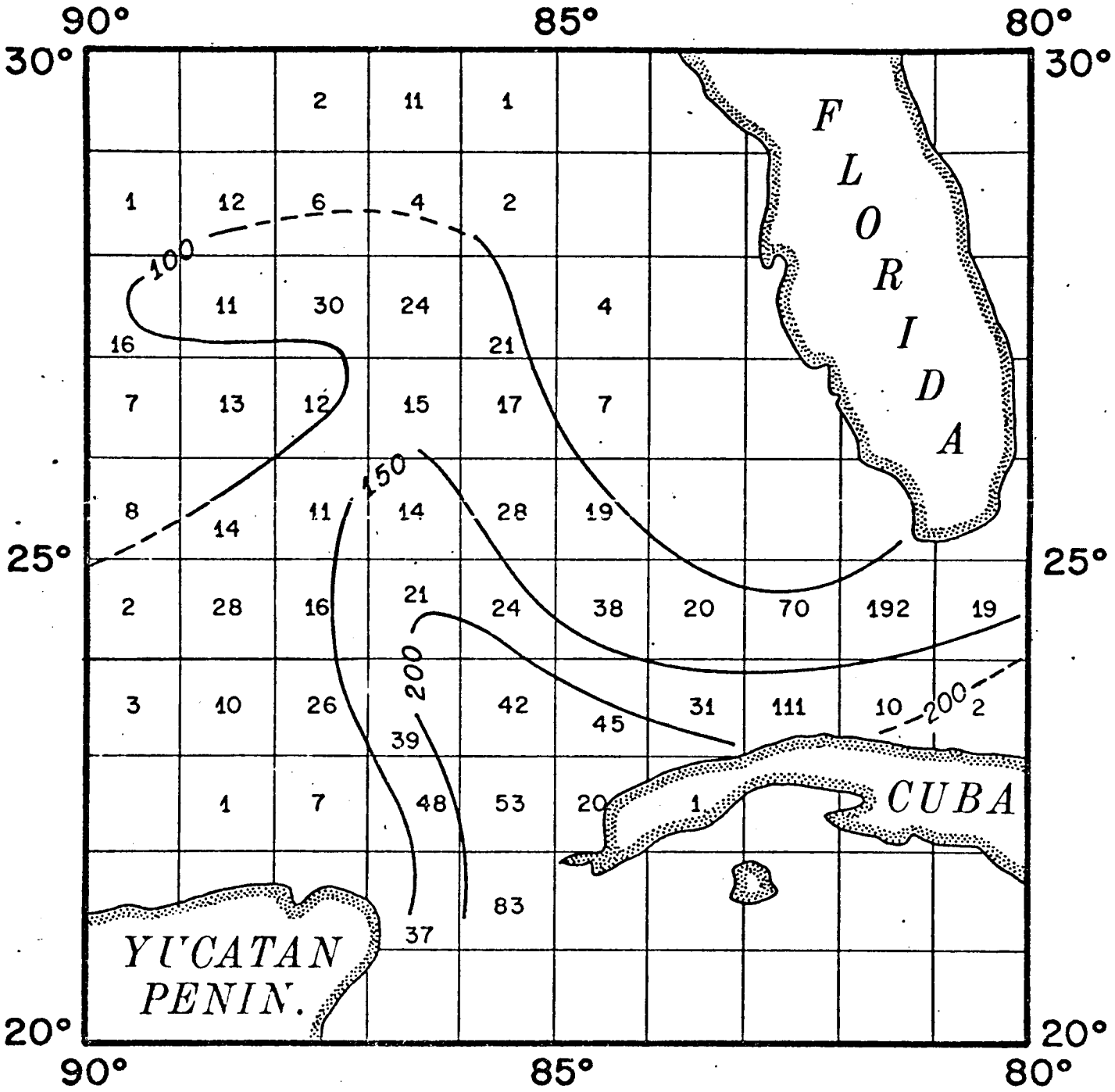

20°C TOPOGRAPHY
NOVEMBER

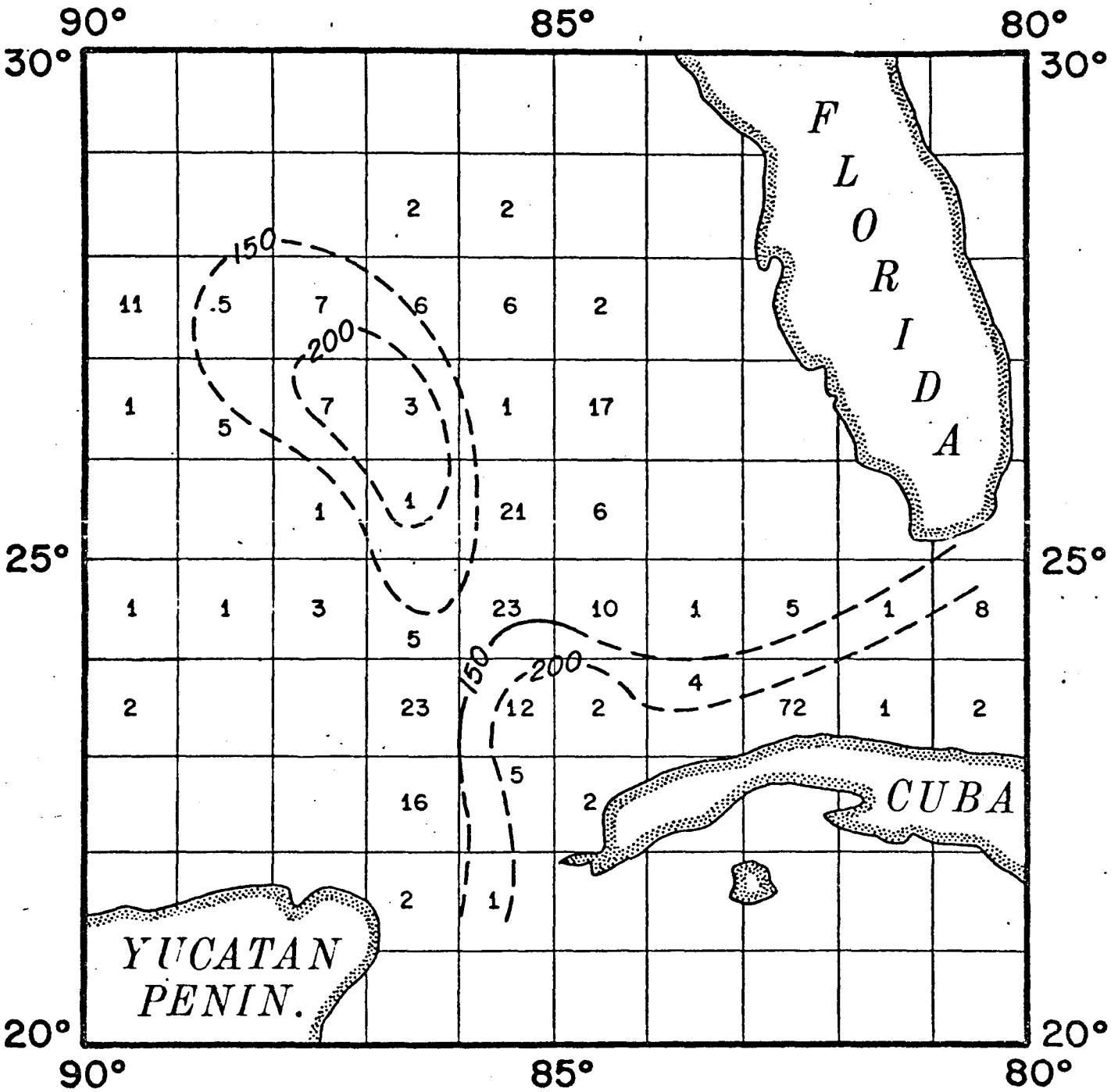

20°C TOPOGRAPHY
DECEMBER

Appendix VI

20 C° Topographies on the MAFLA Shelf during 1964 and 1965

Gaul (1964, 1965, 1966, and 1967) collected temperature data on the continental shelf off Panama City in 1963, 1964, and 1965. The depth of the 20°C isotherm was determined by linearly interpolating between appropriate Nansen bottle values. The topographies which resulted from this analysis are presented in this Appendix.

In addition, the figures also include the results of a drift bottle study. The bottle launch sites are given on the figures, as are the recovery zones. Zone 1 is the east coast of Florida, zone 2 the west coast of Florida, zone 3 the MAFLA shelf to the Mississippi Delta, and zone 4 the region west of the Delta.

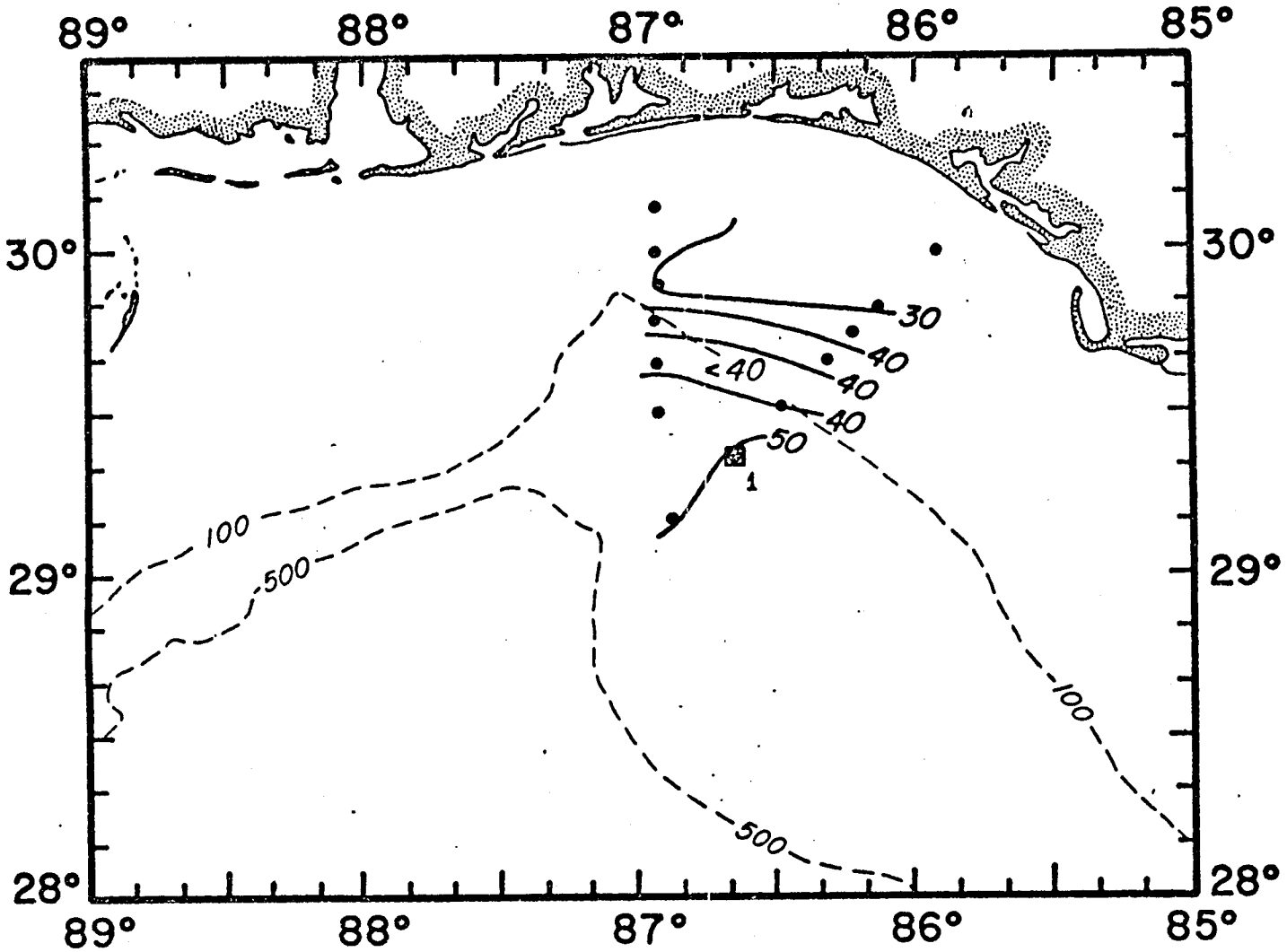

DEPTH (M) OF 20°C ISOTHERMAL SURFACE
CRUISE:
DATE: 5/6-5/7/64

DRIFT BOTTLE DATA

ZONE/SITE	% RECOVERED 1	2	3	SPEED OF FIRST ARRIVAL 1	2	3
1	67			.40		
2						
3	29					
4	4					

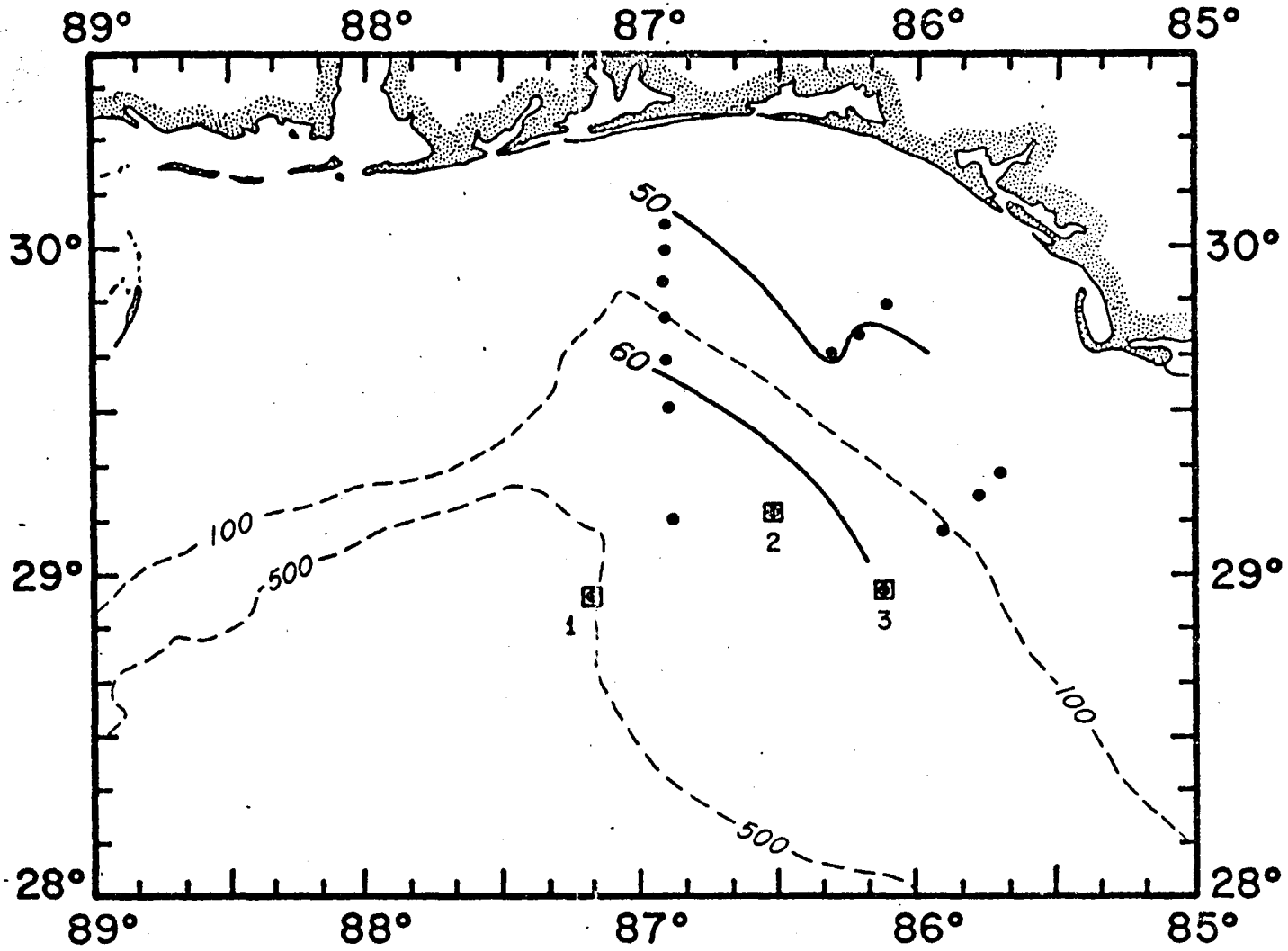

DEPTH (M) OF 20°C ISOTHERMAL SURFACE
CRUISE:
DATE: 6/29-7/3/64

DRIFT BOTTLE DATA

ZONE/SITE	% RECOVERED 1	2	3	SPEED OF FIRST ARRIVAL 1	2	3
1	93	96	90	.66	.38	.40
2	3		4			
3						
4	4	4	6			

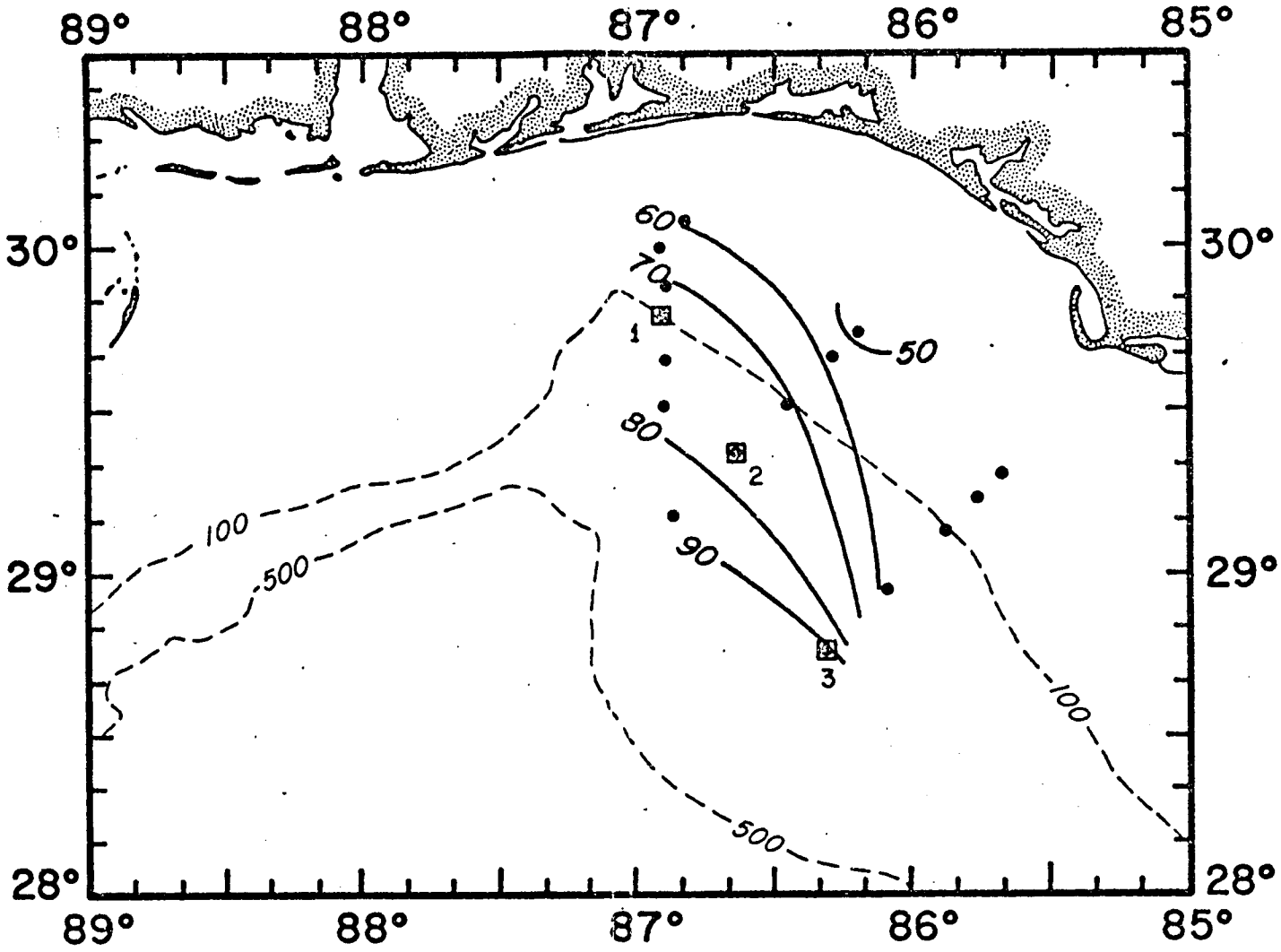

DEPTH (M) OF 20°C ISOTHERMAL SURFACE
CRUISE:
DATE: 8/3-8/7/64

DRIFT BOTTLE DATA

ZONE/SITE	% RECOVERED 1	2	3	SPEED OF FIRST ARRIVAL 1	2	3
1	53	73	100	.57	.41	.29
2	3	5				
3	37	18			.39	
4	7	4			18	

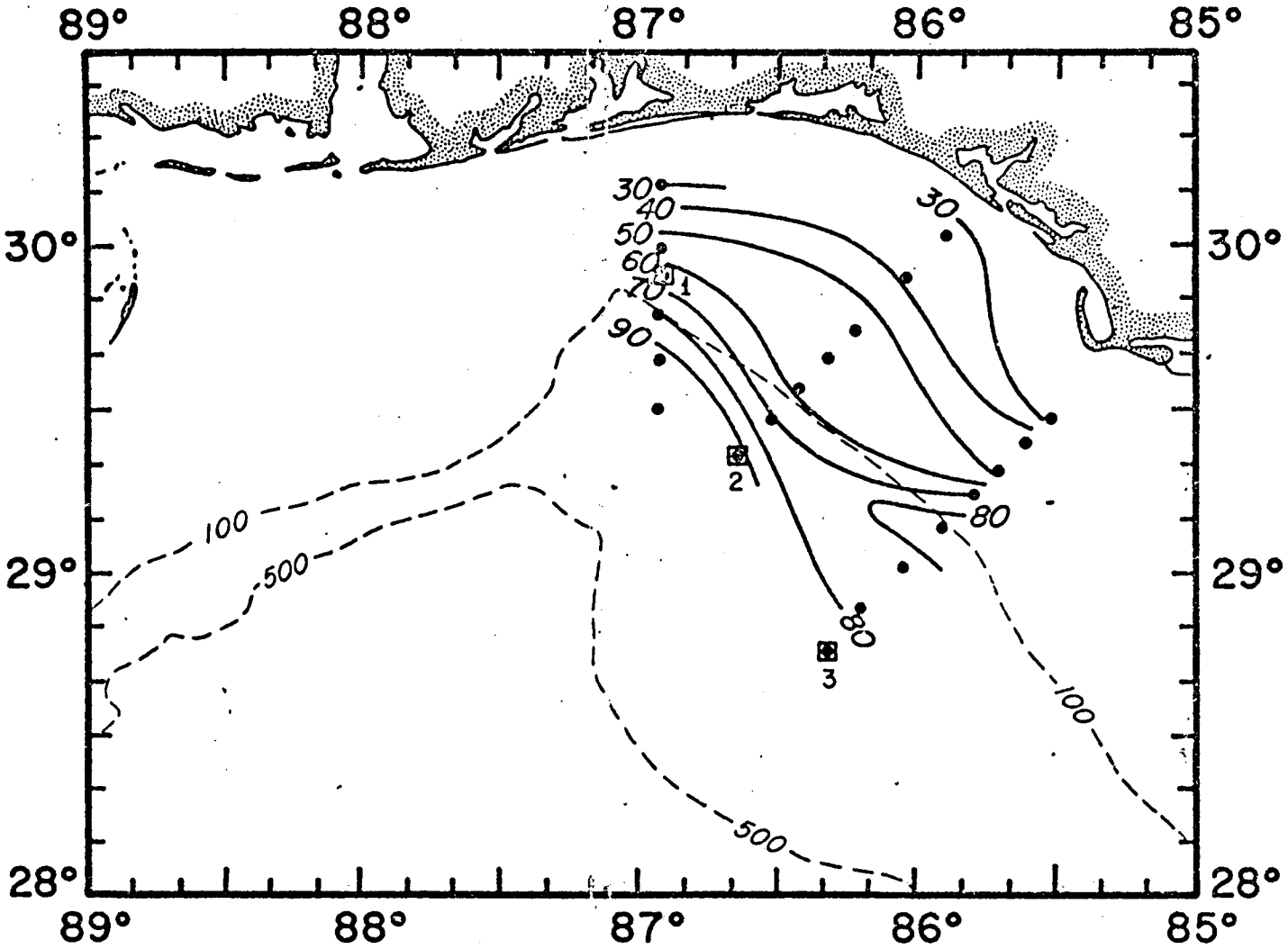

DEPTH (M) OF 20°C ISOTHERMAL SURFACE
CRUISE:
DATE: 8/31-9/4/64

DRIFT BOTTLE DATA

ZONE/SITE	% RECOVERED 1	% RECOVERED 2	% RECOVERED 3	SPEED OF FIRST ARRIVAL 1	SPEED OF FIRST ARRIVAL 2	SPEED OF FIRST ARRIVAL 3
1		5	14		.20	.20
2						
3	33	43			.14	
4	67	52	86	.17	.25	.40

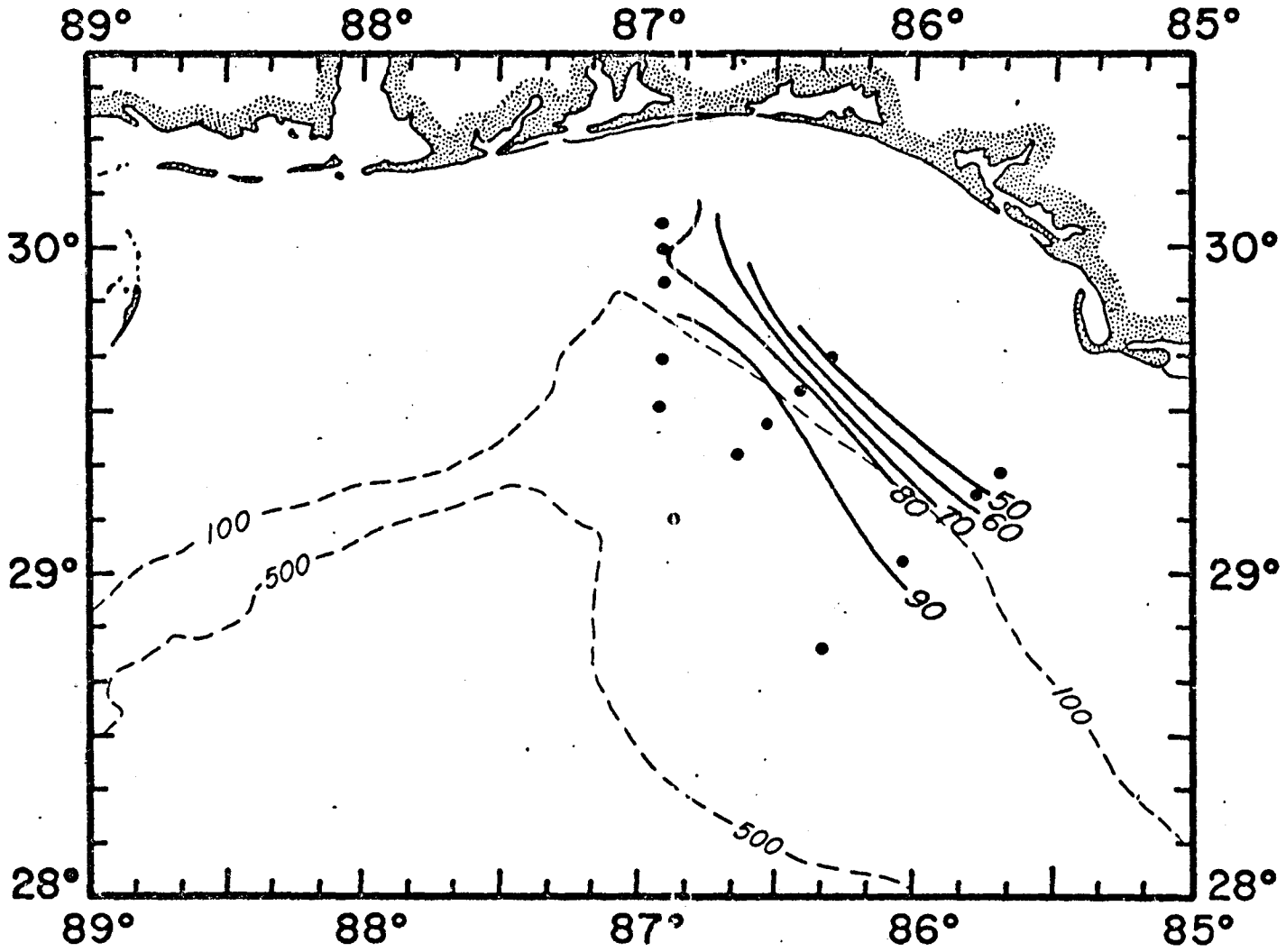

DEPTH (M) OF 20°C ISOTHERMAL SURFACE
CRUISE:
DATE: 11/2-11/6/64

DRIFT BOTTLE DATA

ZONE/SITE	% RECOVERED 1	2	3	SPEED OF FIRST ARRIVAL 1	2	3
1						
2						
3						
4						

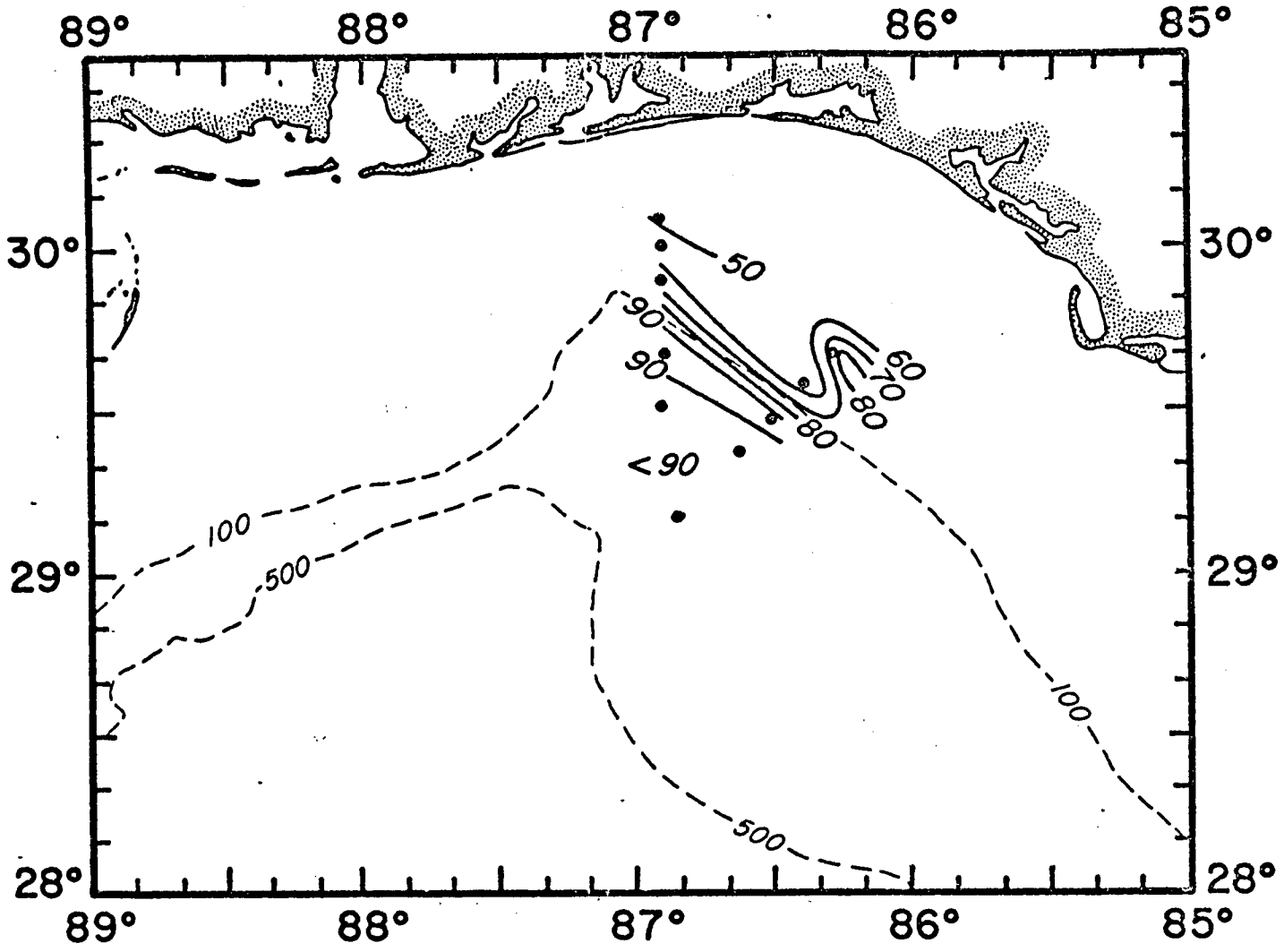

DEPTH (M) OF 20°C ISOTHERMAL SURFACE
CRUISE:
DATE: 12/15-12/16/64 DRIFT BOTTLE DATA

ZONE/SITE	% RECOVERED 1	2	3	SPEED OF FIRST ARRIVAL 1	2	3
1						
2						
3						
4						

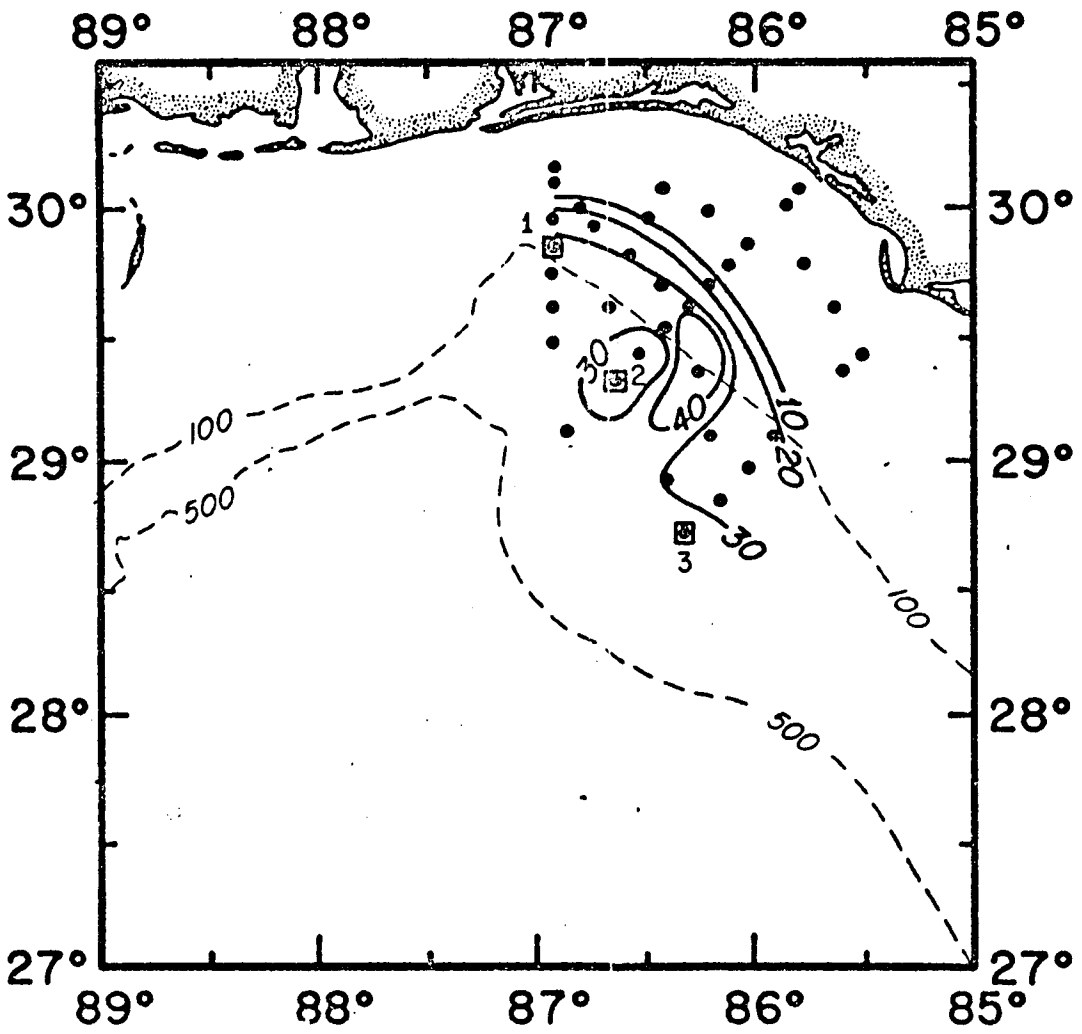

DEPTH (M) OF 20°C ISOTHERMAL SURFACE
CRUISE:
DATE: 4/5-4/9/65

DRIFT BOTTLE DATA

ZONE/SITE	% RECOVERED 1	% RECOVERED 2	% RECOVERED 3	SPEED OF FIRST ARRIVAL 1	SPEED OF FIRST ARRIVAL 2	SPEED OF FIRST ARRIVAL 3
1	19	42	1	.22	.78	.18
2			3			
3	80	58	96	.10	.11	.18
4	1					

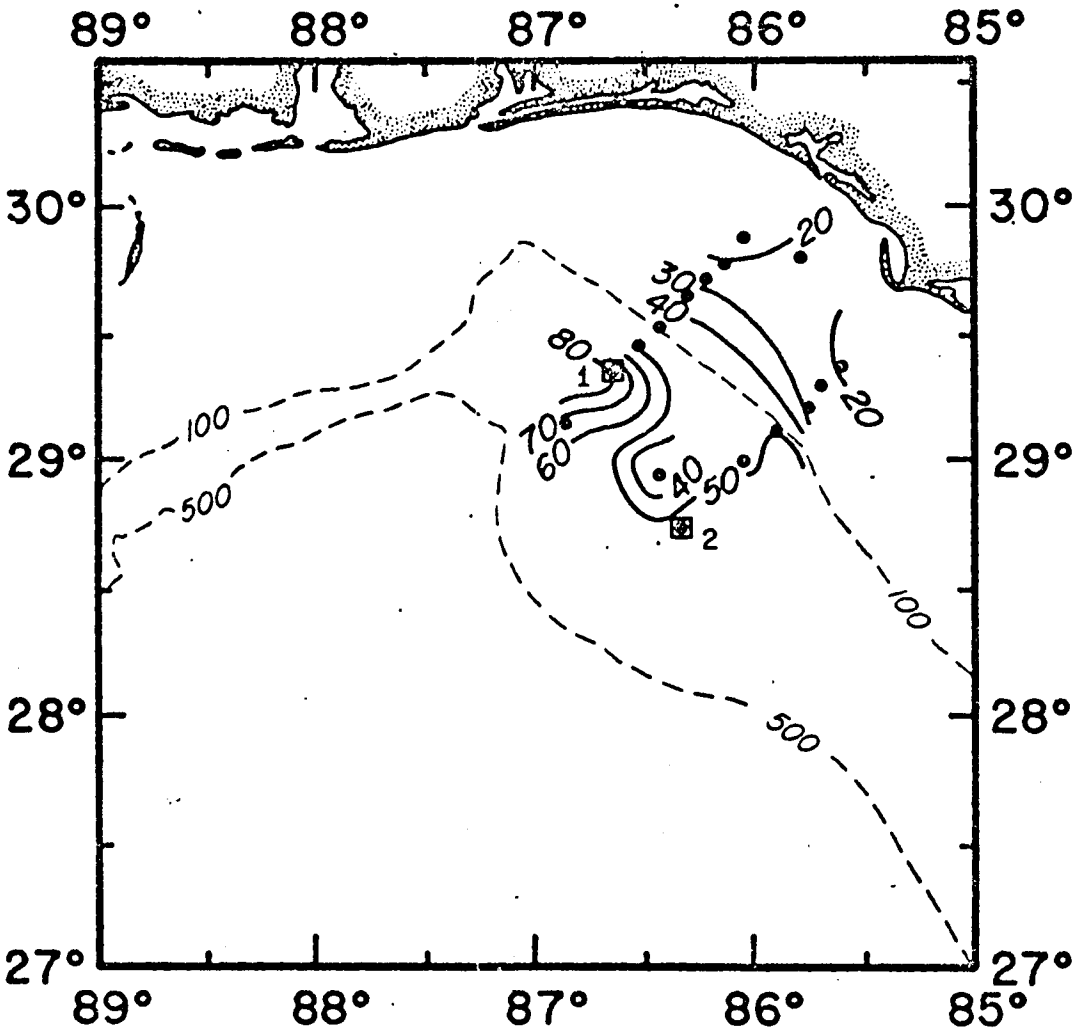

DEPTH (M) OF 20°C ISOTHERMAL SURFACE
CRUISE:
DATE: 5/10-5/11/65 DRIFT BOTTLE DATA

ZONE/SITE	% RECOVERED 1	2	3	SPEED OF FIRST ARRIVAL 1	2	3
1	4	52		.41	.45	
2						
3	95	40		.15	.09	
4	1	3				

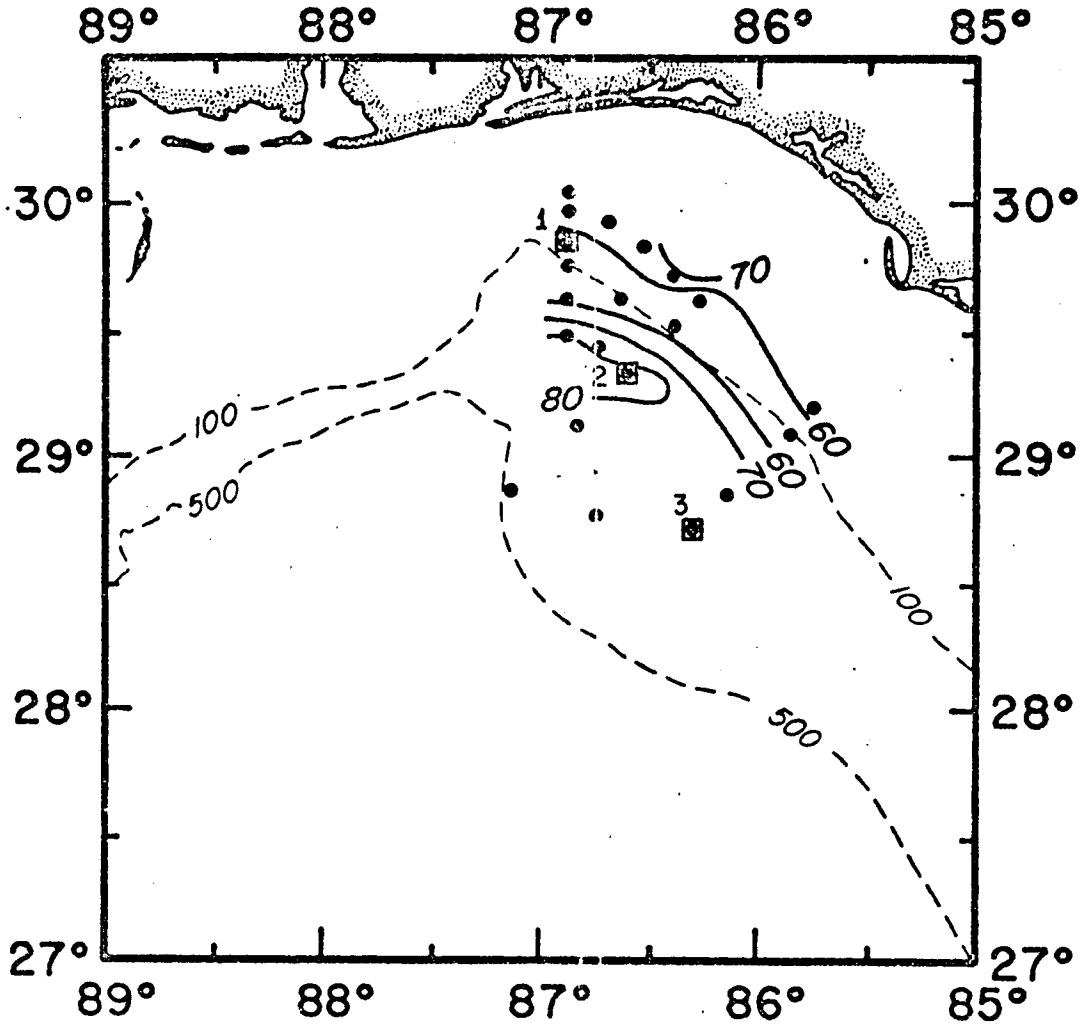

DEPTH (M) OF 20°C ISOTHERMAL SURFACE
CRUISE:
DATE: 6/22-6/26/65 DRIFT BOTTLE DATA

ZONE/SITE	% RECOVERED 1	2	3	SPEED OF FIRST ARRIVAL 1	2	3
1	4	34	58	.29	.39	.54
2						
3	90.	66	27	.17		.08
4	6		15	.19	.35	.25

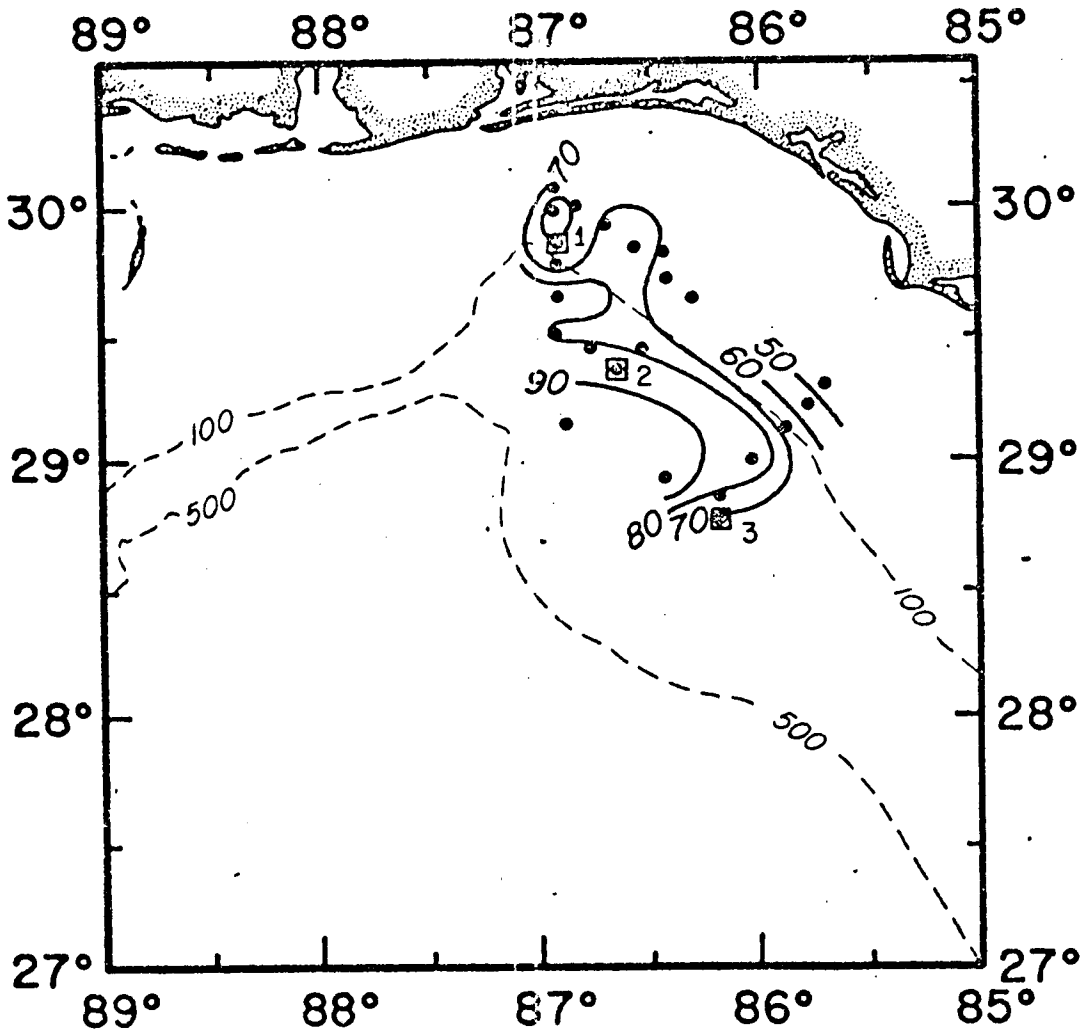

DEPTH (M) OF 20°C ISOTHERMAL SURFACE
CRUISE:
DATE: 7/20-7/22/65 DRIFT BOTTLE DATA

ZONE/SITE	% RECOVERED 1	2	3	SPEED OF FIRST ARRIVAL 1	2	3
1						
2						
3	98	100	90	.25	.36	.20
4	2		10			

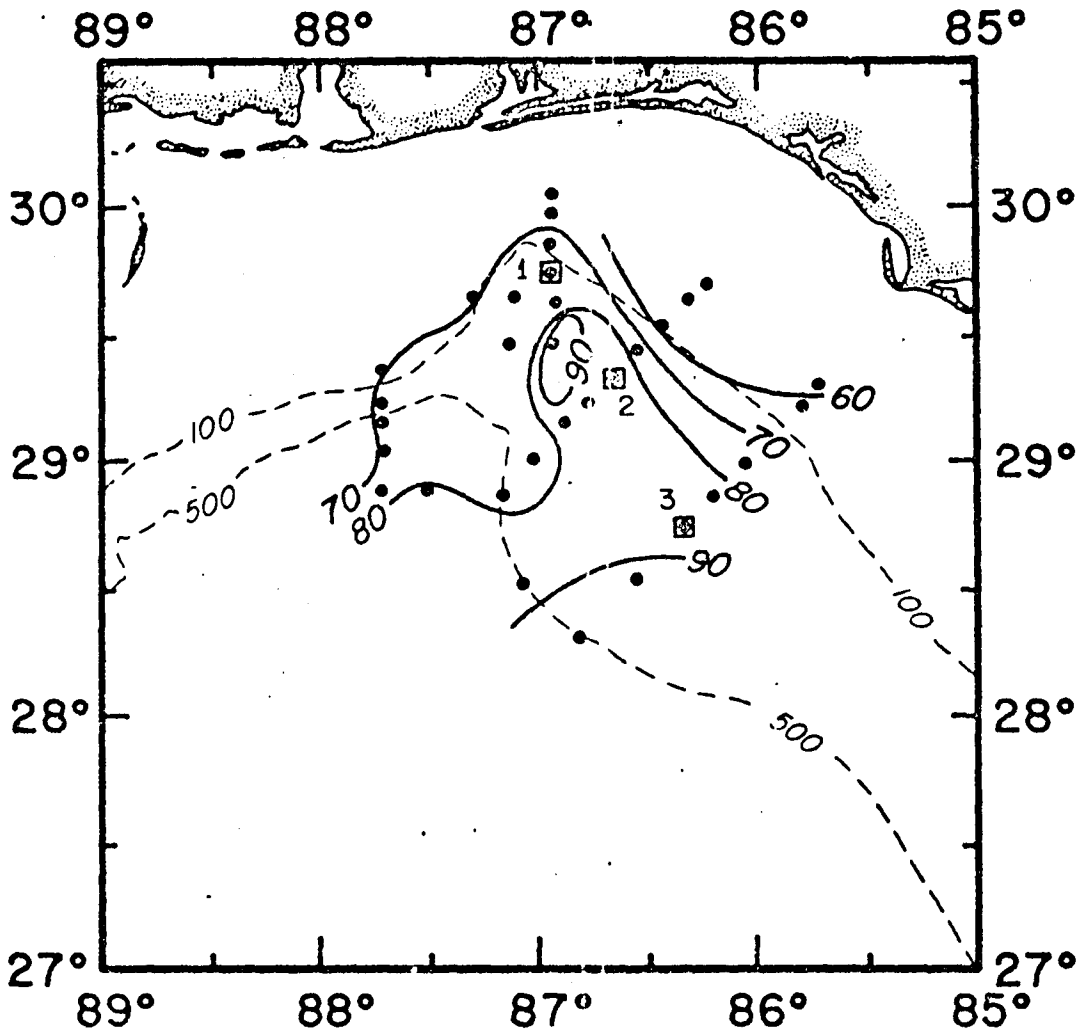

DEPTH (M) OF 20°C ISOTHERMAL SURFACE
CRUISE:
DATE: 8/16-8/25/65 DRIFT BOTTLE DATA

ZONE/SITE	% RECOVERED 1	2	3	SPEED OF FIRST ARRIVAL 1	2	3
1						
2						
3	89	97	96	.26	.20	.25
4	11	3	4	1.21	.34	.24

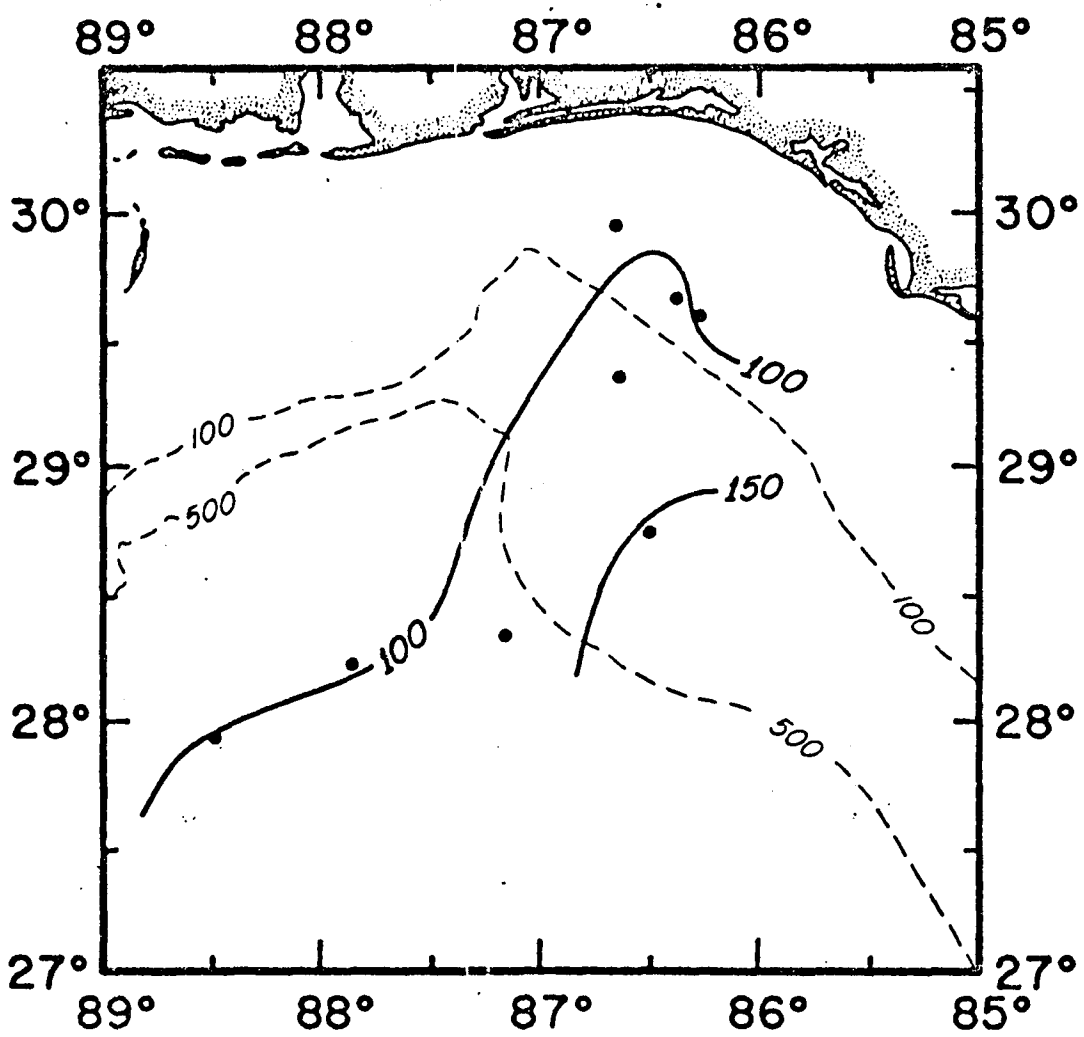

DEPTH (M) OF 20°C ISOTHERMAL SURFACE

CRUISE:

DATE: 9/20-9/23/65 DRIFT BOTTLE DATA

ZONE/SITE	% RECOVERED 1	2	3	SPEED OF FIRST ARRIVAL 1	2	3
1						
2						
3						
4						

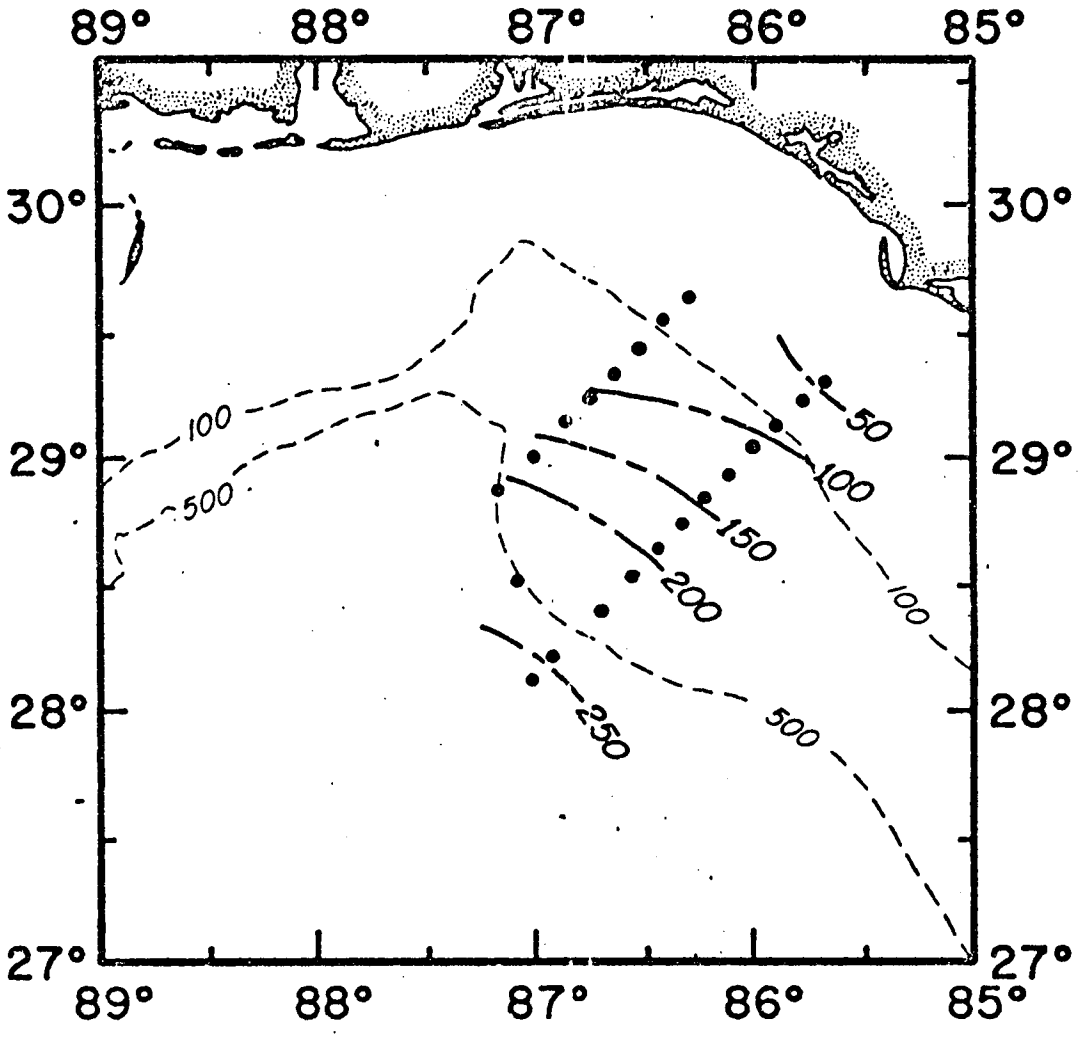

DEPTH (M) OF 20°C ISOTHERMAL SURFACE
CRUISE:
DATE: 10/12-10/13/65

DRIFT BOTTLE DATA

ZONE/SITE	% RECOVERED 1	2	3	SPEED OF FIRST ARRIVAL 1	2	3
1						
2						
3						
4						

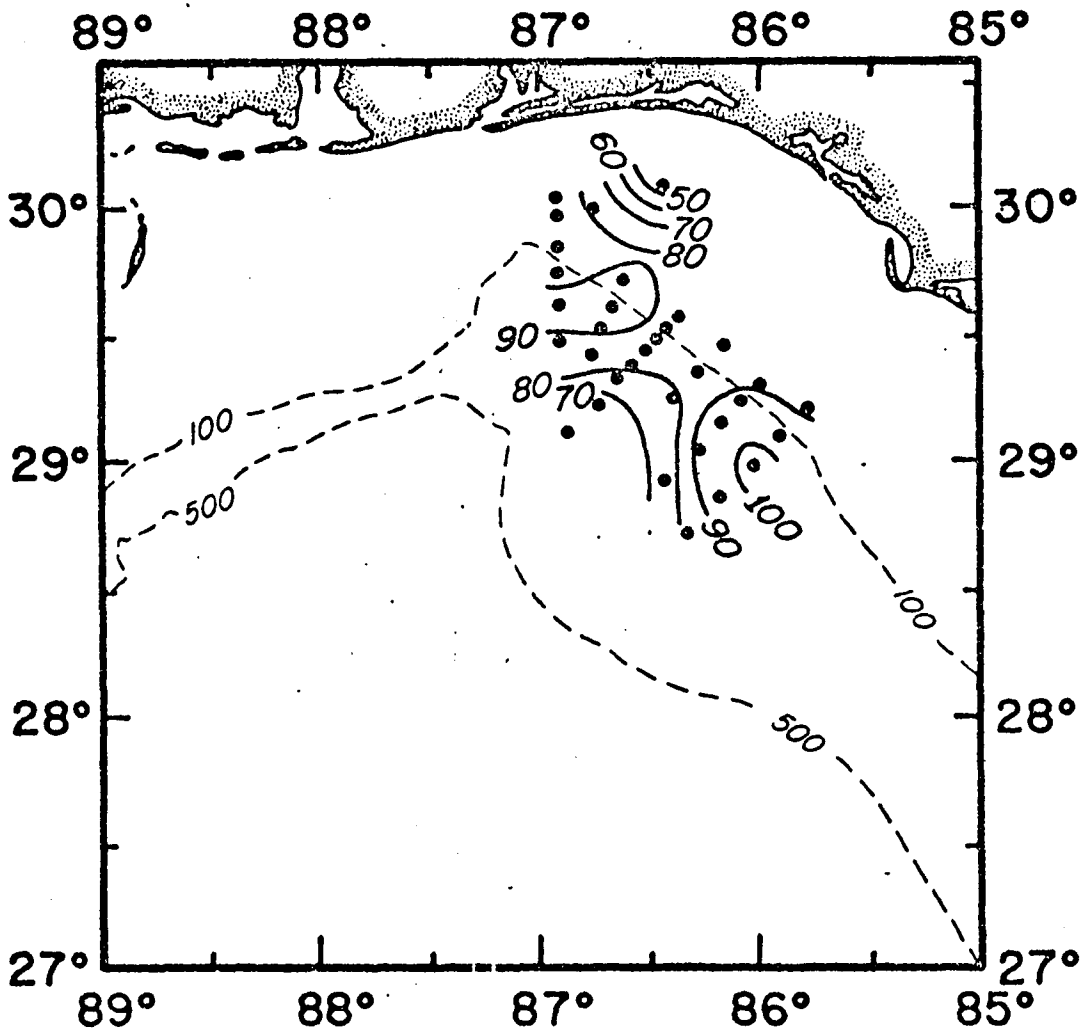

DEPTH (M) OF 20°C ISOTHERMAL SURFACE
CRUISE:
DATE: 12/13-12/17/65 DRIFT BOTTLE DATA

ZONE/SITE	% RECOVERED 1	2	3	SPEED OF FIRST ARRIVAL 1	2	3
1						
2						
3						
4						

Appendix VII

Vertical Sections of Temperature, Salinity, and Sigma-t at 28°30'N, 27°30'N, and 26°00'N

A three-year study of the oceanographic conditions on the west Florida Continental Shelf was conducted in 1971, 1972, and 1973. Data from the Western Florida Continental Shelf Program included the temperature and salinity values used to derive the vertical sections of temperature, salinity, and sigma-t presented in this Appendix.

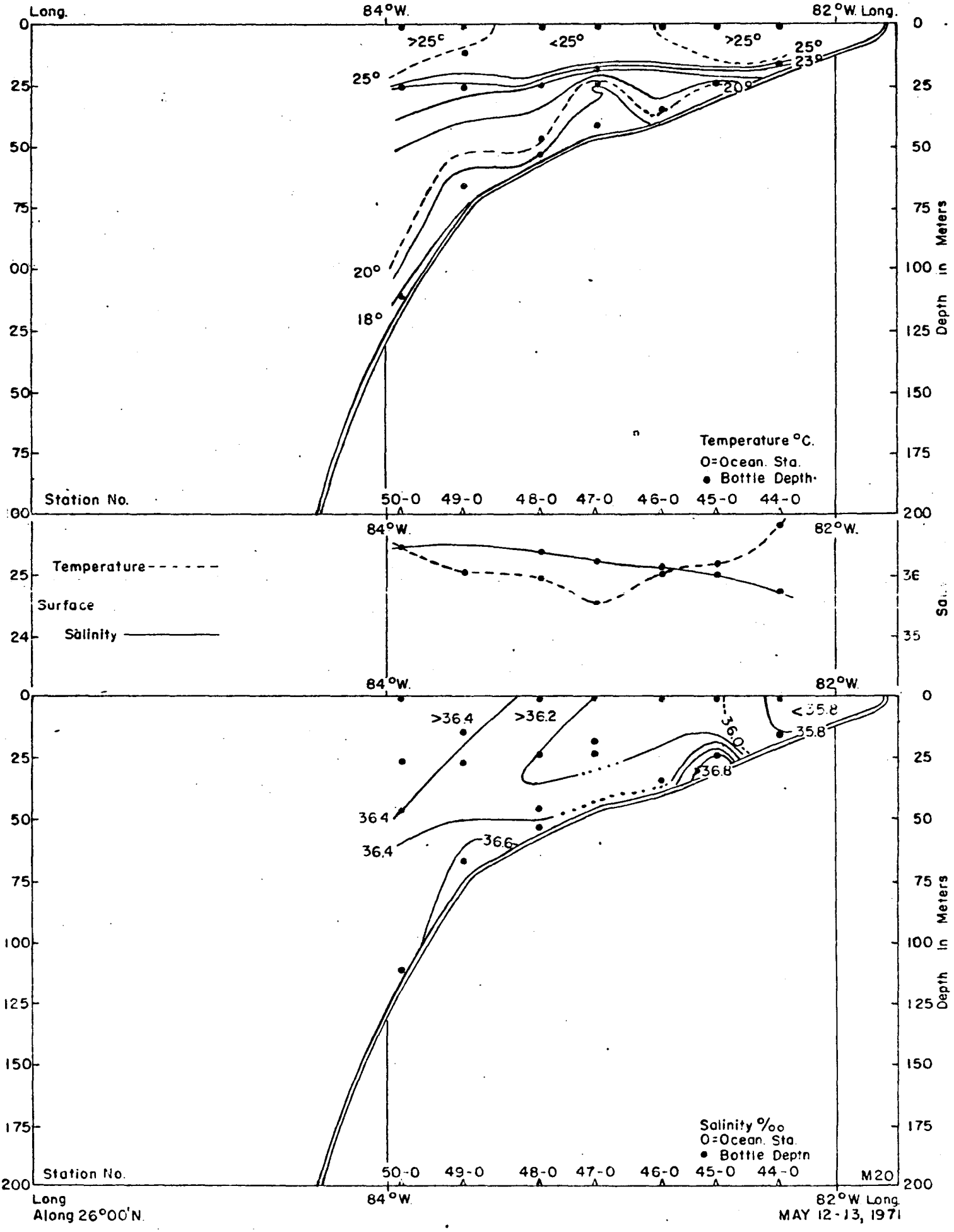

Vertical Distribution Temperature and Salinity - DAN BRAMAN - 7113

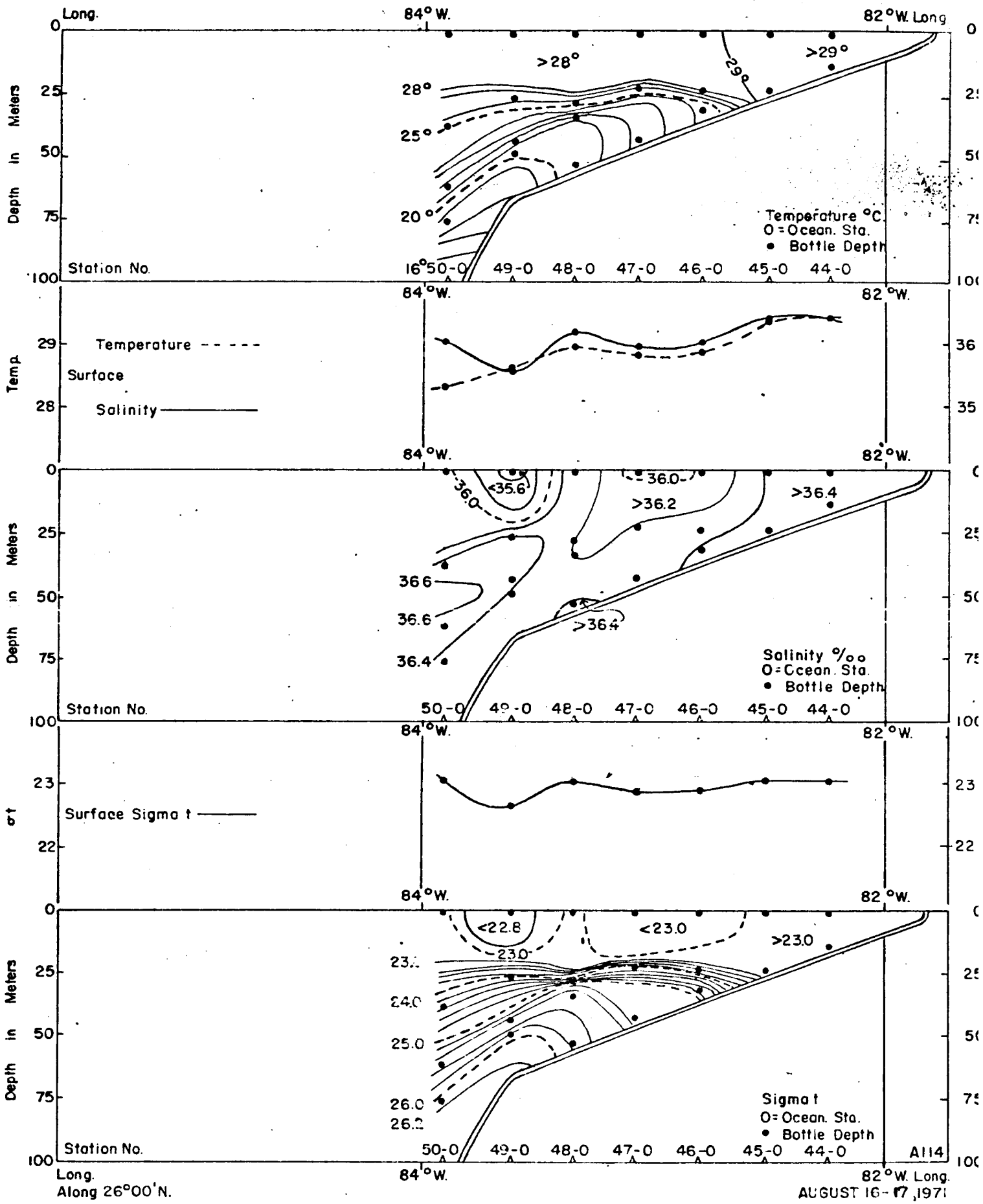

Vertical Distribution Temperature, Salinity and Sigmat - DAN BRAMAN - 7109

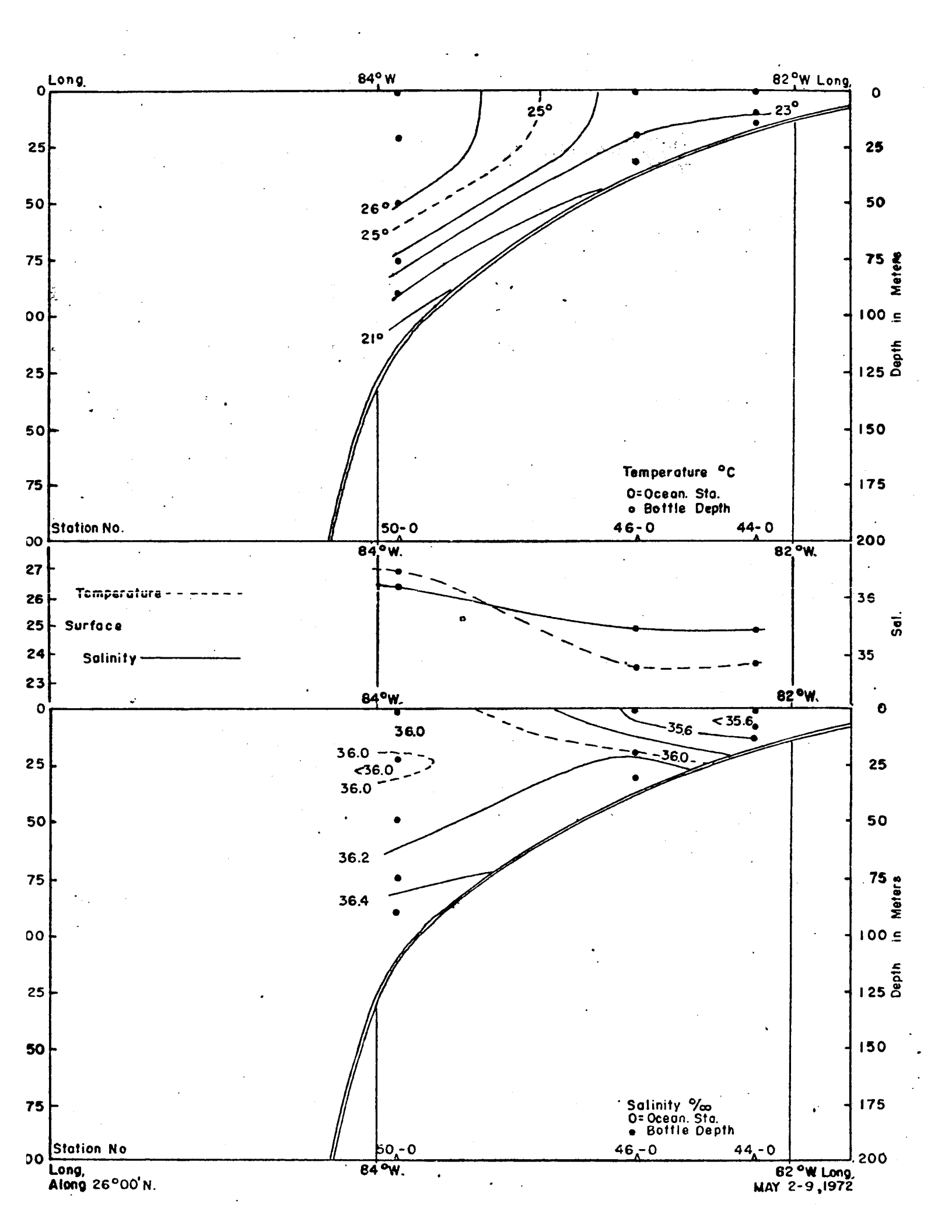
Long.
84°W
82°W Long.
25°
23°
26°
25°
21°
Temperature °C
O=Ocean. Sta.
• Bottle Depth
Station No.
50-0
46-0
44-0
Depth in Meters
84°W.
82°W.
Temperature
Surface
Salinity
Sal.
36.0
35.6
<35.6
<36.0
36.2
36.4
Salinity ‰
O=Ocean. Sta.
• Bottle Depth
Station No
Long.
Along 26°00'N.
MAY 2-9, 1972

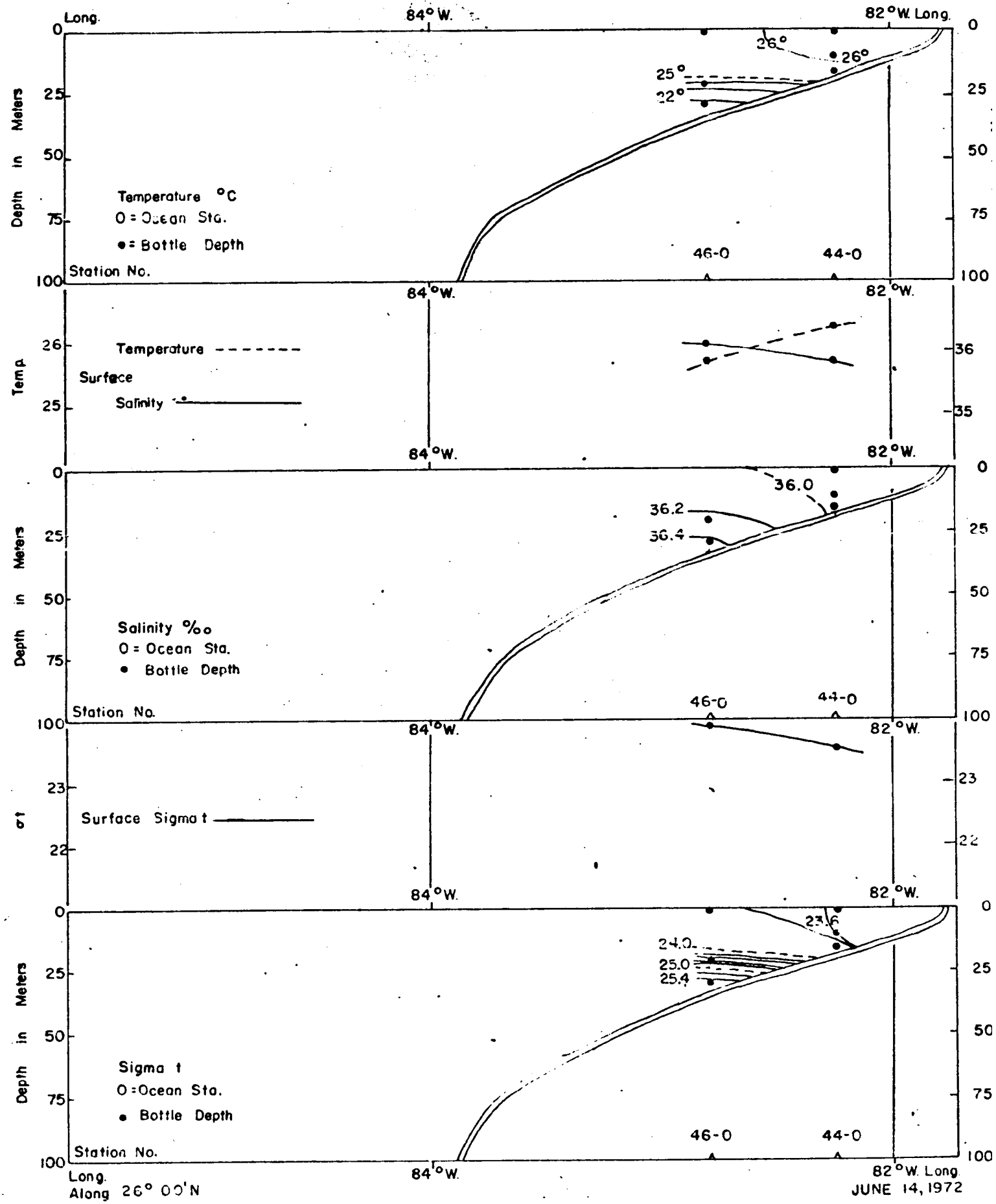

Vertical Distribution Temperature, Salinity and Sigma t - GERDA- 7210

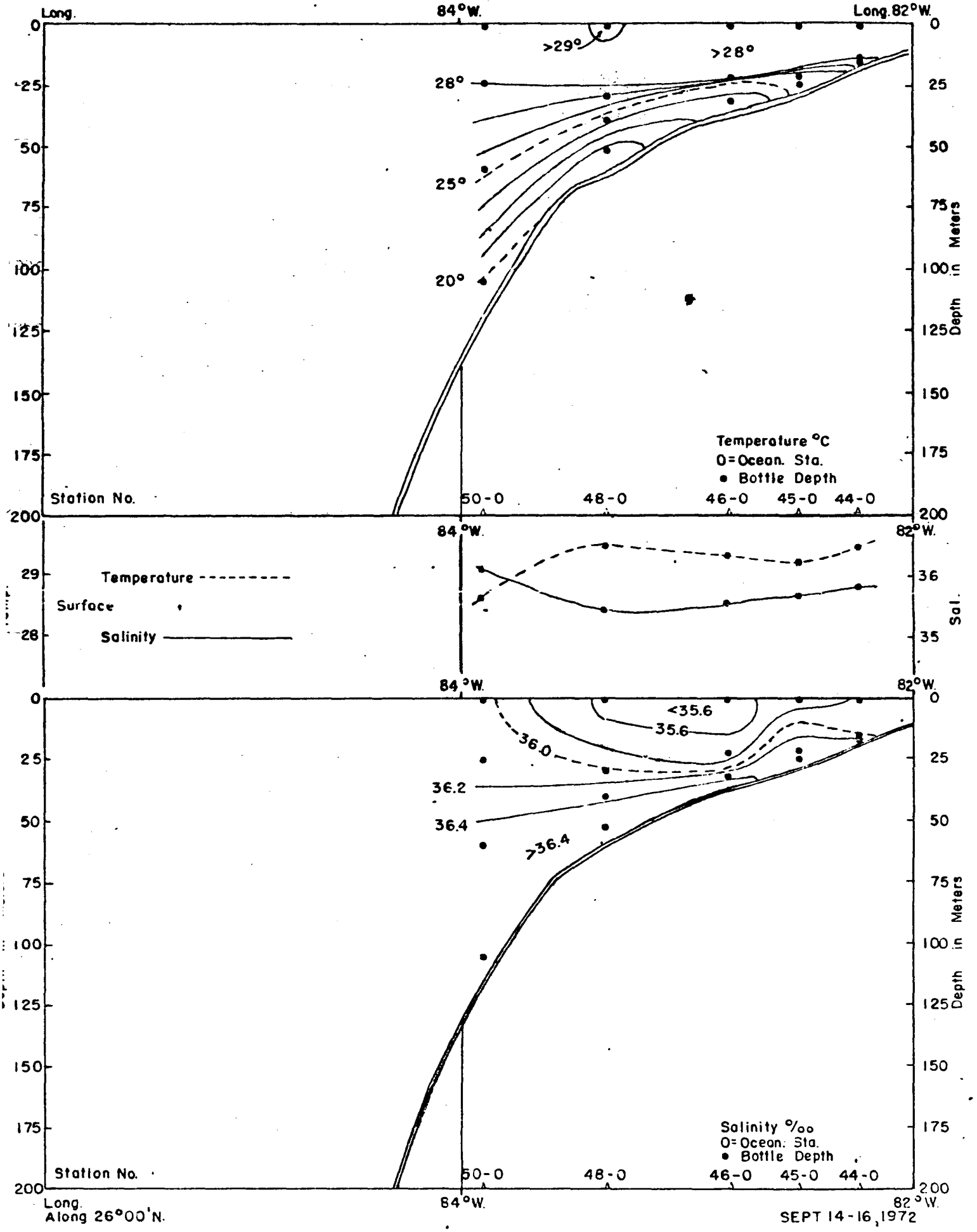

Vertical Distribution -Temperature and Salinity - C. ISELIN - 7205

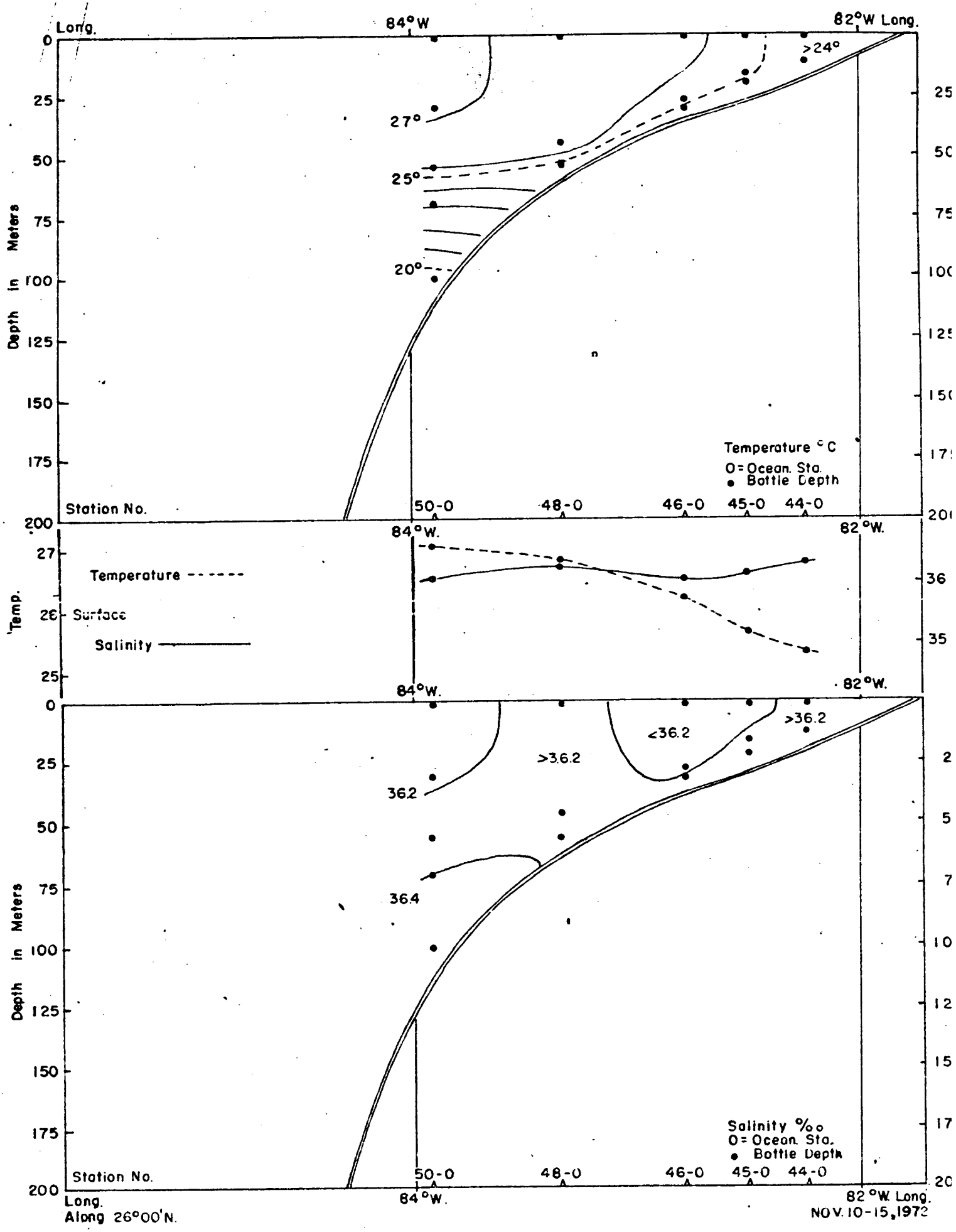

Vertical Distribution - Temperature and Salinity - C. ISELIN - 7209

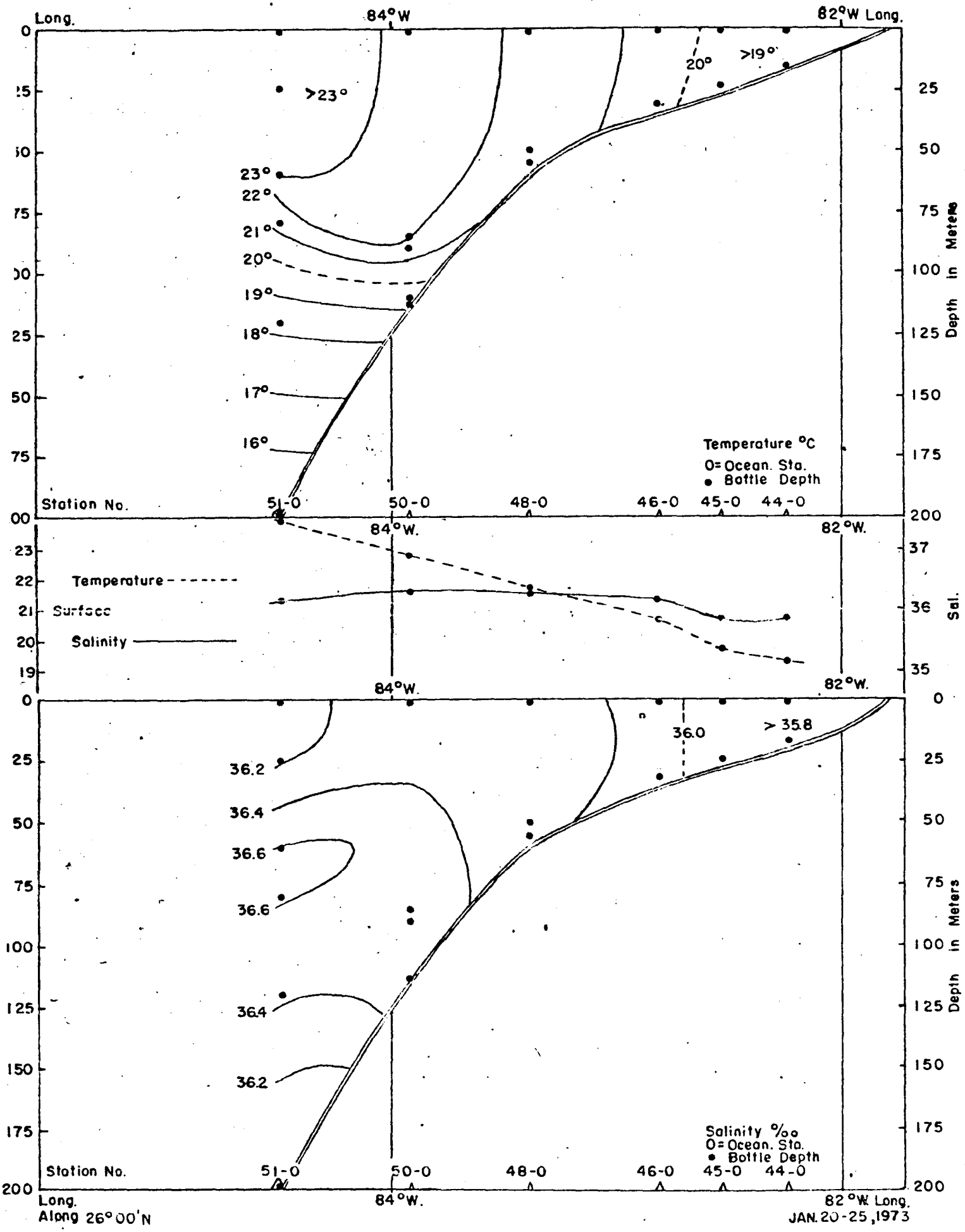

Vertical Distribution - Temperature and Salinity - C. ISELIN - 7303

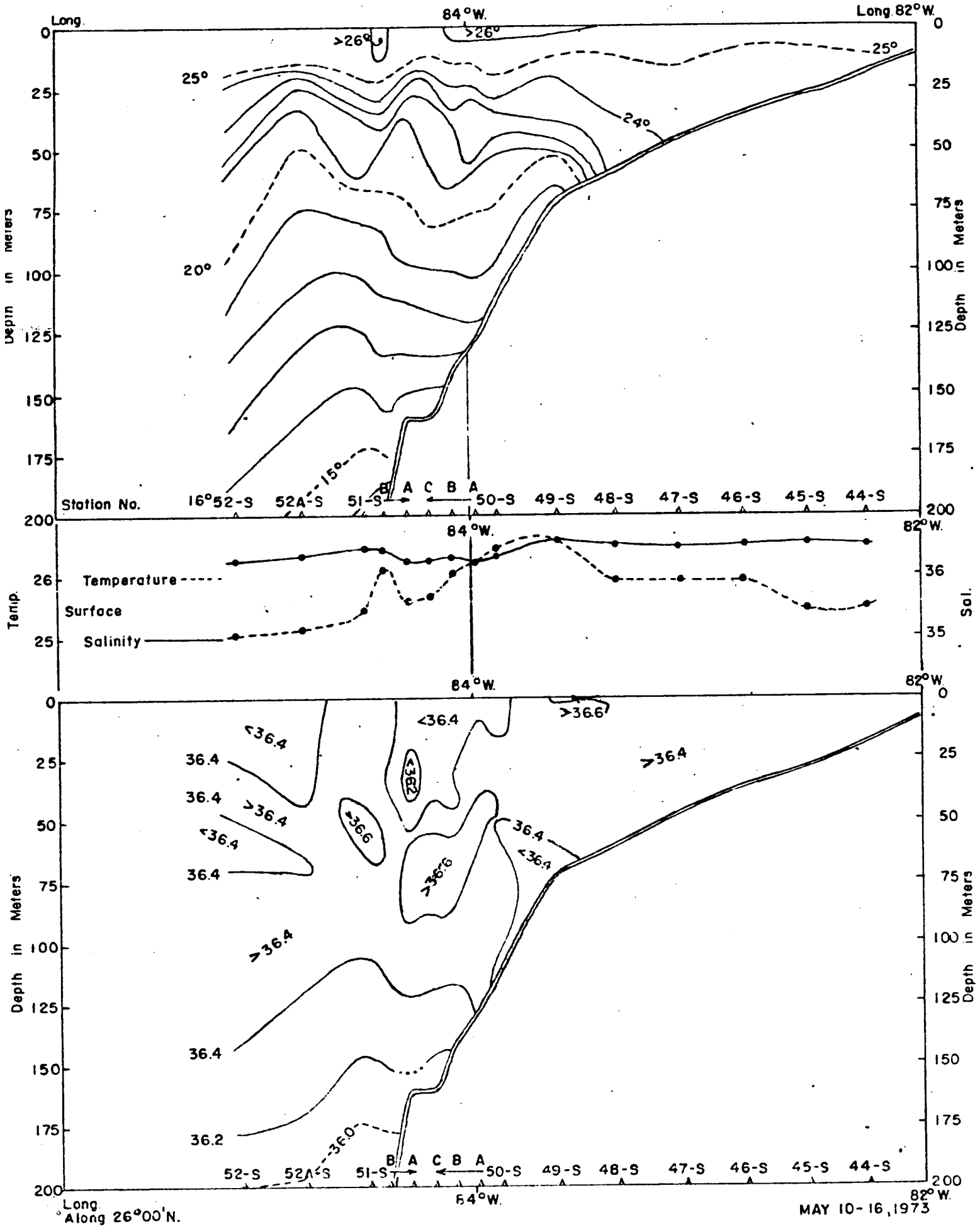

Vertical Distribution Temperature and Salinity - C. ISELIN - 7308

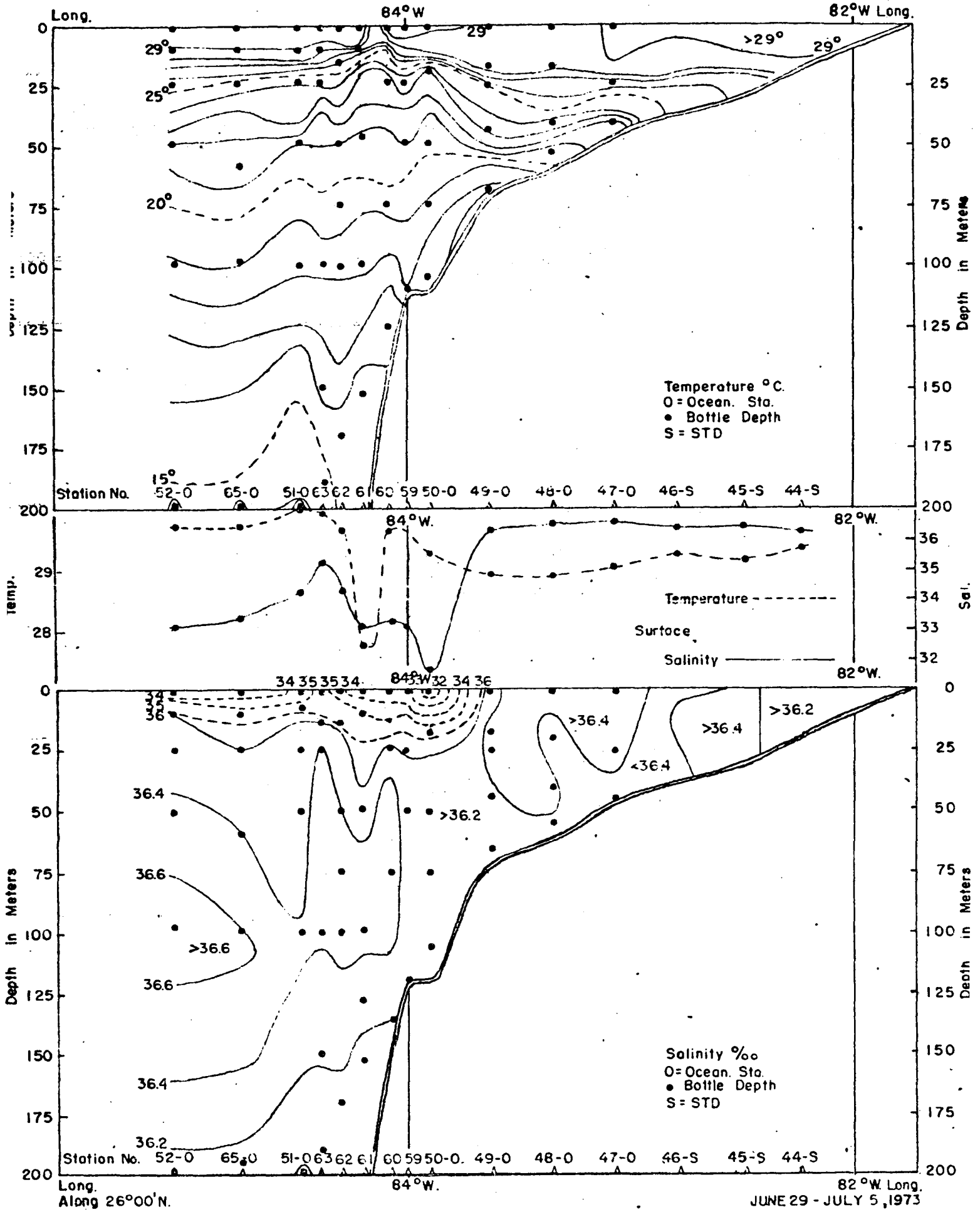

Vertical Distribution - Temperature and Salinity - C. ISELIN - 7311

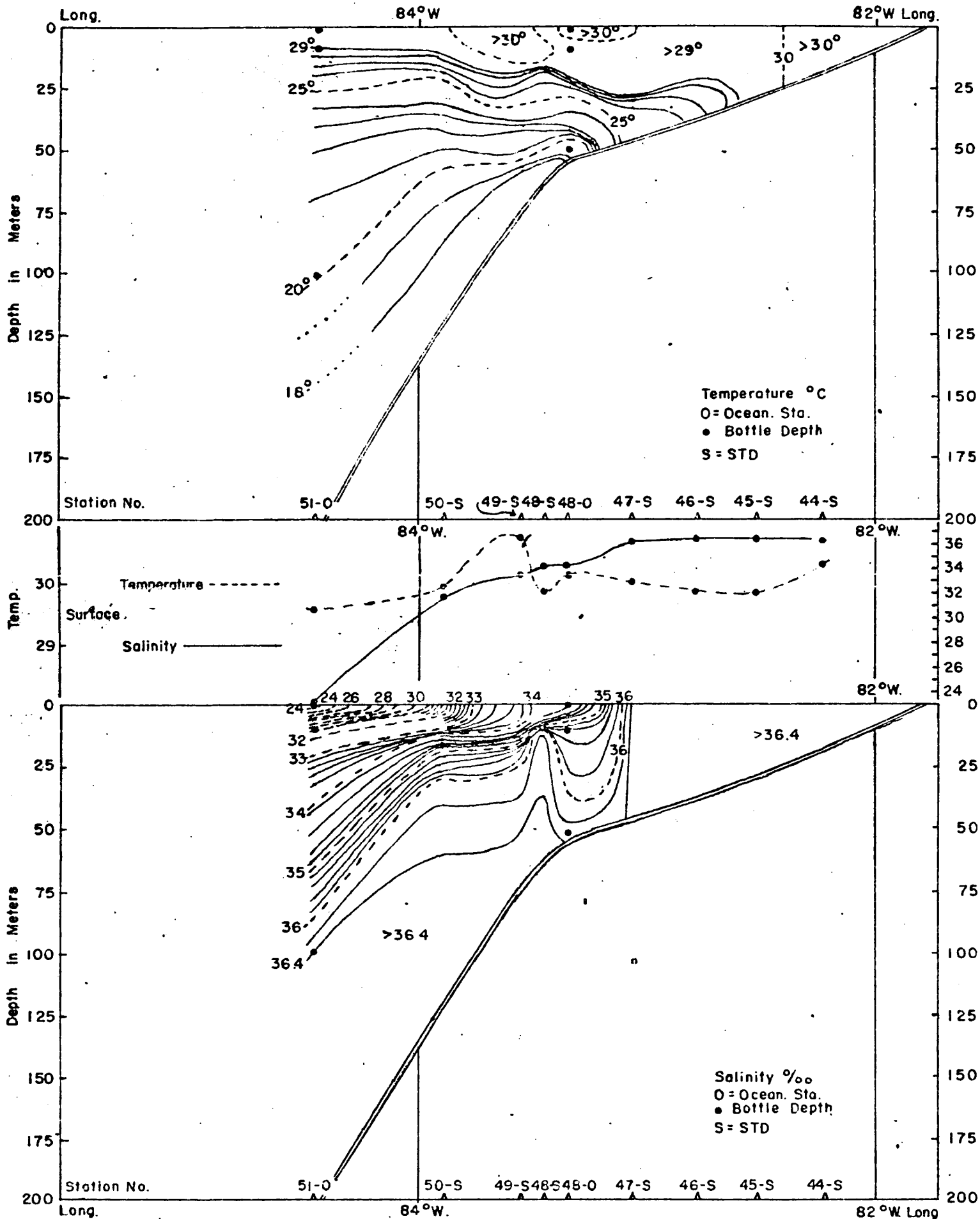
Long.
84°W
82°W Long.
Depth in Meters
29°
25°
20°
18°
>30°
>30°
>29°
30
>30°
25°
Temperature °C
O = Ocean. Sta.
• Bottle Depth
S = STD
Station No.
51-O
50-S
49-S
48-S
48-O
47-S
46-S
45-S
44-S
84°W.
82°W.
Temp.
Temperature
Surface.
Salinity
24 26 28 30 32 33 34 35 36
>36.4
>36 4
36.4
Salinity ‰
O = Ocean. Sta.
• Bottle Depth
S = STD
Long.
Along 26°00'N.
AUG. 6, 1973

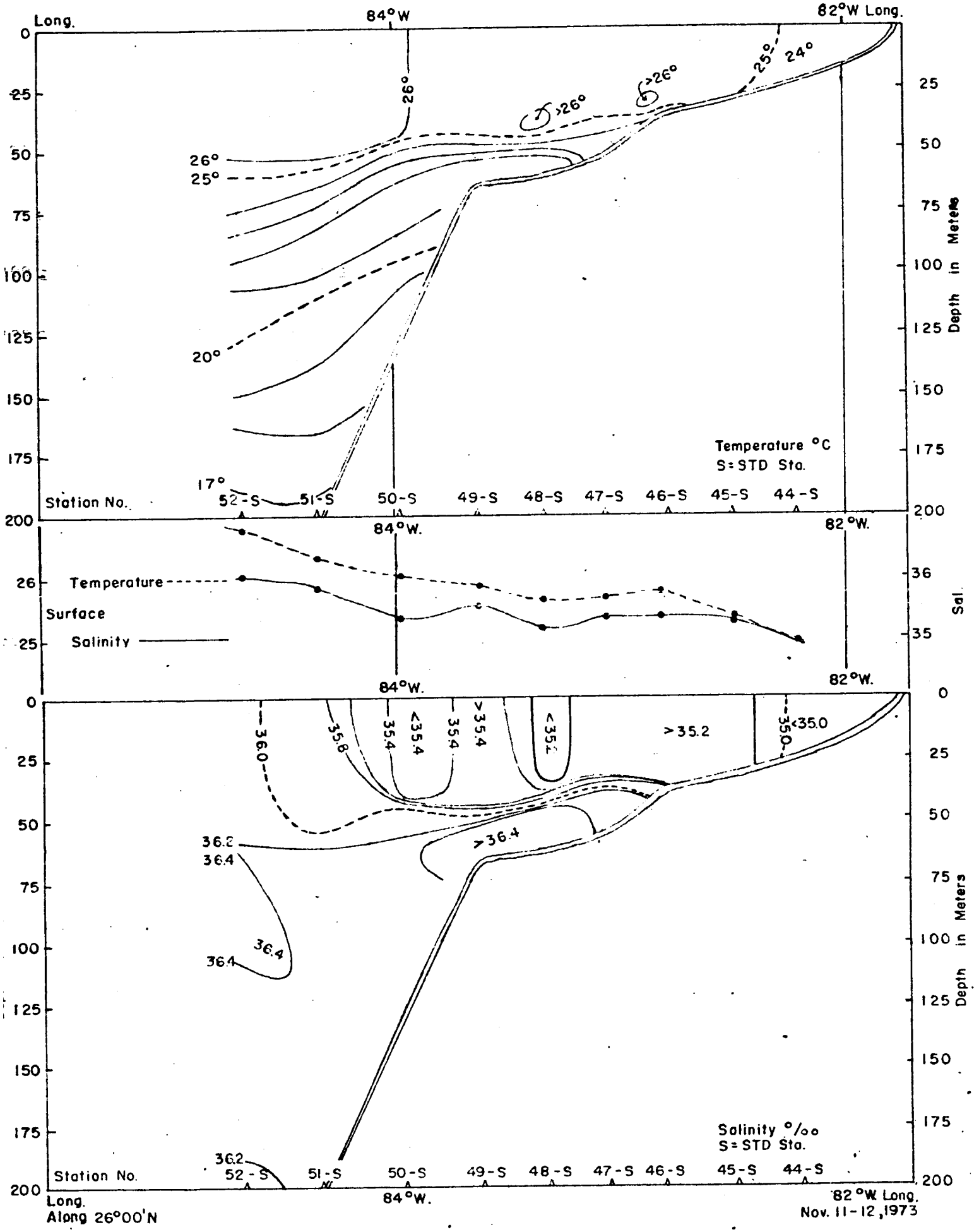

Vertical Distribution - Temperature and Salinity - C. ISELIN - 7320

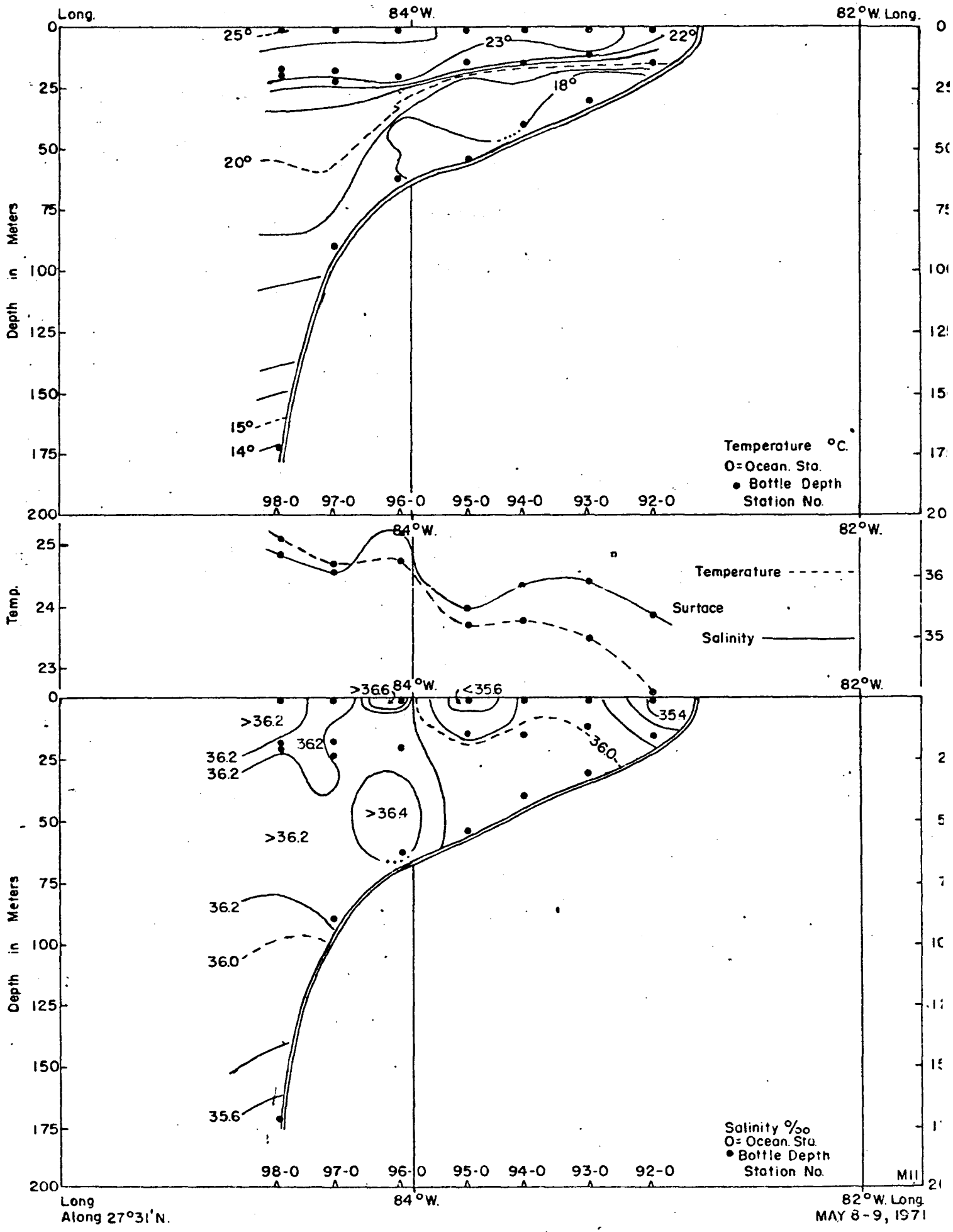

Vertical Distribution Temperature and Salinity- DAN BRAMAN-7113

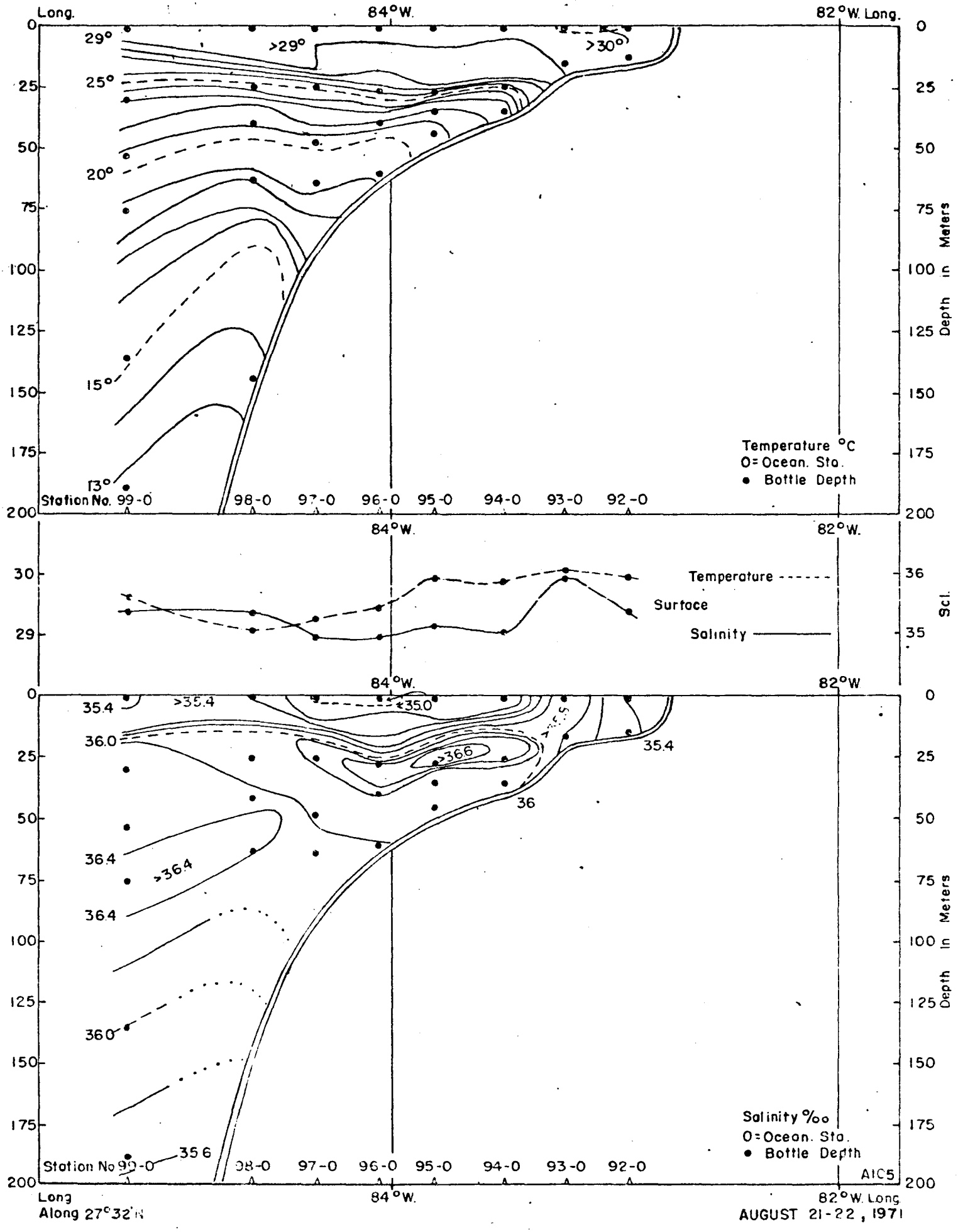

Vertical Distribution - Temperature and Salinity - DAN BRAMAN - 7:09

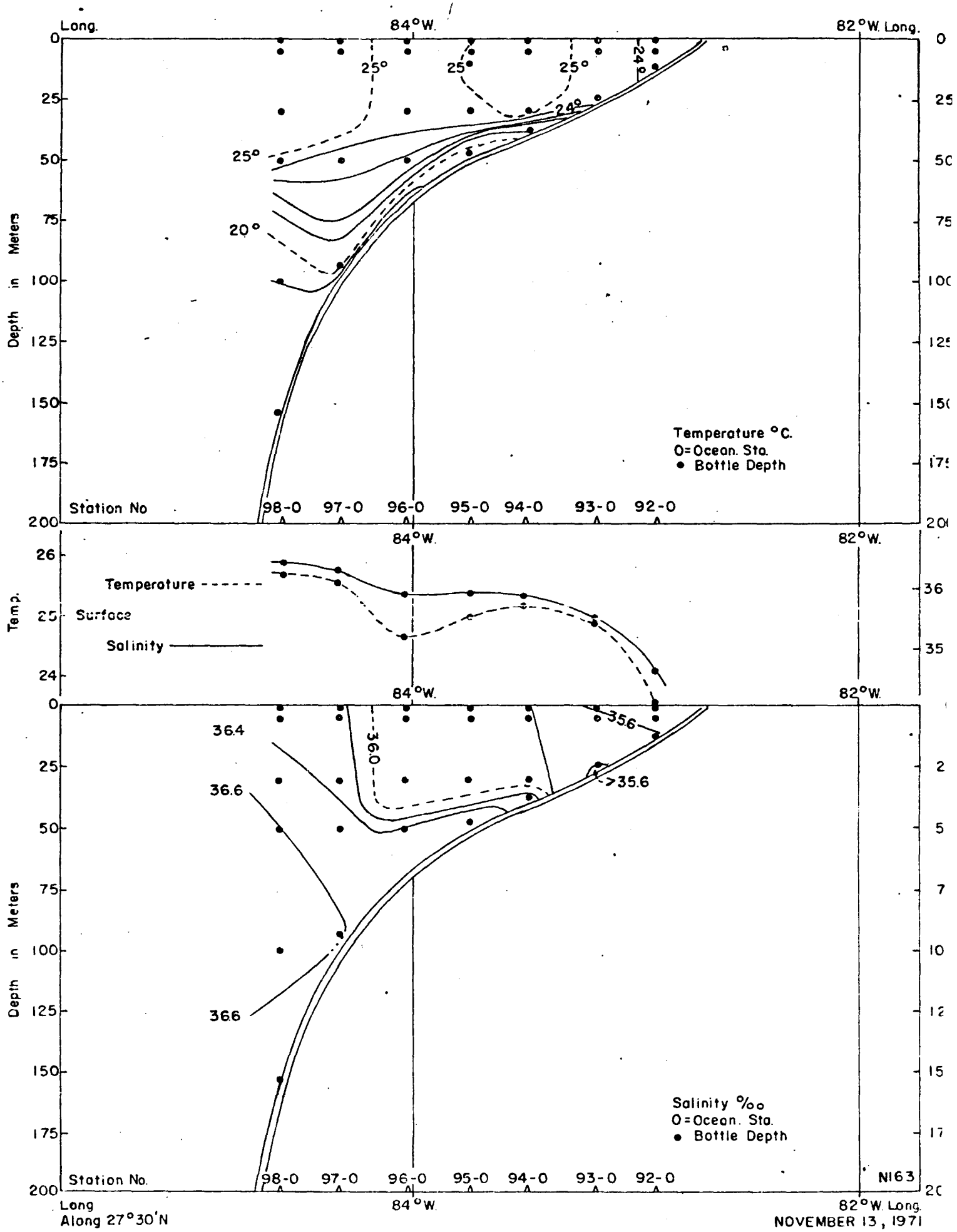

Vertical Distribution - Temperature and Salinity - BELLOWS-7107

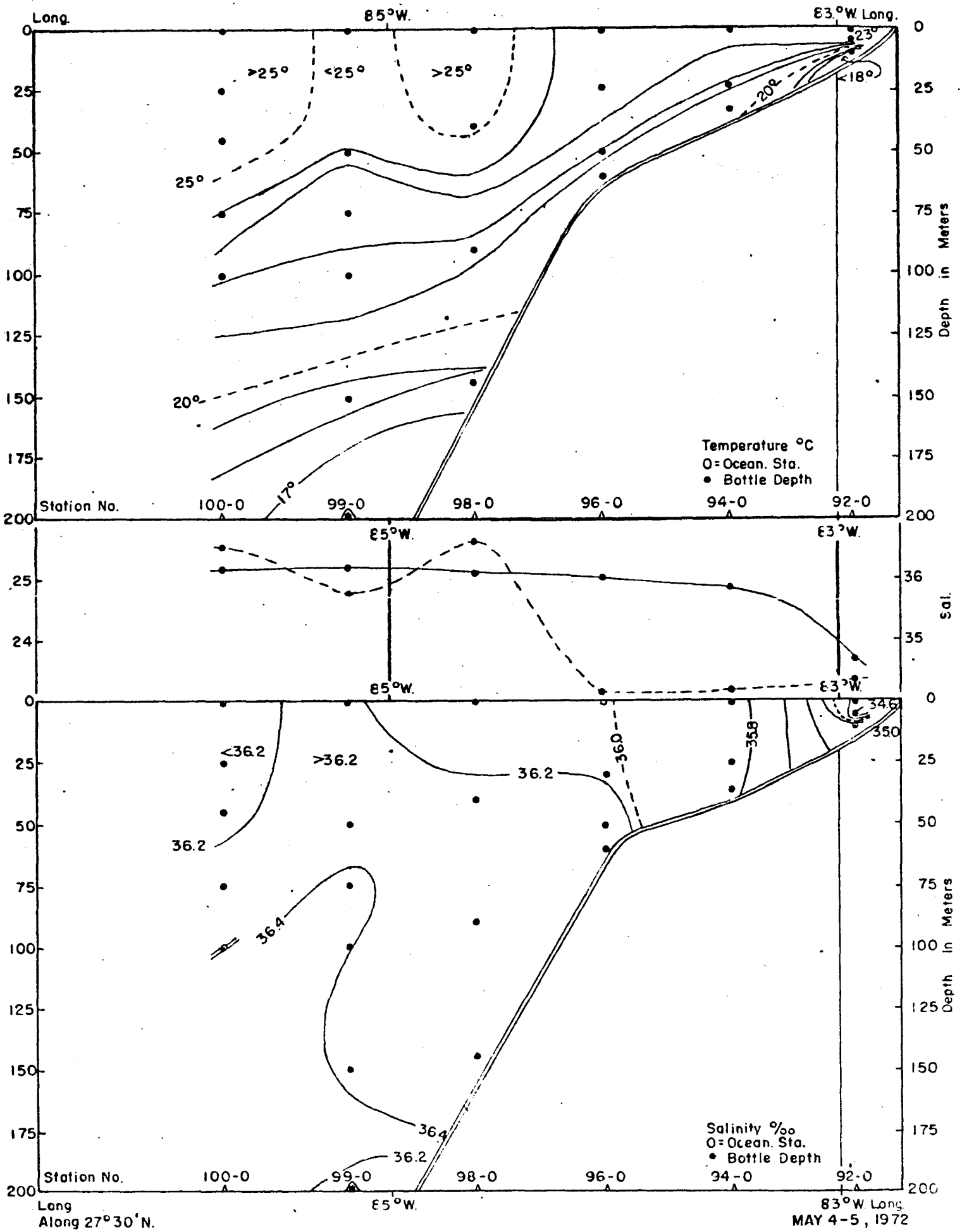

Vertical Distribution Temperature and Salinity - GERDA-7208

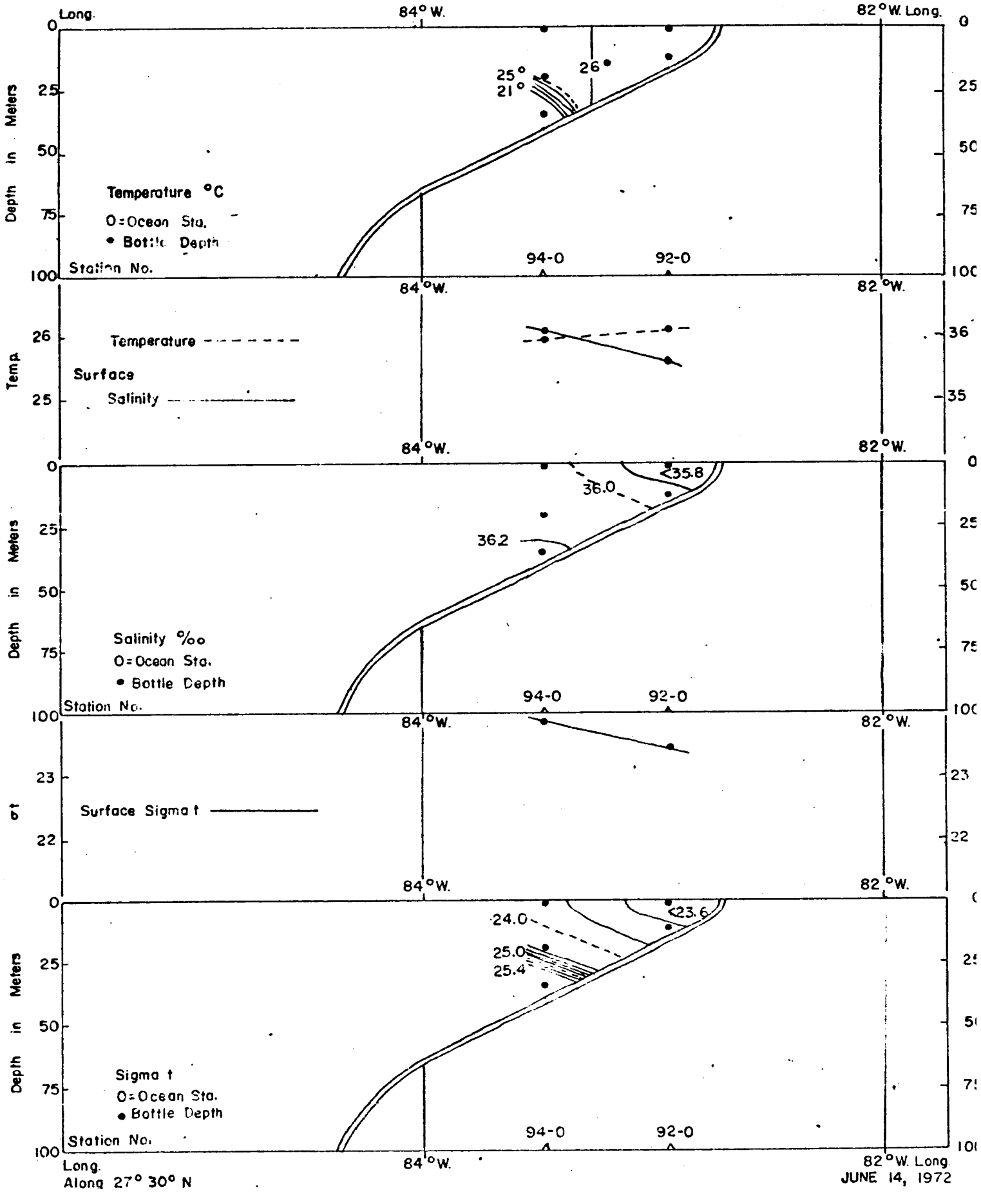
Long.
84° W.
82° W. Long.
Depth in Meters
Temperature °C
O=Ocean Sta.
• Bottle Depth
Station No.
25°
21°
26
94-0
92-0
Temp.
Temperature
Surface
Salinity
36
35
Salinity ‰
<35.8
36.0
36.2
σt
Surface Sigma t
24.0
<23.6
25.0
25.4
Sigma t
Long.
Along 27° 30° N
JUNE 14, 1972

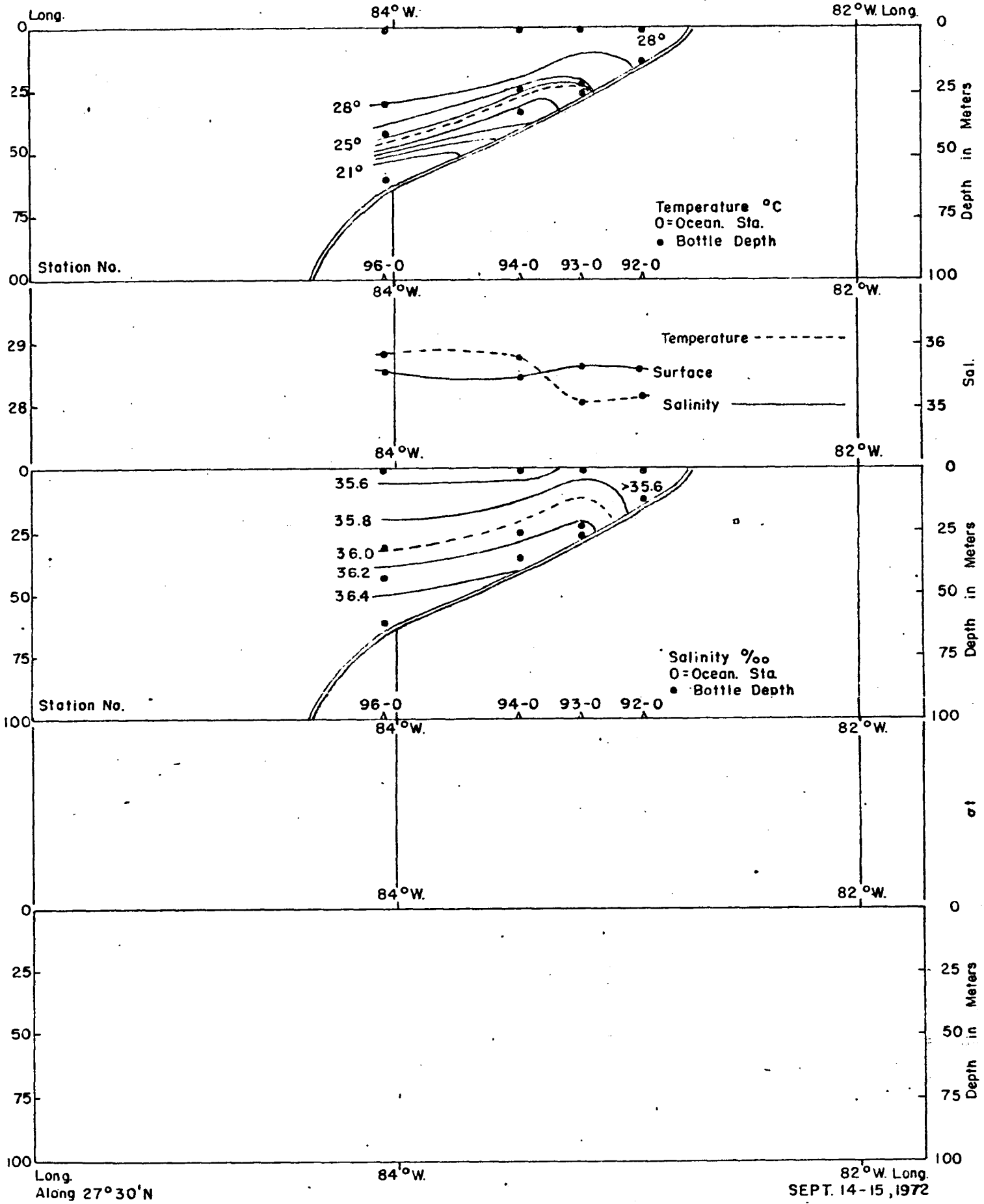

Vertical Distribution Temperature, Salinity and Sigmat - C. ISELIN - 7205

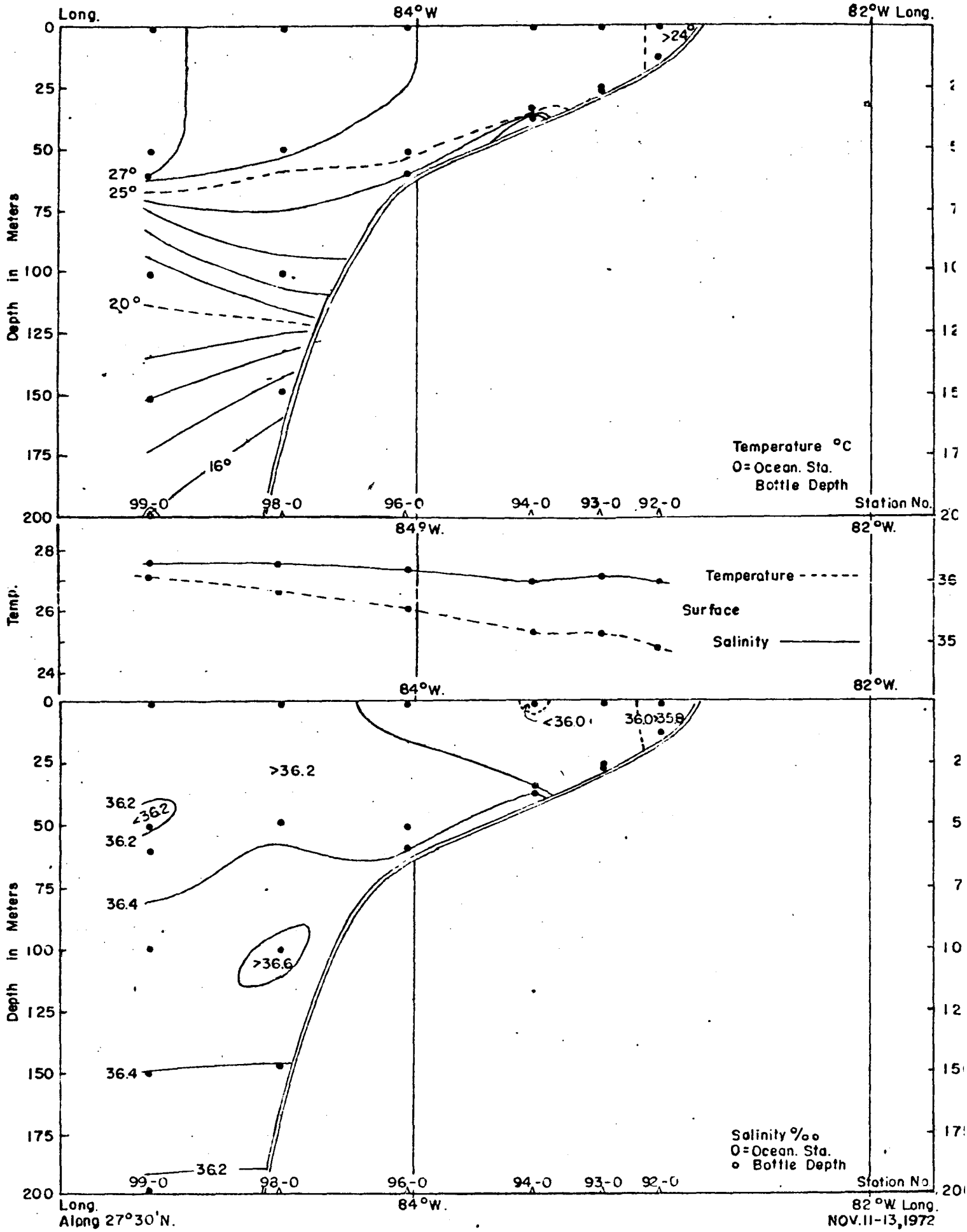

Vertical Distribution - Temperature and Salinity - C. ISELIN - 7209

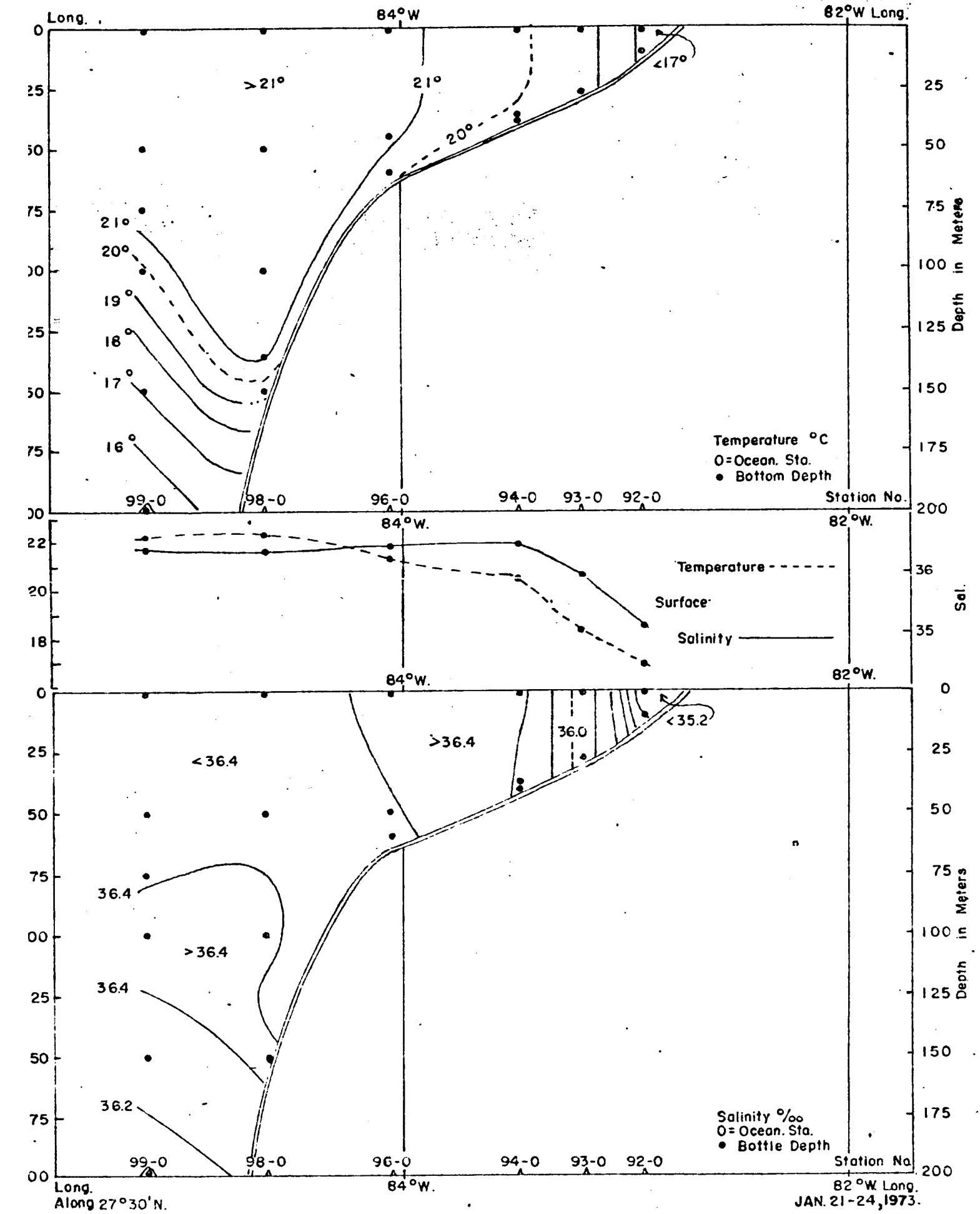

Vertical Distribution - Temperature and Salinity - C. ISELIN - 7303

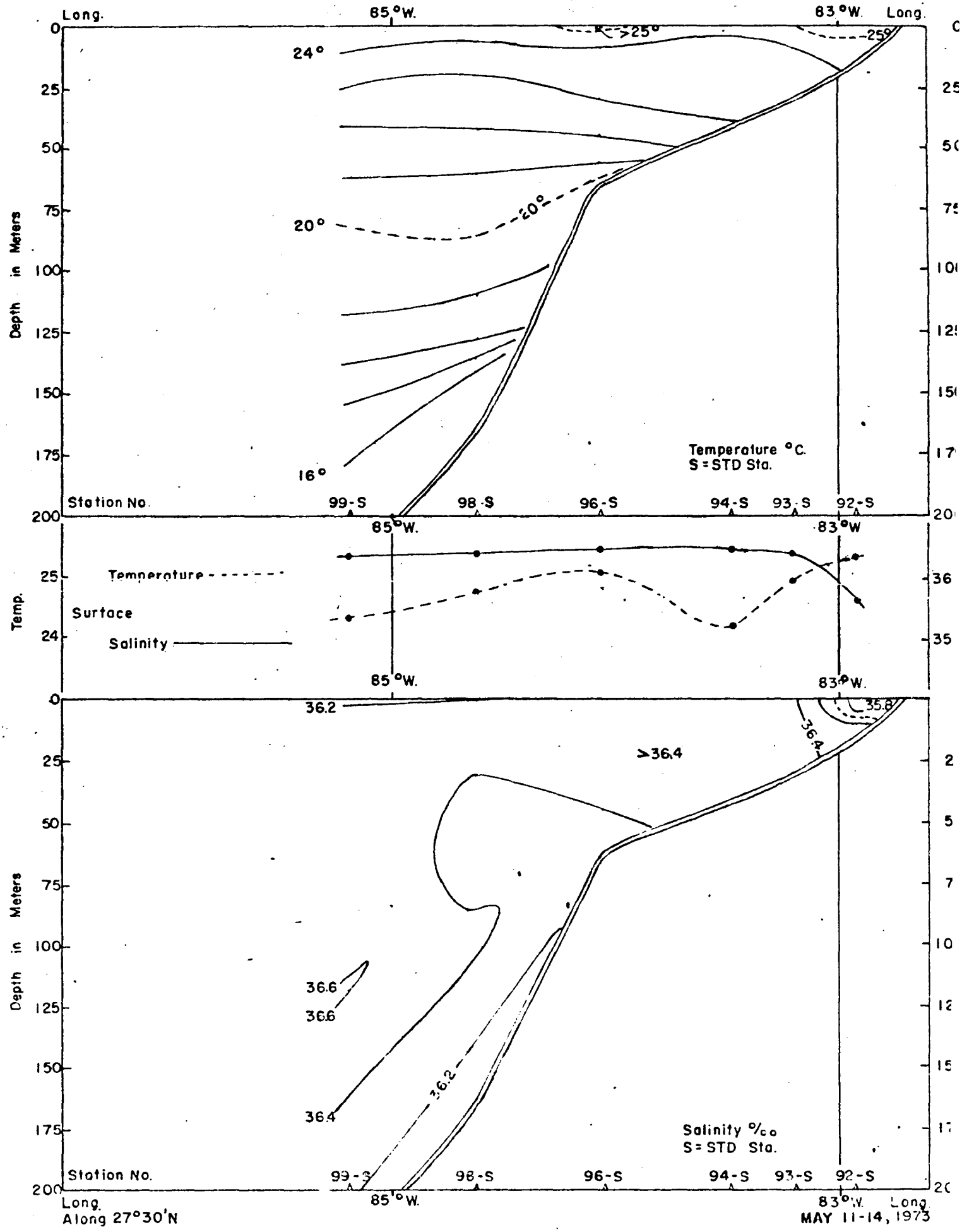
Long.
85°W.
83°W.
Long.
24°
20°
16°
≥25°
25°
≥20°
Depth in Meters
Temperature °C.
S = STD Sta.
Station No.
99-S
98-S
96-S
94-S
93-S
92-S
Temp.
Temperature
Surface
Salinity
36.2
≥36.4
35.8
36.4
36.6
36.6
36.4
36.2
Salinity ‰
S = STD Sta.
Long.
Along 27°30'N
MAY 11-14, 1973

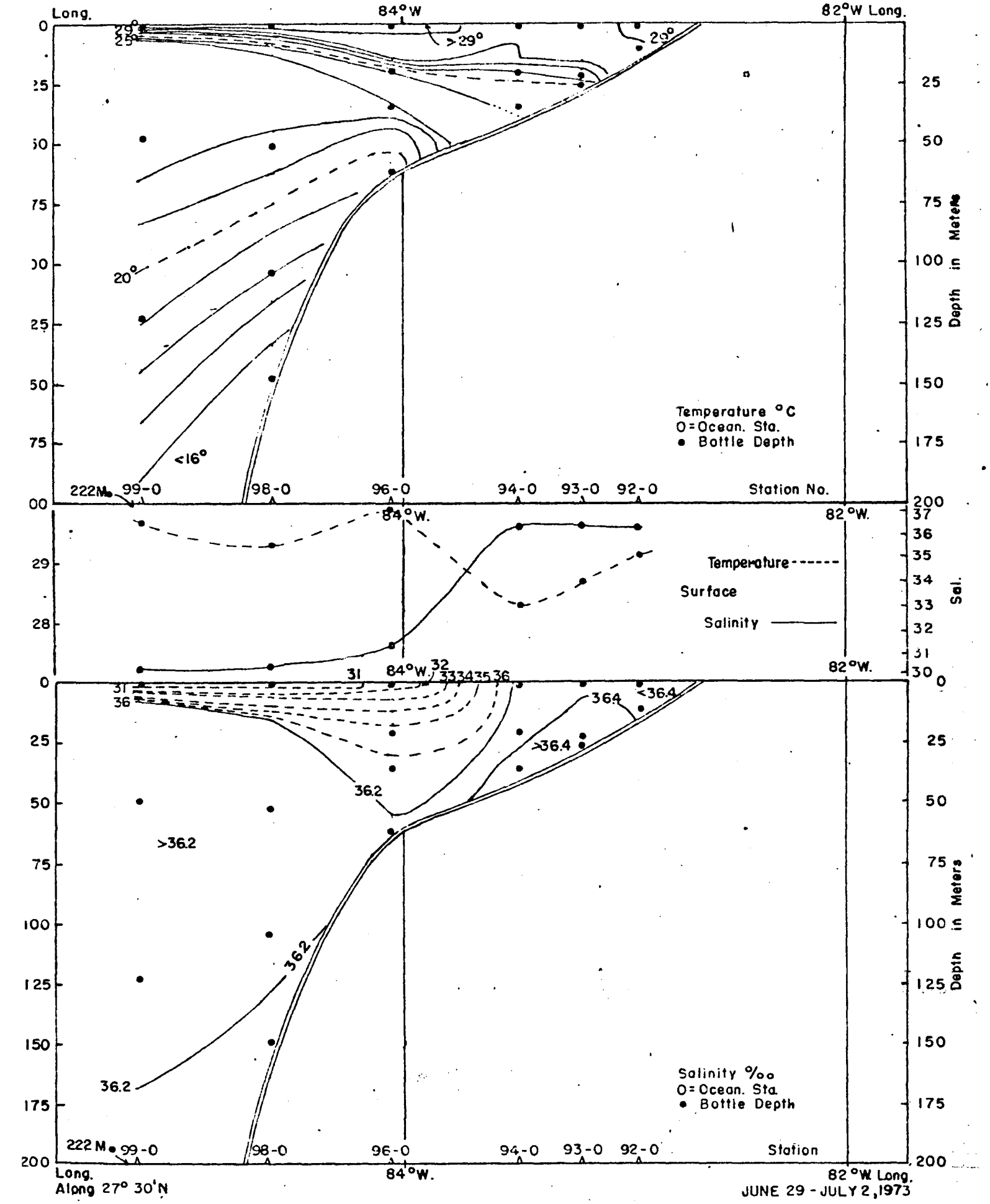

Vertical Distribution - Temperature and Salinity - C. ISELIN - 7311

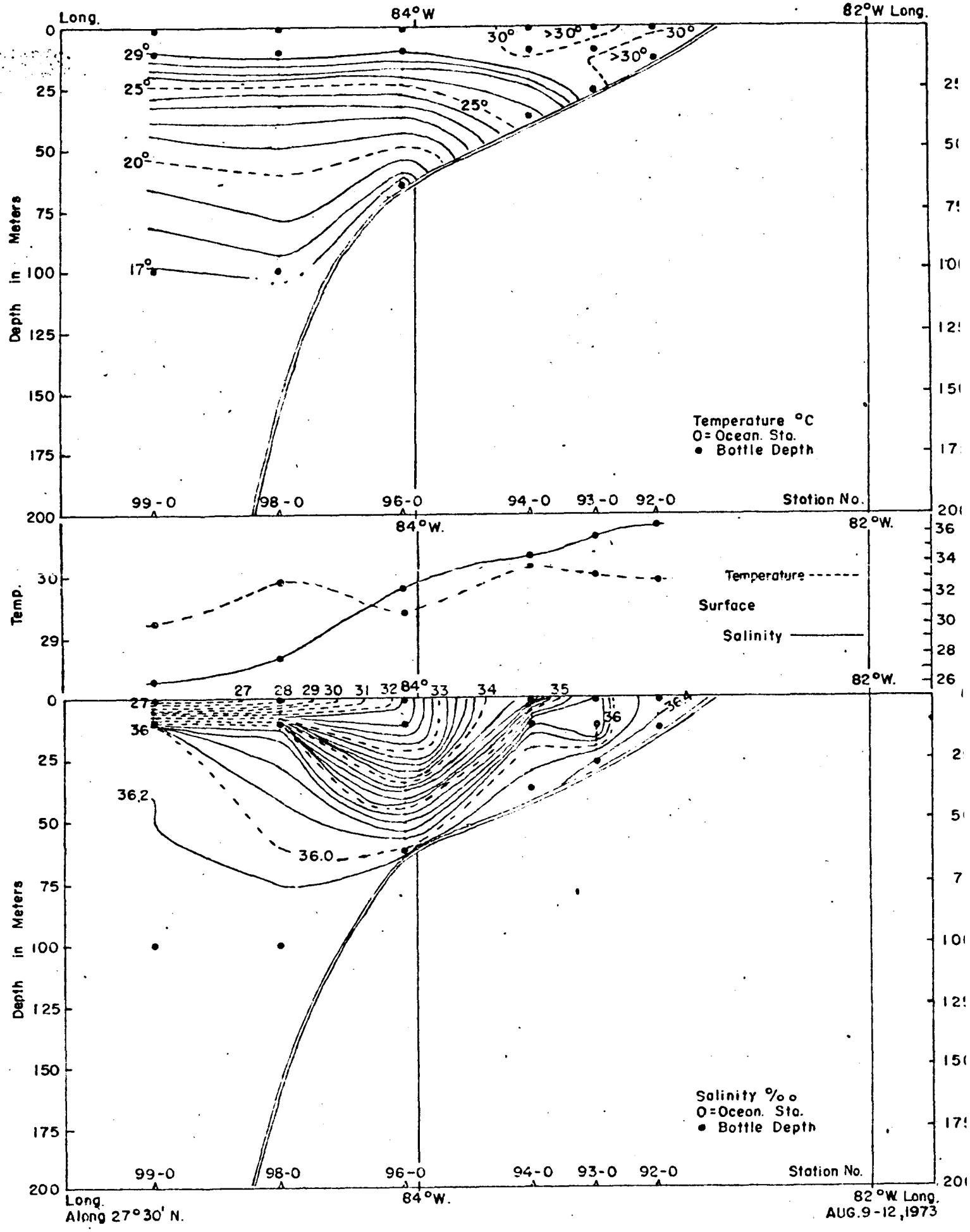
Long.
84°W
82°W Long.
Depth in Meters
29°
25°
20°
17°
30°
>30°
25°
Temperature °C
O= Ocean. Sta.
• Bottle Depth
99-0
98-0
96-0
94-0
93-0
92-0
Station No.
Temp.
Temperature
Surface
Salinity
27 28 29 30 31 32 33 34 35
36
36.2
36.0
Salinity ‰
O=Ocean. Sta.
• Bottle Depth
Long.
Along 27°30' N.
AUG. 9-12, 1973

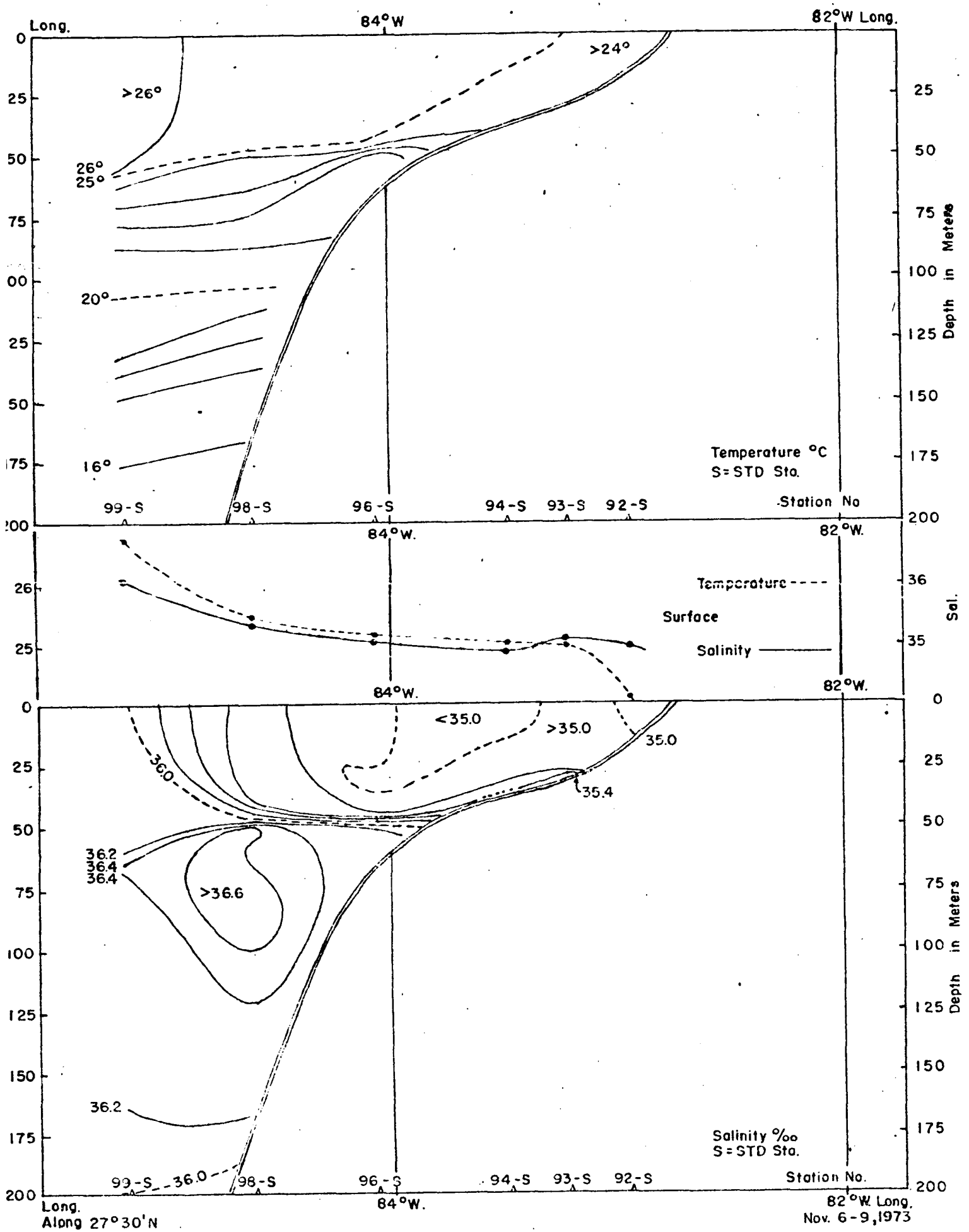

Vertical Distribution - Temperature and Salinity - C. ISELIN - 7320

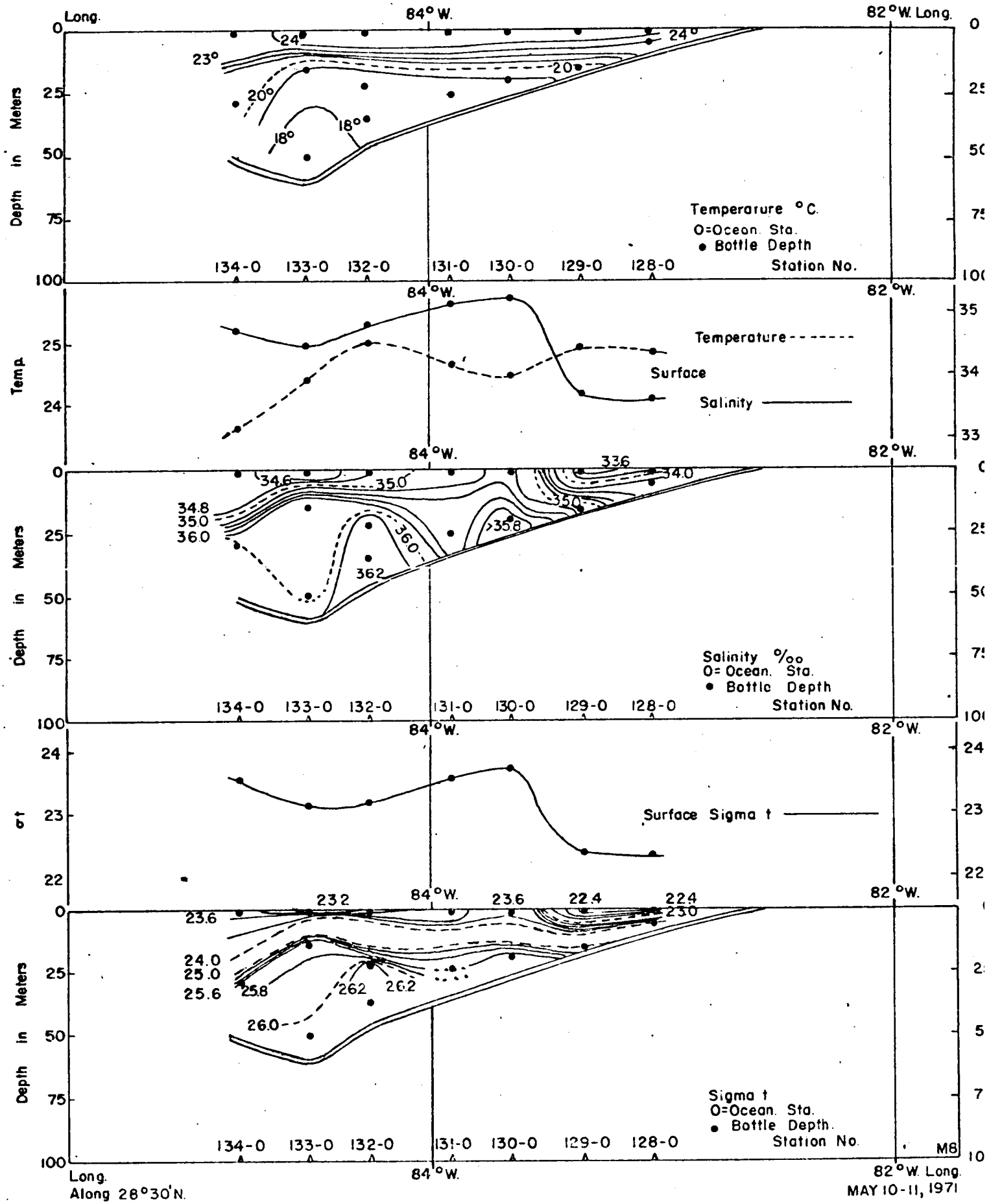

Vertical Distribution Temperature, Salinity and Sigma t- TURSIOPS-7114

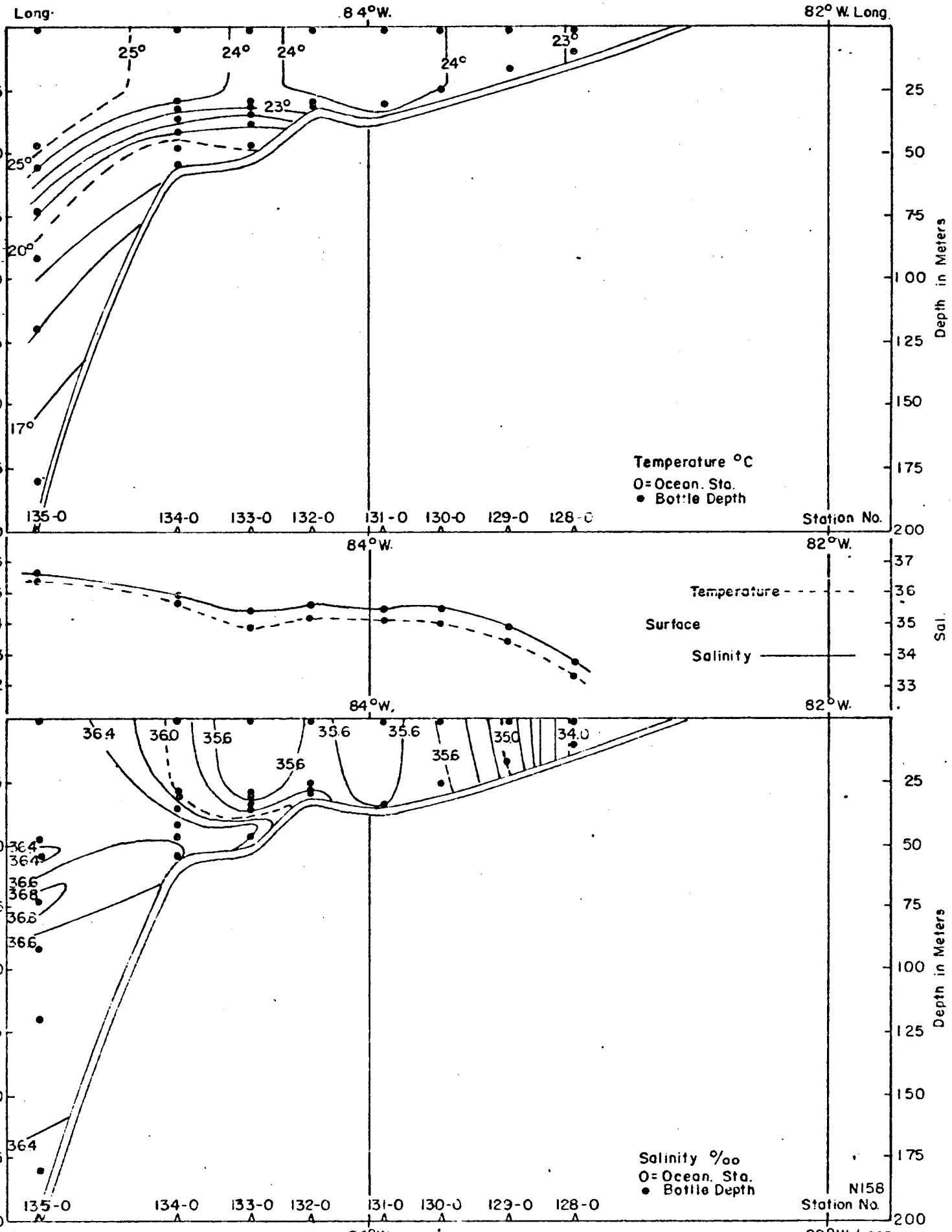
Long.
84°W.
82° W. Long.
25°
24°
24°
24°
23°
23°
25°
20°
17°
Temperature °C
O= Ocean. Sta.
• Bottle Depth
135-0
134-0
133-0
132-0
131-0
130-0
129-0
128-0
Station No.
Depth in Meters
84°W.
82°W.
Temperature
Surface
Salinity
Sal.
84°W.
82°W.
36.4
36.0
35.6
35.6
35.6
35.0
34.0
35.6
36.4
36.4
36.6
36.8
36.6
36.6
36.4
Salinity ‰
O= Ocean. Sta.
• Bottle Depth
N158
135-0
134-0
133-0
132-0
131-0
130-0
129-0
128-0
Station No.
Depth in Meters
Long.
84°W.
82°W. Long.
Alona 28°31'N.
NOVEMBER 14,1971

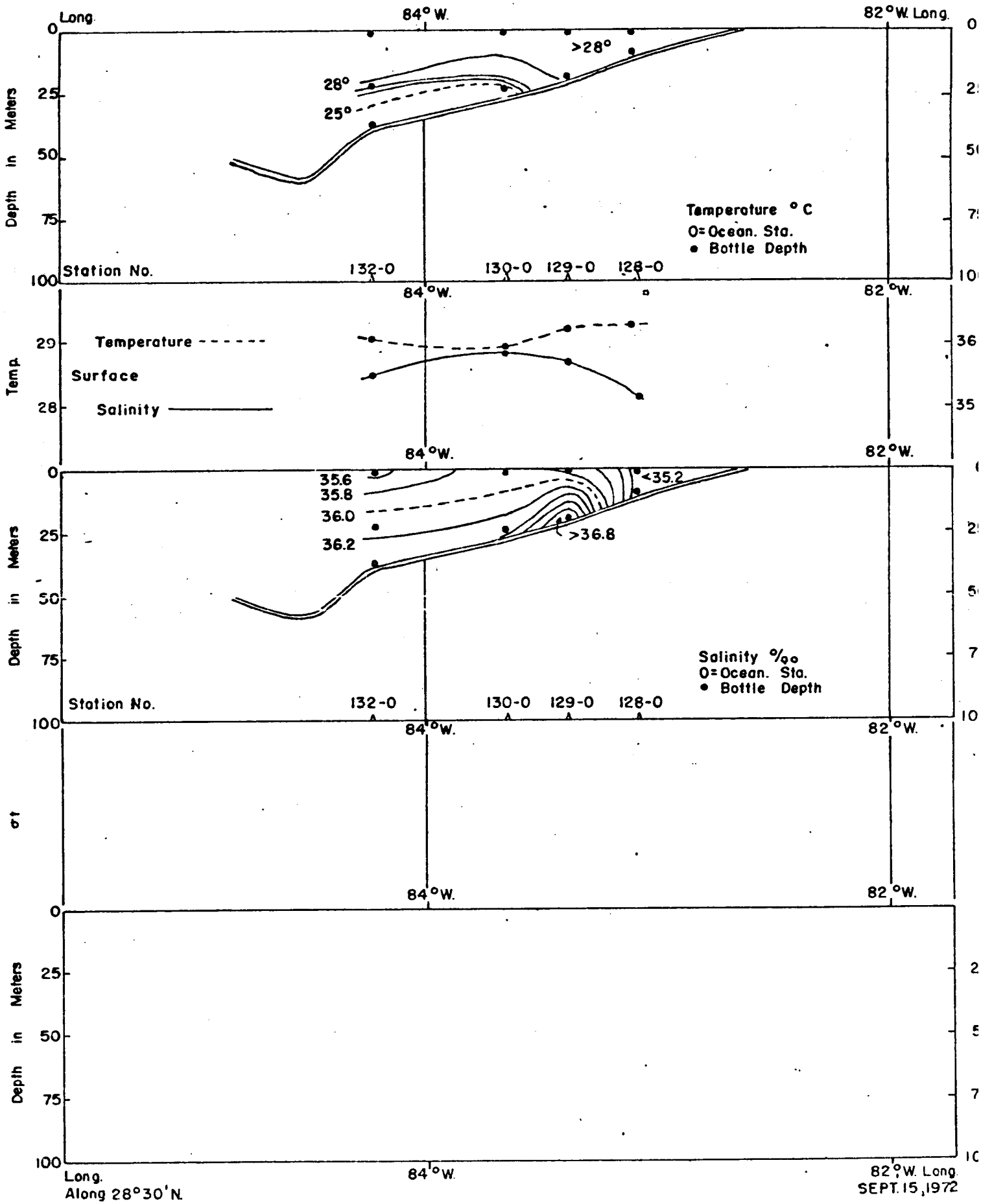

Vertical Distribution Temperature, Salinity and Sigma t - C. ISELIN - 7205

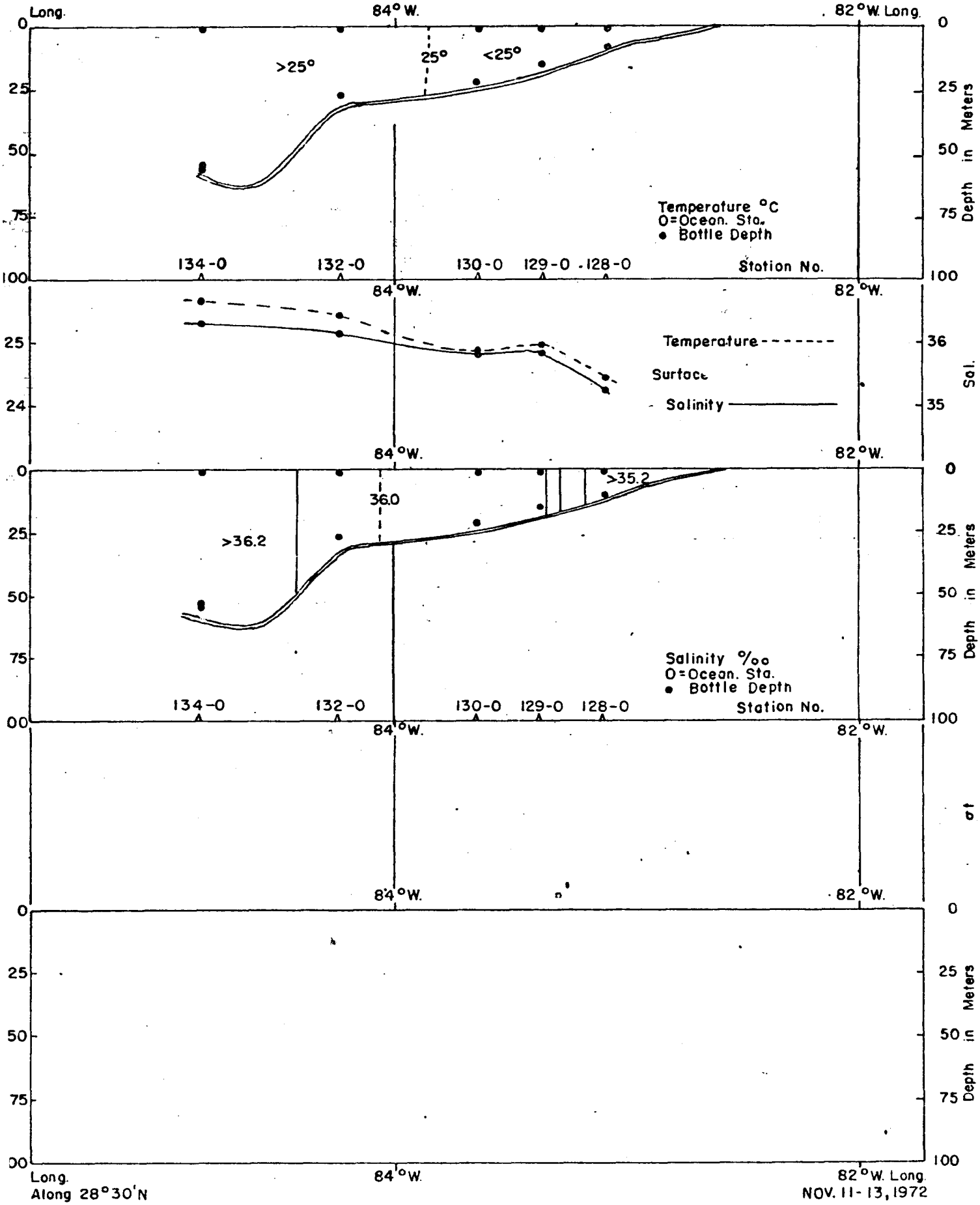

Vertical Distribution Temperature, Salinity and Sigma t - C. ISELIN - 7209

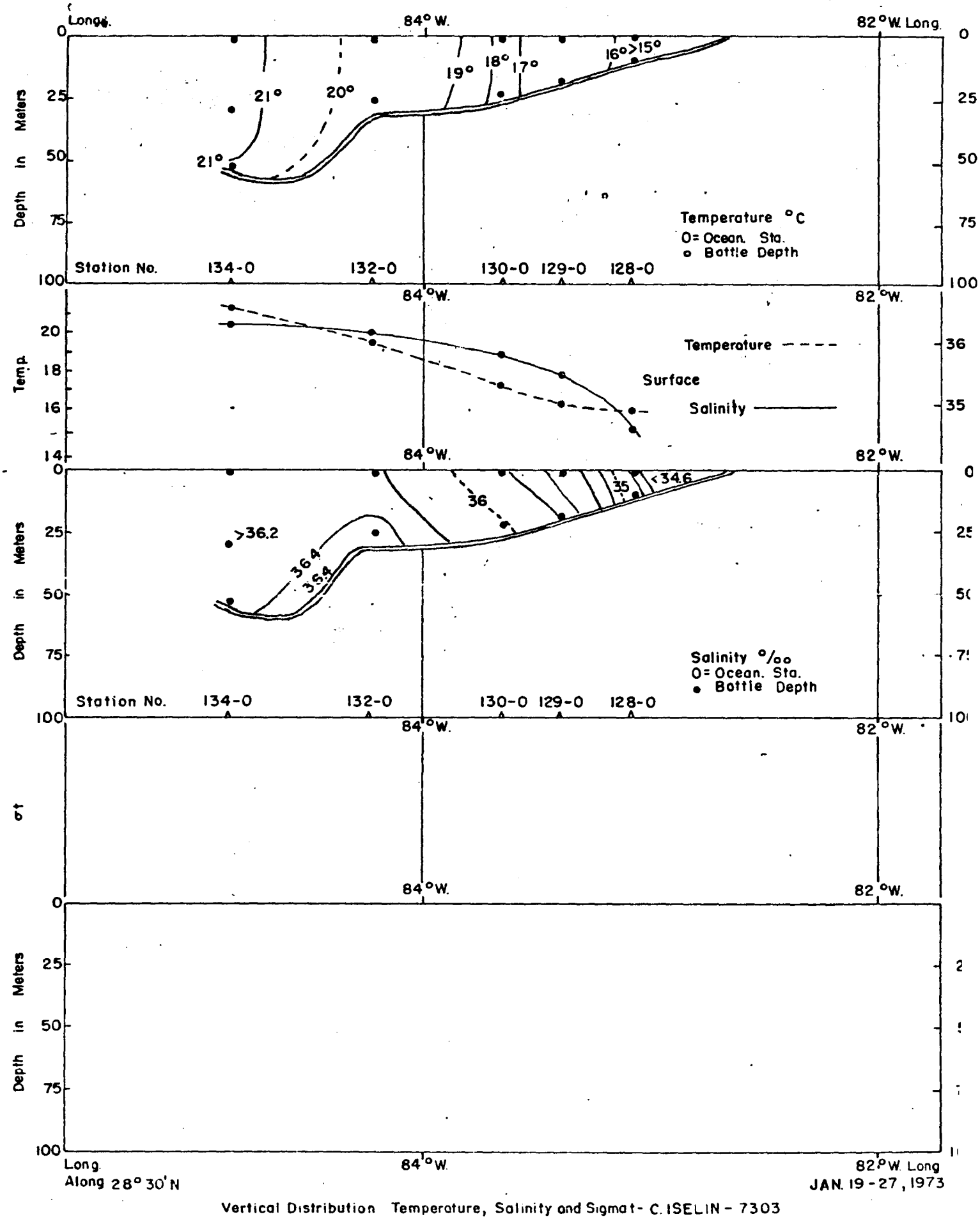

Vertical Distribution Temperature, Salinity and Sigmat - C. ISELIN - 7303

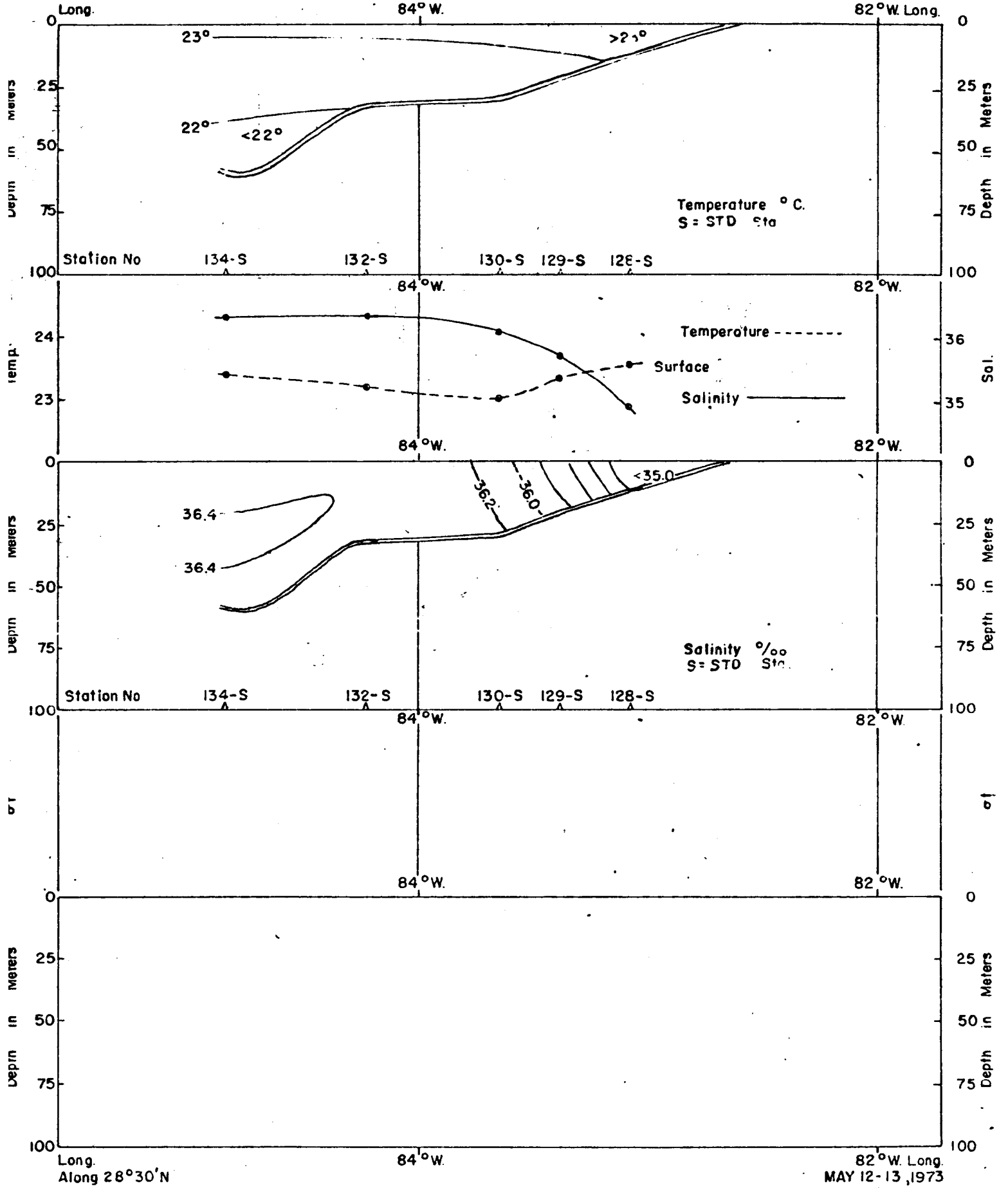

Vertical Distribution Temperature, Salinity and Sigmat-C. ISELIN-7308

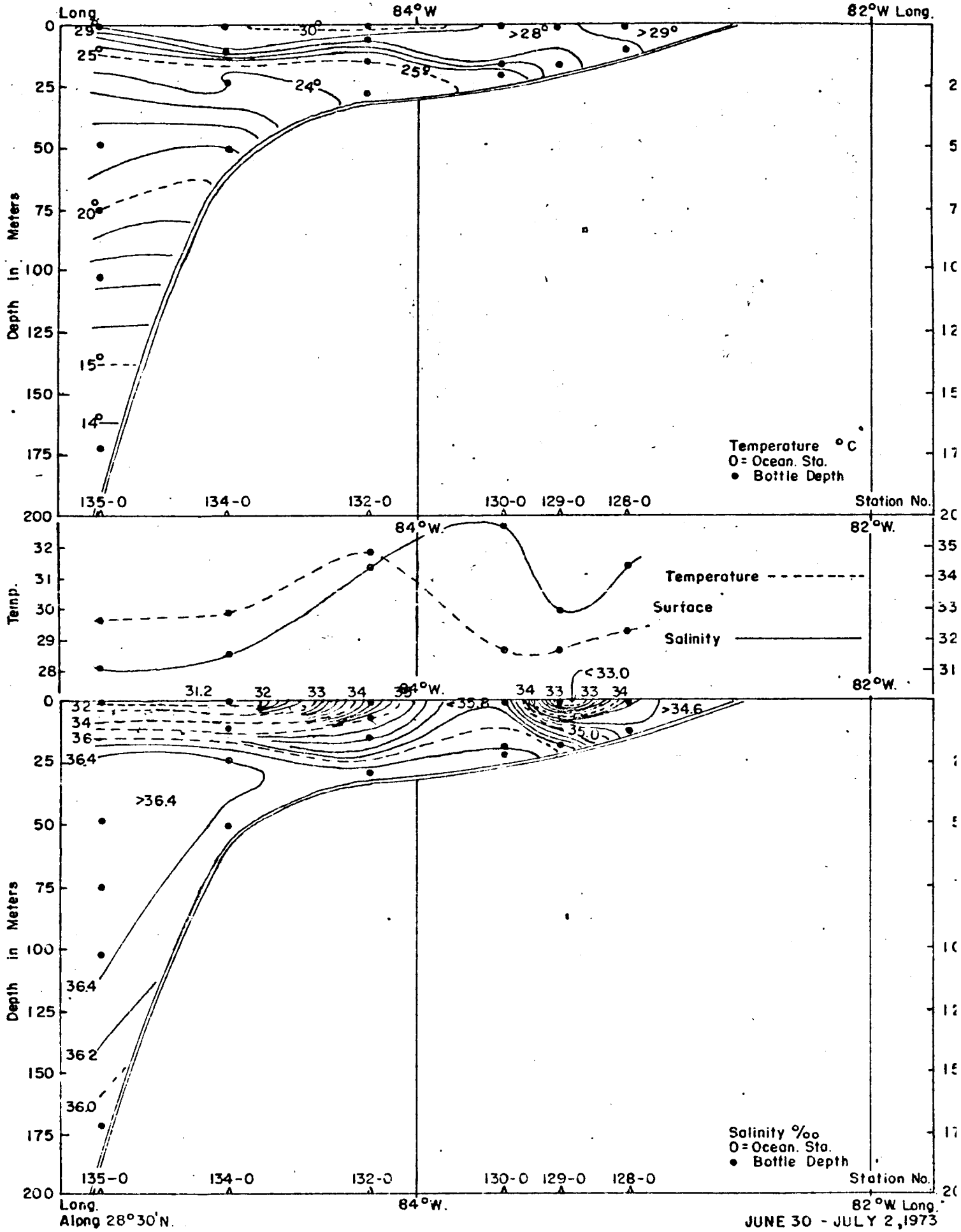

Vertical Distribution - Temperature and Salinity - C. ISELIN - 7311

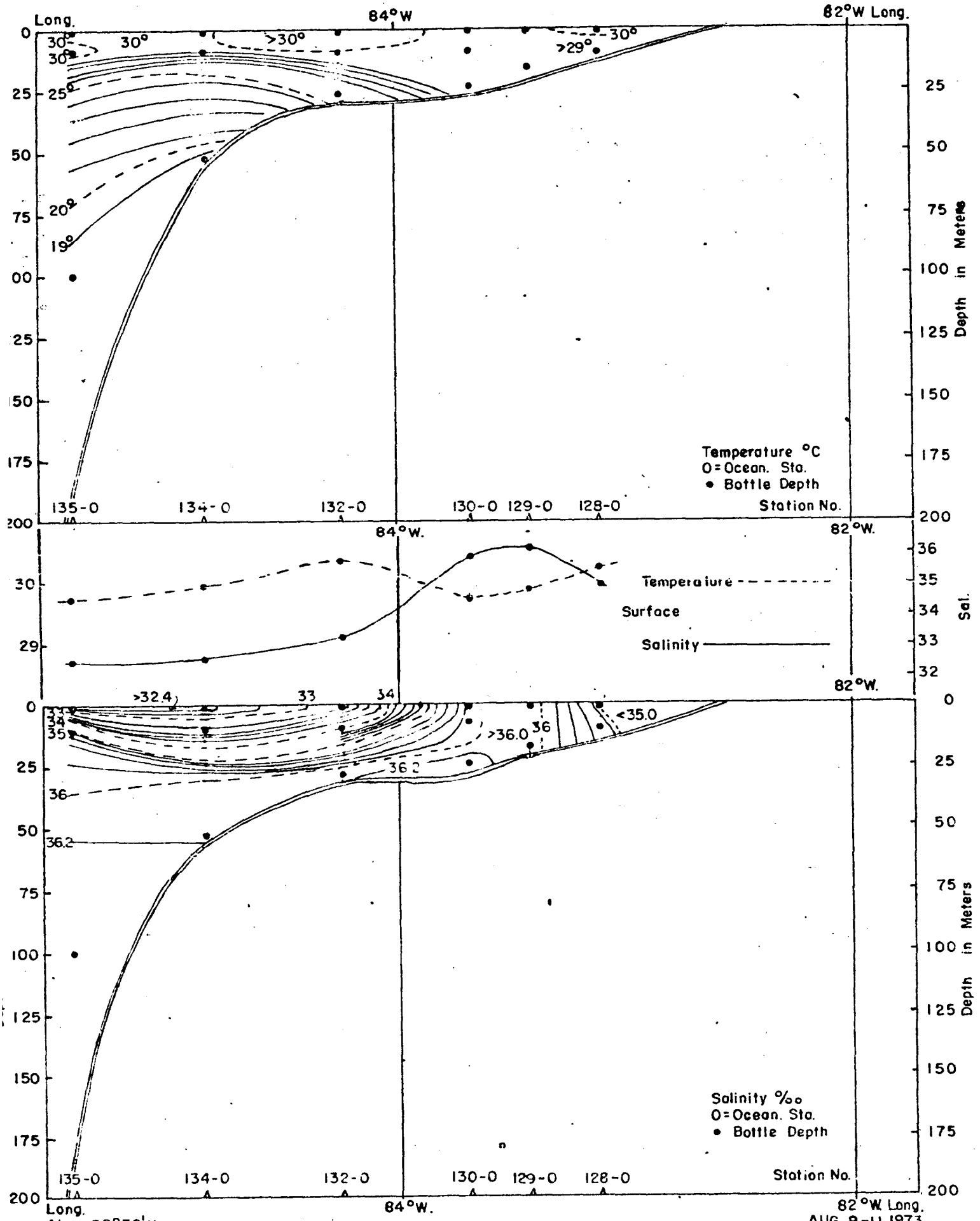
Long.
84°W
82°W Long.
30°
>30°
>29°
25°
20°
19°
Depth in Meters
Temperature °C
0 = Ocean. Sta.
• Bottle Depth
135-0
134-0
132-0
130-0
129-0
128-0
Station No.
84°W.
82°W.
Temperature
Surface
Salinity
Sal.
>32.4
33
34
<35.0
>36.0
36
36.2
Salinity ‰
0 = Ocean. Sta.
• Bottle Depth
Station No.
Long.
Along 28°30'N.
84°W.
82°W Long.
AUG. 9-11, 1973

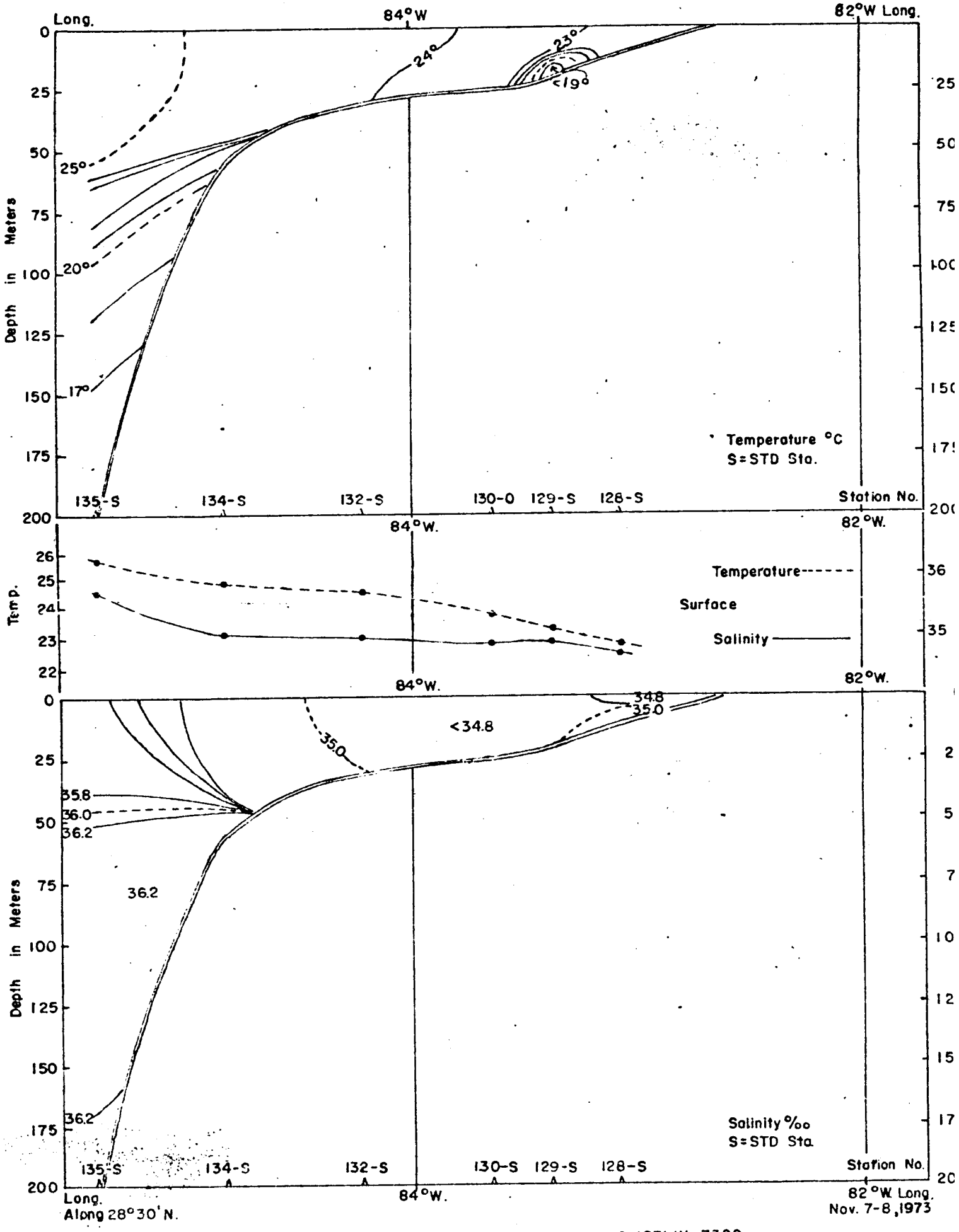

Vertical Distribution - Temperature and Salinity - C. ISELIN - 7320

Appendix VIII

The Basic Characteristics of Modern Recording Current Meters and the Analysis of their Data

James F. Price

Characteristics of Recording Current Meters

Current meters measure and record water temperature, and the direction and speed of the horizontal current at discrete, equally spaced times. The data are recorded internally on magnetic tape. Direct measurement of the very small vertical component of current, though of immense dynamical importance, is not possible with standard techniques at this time. The maximum duration of the record, commonly called a time series, is dependent upon the recording capacity of the particular instrument, and the rate at which samples are recorded. A typical record may have 6 weeks of data recorded at 15-minute intervals. After the current meter is retrieved from the ocean, a number of separate, often time-consuming, procedures are then required to produce useful data. The time from recovery to the first look at the data may be anywhere from several days to several months depending largely upon the degree to which data reduction personnel are experienced and supported by adequate computer facilities. Real time data telemetry is just now becoming feasible, however, the capital cost of such equipment is likely to be considerably higher than the cost of the current meters alone. An example of data reduction techniques and of the data itself may be seen in Price and Mooers (1974).

The percentage of data actually recovered from modern current meters operated by experienced personnel may exceed 80% over a long period. However, the danger always exists that any given mooring and its associated instruments may be lost or that any given instrument may malfunction.

The precision with which a modern current meter can measure current velocity and temperature is quite adequate for most uses. The accuracy of current and temperature measurements depends upon careful recalibration of the sensors at frequent (six months or before each use) intervals.

Time Series Analysis of Current Meter Records

A typical data return from a single current meter may be 5000 points of temperature, of speed, and of direction. Clearly, such large quantities of data must be distilled down to a few conceptually useful statistics before the character of the flow may be deduced.

The most fundamental statistic of all is simply the time average or mean value of the time series. A new time series formed by subtracting the mean from each point of the original series is called the time variable or fluctuating component. The single most important statistic which describes the fluctuating component is its variance (average squared value) or its RMS value (square root of variance). Variance has the units of the parameter squared and is often referred to as energy; for example, in the case of velocity components, the variance of the series is directly proportional to kinetic energy. A number of important

characteristics of a flow may be deduced with variations of the statistics described above. However it is natural to further resolve the fluctuating component into a wide range of frequencies. That is, the time series may be thought to consist of a sum of many independent sinusoidal components. It is then necessary to determine the amplitude of each frequency component. From this point of view the mean value is just the amplitude of the component which has zero frequency or infinite period.

In practice, the amplitudes are found via Fourier transform calculations. The results are often shown as so-called energy spectra and may be displayed in a variety of different formats; Figure IIE-9 is an example. The abscissae of the spectra are frequency, plotted on a log scale in units of cycles per day (cpd), (the corresponding period in days is 1/frequency), and the ordinate is directly proportional to the amplitude squared of the corresponding frequency component times its frequency. Plotted in this manner, the area under the curve is directly proportional to the energy or variance of the corresponding frequency band. The spectra in Figure IIE-9 have further been resolved into components which rotate clockwise and anticlockwise. The total kinetic energy of the horizontal velocity is the sum. Thus, it may be seen (top panel, Figure IIE-9) that the most significant contribution to the total kinetic energy comes from current components which rotate clockwise and which have periods of from 5 to 20 days. The diurnal and semi-diurnal tides appear as sharp spikes at frequencies of 1 and 2 cpd. The area under the tidal spikes, and thus the energy of the tides, is relatively small when compared to that of the low frequency motion.

A great deal of useful information may be obtained by examining the mean and variance of current and temperature. However, still another statistic is needed to describe the linear relation of current or temperature at one location to that at another. The most basic such statistic is the normalized cross correlation function (hereafter referred to as correlation function). The correlation function is computed from two input fluctuation time series and takes on its extreme values of -1 when the two series are exzctly opposite and +1 when they are identical. A correlation near zero(0.2 to+0.2) would indicate the two series were very weakly, if at all, linearly related.

The two input time series may be taken from instruments on the same mooring, in which case the result is a measure of vertical correlation, or from instruments which were at the same depth but on different moorings, in which case the result is a measure of horizontal correlation. An example of such calculations is Figure IIE-10. In general, correlation falls off with increasing separation of the observation points. The distance at which correlation is still significant (approximately0.6) is termed the correlation length or scale.

It is highly desirable that sensors be spaced at distances no greater than the correlation scale. Failure to heed this rule will result in measurements that appear to be unrelated and random. The investigator designing an instrument array must find a balance between the need to take measurements over as large an area as possible and the restraints imposed by the correlation scales of the flow field.

Appendix IX

Salinity Core Maximum Value

Data from the program includes temperature and salinity information from either oceanographic station casts or STD lowerings. The salinity values used to derive the horizontal charts of the maximum salinity distribution came from the station curves, the oceanographic station casts or the STD lowerings themselves. Between May, 1971, and February, 1972, the charts include data from the South Florida Environmental Study by the National Marine Fisheries Service.

The data are from master station locations as indicated by solid circles or by other symbols for cruises run in connection with the Western Florica Continental Shelf Program or within the time frame of such cruises. The data have been contoured at whole parts per thousand of salinity, and matting has been applied for all values in excess of 36.5 °/oo, and such waters are classified as Loop Current waters.

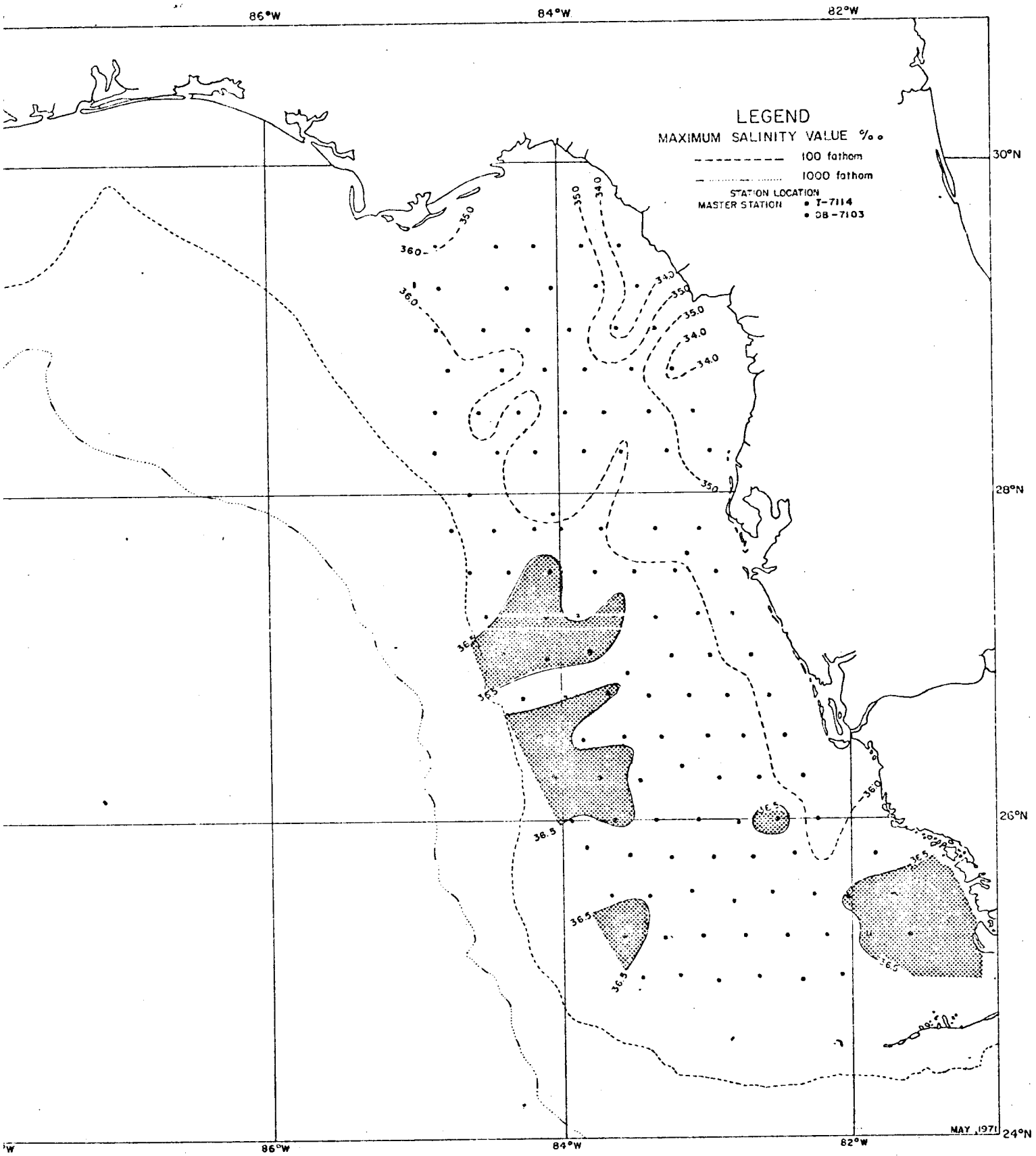
86°W
84°W
82°W
30°N
28°N
26°N
24°N
LEGEND
MAXIMUM SALINITY VALUE ‰
100 fathom
1000 fathom
STATION LOCATION
MASTER STATION
T-7114
DB-7103
35.0
34.0
36.0
36.5
38.5
MAY 1971

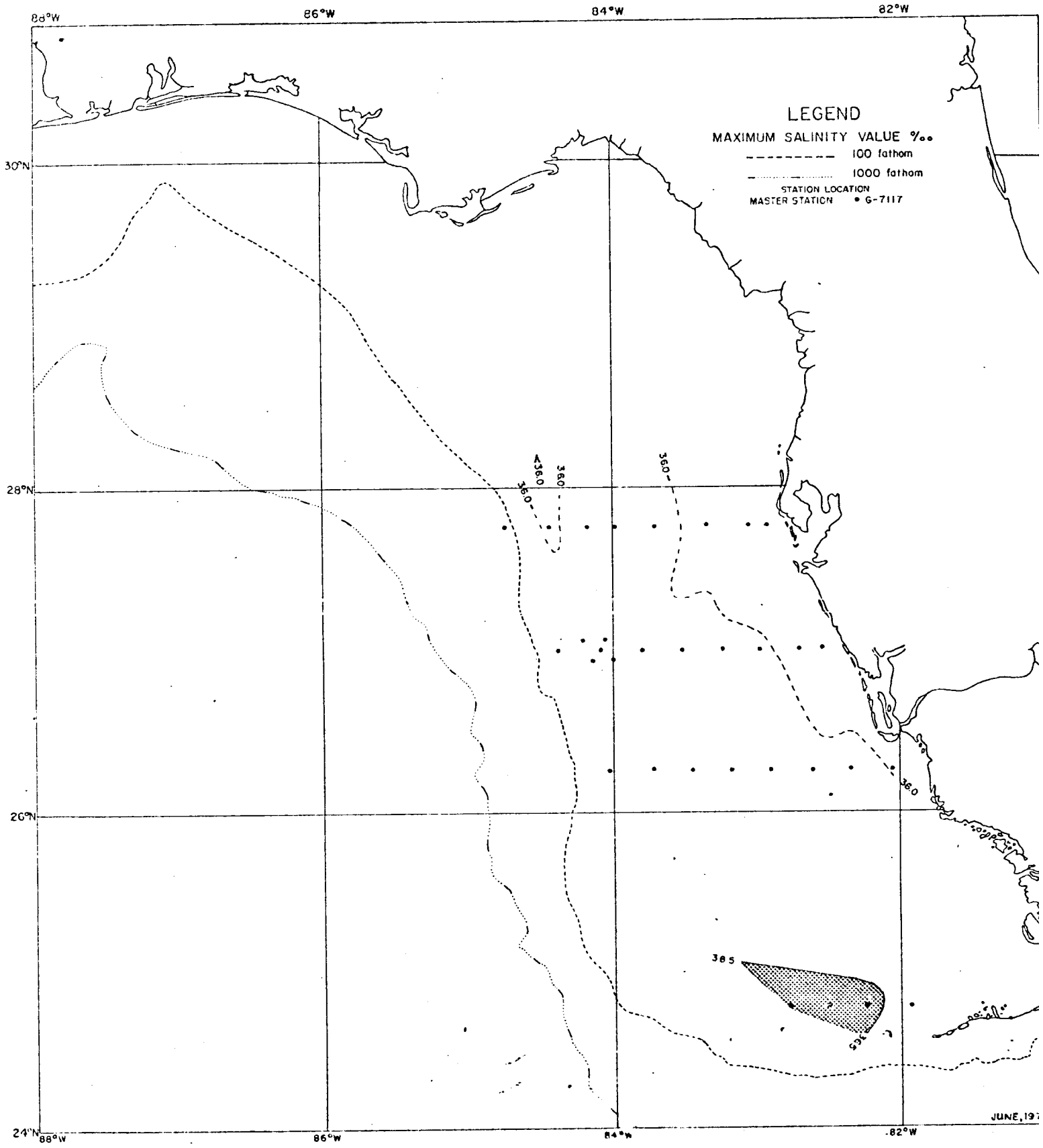
88°W
86°W
84°W
82°W
30°N
28°N
26°N
24°N
LEGEND
MAXIMUM SALINITY VALUE ‰
100 fathom
1000 fathom
STATION LOCATION
MASTER STATION • G-7117
<36.0
36.0
36.5
JUNE, 19

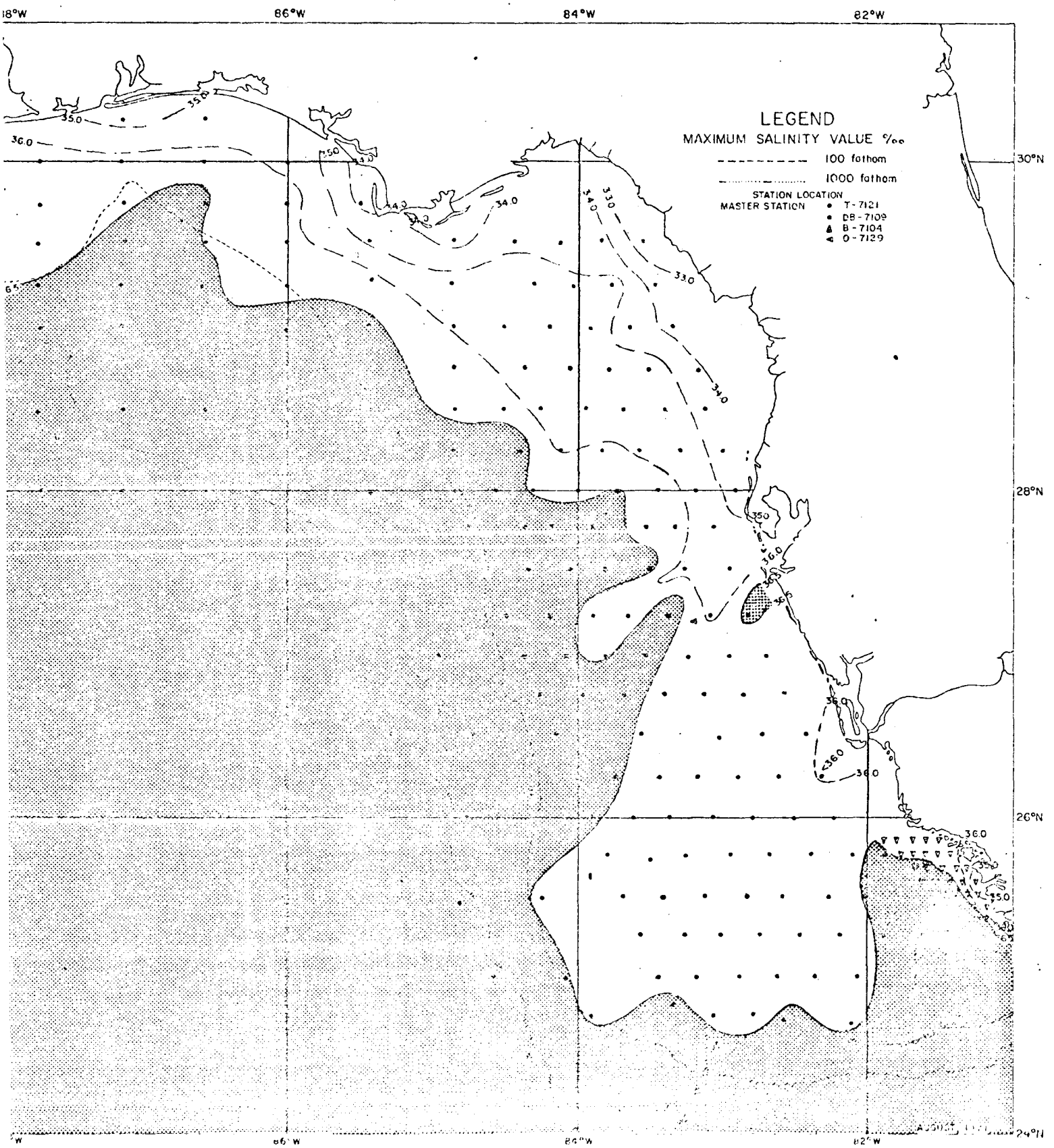
LEGEND
MAXIMUM SALINITY VALUE ‰
100 fathom
1000 fathom
STATION LOCATION
MASTER STATION
T - 7121
DB - 7109
B - 7104
O - 7129
88°W
86°W
84°W
82°W
30°N
28°N
26°N
24°N
35.0
36.0
34.0
33.0
<36.0

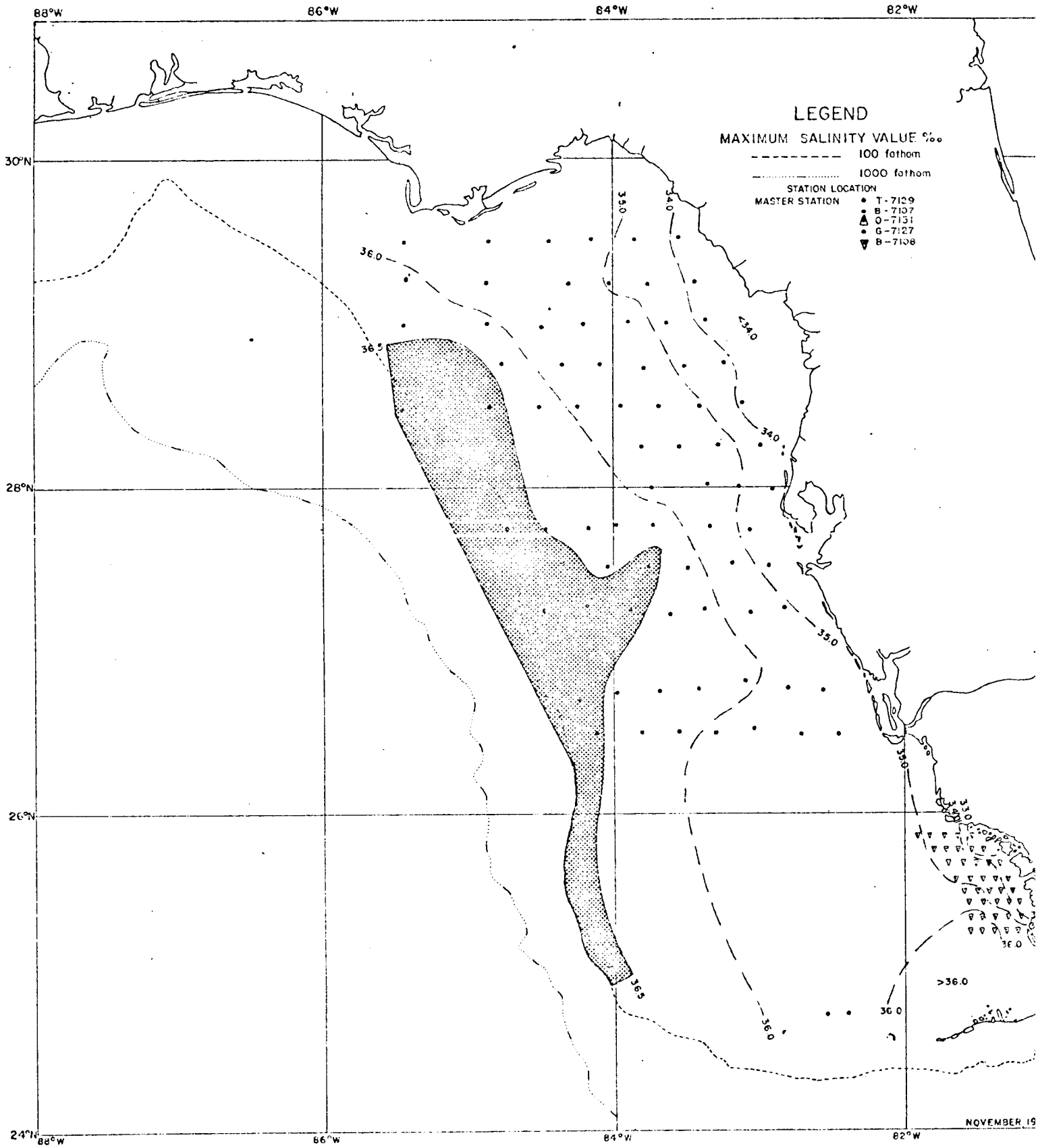
88°W
86°W
84°W
82°W
30°N
28°N
26°N
24°N
LEGEND
MAXIMUM SALINITY VALUE ‰
100 fathom
1000 fathom
STATION LOCATION
MASTER STATION
T-7129
B-7107
O-7131
G-7127
B-7108
35.0
34.0
36.0
36.5
<34.0
34.0
35.0
36.5
36.0
>36.0
36.0
36.0
NOVEMBER 19

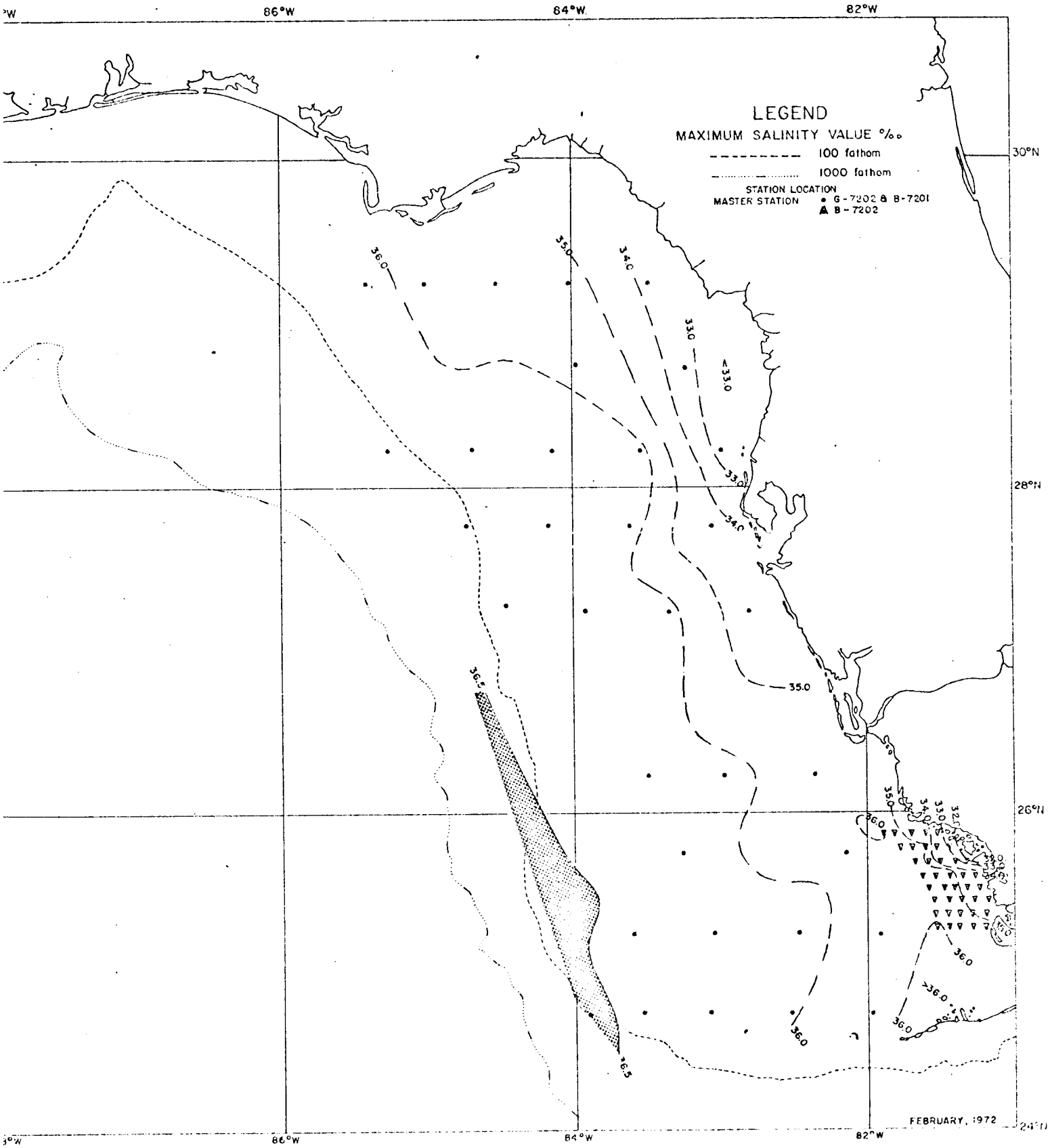
LEGEND
MAXIMUM SALINITY VALUE ‰
100 fathom
1000 fathom
STATION LOCATION
MASTER STATION
G-7202 & B-7201
B-7202
86°W
84°W
82°W
30°N
28°N
26°N
36.0
35.0
34.0
33.0
36.5
FEBRUARY, 1972

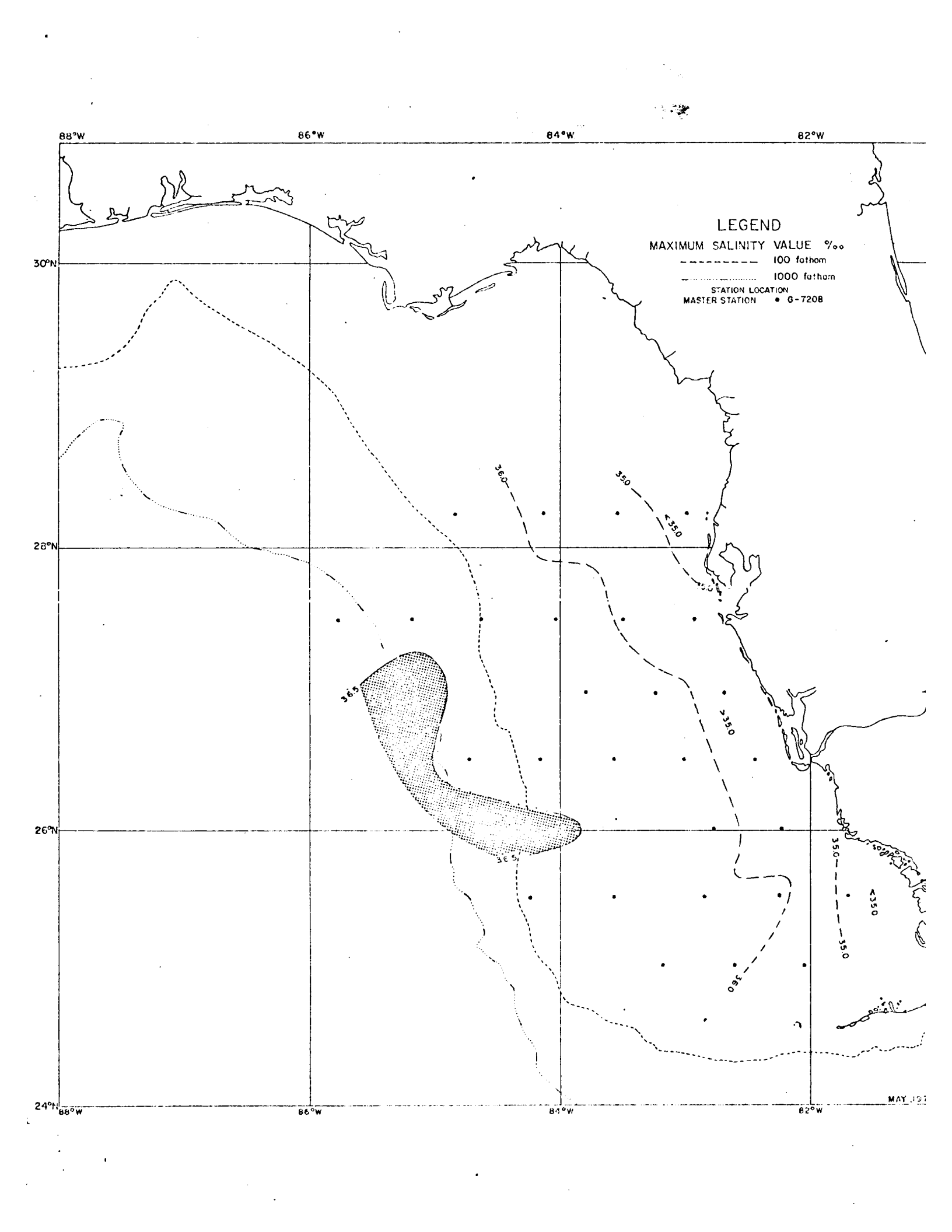
88°W
86°W
84°W
82°W
30°N
28°N
26°N
24°N
LEGEND
MAXIMUM SALINITY VALUE ‰
100 fathom
1000 fathom
STATION LOCATION
MASTER STATION • G-7208
360
350
<350
>350
365
MAY 197

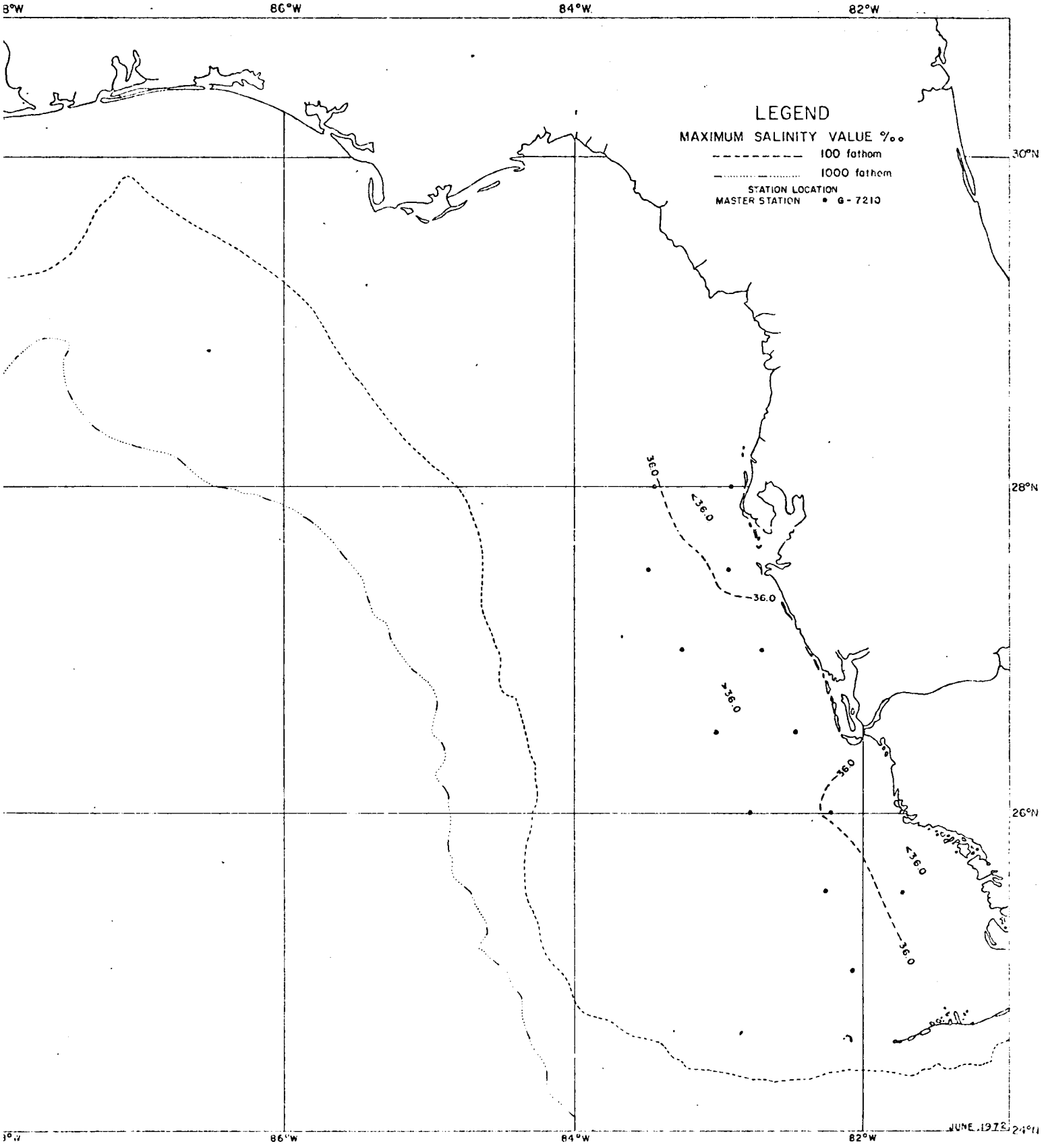
LEGEND
MAXIMUM SALINITY VALUE ‰
100 fathom
1000 fathom
STATION LOCATION
MASTER STATION • G-7210
88°W
86°W
84°W
82°W
30°N
28°N
26°N
24°N
36.0
<36.0
>36.0
JUNE, 1972

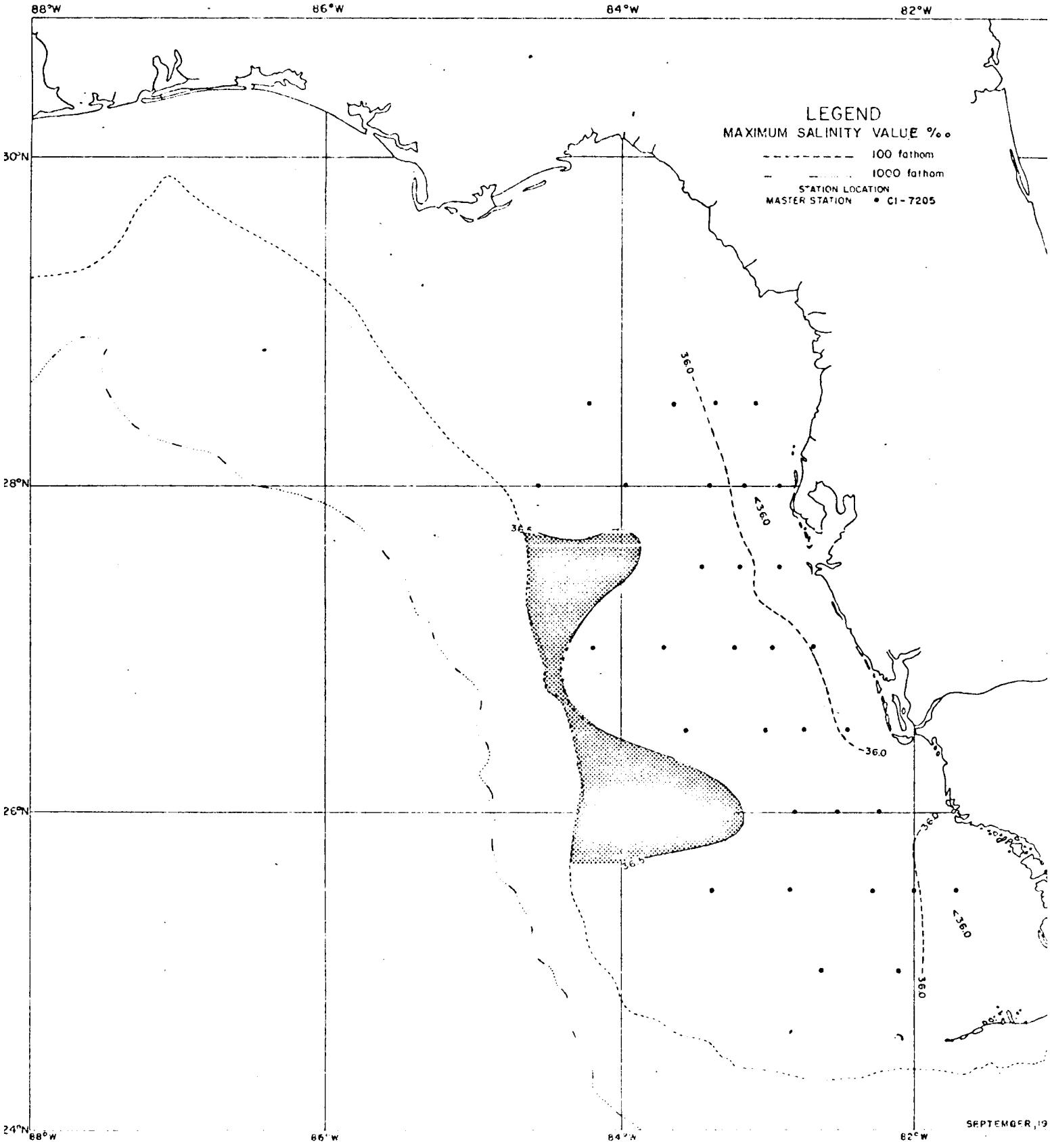
88°W
86°W
84°W
82°W
30°N
28°N
26°N
24°N
LEGEND
MAXIMUM SALINITY VALUE ‰
100 fathom
1000 fathom
STATION LOCATION
MASTER STATION • CI-7205
36.0
<36.0
36.5
SEPTEMBER, 19

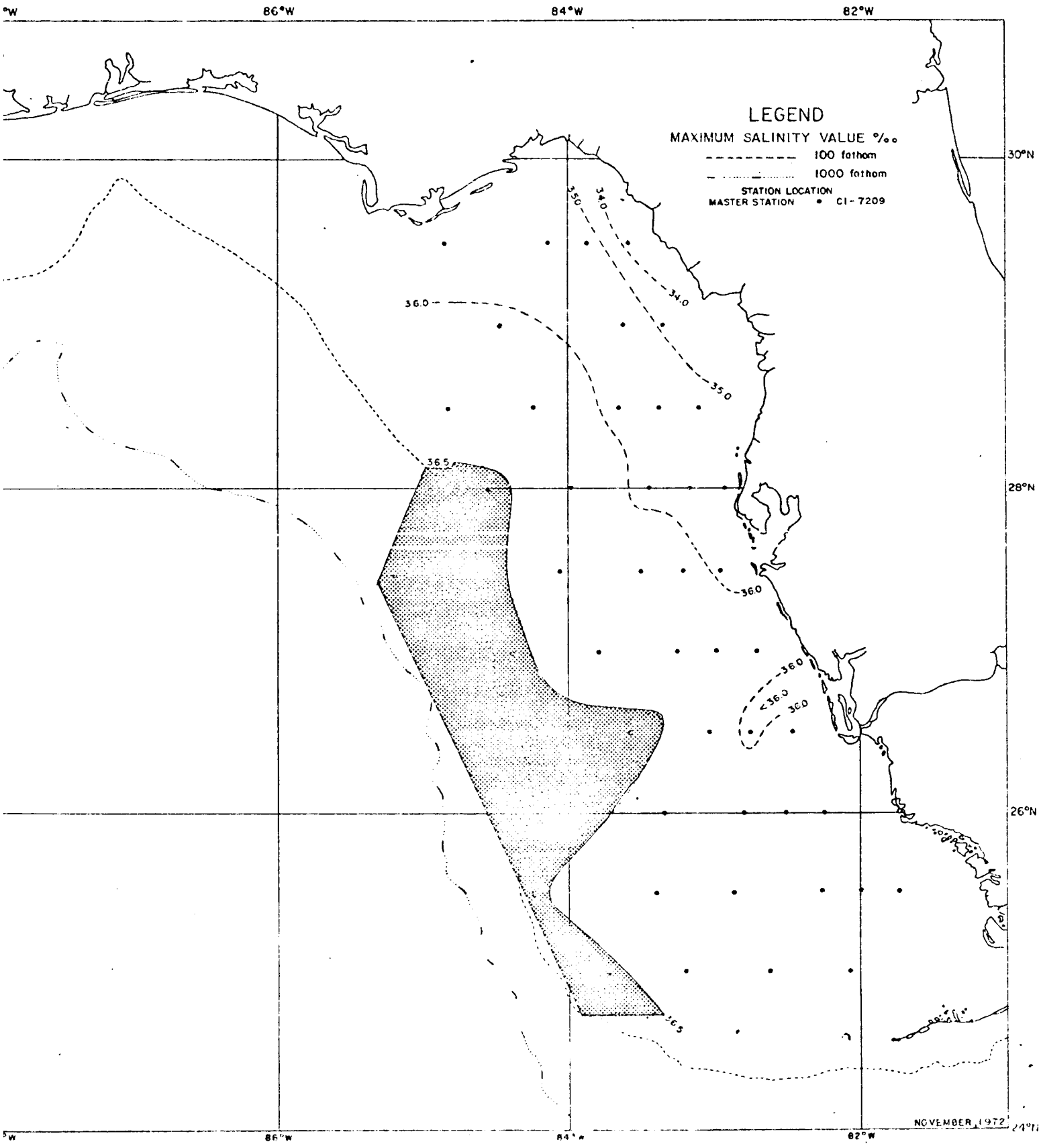
LEGEND
MAXIMUM SALINITY VALUE ‰
100 fathom
1000 fathom
STATION LOCATION
MASTER STATION • CI-7209
86°W
84°W
82°W
30°N
28°N
26°N
35.0
34.0
36.0
36.5
<36.0
NOVEMBER 1972

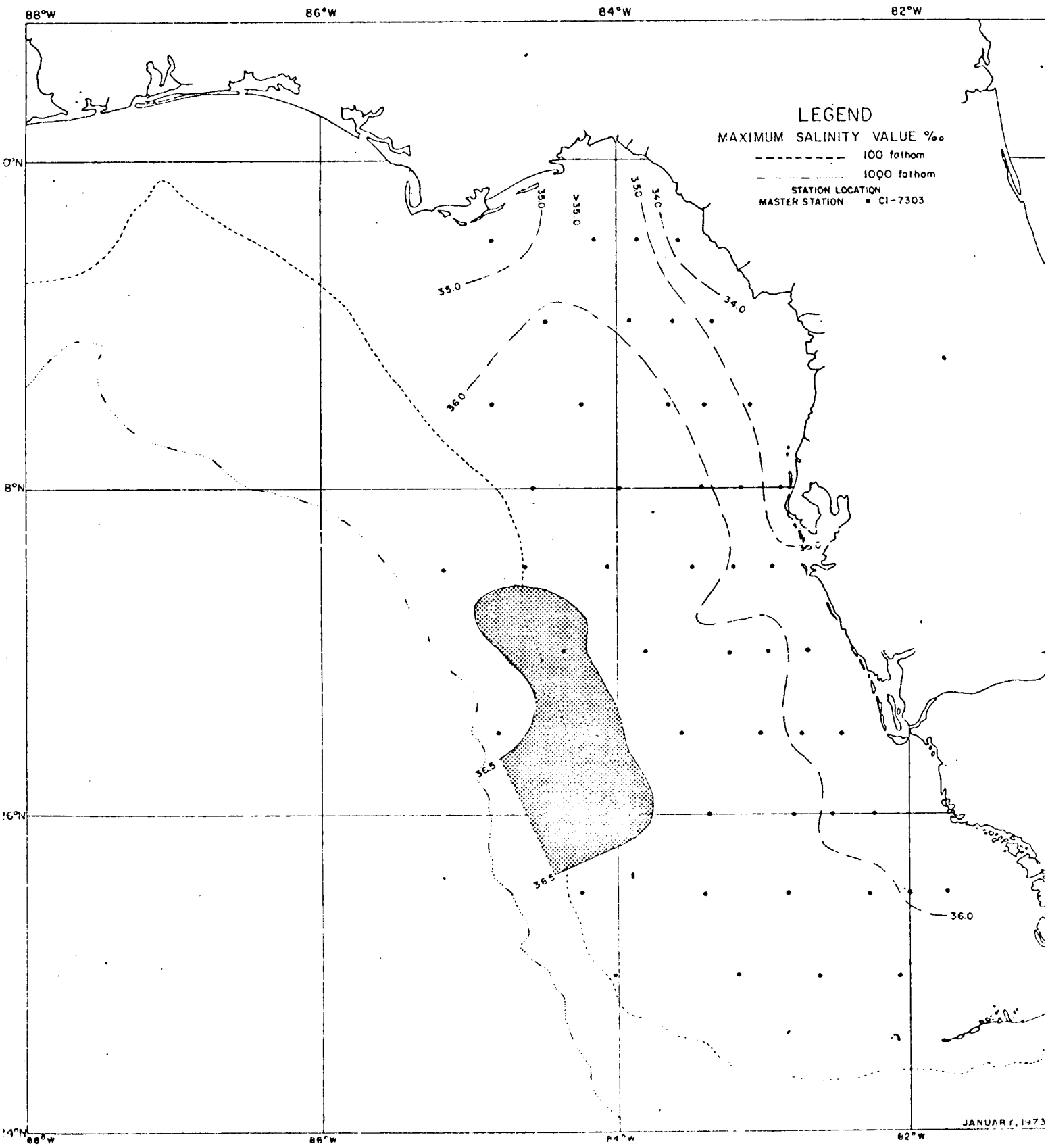
88°W
86°W
84°W
82°W
10°N
8°N
6°N
4°N
LEGEND
MAXIMUM SALINITY VALUE ‰
100 fathom
1000 fathom
STATION LOCATION
MASTER STATION • CI-7303
35.0
34.0
36.0
36.5
JANUARY, 1973

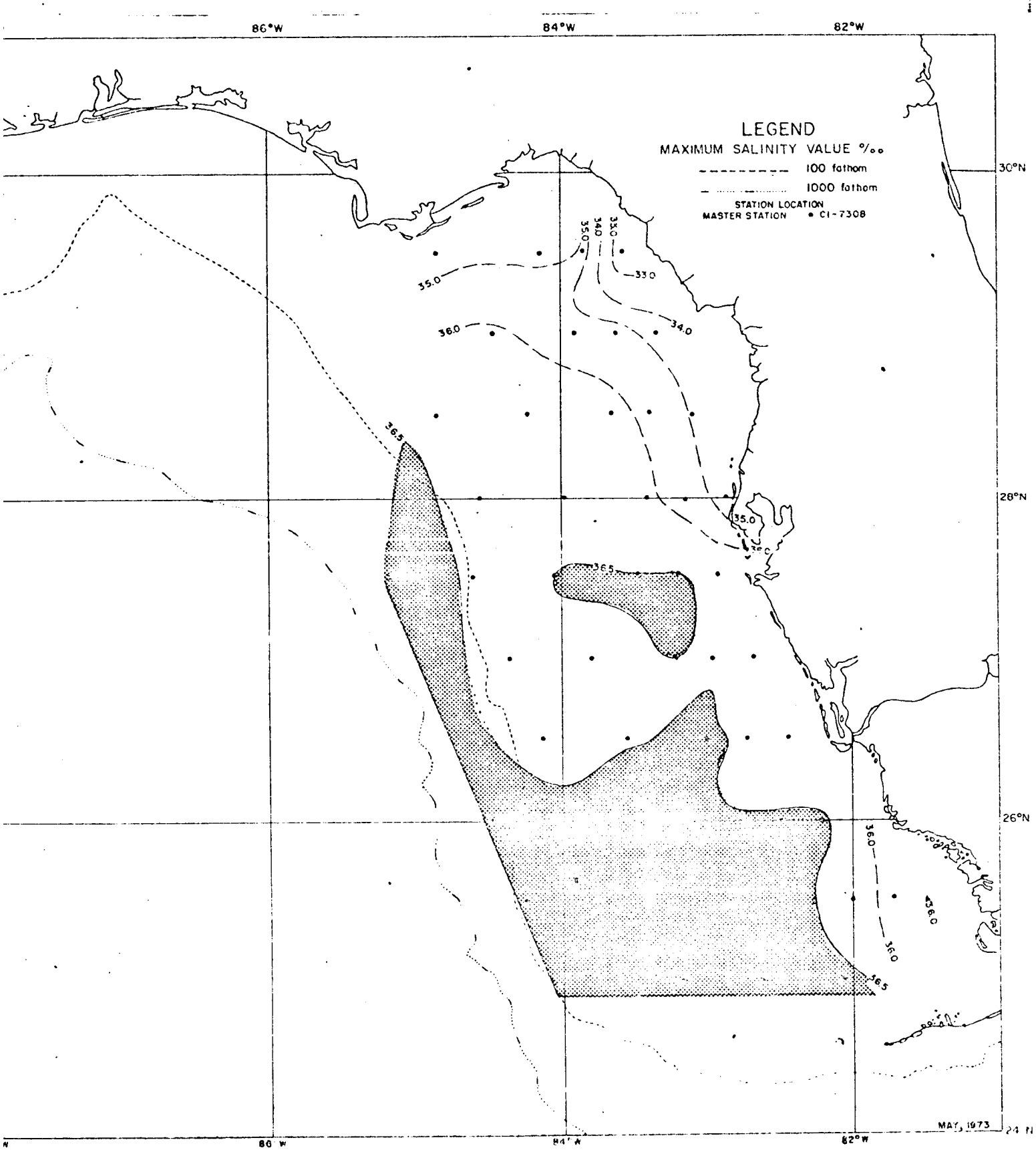
86°W
84°W
82°W
30°N
28°N
26°N
24°N
LEGEND
MAXIMUM SALINITY VALUE °/₀₀
100 fathom
1000 fathom
STATION LOCATION
MASTER STATION • CI-7308
35.0
34.0
33.0
36.5
36.0
MAY, 1973

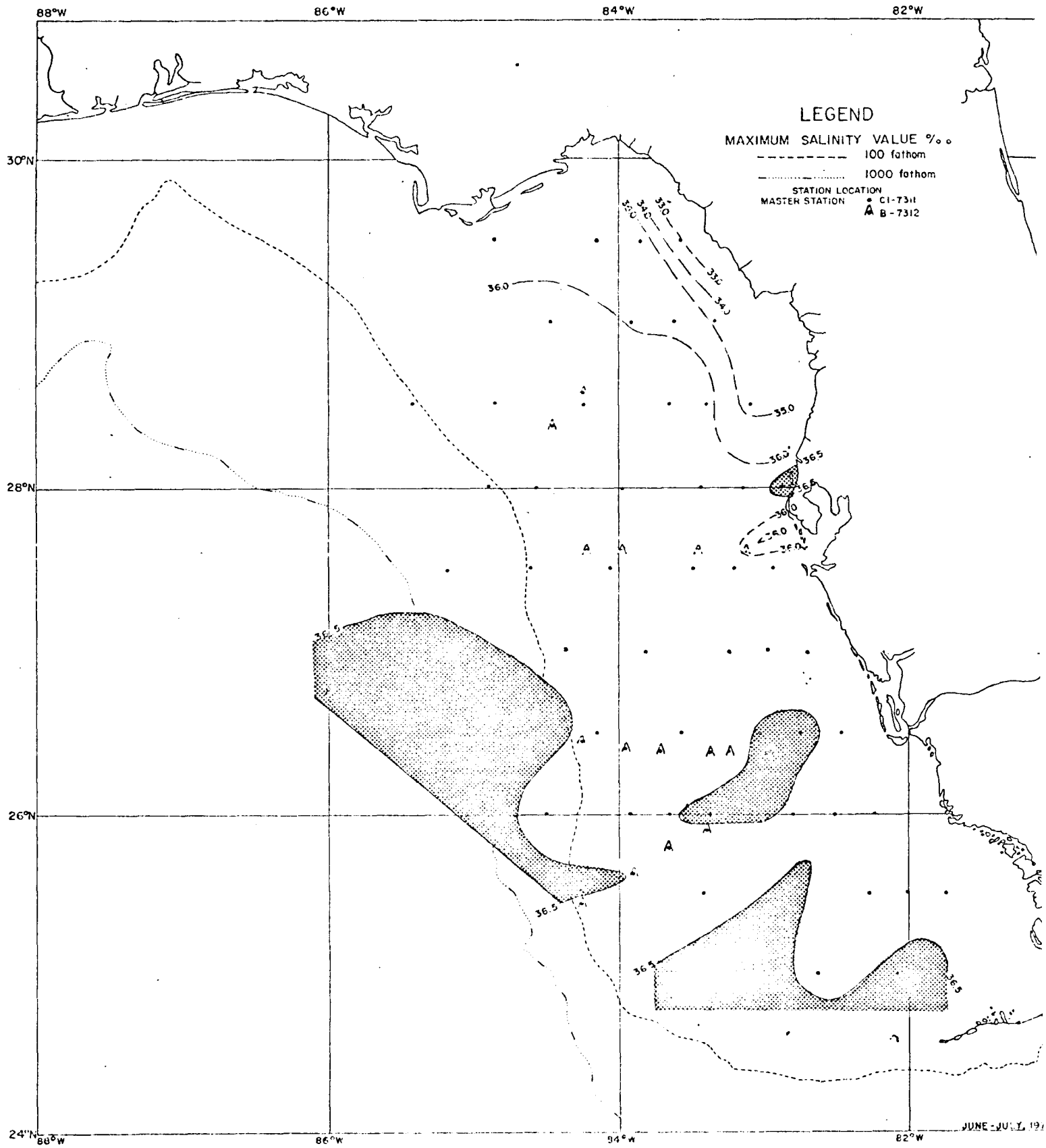
88°W
86°W
84°W
82°W
30°N
28°N
26°N
24°N
LEGEND
MAXIMUM SALINITY VALUE ‰
100 fathom
1000 fathom
STATION LOCATION
MASTER STATION
CI-7311
B-7312
320
330
340
350
360
365
36.5
JUNE-JULY 19

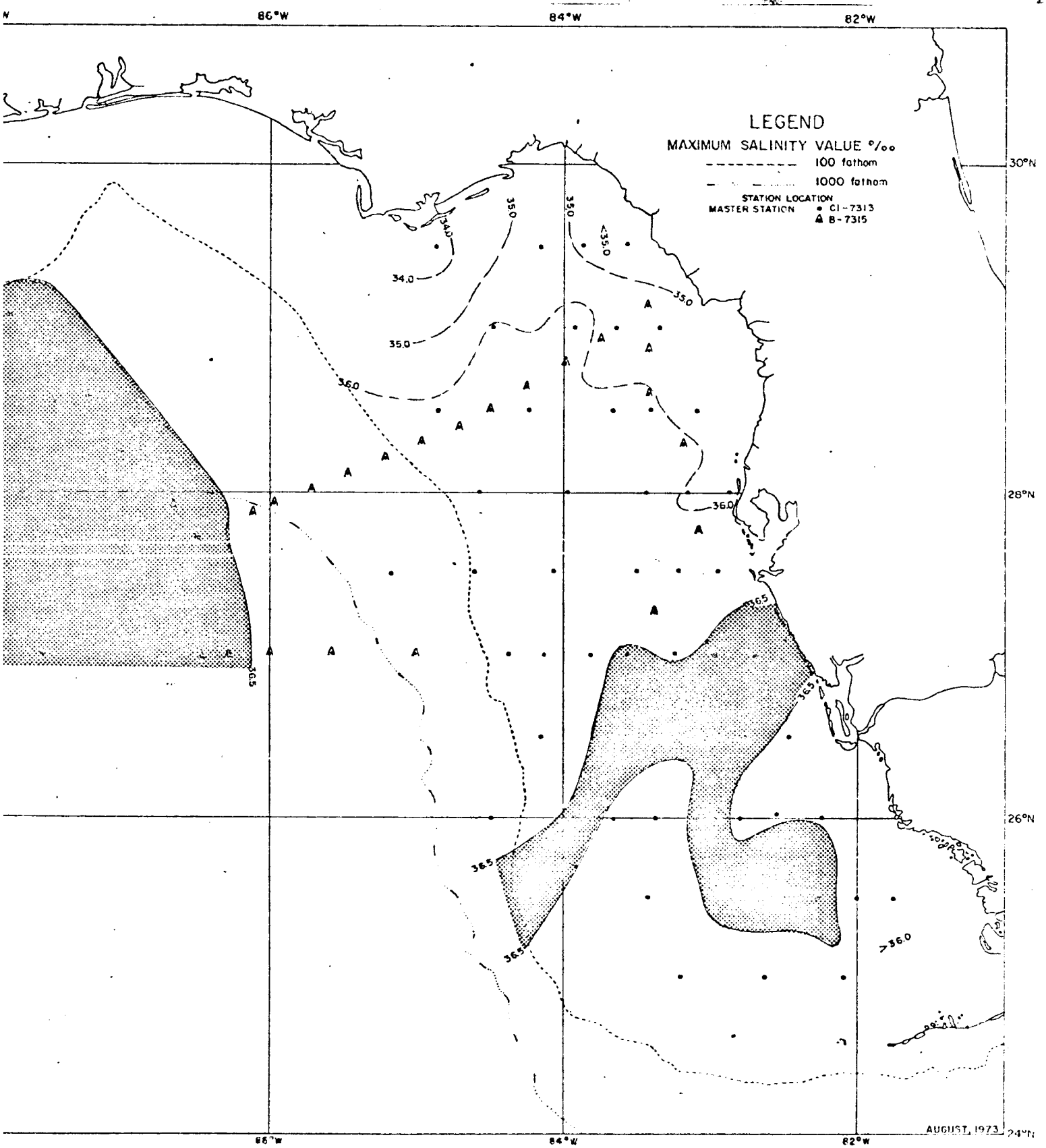
86°W
84°W
82°W
30°N
28°N
26°N
24°N
LEGEND
MAXIMUM SALINITY VALUE °/oo
100 fathom
1000 fathom
STATION LOCATION
MASTER STATION
C1-7313
B-7315
34.0
35.0
<35.0
36.0
36.5
>36.0
AUGUST, 1973

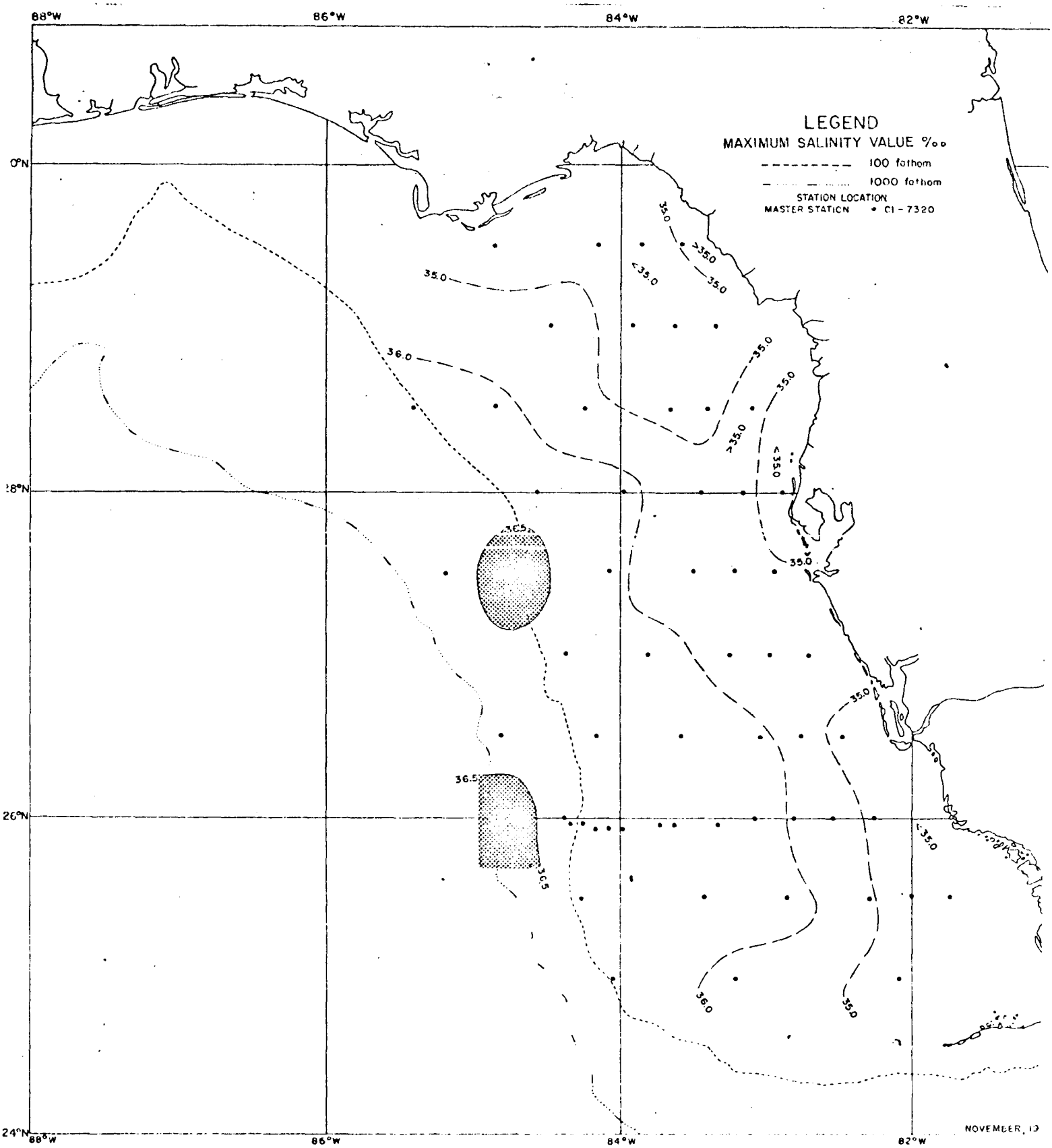
88°W
86°W
84°W
82°W
0°N
28°N
26°N
24°N
LEGEND
MAXIMUM SALINITY VALUE ‰
100 fathom
1000 fathom
STATION LOCATION
MASTER STATION • CI - 7320
35.0
36.0
36.5
NOVEMBER, 19

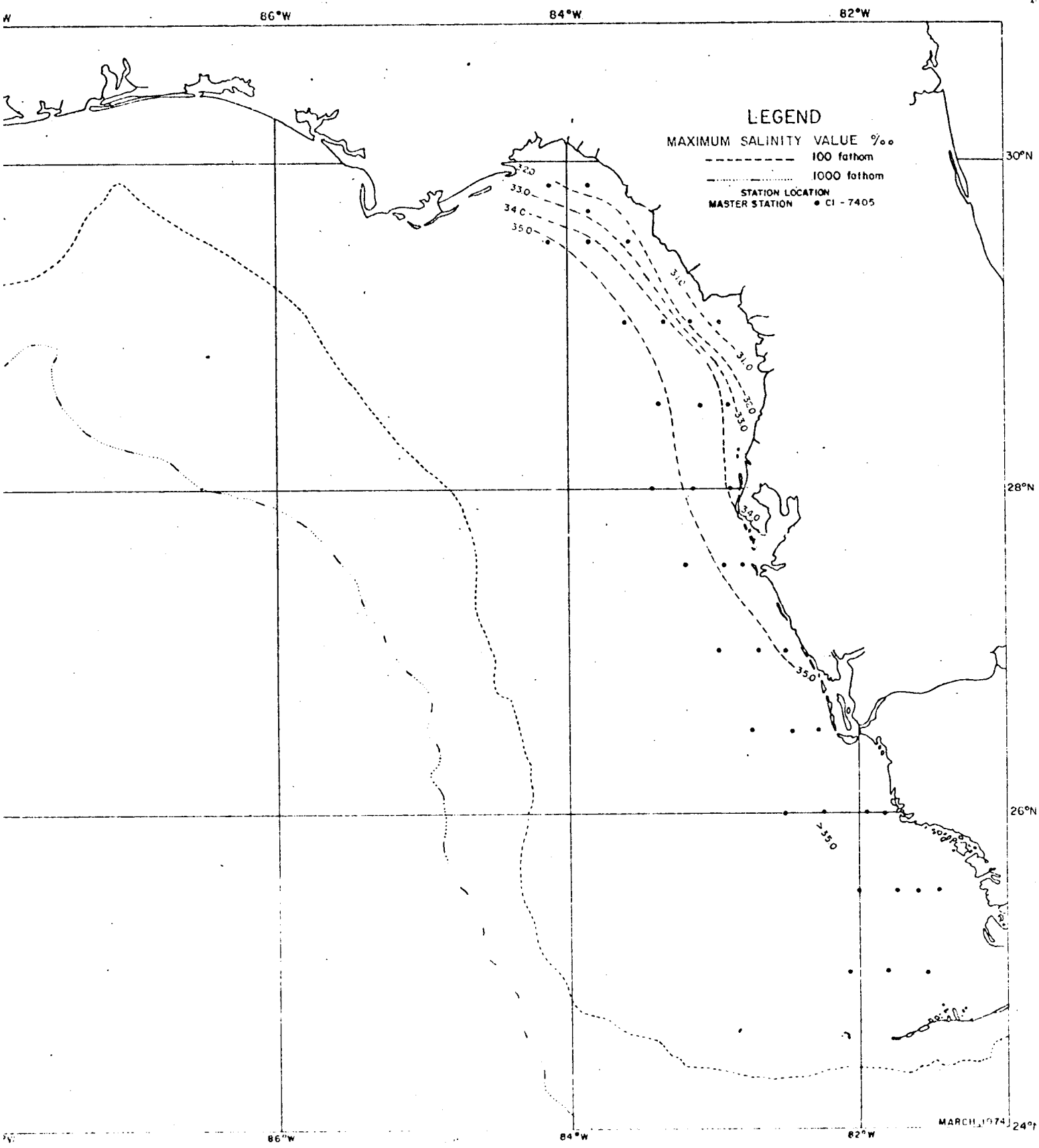
86°W
84°W
82°W
30°N
28°N
26°N
24°N
LEGEND
MAXIMUM SALINITY VALUE ‰
100 fathom
1000 fathom
STATION LOCATION
MASTER STATION • CI - 7405
320
330
340
350
310
310
330
350
340
350
>350
MARCH 1974

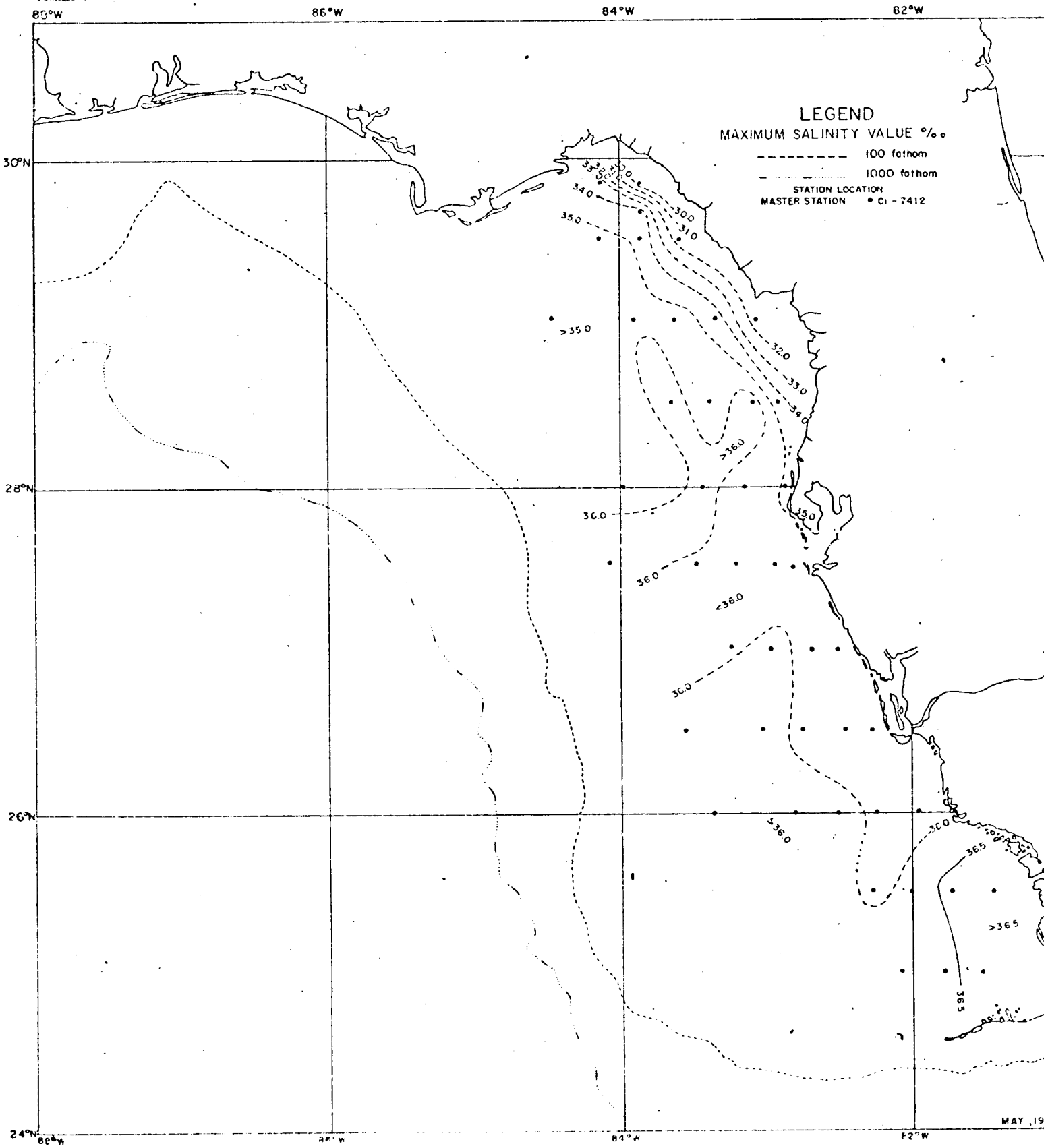
88°W
86°W
84°W
82°W
30°N
28°N
26°N
24°N
LEGEND
MAXIMUM SALINITY VALUE °/oo
100 fathom
1000 fathom
STATION LOCATION
MASTER STATION • CI - 7412
330
340
350
300
310
320
330
340
>350
>360
360
350
360
<360
360
<360
360
365
>365
365
MAY ,19

Appendix X

Meteorological Evaluation of LCB Buoys In the Gulf of Mexico

Jose Fernandez-Partagas
Christopher N. K. Mooers

This study is designed to investigate the performance of NDBO's LCB buoys in terms of producing meteorological observations which are good enough to describe synoptic-scale features affecting the Gulf of Mexico area. The evaluation covers one period in the first half of 1973 and a second period in the second half of 1974 and in the beginning of 1975. Raw data provided by the LCB buoys are edited for complete meteorological observations which include the surface pressure, the temperature, the wind direction, and the wind speed. Complete meteorological observations are then plotted in the form of time series. These time series allow us (1) to intercompare the various buoys' performance; (2) to compare buoy meteorological information with information from other sources; and (3) to investigate the buoys' response to synoptic-scale features. Preliminary results, which are based upon the examination of 1973 and 1974 data, indicate that most LCB buoys tend to intercompare satisfactorily and tend to compare favorably with data from other sources. In general, the preliminary results show, a reasonable response of the buoys' sensors to synoptic-scale features (chiefly atmospheric cold fronts).


90° W
40° N
95° W
35° N
30° N
100° W
25° N
100° W
PIEDMONT
MISS.
G U L F C O A S T A L P L A I N
TEXAS—LOUISIANA SHELF
WESTERN GULF RISE
EAST MEXICO SHELF
EAST MEXICO